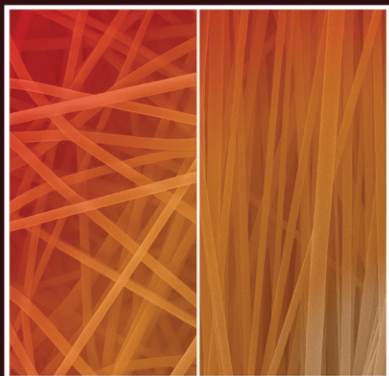


WOODHEAD PUBLISHING SERIES IN BIOMATERIALS



Electrospun Materials for Tissue Engineering and Biomedical Applications

Research, Design and Commercialization

Edited by
Tamer Uyar and Erich Kny

WP
WOODHEAD
PUBLISHING

Electrospun Materials for Tissue Engineering and Biomedical Applications

Related titles

Biomaterials Science 3e
(ISBN: 978-0-12-374626-9)

Electrospinning for Biomedical Applications
(ISBN: 978-1-84569-741-9)

Biomaterials for Biomedical Applications
(ISBN: 978-0-85709-699-9)

Woodhead Publishing Series in Biomaterials

Electrospun Materials for Tissue Engineering and Biomedical Applications

Research, Design and Commercialization

Edited by

Tamer Uyar and Erich Kny



WP

WOODHEAD
PUBLISHING

An imprint of Elsevier

Woodhead Publishing is an imprint of Elsevier
The Officers' Mess Business Centre, Royston Road, Duxford, CB22 4QH, United Kingdom
50 Hampshire Street, 5th Floor, Cambridge, MA 02139, United States
The Boulevard, Langford Lane, Kidlington, OX5 1GB, United Kingdom

© 2017 Elsevier Ltd. All rights reserved.

No part of this publication may be reproduced or transmitted in any form or by any means, electronic or mechanical, including photocopying, recording, or any information storage and retrieval system, without permission in writing from the publisher. Details on how to seek permission, further information about the Publisher's permissions policies and our arrangements with organizations such as the Copyright Clearance Center and the Copyright Licensing Agency, can be found at our website: www.elsevier.com/permissions.

This book and the individual contributions contained in it are protected under copyright by the Publisher (other than as may be noted herein).

Notices

Knowledge and best practice in this field are constantly changing. As new research and experience broaden our understanding, changes in research methods, professional practices, or medical treatment may become necessary.

Practitioners and researchers must always rely on their own experience and knowledge in evaluating and using any information, methods, compounds, or experiments described herein. In using such information or methods they should be mindful of their own safety and the safety of others, including parties for whom they have a professional responsibility.

To the fullest extent of the law, neither the Publisher nor the authors, contributors, or editors, assume any liability for any injury and/or damage to persons or property as a matter of products liability, negligence or otherwise, or from any use or operation of any methods, products, instructions, or ideas contained in the material herein.

Library of Congress Cataloging-in-Publication Data

A catalog record for this book is available from the Library of Congress

British Library Cataloguing-in-Publication Data

A catalogue record for this book is available from the British Library

ISBN: 978-0-08-101022-8 (print)

ISBN: 978-0-08-102222-1 (online)

For information on all Woodhead publications visit our website at <https://www.elsevier.com/books-and-journals>



Working together
to grow libraries in
developing countries

www.elsevier.com • www.bookaid.org

Publisher: Matthew Deans

Acquisition Editor: Laura Overend

Editorial Project Manager: Natasha Welford

Production Project Manager: Poulouse Joseph

Cover Designer: Greg Harris, Asli Celebioglu, Tamer Uyar

Typeset by SPi Global, India

Contents

List of contributors	xi
Preface	xv
Part One Introduction to Electrospinning for Biomedical and Tissue Engineering Applications	1
1 Electrospinning: A versatile processing technology for producing nanofibrous materials for biomedical and tissue-engineering applications	3
<i>A. Senthamizhan, B. Balusamy, T. Uyar</i>	
1.1 Introduction	3
1.2 Biomedical application of electrospun nanofibers	4
1.3 Commercialization prospectus	34
1.4 Conclusion	36
Acknowledgments	38
References	38
2 General requirements of electrospun materials for tissue engineering: Setups and strategy for successful electrospinning in laboratory and industry	43
<i>E. Kijeńska, W. Swieszkowski</i>	
2.1 Electrospinnable materials for TE applications	45
2.2 Electrospinning technologies and set-ups	47
2.3 Basics of industrial upscaling of electrospinning	53
2.4 Conclusions	53
References	54
3 Biomedical applications of electrospinning, innovations, and products	57
<i>J.M. Lagaron, A. Solouk, S. Castro, Y. Echegoyen</i>	
3.1 Innovative technologies with potential for scaling	57
3.2 Brief history of electrospinning	57
3.3 Nozzle-based multijet electrospinning	58
3.4 Electroblowing	60
3.5 Fiber generators in needleless electrospinning	60
3.6 Bubble-electrospinning	64

3.7	Electrospinning-based scaled up developments and commercial products	66
3.8	Future prospects and outlook	69
	References	69
4	Structuring of electrospun nanofiber mats by 3D printing methods	73
	<i>N. Shah Hosseini, N. Khenoussi</i>	
4.1	Introduction	73
4.2	Obtaining oriented nanofibers	74
4.3	Conclusion and future perspectives	83
	References	83
5	Melt electrospinning in tissue engineering	87
	<i>S.M. Willerth</i>	
5.1	Introduction to the process of melt electrospinning	87
5.2	Comparison with solution electrospinning	89
5.3	Applications in tissue engineering	91
5.4	Future directions for the field of melt electrospinning and potential commercial applications	95
	References	96
	Resource List	100
6	In vivo safety evaluations of electrospun nanofibers for biomedical applications	101
	<i>B. Balusamy, A. Senthamizhan, T. Uyar</i>	
6.1	Introduction	101
6.2	Safety evaluations of nanofibers	102
6.3	Conclusions and outlook	112
	Acknowledgments	112
	References	113
Part Two Specific Biomedical and Tissue Engineering Application Areas of Electrospinning		115
7	Electrospun systems for drug delivery	117
	<i>B.A. Minden-Birkenmaier, G.S. Selders, A.E. Fetz, C.J. Gehrman, G.L. Bowlin</i>	
7.1	Introduction	117
7.2	Postelectrospinning modification	119
7.3	Polymer/drug blend electrospinning	125
7.4	Coaxial electrospinning	131
7.5	Electrospinning drug-loaded micro/nanoparticles	132
7.6	Commercialization prospects	134

7.7	Outlook, problems to be overcome	138
7.8	Conclusion	140
	References	141
8	Electrospun nanofibrous materials for wound healing applications	147
	<i>B. Balusamy, A. Senthamizhan, T. Uyar</i>	
8.1	Introduction	147
8.2	Electrospun nanofibrous scaffolds in wound healing	150
8.3	Current challenges and future directions	173
	Acknowledgments	174
	References	174
9	Electrospun biomaterials for dermal regeneration	179
	<i>E.A. Growney Kalaf, K.R. Hixon, P.U. Kadakia, A.J. Dunn, S.A. Sell</i>	
9.1	Overview	179
9.2	Electrospun scaffolds for dermal wound healing	192
9.3	Conclusions and outlook	218
	References	220
10	Electrospun materials for bone and tendon/ligament tissue engineering	233
	<i>N. Bölgen</i>	
10.1	Introduction	233
10.2	Bone structure and bone tissue engineering	234
10.3	Electrospun scaffolds for bone regeneration	235
10.4	Tendon/ligament structure and tendon/ligament tissue engineering	248
10.5	Electrospun scaffolds for tendon/ligament regeneration	248
10.6	Conclusions	252
	Acknowledgment	254
	References	254
11	Electrospun scaffolds for vascular tissue engineering	261
	<i>O. Karaman, M. Şen, E.A. Demirci</i>	
11.1	Introduction	261
11.2	Structure of blood vessels	262
11.3	Biomaterials used for nanofiber fabrication in vascularization	266
11.4	Fabrication parameters for electrospun scaffolds	268
11.5	Biological and mechanical properties of electrospun scaffolds for vascular tissue engineering	270
11.6	In vivo applications of tubular electrospun scaffolds in vascular tissue engineering	276
11.7	Conclusions and future perspectives	279
	Acknowledgments	280
	References	280

12	Electrospun scaffolds for cardiac tissue engineering	289
	<i>A.H. Hekmati, M. Norouzi</i>	
12.1	Introduction	289
12.2	Cardiac patch	290
12.3	Bio-functionalized cardiac patch	292
12.4	Heart valve scaffolds	294
12.5	Conclusion	295
	References	295
13	Electrospun scaffolds for neural tissue engineering	299
	<i>P. Chen, A.E. Rodda, H.C. Parkington, J.S. Forsythe</i>	
13.1	Introduction	299
13.2	3D in vitro platforms to study neuronal physiology	301
13.3	Surface functionalization and drug release	305
13.4	Electrospun fibers for brain repair	309
13.5	Electroactive fibers for nerve stimulation	311
13.6	Commercialization aspects	313
13.7	Future challenges	314
	References	315
14	Coaxial electrospun nanofibers for nanomedicine	321
	<i>K. Vodsed' álková, L. Vysloužilová, L. Berezkinová</i>	
14.1	Introduction	321
14.2	Coaxial electrospinning	322
14.3	Conclusion	332
	References	333
15	Electrospun-based systems in cancer therapy	337
	<i>M. Norouzi, B. Nazari, D.W. Miller</i>	
15.1	Introduction	337
15.2	Chemotherapy	338
15.3	Magnetic hyperthermia therapy	344
15.4	Photothermal-chemotherapy	346
15.5	Gene therapy	347
15.6	Circulating tumor cell capturing	349
15.7	Conclusions and future perspectives	351
	References	351
16	Electrospun nanofibers for regenerative dentistry	357
	<i>D. Pankajakshan, M.T.P. Albuquerque, M.C. Bottino</i>	
16.1	Introduction	357
16.2	Periodontal disease and treatment modalities	358
16.3	Periodontal-specific tissue engineering	358
16.4	Electrospun bioactive membranes for periodontal regeneration	359
16.5	Caries and pulpal disease	370

16.6	Conclusions and future perspectives	374
	Acknowledgments	376
	References	376
17	Electrospinning: A versatile technology to design biosensors and sensors for diagnostics	385
	<i>A. Macagnano, F. De Cesare</i>	
17.1	Introduction	385
17.2	ES-nanosensors for blood analysis	388
17.3	ES-nanosensors for breath analysis	398
17.4	Electronic nose devices for breath analysis	406
17.5	Summary and outlooks	410
	References	413
	Index	419

This page intentionally left blank

List of contributors

M.T.P. Albuquerque Indiana University School of Dentistry, Indianapolis, IN, United States

B. Balusamy Bilkent University, Ankara, Turkey

L. Berezkinová Nanopharma, Pardubice, Czech Republic

N. Bölgen Mersin University, Mersin, Turkey

M.C. Bottino Indiana University School of Dentistry, Indianapolis, IN, United States

G.L. Bowlin University of Memphis, Memphis, TN, United States

S. Castro Novel Materials and Nanotechnology Group, IATA-CSIC, Valencia, Spain

P. Chen Monash University, Melbourne, VIC, Australia

F. De Cesare IIA-National Research Council, Rome, Italy, DIBAF-University of Tuscia, Viterbo, Italy

E.A. Demirci Izmir Katip Celebi University, Izmir, Turkey

A.J. Dunn Saint Louis University, St. Louis, MO, United States

Y. Echegoyen Novel Materials and Nanotechnology Group, IATA-CSIC, Valencia, Spain

A.E. Fetz University of Memphis, Memphis, TN, United States

J.S. Forsythe Monash University, Melbourne, VIC, Australia

C.J. Gehrman University of Memphis, Memphis, TN, United States

E.A. Growney Kalaf Saint Louis University, St. Louis, MO, United States

A.H. Hekmati Islamic Azad University, South Tehran Branch, Tehran, Iran

K.R. Hixon Saint Louis University, St. Louis, MO, United States

- N. Shah Hosseini** Laboratoire de Physique et Mécanique Textiles, Mulhouse, France
- P.U. Kadakia** Saint Louis University, St. Louis, MO, United States
- O. Karaman** Izmir Katip Celebi University, Izmir, Turkey
- N. Khenoussi** Laboratoire de Physique et Mécanique Textiles, Mulhouse, France
- E. Kijęńska** Warsaw University of Technology, Warsaw, Poland
- J.M. Lagaron** Novel Materials and Nanotechnology Group, IATA-CSIC, Valencia, Spain
- A. Macagnano** IIA-National Research Council, Rome, Italy
- D.W. Miller** University of Manitoba, Winnipeg, MB, Canada
- B.A. Minden-Birkenmaier** University of Memphis, Memphis, TN, United States
- B. Nazari** Tehran University of Medical Sciences, Tehran, Iran
- M. Norouzi** University of Manitoba; Kleysen Institute for Advanced Medicine, Winnipeg, MB, Canada
- D. Pankajakshan** Indiana University School of Dentistry, Indianapolis, IN, United States
- H.C. Parkington** Monash University, Melbourne, VIC, Australia
- A.E. Rodda** Monash University, Melbourne, VIC, Australia
- G.S. Selders** University of Memphis, Memphis, TN, United States
- S.A. Sell** Saint Louis University, St. Louis, MO, United States
- M. Şen** Izmir Katip Celebi University, Izmir, Turkey
- A. Senthamizhan** Bilkent University, Ankara, Turkey
- A. Solouk** Amirkabir University of Technology (Tehran Polytechnic), Tehran, Iran
- W. Swieszkowski** Warsaw University of Technology, Warsaw, Poland
- T. Uyar** Bilkent University, Ankara, Turkey

K. Vodsed'áková Nanopharma, Pardubice, Czech Republic

L. Vysloužilova Nanopharma, Pardubice, Czech Republic

S.M. Willerth University of Victoria, Victoria; International Collaboration on Repair Discoveries (ICORD), Vancouver, BC, Canada

This page intentionally left blank

Preface

Electrospinning, an electrohydrodynamic process, is a versatile and promising platform technology for the production of nanofibrous materials for tissue engineering and biomedical applications. This book presents the development of electrospun materials for tissue engineering and biomedical applications. With a strong focus on fundamental materials science and engineering, this book also looks at successful technology transfers to the biomedical industry, highlighting biomedical products already in the market as well as the requirements to successfully commercialize electrospun materials for potential use in tissue engineering and biomedical areas. This book is a valuable resource for materials and biomedical scientists and engineers wishing to broaden their knowledge in the field of tissue engineering and biomedical applications of electrospun fibrous materials.

The first part of this book covers the introduction to electrospinning of nanofibrous materials for biomedical and tissue engineering applications. The general requirements of electrospun materials for biomedical and tissue engineering are summarized. The biomedical industrial applications of electrospinning, and the innovations in the field and the products are listed. In addition, the possibility of creating 3D structures and using printing technologies for electrospun materials are discussed. Although a majority of the electrospun nanofibers are produced from solution-based electrospinning, the advantage of using melt electrospinning for tissue engineering is demonstrated. The last chapter of this part takes into consideration the *In vivo* safety evaluations of electrospun materials. The second part of this book has a focus on specific application areas of electrospun nanofibrous materials in the field of biomedical and tissue engineering. The application areas of electrospun nanofibrous materials and their scaffolds are discussed in detail for drug delivery, wound healing, dermal regeneration, bone and tendon/ligament repair, vascular tissue engineering, cardiac tissue engineering, neural tissue engineering, nanomedicine, cancer therapy, regenerative dentistry and, biosensors and sensors for diagnostics.

The Editors of this book serve as a Chair (Dr. Erich Kny) and Vice-Chair (Prof. Tamer Uyar) of COST Action MP1206—“Electrospun Nano-fibres for bio inspired composite materials and innovative industrial applications” (May 2013–May 2017). The MP1206 scientific network on Electrospinning has grown very extensively by gathering finally more than 400 scientists from 32 countries around the world. Under the MP1206 COST action, numerous international workshops and training schools have been organized, and participation in a number of international conferences has taken place concerning different application fields of electrospun nanofibers including healthcare, sensors, textiles, filtration, food and food packaging, agricultural, and energy. Since tissue engineering and biomedical applications of

electrospun fibrous materials are very promising and important application fields, we decided to publish a book on this topic. This book is one of the fruitful outcomes of our COST Action MP1206.

We are very grateful to Prof. Nabyl Khenoussi, the leader of our working group on “biomedical applications of electrospun nanofibres”, who has supported the idea of publishing such a book very strongly from the very beginning and has organized or coorganized a number of dedicated workshops on the topics of tissue engineering and biomedical applications. With his valuable activities, he has paved the ground and has set the foundations for finally being able to edit a book on biomedical applications of electrospun nanofibers. We are further grateful to all the authors of the individual chapters, who have devoted a lot of time and effort to write the chapters of the book and have responded to our many editorial demands in time and without complaints. Without their very much-valued help, such a collective work would not have been possible. Thank you very much! May this book be a valuable resource for experienced researchers as well as for students and beginners in this field!

Tamer Uyar and Erich Kny

Part One

Introduction to Electrospinning for Biomedical and Tissue Engineering Applications

This page intentionally left blank

Electrospinning: A versatile processing technology for producing nanofibrous materials for biomedical and tissue-engineering applications

1

A. Senthamizhan, B. Balusamy, T. Uyar
Bilkent University, Ankara, Turkey

1.1 Introduction

Design and development of functional materials and tailoring their functionalities in biomedical applications is a great challenge [1]. Electrospinning technique has proved to be a relatively simple and versatile method for producing functional nanofibers and nanofibrous membrane. The fundamentals of electrospinning have been known for a long time, and the effects of various processing parameters on the fibers morphology have been extensively studied [2,3]. The exceptional characteristics of electrospun nanofibrous membrane including high surface area, high porosity, flexibility, and adjustable pore-size distribution make them more suitable candidates in a wide range of applications including biomedical and tissue-engineering applications [3–7].

The designing of hierarchical architecture that mimics the extracellular matrices (ECM) of the native tissues is important for rapid and regeneration of tissues [8]. The electrospinning process gives an opportunity to tailor the scaffold topography [5]. Moreover, surface modification of electrospun nanofibers with bioactive molecules improves the interaction between the scaffolds and cells. Generally, scaffolds provide a temporal support for the regeneration/repair of the tissues. Therefore, it could be highly expected that the scaffolds must fulfill the several requirements. The biocompatibility of the material is considered to be an essential factor for preventing the inflammation and toxicity. The biodegradability of the scaffolds is also a very significant fact because the degradation of the scaffolds and regeneration of the tissues should happen in a timely manner [4].

The diameter and morphology of the nanofibers can be effectively tuned by the number of processing parameters. The collector design has led to tune the orientation of fibers. The uniaxially aligned nanofiber scaffolds can only promote the cell migration along one specific direction and are thus not useful as dural substitutes. In order to promote cell migration from the surrounding tissue to the center of a dural defect and

shorten the time for healing and regeneration of dura mater, a surface patterned with a radially aligned, nanoscale features would be highly desired for an artificial dural substitute. More specifically, scaffolds constructed with radially aligned nanofibers could meet such a demand by guiding and enhancing cell migration from the edge of a dural defect to the center [9]. The dynamic rotating collector is the most widely accepted approach for fabricating aligned fibers from different polymers. The promising use of nanofibers in drug delivery system might result in the salient features such as high loading capacity and concurrent release of diverse therapies. A variety of different drugs ranging from antibiotics and anticancer agents to proteins, aptamer, DNA, and RNA have been successfully incorporated into electrospun fibers [10,11].

The performance of the incorporated biomolecules often loses their activity due to conformational changes in the harsh solvent environment. The modification of the nozzle configuration paves a way to prepare the core-shell morphology. Such a promising system provides a protective environment and sustained drug release because the prepared core-shell fibers have immense potential to preserve the drugs during the electrospinning process. Even though there were a huge number of research reports on the development of electrospun nanofibrous scaffold, researchers are still gaining new insights and developing new ways of utilizing this technique for producing biomedical materials [7].

This chapter highlights the significance of electrospinning approach in fabricating advanced functional nanofibrous scaffolds for biomedical applications including tissue engineering, drug release, wound dressing, and antimicrobial. We do not make any effort to provide library of literature for specific application rather provide a brief view on the advancement of electrospinning approach to prepare a functional nanofibrous biomaterials.

1.2 Biomedical application of electrospun nanofibers

1.2.1 Drug delivery

An ideal drug delivery system should possess the characteristic to enable the controlled release of drugs toward alleviating medical conditions at a defined rate over a definite time period. Electrospun nanofibers are recognized as an advantageous material in drug delivery owing to their higher surface area with interconnected pores, which offer better dissolution and high therapeutics loading capacity. More importantly, the rate of drug release can be tailored by ease tuning of electrospun nanofiber properties including fiber diameter, porosity, and drug-binding mechanism. Until now, a wide variety of drugs and biomolecules have been successfully loaded into electrospun nanofibers using various approaches mainly by coating, embedding, and encapsulating [7,12,13]. The possible three different modes of physical drug-loading method on electrospun nanofiber surface for drug delivery application are given in Fig. 1.1.

A one-step, single-nozzle electrospinning technique was used to fabricate electrospun composite nanofibers containing nanoparticles for the programmable release of dual drugs by Wang et al. [14]. Briefly, dual drug-loaded chitosan (CS)

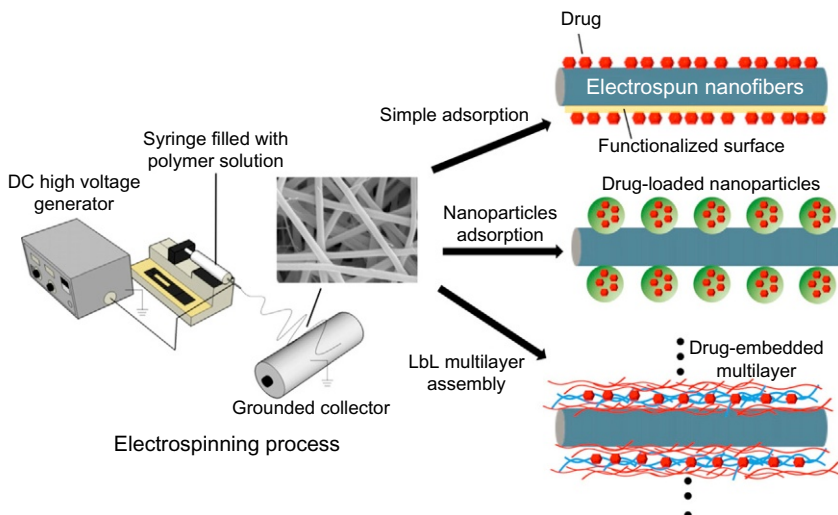


Fig. 1.1 Three modes of physical drug loading on the surface of electrospun nanofibers. Reprinted with permission from Elsevier (Yoo HS, Kim TG, Park TG. Surface-functionalized electrospun nanofibers for tissue engineering and drug delivery. *Adv Drug Delivery Rev* 2009;61:1033–42).

nanoparticle-containing composite nanofibers were prepared for topical drug delivery applications. Fig. 1.2 illustrates the electrospinning setup and the preparation of nanoparticle-containing composite nanofibers. The controlled and programmable release of two drugs was achieved through their different distributions in the shell and core regions of the composite nanofibers, respectively. Fig. 1.3 shows the optical and fluorescence images of the nanofibers encapsulated by the electrospun composite nanofibers. The clear distribution of the rhodamine B-loaded and fluorescein isothiocyanate (FITC)-labeled CS nanoparticles was observed. The laser scanning confocal microscopy (LSCM) imaging revealed the core-shell structure of the composite nanofibers, which consisted of a polycaprolactone (PCL) shell and an array of CS nanoparticles as the core. The release behaviors of the drugs indicated that a controlled release pattern for dual drugs was achieved by adjusting the process used to prepare the electrospinning solution.

In order to overcome the limitations of single-nozzle electrospinning, coaxial electrospinning technique has been attracted much attention for encapsulating fragile, water-soluble bioactive agents and their controlled release. The coaxial electrospinning also controls initial burst release with their core-sheath nanofibers with a blank (drug-free) sheath. In addition, coaxial electrospinning offers the advantage over more sustained release of the encapsulated agents and single-step coencapsulation of multiple drugs with different soluble nature [15]. A study reported by Mickova et al. [16] showed that the liposomes encapsulated with horseradish peroxidase embedded polyvinyl alcohol-core/poly- ϵ -caprolactone-shell nanofibers prepared by

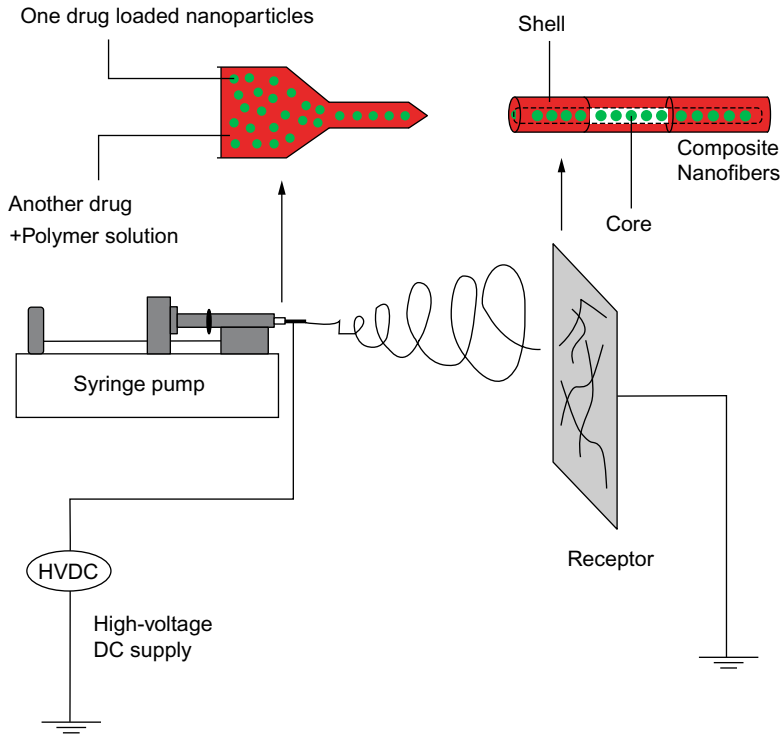


Fig. 1.2 Schematic illustration of the electrospinning setup and the preparation of nanoparticle-containing composite nanofibers.

Reprinted with permission from Nature Publishing Group (Wang Y, Qiao W, Wang B, Zhang Y, Shao P, Yin T. Electrospun composite nanofibers containing nanoparticles for the programmable release of dual drugs. *Polym J* 2011;43:478–83).

coaxial electrospinning revealed enhanced performance than the fibers prepared by blend electrospinning.

Man et al. [17] developed a codelivery system using a polyvinyl pyrrolidone/bovine serum albumin/recombinant human transforming growth factor- β 1 (rhTGF- β 1) composite solution as the core fluid and PCL solution as the sheath fluid. Subsequently, bone marrow-derived stem cell (BMSC)-affinity peptide E7 was conjugated to the coaxial electrospun fibers to develop a codelivery system of rhTGF- β 1 and E7. Fig. 1.4 shows the schematic illustration of the preparation process and working hypothesis for coaxial electrospun fiber scaffolds. The bioactive assay demonstrated that the rhTGF- β 1 released from the peptide-modified scaffolds was at least partially bioactive. Based on the outcome of the study, it is concluded that the prepared rhTGF- β 1 in the core and E7 in the PCL shell of the fibers (CBrhTE) scaffold has several properties that can not only enhance BMSC adhesion and growth but also promote their chondrogenic differentiation in vitro.

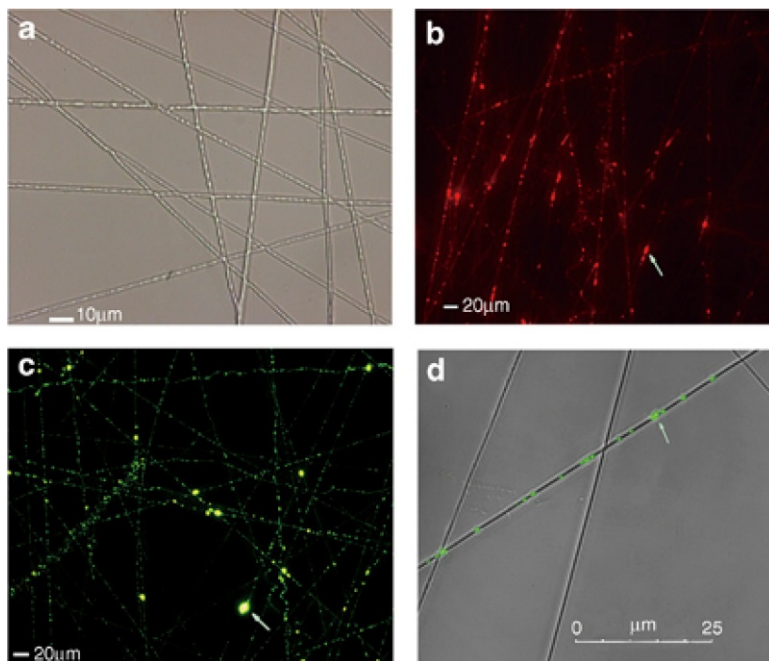


Fig. 1.3 Electrospun composite nanofibers containing chitosan nanoparticles: (A) optical image; (B) and (C) fluorescence images of composite nanofibers containing rhodamine B- and fluorescein isothiocyanate (FITC)-labeled nanoparticles, respectively; and (D) laser scanning confocal microscopy image.

Reprinted with permission from Nature Publishing Group (Wang Y, Qiao W, Wang B, Zhang Y, Shao P, Yin T. Electrospun composite nanofibers containing nanoparticles for the programmable release of dual drugs. *Polym J* 2011;43:478–83).

Recently, Dubey and Gopinath [18] fabricated electrospun poly(ethylene oxide)-poly(caprolactone) composite nanofibers for codelivery of niclosamide (nic) and silver nanoparticles (Ag NPs). Initially, the drugs (niclosamide (nic)) and Ag NPs were loaded separately and together (nic@Ag NPs) into the nanofiber, and their *in vitro* release was investigated. The drug release profile and kinetic studies have been shown in Fig. 1.5. There was a distinct release profile for the drug and nanoparticles released from nic, Ag NPs, and nic@Ag NPs composite nanofibers once brought into contact with the hydrophilic environment. The drug and nanoparticle both showed initial burst release around 15% and 18%, respectively, which could be due to surface adhered particles and initial rapid dissolution of the PEO polymer as shown in Fig. 1.5. The initial rapid phase was followed by slow controlled release of nanofibers, which could be around 43% for the drug and 50% for the nanoparticle in 20 days and 100 h, respectively (Fig. 1.5A and B). Water intrusion into the scaffold is of noteworthy importance for the study of release and degradation kinetics. Thus, diffusion and dissolution are the key players of the drug release mechanism, and the schematic presentation of drug

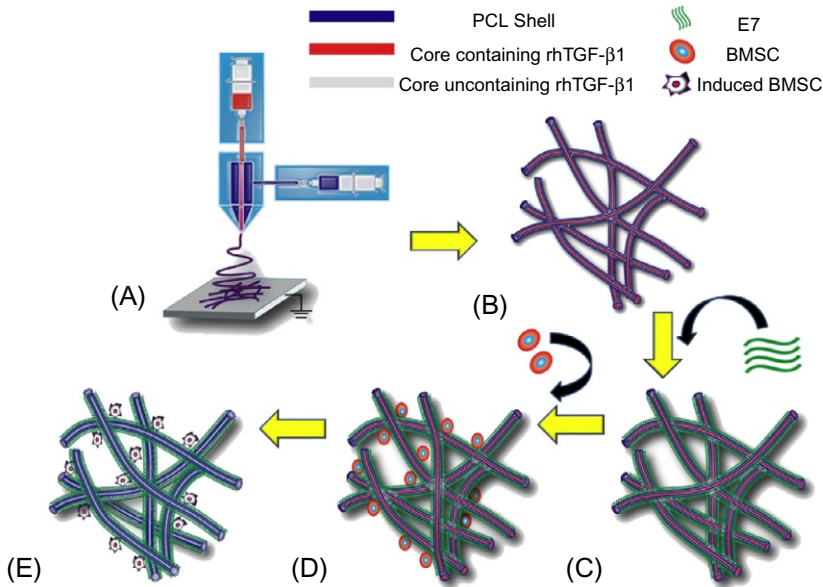


Fig. 1.4 Schematic illustration of the preparation process and working hypothesis for coaxial electrospun fiber scaffolds. (A) The setup of coaxial electrospinning: the spinneret is composed of two concentric needles; the outer needle is used to deliver the shell solution (blue), while the inner needle is used to eject the core solution (red). (B) Scaffold composed of electrospun coaxial fibers, with core (red) and shell (blue) structure. (C) Scaffold conjugated with the BMSC-specific affinity peptide (E7) (green). (D) E7-modified scaffold promoting adhesion of BMSCs onto the scaffold. (E) The rhTGF- β 1 encapsulated in the core of the coaxial fibers could be released in a sustained manner (the core changing from red in D to gray in E) to promote chondrogenic differentiation of BMSCs adhered on the scaffolds.

Reprinted with permission from Elsevier (Man Z, Yin L, Shao Z, Zhang X, Hu X, Zhu J, et al. The effects of co-delivery of BMSC-affinity peptide and rhTGF- β 1 from coaxial electrospun scaffolds on chondrogenic differentiation. *Biomaterials* 2014;35:5250–60).

release from various composite nanofibers has been shown in [Fig. 1.5C](#). It was found that the drug showed sustained and controlled release followed by initial burst release from both drug alone loaded and nic@Ag NPs loaded nanofibers. The codelivery of anticancer drugs nic@Ag NPs from nanofibers displayed superior anticancer potential in vitro when compared with nic alone or Ag NPs composite nanofibers. Additionally, nic@Ag NPs showed better therapeutic efficacy against MCF-7 cells.

A new strategy for creating functional trilayer nanofibers through triaxial electrospinning was demonstrated by Yu et al. [19] in which each layer was based on the same polymer matrix with different functional components or compositions. Ethyl cellulose (EC) was used as the filament-forming matrix in the outer, middle, and inner working solutions and was combined with varied contents of the model active ingredient ketoprofen (KET) in the three fluids, and their dissolution was determined in accordance with the Chinese Pharmacopoeia. A diagram illustrating the

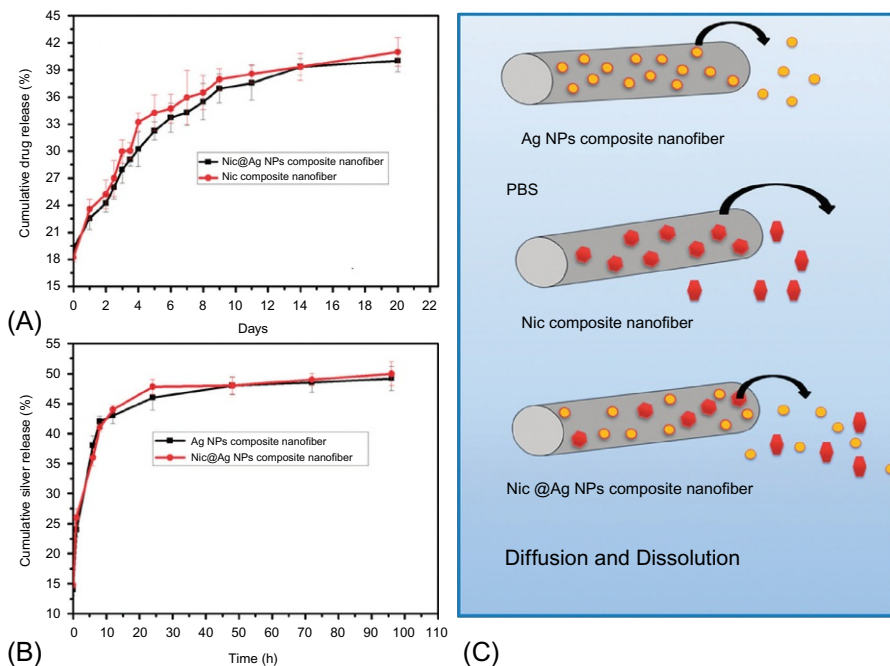


Fig. 1.5 (A) Cumulative drug release profile of the drug released from the drug alone and the nic@Ag NP composite nanofiber. (B) Ag NP release profile from Ag NPs alone and nic@Ag NP composite nanofibers. (C) Schematic illustration of drug released from various composite nanofibers.

Reprinted with permission from The Royal Society of Chemistry (Dubey P, Gopinath P. Fabrication of electrospun poly(ethylene oxide)–poly(capro lactone) composite nanofibers for co-delivery of niclosamide and silver nanoparticles exhibits enhanced anti-cancer effects *in vitro*. *J Mater Chem B* 2016;4:726–42).

triaxial electrospinning process is shown in Fig. 1.6A, and a digital photograph of the triaxial electrospinning process is presented in Fig. 1.6B. Monolithic nanofibers prepared individually from each of the three working solutions using single-fluid electrospinning have similar drug release profiles. An initial burst release is followed by a slowing in the release rate. In sharp contrast, the three-layer nanofibers were able to provide zero-order KET release for over 20 h with a best-fit equation of $Q = 1.73 + 4.24 t$ ($R^2 = 0.9972$), where Q is the drug release percentage, t is the release time, and R is the correlation coefficient. The initial burst release and the slow down at the end of the dissolution process are negative phenomena that inevitably arise with monolithic drug-loaded nanofibers. No burst release was observed from the triaxial nanofibers, and the drug was released at a constant rate for nearly 1 day. This study developed an advanced functional nanofibrous materials using a triaxial electrospinning process and solutions of the same filament-forming polymer matrix for all three working

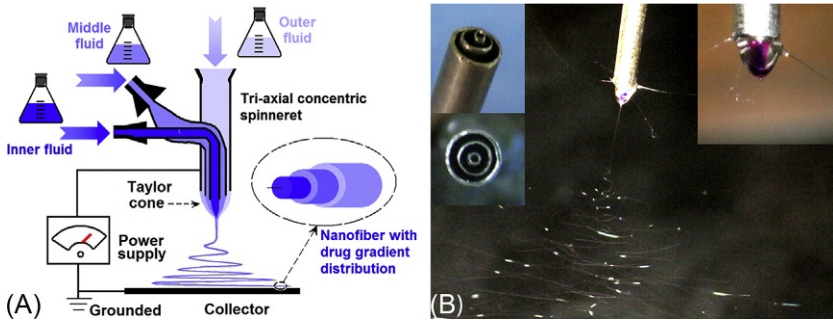


Fig. 1.6 (A) Schematic of the triaxial electrospinning process. (B) Digital photographs of the triaxial electrospinning process. The upper-left insets show the structure of the homemade spinneret, and the upper-right inset show a typical compound Taylor cone. Reprinted with permission from American Chemical Society (Yu DG, Li XY, Wang X, Yang JH, Bligh SWA, Williams GR. Nanofibers fabricated using triaxial electrospinning as zero order drug delivery systems. *ACS Appl Mater Interfaces* 2015;7:18891–7).

fluids. A range of different types of functional nanofibrous materials can be generated from this electrospinning process.

1.2.2 Tissue engineering

The theme of the tissue engineering is dedicated to improve/regenerate the damaged tissues. The exceptional characteristics of electrospun nanofibers including flexibility, highly porous, and interconnected three-dimensional structures mimic the extracellular matrix (ECM) that effectively support the cell adhesion and deliver growth factors. The fibrous structure, pore geometry, and interconnecting pores are significant for cell attachment, migration, growth, and nutrient flow. The biocompatibility and biodegradability of the selected scaffold is an essential parameter in regulating the cell growth rate and preventing the inflammation and toxicity. The architecture of the fibrous scaffolds affects the proliferation and differentiation of the cellular activities. And further, the efficiency of the fibrous scaffold is improved by modifying the fiber surface chemically and physically with bioactive molecules and ligands [5,20,21]. The surface modification not only changes the chemical composition of the surface but also tunes the wetting characteristics of the membrane that can provide the more favorable environment for cellular adhesion. The various surface modification technique for tuning the characteristics of the fiber surface is demonstrated in Fig. 1.7. The plasma treatment is a convenient and cost-effective method that enables the introduction of the various active groups such as carboxyl groups and amine groups on fiber surface. The prepared hydrophilized nanofibers are generally shown to enhance the fibroblast adhesion and proliferation [13]. For example, various kinds of electrospun nanofibers were successfully modified and demonstrated their enhanced performance [20,22,23].

Tian et al. [23] demonstrated the fabrication of poly(lactic acid) (PLA)/silk fibroin/nerve growth factor (PS/N) by encapsulating nerve growth factor (NGF) along with

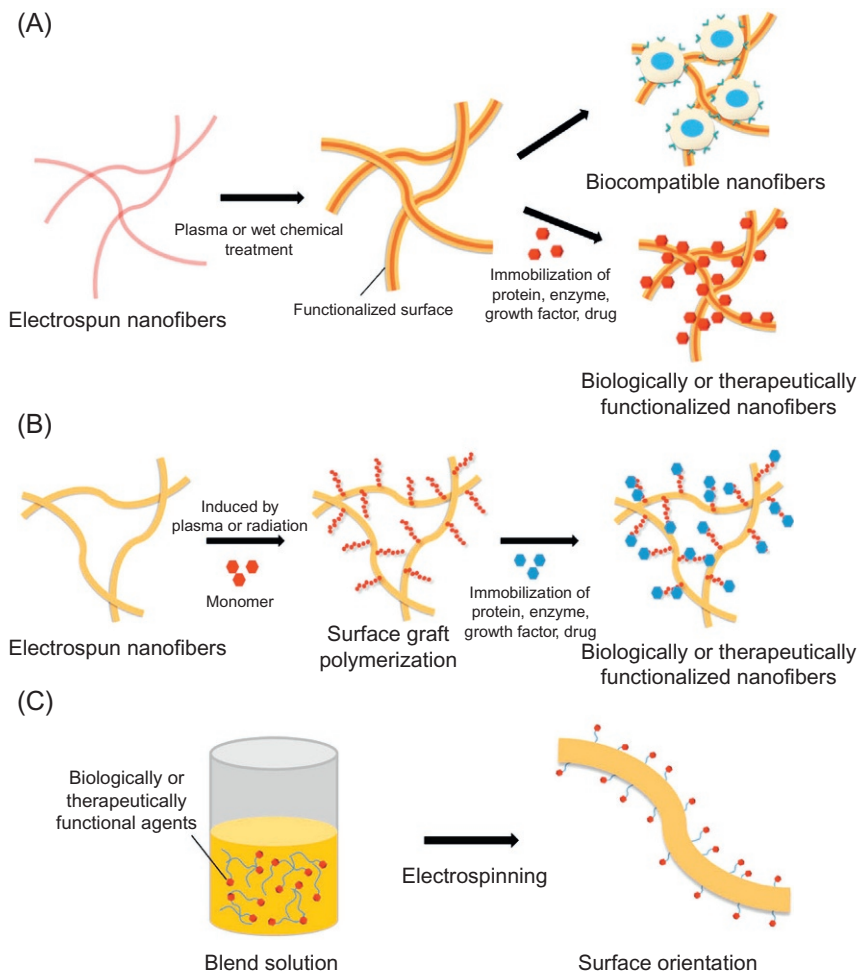


Fig. 1.7 Surface modification techniques of electrospun nanofibers. (A) Plasma treatment or wet-chemical method. (B) Surface graft polymerization. (C) Coelectrospinning. Reprinted with permission from Elsevier (Yoo HS, Kim TG, Park TG. Surface-functionalized electrospun nanofibers for tissue engineering and drug delivery. *Adv Drug Delivery Rev* 2009;61:1033–42).

silk fibroin (SF) as the core of the scaffold. Air plasma treatment was adopted to improve the hydrophilicity of the PS/N surface without causing any damage to the nanofibers. The fibrous scaffold was prepared by using coaxial electrospinning method, and the preparation procedure of p-PS/N scaffold is schematically demonstrated in Fig. 1.8. Initially, pure PLA scaffold was exposed to plasma at various time periods (60, 90, 120, 150, and 180 s). The observed morphological and wetting characteristics suggested that the optimized time period for air plasma treatment was evaluated as 120 s.

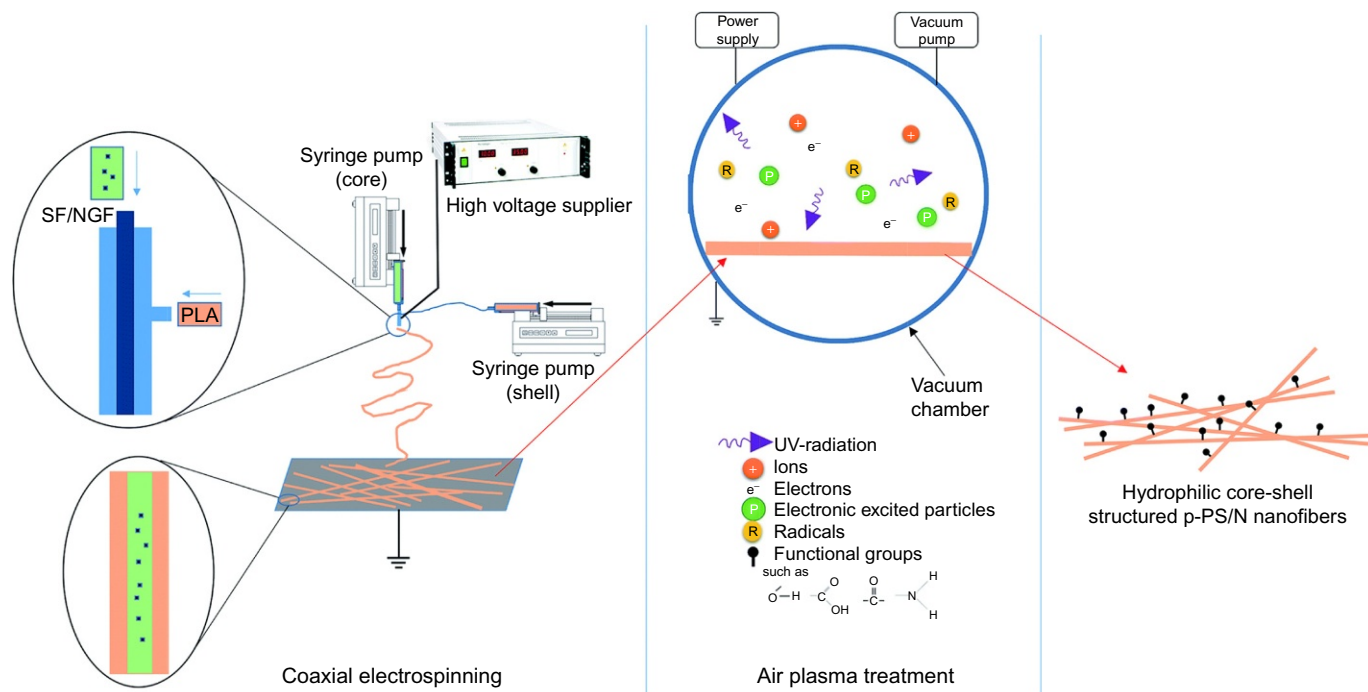


Fig. 1.8 Schematic illustration of the electrospinning and air plasma treatment toward the formation of p-PS/N scaffolds.

Reprinted with permission from Royal Society of Chemistry (Tian L, Prabhakaran MP, Hu J, Chen M, Besenbacher F, Ramakrishna S. Coaxial electrospun poly(lactic acid)/silk fibroin nanofibers incorporated with nerve growth factor support the differentiation of neuronal stem cells. RSC Adv 2015;5:49838–48).

The change in the fiber morphology, surface roughness, and hydrophilicity of PS/N nanofibers before and after plasma treatment was studied, and the results were shown in Fig. 1.9. The observed results suggested that there is no significant change in the fiber diameter. The measured diameters of PS/N and p-PS/N were to be 221 ± 49 and 228 ± 39 nm, respectively. The dramatic change in the water contact angle from 133.60° to 0° proves that the plasma treatment alters the hydrophilicity of the scaffolds significantly ($P \leq 0.05$), by introducing functional groups on the surfaces. But, the plasma treatment does not have any terrible impact on the fibers morphology. The values of average roughness (Ra) for PS/N and p-PS/N were measured to be

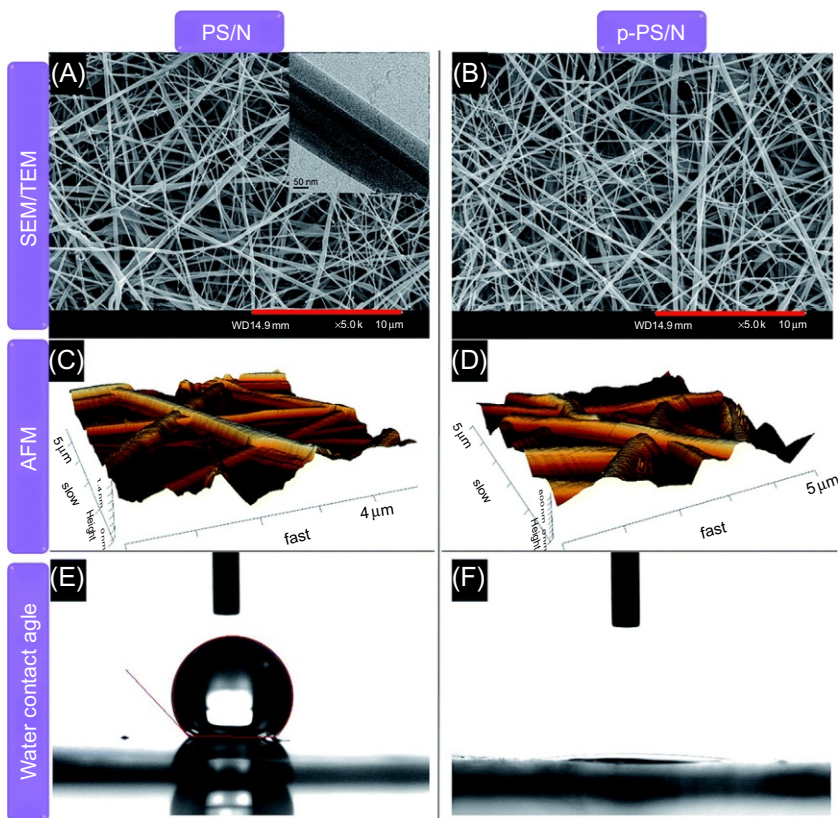


Fig. 1.9 Fiber morphologies, surface roughness and hydrophilicity of PS/N and p-PS/N scaffolds. SEM images of (A) PS/N and (B) p-PS/N scaffolds. The in situ picture shown within (A) is the TEM image, which shows the core-shell structure of the nanofibers. The AFM images of (C) PS/N and (D) p-PS/N scaffolds and the water contact angle of (E) PS/N and (F) p-PS/N scaffolds; the scale bar for (A) and (B) is 10 mm.

Reprinted with permission from Royal Society of Chemistry (Tian L, Prabhakaran MP, Hu J, Chen M, Besenbacher F, Ramakrishna S. Coaxial electrospun poly(lactic acid)/silk fibroin nanofibers incorporated with nerve growth factor support the differentiation of neuronal stem cells. RSC Adv 2015;5:49838–48).

217.97 ± 38.53 and 171.63 ± 32.50 nm, respectively. The surface of the nanofibers became smoother after plasma treatment. Further, MTS assay has been studied to evaluate the PC12 cell proliferation. The gradual increase in the cell proliferation has been noted on tissue culture plate (TCP) for all electrospun nanofibers from day 2 to day 8. After growing the cells for a period of 6 days, the cells were able to contact each other and facilitated the growth of the neighboring cells. NGF is a factor that is supportive toward PC12 cells differentiation, and PC12 stops dividing and proliferating once they are treated with certain concentration of NGF.

The plasma treatment sometime cannot be effectively modified the buried nanofibers surface due to the limited penetration depth of plasma in the nanopores. It is believed that wet-chemical etching approach can offer the flexibility for surface modification of the thick nanofibrous meshes. The concentration of the hydrolyzing agent and hydrolysis time is an important parameter to produce the optimal functional groups on the fiber surface [13,24]. In general, most of the synthetic biodegradable polymers retain their hydrophobic surface nature, but the creation of hydrophilic surface is highly required for ideal cellular responses. Not only surface graft polymerization has been applied to create the surface hydrophilicity, but also it can be used to introduce the various functional groups on the surface of the fibers for enhanced cell adhesion, proliferation, and differentiation [13,25].

In the recent past, much effort has been made to optimize the physiological behavior of cells by designing the suitable three-dimensional (3-D) geometry, chemical composition, and topography. The diameter of the electrospun fibers, alignment of the fibers, can have a great impact on cell adhesion, proliferation, and cell morphology. The aligned fibers are very attractive topographical cues to guide the cell growth with the desired morphology than randomly oriented fibers [26–28]. In addition to that, it has been found that the cellular activities such as cell proliferation and differentiation are modulated through electric stimulation [29]. The recent research reports have been demonstrated that the possible preparation of conductive electrospun fibers is by incorporating the various conductive materials such as polyaniline, carbon nanotubes, and polypyrrole [26,27,29,30]. The study by Chen et al. [26] prepared a nanofibrous scaffold that could simultaneously provide the two types of guidance cues, electric and topographical, to cells.

The prepared scaffold was composed of electrically conductive nanofibers with highly oriented structures and was fabricated by electrospinning a blended solution of poly(ϵ -caprolactone) (PCL) and PANi. PCL has been selected as a core material because of its good biodegradability, biocompatibility, and mechanical properties. The well-aligned electrospun nanofibers are prepared by using two parallel block magnets collector in electrospinning setup. The electrospinning conditions and PANi content on the morphology and alignment of PCL/PANi composite nanofibers were well studied. The SEM images and histograms of the orientation distribution of the PCL/PANi-3 nanofibers at various solution flow rates are shown in Fig. 1.10. The observed results have been well proved that the alignment fibers are increased with decreasing solution flow rate. The optimum fiber alignment was achieved at a flow rate of 0.1 ml h⁻¹, and more than 90% of the fibers were found to be aligned within ±10° of the preferred direction (Fig. 1.10D).

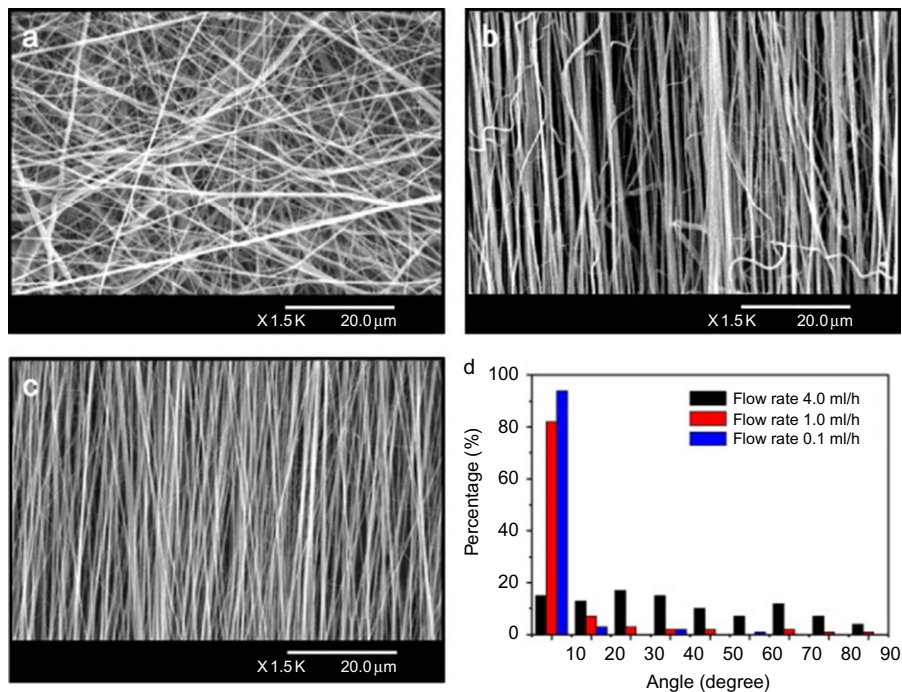


Fig. 1.10 (A–C) The representative SEM micrographs and (D) histograms of the orientation distribution of the PCL/PANi-3 nanofibers fabricated using the MFAES method at solution flow rates of (a) 4.0, (b) 1.0, and (c) 0.1 ml h⁻¹.

Reprinted with permission from Elsevier (Chen MC, Sun YC, Chen YH. Electrically conductive nanofibers with highly oriented structures and their potential application in skeletal muscle tissue engineering. *Acta Biomater* 2013;9:5562–72).

The designing of scaffolds for treating the skeletal muscle defects requires highly aligned fibrous membrane because skeletal muscle has a highly aligned architecture that consists of long, parallel multinucleated myotubes that are formed through the differentiation and fusion of myoblasts [31]. To overcome this problem, the highly aligned PCL/PANi nanofibers are prepared to provide functional scaffolds for engineering the parallel aligned myoblasts and myotubes. Murine skeletal muscle cells (C2C12 myoblasts) have been taken as a model to explore the effects of the electric cues and aligned topography of nanofibrous scaffolds on cell viability and alignment. The representative immunofluorescent images of myotubes differentiated for 5 days on the fibrous scaffolds and immunostained for MHC (green) and DAPI (blue) are demonstrated in Fig. 1.11. The aligned nanofibrous scaffolds (A-PCL and A-PCL/PANi) induced muscle cell alignment and promoted myotube formation compared with the randomly oriented nanofibers (R-PCL). In addition, the incorporation of electrically conductive PANi into the PCL fibers (R-PCL/PANi and A-PCL/PANi) also enhanced myoblast differentiation compared with the R-PCL nanofibers.

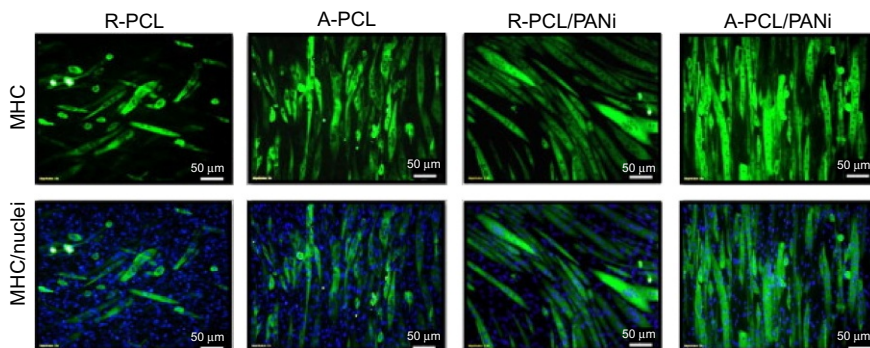


Fig. 1.11 Representative immunofluorescent images of myotubes differentiated for 5 days on random PCL (R-PCL), aligned PCL (A-PCL), random PCL/PANi-3 (R-PCL/PANi), and aligned PCL/PANi-3 (A-PCL/PANi) nanofibers and immunostained for MHC (green) and nucleus (blue). Reprinted with permission from Elsevier (Chen MC, Sun YC, Chen YH. Electrically conductive nanofibers with highly oriented structures and their potential application in skeletal muscle tissue engineering. *Acta Biomater* 2013;9:5562–72).

So far, it has been understood that the electrospun nanofibrous membrane acts as an excellent scaffold for various kinds of tissue engineering. However, the shrinkage and distortion of the electrospun scaffolds restrict the initial cell adhesion and further growth. Ru et al. [32] developed and demonstrated the suspended, shrinkage-free, electrospun. Poly(lactic-co-glycolic acid, PLGA) nanofibrous scaffold for skin tissue engineering. The obtained electrospun PLGA mat is able to maintain its initial shape and size with the auxiliary support from a polypropylene (PP) ring. The used polypropylene (PP) in this study is mechanically strong, chemically stable, and biocompatible. It has a density of 0.91 g/cm^3 enabling the scaffold to suspend in cell culture medium. The use of a PP ring as auxiliary support serves two purposes: (1) to make the overall nanofiber scaffold suspend in liquid, which is necessary for skin cells to be exposed to air during growth, and (2) to prevent nanofiber assemblies from shrinking and maintain long-term membrane integrity. The procedure for constructing the suspending nanofiber scaffolds is schematic illustrated in Fig. 1.12. Initially, the nanofiber assemblies were opened longitudinally and cut into circular membranes with a diameter of 20 mm. And then, an auxiliary plastic ring made of PP paper was heat sealed with the circular PLGA nanofiber membrane. The PLGA membrane fuses onto the PP ring to form a complete scaffold since the melting points of PLGA and PP are approximately 60°C and 170°C , respectively.

The applied high-electric field during the electrospinning process induces the inner stress in the nanofibrous system. The macromolecular chains can rapidly relax when fibrous membrane got immersed into solvent at a temperature higher than 35°C . The result of which induces the shrinkage in the PLGA fibrous assembly. The original and shrunken fibrous assemblies after incubating in PBS at 37°C for 24 h are shown in Fig. 1.13A and B. In contrast, for a PLGA scaffold consisting of a nanofiber assembly fused on a PP ring, no observable shrinkage occurred because of the enhanced

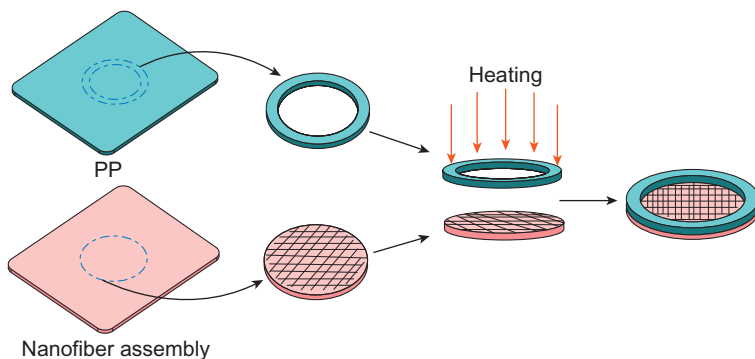


Fig. 1.12 Schematic illustrating steps for constructing suspending nanofiber scaffolds. Reprinted with permission from American Chemical Society (Ru C, Wang F, Pang M, Sun L, Chen R, Sun Y. Suspended, shrinkage-free, electrospun PLGA nanofibrous scaffold for skin tissue engineering. *ACS Appl Mater Interfaces* 2015;7:10872–7).

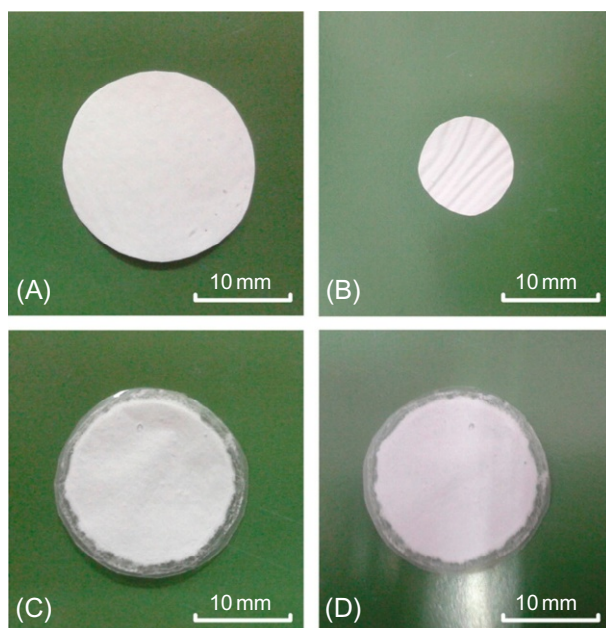


Fig. 1.13 Shrinkage test of fibrous membranes. (A, B) Nanofibrous assembly before and after incubation in PBS at 37°C for 24 h. (C) Scaffold formed by fusing a nanofibrous assembly on a PP ring. (D) The same scaffold after incubation in PBS at 37°C for 24 h. Reprinted with permission from American chemical society (Ru C, Wang F, Pang M, Sun L, Chen R, Sun Y. Suspended, shrinkage-free, electrospun PLGA nanofibrous scaffold for skin tissue engineering. *ACS Appl Mater Interfaces* 2015;7:10872–7).

mechanical property. Fig. 1.13C and D shows an original scaffold and the same scaffold after incubation in PBS at 37°C for 24 h.

The inadequate mechanical properties and low pore-structure controllability of electrospun nanofibrous membrane limit further their performance in tissue engineering. To overcome these limitations, the electrospinning approach has been coupled with various methods including melt-plotting method. The study by Yang et al. [33] demonstrated the fabrication of hybrid scaffold composed of microsized struts by using direct electrospinning writing (DE-writing) coupled with melt-plotting method. The obtained scaffold shows the good mechanical strength, and the width of the electrospun fibrous mat is controllable. Another main part of this study focuses on the creation of pore structure that is believed to have a high impact on cellular behavior. The schematic illustration of preparation method for hybrid scaffolds (HS) is shown in Fig. 1.14. The obtained hybrid scaffolds are comprised of melt-plotted struts and an electrospun fibrous layer.

The morphology of the scaffold structure also severely affects the cell attachment, proliferation, and infiltration in addition to the factors including pore size, porosity, and pore interconnectivity. The morphology of the three different pure melt-plotted polycaprolactone (PCL) scaffold (MC), conventional hybrid scaffold (HS1) consisting of a completely interlayered fibrous mat in the multilayered PCL struts (HS1), and novel hybrid scaffold (HS2) using DE-writing are presented in Fig. 1.15. The observed results clearly show that each scaffold type is composed of melt-plotted PCL layer with a strut diameter and pore size of $701 \pm 63 \mu\text{m}$ and $1.2 \pm 0.2 \text{ mm}$, respectively.

The hybrid scaffold is composed of additional layer, which is generated by DE-writing. The melt-plotted struts and electrospun fibers produced two different pores

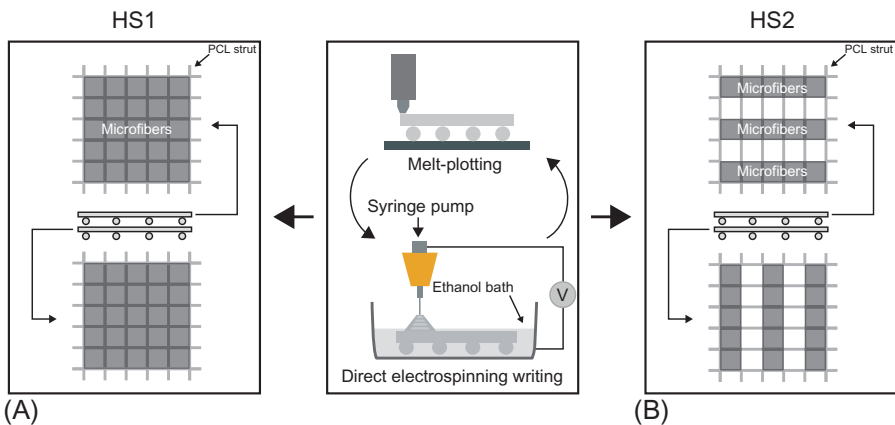


Fig. 1.14 Schematic illustrating generation of the hybrid scaffolds using melt-plotting method and direct electrospinning writing. (A) Fibrous mat covering the whole layer. (B) Fibrous mat covering three lines in the first and second layers horizontally and vertically, respectively. Reprinted with permission from Elsevier (Yang GH, Mun F, Kim G. Direct electrospinning writing for producing 3D hybrid constructs consisting of microfibers and macro-struts for tissue engineering. *Chem Eng J* 2016;288:648–58).

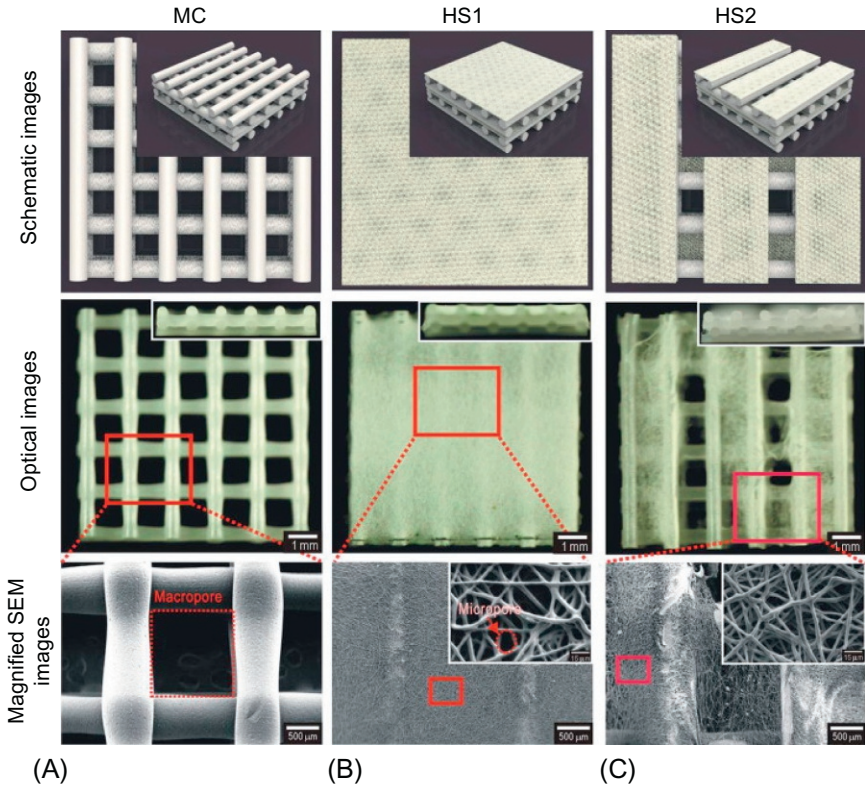


Fig. 1.15 Schematic, optical, and SEM images of (A) the MC scaffold fabricated using the melt-plotting method and two hybrid scaffolds, (B) HS1 and (C) HS2, fabricated using the melt-plotting/direct electrospinning writing. Reprinted with permission from Elsevier (Yang GH, Mun F, Kim G. Direct electrospinning writing for producing 3D hybrid constructs consisting of microfibers and macro-struts for tissue engineering. *Chem Eng J* 2016;288:648–58).

(macropores and micropores) in HS2 scaffolds. The created macropores in the HS2 scaffold could influence the cellular infiltration, nutrient transport, and metabolism, and micropores could enhance the cell attachment and proliferation. Thus, the prepared HS2 scaffold can overcome the limitations found in the HS1 because the insufficient pore size of the interlayered electrospun fibrous mat does not allow the easy migration and proliferation. The *in vitro* cellular activities suggest that the hybrid scaffold (HS2) shows a promise for regenerating hard tissues than conventional hybrid scaffold (HS1).

1.2.3 Wound dressing

The wound-care management is considered to be a serious health-care issue since the skin is the main organ of the body and plays vital role in multiple functions [34]. Depending on the healing time, the wounds are categorized as acute and chronic in

which the chronic wounds are highly exposed to the risk of bacterial infection. Acute wounds are generally caused by traumas, and the wounds are usually healable within 8–12 weeks. This kind of wounds can happen by mechanical damage, stabbing action of hard objects, exposure of extreme heat, irradiation, and so on. But the chronic wounds are formed as a result of chronic diseases such as diabetes, tumors, and severe physiological contaminations. The time period for healing the chronic wound needs more than 12 weeks [35]. According to the appearance, the wounds are further classified in different four types: epithelializing (clean, medium-to-high exudates), granulating (clean and exudating), slough-covered, and necrotic (dry) wounds as seen in Fig. 1.16.

As we look back upon history, the first records of wound care can be found in ancient Sumerians who used to apply poultices of mud, milk, and plants to wound, and Egyptians prepared plasters of honey, plant fibers, and animal fats as bandages for the wounds [36]. The outstanding characteristics of electrospun nanofibrous

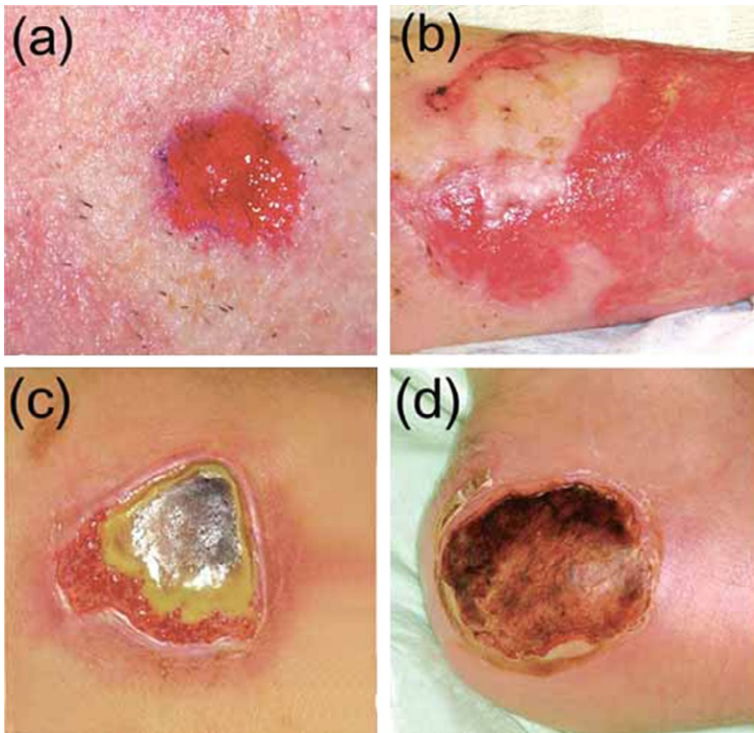


Fig. 1.16 Types of wounds based on their appearances: (A) epithelializing (clean, medium-to-high exudates), (B) granulating (clean and exudating), (C) slough-covered, and (D) necrotic (dry).

Reprinted with permission from John Wiley Sons, Ltd. (Zahedi P, Rezaeian I, Ranaei-Siadat SO, Jafari SH, Supaphol P. A review on wound dressings with an emphasis on electrospun nanofibrous polymeric bandages. *Polym Adv Technol* 2010;21:77–95).

scaffolds including flexibility, high porosity with excellent pore interconnectivity, high surface area, and gas permeation demonstrate their capability as an excellent dressing material for wound healing. The ideal fibrous scaffold should actively initiate the healing process and might reduce the bacterial contamination [36]. Until now, there are a variety of synthetic and natural polymers; chitosan, hyaluronic acid, poly(ethylene oxide) (PEO), poly(lactide) (PLA), poly(caprolactone) (PCL), poly(vinyl alcohol) (PVA), and silk were electrospun due to their nontoxic and biodegradable nature and used for developing a wound-healing scaffolds that can actively support the deposition of healthy tissues [37,38].

The healing process happened through three different stages: (i) inflammation, (ii) new tissue formation, and (iii) remodeling. The first stage in wound repair process happens immediately after tissue damage and multiple biological pathways, that is, coagulation cascade, inflammatory pathways, and immune system that are greatly necessary to prevent the blood and fluid losses, to remove dead and devitalized (dying) tissues, and to prevent infection. The new tissue formation is the second stage of the wound repair and occurs 2–10 days after injury and characterized by cellular proliferation and migration of different cell types. And the third stage of the wound repair is remodeling [39].

The strategy to incorporate the active agents inside/outside the fibers through different approaches is demonstrated in Fig. 1.17. The blending core/shell approach enables the homogeneous distribution of active agents throughout the fiber surface. In such a case, most of the active agents are presented inside the fibers. Typically, modification of electrospun fibers allows the active agents to be present on the outer surface of the fibers. Occasionally, the active agents are very sensitive to the harsh environment [40].

The core/shell fiber scheme provided an efficient platform in which the active agents are fed through the inner channel, and outer shell acts as a protective barrier. The fibrous scaffolds prepared by emulsion approach eliminate the initial burst release and showed the stable release rate. The surface modification of nanofibers facilitates the existence of more active agents on the surface of the fibers. To date, there are different approaches such as dip coating, layer-by-layer assembly, and electrostatic attachment that are adopted to functionalize the fiber surface as demonstrated in Fig. 1.18.

The selected synthetic polymers in making wound-dressing material are mostly because of their desirable mechanical, cytocompatibility properties, and low cost. However, most of the polymeric system lacks to prevent the nonspecific adsorption of proteins resulted in nonspecific cell attachment and bacterial adhesion. The result of which turns to encourage the bacterial infections and pain upon removing the wound-dressing material. In this regard, Unnithan et al. [34] prepared poly(carboxybetaine-co-methyl methacrylate) copolymer (CBMA) for active nonadherent wound-dressing application. They have investigated cell and platelet adhesion behavior in detail. The prepared wound-dressing material can be applied as easy removable, no-pain wound-dressing bandages. The wound-healing ability of the prepared nanofibrous membrane was tested with Wistar rats. The photographs of the in vivo wound-healing study are presented in Fig. 1.19. The results demonstrated that the fibrous mats showed excellent healing capability in the first and second weeks

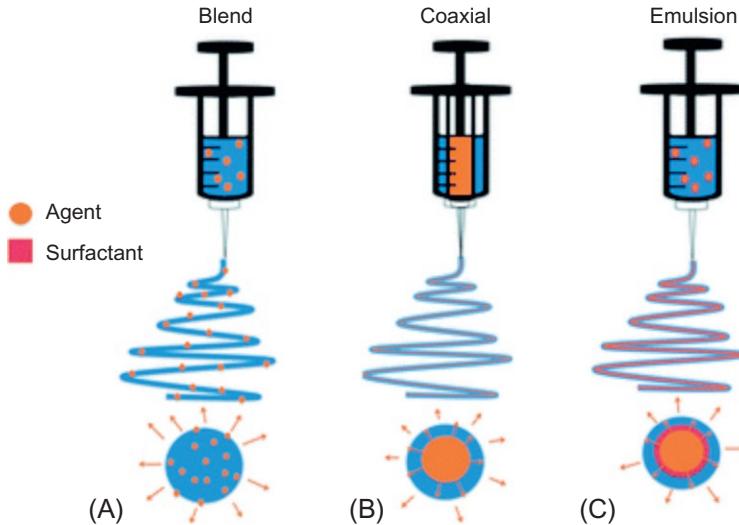


Fig. 1.17 Schematic displays the spinneret loaded with a bioactive agent for (A) blend, (B) coaxial, and (C) emulsion electrospinning. Coaxial electrospinning requires the use of a concentric spinneret configuration. (A) Blend electrospinning often yields fibers that contain the active agent dispersed throughout the fibers, whereas (B) coaxial and (C) emulsion electrospinning lend well to the synthesis of a core/shell morphology. The cross section of an individual fiber produced via the three methods is displayed. Reprinted with permission from Royal Society of Chemistry (Rieger KA, Birch NP, Schiffman JD. Designing electrospun nanofiber mats to promote wound healing—a review. *J Mater Chem B* 2013;1:4531–41).

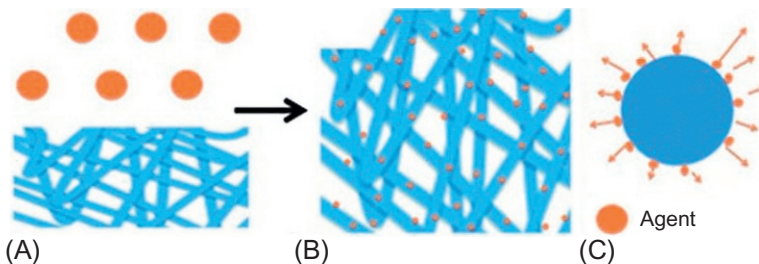


Fig. 1.18 Postproduction, (A) as-spun mats can be modified with functional agents (e.g., polymers, drugs, and biomolecules) to (B) alter their surface chemistry and functionality. (C) A cross section of an individual fiber postmodification displays that the new functional units are located on the surface of the fiber. Reprinted with permission from Royal Society of Chemistry (Rieger KA, Birch NP, Schiffman JD. Designing electrospun nanofiber mats to promote wound healing—a review. *J Mater Chem B* 2013;1:4531–41).

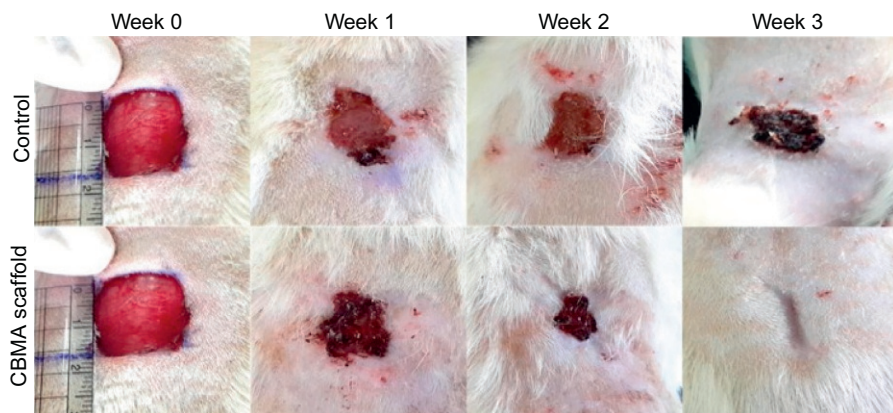


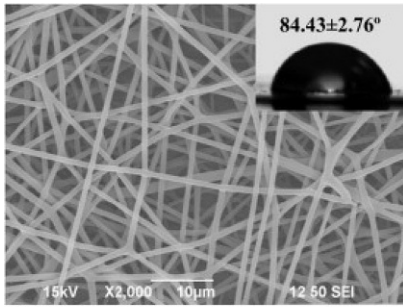
Fig. 1.19 Photographs of the in vivo wound-healing study.

Reprinted with permission from Elsevier (Unnithan AR, Nejad AG, Sasikalaa ARK, Thomas RG, Jeong YY, Murugesan P, et al. Electrospun zwitterionic nanofibers with in situ decelerated epithelialization property for non-adherent and easy removable wound dressing application. *Chem Eng J* 2016;287:640–8).

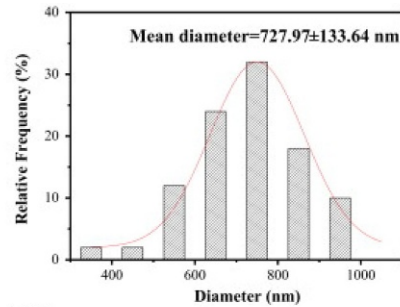
relative to the bare wound. After 3 weeks, the amount of wound closure was observed and evaluated. The obtained results showed that CBMA mat significantly improved the closure at $\sim 92\%$ when compared with bare wounds that showed a wound closure of $\sim 70\%$. After 3 weeks of contact with the CBMA composite mat, the thickness of the granulation layer was similar to that of unwounded skin, indicating optimal healing. They suggested that prepared membranes do not make any pain upon frequent removal. Furthermore, the healing tissue will not be damaged since the newly formed layer of the skin is not disturbed.

It has been well reported that the composite fibers have been widely studied for wound healing owing to the enhanced properties as compared with pristine nanofibrous mat. Later, the interest has been drawn toward to the design of multilayered wound dressing, in which each layer exhibits different functionalities. Tan et al. [41] demonstrated the bilayered nanofibrous mats (BNFs) through sequential electrospinning of polyurethane (PU) and gelatin. Amoxicillin was successfully incorporated into the PU layer to attain the antibacterial function. The morphology and cross-sectional view of the fibrous layer is shown in Fig. 1.20. The prepared BNFs show dual wetting characteristics, that is, the gelatin nanofibrous mats exhibit relative hydrophilicity with WCA of $84.43 \pm 2.76^\circ$, while PUa layer shows hydrophobicity with WCA of $123.07 \pm 8.12^\circ$. The obtained tunable BNFs could be highly recommended as potential wound dressings.

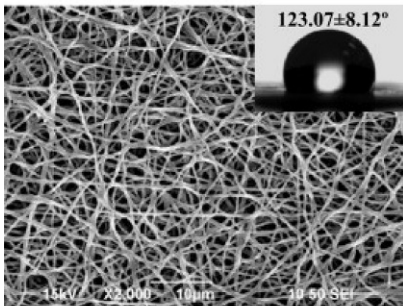
Hajiali et al. [42] combined the effect of two naturally derived compounds, namely, sodium alginate and lavender essential oil, for the development of bioactive nanofibrous dressing. The loaded lavender oil shows an admirable antimicrobial efficiency and also acted to control the induced inflammation. The obtained materials show their excellent efficacy for the treatment of UVB-induced skin injuries. The



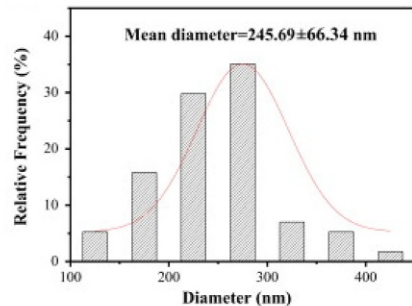
(A1)



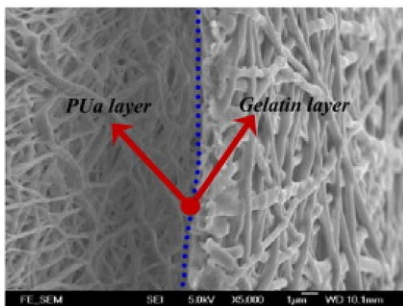
(A2)



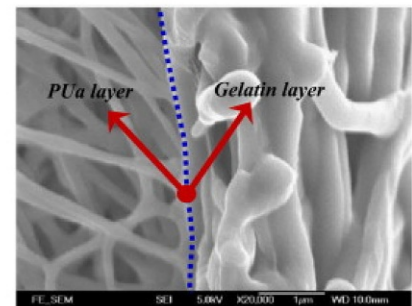
(B1)



(B2)



(C1)



(C2)

Fig. 1.20 SEM images and diameters distribution of gelatin nanofibers (A1 and A2) and polyurethane/amoxicillin nanofibers (B1, B2) and the cross-sectional views of bilayered nanofibrous mats (C1 and C2).

Reprinted with permission from Elsevier (Tan L, Hu J, Zhao H. Design of bilayered nanofibrous mats for wound dressing using an electrospinning technique. *Mater Lett* 2015;156:46–9).

commercially available alginate-based dressing (Tegadermt) was tested for comparison, and the results show that the inhibitory effect of the electrospun nanofibers on cytokine production was higher than that of Tegadermt. Even though there were a huge number of studies that have been evaluated and found electrospun membrane as an efficient wound-dressing material, it remains challenging to prepare a practical

and comfortable nanofibrous dressing. Dong et al. [43] developed an in situ deposition of a personalized nanofibrous dressing by a novel handy e-spinning device and evaluated their skin wound-care properties. Figs. 1.21 and 1.22 demonstrated the probable mechanism for the preparation of the e-spun personalized nanofibrous dressing. The incorporation of appropriate drug into electrospun nanofibrous membrane is a key parameter to produce an active wound-dressing material. They have incorporated the most known mesoporous silica nanoparticles decorated with silver nanoparticles (Ag-MSNs) as additives to the biopolymeric e-spun membranes.

The added Ag-MSNs could release Ag ions continuously and had a long-lasting antibacterial activity. In contrast, the gauze and control groups showed either the remaining scab or an inflamed and unclosed wound. Meanwhile, the wounds covered with e-spun Ag-MSN/PCL nanofibrous membranes presented better fluid retention when compared with the ones covered with gauze. We also found that the nanofibrous membranes were comfortable, flexible, and easier to be handled than the gauze. They



Fig. 1.21 Schematic illustration of the e-spun personalized nanofibrous dressing via a handy e-spinning device for wound healing.

Reprinted with permission from Royal Society of Chemistry (Dong RH, Jia YX, Qin CC, Zhan L, Yan X, Cui L, et al. In situ deposition of a personalized nanofibrous dressing via a handy electrospinning device for skin wound care. *Nanoscale* 2016;8:3482–8).

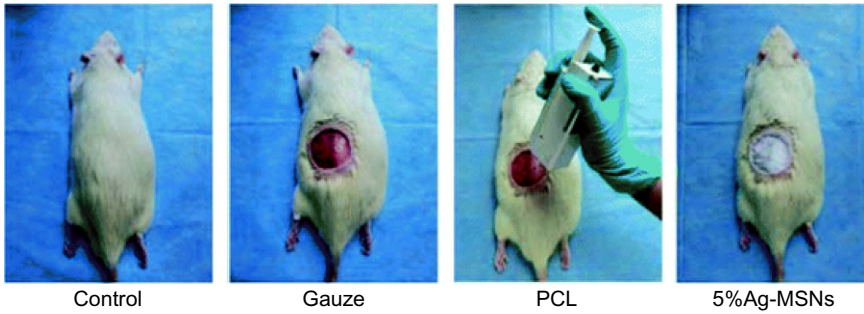


Fig. 1.22 Skin wound healing accelerated by Ag-MSN/PCL nanofibrous membranes.

(A) Exhibition of the entire skin injury model and treatment process in a Wistar rat.

Reprinted with permission from Royal Society of Chemistry (Dong RH, Jia YX, Qin CC, Zhan L, Yan X, Cui L, et al. In situ deposition of a personalized nanofibrous dressing via a handy electrospinning device for skin wound care. *Nanoscale* 2016;8:3482–8).

have studied and compared the performance of conventional gauze, virgin PCL nanofibrous membranes, and Ag-MSN/PCL nanofibrous membranes on the surface of the entire back skin wounds of different groups of Wistar rats. The gross appearance of the skin injury was observed at definite time intervals at 1, 2, 3, 4, and 5 weeks after immediate treatment. The observed results demonstrated that gauze and control groups show either the remaining scab or an inflamed and unclosed wound. At the same time, wounds covered with e-spun Ag-MSN/PCL nanofibrous membranes presented better fluid retention.

In most of the reported studies, the materials and bioactive molecular guidance are concerned to be primary factors to determine the functionality and healing properties of the mat. Despite, the impact of surface morphological properties of nanofibrous to wound dressing has not been considered seriously. The study by Kim et al. [44] developed an advanced electrospinning method that is capable of introducing a specific morphology into the nanofibrous mat. The proposed electrospinning method is mainly for the alteration of the surface morphological properties of electrospun mats. In this approach, the nanofibers are deposited onto a conductive mold with a human skin pattern. Fig. 1.23A and B shows a photograph and SEM image of a fabricated human-skin-patterned mat. The prepared fibers provided morphological guidance for cell growth, which could play a crucial role in the esthetic outcomes of skin tissue regeneration and wound healing. The *in vitro* cell tests (14 days) using a mouse embryonic fibroblast cell line (NIH-3T3) were carried out. The fabricated mat provided excellent morphological guidance of cells along the skin pattern, and as expected, cells cultured thereon exhibited a level of viability equivalent to those cultured on conventional electrospun fibers.

1.2.4 Antimicrobial

The infectious diseases caused by microbes are most significant rationale for human deaths worldwide than any other single cause. A microbe that is capable of causing

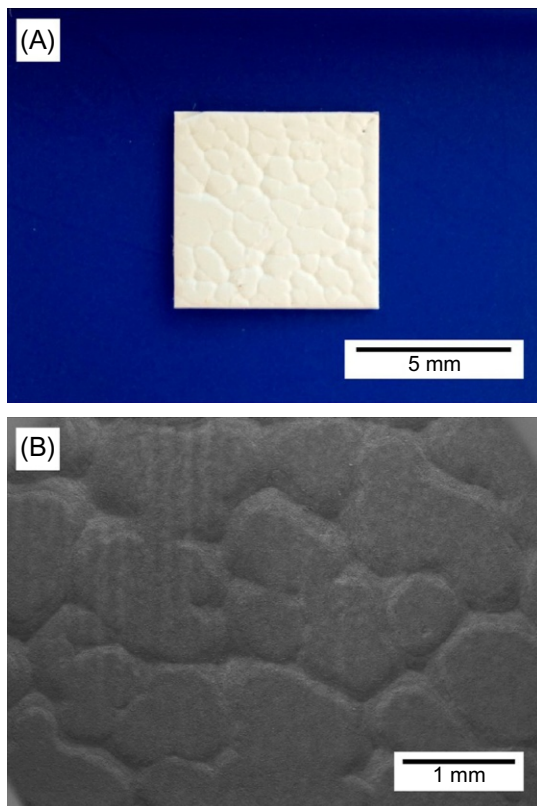


Fig. 1.23 Photograph (A) and SEM image (B) of a human-skin patterned nanofibrous mat. Reprinted with permission from American Chemical Society (Kim JH, Jang J, Jeong YH, Ko TJ, Cho DW. Fabrication of a nanofibrous mat with a human skin pattern. *Langmuir* 2015;31:424–31).

any infectious diseases to the organism is referred as pathogen. The health risks owing to these pathogenic microbial agents remain a challenge, and thus, preparation of effective antimicrobial agents using different approaches is always a great concern. Electrospinning is a cost-effective versatile technique that is used for generation of continuous, one-dimensional nanofibers from a wide variety of materials especially from the polymers and proved to possess a wide range of applications. In recent years, there have been numerous efforts directed toward fabrication of electrospun nanofibers with antimicrobial properties using various approaches, namely, encapsulation of antimicrobial agents, functionalization, and surface modification owing to their unique features. The properties of electrospun nanofibers such as fiber diameter, specific surface area, composition of the polymer, and porosity significantly play vital role in the release profile of encapsulated agent. An antimicrobial agent is a molecule of natural, semisynthetic or synthetic origin, which inhibits the growth of the microbes or kills with minimal or no adverse effect to the host. There is particularly a significant focus on the incorporation of drugs, nanoparticles, and plant-derived compounds in nanofibers, which exhibit antimicrobial property. To date, numerous active antimicrobial agents have been successfully encapsulated into nanofibrous membranes and demonstrated their potency in controlling the microbial growth including

antibiotics, triclosan, essential oils, chlorhexidine, silver nanoparticles, and metal oxide nanoparticles.

In an overview, encapsulation of active agents in electrospun nanofibers can be achieved by blending in polymer solution before electrospinning, confining in core of the nanofiber using coaxial electrospinning, dispersing the nanostructures in electrospinning solution, converting a precursor into active agent through post-treatment process, and attaching on the nanofiber surface as indicated by Gao et al. [45]. A graphic illustration on different methods of incorporating biocides into electrospun nanofibers is presented in Fig. 1.24. However, during encapsulation of antibiotics, the close relationship between the polymer solution and hydrophilicity/hydrophobicity nature of the antibiotics should be taken into account to result in successful encapsulation of antibiotics in nanofibers. For instance, if a hydrophilic polymer is chosen to encapsulate hydrophilic drug, which might result in complete encapsulation, then a hydrophobic drug might not be fully encapsulated.

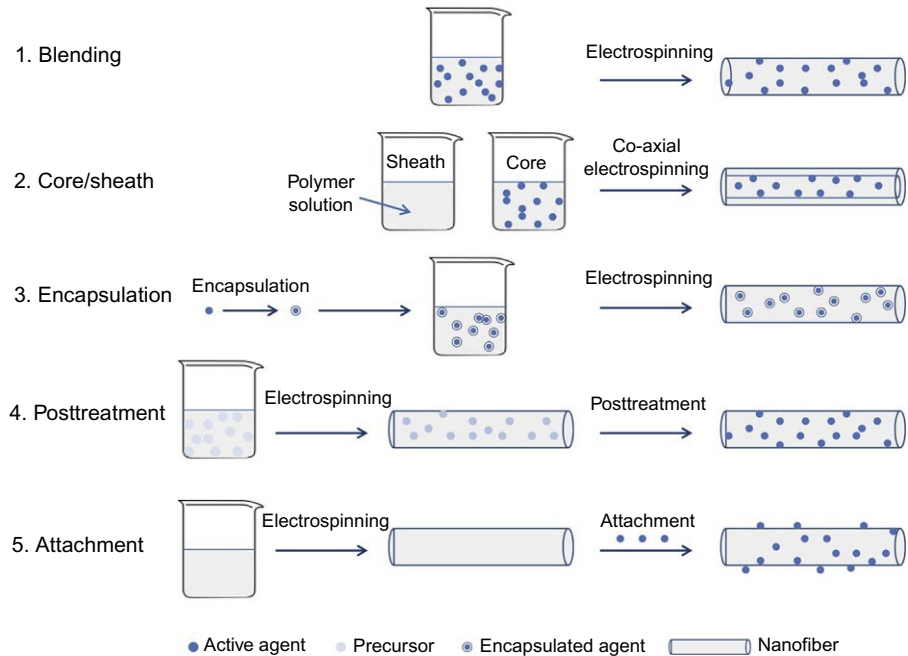


Fig. 1.24 Various methods of incorporating biocides into electrospun nanofibers. (1) Blending/dispersion of the active agent in the polymer solution prior to electrospinning, (2) confinement of the active agent in the core of the fiber through coaxial electrospinning, (3) encapsulation/adsorption of the active agent in nanostructures before dispersion in the electrospinning solution, (4) conversion of a precursor to active agent in the nanofibers after electrospinning, and (5) attachment of the active agent onto the nanofibers after electrospinning. Reprinted with permission from Wiley Periodicals, Inc. (Gao Y, Truong YB, Zhu Y, Kyratzis IL. Electrospun antibacterial nanofibers: Production, activity, and *in vivo* applications. *J Appl Polym Sci* 2014;131:40797).

Recently, Yang et al. [46] prepared agar/polymer electrospun hybrid to couple the advantage of both agar and electrospun fibers to achieve a novel composite with enhanced, comprehensive properties and a high potential for drug delivery. Ampicillin (AMC)-loaded, agar-doped polyacrylonitrile (PAN) composite nanofibers were prepared, and their performance in bioactivity assays against *Escherichia coli* bacteria was studied using disc diffusion method. The preparation of electrospun nanofiber using agar as an additive is illustrated in Fig. 1.25. In addition, the relationship between the spinnability and agar concentration in order to determine the critical factors in achieving a successful electrospinning.

The antimicrobial properties of silver have been noted since ancient times. Silver nanoparticles (AgNPs) are well known as a broad spectrum of antibiotic with strong antibacterial properties against many potential pathogens. Due to their excellent antimicrobial activities, preparation of silver nanoparticles containing electrospun nanofibers attracted intensive research interest. Xu et al. [47] demonstrated the preparation of biodegradable poly(l-lactide) (PLA) ultrafine fibers containing nanosilver particles via electrospinning technique. The *in vitro* antibacterial activities of PLA fibers with silver nanoparticles were studied. The observation shows that the silver is released steadily, and thus, the antibacterial activity is durable.

To minimize the aggregation of silver nanoparticles in polymeric solution and avoid environmentally hazardous chemicals, an effort was made by reducing silver through atmospheric plasma treatment. Thus, silver/polyacrylonitrile (Ag/PAN) hybrid nanofibers were prepared by coupling atmospheric plasma treatment and electrospinning. Further, the antibacterial efficiency was investigated against a gram-negative enteric pathogen *E. coli* O157:H7 (B179) and a spore-forming gram-positive pathogen *Bacillus cereus* (B002). As a result, PAN nanofibers without silver or silver compounds showed no significant antibacterial activity. Conversely,

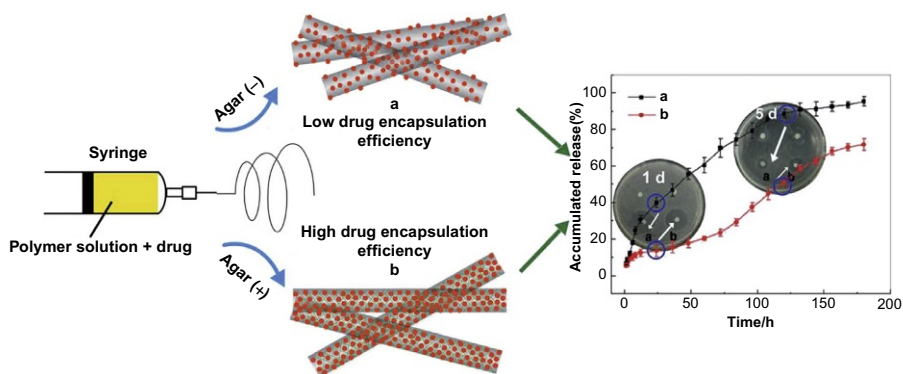


Fig. 1.25 Schematic illustration for the drug delivery systems by means of the agar doped electrospun fibers.

Reprinted with permission from Royal Society of Chemistry (Yang H, Gao PF, Wu WB, Yang XX, Zeng QL, Li C, et al. Antibacterials loaded electrospun composite nanofibers: release profile and sustained antibacterial efficacy. *Polym Chem* 2014;5:1965–75).

Ag/PAN hybrid nanofibers showed complete inhibition of both gram-negative and gram-positive microorganisms, indicating that the nanofibers are endowed with excellent antibacterial properties due to the introduction of Ag nanoparticles [48].

The incorporation of silver nanoparticles in electrospun chitosan nanofibers has been shown to improve their antibacterial performance. This modification has been achieved by loading prefabricated silver nanoparticles into the electrospinning chitosan solution or by adding a silver precursor to the formulation and then performing the thermally induced synthesis of silver nanoparticles. However, the antibacterial performance of these silver nanoparticles is often restricted because they are uniformly distributed and mostly embedded below the nanofiber surface. To ensure the maximum exposure of silver nanoparticles, the reduction reaction of the precursor should be directed or confined to the nanofiber surfaces. Annur et al. [49] recently reported the argon-plasma synthesis of silver nanoparticles for the surface immobilization of silver nanoparticles without the use of additional chemical reagents. Argon plasma etching and nanofiber thinning also promoted the further accumulation and exposure of silver nanoparticles on the nanofiber surfaces.

The antibacterial performances of chitosan nanofibers with and without surface-immobilized silver nanoparticles were investigated by the disk diffusion method using *E. coli* as the model bacteria. Inhibition zone improvements were observed in the silver nanoparticle-immobilized C10Ag (silver nitrate (AgNO_3) 1.0 wt%) and C20Ag (AgNO_3 2.0 wt%) nanofibers after the argon-plasma bombardment. For the 0.5 and 1 min plasma exposure time, both samples demonstrated increased inhibition zone sizes to 0.36 and 0.48 mm, respectively. When treated with 1.5 min of argon plasma, the C10Ag and C20Ag samples had the maximum antibacterial activity and inhibited bacterial growth up to a distance of 0.78 mm. These results for the C0, C10Ag, and C20Ag samples are summarized in Fig. 1.26 as a function of the plasma dosage.

Among other metal oxides, zinc oxide (ZnO) and titanium dioxide (TiO_2) have been considered as versatile and eco-friendly materials owing to their exceptional physicochemical properties. The ZnO nanostructures were extensively studied for their antimicrobial activities; a considerable attention was paid on the preparation of ZnO -incorporated nanofiber via electrospinning process. In addition, ZnO is listed as a generally regarded as safe (GRAS) by the US Food and Drug Administration, which has been used in many personal and health-care products. Anitha et al. [50] reported the in situ generation of ZnO nanoparticles in cellulose acetate (CA) fibrous membrane and their excellent antibacterial activity.

Lee et al. [51] developed a facile two-step fabrication method to enhance the surface area of electrospun TiO_2 nanofibers by subsequent hydrothermal synthesis of TiO_2 nanowires. Furthermore, the uniform deposition of a large quantity of silver nanoparticles on the surface of the TiO_2 nanofibers ensured a significant enhancement of the antibacterial performance, even under dark conditions. The schematic illustration of the preparation procedure is shown in Fig. 1.27.

The hierarchical TiO_2 nanofibers were prepared through a hydrothermal synthesis of TiO_2 nanowires on pure TiO_2 nanofibers prepared via electrospinning, followed by calcination. The morphology of pure and hierarchical TiO_2 nanofibers is shown in

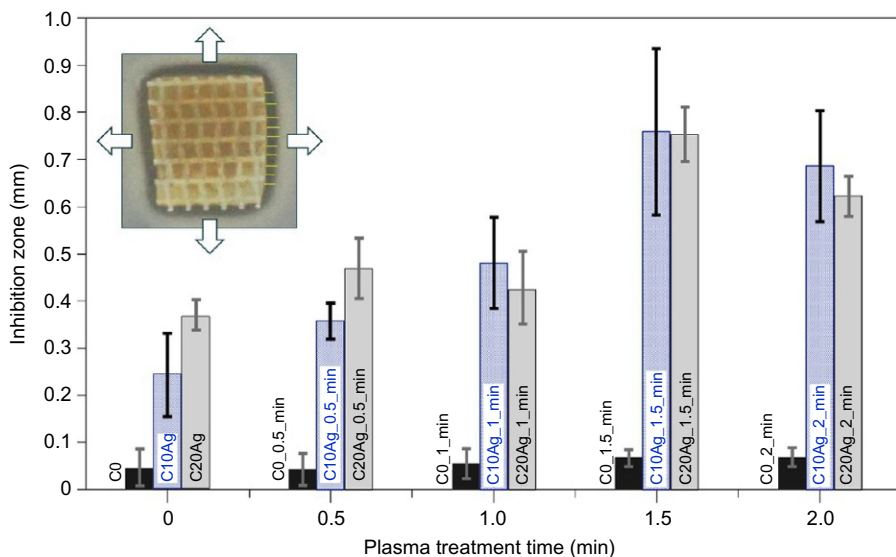


Fig. 1.26 Antibacterial inhibition zone measurements for C0, C10Ag, and C20Ag samples versus the argon-plasma dosages. The inset shows an example of the inhibited-growth zones surrounding the nanofiber sample.

Reprinted with permission from American Chemical Society (Annur D, Wang ZK, Liao JD, Kuo C. Plasma-synthesized silver nanoparticles on electrospun chitosan nanofiber surfaces for antibacterial applications. *Biomacromolecules* 2015;16:3248–55).

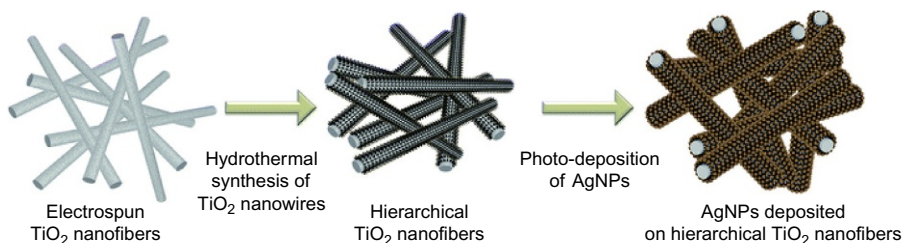


Fig. 1.27 Schematic illustration of the approaches used to achieve enhanced antibacterial activity of TiO₂ NFs. Hierarchical structures prepared by electrospinning, pyrolysis, hydrothermal synthesis of nanowires, and deposition of silver nanoparticles.

Reprinted with permission from Royal Society of Chemistry (Lee WS, Park YS, Cho YK. Significantly enhanced antibacterial activity of TiO₂ nanofibers with hierarchical nanostructures and controlled crystallinity. *Analyst* 2015;140:616–22).

Fig. 1.28. The prepared structures exhibited a highly enhanced photocatalytic effect owing to an increased surface area and an improved crystallinity of the surface. This enhanced photocatalytic effect led to a highly enhanced antibacterial activity of $89.90 \pm 2.02\%$ in the presence of UV light, even for a very short irradiation time

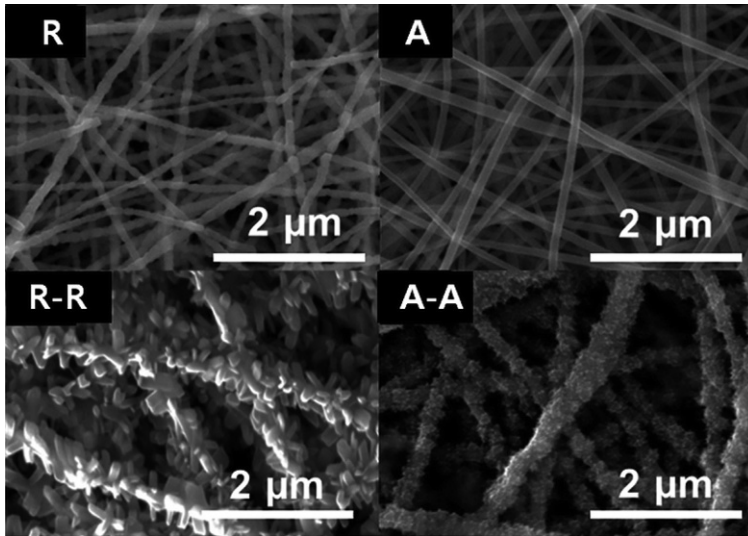


Fig. 1.28 SEM images of TiO_2 nanofibers with various crystalline phases and nanostructures: (R) pure TiO_2 nanofibers with rutile phase, (A) pure TiO_2 nanofibers with anatase phase, (R–R) hierarchical TiO_2 rutile nanofibers with rutile– TiO_2 nanowires, and (A–A) hierarchical TiO_2 anatase nanofibers with anatase TiO_2 nanowires.

Reprinted with permission from Royal Society of Chemistry (Lee WS, Park YS, Cho YK. Significantly enhanced antibacterial activity of TiO_2 nanofibers with hierarchical nanostructures and controlled crystallinity. *Analyst* 2015;140:616–22).

(1.5 min). Furthermore, Ag/TiO_2 nanofiber composites were prepared via photoreduction synthesis of Ag NPs that were deposited on the hierarchical anatase TiO_2 nanofibers under UV illumination.

Airborne fine particulates raise severe health and safety issues as they can be inhaled and may also cause explosions. It is vital to improve the indoor air quality by controlling these particulates under a certain concentration both in industry and in our daily life. Zhong et al. [52] prepared an air filter by growing one-dimensional ZnO nanorods on the three-dimensional porous networks of expanded polytetrafluoroethylene (ePTFE). The schematic for the preparation process and the morphologies of the filter at different stages are shown in Fig. 1.29. The preparation of the filters contains two simple steps: seeding of ZnO nanoparticles on the ePTFE networks and hydrothermal growth of ZnO nanorods on the seeding layer. They have adopted atomic layer deposition (ALD) to uniformly seed ZnO on the surface of ePTFE matrix and then synthesize well-aligned ZnO nanorods with tunable widths and lengths from the seeds under hydrothermal conditions. The resultant filters show ultrahigh efficiency and an interesting antibacterial functionality because of the conjunction of ZnO NRs on the network of ePTFE.

A recent report by Song et al. [53] has shown a route to fabricate low-cost porous carbon nanofibers (CNFs) using biomass tar, polyacrylonitrile (PAN), and silver

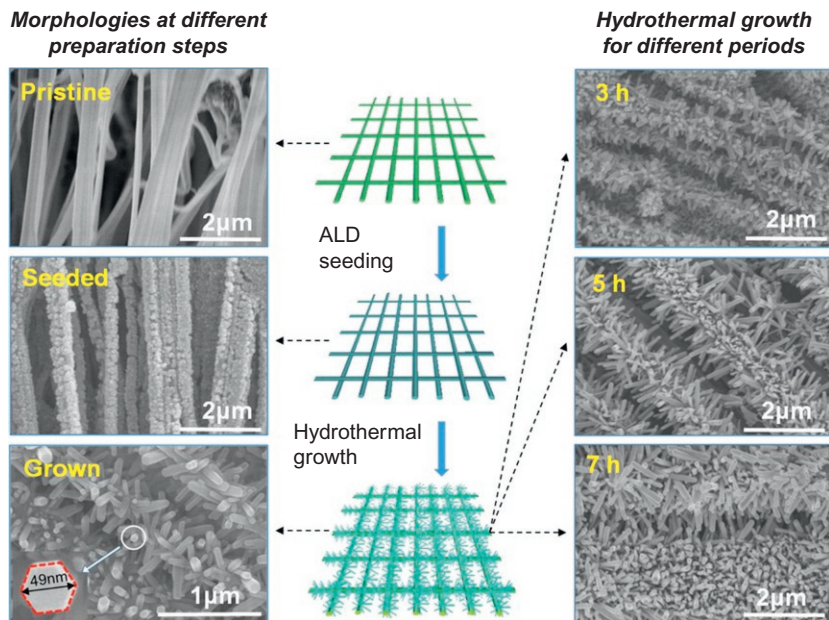


Fig. 1.29 Schematic of the preparation process of the ZnO-functionalized ePTFE filters and the SEM images of the filters at different stages. The inset shows the magnified top-view SEM image of an individual ZnO NR prepared with a hydrothermal growth period for 3 h. Reprinted with permission from American Chemical Society (Zhong Z, Xu Z, Sheng T, Yao J, Xing W, Wang Y. Unusual air filters with ultrahigh efficiency and antibacterial functionality enabled by ZnO nanorods. *ACS Appl Mater Interfaces* 2015;7:21538–44).

nanoparticles by coupling electrospinning technique, subsequent stabilization, and carbonization processes. The resultant membrane exhibited high specific surface area ($>400 \text{ m}^2/\text{g}$) and microporosity. A schematic illustration for fabricating the porous tar-derived CNFs through electrospinning is presented in Fig. 1.30. The porous characteristics of nanofibers increased the exposures and contacts of silver nanoparticles to the bacteria, leading to excellent antimicrobial performances.

Cyclodextrins (CDs) are cyclic oligosaccharides consisting of $\alpha(1,4)$ -linked glucopyranose units having a truncated cone-shaped molecular structure. Due to their unique molecular structure, CDs can form intriguing supramolecular assemblies by forming noncovalent host-guest inclusion complexes with a variety of small molecules and macromolecules. Hence, CDs are applicable in many areas including antibacterial application [54,55]. Celebioglu and Uyar [56] established the first studies on electrospinning of CD nanofibers by itself without the use of a carrier polymer matrix. Essential oils (EOs) are volatile compounds and well known for their antimicrobial and antioxidant properties. Owing to their volatile nature, encapsulation/inclusion is considered very necessary for their effective utilization in different applications. A recent study by Aytac et al. [57] reported that geraniol (which is a

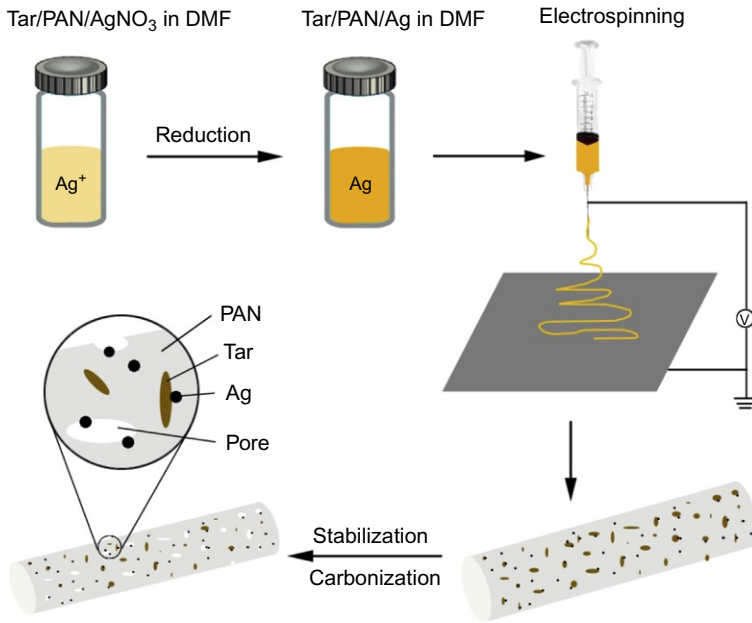


Fig. 1.30 A schematic illustrating the fabrication of the porous tar-derived CNFs through electrospinning followed by stabilization and carbonization processes. Reprinted with permission from American Chemical Society (Song K, Wu Q, Zhang Z, Ren S, Lei T, Negulescu II, et al. Porous carbon nanofibers from electrospun biomass tar/polyacrylonitrile/silver hybrids as antimicrobial materials. *ACS Appl Mater Interfaces* 2015;7:15108–16).

well-known volatile essential oil compound) was effectively encapsulated into three different cyclodextrins (CDs), namely, hydroxypropyl-beta-cyclodextrin (HP β CD), methylated-beta-cyclodextrin (M β CD), and hydroxypropyl-gamma-cyclodextrin (HP γ CD), which is a cyclic oligosaccharide. The schematic representation of the experimental procedure is shown in Fig. 1.31. The cyclodextrin/geraniol-inclusion complex (CD/geraniol-IC) furthers electrospun as a free-standing nanofibrous webs CD/geraniol-IC-NF. The antibacterial studies indicated that prepared CD/geraniol-IC-NFs possessed strong antibacterial activity.

1.3 Commercialization prospectus

So far, the electrospun nanofibers have been well demonstrated for their potentiality in a variety of biomedical applications. To date, numerous electrospinning-based technologies were already transferred out of the laboratories, and products are commercialized in a wide range of industrial sectors including filtration, energy storage, and tissue engineering. Persano et al. [3] reviewed the status of electrospinning in industrialization

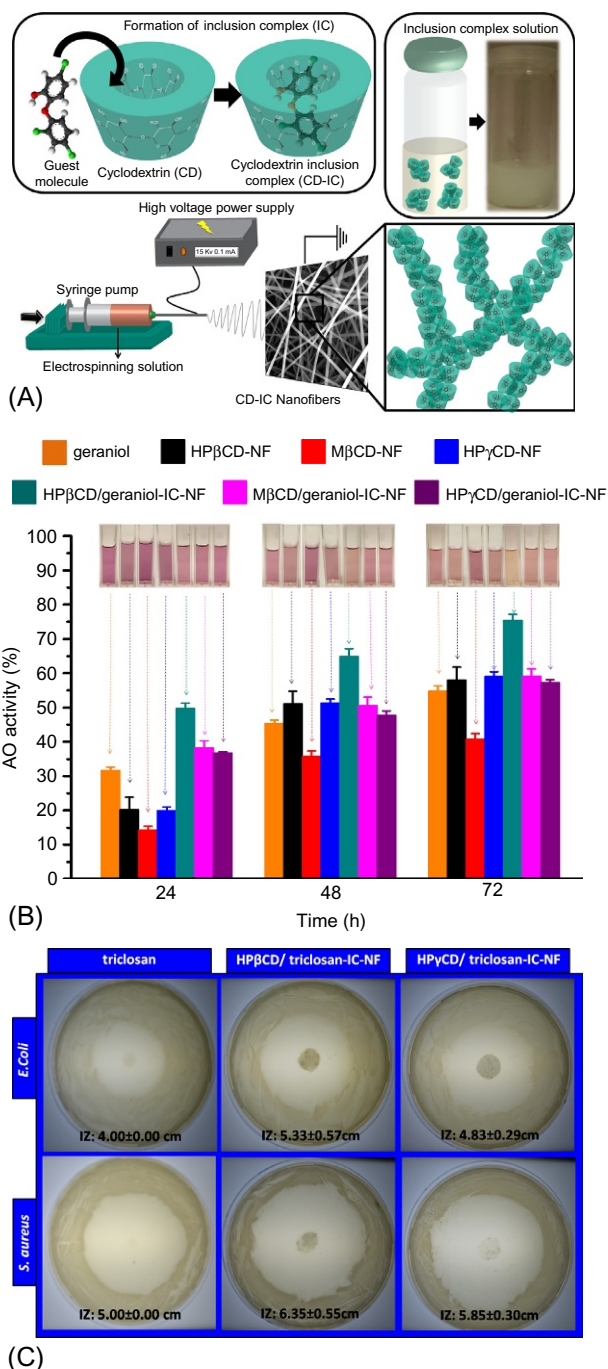


Fig. 1.31 (A) Schematic representation of IC formation and IC solution; illustration of electrospinning of CD-IC nanofibers. (B) The antioxidant (AO) activity (%) of geraniol, HPβCD-NF, MβCD-NF, HPγCD-NF, HPβCD/geraniol-IC-NF, MβCD/geraniol-IC-NF, and HPγCD/geraniol-IC-NF and the photographs of DPPH solutions in which geraniol, HPβCD-NF, MβCD-NF, HPγCD-NF, HPβCD/geraniol-IC-NF, MβCD/geraniol-IC-NF, HPγCD/geraniol-IC-NF were immersed, respectively. (C) The representative photographs of antibacterial test plates with the average inhibition zone (IZ) and standard deviation calculations for *E. coli* and *S. aureus* treated with pure triclosan, HPβCD/triclosan-IC-NF, and HPγCD/triclosan-IC-NF.

perspectives and listed the companies involved in supplying industrial-scale electrospinning equipment and nanofiber-based products. A list of representative companies providing industrial-scale electrospinning equipment includes Elmarco (www.elmarco.com), Holmarc Opto-Mechatronics (www.holmarc.com), NaBond (www.electro-spinning.com), E-Spin Nanotech (www.espinnanotech.com), Electrospinz (www.electrospinz.co.nz), Electrospunra (www.electrospunra.com), Linari Engineering (www.linaribiomedical.com), Mecc Co. (www.mecc.co.jp), Kato Tech (www.keskato.co.jp), Inovenso (www.inovenso.com), Toptec (www.toptec.co.kr), IME Technologies (www.imetechnologies.nl), and Yflow (www.yflow.com). And also, a list of companies involved in supplying electrospun products for different fields of application includes Ahlstrom Corporation (www.ahlstrom.com), Donaldson (www.donaldson.com), DuPont (www.dupont.com), eSpin Technologies (www.espintechnologies.com), Esfil Tehno AS (www.esfiltehno.ee), HemCon Medical Technologies, Inc (www.hemcon.com), Johns Manville (www.jm.com), Finetex Technology (www.finetextech.com), Hollingsworth and Vose Company (www.hollingsworthvose.com), Japan Vilene Company (www.vilene.co.jp), Nanofiber Solutions (www.nanofibersolutions.com), Kertak Nanotechnology (www.kertaknanotechnology.com), Nano109 (www.nano109.com), NanoSpun (www.nanospuntech.com), Soft Materials and Technologies S.r.l (www.smtnano.com), Polynanotec (www.polynanotec.com), Yflow (www.yflow.com), and SNS Nano-Fiber Technology (www.snsnano.com). In addition, the ElectrospinTech listed variety of companies involved in electrospinning-based products/service suppliers [58]. The list of selected companies involved in tissue-engineering products services is presented in Table 1.1.

Even though the technical specification and requirements in instruments have been solved to produce nanofibers in industrial scale, it is more important that the produced material should possess the biological compatibility to further apply in tissue-engineering applications. Another key challenge is quality control; most importantly, these materials need to be produced by following the good manufacturing practice (GMP) conditions to meet FDA and other regulatory standards. Therefore, the innovations at laboratory scale related to biomedical applications must travel through in line with industrial requirements to avoid failure at later stage.

1.4 Conclusion

In this chapter, we highlighted the advancement of nanofibrous membrane in biomedical applications. The outstanding uniqueness of electrospun nanofibrous membrane provides a wide range of opportunities for their use in many different biomedical applications. The easy functionalization of nanofibrous assembly yielding significant advancements in the development of functional nanofibrous scaffolds. An obvious advantage of core-shell fibrous assembly has led the burst and sustained release of bioactive molecules. Besides controlled nanofibrous structures, hydrophilicity of the fibrous membrane also provides the more favorable environment for cellular adhesion. The wetting characteristics of the nanofibrous scaffold are also efficiently

Table 1.1 List of companies involved in tissue-engineering products service

S. No.	Company name	Product/service	Country	Website
1	Ahlstrom Corporation	Nanofiber-based products for medical care, life science and diagnostics	Finland	www.ahlstrom.com
2	3-D Biotek	Cell culture device	The United States	www.3dbiotek.com
3	BioSurfaces Inc.	Drug-loaded electrospun fibers for implantable and nonimplantable devices	The United States	www.biosurfaces.us
4	Biotronik	Covered Stent	Germany	www.biotronik.com
5	Espin Technologies	Nanofiber-based products for regenerative medicine and drug delivery	The United States	www.espintechologies.com
6	HemCon Medical Technologies, Inc	Nanofiber-based products for wound care	The United States	www.hemcon.com
7	Nanofiber Solutions	3-D cell culture consumables and scaffolds for tissue engineering	The United States	www.nanofibersolutions.com
8	Neotherix	Nanofiber scaffold for tissue regeneration	The United Kingdom	www.neotherix.com
9	Nicast Ltd	Nanofiber implants	Israel	www.nicast.com
10	Sigma-Aldrich	Nanofiber culture plates	The United States	www.sigmaaldrich.com
11	Soft Materials and Technologies S.r.l.	Fibrous tissues	Italy	www.smtnano.com
12	Stellenbosch Nanofiber Company	Nanofiber-based materials for medical applications	South Africa	www.sncfibers.com
13	The Electrospinning Company	Nanofiber scaffold for tissue regeneration	The United Kingdom	www.electrospinning.co.uk

modified via plasma treatment and chemical-etching treatment. The shrinkage and distortion of the electrospun scaffolds restrict the initial cell adhesion and further growth, and therefore, suspended, shrinkage-free electrospun scaffold has been developed. A hybrid scaffold has also been well demonstrated to enhance the cellular infiltration and nutrient transport. The practical and comfortable wound dressing is a critical challenge even though there were a huge number of studies that have been evaluated and found electrospun membrane as an efficient wound-dressing material. The novel handy e-spinning device has also been demonstrated to develop a personalized nanofibrous dressing. The research may extent to incorporate the sensor to monitor the wound management. It may give necessary information on infection feedback, which may help to change the dressing material if necessary. The successful clinical translation of such demonstrated nanofibrous scaffold may provide their effectiveness in biomedical field. Therefore, the toxic profile of nanofibrous membrane should be carefully studied. The potential of nanofibrous scaffold provides the improved performances in biomedical applications, suggesting that their participant remains promising.

Acknowledgments

A.S. acknowledges the Scientific and Technological Research Council of Turkey (TUBITAK)-BIDEB 2221—Fellowships for Visiting Scientists and Scientists on Sabbatical Leave for the fellowship. B.B. acknowledges TUBITAK-BIDEB 2216, Research Fellowship Programme for Foreign Citizens for postdoctoral fellowship. T.U. acknowledges the Turkish Academy of Sciences — Outstanding Young Scientists Award Program (TUBA-GEBIP).

References

- [1] Wade RJ, Burdick JA. Advances in nanofibrous scaffolds for biomedical applications: From electrospinning to self-assembly. *Nano Today* 2014;9:722–42.
- [2] Huang ZM, Zhang YZ, Kotaki M, Ramakrishna S. A review on polymer nanofibers by electrospinning and their applications in nanocomposites. *Compos Sci Technol* 2003;63:2223–53.
- [3] Persano L, Camposeo A, Tekmen C, Pisignano D. Industrial upscaling of electrospinning and applications of polymer nanofibers: a review. *Macromol Mater Eng* 2013;298:504–20.
- [4] Agarwal S, Wendorff JH, Greiner A. Use of electrospinning technique for biomedical applications. *Polymer* 2008;49:5603–21.
- [5] Jiang T, Carbone EJ, Lo KWH, Laurencin CT. Electrospinning of polymer nanofibers for tissue regeneration. *Prog Polym Sci* 2015;46:1–24.
- [6] Senthamizhan A, Balusamy B, Uyar T. Glucose sensors based on electrospun nanofibers: a review. *Anal Bioanal Chem* 2016;408:285–1306.
- [7] Sill TJ, von Recum HA. Electrospinning: Applications in drug delivery and tissue engineering. *Biomaterials* 2008;29:1989–2006.
- [8] Saracino GAA, Cigognini D, Silva D, Caprini A, Gelain F. Nanomaterials design and tests for neural tissue engineering. *Chem Soc Rev* 2013;42:225–62.

- [9] Xie J, MacEwan MR, Ray WZ, Liu W, Siewe DY, Xia Y. Radially aligned, electrospun nanofibers as dural substitutes for wound closure and tissue regeneration applications. *ACS Nano* 2010;4:5027–36.
- [10] Shi J, Votruba AR, Farokhzad OC, Langer R. Nanotechnology in drug delivery and tissue engineering: from discovery to applications. *Nano Lett* 2010;10:3223–30.
- [11] Zamani M, Prabhakaran MP, Ramakrishna S. Advances in drug delivery via electrospun and electrosprayed nanomaterials. *Int J Nanomed* 2013;8:2997–3017.
- [12] Hu X, Liu S, Zhou G, Huang Y, Xie Z, Jing X. Electrospinning of polymeric nanofibers for drug delivery applications. *J Controlled Release* 2014;185:12–21.
- [13] Yoo HS, Kim TG, Park TG. Surface-functionalized electrospun nanofibers for tissue engineering and drug delivery. *Adv Drug Delivery Rev* 2009;61:1033–42.
- [14] Wang Y, Qiao W, Wang B, Zhang Y, Shao P, Yin T. Electrospun composite nanofibers containing nanoparticles for the programmable release of dual drugs. *Polym J* 2011;43:478–83.
- [15] Jiang H, Wang L, Zhu K. Coaxial electrospinning for encapsulation and controlled release of fragile water-soluble bioactive agents. *J Controlled Release* 2014;193:296–303.
- [16] Mickova A, Buzgo M, Benada O, Rampichova M, Fisar Z, Filova E, et al. Core/shell nanofibers with embedded liposomes as a drug delivery system. *Biomacromolecules* 2012;13:952–62.
- [17] Man Z, Yin L, Shao Z, Zhang X, Hu X, Zhu J, et al. The effects of co-delivery of BMSC-affinity peptide and rhTGF- β 1 from coaxial electrospun scaffolds on chondrogenic differentiation. *Biomaterials* 2014;35:5250–60.
- [18] Dubey P, Gopinath P. Fabrication of electrospun poly(ethylene oxide)–poly(caprolactone) composite nanofibers for co-delivery of niclosamide and silver nanoparticles exhibits enhanced anti-cancer effects *in vitro*. *J Mater Chem B* 2016;4:726–42.
- [19] Yu DG, Li XY, Wang X, Yang JH, Bligh SWA, Williams GR. Nanofibers fabricated using triaxial electrospinning as zero order drug delivery systems. *ACS Appl Mater Interfaces* 2015;7:18891–7.
- [20] Chen JP, Su CH. Surface modification of electrospun PLLA nanofibers by plasma treatment and cationized gelatin immobilization for cartilage tissue engineering. *Acta Biomater* 2011;7:234–43.
- [21] Rim NG, Shin CS, Shin H. Current approaches to electrospun nanofibers for tissue engineering. *Biomed Mater* 2013;8:014102.
- [22] Jeon HJ, Lee H, Kim GH. Fabrication and characterization of nanoscale-roughened PCL/collagen micro/nanofibers treated with plasma for tissue regeneration. *J Mater Chem B* 2015;3:3279–87.
- [23] Tian L, Prabhakaran MP, Hu J, Chen M, Besenbacher F, Ramakrishna S. Coaxial electrospun poly(lactic acid)/silk fibroin nanofibers incorporated with nerve growth factor support the differentiation of neuronal stem cells. *RSC Adv* 2015;5:49838–48.
- [24] Croll TI, O'Connor AJ, Stevens GW, Cooper-White JJ. Controllable surface modification of Poly(lactic-co-glycolic acid) (PLGA) by hydrolysis or aminolysis I: physical, chemical, and theoretical aspects. *Biomacromolecules* 2004;5:463–73.
- [25] Ma Z, Kotaki M, Yong T, He W, Ramakrishna S. Surface engineering of electrospun polyethylene terephthalate (PET) nanofibers towards development of a new material for blood vessel engineering. *Biomaterials* 2005;26:2527–36.
- [26] Chen MC, Sun YC, Chen YH. Electrically conductive nanofibers with highly oriented structures and their potential application in skeletal muscle tissue engineering. *Acta Biomater* 2013;9:5562–72.

- [27] Prabhakaran MP, Ghasemi-Mobarakeh L, Jin G, Ramakrishna S. Electrospun conducting polymer nanofibers and electrical stimulation of nerve stem cells. *J Biosci Bioeng* 2011;112:501–7.
- [28] Zhang J, Qiu K, Sun B, Fang J, Zhang K, El-Hamshary H, et al. The aligned core–sheath nanofibers with electrical conductivity for neural tissue engineering. *J Mater Chem B* 2014;2:7945–54.
- [29] Shao S, Zhou S, Li L, Li J, Luo C, Wang J, et al. Osteoblast function on electrically conductive electrospun PLA/MWCNTs nanofibers. *Biomaterials* 2011;32:2821–33.
- [30] Balint R, Cassidy NJ, Cartmell SH. Conductive polymers: Towards a smart biomaterial for tissue engineering. *Acta Biomater* 2014;10:2341–53.
- [31] Shimizu K, Fujita H, Nagamori E. Alignment of skeletal muscle myoblasts and myotubes using linear micropatterned surfaces ground with abrasives. *Biotechnol Bioeng* 2009;103:631–8.
- [32] Ru C, Wang F, Pang M, Sun L, Chen R, Sun Y. Suspended, shrinkage-free, electrospun PLGA nanofibrous scaffold for skin tissue engineering. *ACS Appl Mater Interfaces* 2015;7:10872–7.
- [33] Yang GH, Mun F, Kim G. Direct electrospinning writing for producing 3D hybrid constructs consisting of microfibers and macro-struts for tissue engineering. *Chem Eng J* 2016;288:648–58.
- [34] Unnithan AR, Nejad AG, Sasikalaa ARK, Thomas RG, Jeong YY, Murugesan P, et al. Electrospun zwitterionic nanofibers with *in situ* decelerated epithelialization property for non-adherent and easy removable wound dressing application. *Chem Eng J* 2016;287:640–8.
- [35] Zahedi P, Rezaeian I, Ranaei-Siadat SO, Jafari SH, Supaphol P. A review on wound dressings with an emphasis on electrospun nanofibrous polymeric bandages. *Polym Adv Technol* 2010;21:77–95.
- [36] Abrigo M, McArthur SL, Kingshott P. Electrospun nanofibers as dressings for chronic wound care: advances, challenges, and future prospects. *Macromol Biosci* 2014;14:772–92.
- [37] Morgado PI, Lisboa PF, Ribeiro MP, Miguel SP, Simões PC, Correia IJ, et al. Poly(vinyl alcohol)/chitosan asymmetrical membranes: Highly controlled morphology toward the ideal wound dressing. *J Membr Sci* 2014;469:262–71.
- [38] Sarhan WA, Azzazy HM, El-Sherbiny IM. Honey/Chitosan nanofiber wound dressing enriched with *Allium sativum* and *Cleome droserifolia*: Enhanced antimicrobial and wound healing activity. *ACS Appl Mater Interfaces* 2016;8:6379–90.
- [39] Gurtner GC, Werner S, Barrandon Y, Longaker MT. Wound repair and regeneration. *Nature* 2008;453:314–21.
- [40] Rieger KA, Birch NP, Schiffman JD. Designing electrospun nanofiber mats to promote wound healing—a review. *J Mater Chem B* 2013;1:4531–41.
- [41] Tan L, Hu J, Zhao H. Design of bilayered nanofibrous mats for wound dressing using an electrospinning technique. *Mater Lett* 2015;156:46–9.
- [42] Hajiali H, Summa M, Russo D, Armirotti A, Brunetti V, Bertorelli R, et al. Alginate–lavender nanofibers with antibacterial and anti-inflammatory activity to effectively promote burn healing. *J Mater Chem B* 2016;4:1686–95.
- [43] Dong RH, Jia YX, Qin CC, Zhan L, Yan X, Cui L, et al. *In situ* deposition of a personalized nanofibrous dressing via a handy electrospinning device for skin wound care. *Nanoscale* 2016;8:3482–8.
- [44] Kim JH, Jang J, Jeong YH, Ko TJ, Cho DW. Fabrication of a nanofibrous mat with a human skin pattern. *Langmuir* 2015;31:424–31.

- [45] Gao Y, Truong YB, Zhu Y, Kyrtzlis IL. Electrospun antibacterial nanofibers: Production, activity, and *in vivo* applications. *J Appl Polym Sci* 2014;131:40797.
- [46] Yang H, Gao PF, Wu WB, Yang XX, Zeng QL, Li C, et al. Antibacterials loaded electrospun composite nanofibers: release profile and sustained antibacterial efficacy. *Polym Chem* 2014;5:1965–75.
- [47] Xu X, Yang Q, Wang Y, Yu H, Chen X, Jing X. Biodegradable electrospun poly(l-lactide) fibers containing antibacterial silver nanoparticles. *Eur Polym J* 2006;42:2081–7.
- [48] Shi Q, Vitichuli N, Nowak J, Caldwell JM, Breidt F, Bourham M, et al. Durable antibacterial Ag/polyacrylonitrile (Ag/PAN) hybrid nanofibers prepared by atmospheric plasma treatment and electrospinning. *Eur Polym J* 2011;47:1402–9.
- [49] Annur D, Wang ZK, Liao JD, Kuo C. Plasma-synthesized silver nanoparticles on electrospun chitosan nanofiber surfaces for antibacterial applications. *Biomacromolecules* 2015;16:3248–55.
- [50] Anitha S, Brabu B, Thiruvadigal DJ, Gopalakrishnan C, Natarajan TS. Optical, bactericidal and water repellent properties of electrospun nano-composite membranes of cellulose acetate and ZnO. *Carbohydr Polym* 2013;97:856–63.
- [51] Lee WS, Park YS, Cho YK. Significantly enhanced antibacterial activity of TiO₂ nanofibers with hierarchical nanostructures and controlled crystallinity. *Analyst* 2015;140:616–22.
- [52] Zhong Z, Xu Z, Sheng T, Yao J, Xing W, Wang Y. Unusual air filters with ultrahigh efficiency and antibacterial functionality enabled by ZnO nanorods. *ACS Appl Mater Interfaces* 2015;7:21538–44.
- [53] Song K, Wu Q, Zhang Z, Ren S, Lei T, Negulescu II, et al. Porous carbon nanofibers from electrospun biomass tar/polyacrylonitrile/silver hybrids as antimicrobial materials. *ACS Appl Mater Interfaces* 2015;7:15108–16.
- [54] Celebioglu A, Uyar T. Electrospinning of polymer-free nanofibers from cyclodextrin inclusion complexes. *Langmuir* 2011;27:6218–26.
- [55] Celebioglu A, Umu OCO, Tekinay T, Uyar T. Antibacterial electrospun nanofibers from Triclosan/Cyclodextrin inclusion complexes. *Colloids Surf B Biointerfaces* 2014;116:612–9.
- [56] Celebioglu A, Uyar T. Cyclodextrin nanofibers by electrospinning. *Chem Commun* 2010;46:6903–5.
- [57] Aytac Z, Yildiz ZI, Kayaci-Senirmak F, Keskin NOS, Tekinay T, Uyar T. Electrospinning of polymer-free cyclodextrin/geraniol–inclusion complex nanofibers: enhanced shelf-life of geraniol with antibacterial and antioxidant properties. *RSC Adv* 2016;6:46089–99.
- [58] ElectrospinTech. <<http://electrospintech.com/epin-companies.html#.V7wjIDWhovV>> (accessed 23.08.2016).

This page intentionally left blank

General requirements of electrospun materials for tissue engineering: Setups and strategy for successful electrospinning in laboratory and industry

E. Kijeńska, W. Swieszkowski

Warsaw University of Technology, Warsaw, Poland

Regenerative medicine based on tissue engineering (TE) along with sophisticated biomedical devices combines knowledge from many scientific fields like biology, materials science, and chemistry to develop novel therapies for damaged tissues and organ malfunctions [1,2]. This multidisciplinary approach aims to provide sufficient habitat for cells or stable microenvironment for tissue self-healing, in a form of tissue-engineered scaffold, wound dressing, or drug delivery carrier [3–5]. These types of constructs must comply with specific criteria matching the characteristics and properties of the tissue at the implantation site [6]. Certain requirements refer to properties of tissue-engineered scaffolds. They should exhibit mechanical properties similar to those of native tissue, providing optimal support to withstand the forces occurring in physiological body conditions [6]. However, scaffold should lose its strength parallel to tissue formation during regeneration [7]. Other important aspects are scaffolds' architecture and morphology. Structure should distinguish itself with high porosity, high surface area, and interconnected pores to ensure cell penetration, exchange of the nutrients/O₂ and wastes/CO₂ [8], and vascularization of the regrowing region. The size of the pores is crucial. The pores should be not only large enough to allow cells to migrate toward the structure but also small enough to allow efficient binding of the cells [9]. In general, there is no optimal pore size for all tissue regeneration. The sufficient pore sizes for versatile tissues are in a range of 20–350 μm [10]. The structure of ideal tissue-engineered construct should distinguish itself with heterogeneous morphology possessing both nanoscaled elements allowing attachment and accommodation of the cells and macroscale pores permitting their infiltration and propagation within the structure [11].

Adverse to implants, scaffolds are not intended for long-term use and permanent presence within the body. They should be degradable, and the time of their degradation should not exceed the period of the new tissue formation [7]. Native extracellular matrix (ECM) of most tissues exhibits intricate organization build of nano- and microstructured protein and proteoglycanous fibers [12] with 50–500

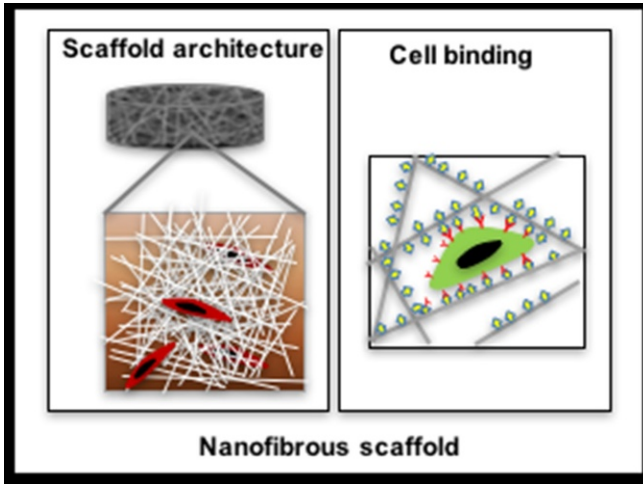


Fig. 2.1 Schematic diagram of effect of nanofibrous scaffold architecture on cell binding based on [15].

nm collagen fibrils [13]. Thus, it is believed that nanoscaled environment promotes uniform cell distribution and allows for intramolecular interactions, which in turn affects morphological and functional development of the cells. Scaffolds composed of nanofibers exhibit high surface area to volume ratio [14], which improves adsorption of the protein by providing more binding sites, thus mimicking specific ligands and topography of native ECM (Fig. 2.1). There are a number of methods like phase separation [16], self-assembly [17], and electrospinning [18] that have been used to obtain nanofibrous constructs for TE applications. However, electrospinning technique seems to be the most effective and versatile method of its fabrication. Other aspects making this method very attractive to utilize are the simplicity and low price of the applied setup [19].

The essential mechanism of electrospinning process is based on drawing of the fluid (polymer solution or melt) using electrostatic field [18]. When a high voltage is applied to polymer solution through flattened needle, charges within the fluid undergo induction. When they reach a critical amount, the jet starts erupting from the droplet at the tip of the needle, and Taylor cone is formed. The jet is traveling toward grounded collector, where the potential gradient is located. During the flight, solution evaporates, and solidified fibers are collected on the collector [18,20].

There are a great number of different types of polymers, precursors, and other bio-active substances that can undergo electrospinning to form nanofibers [21]. In general, the choice of the material to be electrospun depends on the applications of the resultant fibers and fibrous structures. However, there are some certain conditions that must be met by particular material regardless of the applications of the fibrous structures. The main property of the utilized substrate is its biocompatibility, understood as the ability of providing sufficient cellular environment. It should not cause any immune reaction or inflammation of the body after implantation, resulting to its rejection or disturbing

the healing process. Materials should be degradable, and the by-products of the degradation should be nontoxic and possess the ability of exiting the body without any interference with other tissues and organs [9].

2.1 Electrospinnable materials for TE applications

Research into the use of polymer nanofibers has increased significantly, and electrospun fibrous constructs have been established as a potential substratum for TE scaffolds. Wide range of versatile materials can be utilized within the process to develop diverse implants. In this chapter, the most commonly available materials that can undergo electrospinning for biomedical purposes will be briefly discussed along with the basic requirements of utilized solvents and other additives.

2.1.1 *Synthetic and natural polymers used in electrospinning for biomedical applications*

There are various polymers that have been investigated to produce electrospun nanofibrous scaffolds, including synthetic, natural, and their blends [22]. For tissue engineering scaffolds, bioabsorbable polymers are preferred, due to their degradability and possibility to employ them as temporary supporting systems, which can be replaced by newly formed tissue [23]. Biomedical application of materials imposes also some other conditions influencing their selection. Most of them are related to the biomaterial chemical composition, its molecular weight, crystal structure, hydrophilic nature, lubricity, catalytic degradation in water-based conditions, and mechanism of its erosion [10]. On the other hand, polymers used for electrospinning must distinguish themselves with some specific properties that allow utilized material to form fibers. One of the most significant factors is the molecular weight of the polymer. This parameter indicates the number of chains that can be entangled, which further affects the formation of smooth uniform nanofibers. Low molecular weight might cause droplet formation (electrospray) or the presence of beads within the fibers [18]. If the molecular weight of polymer is too low and there is no possibility of obtaining the same polymer with higher value of this factor, it is recommended to blend it with polymer holding higher molecular weight or increase significantly the concentration of the polymer solution. Recently, the most interesting synthetic polymers used for tissue engineering scaffold and drug/growth factor delivery carriers are FDA-approved polyesters like poly(L-lactide) (PLLA), poly(ϵ -caprolactone) (PCL), poly(glycolic acid) (PGA), and their copolymers like poly(L-lactide-co- ϵ -caprolactone) (PLCL) or poly(lactic-co-glycolic acid) (PLGA) with different ratios of their components [24]. However, synthetic polymers alone might not meet all the requirements of an artificial tissue construct since they lack recognition sites for cell adhesion [25]. Commonly used polymers of natural origin such as collagen, gelatin silk, and alginate can provide a suitable matrix for cells, since their structure is enriched with binding sites and ligands influencing attachment, proliferation, survival, and differentiation of the cells [26]. However, the main disadvantage of their use is

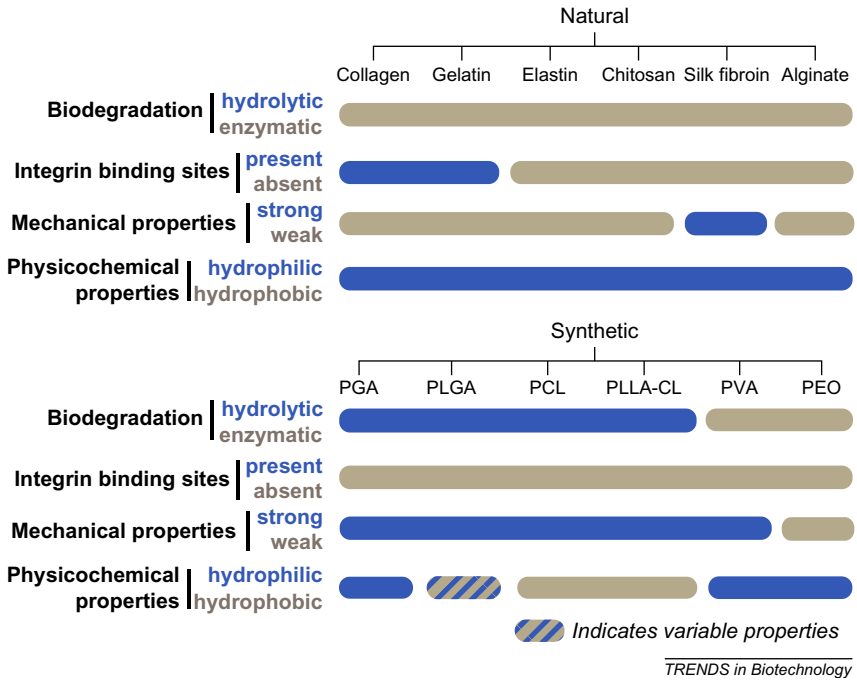


Fig. 2.2 Properties of selected polymers used for biomedical applications. Reprinted with permission from Elsevier (Gunn J, Zhang M. Polyblend nanofibers for biomedical applications: perspectives and challenges. *Trends Biotechnol* 2010;28(4):189–97).

connected to low mechanical properties, poor stability of the proteins in aqueous environment, and low thermal stability in general. Therefore, electrospun nanofibrous scaffolds composed of both synthetic polymer and protein might overcome the limitations of single component nanofibrous systems and provide suitable substrates for TE [25].

Fig. 2.2 provides concise information about biological, mechanical, and physicochemical properties of polymers most commonly used in biomedical application.

2.1.2 Requirements for solvents

In the traditional electrospinning from the polymer solution, the choice of sufficient solvent is critical for formation of the fibers and their resultant morphology. When selecting a solvent for manufacturing of nanofibrous scaffolds for TE application or drug delivery, the most important, along with obtaining of desired morphology of the fibers, is possible toxicity of the solvent residuals within fabricated structures. The venom remaining might influence cell behavior or even indicate cell apoptosis. Thus, water, nontoxic, and/or highly evaporating liquids are preferable. From the technological point of view of the process, the most relevant aspects for consideration are the solubility of individual polymer and the volatility of used solvent [27].

Electrospinning process involves evaporation of the solvent and separation of the phases during the time when the jet is traveling from the capillary tip toward the grounded collector [28]. Generally, the more volatile is the solvent, the faster polymer solution jet dries. On the other hand, when the evaporation rates are too high, fluid tends to shrivel fast and clogs nozzle disrupting the flow rate of the solution [27]. Numerous studies have been conducted toward investigation of the influence of the versatile solvents on the morphology and porosity of the electrospun fibers [29–31]. It has been observed that solvents with high boiling point like DMF, which do not fully evaporate during electrospinning, result in flat or coagulated fibers in the point of contact [27]. On the other hand, use of solvents with high volatility allows to obtain nanofibers with large pores on their surface [30], which might be beneficial for fibers used as a drug delivery carriers. Utilization of mixture of solvents with different boiling points and vapor pressures like THF and DMF and variations of volume ratios in-between them enables tailoring of the size and the density of the pores on the fibers' surface [29]. Less volatile is the solvents' mixture, resultant fibers will be smoother and opposite, more volatile is the solution, and larger is the size of the pores and their density. Other properties of the solvents having impact on the process are their dielectric constant and conductivity. Utilization of solvent with higher dielectric constant results with decrease in beads formation and reduction of fibers' diameters. Low dielectric constant and high surface tension of the fluid, like for DCM-based solutions, causing lower charge repulsion within the jet, result in beads formation. Solution prepared with solvents possessing higher conductivity allows to obtain fibers with smoother morphology without beads [18]. Low conductivity of the polymer solution can be overcome by the addition of the ions from salts like KH_2PO_4 , NaH_2PO_4 , or NaCl . This increases the charge carrying capacity of the fluid; extends deposition area by increase of bending instability of the fluid, which all together cause less beads formation; and decreases in the fibers' diameter [32].

In conclusion, nanofiber morphology and their surface porosity can be regulated by the use of particular solvent or compound of solvents allowing for obtaining desired morphology and diameter of the nanofibers. Some of the solvents commonly used in electrospinning for biomedical application and their properties have been listed in Table 2.1.

Schematic graph summarizing the basic strategies for successful electrospinning of nanofiber for TE applications has been presented in Fig. 2.3.

2.2 Electrospinning technologies and set-ups

Recently, electrospinning evolved as an effectual tool for fabrication of tissue-engineered manufactures [35]. This fiber fabrication technique provides the possibility of obtaining nanofibrous structures with various shapes and diverse properties of the fibers. The morphology of the fibers and their composition and orientation, along with the geometry and porosity of obtained structures, can be tailored by customization of electrospinning process [21]. The laboratory strategies of TE products and drug delivery system development defy mainly on customization of basic electrospinning

Table 2.1 Solvent properties

Solvent type	Boiling point (°C)	Dielectric constant (dyn/cm)	Basic characteristics
DCM	39.8	8.93	High surface tension
HFP	59	16.7	High dipole moment, good conductivity
Chloroform	61.2	4.8	High intrinsic viscosity
Methanol	64.7	32.6	High surface tension
THF	66	7.47	High dipole moment, good conductivity
Ethanol	78.3	24.55	Low surface tension, high intrinsic viscosity
Water	100	80.2	Low intrinsic viscosity
DMF	153	36.71	High dipole moment, high conductivity

DCM, dichloromethane; HFP, 1,1,1,3,3,3-hexafluoro-2-propanol; THF, tetrahydrofuran; DMF, dimethylformamide). Based on Ramakrishna S. An introduction to electrospinning and nanofibers. World Scientific Publishing Company Incorporated, 2005; Pillay V, et al. A review of the effect of processing variables on the fabrication of electrospun nanofibers for drug delivery applications. J Nanomater, 2013, p. 22; <http://stenutz.eu/chem/solv6.php?name=1%2C1%2C1%2C3%2C3%2C3-hexafluoropropan-2-ol>, 26.10.2016; Gualandi C. Porous polymeric bioresorbable scaffolds for tissue engineering. Berlin, Heidelberg: Springer; 2013 [18,27,33,34].

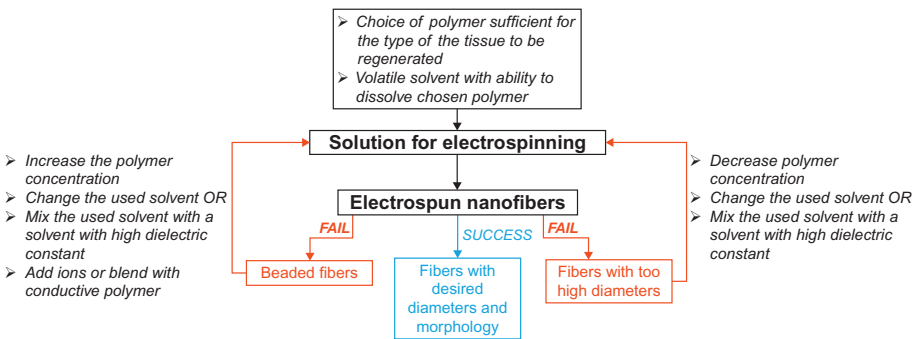


Fig. 2.3 Schematic flowchart for electrospinning basic strategy.

Partially based on Teo W-E. Electrospinning nanofiber flowchart, http://electrospintech.com/espinflowchart.html#_WBCVE8mr_iB.

setups. Modification of utilized collectors allows to produce more complicated structures with different orientations of the fibers, and versatile spinnerets enable to obtain fibers with nonhomogenous fiber composition. Others employed procedures based on postprocessing functionalization of the nanofibers, for example, to increase the bioactivity of the surfaces or to change the porosity of the constructs [36].

2.2.1 Fabrication of the structures with different orientation of the fibers

Development of engineered nanofibrous scaffolds with topographical features mimicking native ECM of the tissue is still a challenge. Electrospinning method allows for obtaining nonwoven structures with an extremely high ratio of surface to volume and structure of interconnected pores. This provides better cellular adhesion and influence in a positive manner spreading and growth of the cells [37]. Basically, using standard electrospinning method, two types of the fibers' orientation can be obtained, namely, random and aligned [38]. Nanofibrous structures with uniaxial orientation of the fibers exhibit anisotropic mechanical properties, very similar to those of native ECM. Also on the biomolecular level, this type of topography might selectively enhance endocytosis, adhesion, and proliferation of cells [39]. Moreover, cell spreading and proliferation can be oriented along the nanofibers orientation [40]. Thus, nanofibrous scaffolds should be designed with respect to the regeneration of the tissues with oriented texture. For example, smooth muscle cells, neural cells, osteoblasts, and fibroblasts can display aligned actin fiber organization caused by predominated nanofibrous orientation [41].

In standard electrospinning setup, utilization of flat collector results in obtaining randomly oriented fibers (Fig. 2.4A). Employment of collectors based mainly on rotating movement like rotating drum or disk or parallel electrodes enables to obtain aligned orientation of the fibers within the mesh (Fig. 2.4B). Selected types of setups with various collecting devices are shown in Fig. 2.5.

Collectors presented in Fig. 2.5 can be characterized by their simplicity, and there are many advantages of their utilization to produce biomedical products. However, in case of fabrication of aligned fibers, there are some limitations. Usage of rotating drum allow to obtain large area of nanofibrous meshes, but the high alignment of the fibers might be not accurate within whole structure. On the other hand, the use of two parallel electrodes results in high alignment of the fibers, but it is not possible to produce thick membranes. Employment of sharp-edged disk gives good alignment but only for some range of diameter of the fibers [38].

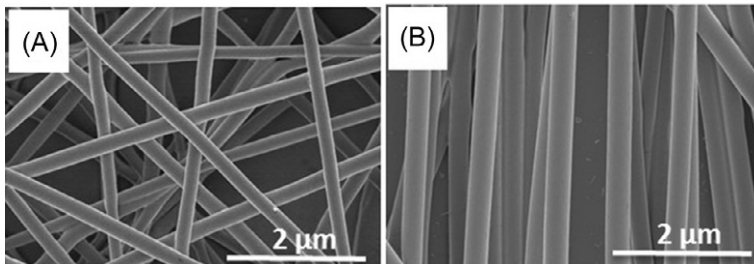


Fig. 2.4 Morphology of randomly oriented (A) and aligned (B) nanofibrous meshes.

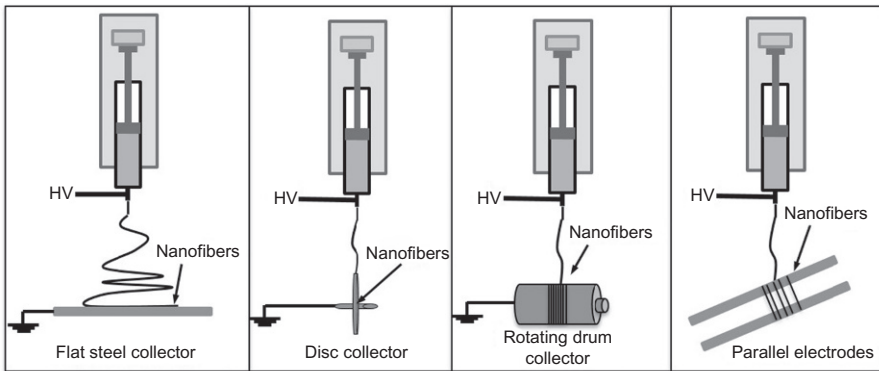


Fig. 2.5 Selected types of nanofibers collecting devices.

2.2.2 Production of fibrous structures with non-homogenous composition of fibers or with diverse composition of layers

Biomedical applications of the nanofibers are not only limited to tissue engineering scaffolds. Electrospun nanofibers can be also adapted as various drug and growth factor delivery carriers allowing for sustained release of labile bioactive agent without their degradation [42]. The advantage of electrospinning process is a possibility of employment of several types of spinnerets (i.e., needle in needle and two needles in a row) enabling to obtain fibers with core-shell or hollow structures or simultaneous spinning of different materials. Utilization of coaxial electrospinning allows to obtain electrospun nanofibrous scaffolds with active biomolecules enclosed within the fibers [41]. Simultaneous spinning of different solutions (double spinning) provides possibility of obtaining nonwovens with different layers in terms of material type, possessing different properties [43]. Utilization of multispinning spinnerets (Fig. 2.6B) also provides a potentiality of overcoming obstacles related to small pore diameters within the nanofibrous structures and high packing density of the meshes. Electrospinning of the same polymer from two different solvents with particular properties (like volatility) results as if fibers are obtained with, for example, different nano- and microdimensions and morphology. Received nanofibrous structures exhibit intermixed pore-size distribution enhancing cellular infiltration, which is usually limited with small pores within the scaffolds [11]. Fig. 2.6 shows two basic setups for coaxial (Fig. 2.6A) and double electrospinning (Fig. 2.6B).

2.2.3 Strategies for fabrication of 3D electrospun constructs

Electrospinning method is not limited only to fabrication of nanofibrous semi-3-D membranes. Tissue engineering applications often require 3-D constructs with a larger thickness, which are difficult to obtain and time-consuming using standard electrospinning. Recent progress in technology results in the development of several methods for production of 3-D scaffolds based on electrospun nanofibers. Some of the

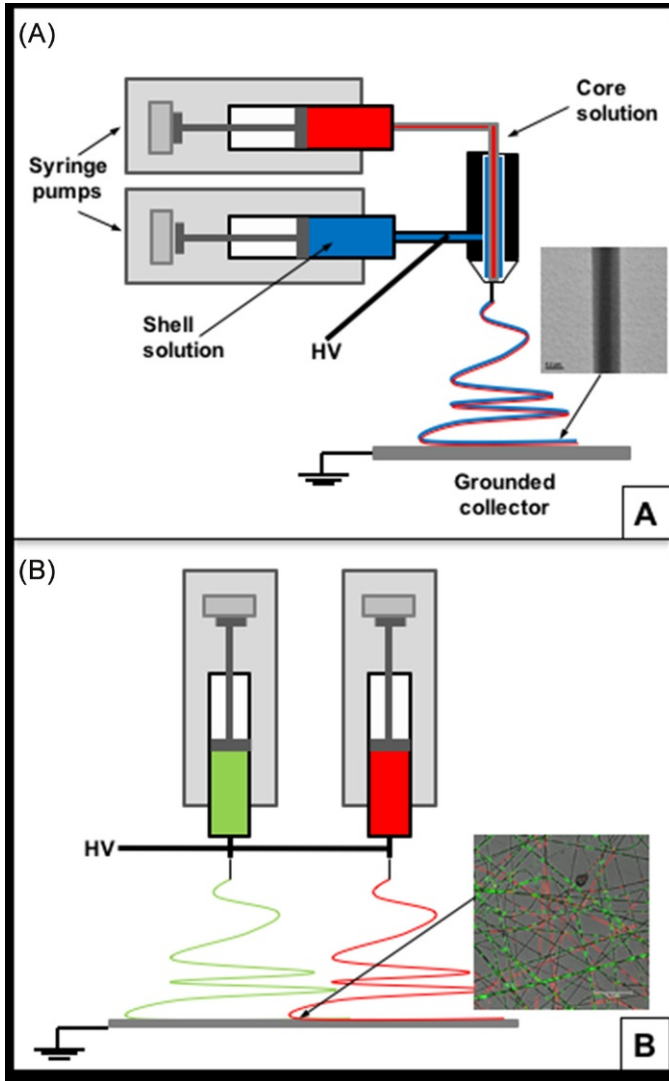


Fig. 2.6 Electrospinning setups for (A) coaxial and (B) double electrospinning.

basic strategies of 3-D nanofibrous scaffold fabrication using standard or modified electrospinning setups will be briefly explained below.

The most simple method of 3-D nanofibrous scaffold fabrication is based on vertically stacking layers (membranes) of fibers (Fig. 2.7A). Utilized membranes might be composed of the different materials and possess different orientations of the fibers, causing variation of the porosity and pore size within the volume of whole structure. Another possible way is rolling membrane to obtain cylindrical multilayered shape (Fig. 2.7B) [44]. In both methods, it is possible to seed the cells on the particular layers

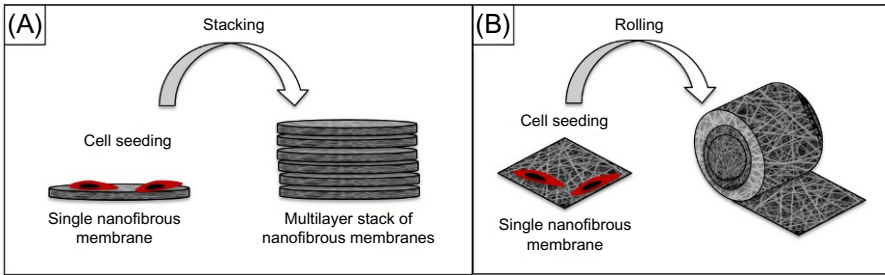


Fig. 2.7 3-D structure obtained by (A) stacking and (B) manual rolling of single nanofibrous membranes.

while constructing 3-D shapes, obtaining even distribution of the cells within whole volume of scaffolds [45,46].

Three-dimensional cylindrical shape of nanofibrous structure, which finds its application for nerve conduits and vascular grafts [47,48], can be obtained with use of rotating mandrel collector (Fig. 2.8A).

Another modification of the standard setup to obtain 3-D structure is the use of liquid reservoir as a collector (Fig. 2.8B). This method increases the internal pore size of the nanofibrous structures. The pack density of obtained meshes using standard electrospinning setup is mainly attributed to the process itself, where produced fibers impact preceding fibers collected on the steel collector [44]. Utilization of low-surface-tension liquid, which causes sinking of the fibers below its surface upon the contact, overcomes the affection of the oncoming fibers on already collected fibers. In turn, this will result in loose of packaging density of the fibers [49]. The choice of the liquid should be dictated by its surface tension and by hydrophilic nature

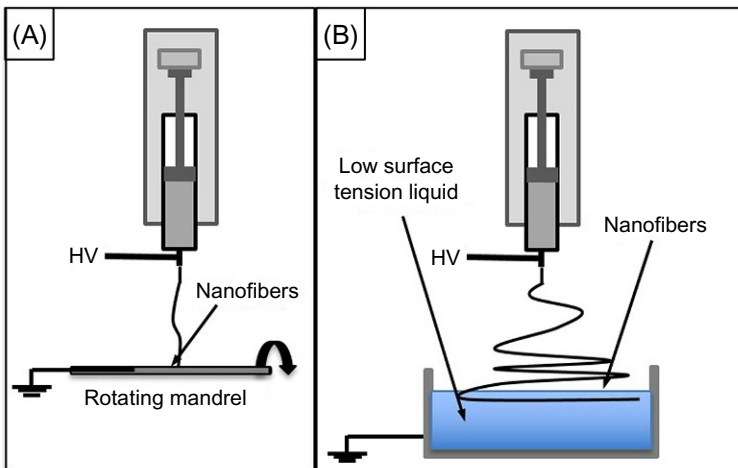


Fig. 2.8 Electrospinning setup with (A) mandrel (B) liquid collectors.

of the polymer used for fabrication of the fibers, preventing fibers from floating on the surface of the liquid [44]. It has been observed that constructs obtained by these methods demonstrate good penetration of the cells [50].

Three-dimensional scaffolds containing electrospun nanofibers can also be produced by development of hybrid structures composed of electrospun nanofibers and microfibers [51], nanofibrous meshes combined with rapid-prototyped scaffolds [52], or nanofibers mixed with hydrogels [53].

2.3 Basics of industrial upscaling of electrospinning

The aforementioned methods and setups listed in the previous part of this chapter are effective ways to produce nanofibrous constructs for biomedical applications in a laboratory scale. When the main aim of research is a development of tailor-made patient-specific tissue-engineered scaffold, the small laboratory scale is efficient enough. However, for the biomedical products, targeting mass-scale production, like patches for wound healing or multipurpose drug delivery carriers, the productivity of used devices and equipment must possess relatively high production rates (sufficient for targeted implementation area). Persano et al. [54] suggested that when the fabrication of nanofibrous structures is planned to be moved to industrial scale, some specific requirements have to be met. Designing of the process should focus on assurance of large volume processing, the accuracy and reproducibility of the produced manufactures, good capacity of process monitoring and inline quality control, and on the ensuring of the environmental safety. Thus, some systems of spinnerets and collectors designed for laboratory research may not apply for mass-scale production. Laboratory equipment based on so-called “needle-type” spinneret setups fails in a large scale due to clogging of the nozzle while spinning highly concentrated or particle consisting solutions [55]. The other problem is very small efficiency and productivity of the process performed using this type of apparatus with only 0.005–0.01 g of fiber per hour per needle [56]. Most of the commercially available high-productivity equipment encompass use of free surface electrospinning or multinozzle nonneedle spinnerets [54]; this allows to obtain larger density of the jets that can be formed, thus increasing the efficiency of the process. Furthermore, industrial systems contrary to laboratory setups use mainly rotating drum for fiber collecting, which allows to obtain large area of produced nanofibrous structures. Another important aspect is the use of volatile solvents for electrospinning, which residues might be present in resultant fibers, and in mass scale, the problem of the toxicity of the wastes occurs. Taking into account all mentioned aspects, planning commercialization and industrial scale of fabrication of product for biomedical application needs a detailed strategy on the possible devices that can be used for their production.

2.4 Conclusions

Electrospinning technique allows for obtaining of advanced structures for biomedical applications like tissue-engineered scaffolds, wound dressing, or delivery carriers. Successful strategies for development of electrospun constructs for biomedical applications

should be based on the knowledge of characteristics of tissue to be regenerated, properties of applied polymers and solvents, and optimal design of the nanofibrous structures sufficient for its application. Planning of the technology of fabrication and utilized setups should not only focus on *in vitro* laboratory or *in vivo* preclinical research but also anticipate an adaptation of the manufacturing process into the industrial scale.

References

- [1] Chan BP, Leong KW. Scaffolding in tissue engineering: general approaches and tissue-specific considerations. *Eur Spine J* 2008;17(suppl 4):467–79.
- [2] Rustad KC, et al. Strategies for organ level tissue engineering. *Organogenesis* 2010;6(3):151–7.
- [3] Idaszek J, et al. How important are scaffolds and their surface properties in regenerative medicine. *Appl Surf Sci* 2016;388(part B):762–74.
- [4] Zhong SP, Zhang YZ, Lim CT. Tissue scaffolds for skin wound healing and dermal reconstruction. *Wiley Interdiscip Rev Nanomed Nanobiotechnol* 2010;2(5):510–25.
- [5] Biondi M, et al. Controlled drug delivery in tissue engineering. *Adv Drug Deliv Rev* 2008;60(2):229–42.
- [6] Hutmacher DW. Scaffold design and fabrication technologies for engineering tissues—state of the art and future perspectives. *J Biomater Sci Polym Ed* 2001;12(1):107–24.
- [7] Liao SS, Cui FZ. *In vitro* and *in vivo* degradation of mineralized collagen-based composite scaffold: nanohydroxyapatite/collagen/poly(L-lactide). *Tissue Eng* 2004;10(1–2):73–80.
- [8] Bártolo P, et al. 3rd International conference on tissue engineering, ICTE2013 permeability evaluation of lay-down patterns and pore size of Pcl scaffolds. *Procedia Eng* 2013;59:255–62.
- [9] O'Brien FJ. Biomaterials & scaffolds for tissue engineering. *Mater Today* 2011;14(3):88–95.
- [10] Dhandayuthapani B, Yoshida Y, Maekawa T, Sakthi Kumar D. Polymeric scaffolds in tissue engineering application: a review. *Int J Polym Sci* 2011;2011. Article 290602, 19p.
- [11] Khorshidi S, et al. A review of key challenges of electrospun scaffolds for tissue-engineering applications. *J Tissue Eng Regen Med* 2016;10(9):715–38.
- [12] Ma Z, et al. Potential of nanofiber matrix as tissue-engineering scaffolds. *Tissue Eng* 2005;11(1–2):101–9.
- [13] Li W, et al. Electrospun nanofibers immobilized with collagen for neural stem cells culture. *J Mater Sci Mater Med* 2008;19(2):847–54.
- [14] John MJ, Thomas S. Biofibres and biocomposites. *Carbohydr Polym* 2008;71(3):343–64.
- [15] Stevens MM, George JH. Exploring and engineering the cell surface interface. *Science* 2005;310(5751):1135–8.
- [16] Woo KM, Chen VJ, Ma PX. Nano-fibrous scaffolding architecture selectively enhances protein adsorption contributing to cell attachment. *J Biomed Mater Res A* 2003;67(2):531–7.
- [17] Forns P, et al. Induction of protein-like molecular architecture by monoalkyl hydrocarbon chains. *Biopolymers* 2000;54(7):531–46.
- [18] Ramakrishna S. An introduction to electrospinning and nanofibers. Singapore: World Scientific Publishing; 2005.
- [19] Pham QP, Sharma U, Mikos AG. Electrospinning of polymeric nanofibers for tissue engineering applications: a review. *Tissue Eng* 2006;12(5):1197–211.

- [20] Taylor G. Electrically driven jets. *Proc R Soc Lond A: Math Phys Eng Sci* 1969;313(1515):453–75.
- [21] Peng S, et al. Multi-functional electrospun nanofibres for advances in tissue regeneration, energy conversion & storage, and water treatment. *Chem Soc Rev* 2016;45(5):1225–41.
- [22] Zhang Y, et al. Recent development of polymer nanofibers for biomedical and biotechnological applications. *J Mater Sci Mater Med* 2005;16(10):933–46.
- [23] Ashammakhi N, et al. Biodegradable nanomats produced by electrospinning: expanding multifunctionality and potential for tissue engineering. *J Nanosci Nanotechnol* 2006;6(9-10):2693–711.
- [24] Gunn J, Zhang M. Polyblend nanofibers for biomedical applications: perspectives and challenges. *Trends Biotechnol* 2010;28(4):189–97.
- [25] Kijeńska E, et al. Electrospun bio-composite P (LLA-CL)/collagen I/collagen III scaffolds for nerve tissue engineering. *J Biomed Mater Res B Appl Biomater* 2012;100(4):1093–102.
- [26] Kijeńska E, et al. Nano-engineered biocomposite tricomponent polymer based matrices for bone tissue engineering. *Int J Polym Mater Polym Biomater* 2016;65(16):807–15.
- [27] Pillay V, et al. A Review of the Effect of Processing Variables on the Fabrication of Electrospun Nanofibers for Drug Delivery Applications. *J Nanomater* 2013;2013:22.
- [28] Subbiah T, et al. Electrospinning of nanofibers. *J Appl Polym Sci* 2005;96(2):557–69.
- [29] Megelski S, et al. Micro- and nanostructured surface morphology on electrospun polymer fibers. *Macromolecules* 2002;35(22):8456–66.
- [30] Bognitzki M, et al. Nanostructured fibers via electrospinning. *Adv Mater* 2001;13(1):70–2.
- [31] Jarusuwanpoom T, et al. Effect of solvents on electro-spinnability of polystyrene solutions and morphological appearance of resulting electrospun polystyrene fibers. *Eur Polym J* 2005;41(3):409–21.
- [32] Zong X, et al. Structure and process relationship of electrospun bioabsorbable nanofiber membranes. *Polymer* 2002;43(16):4403–12.
- [33] <http://stenutz.eu/chem/solv6.php?name=1%2C1%2C1%2C3%2C3%2C3-hexafluoropropan-2-ol>, 26.10.2016.
- [34] Gualandi C. Porous polymeric bioresorbable scaffolds for tissue engineering. Berlin, Heidelberg: Springer; 2013.
- [35] Ladd MR, et al. Electrospun nanofibers in tissue engineering. In: Li DT, editor. *Nanofibers-production, properties and functional applications*. InTech; 2011.
- [36] Agarwal S, Wendorff JH, Greiner A. Use of electrospinning technique for biomedical applications. *Polymer* 2008;49(26):5603–21.
- [37] Chen D, Li M, Fang Q. Application of electrostatic spinning technology in nano-structured polymer scaffold. *Zhongguo Xiu Fu Chong Jian Wai Ke Za Zhi* 2007;21(4):411–5.
- [38] Murugan R, Ramakrishna S. Design strategies of tissue engineering scaffolds with controlled fiber orientation. *Tissue Eng* 2007;13(8):1845–66.
- [39] Kai D, Liow SS, Loh XJ. Biodegradable polymers for electrospinning: towards biomedical applications. *Mater Sci Eng C* 2014;45:659–70.
- [40] Xu CY, et al. Aligned biodegradable nanofibrous structure: a potential scaffold for blood vessel engineering. *Biomaterials* 2004;25(5):877–86.
- [41] Mo X, et al. Electrospun nanofibers for tissue engineering. *J Fiber Bioeng Informat* 2013;6(3):225–35.
- [42] Kijeńska E, et al. Interaction of Schwann cells with laminin encapsulated PLCL core-shell nanofibers for nerve tissue engineering. *Eur Polym J* 2014;50:30–8.
- [43] Liang D, Hsiao BS, Chu B. Functional electrospun nanofibrous scaffolds for biomedical applications. *Adv Drug Deliv Rev* 2007;59(14):1392–412.

- [44] Teo W-E. 3D nanofibrous structures. <http://electrospintech.com/3D-nano-structure.html#.WBnty8k23iA>].
- [45] He X, et al. Electrospun gelatin/polycaprolactone nanofibrous membranes combined with a coculture of bone marrow stromal cells and chondrocytes for cartilage engineering. *Int J Nanomed* 2015;10:2089–99.
- [46] Joshi V, et al. Macro-porosity enhances vascularization of electrospun scaffolds. *J Surg Res* 2013;183(1):18–26.
- [47] Koh HS, et al. In vivo study of novel nanofibrous intra-luminal guidance channels to promote nerve regeneration. *J Neural Eng* 2010;7(4):046003.
- [48] He W, et al. Tubular nanofiber scaffolds for tissue engineered small-diameter vascular grafts. *J Biomed Mater Res A* 2009;90A(1):205–16.
- [49] Kostakova E, et al. Study of polycaprolactone wet electrospinning process. *Exp Polym Lett* 2014;8:554–64.
- [50] Coburn JM, et al. Bioinspired nanofibers support chondrogenesis for articular cartilage repair. *Proc Natl Acad Sci* 2012;109(25):10012–7.
- [51] Shim IK, et al. Chitosan nano-/microfibrous double-layered membrane with rolled-up three-dimensional structures for chondrocyte cultivation. *J Biomed Mater Res A* 2009;90(2):595–602.
- [52] Kijenska E, et al. The interaction between nanofibers mesh covered scaffolds and chondrocytes. In *Tissue Engineering Part A*, 2008. Mary Ann Liebert Inc, 140 Huguenot Street, 3rd fl, New Rochelle, NY 10801, USA.
- [53] Kai D, et al. Mechanical properties and in vitro behavior of nanofiber-hydrogel composites for tissue engineering applications. *Nanotechnology* 2012;23(9):095705.
- [54] Persano L, et al. Industrial upscaling of electrospinning and applications of polymer nanofibers: a review. *Macromol Mater Eng* 2013;298(5):504–20.
- [55] Li L, Frey MW, Green TB. Modification of air filter media with nylon-6 nanofibers. *J Eng Fibers Fabr* 2006.
- [56] Ramakrishnan R, et al. Needleless electrospinning technology—an entrepreneurial perspective. *Indian J Sci Technol* 2016;9(15):1–11.

Biomedical applications of electrospinning, innovations, and products

3

*J.M. Lagaron**, *A. Solouk[†]*, *S. Castro**, *Y. Echevoyen**

*Novel Materials and Nanotechnology Group, IATA-CSIC, Valencia, Spain, [†]Amirkabir University of Technology (Tehran Polytechnic), Tehran, Iran

3.1 Innovative technologies with potential for scaling

Electrospinning is an electrohydrodynamic-based technique capable of generating controlled fibers with diameters well below the micron. However, the low typical throughput of a single Taylor cone demands the use multicone sources for industrial applications. Two alternatives with their advantages and drawbacks have been developed: multinozzle injectors and later needleless spinnerets.

3.2 Brief history of electrospinning

The first record of an electrohydrodynamic process dates from the 17th century. During the early 20th century, Zeleny focused on the study of fluid droplets in an electric field placed at the end of metallic capillaries. In the 1930s and 1940s, Anton Formhals described the phenomenon of electrospinning in a series of patents [1], and Rozenblum and Petryanov-Sokolov fabricated a filtering material out of electrospun fibers. In the 1960s, Taylor described mathematically the shape of the so-called Taylor cone. Initial characterization of the mechanism and development of the technique required a highly controlled quasi-static geometry; therefore, using a nozzle to generate and hold the Taylor cone was necessary at the time. It took 20 more years for a needleless electrospinning system using a ring spinneret to be patented for the electrostatic production of fleece fibers [2]. The attention of the scientific community focused on the electrospinning process in the early 1990s, after Reneker and coworkers demonstrated that electrospinning was a suitable technique to generate nanofibers [3], probably prompted by the development of its cousin technique, electrospray, to generate gas-phase nonvolatile proteins [4], which was a revolution in the mass spectrometry community at the time and granted John B. Fenn a Nobel prize for his discovery. Fifteen years later, needleless electrospinning began to exhibit its potential in the mass production of nanofibers and began its own flourishing period in the electrospinning community. In 2004, a magnetic-field-assisted needleless electrospinning was reported. A magnetic field was used to induce the formation of protuberances on the flat solution surface, which concentrated the electric field triggering the electrospinning process [5]. Although

rings were first invented as a needleless electrospinning spinneret [2], needleless electrospinning began to attract attentions since Jirsak et al.'s invention in 2005 of a metal roller as a spinneret [6]. The main advantage of this technology is that the jets are initiated naturally in the optimal positions. This rotating roller was used as a fiber generator for the mass production of electrospinning nanofibers [6]. This technique was commercialized by Elmarco Co. with the brand name "Nanospider." Several approaches were used to trigger Taylor cones and initiate electrospinning from a free surface, including air bubbles [7], a conical wire coil [8], a metal plate [9], a splashing spinneret [10], a rotary cone [11], a cylinder [12], a bowel edge [13], and moving bead chain [14]. The influence of the spinneret geometry on the electrospinning process and fiber quality was determined by Niu et al. [15].

The main drawback of single nozzle compared to needleless injectors is its low throughput. However, it offers a better control on the fiber diameter and distribution, offering homogeneous film porosity, critical feature, for example, for the growth of cells for biomedical applications. In needleless electrospinning, a multitude of jets are formed simultaneously from the needleless fiber generator without the influence of capillary effect that is normally associated with nozzle-based injectors. Because the cone-jet generation in needleless electrospinning is a self-triggered process occurring on a free liquid surface, the spinning process is hard to control. Multinozzle injectors with different geometries, mainly planar and linear, have been developed to increase the nozzle-based injector throughput. Furthermore, multijets can be issued as well from a single nozzle. However, this approach, like needleless spinnerets, lacks fibers control.

3.3 Nozzle-based multijet electrospinning

Multijet technology is a necessary approach to increase the throughput of the electrospinning process [16–18]. Although multijet electrospinning is a more complex process than the single jet, it has been demonstrated to be a better approach to enhance electrospinning productivity rather than substantially increasing the throughput of a single spinneret. Modified single-nozzle, multinozzle, and needleless systems, explained below in detail, have been developed to obtain multiple jets and thus to increase the system throughput.

Multijet electrospinning was first accomplished using a single nozzle with a grooved tip, from the branches of which multijets were formed [19]. This multicone technique proved to improve the productivity of the single-nozzle electrospinning process. However, the process is rather chaotic due to the poor control of the polymeric solution flow rate through each of the cones generated.

Further, the mechanism behind fiber formation has not been examined. Later, the use of curved collectors on single-nozzle configuration to generate multiple Taylor cones was proposed as an alternative to enhance the throughput [20]. Two possible mechanisms for this phenomenon were provided including electric field distribution and clogging of the passageway of the polymer solution. However, there are still a number of unsolved issues related to electrospun webs, including fiber morphology and diameter. No public reports have been to date published on mass production of nanofibers by this approach.

An alternative procedure considered to increase the throughput of the single nozzle was to split the polymer jet into two separate subfilaments during its flight to the fiber collector by applying a sufficiently large tangential stress [21].

The most direct method to increase the electrospinning injector throughput relies on the use of a bundle of nozzles. Nozzle configuration, nozzle number, and nozzle spacing are the three key parameters to design a multinozzle injector. The multinozzle injector can be organized into linear arrays [22–25] and two-dimensional arrays [22–25], that is, square [22,24], circular and elliptic [25], hexagonal [26], and triangular [27].

A linear array of nozzles is the simplest multinozzle configuration. Several examples have been reported in the last few years. For example, linear multinozzle electrospinning setups composed of four nozzles were designed to produce nanofibers [23]. It was shown that the nanofibers were unevenly deposited onto fibrous substrates probably because of the distorted electric field effect due to the finite boundary conditions. Further, spinnerets with arrays of seven and nine nozzles were employed to examine the behavior of jets in multinozzle electrospinning [17]. Experimental results and simulations showed a contrasting behavior between outer and inner jets, such as bending direction and envelope cone. However, each jet was subjected to the typical bending instabilities observed in single-jet electrospinning. Electric field shielding at the inner nozzles was observed in a 26-nozzle injector with a linear arrangement. It was observed that only the outer nozzles were active, whereas the inner ones did not generate the Taylor cone [25]. An additional electrode is necessary in order to compensate for the boundary effect and homogenize the overall electric field [28]. Most investigations on multinozzle electrospinning have been focused on two-dimensional arrays. For example, multinozzle injectors with elliptic and circular configurations were designed to improve the process stability and throughput [25]. It was shown the circular configuration was a more stable process and obtained a higher throughput for polyvinyl alcohol (1 vs. 0.4 mg/min per nozzle). Yang et al. developed a seven-nozzle (10 mm spacing) injector arranged as a regular hexagon with one nozzle located in the center [26]. They observed that the six outer jets bent outward due to the repulsion from center one. The lack of symmetry in the electric field in the 2-D arrays triggered a similar bending behavior as in linear arrays. Theron et al. reported a slightly more complex nine-nozzle design placed in a 3×3 matrix [22]. The throughput observed for this nine-nozzle injector ranged from 22.5 mL/(cm² min) to 22.5 L/(cm² min). Kim and Park [29] patented a more advanced multinozzle device designated conjugated electrospinning. This design was able to mass-produce composite nanofiber webs from several kinds of polymer solutions. More recently, an industrial multinozzle injector composed of 1000 nozzles was reported [30]. Finally, Lagaron et al. [31] developed a coaxial high-throughput multinozzle injector technology that allows low viscous solutions to be more efficiently processed. This technology is especially suitable for encapsulation of active and bioactive ingredients.

The company Bioinicia SL, Spain (www.bioinicia.com), through their engineering division Fluidnatek, has launched since 2012 a range of high-throughput multinozzle equipment for pilot plant and manufacturing purposes, called LE-500 and LE-1000, respectively. These tools that come with climate control, for example, temperature and

%RH control, are designed to, for instance, meet the existing stringent legislation criteria in the biospace and to provide complete flexibility for the manufacturing of electrospun/electrosprayed products. The equipment was designed to be integrated in industrial production lines that involve roll-to-roll collection or any other type of collection, pre- or postprocessing steps. The company has also built two demonstration/contract manufacturing electrohydrodynamic processing plants in Valencia, Spain, that are currently capable of manufacturing a minimum of 2 ton/year of nanofiber-based products with pharma/biomedicine legislation compliancy and a minimum of 1 kg/h of powder-based products for cosmetic, agrochemical, and food applications.

3.4 Electroblowing

A sheath gas, to provide an additional drawing force, has been widely used in electrospinning to stabilize the process. Electroblowing, also known as electroblown spinning, is the conjugation of a pneumatic and an electrohydrodynamic force to generate fibers. This technique has demonstrated a significant improvement in the production rate of polymeric nanofibers. The technique obtained higher production rates than conventional single-nozzle electrospinning due to the additional pneumatic driving force that enabled an extra increase in the polymeric solution flow rate without significant loss of fiber quality. Kim and Park [29] successfully designed a high-throughput electrospinning spinneret with an air nozzle to produce nanofiber webs from thermoplastic or thermosetting polymers. However, several problems such as the high applied voltage required complex electric insulation and coupling of working distance to applied voltage needed to be addressed. However, a patent by Bryner et al. [32] upgraded the electroblowing process by directly applying the voltage to a pair of electrodes located parallel to the surface of a grounded spinneret, which overcame some of those obstacles caused by the conventional application of the voltage. An enhanced throughput five times higher than that obtained with electrospinning was demonstrated.

3.5 Fiber generators in needleless electrospinning

The central image in Fig. 3.1 shows a single-nozzle electrospinning setup, which is composed of a syringe that usually contains a polymeric solution to be electrospun, a nozzle and a counterelectrode collector, and a high-voltage power supply connected between the nozzle or solution and the collector to apply the appropriate electric field to generate the Taylor cone [33]. The solution is issued from the tip of “Taylor cone” in the form of a charged jet. Initially, this thin jet stretches further due to the interaction between the electric field applied and its charge and to the internal repulsion between charges. Solvent evaporation leads to the solidification of the filament into fibers, which are finally deposited on the collector usually forming a randomly oriented fiber web. Similar setups to the one described above have been widely used in hundreds of laboratories around the world for multitude of research projects.

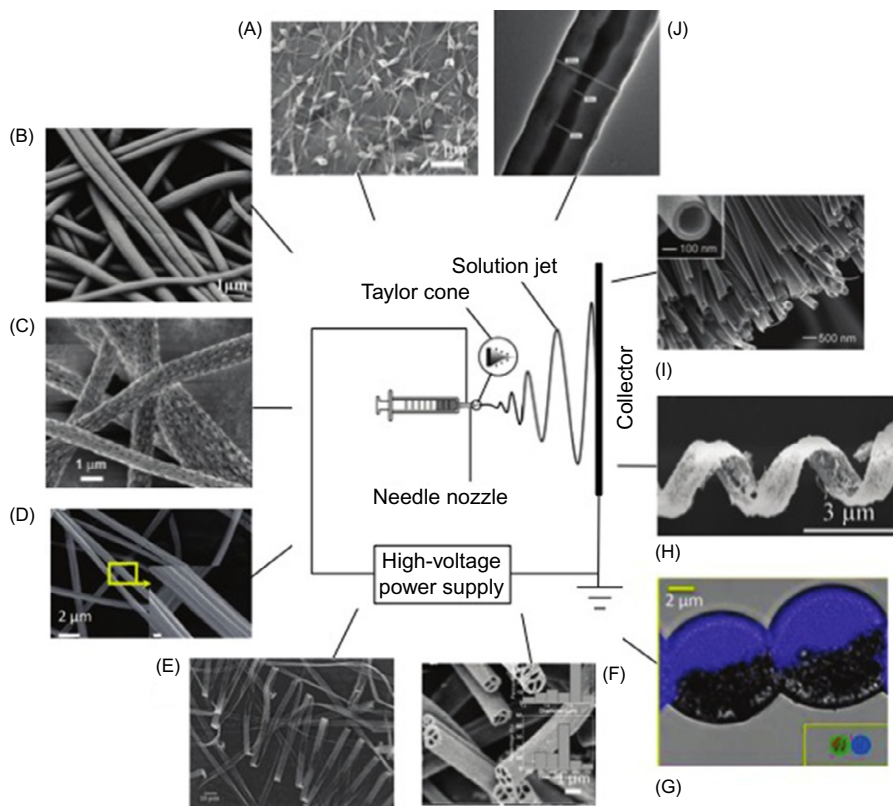


Fig. 3.1 (Central) a typical apparatus for nozzle electrospinning and (outer) images of electrospun nanofibers with various morphologies, (A) beaded fiber, (B) round fiber, (C) fiber with a porous surface, (D) grooved fiber, (E) ribbon, (F) multichannel fiber, (G) side-by-side fiber, (H) crimped fiber, (I) hollow fiber, and (J) core-sheath fiber. (A–F) are prepared by conventional nozzle electrospinning, and (G–J) are electrospun mainly by a special nozzle spinneret. From Niu HT, Lin T. Fiber generators in needleless electrospinning. *J Nanomater* 2012;2012:725950.

Electrospinning is mainly suitable for processing thermoplastic polymers and electrospun fibers that are typically in the range of several nanometers to a few microns in diameter. Electrospinning enables control of the fiber diameter through the solution properties and experimental variables such as solution flow rate and flight distance (nozzle to collector distance).

Most electrospun nanofibers show a round cross section with a smooth surface. However, nanofibers with different morphologies can also be produced choosing an appropriate polymer, polymer solution properties, nozzle configuration, or operating conditions. Beaded fibers can be observed in almost all spinnable polymers [34]. Additional geometries such as fibers with a porous surface [35], ribbons [36], helices [37], or grooved fibers [38,39] have been observed. Further, more complex

bicomponent fibers with different cross-sectional configuration, such as hollow fibers [40], core/shell configuration [41], side-by-side fibers [42], or crimped structures [42], can be as well generated using specific nozzles having two or more channels to feed different polymer solutions (Fig. 3.1).

Electrospinning enables nanofibers with exceptional features, such as the abovementioned controlled fiber diameter, morphology, and structure as well as their high surface area and the ability to generate highly porous membranes with excellent pore interconnectivity. Further, the intrinsic high tunability of polymers enables extensive fiber functionalization. Such unique features open electrospun nanofibers to multiple applications in various fields. Some important applications of electrospun nanofibers include tissue-engineering scaffolds [44], filtration [45], catalyst and enzyme carriers [46,47], release control [48], sensors [49], energy storage [50], affinity membranes [51], and recovery of metal ions [52–54].

Needleless electrospinning relies on the use of an external perturbation to locally concentrate the electric field on a free liquid surface up to the intensity needed to initiate a Taylor cone. In the case of stationary spinnerets, conical spikes are often generated using an external force, such as magnetic force, high-pressure gas flow, or gravity. Fig. 3.2 lists the stationary spinnerets reported. In the case of rotating

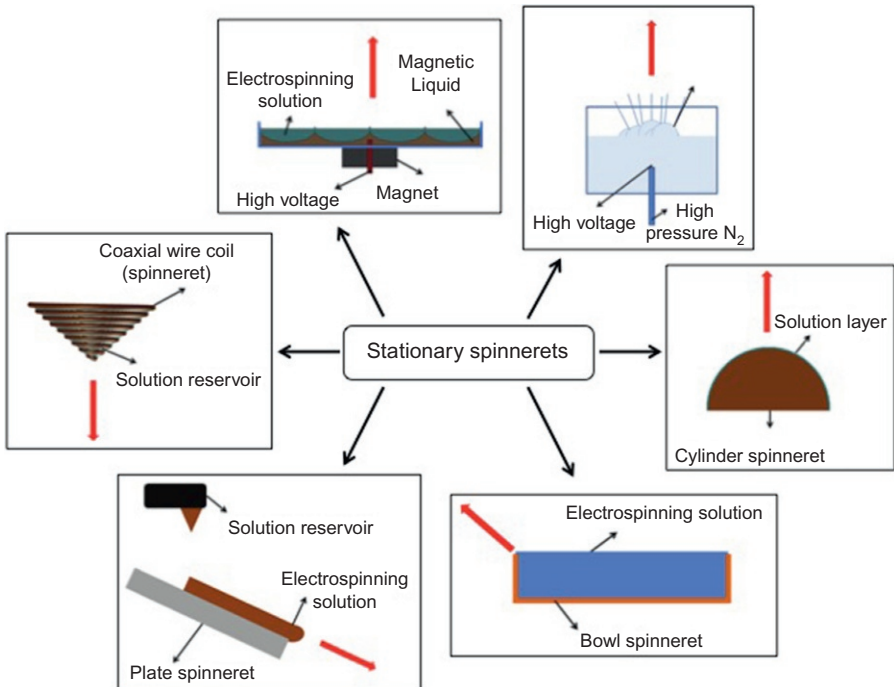


Fig. 3.2 Schematic summary of stationary needleless spinnerets (electrospinning direction along the red arrow).

From Niu HT, Lin T. Fiber generators in needleless electrospinning. *J Nanomater* 2012;2012:725950.

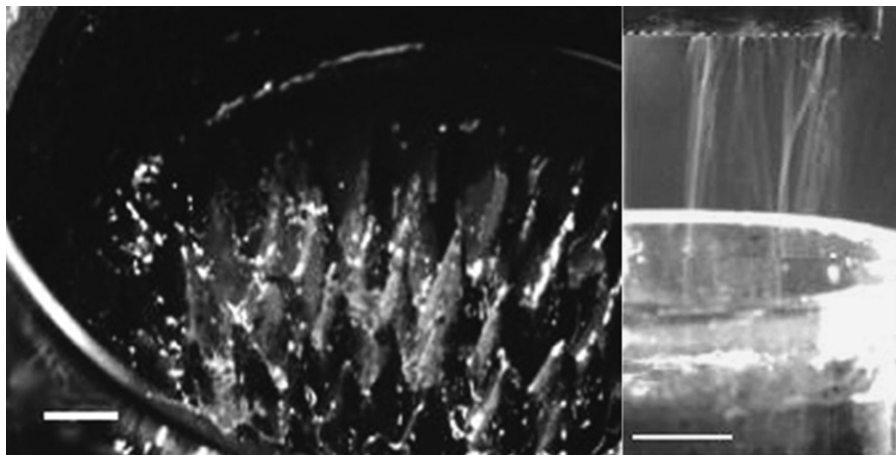


Fig. 3.3 (A) Magnetic-field-assisted needleless electrospinning setup and (B) multiple jets ejected toward the counterelectrode.

From Yarin AL, Zussman E. Upward needleless electrospinning of multiple nanofibers. *Polymer* 2004;45(9):2977–80.

spinnerets, rotation is usually used to feed the Taylor cones with the polymeric solution. The Taylor cones are generated at a certain position, usually away from the solution container, where the electric field is intense enough.

Yarin and Zussman reported a needleless electrospinning system that used a magnetic field to initiate the Taylor cone formation [5]. The system was composed of a bottom layer of ferromagnetic fluid and an upper layer of polymer solution (Fig. 3.3A).

Vertical ferromagnetic fluid spikes were generated applying a magnetic field; such spikes perturbed the top polymeric solution layer, which under the influence of an additional electric field generated a Taylor cone (and consequently nanofibers) positioned on top of each of the ferromagnetic spike (Fig. 3.3B).

In order to prevent spinning solution from dropping onto the fiber mat, an upward electrospinning configuration is used. The rotation of the spinneret transfers the polymer solutions to the electrospinning sites of appropriate electric field, ensuring the production continuously. In the case of roller and cone electrospinning, the polymeric solution is fed from separated containers. The nanofiber formation in needleless electrospinning has been proposed to follow four steps: (1) A film of polymer solution is continuously transferred onto the partially immersed spinneret surface as a result of the rotation; (2) the highly viscous film generated during the rotation of the spinneret shows some rugosity by the time it reaches the area of optimal electric field; (3) such rugosities concentrate the electric forces intensifying it to the range at which Taylor cones are formed; and (4) nanofibers form upon the solidification of the jets issued from each Taylor cone formed.

Fig. 3.4 shows a list of the reported rotating spinnerets. Different configurations, cylinder, ball, disk, coil, and beaded chain, are used to control the flow rate of polymer solution fed to the Taylor cones. These spinnerets are connected to a high voltage

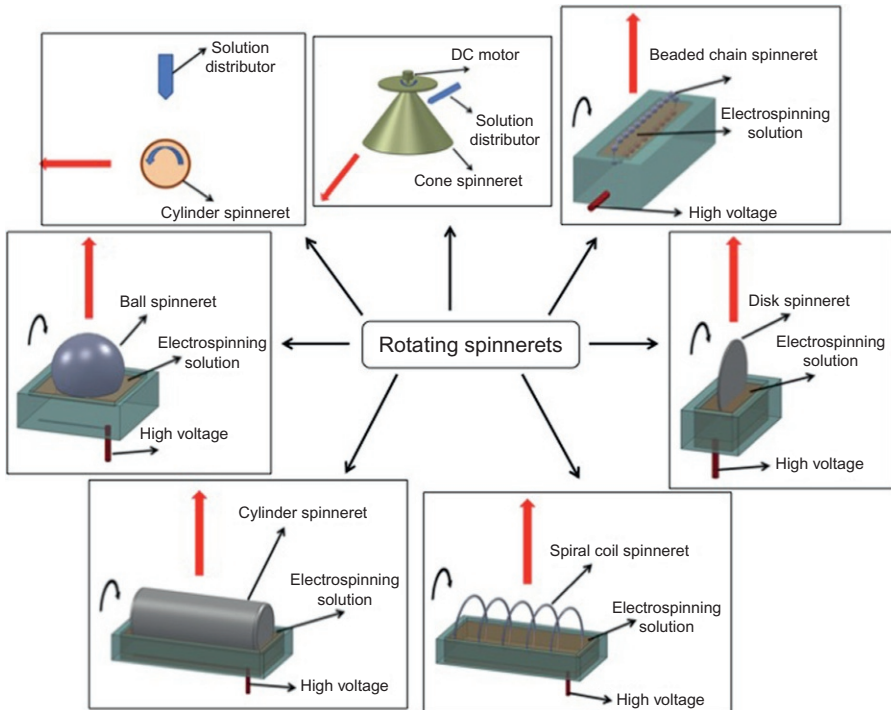


Fig. 3.4 Schematic summary of needleless rotating spinnerets (electrospinning direction along the red arrow).

From Niu HT, Lin T. Fiber generators in needleless electrospinning. *J Nanomater* 2012;2012:725950.

submerged in the spinning solution while rotating. The Taylor cones are generated at the point or area of maximum electric field. Niu et al. compared some of these configurations and observed significant variations on fiber diameters under the same working conditions (cylinder, 357 ± 127 nm; disk, 257 ± 77 nm; and ball spinnerets, 344 ± 105 nm) and throughput (cylinder, 8.6 g/h; disk, 6.2 g/h; and ball, 3.1 g/h).

Fig. 3.5 shows a coil spinneret and a nanofiber mat generated with this configuration. Multiple polymeric jets are generated from the wire coil. The nanofibers produced from the coil spinneret are thinner and show a narrower fiber diameter distribution than that observed in typical nozzle electrospinning processes.

3.6 Bubble-electrospinning

Bubble electrospinning was developed in 2007 [55]. In contrast to the classical electrospinning process, where the electrospinning ability relies strongly on the solution properties, bubble electrospinning depends mainly on the size of produced bubbles.

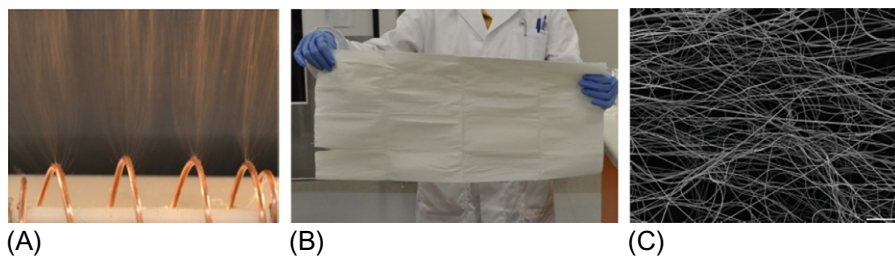


Fig. 3.5 (A) Photograph of the spiral coil spinneret and electrospinning process, (B) photograph of polyacrylonitrile (PAN) nanofiber mat produced by coil electrospinning, and (C) SEM image of coil electrospun PAN nanofibers (scale bar 10 μm).

From Niu HT, Lin T. Fiber generators in needleless electrospinning. *J Nanomater* 2012;2012:725950.

When no voltage is applied, the surface tension depends on the size of the bubble. When an electric field is present, it induces charges onto the surface of the bubbles. The surface charge coupling and the external electric field create a tangential stress, leading to the deformation of the bubble into a protuberance-induced upward-directed reentrant jet, as shown in Fig. 3.6. Once the electric field exceeds the critical value needed to overcome the surface tension, a fluid jet is ejected from the apex of the conical bubble. When the bubble breaks, the surface charges will be redistributed, and the bubble surface is pulled upwards again by the electric force; thus, multiple jets are

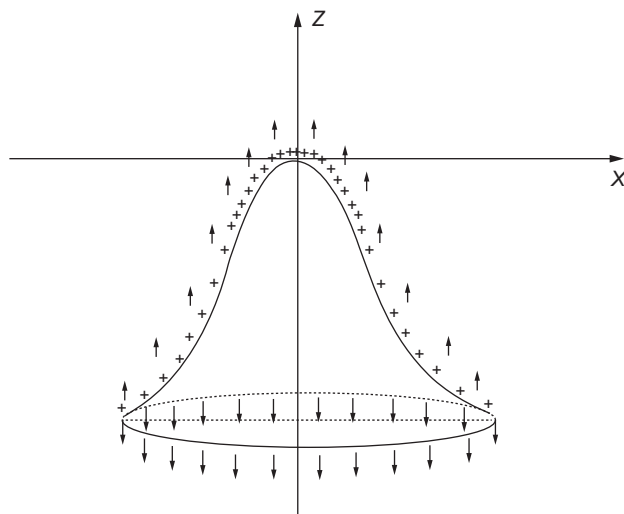


Fig. 3.6 Deformation of polymer bubble under electric force.

formed in a very short period. In the case of bubbles with dimensions tending to the nanoscale, the surface tension becomes extremely small and the generation of nanofibers is promoted. This technology was demonstrated to produce nanofibers as small as 50 nm [55].

3.7 Electrospinning-based scaled up developments and commercial products

The use of biocompatible polymers in the biomedical industry has promoted the fabrication of artificial tissue and the development of drug delivery and targeting vehicles. Polymers are an extensive family of materials that can be engineered or selected, for example, to be bioabsorbable or to offer a low immune system rejection risk, or posttreated to carry out specific functions. Electrospinning is the most promising emerging processing technologies for the production of multiple nanofiber-based polymeric biomedical products. Electrospinning nanofibers offer controlled composition and morphology—especially when made from nozzles—and are currently being used in both upstream and downstream production. These nanofibers can be used to fabricate artificial tissue structures that mimic natural scaffolds and controlled drug-release patches or to cover implants reducing their immune system rejection, among other uses.

Many companies have emerged in the last few years offering electrospinning-based products that could be used for biomedical applications (Table 3.1). Many of them make use of nozzle-based technologies to achieve maximum fiber control and emphasize the excellent properties of electrospinning fibers to be exploited as drug delivery products or artificial scaffolds. This far upstream product portfolio, although necessary, is in many cases in a proof of concept stage or in certification trials and hence one step behind producing actual biomedical commercial products. Below are some examples of products that are downstream at or near a commercialization stage.

Nicast's AVflo is an artificial vascular access graft used for hemodialysis patients. AVflo is made with medical grade biocompatible polycarbonateurethane and silicone copolymers electrospun nanofibers. It is formed by four distinctive layers: The inner layer is in contact with the blood and is designed to minimize platelets adhesion. The high tunability of biopolymer nanofibers enables the design of fibers with reduced affinity to specific cells; the middle layer has elastic features that mimic a blood vessel and provides self-healing properties to the vessel reducing bleeding time after nozzle removal. The fibers open up during nozzle penetration and close back quickly upon nozzle extraction, the reduced porosity of the barrier layer prevents the diffusion of serum and molecules and provides strength and flexibility, and the outer layer favors the growth of surrounding tissue and adds on to the self-healing feature [56]. Polymer nanofibers are tuned in this occasion to favor cell attachment and growth. Patients with chronic renal failure, more than 450,000 are under treatment in the United States alone, need 2–3 dialysis sessions per week [57]. One of the most recommended surgeries to enable hemodialysis is the creation of a communication between a native

Table 3.1 List of electrospinning-based companies and biomedical products developed

Company name	Country	Product	Website
Arsenal Medical	The United States	Core-shell fibers	www.arsenalmedical.com
Bioincia	Spain	RIVELIN Drug delivery nanofiber-based patch	www.bioincia.com
Biomimetic Electrospinning Technologies Inc.	The United States	Customized scaffold for biomedical application	www.biomimeticspintech.com
BioSurfaces Inc.	The United States	Drug-loaded electrospun fibers for medical applications	www.biosurfaces.us
Biotronik	Germany	Covered stent	www.biotronik.com
Medprin	Germany	ReDura dural patch	www.medprin.com
Nanofiber Solutions Inc.	The United States	Nanofiber-based scaffolds for medical applications	www.nanofibersolutions.com
NanoSpun Technologies	Israel	Porous nanofibers for medical application	www.nanospuntech.com
Neotherix	The United Kingdom	Manufactures nanofiber scaffold for tissue regeneration	www.neotherix.com
Nicast	Israel	Nanofiber implants	www.nicast.com
Ortho Rebirth	Japan	ReBOSSIS, synthetic bone	www.orthorebirth.com
PolyRemedy	The United States	HealSmart Personalized Antimicrobial Dressings	www.polyremedy.com
SKE Advanced Therapies	Italy	Silk Fibroin tubular scaffold, flat sheet scaffold, disk	www.ske.it
SNS Nanofiber Technology LLC	The United States	Nanofiber-based materials for medical applications	www.snsnano.com
Stellenbosch Nanofiber Company	South Africa	Nanofiber-based materials for medical applications	www.sncfibers.com
The Electrospinning Company	The United Kingdom	Manufactures nanofiber scaffold for tissue regeneration	www.electrospinning.co.uk
Zeus	The United States	Bioweb biomedical encapsulation material	www.zeusinc.com

artery and a vein of an extremity, for example, a native arteriovenous (AV) fistula. AVflo serves as such artery-vein communication. AVflo can be easily sutured to the blood vessels and offers an unobstructed blood flow and, thanks to the self-healing nature of nanofibers, a rapid sealing after suture and puncture (less than 5 min) compared to native AV fistulas, which usually takes longer [58].

Another interesting intercompany joint development is the RIVELIN Patch, which is being currently commercialized by Dermtreat ApS, Denmark, which was codeveloped by Bioinicia SL, Spain, and that is currently being manufactured in the unique scaled-up facilities of Bioinicia SL in Valencia, Spain. Despite millions worldwide suffering from severe and painful oral lesions requiring treatment, there is currently no licensed product available. RIVELIN offers a product for treatment of these lesions based on a mucosal adhesive patch technology with targeted drug delivery, aimed to service this large unmet market. The product is based on “repositioning”—that is, using excipients and active drugs already approved by the authorities. This brings significantly reduced risks, costs, and time to market compared to conventional pharma developments but with similar opportunities for market positioning. The product targets severe inflammatory diseases in the mouth—to be treated with a steroid, known from literature and studies to have significant clinical efficacy. This represents an estimated market in excess of USD 1 bill.

RIVELIN is an electrospun, two-layer patch including a mucoadhesive layer, which includes the drug and a protective layer ensuring occlusion and unidirectional drug delivery into the mucosal lesion. The mucoadhesive ability of the patch provides a unique feature of a direct, controlled, and longer-term drug delivery. Direct topical delivery of drugs ensures higher efficacy, lower dose, and less bystander toxicity.

US Patent 8,431,151 B2 proposes a method to manufacture a hydrogel antimicrobial nonwoven fibrous dressing with controlled release of silver ions. The inventors describe a PEG-based multiblock thermoplastic polyurethane incorporating polyhedral oligomeric silsesquioxane, forming organic-inorganic hybrid hydrogels with unique mechanical properties and adjustable swelling ratios. In this case, a nanofiber network, produced with the electrospinning technique, was used to deliver silver ions. AgNO₃ was directly incorporated into polymer/dimethylformamide solutions to prepare the antimicrobial scaffolds [59].

Nanofiber Solutions Inc. 3-D scaffolds are electrospun developments for soft tissue and organ replacement, eliminating the need for organ donation, immune suppression, and the risk of transplant rejection. The company has developed complex shapes/geometries to model different organs throughout the body and recently designed the first synthetic tracheas implanted into human patients. The physical properties of the scaffolds depend upon the type of polymer used in the manufacturing process, that is, if they are made from polyurethane (PU), the scaffolds will be very elastomeric like a rubber band, while something made from polyglycolic acid (PGA) will initially be more rigid and stiff. There is also the possibility of obtaining random and aligned orientation of the fibers. In addition to tissue engineering, these products are used in regenerative medicine as a means to increase stem cell expansion rates for cellular therapy companies working to bring the promise of personalized stem cell treatments closer to reality.

The company ORTHOREBIRTH has developed a new product named ReBOSSIS. It is a cottony type, synthetic bone-void-filling material, whose main ingredients include β -tricalcium phosphate (β -TCP) that is excellent in bioabsorbable property, polylactic acid (PLLA), and silicone-containing calcium carbonate that promotes the bone formation. It contains 1% silicon by weight, a level similar to that present in normal growing bone. The diameter of the fibers in the PLLa scaffold ranges from 10 to 50 μm . The interconnected macro- and microporous structure allows for formation of new bone and the growth of capillary blood vessels throughout the network of interconnecting pores. The product form allows for versatility in handling and ease of use. The basic technology, on which ReBOSSIS has been based, was initially developed by Professor Toshihiro Kasuga of Nagoya Institute of Technology (NIT) and his research team. Back in 2011, Dr. Kasuga and his team started to study on artificial bones for dental care and contrived an artificial bone to be used for dental implantation. This artificial bone was mainly made of calcium chloride, PLLa, and silicone just like the current ReBOSSIS. The initial type of this artificial bone was based on non-woven material. Then, they developed it into fabric-based artificial bone by using electrospinning method. In this method, a solution mixed with calcium chloride, PLLa, and silicone turned into a fabric-based material. The research team made repeated trials and errors until they successfully made the fabric-based material into a cottony material of very fine fibers of micrometer in size just like ReBOSSIS. The team needed a great amount of time in determining a proper diameter and thickness of the fiber for effectively activating the growth of osteoblast.

Taking over the successful technology from NIT, ORTHOREBIRTH repeatedly improved the artificial bone into the current ReBOSSIS. In October 2014, the company officially obtained FDA 510(k) clearance and started to sell ReBOSSIS in the United States in April 2015.

3.8 Future prospects and outlook

Electrospinning is no longer a lab technology. Many advances in scaling up and industrialization have been carried out over the last few years by some pioneering companies across the globe. Biomedical products due to relatively low volumes and high margins have been the first to be scaled up. The challenge of setting up manufacturing facilities with certification compliancy has been surpassed already, and industrial activity in the area will continue to grow in the years to come.

References

- [1] Formhals A. Process and apparatus for preparing artificial threads. Google Patents; 1934.
- [2] Simm W, Gosling C, Bonart R, Falkai BV. Fibre fleece of electrostatically spun fibres and methods of making same. Google Patents; 1979.
- [3] Doshi J, Reneker DH. [Electrospinning process and applications of electrospun fibers.](#) *J Electrostat* 1995;35(2–3):151–60.

- [4] Fenn JB, Mann M, Meng CKAI, Wong SF, Whitehouse CM. Electrospray ionization for mass spectrometry of large biomolecules. *Science* 1989;246:64–71.
- [5] Yarin AL, Zussman E. Upward needleless electrospinning of multiple nanofibers. *Polymer* 2004;45(9):2977–80.
- [6] Jirsak O, Sanetnik F, Lukas D, Kotek V, Martinova L, Chaloupek J. A method of nanofibres production from a polymer solution using electrostatic spinning and a device for carrying out the method. WO 2005/024101 A1; 2005.
- [7] Liu Y, He J-H, Xu L, Yu J-Y. The principle of bubble electrospinning and its experimental verification. *J Polym Eng* 2008;28:55–66.
- [8] Lin T, Wang X, Wang X, Niu H. Electrostatic spinning assembly. WO 2010/043002; 2010.
- [9] Thoppey NM, Bochinski JR, Clarke LI, Gorga RE. Unconfined fluid electrospun into high quality nanofibers from a plate edge. *Polymer* 2010;51:4928–36.
- [10] Tang S, Zeng Y, Wang X. Splashing needleless electrospinning of nanofibers. *Polym Eng Sci* 2010;50(11):2252–7.
- [11] Lu B, Wang Y, Liu Y, Duan H, Zhou J, Zhang Z, et al. Superhigh-throughput needleless electrospinning using a rotary cone as spinneret. *Small* 2010;6:1612–6.
- [12] Wu D, Huang X, Lai X, Sun D, Lin L. High throughput tip-less electrospinning via a circular cylindrical electrode. *J Nanosci Nanotechnol* 2010;10:4221–6.
- [13] Thoppey N, Bochinski JR, Clarke LI, Gorga RE. Edge electrospinning for high throughput production of quality nanofibers. *Nanotechnology* 2011;22:345301.
- [14] Green TB, King SL, Li L. Fine fiber electro-spinning equipment, filter media systems and methods. Google Patents; 2011.
- [15] Niu H, Lin T, Wang X. Needleless electrospinning. I. A comparison of cylinder and disk nozzles. *J Appl Polym Sci* 2009;114:3524–30.
- [16] Dzenis Y. Spinning continuous fibers for nanotechnology. *Science* 2004;304:1917.
- [17] Burger C, Hsiao BS, Chu B. Nanofibrous materials and their applications. *Annu Rev Mater Res* 2006;36:333.
- [18] Greiner A, Wendorff JH. Electrospinning: a fascinating method for the preparation of ultrathin fibres. *Angew Chem Int Ed* 2007;46:5670–703.
- [19] Yoshihiro Y, Ko F, Akira T, Hajime M. Characteristics of elastomeric nanofiber membranes produced by electrospinning. *J Text Eng* 2007;53:137.
- [20] Vaseashta A. Controlled formation of multiple Taylor cones in electrospinning process. *Appl Phys Lett* 2007;90:093115/1.
- [21] Paruchuri S, Brenner MP. Splitting of a liquid jet. *Phys Rev Lett* 2007;98:134502.
- [22] Theron SA, Yarin AL, Zussman E, Kroll E. Multiple jets in electrospinning: experiment and modeling. *Polymer* 2005;46:2889.
- [23] Bowman J, Taylor M, Sharma V, Lynch A, Chadha S. Multispinneret methodologies for high throughput electrospun nanofiber. *Mater Res Soc Sym Proc* 2003;752:AA1.5.1.
- [24] Yamashita Y, Miyakeb H, Higashiyamab A, Tanakaa A. In: 9th Asian textile conference, Taiwan; 2007.
- [25] Tomaszewski W, Szadkowski M. Investigation of electrospinning with the use of a multi-jet electrospinning head. *Fibers Text East Eur* 2005;13(22).
- [26] Yang Y, Jia Z, Li Q, Hou L, Gao H, Wang L, et al. In: 8th International conference on properties and applications of dielectric materials, Bali; 2006. p. 940.
- [27] Yamashita Y, Tanaka A, Ko F. In: International fiber conference 2006, Seoul; 2006. p. 87.
- [28] Yang Y, Jia Z, Li Q, Hou L, Liu J, Wang L, et al. A shield ring enhanced equilateral hexagon distributed multi-needle electrospinning spinneret. *IEEE Trans Dielectr Electr Insul* 2010;17:1592–601.

- [29] Kim HY, Park JC. KR Patent WO2007035011; 2007.
- [30] Yamashita Y, Ko F, Miyake H, Higashiyama A. Establishment of nanofiber preparation technique by electrospinning. *Sen'i Gakkaishi* 2008;64(24).
- [31] Lagaron JM, et al. Nozzle with multiple outlets. Patent Application WO2016083643; 2014.
- [32] Bryner MA, Armantrout JE, Johnson BS. US Patent 20060138710; 2006.
- [33] Li D, Xia Y. Electrospinning of nanofibers: reinventing the wheel? *Adv Mater* 2004;16:1151–70.
- [34] Fong H, Chun I, Reneker D. Beaded nanofibers formed during electrospinning. *Polymer* 1999;40:4585–92.
- [35] Koombhongse S, Liu W, Reneker DH. Flat polymer ribbons and other shapes by electrospinning. *J Polym Sci B Polym Phys* 2001;39:2598–606.
- [36] Chen H, Di J, Wang N, Dong H, Wu J, Zhao Y, et al. Fabrication of hierarchically porous inorganic nanofibers by a general microemulsion electrospinning approach. *Small* 2011;7:1779–83.
- [37] Chang G, Shen J. Helical nanoribbons fabricated by electrospinning. *Macromol Mater Eng* 2011;296:1071–4.
- [38] Huang C, Tang Y, Liu X, Sutti A, Ke Q, Mo X, et al. Electrospinning of nanofibres with parallel line surface texture for improvement of nerve cell growth. *Soft Matter* 2011;7:10812–7.
- [39] Bognitzki M, Czado W, Frese T, Schaper A, Hellwig M, Steinhart M, et al. Nanostructured fibers via electrospinning. *Adv Mater* 2001;13:70–2.
- [40] Li D, Xia Y. Direct fabrication of composite and ceramic hollow nanofibers by electrospinning. *Nano Lett* 2004;4:933–8.
- [41] Sun Z, Zussman E, Yarin AL, Wendorff JH, Greiner A. Compound core-shell polymer nanofibers by co-electrospinning. *Adv Mater* 2003;15:1929–32.
- [42] Lin T, Wang H, Wang X. Self-crimping bicomponent nanofibers electrospun from polyacrylonitrile and elastomeric polyurethane. *Adv Mater* 2005;17:2699–703.
- [43] Niu HT, Lin T. Fiber generators in needleless electrospinning. *J Nanomater* 2012;2012:725950.
- [44] Pham QP, Sharma U, Mikos AG. Electrospinning of polymeric nanofibers for tissue engineering applications: a review. *Tissue Eng* 2006;12:1197–211.
- [45] Gopal R, Kaur S, Ma Z, Chan C, Ramakrishna S, Matsuura T. Electrospun nanofibrous filtration membrane. *J Membr Sci* 2006;281:581–6.
- [46] Kedem S, Schmidt J, Paz Y, Cohen Y. Composite polymer nanofibers with carbon nanotubes and titanium dioxide particles. *Langmuir* 2005;21:5600–4.
- [47] Jia H, Zhu G, Vugrinovich B, Kataphinan W, Reneker DH, Wang P. Enzyme-carrying polymeric nanofibers prepared via electrospinning for use as unique biocatalysts. *Biotechnol Prog* 2002;18:1027–32.
- [48] Abidian MR, Kim DH, Martin DC. Conducting-polymer nanotubes for controlled drug release. *Adv Mater* 2006;18:405–9.
- [49] Wang X, Drew C, Lee S-H, Senecal KJ, Kumar J, Samuelson LA. Electrospun nanofibrous membranes for highly sensitive optical sensors. *Nano Lett* 2002;2:1273–5.
- [50] Thavasi V, Singh G, Ramakrishna S. Electrospun nanofibers in energy and environmental applications. *Energy Environ Sci* 2008;1:205–21.
- [51] Ma Z, Kotaki M, Ramakrishna S. Electrospun cellulose nanofiber as affinity membrane. *J Membr Sci* 2005;265:115–23.
- [52] Saeed K, Haider S, Oh T-J, Park S-Y. Preparation of amidoxime-modified polyacrylonitrile (PAN-oxime) nanofibers and their applications to metal ions adsorption. *J Membr Sci* 2008;322:400–5.

- [53] Fang J, Niu H, Lin T, Wang X. Applications of electrospun nanofibers. *Chin Sci Bull* 2008;53:2265–86.
- [54] Lu X, Wang C, Wei Y. One-dimensional composite nanomaterials: synthesis by electrospinning and their applications. *Small* 2009;5:2349–70.
- [55] Liu Y, He J-H. Bubble electrospinning for mass production of nanofibers. *Int J Nonlinear Sci Numer Simul* 2007;8:393–6.
- [56] Wijeyaratne SM, Kannangara L. Safety and efficacy of electrospun polycarbonate-urethane vascular graft for early hemodialysis access: first clinical results in man. *J Vasc Access* 2011;12:28–35.
- [57] <http://www.niddk.nih.gov/health-information/health-topics/kidney-disease/hemodialysis/Pages/facts.aspx>.
- [58] Boulanger H, Ahriz-Saksi S, Flamant M, Vigerel P. Evaluation of post-puncture bleeding time of arteriovenous fistulas with IRIS (R) bandage. *J Vasc Access* 2014;15(2):102–7.
- [59] Mather P, Wu J, Ren D, Hou S. US Patent 8,431,151 B2; 2013.

Structuring of electrospun nanofiber mats by 3D printing methods

4

N. Shah Hosseini, N. Khenoussi

Laboratoire de Physique et Mécanique Textiles, Mulhouse, France

4.1 Introduction

Electrospinning is a low-cost, simple, and efficient technique, among others, spinning methods such as drawing, template synthesis, phase separation, and self-assembly to produce nanofibers in nanoscale diameters. In this process, a positively charged polymer solution jet is drawn through a spinneret by applying a high-voltage electrostatic force; then, nanofibers are collected over a grounded metallic collector [1].

Nanofibers are being utilized for a wide range of applications in various fields such as high-performance filtration, protective material, fiber-based sensors, and biomedical applications [2,3]. Today, due to their main interesting properties and specifically large surface area to volume ratio, biomedical applications attract more and more interest from the scientific community. One of the most important areas is tissue engineering in which it is needed to provide a scaffold to mimic the natural extracellular matrix (ECM). These nanofibrous scaffolds provide a structural support for cells to be guided and accommodated in the three-dimensional space to regenerate the function of damaged tissue [4,5]. Nanofibrous materials are good candidates for this kind of application and fiber orientation considered as an important feature, which affect cell attachment and proliferation [6]. Thus, nanofibrous scaffolds formed by electrospinning could represent favorable structures for biomedical applications because of their similarity to natural ECM and use of various polymeric materials. Recently, many studies are working on optimization of tissue scaffolds with ordered and defined organizations of nanofibers. Since some cells in certain tissue, such as nerve, prefer to be aligned in the direction of the fiber orientation, well-controlled organization of fibers is necessary [7].

The electrospinning setup can be modified in different ways to combine material properties with different morphological structures for diverse applications ranging from tissue engineering to nanocomposite fabrication; however, electrospun nanofibers are generally deposited randomly, which limit their applications. In electrospinning process, there are a few variables that can affect the deposition of nanofibers. One of the critical variables is collector design that plays an important role to determine the nanofibers arrangement in an electrospun nanoweb.

The aim of this chapter is to highlight several methods to control the arrangement of 2D/3D nanofibers, such as the use of mechanical devices and parallel electrode collectors. Additive manufacturing (AM) methods are presented to describe innovative methods to achieve various geometries of collectors to be used to produce complex nanofibrous architectures during electrospinning.

By changing three key elements, including surface chemistry, topography, and structuration of nanofibers, desired applications can be achieved. This review highlights the current state of the art methods for producing patterned electrospun materials, focusing on structuration of nanofibers and their effects on cell growth.

Typically, electrospun nanofibers are deposited on a metallic flat substrate as random nanofibers with no preferential organization of fibers. Different collector types with different designs such as static plate, rotating drum, parallel electrode, and rotating disk have been developed [8]. Depending on the collector type, nanofiber orientation can be changed from totally random to highly oriented or 2D to 3D arrangement [9,10].

4.2 Obtaining oriented nanofibers

Some specific connective tissues are composed of oriented collagen fibers. In terms of mimicking that structure, a variety of studies were performed to evaluate the effect of fiber alignment on cell behavior in tissue engineering area. Several polymers including poly(L-lactic-co- ϵ -caprolactone), poly(lactic acid), and poly(esterurethane urea) were electrospun in aligned or random form for tissue engineering applications. The cellular activities were demonstrated to be highly affected by nanofibers [11–13].

Since the orientation of nanofibers in a scaffold is a main interest for many applications, upcoming paragraphs describe several methods, which have been investigated to produce aligned electrospun mats. Orientation or patterning of nanofibers is generally obtained via two general methods: dynamic devices and manipulation of the electrostatic field during the electrospinning process.

4.2.1 Manipulation of the electrostatic field

Using conductive electrode(s) or different collector geometries can do manipulation of the electric field in the electrospinning apparatus. The electrospun nanofibers are guided by altering the static electric field and their travel patterns during the electrospinning process [14].

The parallel electrode concept is the simplest method to produce highly aligned nanofibers. The air gap between two electrodes encourages the electrospinning jet to swing between them to generate greatly aligned nanofibers. This method has some limitations such as the length of the nanofibers path, the thickness of the oriented electrospun mat, and the difficulty of transferring the samples for further processing.

Xie and Li et al. have reported a designed collector based on manipulation of the electrostatic field to produce nanofiber mat containing both aligned and random portions, Fig. 4.1. The fabricated collector is composed of two stapler-shaped metal

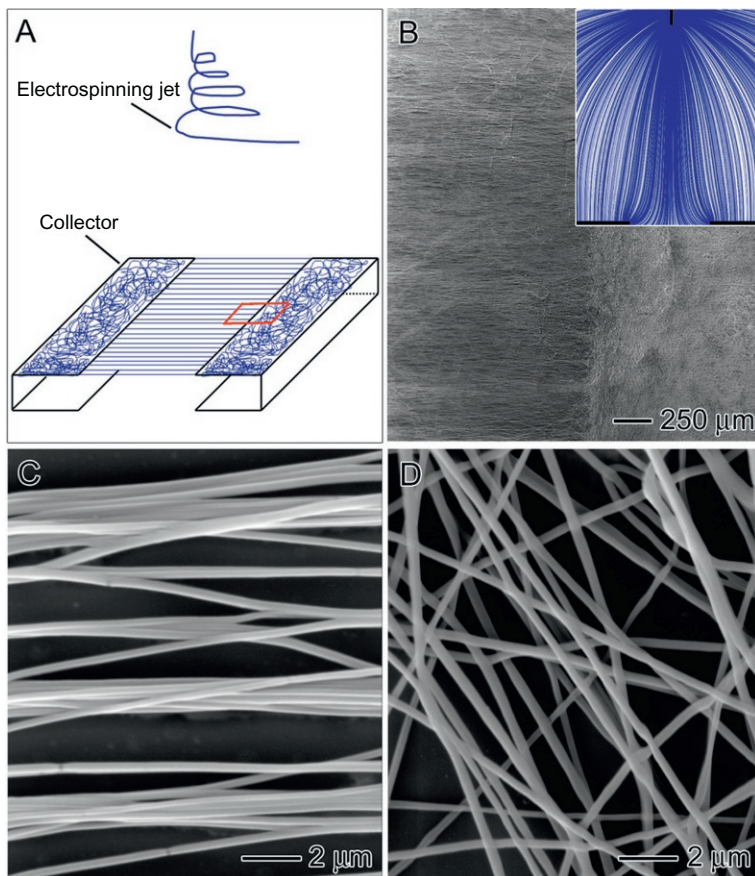


Fig. 4.1 A) Schematic illustrating the experimental setup for the fabrication of aligned-to-random nanofiber scaffolds. (B) SEM images of nanofiber scaffolds consisting of random and uniaxially aligned PLGA (50:50) nanofibers on the left and right, respectively, or the small region of boxed in (A). Inset, streamline plot of electric field between the needle and collector. (C, D) High-magnification views of the random and aligned portions of the scaffold in (B). Reused with permission from Xie J, Li X, Lipner J, Manning CN, Schwartz AG, Thomopoulos S, et al. "Aligned-to-random" nanofiber scaffolds for mimicking the structure of the tendon-to-bone insertion site. *Nanoscale* 2010;2:923–26, copyright Nanoscale publisher.

frames. Nanofibers are deposited randomly on the metal frame and aligned across the air gap. After performing a biological test, it has been shown that cells were oriented along the direction of fiber alignment, while cells were randomly oriented on the random portion of the electrospun mat. Afterward, it has been proved that fabrication of aligned-to-random scaffold could mimic the collagen fibers in the human body [15].

Zhang and Chang have studied the use of electroconductive wire with protrusions as collectors to control the arrangement of electrospun nanofibers, as it is presented in Fig. 4.2.

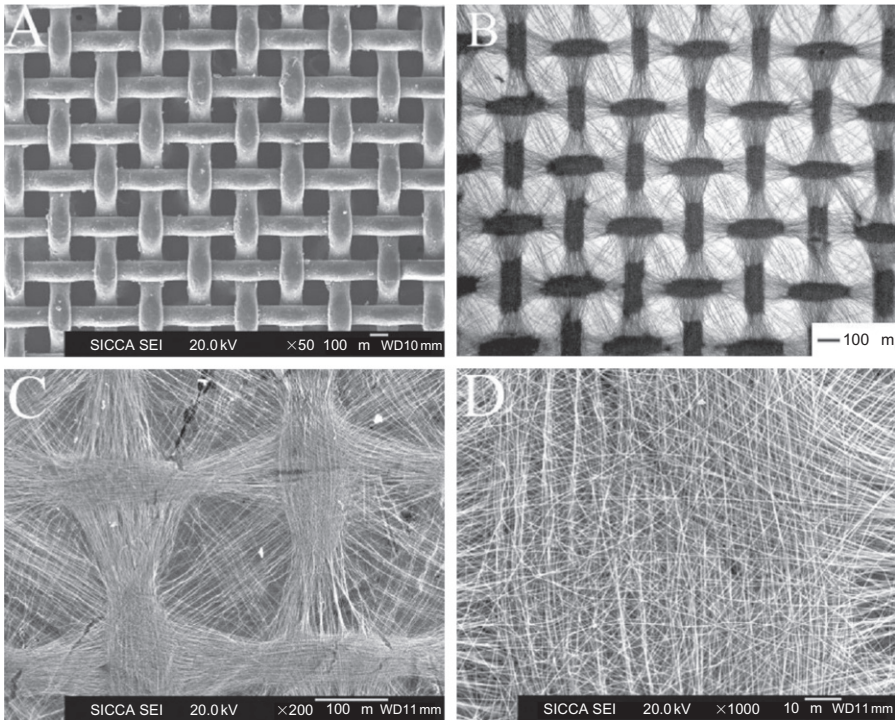


Fig. 4.2 (A) SEM image of a patterned collector. (B) Optical image of electrospun mat collected using the collector in (A). (C) SEM image of a typical unit in the electrospun mat collected using the collector in (A). (D) SEM image of the cross point in the electrospun mat. Reused with permission from Zhang D, Chang J. Patterning of electrospun fibers using electroconductive templates. *Adv Mater* 2007;19:3664–7, copyright Advanced Materials publisher.

They have concluded that the patterned collector obviously affects the deposition and arrangement of the fibers and the architecture of the electrospun mats [16].

4.2.2 Dynamic devices

It has been suggested to use mechanical forces to collect aligned electrospun nanofibers. For example, by rotating a cylindrical collector at a very high speed (up to thousands of rpm), radially oriented nanofibers can be obtained. The rotating speed of rotating collectors can change the diameter of nanofibers and determine the degree of alignment of the nanofibers [14]. In another study, Subramanian et al. have presented highly aligned electrospun nanofibers of PLGA produced by using rotating mandrel (3 mm in diameter) with a maximum speed of 2500 rpm. Fig. 4.3 illustrates the produced tubular scaffold consisting longitudinally oriented nanofibers by electrospinning [17].

It has been shown that fully aligned fibers have fewer defects and may help to the progress of neurite outgrowth and their elongation in nerve regeneration. The

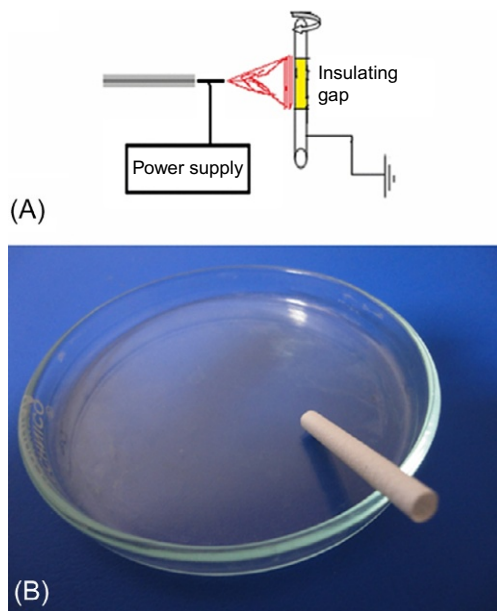


Fig. 4.3 (A) Electrospinning setup used for the fabrication of the longitudinally oriented tubular scaffold. (B) Tubular scaffold.

Reused with permission from Subramanian A, Krishnan UM, Sethuraman S. Fabrication of uniaxially aligned 3D electrospun scaffolds for neural regeneration. *Biomed Mater* 2011;6:025004, copyright Biomedical Materials publisher.

longitudinally oriented scaffold has presented good flexibility, less pore size, and better cell proliferation rate compared with random fibers [17,18].

Compared with the parallel electrode, by using dynamic collectors, large area of oriented nanofibers could be achieved. In general, in order to produce uniform and highest alignment possible, the rotational speed should be optimized to prevent fiber breakage [19].

4.2.3 Complex patterned architectures by additive manufacturing methods (AM)

Recently, producing patterned electrospun nanofibers has been the main interest for various applications such as micro- or nanodevices and biomedical fields. It has been proved that 3D patterned scaffolds with different nanofiber orientations and alignments can provide a structure able to mimic better the natural ECM environment.

Even though there have been different methods for achieving patterned and oriented nanofibers, there is still a challenge for accurately controlling the structure of nanofibers by choosing a reproducible, scalable, and flexible method. Hence, AM has attracted great interest in design and fabrication of collectors for electrospinning to produce patterned scaffolds over the past year.

AM is the general name for a number of methods in which complex and precise 3D structures can be formed layer-by-layer manner according to computer-aided design

(CAD) [20]. Several studies have been done with combining electrospinning and AM techniques, such as photolithography, stereolithography, inkjet printing processes, and 3D printing [21].

Photolithography is the method in which UV light is used to generate a pattern on the substrate from a photomask to a light-sensitive chemical photoresist. Thus, different micro- or nanopattern dimensions can be assembled on flat substrate.

In the Wittmer et al. study, honeycomb micropatterns of electrospun fibers were obtained on micropatterned collectors on the silicon wafers using photolithographic methods (Fig. 4.4).

They used a combination of electrospinning and electro spraying methods for fabricating micropatterned collectors to produce the composite of fibers and microparticles highly organized in 3D structure. They have obtained 3D nanofibrous PCL microstructured scaffolds during the electrospinning process with various

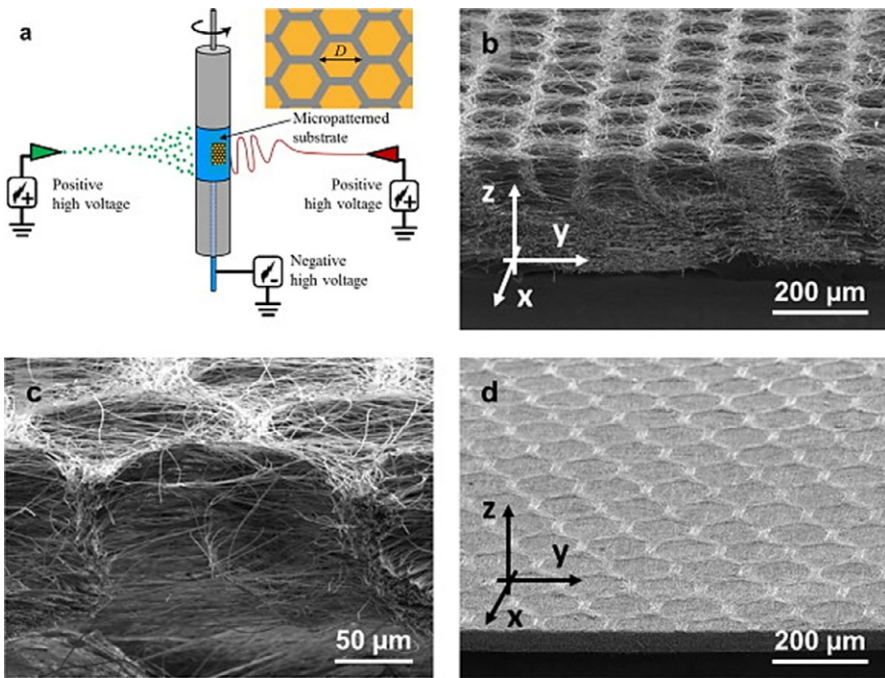


Fig. 4.4 (A) Schematic of the process. The diameter D of the honeycombs was 40 μm , 80 μm , 160 μm , or 360 μm . The width and the height of honeycomb walls were, respectively, 20 μm and 60 μm . (B) 3D columnar structures obtained for $D=160 \mu\text{m}$ after 1 h of production. (C) 3D columnar structure obtained after 15 min of production. (D) Fibrous structure obtained with the same operating conditions and time of production than for (B) but without electro spraying. No internal 3D microstructure can be achieved in this case. Reused with permission from Wittmer CR, Hébraud A, Nedjari S, Schlatter G. Well-organized 3D nanofibrous composite constructs using cooperative effects between electrospinning and electro spraying. *Polymer* 2014;55:5781–7, copyright Biomedical Materials publisher.

porosity gradients. This novel technique could be used for producing 3D scaffolds with tunable pore size according to the desired application [22].

Another method *stereolithography* (Vaquette et al.) can be applied, which is based on layer-by-layer photosensitive resin polymerization using UV light. In their study, Rogers et al. used microstereolithography to generate the patterned resin from a simple sinusoidal wave to a more complex honeycomb with feature size ranging from 100 to 1000 μm . They have studied the behavior of 3T3 fibroblasts on 3D patterned hybrid sinusoidal electrospun PLGA scaffold in vitro. They produced electrospun nanofibers scaffold using tailored resin collectors produced by the AM approaches. Fig. 4.5 presents oriented and randomly oriented microfibers in complex patterned scaffold such as sawtooth, hexagonal, and reentrant honeycomb, which followed the tailored collectors [23,24].

Rogers believed that the mentioned methods have main limitations such as lack of versatility, reproducibility, and scalability in the design and fabrication. So, they have presented a novel method to fabricate electrospun scaffolds with tailored geometries using a precise, robust, and scalable AM approach.

According to patent of Claeysens et al. [25], a template consisting of aluminum sheet having a nonconductive 3D pattern thereon has been formed by microstereolithography. Since the inventors have observed that electrospun nanofibers were mostly gathered onto a nonconductive surface, they have provided a patterned nonconductive collector on a conductive collector. This invention is presenting a technique for producing an electrospun scaffold having defined cavities, which makes it possible to act as a stem cell niche to house cells. The stem cells could be located in the microenvironments called niches, which are chemically and biologically well characterized. The ability of producing scaffolds with complex 3D architecture may be used in treating an ocular injury, a skin wound, corneal replacement, etc. as a medicament [26].

Although the above methods enable the production of 3D electrospun materials, they have some drawbacks including low control of the 3D structure, long production time, and imprecision. In order to overcome these disadvantages, new methods, which assure fast, precise, and controllable production of 3D collectors, have to be developed [27].

3D printer technology is another technique among AM approaches to fabricate a 3D object of almost any shape by using CAD so it can be a good way to fabricate different patterned collectors. The primary substance that is used in 3D printing and inkjet printing is different. In 3D printers, layers of curable liquid photopolymer jet onto a build tray instead of using ink drops. This 3D printer system jets layers of liquid photopolymer resin onto a build tray and instantly cures them with UV light. It also jets a gel-like support material to maintain the complex geometries. This method has some advantages such as fine detail, high speed of processing, precision, and no postcuring needed. The process contains three steps, preprocessing, production, and support removal:

- Preprocessing: 3D CAD model is uploaded into the machine via its software. The software finds appropriate place to put the material automatically.

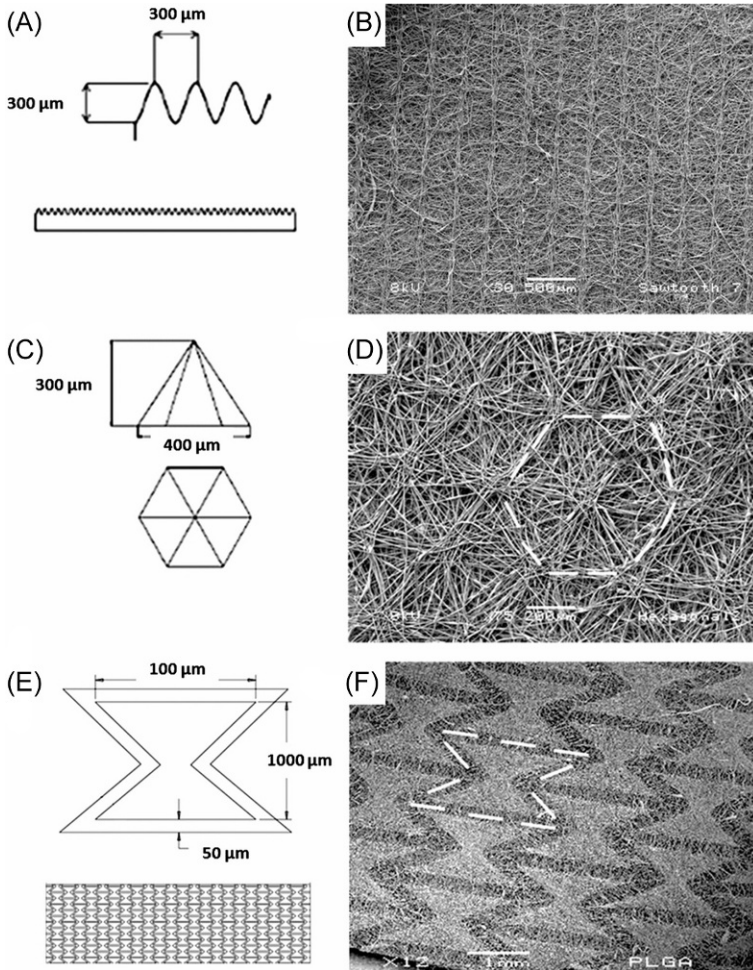


Fig. 4.5 The versatility of the RP approach to produce formers with various 3D geometries and the resulting patterned scaffolds. Representative images of the sawtooth (A and B), hexagonal (C and D), and reentrant honeycomb (E and F) CAD models and electrospun scaffolds. Reused with permission from Rogers CM, Morris GE, Gould TW, Bail R, Toumpaniari S, Harrington H, et al. A novel technique for the production of electrospun scaffolds with tailored three-dimensional micro-patterns employing additive manufacturing. *Biofabrication* 2014;6:035003, copyright Biofabrication publisher.

- Production: Once the 3D printer jets the drops of photopolymer, the UV cures them in shape of layers on the tray to create the 3D models. It jets removal of gel-like material to support the complex shapes.
- Support removal: The supportive material can be removed easily with water, and no post-curing is needed.

Shah Hosseini et al. [28] have focused on AM method to generate 3D electrospun scaffolds by using patterned resin collectors produced using 3D printer technology in combination with electrospinning. A preliminary study on design and fabrication of 3D collectors for electrospinning of nanofibers was conducted. This study has shown the feasibility of this method. Fig. 4.6 presents the CAD models of collector, which had been uploaded in 3D printer.

The collectors have been firstly observed by scanning electron microscope (SEM) to refine the choices in the final topography. Eight collectors have been produced with different topographies such as holes, pillars, or grooves. Geometric dimensions are reported in Table 4.1.

Dimension has been chosen regarding optimum resolution of 3D printer. For each geometry, two dimensions have been realized to make a comparison to optimize the process.

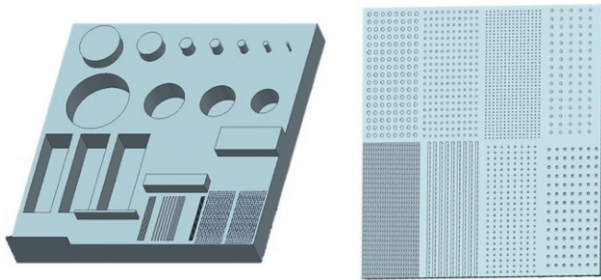


Fig. 4.6 CAD model collector.

Table 4.1 Dimensions of produced collectors in different forms

Collector number	Design	Diameter/width (μm)	Longitudinal pitch (μm)	Track pitch (μm)	Height (μm)
1	Cylindrical hole	700	2100	2100	50
2	Cylindrical hole	400	1200	1200	50
3	Cylindrical stud	200	600	800	50
4	Cylindrical stud	400	1200	1600	50
5	Groove	200	600	600	50
6	Groove	500	1500	1500	50
7	Hemispheric stud	350	1400	1050	50
8	Hemispheric stud	550	1650	1650	50

Once the production of collectors has been completed, they were coated by a very thin layer of gold to be conductive. Afterward, electrospinning has been performed on these collectors with different patterns (holes, grooves, etc.). Fig. 4.7 presents the polyamide 66 nanofibers mat on the fabricated patterned collector 1, 4, 6, and 8.

The electrospun nonwovens have been characterized by SEM. Figs. 4.8 and 4.9 represent the micrographs from the obtained patterned nanoweb using collectors 5 and 8 with groove and hemispheric stud patterns.

The results show that patterned collectors allow producing nanoweb templates made of nanofibers with alternative pattern of oriented and nonoriented area, which can provide an appropriate surface for cell growth.

By using the similar processing conditions described earlier, from the same author, a 3D patterned scaffold composed of oriented and nonoriented nanofibers has been produced. Different 3D grooved collectors, which have been obtained by a 3D printing



Fig. 4.7 Coated patterned collectors and electrospinning on coated collectors.

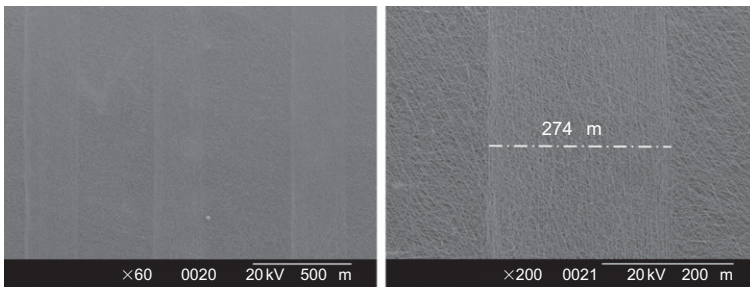


Fig. 4.8 Nonwoven obtained on groove structure with two different magnifications.

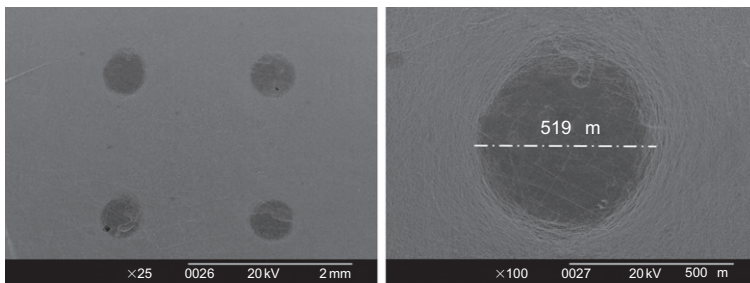


Fig. 4.9 Nonwoven obtained on pillar structure with two different magnifications.

technique, were used in an electrospinning system as collectors to produce polyamide 66 (PA66) scaffolds. The characterization results have shown that the PA66 nanofibers followed both the geometries and dimensions of the fabricated 3D collectors. So, it has been proved that different scaffold designs can be obtained from 3D printing, with repeatable 3D geometry. This provides the possibility of having interconnected porous net that can be used in tissue engineering [29].

4.3 Conclusion and future perspectives

Different 3D patterning of electrospun nanofibers fabricated by different methods has been demonstrated. AM techniques were demonstrated to be very important to achieve the precise and reproducible method to produce patterned or aligned electrospun fibers.

The design of scaffolds for tissue engineering applications that are able to maintain the tissues' structure and biological properties lies at mimicking the native connective tissue fibers. In terms of mimicking that structure, a variety of studies were performed to develop organized 3D electrospun nanofibers. Electrospinning has been used to prepare 3D scaffolds by collecting nanofibers on patterned collectors. Patterned collectors can be capable of constructing 3D electrospun structures that may be very useful for some tissue engineering applications where ordered fiber organizations are required. The potential of 3D printing technology has been shown when it is combined with the electrospinning method to produce 3D scaffolds in nanoscale.

Most methods of the presented applications have not reached the level of maturity required for industrial application but just at a laboratory research. It should be mentioned that the current methods are novel and there is not much information on commercial aspects of 3D patterned electrospun scaffolds, but there is a great possibility of attracting attentions and investments from academia, governments, and industry all over the world.

Although significant progress has been made to develop electrospun nanofibrous materials for biomedical applications, there are very few products in the market, mainly due to the limitation of electrospun scaffolds for 3D applications. AM techniques and combination of electrospinning with 3D printed collectors can enable the construction of new materials to enter the market for clinical tissue engineering applications.

References

- [1] Hekmati AH, Rashidi A, Ghazisaeidi R, Drean JY. Effect of needle length, electrospinning distance, and solution concentration on morphological properties of polyamide-6 electrospun nanowebs. *Text Res J* 2013;83:1452–66.
- [2] Fang J, Niu H, Lin T, Wang X. Applications of electrospun nanofibers. *Chin Sci Bull* 2008;53:2265.
- [3] Sill TJ, Von Recum HA. Electrospinning: applications in drug delivery and tissue engineering. *Biomaterials* 2008;29:1989–2006.

- [4] Pham QP, Sharma U, Mikos AG. Electrospinning of polymeric nanofibers for tissue engineering applications: a review. *Tissue Eng* 2006;12:1197–211.
- [5] Subramony SD, Dargis BR, Castillo M, Azeloglu EU, Tracey MS, Su A, et al. The guidance of stem cell differentiation by substrate alignment and mechanical stimulation. *Biomaterials* 2013;34:1942–53.
- [6] Ng R, Zang R, Yang KK, Liu N, Yang S-T. Three-dimensional fibrous scaffolds with microstructures and nanotextures for tissue engineering. *RSC Adv* 2012;2:10110.
- [7] Murugan R, Ramakrishna S. Design strategies of tissue engineering scaffolds with controlled fiber orientation. *Tissue Eng* 2007;13:1845–66.
- [8] Teo WE, Ramakrishna S. A review on electrospinning design and nanofibre assemblies. *Nanotechnology* 2006;17:R89.
- [9] Lavielle N, Hébraud A, Mendoza-Palomares C, Ferrand A, Benkirane-Jessel N, Schlatter G. Structuring and molding of electrospun nanofibers: effect of electrical and topographical local properties of micro-patterned collectors. *Macromol Mater Eng* 2012;297:958–68.
- [10] Wu Y, Dong Z, Wilson S, Clark RL. Template-assisted assembly of electrospun fibers. *Polymer* 2010;51:3244–8.
- [11] Anselme K, Davidson P, Popa AM, Giazzon M, Liley M, Ploux L. The interaction of cells and bacteria with surfaces structured at the nanometer scale. *Acta Biomater* 2010;6:3824–46.
- [12] Cardwell RD, Dahlgren LA, Goldstein AS. Electrospun fiber diameter, not alignment, affects mesenchymal stem cell differentiation into the tendon/ligament lineage. *J Tissue Eng Regen Med* 2014;8:937–45.
- [13] Vaquette C, Kahn C, Frochot C, Nouvel C, Six JL, De Isla N, et al. Aligned poly(L-lactico-e-caprolactone) electrospun microfibers and knitted structure: a novel composite scaffold for ligament tissue engineering. *J Biomed Mater Res A* 2010;94:1270–82.
- [14] Haseeb B. Controlled deposition and alignment of electrospun PMMA-g-PDMS nanofibers by novel electrospinning setups. Master of Science Thesis, Stockholm, Sweden, 2011.
- [15] Xie J, Li X, Lipner J, Manning CN, Schwartz AG, Thomopoulos S, et al. “Aligned-to-random” nanofiber scaffolds for mimicking the structure of the tendon-to-bone insertion site. *Nanoscale* 2010;2:923–6.
- [16] Zhang D, Chang J. Patterning of electrospun fibers using electroconductive templates. *Adv Mater* 2007;19:3664–7.
- [17] Subramanian A, Krishnan UM, Sethuraman S. Fabrication of uniaxially aligned 3D electrospun scaffolds for neural regeneration. *Biomed Mater* 2011;6:025004.
- [18] Venugopal J, Low S, Choon AT, Ramakrishna S. Interaction of cells and nanofiber scaffolds in tissue engineering. *J Biomed Mater Res B Appl Biomater* 2008;84:34–48.
- [19] Beilke MC, Zewe JW, Clark JE, Olesik SV. Aligned electrospun nanofibers for ultra-thin layer chromatography. *Anal Chim Acta* 2013;761:201–8.
- [20] Dalton PD, Vaquette C, Farrugia BL, Dargaville TR, Brown TD, Hutmacher DW. Electrospinning and additive manufacturing: converging technologies. *Biomater Sci* 2013;1:171–85.
- [21] Vaezi M, Seitz H, Yang S. A review on 3D micro-additive manufacturing technologies. *Int J Adv Manuf Technol* 2013;67:1721–54.
- [22] Wittmer CR, Hébraud A, Nedjari S, Schlatter G. Well-organized 3D nanofibrous composite constructs using cooperative effects between electrospinning and electrospraying. *Polymer* 2014;55:5781–7.

-
- [23] Rogers CM, Morris GE, Gould TW, Bail R, Toumpaniari S, Harrington H, et al. A novel technique for the production of electrospun scaffolds with tailored three-dimensional micro-patterns employing additive manufacturing. *Biofabrication* 2014;6:035003.
 - [24] Wang Y, Wang G, Chen L, Li H, Yin T, Wang B, et al. Electrospun nanofiber meshes with tailored architectures and patterns as potential tissue-engineering scaffolds. *Biofabrication* 2009;1:015001.
 - [25] Claeysens F, Ortega I, Macneil S, Ryan A, inventors, Scaffold, Patent EP2844308A1, 2013.
 - [26] Fuchs E, Tumber T, Guasch G. Socializing with the neighbors: stem cells and their niche. *Cell* 2004;116:769–78.
 - [27] Barclift MW, Williams CB. Examining variability in the mechanical properties of parts manufactured via polyjet direct 3d printing. In: *International Solid Freeform Fabrication Symposium*, August, 2012; 2012. p. 6–8.
 - [28] Shah Hosseini N, Khenoussi N, Dominique Adolphe, Amir Houshang Hekmati, Laurence Schache, Nimet Bölgen, 2014b. Producing electrospun 3D scaffold by using 3D collectors for controlling cell response, The Fiber Society Philadelphia, Pennsylvania, USA.
 - [29] Shah Hosseini N, Bolgent N, Yetkin D, Şakir Necat Yilmaz, Nabyl Khenoussi, Dominique Adolphe, Amir Houshang Hekmati, Yenne Heitter, Laurence Schacher, 2014a. Novel patterned 3D electrospun scaffolds and their effect on cartilage cell attachment. *Biomedical Electrospun Materials & Applications (BEMA 2014)*, Université de Haute Alsace (UHA).

This page intentionally left blank

Melt electrospinning in tissue engineering

5

S.M. Willerth^{*,†}

^{*}University of Victoria, Victoria, BC, Canada, [†]International Collaboration on Repair Discoveries (ICORD), Vancouver, BC, Canada

5.1 Introduction to the process of melt electrospinning

This chapter focuses on how the technique of melt electrospinning can be used to generate reproducible 3-D fiber scaffolds for applications in tissue engineering. Fibers are threadlike structures possessing a length far greater than their width. This property makes them useful for a wide variety of applications in textile engineering, energy systems, and biomedical systems [1–4]. The properties of fibers can vary and include length, cross-sectional shape, construction material, and method of fabrication. These parameters can be modified during the fabrication process to ensure optimal fiber function and performance based on the desired application. While this book focuses on electrospinning for producing fibers, other fiber production techniques exist that can generate fiber-based scaffolds for tissue engineering applications as reviewed recently by Tamayol et al. [5]. The process of microfluidic spinning serves as an interesting alternative to the use of electrospinning when engineering tissues as reviewed recently [6]. In this process, microfluidic devices are used to fabricate fibers through a polymerization reaction. The device controls the flow rate and mixing speed of the polymer solution and the agent used to cross-link the solution to form a fiber. Altering these parameters will determine the properties of the fibers produced. This technique does not require the use of an electric field and can generate both nanofibers and microfibers.

Unlike the microfluidic spinning method of fiber production, electrospinning requires an electric field to charge the polymer solution from which the fibers are drawn—hence the prefix “electro” [7]. Electrospinning shares many common features with the process of electro spraying. The major difference between the two processes is that electro spraying generates fine droplets from a charged polymer solution instead of producing a series of fibers [8]. The majority of literature around electrospinning has focused on solution electrospinning, a fabrication process where a polymer is dissolved in a solvent with the resulting solution being electrospun into fibers that are collected on the surface charged by the counter electrode [7]. Unlike solution electrospinning, melt electrospinning requires that the polymer be heated up until it becomes liquid [9,10]. Once it is liquid, the resulting polymer melt is charged with an electric field and then used to fabricate fibers. The nozzle extruding the melt can be moved, or the collector can be manipulated in order to control the morphology of the deposited fibers [11–13].

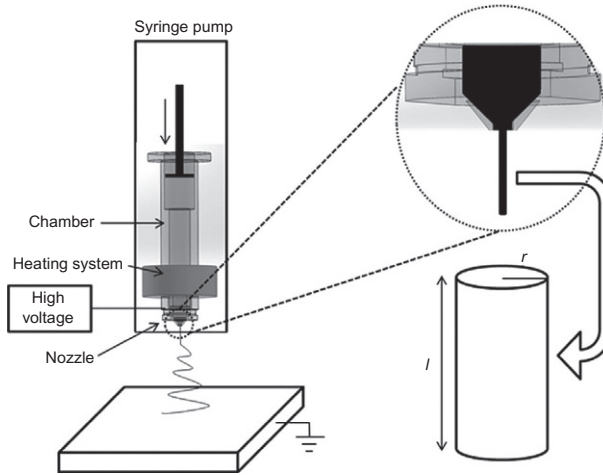


Fig. 5.1 Schematic of a custom-designed melt electrospinning device showing the syringe pump, the chamber where the polymer is melted, the heating system, the nozzle, and where the electric field is applied.

From Ko J, Mohtaram NK, Ahmed F, Montgomery A, Carlson M, Lee PC, et al. Fabrication of poly(-caprolactone) microfiber scaffolds with varying topography and mechanical properties for stem cell-based tissue engineering applications. *J Biomater Sci Polym Ed* 2014;25(1):1–17.

Fig. 5.1 shows a schematic of a typical melt electrospinning set-up taken from Ko et al. [11]. The major features of the set-up include the chamber where the polymer is loaded, the heating system, the nozzle for melt extrusion, the high-voltage power source, and the collector. This technique has become increasingly popular in recent years as it provides a way to directly fabricate scaffolds with defined structures in a process similar to 3-D printing [10]. Dr. Paul Dalton (presently at the University of Würzburg) has been one of the prominent advocates of using melt electrospinning to fabricate scaffolds for tissue engineering. His website serves an excellent resource for the field, and the URL can be found in the resource list at the end of the chapter. Other prominent research groups using melt electrospinning for tissue engineering include Dr. Dietmar Hutmacher's group and Dr. Mia Woodruff's group at the Queensland University of Technology and Dr. Groll's group at the University of Würzburg.

In addition to the experimental studies detailed later in this chapter, several studies have modeled the process of melt electrospinning using physical principles [14–16]. Ko et al. developed a model for the melt electrospinning process based on the physics of the melt using the following parameters: nozzle size, counter electrode distance, and applied voltage [14]. In melt electrospinning, the fibers produced tend to be much smaller than the nozzle size used due to the effects of the electric field combined with gravity. For example, using a nozzle with a $150\ \mu\text{m}$ diameter produces melt electrospun fibers that are $12 \pm 1\ \mu\text{m}$ in size, while using a much larger nozzle with a $1700\ \mu\text{m}$ diameter yields fibers with a width of $220 \pm 9\ \mu\text{m}$. The resulting

mathematical model was able to recreate these observations. Also, the model predicted that increasing the electric field would decrease fiber diameter and that increasing the collection distance would increase fiber size. These predictions correlated well with the experimentally collected data. In the same paper, a model for the 3-D deposition process was also developed, showing that the transition speed of the computer numerical control controller plays an important role in determining fiber density. The scaffold porosity could be predicted by this mathematical model when the aforementioned parameters were incorporated into it. A follow-up study further extended this model to include the effects of temperature and linear transitional speed [15]. The resulting fiber size decreases as the temperature of the melt increases. A 2013 study by Wang and colleagues used simulations to determine how the electric field distribution influences the fiber deposition during the melt electrospinning process [16]. In particular, they used dissipative particle dynamics to simulate the electrospinning process and found that polymer viscosity, melt temperature, and electric field all influence fiber production. Overall, these models illustrate the major parameters that influence the process of melt electrospinning and how they can be manipulated to produce scaffolds with the desired fiber size and topography.

5.2 Comparison with solution electrospinning

While solution electrospinning has been commonly used to fabricate scaffolds for tissue engineering applications, the use of melt electrospinning for these applications has been increasing in recent years [17]. As other chapters of this book describe the use of solution electrospinning in depth, here, a comparison of the advantages and disadvantages of each of these methods is detailed. One of the major differences that contribute to these differences between the two processes is how the production of the polymer solution occurs. For solution electrospinning, polymers are dissolved into solvents to prepare the solution used during the spinning process. These solvents can often be volatile and toxic—examples include the use of 1,1,1,3,3,3-hexafluoro-2-propanol (HFIP) and trifluoroacetic acid (TFA) [18]. However, progress has been made to eliminate the need for such solvents by using weak acids during electrospinning [19,20]. These alternatives can yield less than desirable morphologies and require further optimization. In contrast, melt electrospinning uses a liquid derived from heating up the polymer until it transitions into a liquid state, avoiding the use of such solvents [9]. One limitation of the melt electrospinning process is that the polymer used must exhibit a glass transition temperature, making it incompatible with thermoset polymers and biologically sourced proteins.

In solution electrospinning, the resulting solution is first spun into fibers and then collected to form fibrous scaffolds. The collection method can be altered to enable fabrication of scaffolds with different topographies [21–23]. Spinning parameters, such as applied voltage and collection distance, can be altered to obtain scaffolds with fiber sizes ranging from nanoscale to microscale [24]. One of the major advantages of solution electrospinning is that this process can be used to produce fibrous scaffolds

that can deliver bioactive molecules—an important factor when engineering tissues [25–27]. For example, proteins can be mixed directly into a polymer solution to encapsulate them into nanofibers [28] or added to the surface of nanofibers through chemical functionalization schemes [29]. Oftentimes, coaxial electrospinning is used to encapsulate bioactive factors inside of electrospun nanofibers [30]. Coaxial electrospinning uses two different solutions during the spinning process to generate a core layer and a shell layer with the bioactive factors being located in the more compatible solvent found in the middle of the nanofiber. This process helps to retain the activity of these incorporated bioactive factors. Scaffolds can be fabricated from natural biomaterials when using solution electrospinning as well, greatly expanding the versatility of this technique compared with melt electrospinning [31,32].

However, solution electrospinning can be a temperamental process with a number of factors affecting the consistency of the process. These factors include humidity, incorporation of bioactive factors into the polymer solution, distance to collector, solution preparation, and voltage applied [33,34]. Obtaining consistent fiber sizes can be challenging as the resulting fibers often vary in diameter along their length as my group has observed [28,35]. The incorporation of bioactive factors also leads to a greater distribution of fiber sizes and influences the resulting fiber size as detailed in the aforementioned studies. The size of the molecule being incorporated, the charge of the molecule, and its polarity all affect the properties of the polymer solution being spun, causing these effects to be observed. Another disadvantage of solution electrospinning is that when collecting nanofibers, the level of charge can accumulate in the scaffold, restricting the thickness of the resulting scaffolds to 3–4 mm [36].

The process of melt electrospinning enables a greater degree of control over the writing of the melted polymer, which allows for direct writing of scaffold topography by moving the collector as the polymer is deposited on the surface [37]. This feature makes the process more reproducible and precise when compared with solution electrospinning. However, it remains challenging to make nanoscale fibers as polymer melts tend to be more viscous than polymer solutions [38]. The recent lower limit on the size of fibers produced using melt electrospinning was reported as 817 ± 165 nm [39]. Also, thicker scaffolds can be printed using melt electrospinning as the viscosity of the solution can overcome the effects of the charge gradient on the collector. A recent study has increased the thickness of the scaffolds that can be produced using melt electrospinning [40]. As the polymers are directly melted, there is no need for using toxic solvents, making these scaffolds suitable for tissue engineering applications [41,42]. The use of heat makes it difficult to incorporate bioactive proteins and growth factors into the fibers generated using this process, but the resulting scaffolds could be functionalized with such molecules after fabrication. In the case of melt electrospinning, a coaxial process has been used to fabricate fibers with phase changes inside of their core [43]. Other groups have incorporated cellulose into melt electrospun scaffolds to improve their mechanical properties [44]. A series of studies have investigated the use of different melt electrospinning formulations to deliver a small-molecule beta-blocker, indicating the suitability of melt electrospinning for certain drug delivery applications [45–47].

Unlike solution electrospinning, most of the reported studies using melt electrospinning involve poly(ϵ -caprolactone) (PCL) as it has a melting temperature that ranges from 60 to 80°C [9,12]. Often, studies have added other polymers, such as poly(ethylene glycol) (PEG), poly(ethylene oxide) (PEO), or bioactive glass, to these PCL melts to alter their properties [48–53]. Also, a recent report discusses the use of poly(L-lactide-*co*- ϵ -caprolactone-*co*-acryloyl carbonate) (poly(LLA-*e*-CL-AC)) for melt electrospinning applications [54]. However, exploration of other polymer melts remains a key area for future investigation in the field of melt electrospinning.

5.3 Applications in tissue engineering

Tissues are composed of the extracellular matrix, a network of proteins and polysaccharides that ensure the proper functioning of the cells embedded in them, and different types of cells that work together to perform specific functions. It is logical to use healthy tissue as a blueprint for how to engineer replacements for diseased and damaged versions of the same tissue [55]. Key features of the extracellular matrix include porosity, nano- and microscale features, mechanical stiffness, and bioactive sites for cell adhesion [56]. A successful melt electrospun scaffold should replicate these desirable features of the extracellular matrix so that it can support cell growth and function. Normally, a melt electrospun scaffold with defined properties is used in combination with a cellular component when engineering replacement tissues. The following sections review the different types of tissues that can be engineered using melt electrospun scaffolds as substrates and the characteristics of these scaffolds.

5.3.1 Neural tissue

The nervous system is composed of the cells that enable the brain to transmit and receive information, enabling people to respond to stimuli in the environment. Engineering neural tissue poses a significant challenge as these complex systems of cells must be replicated when engineering substitutes [57–59]. My group, along with our close collaborators at the University of Victoria, Dr. Martin Jun's Laboratory for Advanced Multiscale Manufacturing, has investigated the use of melt electrospun scaffolds as substrates for engineering tissue from pluripotent stem cells. As pluripotent stem cells can form any type of cell found in an organism, they require cues to instruct them to become the desired phenotypes [60]. For neural tissue engineering applications, we focused on the generation of neurons from pluripotent stem cells seeded on melt electrospun scaffolds [11,13]. Our first study used melt electrospinning to generate scaffolds from a PCL melt with a loop mesh microfiber morphology consisting of overlapping ovals [11]. We found that changing the nozzle size of the melt extruder would change fiber diameter as expected, and we could use this property to alter scaffold porosity. We then seeded these scaffolds with aggregates consisting of mouse R1 embryonic stem cells treated with retinoic acid. These cells

could survive 14 days of culture on these scaffolds, and they were able to differentiate into neurons.

Building upon this work, we conducted a follow-up study where we looked at the effect of both loop mesh topography and biaxial aligned topography (Fig. 5.2) on pluripotent stem cell behavior [13]. We then seeded neural aggregates derived from human-induced pluripotent stem cells upon these scaffolds, cultured them for 12 days, and assessed the effect of topography on the resulting stem cell behavior. These cells were able to survive and differentiate into neurons. As seen in Fig. 5.2, the biaxial aligned scaffolds directed neurite extension to a much greater degree than what was observed with the cultures seeded on the loop mesh scaffolds. These results suggest that the aligned microfibers can be used to organize cells in structures similar to those found in native neural tissue and that these aligned microfibers promote neurite outgrowth. This pair of studies shows the utility of melt electrospun scaffolds for neural tissue engineering applications using pluripotent stem cells. Additionally, the microfiber scaffolds could be used as *in vitro* substrates for culturing pluripotent stem cell-derived neurons, which could then be employed for drug screening applications.

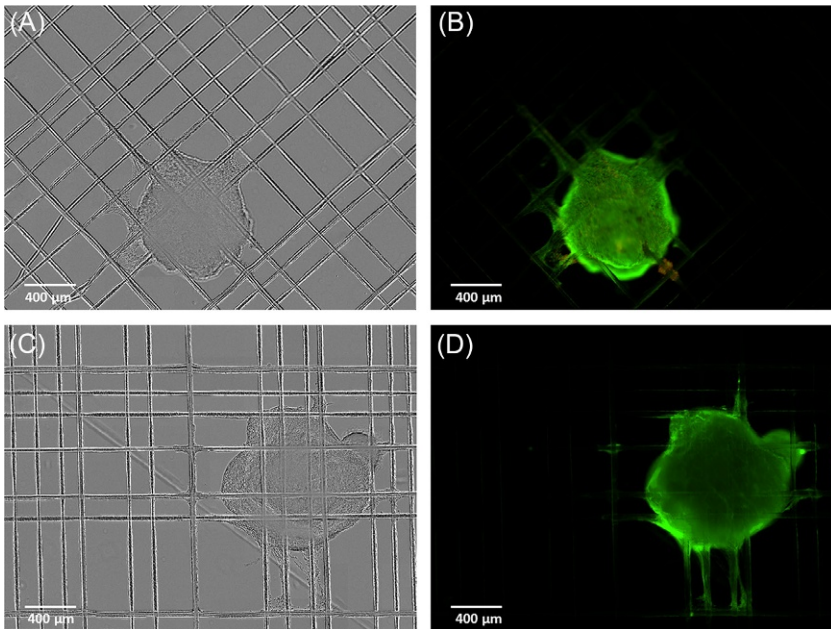


Fig. 5.2 Neural progenitors seeded on biaxial aligned scaffolds fabricated using a 200 mm nozzle after 12 days of culture. (A, B) Bright field image and fluorescence image showing live and dead staining of cells. (C, D) Bright field image and fluorescence image showing staining for the neuronal marker Tuj-1 expressed by cells.

From Mohtaram NK, Ko J, King C, Sun L, Muller N, Jun MB, et al. Electrospun biomaterial scaffolds with varied topographies for neuronal differentiation of human-induced pluripotent stem cells. *J Biomed Mater Res A* 2015;103(8):2591–601.

5.3.2 Muscle tissue

While muscle has an inherent regenerative capacity, severe injuries can necessitate the generation of artificial replacements [61]. Additionally, such substitutes could be used to treat musculoskeletal disorders [62]. It is possible to engineer such replacement tissues by seeding melt electrospun scaffolds with cells. In one of the pioneering studies on melt electrospinning-based tissue engineering, Dalton and colleagues showed that scaffolds consisting of a blend of PEO-block-PCL and pure PCL could be melt electrospun onto fibroblasts and influence their behavior [48]. The fibroblasts shift from a flat morphology to a spindle-like morphology similar to that observed in muscle tissue. A follow-up study fully characterized the effects of temperature and molecular weight of these copolymers consisting of PEG-b-PCL on the morphology of the resulting melt electrospun scaffolds [49]. Additional work indicated that the flow rate of the melt influences fiber quality during the process and confirmed that fiber morphology influenced fibroblast morphology [42]. Other work in soft tissue engineering from the Ratner and Sanders groups showed that different polyurethane blends could successfully be melt electrospun into 3-D structures [63]. These 3-D polyurethane scaffolds could support the growth of human fetal foreskin fibroblasts when coated with fibronectin. These studies all provide excellent examples of how melt electrospinning can be applied to engineering muscle tissue.

5.3.3 Cartilage tissue

Cartilage serves as connective tissue that links together bones, which is often found at joints [64]. It plays a vital role in allowing bone to bear weight while reducing the effects of friction. Cartilage contains cells called chondrocytes, which have a low regenerative potential—making it a difficult tissue to repair without surgical intervention [65]. Park and colleagues used a direct deposition melt electrospinning set-up to fabricate dual-scale fibrous scaffolds for applications in engineering cartilage tissue [41]. They used computer-aided design to control the fiber size, the pore size, and interconnectivity to ensure the scaffolds would mimic the ECM. They spun blended PCL/collagen nanofibers onto the PCL melt electrospun microfiber scaffolds, which enabled successful chondrocyte adhesion and growth. These results are important as chondrocytes can be hard to culture in manner that maintains their biological function. Also, the use of dual-scale scaffolds enabled melt electrospun scaffolds to be combined with protein functionalization, extending the utility of these scaffolds.

5.3.4 Bone tissue

Bone tissue plays an important role in supporting the body, and these tissues are often damaged. Electrospinning can be used to fabricate substitutes for damaged bone tissue [66]. For example, 3-D PCL melt electrospun microfibers that were further functionalized with silk could support the adhesion and survival of mesenchymal stem cells, which could be further extended for applications in bone tissue engineering [67]. In a similar approach, Kim et al. showed the melt electrospun PCL fibers could be coated with silk nanofibers to create a composite scaffold that supported human

mesenchymal stem cell growth and differentiation [68]. This study showed that silk nanofiber content correlated with bone regeneration in a rabbit bone defect model. Yeo and colleagues were able to melt electrospun 3-D microfiber scaffolds from a PCL- β -tricalcium phosphate mix, which they then coated with collagen nanofibers [50]. These novel scaffolds presented favorable conditions for the culture of osteoblast-like cells compared with scaffolds without the collagen nanofibers present. In 2009, Brown et al. showed that tubular scaffolds fabricated from PCL could support both human and mouse osteoblasts as a way to engineer bone tissue [69]. In this case, advanced collection methods were used to fabricate the tubular structures from the melt electrospun fibers.

The Woodruff group published a set of papers showing that strontium-substituted bioactive glass could be successfully incorporated in PCL melts to produce scaffolds for bone regeneration [51,53]. These scaffolds had an interconnected porous architecture and could support the culture of mouse preosteoblasts cells. The incorporation of the strontium-substituted bioactive glass further enhanced the alkaline phosphate activity of the cells seeded on these novel scaffolds, indicating proper cell function (Fig. 5.3). A similar process was used to generate bone tissue for periodontal applications by the Hutmacher group [52]. They produced a biphasic scaffold using melt electrospinning, which was coated in calcium phosphate followed by seeding with osteoblasts. The construct was cultured in vitro for 6 weeks before implantation into the periodontal ligament sheets of athymic mice where they became vascularized and attached at the dentin interface.

5.3.5 Skin tissue

Using allografts and autografts to replace damaged regions of the skin cannot keep up with the high demand for such tissues. As a result, researchers have turned to biomaterial-based strategies to generate replacements [70]. Electrospinning scaffolds provide a popular strategy for generating replacements for damaged skin as it can generate the high levels of porosity needed to support dermal fibroblasts [71]. Work by Farrugia et al. has shown that 3-D PCL melt electrospun scaffolds can be generated with a high degree of porosity (87%) when using the direct writing method [72]. Not only did dermal fibroblasts infiltrate and survive inside of these scaffolds, but also they began to deposit ECM proteins, including type I collagen and fibronectin. The end goal of such work would be to use this combination of a novel 3-D directly written scaffold seeded with dermal fibroblasts to repair damaged skin tissue.

5.3.6 Tendon tissue

Tendons serve as the tissues that connect muscle to bone, and their structure reflects this function [62]. An et al. were able to mimic the structural components of tendons by using melt electrospinning to make bundles of fibers [73]. These scaffolds supported human dermal cell attachment and survival for 7 days. These scaffolds were then evaluated in an Achilles tendon rabbit model. Once these scaffolds were implanted in vivo, they were infiltrated by tendon tissue after a month, and the resulting tissue appeared to align in a manner similar to healthy tissue. Most of the aforementioned

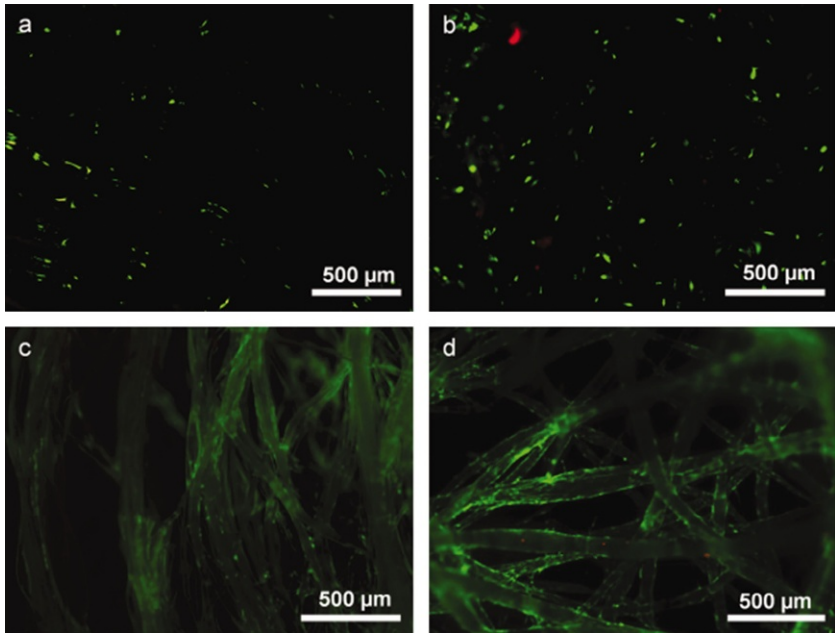


Fig. 5.3 Live/dead staining of MC3T3 osteoblast precursor cells cultured on melt electrospun scaffolds. (A) PCL and (B) PCL-strontium-substituted bioactive glass (SrBG) after 1-day culture, and (C) PCL and (D) PCL-SrBG are after 7-day culture. *Green* fluorescence indicates live cells, while *red* fluorescence indicates dead cells.

From Ren J, Blackwood KA, Doustgani A, Poh PP, Steck R, Stevens MM, et al.

Melt-electrospun polycaprolactone strontium-substituted bioactive glass scaffolds for bone regeneration. *J Biomed Mater Res A* 2014;102(9):3140–53.

studies in this chapter discuss the use of PCL for melt electrospinning engineered scaffolds. However, a collaboration between the Amsden, Dalton, and Groll groups recently showed that the photo cross-linkable polymer—poly(LLA-*ε*-CL-AC)—could be melt electrospun into scaffolds for tissue engineering applications [54]. These scaffolds have higher strength than the typical melt electrospun scaffolds and could be used for engineering tissue similar to that found in tendons.

5.4 Future directions for the field of melt electrospinning and potential commercial applications

Overall, this chapter has reviewed a number of exciting studies detailing how melt electrospinning can be used to engineering a wide variety of tissues. However, much of the potential of melt electrospun scaffolds remains to be unlocked. For example, a recent study demonstrated how such defined 3-D melt electrospun scaffolds could be combined with gelatin-methyl acrylate hydrogels to engineer cartilage [74]. This approach enabled researchers to take advantage of the properties of hydrogels while

getting the structural benefits of melt electrospinning. This combinatorial approach can better replicate the structures and complexity found in native tissue. Another recent study showed it was feasible to directly write melt electrospun scaffolds onto paper [75], which further promises to expand the field by making such scaffolds easier to fabricate and extending the potential methods for collection of the melt fibers extruded.

Translating melt electrospun scaffolds for commercial applications would be the next logical step based on the current state of research in this field. Though no melt electrospun scaffolds are currently available on the market, setups for melt electrospinning can be purchased from the company Spraybase. However, scaffold production using melt electrospinning would benefit from the reproducibility of the process and the ability to print such scaffolds in a high-throughput manner by controlling the method of collection. Based on the studies detailed in this chapter, it is likely that commercial products could be made by printing cell culture substrates with different topographies in the near future. Tissue-engineered products combining cells with melt electrospun scaffolds would require more effort to commercialize.

Despite these significant advances in recent years, a number of challenges still remain when using melt electrospinning. One of the major areas for future research involves evaluating a wider range of natural and synthetic polymers for melt electrospinning applications. Also, obtaining nanoscale-level resolution of fibers would further enhance melt electrospinning's attractiveness compared with less precise control offered by solution electrospinning. Another challenge is obtaining successful incorporation of heat-sensitive, bioactive molecules, such as proteins, into such scaffolds. Determining methods that allow melt electrospun scaffolds to release bioactive proteins would represent a significant advance over the current technology. It might be feasible to use a type of coaxial electrospinning or develop an encapsulation strategy for achieving this goal. Further evaluation of the compatibility of these scaffolds with pluripotent stem cells would also be beneficial as these cells can be used to engineer any type of tissue. In particular, the ability to generate patient-specific-induced pluripotent stem cell lines makes it possible to engineer tissue from a patient's own cells [60], which is an attractive option for clinical applications in tissue engineering. Finally, as with all of tissue engineering, the true test of the utility of melt electrospinning will be to have these scaffolds validated for clinical applications. If such a goal was realized, melt electrospinning provides a natural avenue for high-throughput manufacturing of scaffolds for tissue engineering applications, which could also be translated for commercial applications. Overall, melt electrospinning has the potential to greatly advance the field of tissue engineering.

References

- [1] Hu J, Meng H, Li G, Ibekwe SI. A review of stimuli-responsive polymers for smart textile applications. *Smart Mater Struct* 2012;21(5):053001.
- [2] Snyder JF, Wong EL, Hubbard CW. Evaluation of commercially available carbon fibers, fabrics, and papers for potential use in multifunctional energy storage applications. *J Electrochem Soc* 2009;156(3):A215–24.

- [3] Liang D, Hsiao BS, Chu B. Functional electrospun nanofibrous scaffolds for biomedical applications. *Adv Drug Deliv Rev* 2007;59(14):1392–412.
- [4] Yetisen AK, Qu H, Manbachi A, Butt H, Dokmeci MR, Hinstroza JP, et al. Nanotechnology in textiles. *ACS Nano* 2016;10(3):3042–68.
- [5] Tamayol A, Akbari M, Annabi N, Paul A, Khademhosseini A, Juncker D. Fiber-based tissue engineering: progress, challenges, and opportunities. *Biotechnol Adv* 2013;31(5):669–87.
- [6] Jun Y, Kang E, Chae S, Lee S-H. Microfluidic spinning of micro- and nano-scale fibers for tissue engineering. *Lab Chip* 2014;14(13):2145–60.
- [7] Bhardwaj N, Kundu SC. Electrospinning: a fascinating fiber fabrication technique. *Biotechnol Adv* 2010;28(3):325–47.
- [8] Yurteri CU, Hartman RP, Marijnissen JC. Producing pharmaceutical particles via electro-spraying with an emphasis on nano and nano structured particles—a review. *KONA Powder Part J* 2010;28:91–115.
- [9] Hutmacher DW, Dalton PD. Melt electrospinning. *Chem Asian J* 2011;6(1):44–56.
- [10] Muerza-Cascante ML, Haylock D, Hutmacher DW, Dalton PD. Melt electrospinning and its technologization in tissue engineering. *Tissue Eng Part B Rev* 2015;21(2):187–202.
- [11] Ko J, Mohtaram NK, Ahmed F, Montgomery A, Carlson M, Lee PC, et al. Fabrication of poly(ϵ -caprolactone) microfiber scaffolds with varying topography and mechanical properties for stem cell-based tissue engineering applications. *J Biomater Sci Polym Ed* 2014;25(1):1–17.
- [12] Brown TD, Dalton PD, Hutmacher DW. Direct writing by way of melt electrospinning. *Adv Mater* 2011;23(47):5651–7.
- [13] Mohtaram NK, Ko J, King C, Sun L, Muller N, Jun MB, et al. Electrospun biomaterial scaffolds with varied topographies for neuronal differentiation of human-induced pluripotent stem cells. *J Biomed Mater Res A* 2015;103(8):2591–601.
- [14] Ko J, Bhullar S, Mohtaram N, Willerth S, Jun M. Using mathematical modeling to control topographical properties of poly(ϵ -caprolactone) melt electrospun scaffolds. *J Micromech Microeng* 2014;24(6):065009.
- [15] Ko J, Mohtaram NK, Lee PC, Willerth SM, Jun MB. Mathematical model for predicting topographical properties of poly(ϵ -caprolactone) melt electrospun scaffolds including the effects of temperature and linear transitional speed. *J Micromech Microeng* 2015;25(4):045018.
- [16] Wang X, Liu Y, Zhang C, An Y, He X, Yang W. Simulation on electrical field distribution and fiber falls in melt electrospinning. *J Nanosci Nanotechnol* 2013;13(7):4680–5.
- [17] Dalton PD, Muerza-Cascante ML, Hutmacher DW. Design and fabrication of scaffolds via melt electrospinning for applications in tissue engineering. In: Mitchell GR, editor. *Electrospinning: principles, practice and possibilities*. London, UK: Royal Society of Chemistry; 2015.
- [18] Agarwal S, Wendorff JH, Greiner A. Progress in the field of electrospinning for tissue engineering applications. *Adv Mater* 2009;21(32–33):3343–51.
- [19] Song J-H, Kim H-E, Kim H-W. Production of electrospun gelatin nanofiber by water-based co-solvent approach. *J Mater Sci Mater Med* 2008;19(1):95–102.
- [20] Sisson K, Zhang C, Farach-Carson MC, Chase DB, Rabolt JF. Evaluation of cross-linking methods for electrospun gelatin on cell growth and viability. *Biomacromolecules* 2009;10(7):1675–80.
- [21] Xie J, Macewan MR, Willerth SM, Li X, Moran DW, Sakiyama-Elbert SE, et al. Conductive core-sheath nanofibers and their potential application in neural tissue engineering. *Adv Funct Mater* 2009;19(14):2312–8.
- [22] Xie J, Willerth SM, Li X, Macewan MR, Rader A, Sakiyama-Elbert SE, et al. The differentiation of embryonic stem cells seeded on electrospun nanofibers into neural lineages. *Biomaterials* 2009;30(3):354–62.

- [23] Agbay A, Mohtaram NK, Willerth SM. Controlled release of glial cell line-derived neurotrophic factor from poly(epsilon-caprolactone) microspheres. *Drug Deliv Transl Res* 2014;4(2):159–70.
- [24] Pham QP, Sharma U, Mikos AG. Electrospun poly(epsilon-caprolactone) microfiber and multilayer nanofiber/microfiber scaffolds: characterization of scaffolds and measurement of cellular infiltration. *Biomacromolecules* 2006;7(10):2796–805.
- [25] Prabakaran M, Jayakumar R, Nair S. Electrospun nanofibrous scaffolds-current status and prospects in drug delivery. In: *Biomedical applications of polymeric nanofibers*. New York: Springer; 2011. p. 241–62.
- [26] Mohtaram NK, Montgomery A, Willerth SM. Biomaterial-based drug delivery systems for the controlled release of neurotrophic factors. *Biomed Mater* 2013;8(2):022001.
- [27] Ji W, Sun Y, Yang F, van den Beucken JJ, Fan M, Chen Z, et al. Bioactive electrospun scaffolds delivering growth factors and genes for tissue engineering applications. *Pharm Res* 2011;28(6):1259–72.
- [28] Mohtaram N, Ko J, Agbay A, Rattray D, Neill P, Rajwani A, et al. Development of a glial cell-derived neurotrophic factor-releasing artificial dura for neural tissue engineering applications. *J Mater Chem B* 2015;3(40):7974–85.
- [29] Oliveira C, Costa-Pinto AR, Reis RL, Martins A, Neves NM. Biofunctional nanofibrous substrate comprising immobilized antibodies and selective binding of autologous growth factors. *Biomacromolecules* 2014;15(6):2196–205.
- [30] Yarin A. Coaxial electrospinning and emulsion electrospinning of core-shell fibers. *Polym Adv Technol* 2011;22(3):310–7.
- [31] Sell SA, Wolfe PS, Garg K, McCool JM, Rodriguez IA, Bowlin GL. The use of natural polymers in tissue engineering: a focus on electrospun extracellular matrix analogues. *Polymers* 2010;2(4):522–53.
- [32] Li M, Mondrinos MJ, Gandhi MR, Ko FK, Weiss AS, Lelkes PI. Electrospun protein fibers as matrices for tissue engineering. *Biomaterials* 2005;26(30):5999–6008.
- [33] Beachley V, Wen X. Effect of electrospinning parameters on the nanofiber diameter and length. *Mater Sci Eng C* 2009;29(3):663–8.
- [34] Jacobs V, Anandjiwala RD, Maaza M. The influence of electrospinning parameters on the structural morphology and diameter of electrospun nanofibers. *J Appl Polym Sci* 2010;115(5):3130–6.
- [35] Mohtaram NK, Ko J, Montgomery A, Carlson M, Sun L, Wong A, et al. Multifunctional electrospun scaffolds for promoting neuronal differentiation of induced pluripotent stem cells. *J Biomater Tissue Eng* 2014;4(11):906–14.
- [36] Vaquette C, Cooper-White J. The use of an electrostatic lens to enhance the efficiency of the electrospinning process. *Cell Tissue Res* 2012;347(3):815–26.
- [37] Dalton PD, Klinkhammer K, Salber J, Klee D, Moller M. Direct in vitro electrospinning with polymer melts. *Biomacromolecules* 2006;7(3):686–90.
- [38] Lyons J, Li C, Ko F. Melt-electrospinning part I: processing parameters and geometric properties. *Polymer* 2004;45(22):7597–603.
- [39] Hochleitner G, Jüngst T, Brown TD, Hahn K, Moseke C, Jakob F, et al. Additive manufacturing of scaffolds with sub-micron filaments via melt electrospinning writing. *Biofabrication* 2015;7(3):035002.
- [40] Ristovski N, Bock N, Liao S, Powell SK, Ren J, Kirby GT, et al. Improved fabrication of melt electrospun tissue engineering scaffolds using direct writing and advanced electric field control. *Biointerphases* 2015;10(1):011006.
- [41] Park SH, Kim TG, Kim HC, Yang DY, Park TG. Development of dual scale scaffolds via direct polymer melt deposition and electrospinning for applications in tissue regeneration. *Acta Biomater* 2008;4(5):1198–207.

- [42] Dalton PD, Joergensen NT, Groll J, Moeller M. Patterned melt electrospun substrates for tissue engineering. *Biomed Mater* 2008;3(3):034109.
- [43] McCann JT, Marquez M, Xia Y. Melt coaxial electrospinning: a versatile method for the encapsulation of solid materials and fabrication of phase change nanofibers. *Nano Lett* 2006;6(12):2868–72.
- [44] Martínez-Sanz M, Lopez-Rubio A, Lagaron JM. Optimization of the dispersion of unmodified bacterial cellulose nanowhiskers into polylactide via melt compounding to significantly enhance barrier and mechanical properties. *Biomacromolecules* 2012; 13(11):3887–99.
- [45] Nagy ZK, Balogh A, Dravavolgyi G, Ferguson J, Pataki H, Vajna B, et al. Solvent-free melt electrospinning for preparation of fast dissolving drug delivery system and comparison with solvent-based electrospun and melt extruded systems. *J Pharm Sci* 2013;102(2): 508–17.
- [46] Balogh A, Dravavolgyi G, Farago K, Farkas A, Vigh T, Soti PL, et al. Plasticized drug-loaded melt electrospun polymer mats: characterization, thermal degradation, and release kinetics. *J Pharm Sci* 2014;103(4):1278–87.
- [47] Balogh A, Farkas B, Farago K, Farkas A, Wagner I, Van Assche I, et al. Melt-blown and electrospun drug-loaded polymer fiber mats for dissolution enhancement: a comparative study. *J Pharm Sci* 2015;104(5):1767–76.
- [48] Dalton PD, Lleixà Calvet J, Mourran A, Klee D, Möller M. Melt electrospinning of poly-(ethylene glycol-block- ϵ -caprolactone). *Biotechnol J* 2006;1(9):998–1006.
- [49] Dalton PD, Lleixa Calvet J, Mourran A, Klee D, Moller M. Melt electrospinning of poly-(ethylene glycol-block- ϵ -caprolactone). *Biotechnol J* 2006;1(9):998–1006.
- [50] Yeo M, Lee H, Kim G. Three-dimensional hierarchical composite scaffolds consisting of polycaprolactone, β -tricalcium phosphate, and collagen nanofibers: fabrication, physical properties, and in vitro cell activity for bone tissue regeneration. *Biomacromolecules* 2010;12(2):502–10.
- [51] Ren J, Blackwood KA, Doustgani A, Poh PP, Steck R, Stevens MM, et al. Melt-electrospun polycaprolactone-strontium substituted bioactive glass scaffolds for bone regeneration. *J Biomed Mater Res A* 2013;102(9):3140–53.
- [52] Costa PF, Vaquette C, Zhang Q, Reis RL, Ivanovski S, Hutmacher DW. Advanced tissue engineering scaffold design for regeneration of the complex hierarchical periodontal structure. *J Clin Periodontol* 2014;41(3):283–94.
- [53] Ren J, Blackwood KA, Doustgani A, Poh PP, Steck R, Stevens MM, et al. Melt-electrospun polycaprolactone strontium-substituted bioactive glass scaffolds for bone regeneration. *J Biomed Mater Res A* 2014;102(9):3140–53.
- [54] Chen F, Hochleitner G, Woodfield T, Groll J, Dalton PD, Amsden BG. Additive manufacturing of a photo-cross-linkable polymer via direct melt electrospinning writing for producing high strength structures. *Biomacromolecules* 2016;17(1):208–14.
- [55] Atala A. Engineering tissues and organs. *Curr Opin Urol* 1999;9(6):517–26.
- [56] Khetani SR, Bhatia SN. Engineering tissues for in vitro applications. *Curr Opin Biotechnol* 2006;17(5):524–31.
- [57] Schmidt CE, Leach JB. Neural tissue engineering: strategies for repair and regeneration. *Annu Rev Biomed Eng* 2003;5(1):293–347.
- [58] Willerth SM, Sakiyama-Elbert SE. Approaches to neural tissue engineering using scaffolds for drug delivery. *Adv Drug Deliv Rev* 2007;59(4):325–38.
- [59] Chew SY, Wen J, Yim EK, Leong KW. Sustained release of proteins from electrospun biodegradable fibers. *Biomacromolecules* 2005;6(4):2017–24.
- [60] Willerth SM. Neural tissue engineering using embryonic and induced pluripotent stem cells. *Stem Cell Res Ther* 2011;2(2):17.

- [61] Wolf MT, Dearth CL, Sonnenberg SB, Lobo EG, Badylak SF. Naturally derived and synthetic scaffolds for skeletal muscle reconstruction. *Adv Drug Deliv Rev* 2015;84:208–21.
- [62] Rodrigues MT, Reis RL, Gomes ME. Engineering tendon and ligament tissues: present developments towards successful clinical products. *J Tissue Eng Regen Med* 2013;7(9):673–86.
- [63] Karchin A, Simonovsky FI, Ratner BD, Sanders JE. Melt electrospinning of biodegradable polyurethane scaffolds. *Acta Biomater* 2011;7(9):3277–84.
- [64] Camarero-Espinosa S, Rothen-Rutishauser B, Foster EJ, Weder C. Articular cartilage: from formation to tissue engineering. *Biomater Sci* 2016;4(5):734–67.
- [65] Zhang W, Ouyang H, Dass CR, Xu J. Current research on pharmacologic and regenerative therapies for osteoarthritis. *Bone Res* 2016;4:15040.
- [66] Ghasemi-Mobarakeh L, Prabhakaran MP, Balasubramanian P, Jin G, Valipouri A, Ramakrishna S. Advances in electrospun nanofibers for bone and cartilage regeneration. *J Nanosci Nanotechnol* 2013;13(7):4656–71.
- [67] Yoon H, Ahn S, Kim G. Three-dimensional polycaprolactone hierarchical scaffolds supplemented with natural biomaterials to enhance mesenchymal stem cell proliferation. *Macromol Rapid Commun* 2009;30(19):1632–7.
- [68] Kim BS, Park KE, Kim MH, You HK, Lee J, Park WH. Effect of nanofiber content on bone regeneration of silk fibroin/poly(epsilon-caprolactone) nano/microfibrous composite scaffolds. *Int J Nanomedicine* 2015;10:485–502.
- [69] Brown TD, Slotosh A, Thibaudeau L, Taubenberger A, Loessner D, Vaquette C, et al. Design and fabrication of tubular scaffolds via direct writing in a melt electrospinning mode. *Biointerphases* 2012;7(1–4):13.
- [70] Priya SG, Jungvid H, Kumar A. Skin tissue engineering for tissue repair and regeneration. *Tissue Eng B Rev* 2008;14(1):105–18.
- [71] Zhu X, Cui W, Li X, Jin Y. Electrospun fibrous mats with high porosity as potential scaffolds for skin tissue engineering. *Biomacromolecules* 2008;9(7):1795–801.
- [72] Farrugia BL, Brown TD, Upton Z, Hutmacher DW, Dalton PD, Dargaville TR. Dermal fibroblast infiltration of poly(epsilon-caprolactone) scaffolds fabricated by melt electrospinning in a direct writing mode. *Biofabrication* 2013;5(2):025001.
- [73] An J, Chua CK, Leong KF, Chen CH, Chen JP. Solvent-free fabrication of three dimensionally aligned polycaprolactone microfibers for engineering of anisotropic tissues. *Biomed Microdevices* 2012;14(5):863–72.
- [74] Visser J, Melchels FP, Jeon JE, van Bussel EM, Kimpton LS, Byrne HM, et al. Reinforcement of hydrogels using three-dimensionally printed microfibres. *Nat Commun* 2015;6:6933.
- [75] Luo G, Teh KS, Liu Y, Zang X, Wen Z, Lin L. Direct-write, self-aligned electrospinning on paper for controllable fabrication of three-dimensional structures. *ACS Appl Mater Interfaces* 2015;7(50):27765–70.

Resource List

Dr. Paul Dalton's website on melt electrospinning: <http://daltonlab.com/electrospinning-writing/>.

In vivo safety evaluations of electrospun nanofibers for biomedical applications

6

B. Balusamy, A. Senthamizhan, T. Uyar
Bilkent University, Ankara, Turkey

6.1 Introduction

Electrospinning has emerged as one of the most attractive processing techniques to produce nanoscale fibers that can closely mimic the extracellular matrix (ECM) components and to stimulate the natural functionalization of the cells. Electrospun nanofibers of various natural and synthetic polymers were extensively investigated for their potential in biomedical and pharmaceutical applications especially for skin tissue engineering, wound healing, and controlled drug delivery. The nanofibers have unique properties including high surface area and enhanced cellular interactions and protein absorption for facilitating binding sites of cell receptors. They have been highlighted as promising materials for cartilage, bone, vascular, bladder, and tissue engineering applications [1]. To date, numerous clinical applications of electrospun nanofibers are being considered, and thereby, concerns on the safety of these nanofibrous membranes are significantly increased. The nanotoxicology research is mainly foreseeable to address the requirements of regulatory agencies including US Food and Drug Administration (US FDA) and also biosafety needs. Cipitria et al. [2] reviewed and presented the biocompatibility characteristics of poly(ϵ -caprolactone) (PCL) electrospun nanofibers.

Biocompatibility is generally defined as the compatible nature of any foreign agents with living system or tissue not causing any toxic effects and immunologic rejection and physiologically reactive. The biocompatibility evaluation of a material is generally critical due to their variations in intended use, nature of body, time, and duration. The biocompatible material should not cause any adverse effects including local or systemic, genotoxicity, and developmental toxicity either directly or due to their leachable chemicals. Therefore, the safety of a material that is intended for human use should be systematically investigated in accordance to well-established standard testing guidelines to fulfill the requirements regulatory agencies.

The biological evaluation of a material that is intended for human use shall take part in structured biological evaluation program within a risk management process according to the International Organization for Standardization (ISO) ISO 14971:2007 [3], which particularly addresses the risks associated with medical devices. The ISO (10993-1:2010) [4] standard addresses the biological evaluation

of medical devices with a series of testing guidelines to deal with a range of possible short-term effects such as acute toxicity; irritation in the skin, eye, and mucous membranes; thrombogenicity; and hemolysis. And also, the standard addresses long-term/specific toxic effects such as subchronic and chronic effects, sensitization, genotoxicity, tumorigenicity, and teratogenicity using various preclinical studies. Following the successful completion of preclinical evaluations, clinical studies in two main types (i) clinical trials (interventional studies) and (ii) observational are conducted in human volunteers to add medical knowledge, which should be in compliance with regulatory agency.

Although numerous *in vitro* studies have been devoted to investigate the safety of nanofibrous membranes, the rationale of investing in *in vivo* safety studies is comparatively lesser, which obviously slows down further the progress of bedside research [5,6]. However, the true effects of a testing material cannot be proved only through animal models, and clinical studies will play vital role in conforming the findings in humans. This chapter highlighted about the *in vivo* studies conducted on electrospun nanofibers that are used for various applications and their toxicity outcomes. And also, the chapter discusses about the clinical trials conducted using electrospun nanofibers. We made an effort to provide overview on both cases rather than presenting an in-depth literature survey.

6.2 Safety evaluations of nanofibers

6.2.1 *In vivo studies in animal models*

The exceptional characteristics of electrospun nanofibrous membrane show an excellent *in vitro* performance in terms of cell attachment, spreading, and differentiation. The reason for the tremendous growth of electrospun scaffolds in biomedical applications might be due to three main variables: (1) fiber diameter, (2) chemistry, and (3) fiber orientation. However, although electrospun materials show excellent cell and tissue response, a major drawback is their poor mechanical properties, thought to be critical to the success of the surgical repair of tendons. Hakimi et al. [7] developed a bonding technique that enables the processing of electrospun sheets into multilayered, robust, implantable fabrics. The tissue reaction to the patch after implantation in a rat's shoulder is assessed. This animal study was performed to demonstrate safety rather than efficacy of the layered design. Preliminary *in vivo* evaluation of the assembled patch was carried out for periods of 1, 2, 4, 6, and 12 weeks.

Fig. 6.1 shows the proposed possible mechanism by which the scaffold may be integrated *in vivo*, based on gross and histological observation. During the first 4 weeks, it is proposed that cells surrounding the scaffold respond to the morphology of the electrospun layer to align along the nanofibers. At the next phase, around 4–6 weeks, the woven component is increasingly integrated by the tissue. Foreign-body giant cell numbers peak at week 4, as the electrospun component degrades, and are gradually replaced by more organized cell arrays. At the last time point, at week 12, the remaining scaffold is tightly embedded in dense tissue, inflammation is resolved, and the surrounding tissue begins to remodel. Importantly, it

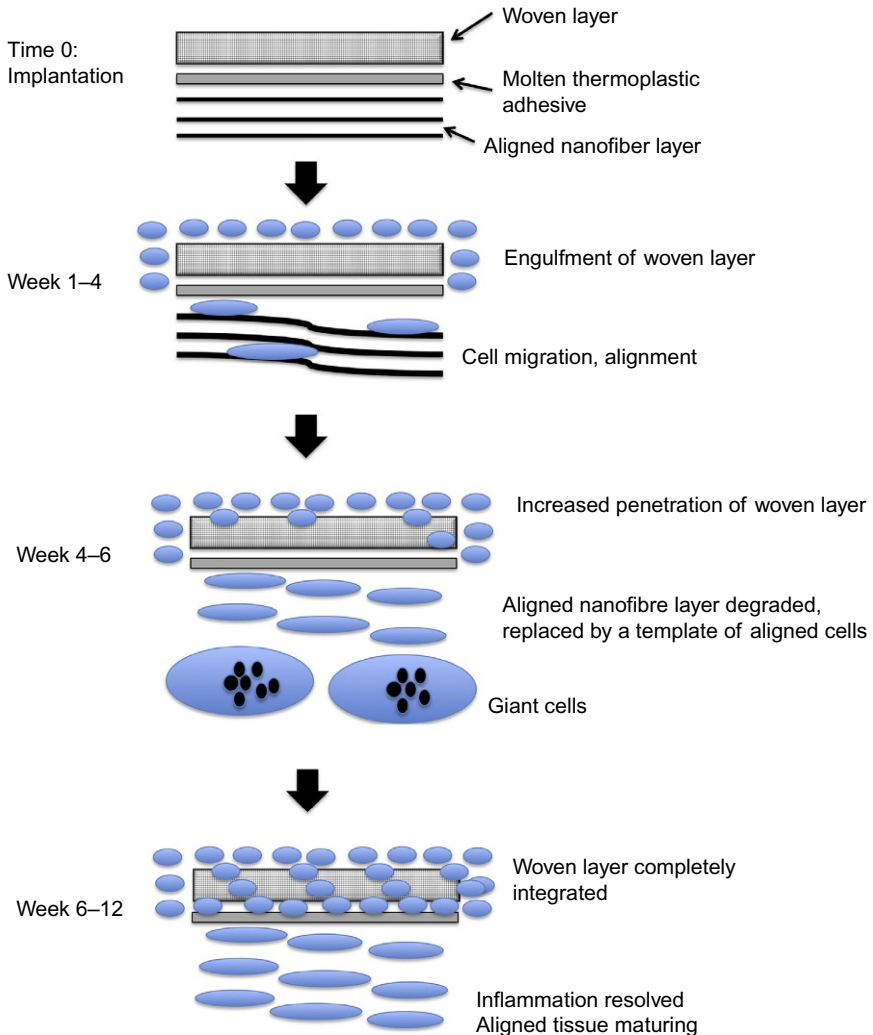


Fig. 6.1 A schematic representation of tissue reaction to the scaffold based on in vivo observations.

Reproduced with permission from Hakimi O, Mouthuy PA, Zargar N, Lostis E, Morrey M, Carr A. A layered electrospun and woven surgical scaffold to enhance endogenous tendon repair. *Acta Biomater* 2015;26:124–35, with permission from Elsevier.

should be acknowledged that this proposed mechanism is an interpretation of biocompatibility data collected in a rat model. The efficacy reported in the study is based on the animal model, and it is certain that rate and true efficacy cannot be proved in an animal model, and a clinical trial will be vital to confirm our findings in humans. These compelling results warrant further research and development of the scaffold for human application.

The bare electrospun fibrous membrane, for example, bacterial cellulose (BC), has received considerable interest as wound-dressing material. The insufficient antimicrobial activity is considered to be a critical skin-barrier function in wound healing. The additional active agents have been introduced to solve this problem so far. The strong antimicrobial activities of silver nanoparticles (AgNPs) against many different bacteria, fungi, and viruses have been known for long time. The work has been initiated to incorporate the AgNPs into the bare electrospun nanofibrous membrane. However, the adhesion of anchored nanoparticles is usually very weak. In such a case, the release of nanoparticles is quite normal, and it could cause the cellular toxicity. It has been already well reported that silver is a recognized cause of argyrosis and argyria, and high-level exposure of silver nanoparticles is toxic to mammalian cells [8].

Tseng et al. [9] developed biodegradable vancomycin-loaded poly[lactic-co-glycolic acid] (PLGA) nanofibrous membranes for vancomycin release in the cerebral tissue of rats. Following the results from in vitro drug release study, the biodegradable nanofibrous membranes embedded with vancomycin were then placed into the brain surface of rats after operative craniectomy was performed, and the characteristics of vancomycin release from the membranes in vivo were investigated. Fig. 6.2 indicated the gross wound

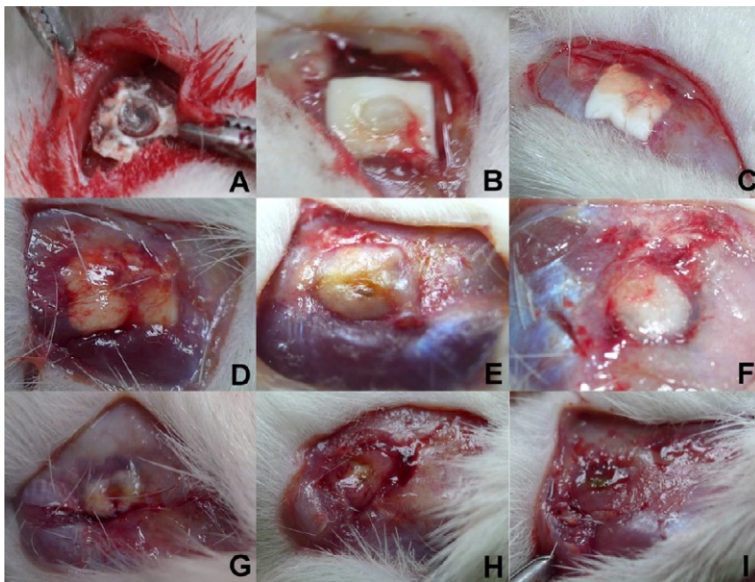


Fig. 6.2 Gross wound conditions: (A) 3 days, (B) 1 week, (C) 2 weeks, (D) 3 weeks, (E) 4 weeks, (F) 5 weeks, (G) 6 weeks, (H) 7 weeks, and (I) 8 weeks. The scalp wound and brain tissue were quite clear, and no infection (exudate, pus, or granulation formation) was noticed during the whole experimental period. By week 8, the PLGA/vancomycin nanomembranes were nearly completely dissolved.

Reproduced with permission from Tseng YY, Kao YC, Liao JY, Chen WA, Liu SJ. Biodegradable drug-eluting poly[lactic-co-glycolic acid] nanofibers for the sustainable delivery of vancomycin to brain tissue: in vitro and in vivo studies. *ACS Chem Neurosci* 2013;4: 1314–21, with permission from American Chemical Society.

condition and gradual degradation of the vancomycin-loaded biodegradable PLGA nanofibrous membrane. The scalp wounds and brain tissues were clear, and no infection (exudate, pus, or granulation formation) was noticed grossly. The biodegradable PLGA/vancomycin nanofibrous membranes degraded gradually after operative implantation and were almost completely diminished by 8 weeks. The histological examination also showed no obvious inflammation reaction of the brain tissues.

Lowe et al. [10] prepared a novel acrylonitrile (AN)-based terpolymers and adopted electrospinning method to prepare nonwoven sheets of bandage/wound-dressing-type materials for storage and delivery applications of nitric oxide (NO) for wound healing, which release NO upon contact to a humidified or physiological environment that binds and releases NO. Fig. 6.3 shows the digital images of NO-treated and control-treated wounds from days 0, 7, and 14. No significant adverse effects on surrounding skin or wound margins were noted following the treatment with NO or control dressings. Further, the histopathology examinations indicated that the average capillary density was significantly higher at $\sim 60\%$ for the NO-treated wounds as compared with control-treated wounds. They further suggested that daily bandage changes will significantly enhance healing progression as soon as 4 days. In this novel, NO dressings are easy to apply and change, thus making multiple applications each week possible.

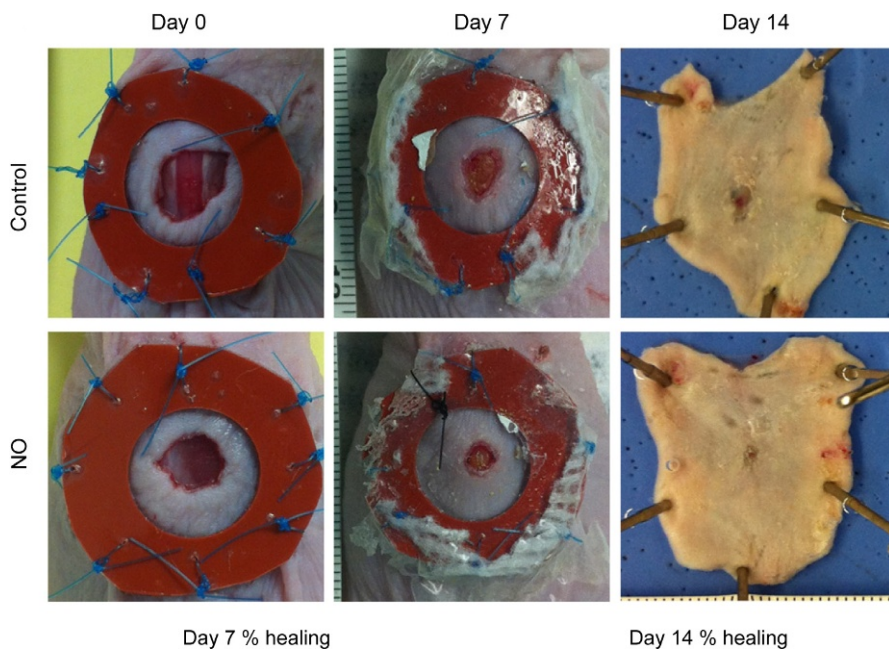


Fig. 6.3 Weekly administration of NO-releasing dressings improves wound closure. Representative digital images of NO and control wounds at days 0, 7, and 14 in the first study. Images are presented at equivalent scale.

Reproduced with permission from Lowe A, Bills J, Verma R, Lavery L, Davis K, Balkus KJ. Electrospun nitric oxide releasing bandage with enhanced wound healing. *Acta Biomater* 2015;13: 121–30, with permission from Elsevier.

The study demonstrated the compatibility of NO of incorporating the electrospun nanofibers in breached skin of the mouse.

The insufficient concentration and nonspecific distribution of the antitumor drugs are the major limitations of the conventional tumor chemotherapy. In the recent past, research has been shown that biodegradable electrospun nanofibers are considered as very promising drug carriers for localized and controlled delivery of antitumor drugs. This might be due the following reasons: biodegradable carriers capable of undergoing gradual decomposition into carbon dioxide, water, and finally disappearing *in vivo*; maximization of local drug concentration in the immediate tumor environment and minimization of nontarget organ toxicity; delayed release of the drugs at cytotoxic concentrations that are sustained for longer periods at much lower total doses than can be achieved with typical systemic chemotherapeutic regimes; increase in the duration of tumor exposure to the drug; reduction of the frequency of drug administration; and convenience of being cut to almost any size and fabricated into other shapes using different target geometries for clinical applications [11,12]. Liu et al. [11] demonstrated the possibility and feasibility of nanofiber-based local drug delivery system and low-cost therapeutic option supplementary to currently limited clinical protocols for patients with hepatocellular carcinoma (HCC) or secondary hepatic carcinoma (SHCC). The therapeutic process of nanofibers in the treatment of mice is shown in Fig. 6.4.

The doxorubicin hydrochloride (Dox) was chosen as model of antitumor drug due to their broad spectrum antitumor activity and fluorescent property suitable for *in vivo* tracing. The *in vivo* antitumor efficacy of Dox fibers was studied in Balb/c mice

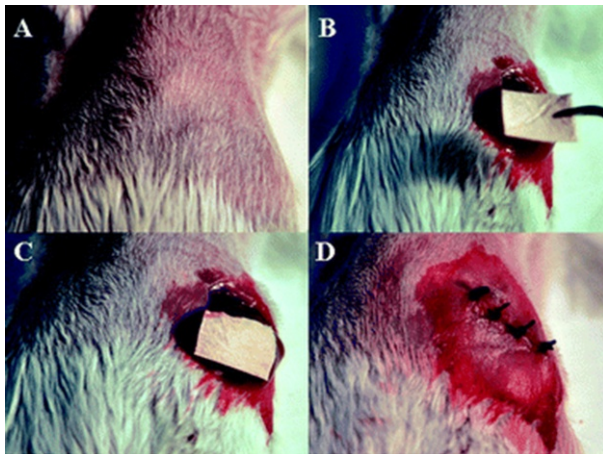


Fig. 6.4 Therapeutic process of nanofibers in the treatment of mice: (A) anesthetization of mice, (B) exposure of the liver after laparotomy, (C) direct placement of drug-loaded nanofibers on the tumor site, and (D) abdominal closure.

Reproduced with permission from Liu S, Zhou G, Liu D, Xie Z, Huang Y, Wang X, Wu W, Jing X. Inhibition of orthotopic secondary hepatic carcinoma in mice by doxorubicin-loaded electrospun polylactide nanofibers. *J Mater Chem* 2013;B1: 101–9, with permission from Royal Society of Chemistry.

bearing nodular SHCC (NSHCC). Seven days after the cell injection, whitish and irregular tumor nodules were observed in the liver lobe during explorative laparotomy of the mice as clearly seen in Fig. 6.5A. After the identification of NSHCC, a 6% Dox fiber-mat of required size and shape was placed on the surface of the tumor nodule. Although the animals underwent second surgery within a week, they soon returned to their preoperative physical state. On day 30, all animals were still alive. Then, they were sacrificed and their livers were harvested. Macroscopic observation showed that most of the livers (5/6) in Dox fibers group displayed the appearance of normal liver tissue except the tumor site covered by the fiber-mat (Fig. 6.5B), whereas the tumor nodule was big and took a quite fraction of the liver in the control group (Fig. 6.5C). Pasting of 6% Dox fibers did cause a statistically marked reduction in tumor burden in the liver ($P < .01$), the ratio of aspartate aminotransferase over alanine transaminase in serum (AST/ALT), a clinical indicator used in differentiating between causes of liver damage, $P < .01$, and the AST activities ($P < .05$) compared with those of the control group (Fig. 6.5D).

Jiang et al. [13] fabricated a three-dimensional aligned layer-by-layer nanofibrous scaffold by incorporation of poly(ϵ -caprolactone)-poly(ethylene glycol) (PCE) copolymer nanofibers into porous chitosan (CHI) to dictate the oriented regeneration of periodontium with aligned periodontal ligament (PDL) fibers perpendicular to the root surface. In vivo evaluation of the prepared scaffolds was conducted in rats (Sprague-Dawley) model having periodontal defects in four groups. The surgical process performed during the study is presented in Fig. 6.6. Two months following

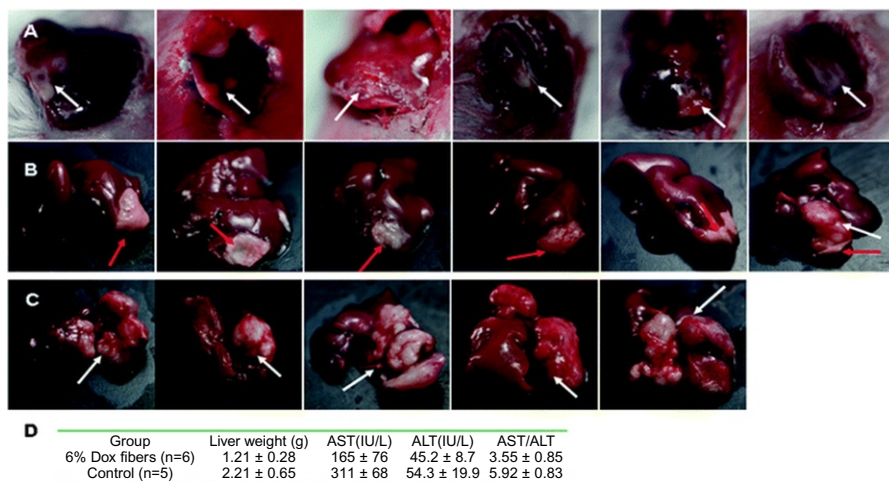


Fig. 6.5 Dox fibers inhibited NSHCC in Balb/c mice. Photographs of NSHCC before fiber-mat placement (A), 23 days after 6% Dox fiber placement (B), and 30 days without any treatment (control) (C). The white arrow indicates the site of tumor and the red arrow indicates the site of Dox fiber-mat. (D) Antitumor effects of 6% Dox fibers in mice bearing NSHCC.

Reproduced with permission from Liu S, Zhou G, Liu D, Xie Z, Huang Y, Wang X, Wu W, Jing X. Inhibition of orthotopic secondary hepatic carcinoma in mice by doxorubicin-loaded electrospun polylactide nanofibers. *J Mater Chem* 2013;B1: 101–9, with permission from Royal Society of Chemistry.

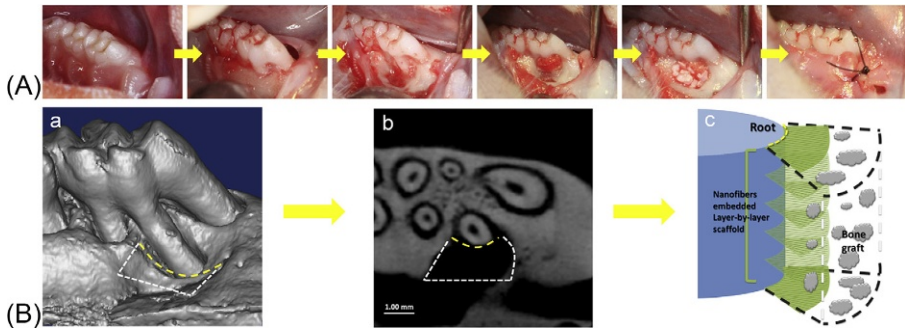


Fig. 6.6 Establishment of the rat periodontal defect model. (A) Surgical procedures of the periodontal fenestration defect at the maxillary first molar. (B) micro-CT reconstructed image scan (a), micro-CT transverse view (b), and schematic diagram (c) of the standardized defect with layers of fibers placed perpendicular against the root surface.

Reproduced with permission from Jiang W, Li L, Zhang D, Huang S, Jing Z, Wu Y, Zhao Z, Zhao L, Zhou S. Incorporation of aligned PCL–PEG nanofibers into porous chitosan scaffolds improved the orientation of collagen fibers in regenerated periodontium. *Acta Biomater* 2015;25:240–52, with permission from Elsevier.

the surgery, the ligament tissue organization from different groups was examined using hematoxylin and eosin (H&E) staining as illustrated in Fig. 6.7. The histological images show that the distinct topological structures of three scaffolds led to different morphological patterns of PDL healing. The topographic guidance of scaffolds for regenerated tissue was strong. Disorderly and unsystematic regeneration was generated in blank control group, with irregular fibers along the root surface. The fibers in porous control group were more compact than that in blank control group but were still in random arrangement. In contrast, the PCE nanofiber-embedded scaffolds (i.e., 3D-RD and 3D-AL) presented much more defined orientation of regenerated tissues, as blank arrows with dash line indicated in Fig. 6.7 A(c and d) in which the fibers of 3D-AL were more parallel and PDL-like than that of 3D-RD. Moreover, cementum-like tissue layers were deposited on the dentin surfaces in 3D-AL scaffold, as the yellow arrows indicate. The developed scaffold has a great capacity of providing topographic cues and subsequently guiding the oriented regeneration of periodontal tissue *in vivo*.

6.2.2 Clinical studies in human

Despite many efforts have been paid in recent past for developing functional nanofibers to suit different biomedical applications, the studies in clinical phase are very limited and need further insight. Kossovich et al. [14] demonstrated the preparation of chitosan/polyethylene oxide(PEO) nanofibers by electrospinning method, and clinical trial study was conducted in patients with II, IIIa, and IIIb degree burns. The nanofibrous membranes of thickness 200 μm were applied onto burns, and their wound-healing behavior was studied. The clinical trial results indicated that chitosan nanofibrous dressing reduces the pain from dressing removal, absorption of exudate, ventilation of the wound, protection from infection, and further stimulates the process of skin tissue regeneration

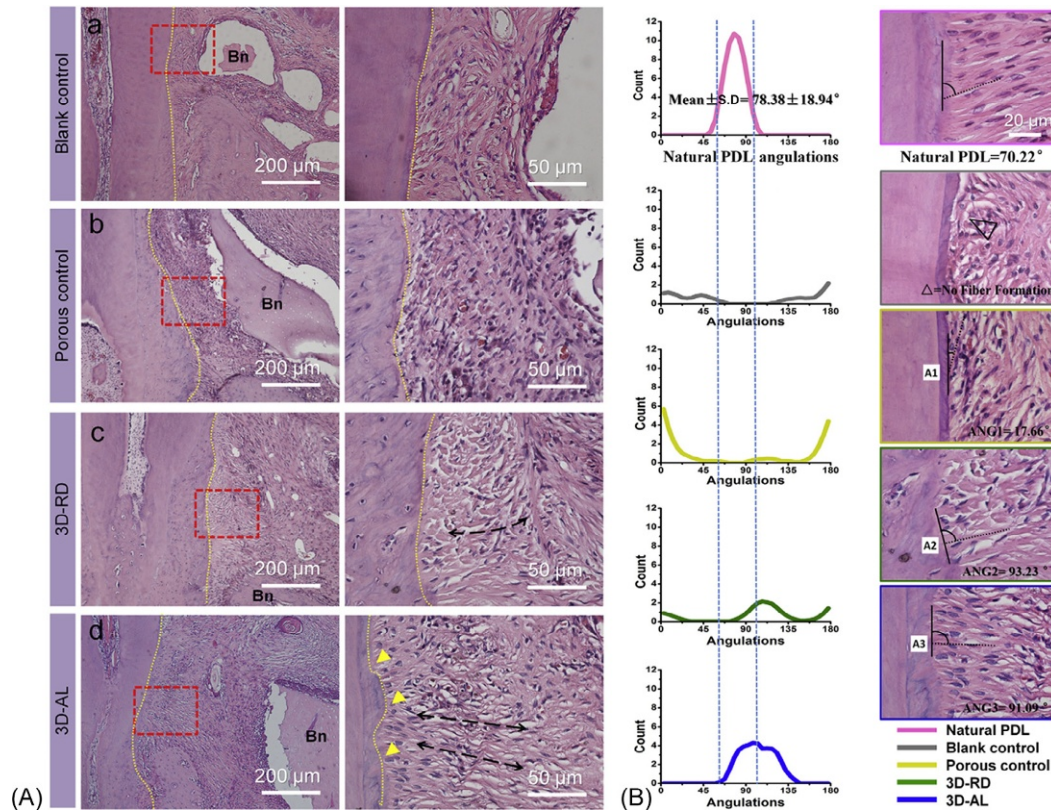


Fig. 6.7 In vivo-regenerated PDL-like tissue arrangement after 2 months. (A) Hematoxylin and eosin (H&E) staining (a–d) to determine the arrangement of PDL-like fibrous connective tissue against the root surfaces. The images on the right are higher magnifications of images in the red frames on the left. Black dash lines indicated the orientation of regenerated PDL-like tissues. Yellow arrows indicate the newly formed cementum. Green arrows indicate the intensive collagen formation against the root surfaces. (B) The angular distribution of each experimental group, compared with the natural PDL ligament as a reference (average angular value = $78.38 \pm 18.94^\circ$), and the angular values of each representative image: natural PDL, no fiber formation, and angulated ligament tissues.

Reproduced with permission from Jiang W, Li L, Zhang D, Huang S, Jing Z, Wu Y, Zhao Z, Zhao L, Zhou S. Incorporation of aligned PCL–PEG nanofibers into porous chitosan scaffolds improved the orientation of collagen fibers in regenerated periodontium. *Acta Biomater* 2015;25:240–52, with permission from Elsevier.

(Figs. 6.8 and 6.9). Further, the degradation of this fibrous membrane prevents the mechanical damage of wound during removing dressings.

It is worth to note that few electrospun nanofibrous products are commercialized. The AVflo is a CE-certified electrospun nanofibrous-based polyurethane vascular access graft developed by Nicast Ltd, Israel, which is currently available in Asian countries, European Union market, and Israel [15]. The clinical trial studies of AVflo were conducted in patients and well reported [16]. The company is in further progress of developing nanofiber-based products such as nanostructured bioactive small-diameter vascular graft, biodegradable implant toward a better therapy for visual sensory impairments, biomimetic nanofiber-based nucleus pulposus regeneration for the treatment of degenerative disk disease, and NovaMesh Ventral Hernia Mesh.

Only few more efforts have been made to study the clinical effects of electrospun nanofiber-based products. The clinical trial website [17] was used to find out the list of clinical trials that were conducted on electrospun nanofiber-based products. The search results using the terms electrospinning and nanofibers are presented in Table 6.1. As summarized, the patches and nanofibers prepared by electrospinning technique were investigated in different phase studies to treat various conditions.



Fig. 6.8 Example of healing of IIIa burn: (A) sample of chitosan nanofiber dressing, (B) IIIa burn before covering, (C) after covering, (D) 5 days after covering, (E) 10 days after covering, and (F) 14 days after covering.

Reproduced with permission from Kossovich LY, Salkovskiy Y, Kirillova IV. Electrospun chitosan nanofiber materials as burn dressing. IFMBE Proc 2010;31:1212–14, with permission from Springer.



Fig. 6.9 Donor wound: (A) before covering, (B) after covering, (C) 12 days after covering, and (D) 14 days after covering.

Reproduced with permission from Kossovich LY, Salkovskiy Y, Kirillova IV. Electrospun chitosan nanofiber materials as burn dressing. IFMBE Proc 2010;31:1212–14, with permission from Springer.

Table 6.1 Summary of clinical trials conducted on electrospun nanofibers and patches

ClinicalTrials.gov Identifier:	Study title	Condition	Status
NCT00317629	Controlled Nitric Oxide Releasing Patch Versus Meglumine Antimoniate in the Treatment of Cutaneous Leishmaniasis	Cutaneous leishmaniasis	Terminated
NCT00428727	Clinical Trial for the Treatment of Diabetic Foot Ulcers Using a Nitric Oxide Releasing Patch: PATHON	Diabetic foot	Completed
NCT02237287	Combination of Taliderm [®] and Vacuum-assisted Closure (VAC) for Treatment of Pressure Ulcers	Wounds Pressure ulcer	Terminated
NCT02255188	Experimental Study of the Vascular Prosthesis Manufactured by Electrospinning	Arterial occlusive disease	Ongoing
NCT02680106	Evaluation of the SPINNER Device for the Application of Wound Dressing: Treatment of Split Skin Graft Donor Sites (SPINNER01)	Wound of skin	Ongoing

6.3 Conclusions and outlook

In this chapter, we have presented an overview on the different types of *in vivo* studies and clinical trials conducted using electrospun nanofibrous materials, which are intended for various biomedical applications. To date, there are various hindrances in transferring lab-scale research to practical applications. The use of electrospun nanofibers in clinical applications is still in its infancy because of various issues including animal use, reliable correlation between *in vitro*-*in vivo* experiments, and high cost, which need to be addressed. *In vivo* testing of electrospun nanofibers is very few when compared with *in vitro* tests. However, most of the conducted *in vivo* studies in research laboratories are mainly not in accordance with standard safety guidelines to fulfill the requirements of the regulatory agencies. There is a great interest on generating toxicity data according to well-established regulatory guidelines [18], whereas there is no standard that specifically addresses the biological evaluation of medical devices containing nanomaterials till now. But, a new standard ISO 10993-Part 22 is under development for this purpose.

Considering the toxicity evaluation of electrospun nanofibers, factors including interaction of cells and nanoscaffolds, fiber diameter and pore size, surface patterning and topography, nanofiber alignment, fiber composition-wettability, and cellular response to electrospun scaffolds play critical role in study outcome. And also, it is recommended that designing of both *in vitro* and *in vivo* toxicity studies should follow the requirements of ISO 10993-Part 1:2010 standard in which the devices are classified under three main categories such as surface device (skin, mucosal membrane, breached, or compromised surface), external communicating device (blood path indirect, tissue/bone/dentin, and circulating blood), and implant device (tissue/bone and blood) based on their contact with the human body, directly or indirectly. In addition, the type of studies to be conducted is also based on their duration of exposure with the human body in which exposure duration is categorized as limited (≤ 24 h), prolonged (24 h to 30 days), and permanent (> 30 days). Based on these factors, studies need to be conducted in line with established standards of ISO 10993. Most importantly, the FDA recommends that these studies need to be conducted in good laboratory practice (GLP) certified or ISO/IEC 17025-accredited laboratories.

Acknowledgments

B. B. acknowledges TUBITAK-BIDEB 2216, Research Fellowship Programme for Foreign Citizens for postdoctoral fellowship. A. S. acknowledges the Scientific and Technological Research Council of Turkey (TUBITAK), BIDEB 2221-Fellowships for Visiting Scientists, and Scientists on Sabbatical for the fellowship. T. U. acknowledges the Turkish Academy of Sciences-Outstanding Young Scientists Award Program (TUBA-GEBIP).

References

- [1] Zhang L, Webster TJ. Nanotechnology and nanomaterials: Promises for improved tissue regeneration. *Nano Today* 2009;4:6680.
- [2] Cipitria A, Skelton A, Dargaville TR, Dalton PD, Hutmacher DW. Design, fabrication and characterization of PCL electrospun scaffolds—a review. *J Mater Chem* 2011;21:9419–53.
- [3] ISO 14971:2007. Medical devices – Application of risk management to medical devices.
- [4] ISO 10993-1:2010. Biological evaluation of medical devices – Part 1, Evaluation and testing within a risk management process.
- [5] Goonoo N, Bhaw-Luximon A, Jhurry D. *In vitro* and *in vivo* cytocompatibility of electrospun nanofiber scaffolds for tissue engineering applications. *RSC Adv* 2014;4:31618–42.
- [6] Ong CT, Zhang Y, Lim R, Samsonraj R, Masilamani J, Phan THH, et al. Preclinical evaluation of Tegaderm™ supported nanofibrous wound matrix dressing on porcine wound healing model. *Adv Wound Care* 2015;4:110–8.
- [7] Hakimi O, Mouthuy PA, Zargar N, Lostis E, Morrey M, Carr A. A layered electrospun and woven surgical scaffold to enhance endogenous tendon repair. *Acta Biomater* 2015;26:124–35.
- [8] Rosenman KD, Moss A, Kon S. Argyria: clinical implications of exposure to silver nitrate and silver oxide. *J Occup Med* 1979;21:430–5.
- [9] Tseng YY, Kao YC, Liao JY, Chen WA, Liu SJ. Biodegradable drug-eluting poly [lactic-co-glycol acid] nanofibers for the sustainable delivery of vancomycin to brain tissue: *in vitro* and *in vivo* studies. *ACS Chem Neurosci* 2013;4:1314–21.
- [10] Lowe A, Bills J, Verma R, Lavery L, Davis K, Balkus KJ. Electrospun nitric oxide releasing bandage with enhanced wound healing. *Acta Biomater* 2015;13:121–30.
- [11] Liu S, Zhou G, Liu D, Xie Z, Huang Y, Wang X, et al. Inhibition of orthotopic secondary hepatic carcinoma in mice by doxorubicin-loaded electrospun polylactide nanofibers. *J Mater Chem B* 2013;1:101–9.
- [12] Toshkova R, Manolova N, Gardeva E, Ignatova M, Yossifova L, Rashkov I, et al. Anti-tumor activity of quaternized chitosan-based electrospun implants against Graffi myeloid tumor. *Int J Pharm* 2010;400:221–33.
- [13] Jiang W, Li L, Zhang D, Huang S, Jing Z, Wu Y, et al. Incorporation of aligned PCL–PEG nanofibers into porous chitosan scaffolds improved the orientation of collagen fibers in regenerated periodontium. *Acta Biomater* 2015;25:240–52.
- [14] Kossovich LY, Salkovskiy Y, Kirillova IV. Electrospun chitosan nanofiber materials as burn dressing. *IFMBE Proc* 2010;31:1212–4.
- [15] Nicast Homepage. <http://www.nicast.com/index.aspx?> [accessed 14.06.16].
- [16] Wijeyaratne SM, Kannangara L. Safety and efficacy of electrospun polycarbonate-urethane vascular graft for early hemodialysis access: first clinical results in man. *J Vasc Access* 2011;12:28–35.
- [17] Clinical Trials Homepage. <http://www.clinicaltrials.gov/> [accessed 14.06.16].
- [18] Brabu B, Haribabu S, Revathy M, Anitha S, Thangapandiyan M, Navaneethakrishnan KR, et al. Biocompatibility studies on lanthanum oxide nanoparticles. *Toxicol Res* 2015; 2015(4):1037–44.

This page intentionally left blank

Part Two

Specific Biomedical and Tissue Engineering Application Areas of Electrospinning

This page intentionally left blank

Electrospun systems for drug delivery

7

B.A. Minden-Birkenmaier, G.S. Selders, A.E. Fetz, C.J. Gehrman, G.L. Bowlin
University of Memphis, Memphis, TN, United States

7.1 Introduction

In the clinical setting, the vast majority of therapeutic agents are delivered systemically, either taken orally or injected intravenously. While it is beneficial for treatments that require dispersion of these agents throughout the body, systemic delivery has significant drawbacks when attempting to target a specific area within the body, such as a wound site or a tumor. By necessity, the dose delivered through this route must be significantly higher than that required by the target tissue because much of the drug will be taken up by other tissues or be cleared by the liver and kidneys. This uptake by untargeted tissues can lead to unfavorable interactions, causing wide ranges of unpleasant side effects that limit the useable dosage. Thus, in many applications, a more localized form of delivery would provide significant benefits, including increasing the efficacy and precision of the delivered dosage and reducing uptake by untargeted tissues [1–4].

Due to the versatility of their fabrication and unique structural properties, electrospun meshes are ideal drug delivery vehicles for many applications. Their biocompatibility allows them to be placed in a wide variety of locations within the body, near or within the target tissue, enabling local drug delivery to the tissue. The wide variety of methods for attaching or encapsulating bioactive molecules within the fibrous structures enables the delivery of many different types of pharmaceutical agents, potentially simultaneously delivered from the same mesh [5]. Additionally, the high surface-area-to-volume ratio and the tailorability of the structure with regard to polymer type, fiber size and orientation, and biodegradability allow for a high loading capacity and great control over the delivery of these agents over time. The following chapter describes the common methods used to create electrospun systems for drug delivery, their applications in the field today, the immediate outlook of the field, and likely commercialization prospects in the near future. In this chapter, “drug” refers to any therapeutic agent that does not directly alter the cell’s genetic structure. Thus, proteins, small molecules, synthetic pharmaceutical agents, and antibiotics are included, but nucleic acids are excluded from this definition.

The methods of incorporating drug molecules into electrospun scaffolds can be divided into four main categories. Drugs can be attached using postspinning modifications such as drug adsorption, layer-by-layer (LBL) assembly, and covalent binding, which attach the drug molecules to the outside of the fibers. Alternatively, polymer/drug blend electrospinning can be used to incorporate the drug molecules throughout

the fiber interior. In a more sophisticated variation of this method, coaxial electrospinning is used to incorporate the drug molecules into a drug/polymer core within a shell of a different polymer composition. The properties of this shell can be tailored to delay and control levels of drug release from the inner core. Another way to exert additional control over drug release is by electrospinning drug-loaded particles, which results in encapsulation of the particles within the fibers or binding of them to the fiber surface. The properties of the particles can be tailored to delay and control drug release, and if the particles are encapsulated in the fiber interior, the fiber properties can be tailored to delay and control drug release as well. These methods of drug incorporation in electrospun meshes are depicted in Fig. 7.1.

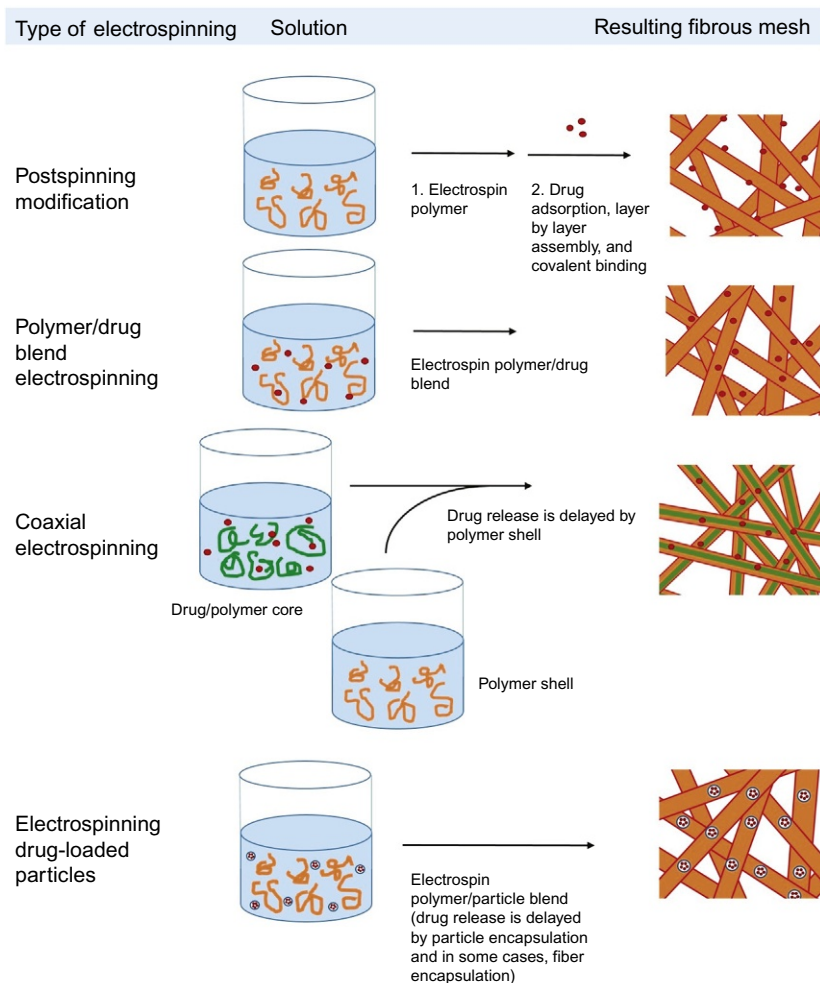


Fig. 7.1 Common methods of incorporating drug molecules into electrospun meshes.

7.2 Postelectrospinning modification

Many drug delivery applications require drug molecules to be attached to the fibrous mesh after the electrospinning process is completed. Postelectrospinning modification (Fig. 7.1) avoids exposing sensitive molecules, like proteins, to the harsh solvents and voltage conditions involved in the electrospinning process. By avoiding these conditions, postelectrospinning modification protects the molecular structure and activity of therapeutic agents and prevents charged molecules from aggregating in the organic solvents used during electrospinning [6].

7.2.1 Drug adsorption

The simplest method of attaching bioactive molecules to electrospun meshes is to adsorb the molecules directly onto the surface of the fibers. Adsorption, which involves the binding of molecules to surfaces through electrostatic and van der Waals interactions, allows the protein to be directly immobilized on the fiber surface without the use of a covalent linker [7]. This method of attachment usually has a burst release within the first few hours of implantation, sometimes followed by a lower level sustained release over a period of days [8]. In addition, adsorption creates little-to-no interference with the structure and activity of the adsorbed molecules. An example of this direct immobilization is the adsorption of platelet-derived growth factor (PDGF) to bone-mimetic meshes for bone repair [9]. In order to overcome the short *in vivo* half-life, PDGF was adsorbed onto electrospun polycaprolactone (PCL) and PCL/collagen/hydroxyapatite (HA) meshes by soaking in a PDGF solution over a period of 24 h. Upon incubating these meshes in phosphate-buffered saline (PBS), Phipps et al. saw an initial burst release of the PDGF within the first 4 days, followed by sustained delivery over a period of 10–20 days [9]. As expected, due to previous studies showing the high capacity of HA for protein adsorption, the PCL/collagen/HA meshes adsorbed more PDGF than the PCL controls, which translated to higher levels of sustained PDGF release from the meshes. As another typical example of drug-adsorbed meshes, Bölgen et al. created antibiotic-loaded PCL meshes for the prevention of postsurgery abdominal adhesions [10]. Meshes were electrospun from a solution of PCL and dimethylformamide (DMF), and subsequently a solution containing ornidazole, a common antibiotic, was dropped onto the mesh and evenly distributed across the mesh surface. The release profile of the meshes showed a high initial burst release during which 80% of the total loaded antibiotic was released within the first 18 h [10].

The surface of electrospun fibers can also be treated to facilitate easier adsorption of drugs. Common treatments involve binding or coating fiber surfaces with molecules such as heparin, perlecan, or cationized gelatin (CG), which facilitate the binding of growth factors to the fiber surface [11,12]. In a particularly in-depth study, Lu et al. used coaxial electrospinning to create fibers with a PCL core to provide tensile strength, surrounded by a CG outer layer to provide positive charges, thus facilitating adsorption. The outer CG layer was cross-linked by exposure to glutaraldehyde vapor for different time periods, and it was found that longer cross-linking times decreased

the degree of fiber swelling when placed in an aqueous solution. In general, fiber swelling increases the diffusion rate of hydrophilic drugs from the fiber interior. Thus, the decrease in swelling caused by the longer cross-linking times decreases the initial burst release. Meshes were then placed in solutions of fluorescein isothiocyanate (FITC)-labeled bovine serum albumin (BSA), vascular endothelial growth factor (VEGF), or FITC-labeled heparin for adsorption. The CG outer layer was shown to significantly increase adsorbed levels of BSA.

Release profiles of both BSA and heparin showed a slight burst release within the first 2 h, followed by negligible release after 100 min (Fig. 7.2A). As shown in Fig. 7.2B, longer cross-linking times translated to a flatter, more prolonged release profile of heparin, with the 4-day cross-linked fibers having a release duration of more than 3 days.

VEGF was adsorbed onto CG-coated membranes with and without heparin adsorbed to their surface by pipetting VEGF solution directly onto the meshes. Release profiles, shown in Figs. 7.2A, B and 7.3A, demonstrate that the heparin-adsorbed meshes had a smaller burst release and much more sustained release of VEGF over time as compared with the membranes without heparin. Due to the shielding effect of heparin, released VEGF maintained its ability to stimulate growth in human dermal microvascular endothelial cells (HDMECs) (Fig. 7.3B) [12]. This study demonstrates the advantages of preadsorption surface modifications, both in increasing adsorption efficiency and in creating controlled, sustained release profiles while maintaining drug bioactivity.

7.2.2 LBL assembly

Another common method of loading electrospun meshes with bioactive particles is LBL assembly. In this method, the surface of the electrospun structure is imbued with charged molecules driven by electrostatic forces to create a self-assembled layer adsorbed onto the structure. Layers are deposited by alternating immersion in polycations and polyanions in order to create molecular strata in which bioactive drug molecules can be incorporated and bound [13]. A good example of drug loading by this method is the creation of methylene blue-loaded polyacrylic acid (PAA)/poly(allylamine hydrochloride) (PAH) electrospun meshes in a 2007 study by Chunder et al. These meshes consisted of fibers with negatively charged carboxylate groups, which, following a soak in 0.05 M NaOH to deprotonate the carboxylate groups, facilitated the adsorption of cationic methylene blue molecules onto the surface and the deposition of alternating layers of PAA and poly(*N*-isopropylacrylamide) (PNIPAAm) over the initial methylene blue layer. In nonbuffered solution, methylene blue release from the mesh was modulated by altering the pH of the solution. At high pH levels, between 6.5 and 10, no methylene blue release was observed. When the pH was shifted to 6 or less, carboxylate groups became increasingly protonated, resulting in the increased release of methylene blue as the pH decreased further and further. This mechanism thus allows for interesting tailorability of the release profile of methylene blue which may be translated to tailorable drug release [14]. When this release study was repeated in a buffered solution, all of the methylene blue was released within the first 10 min, regardless of pH. This fast release is hypothesized to be the

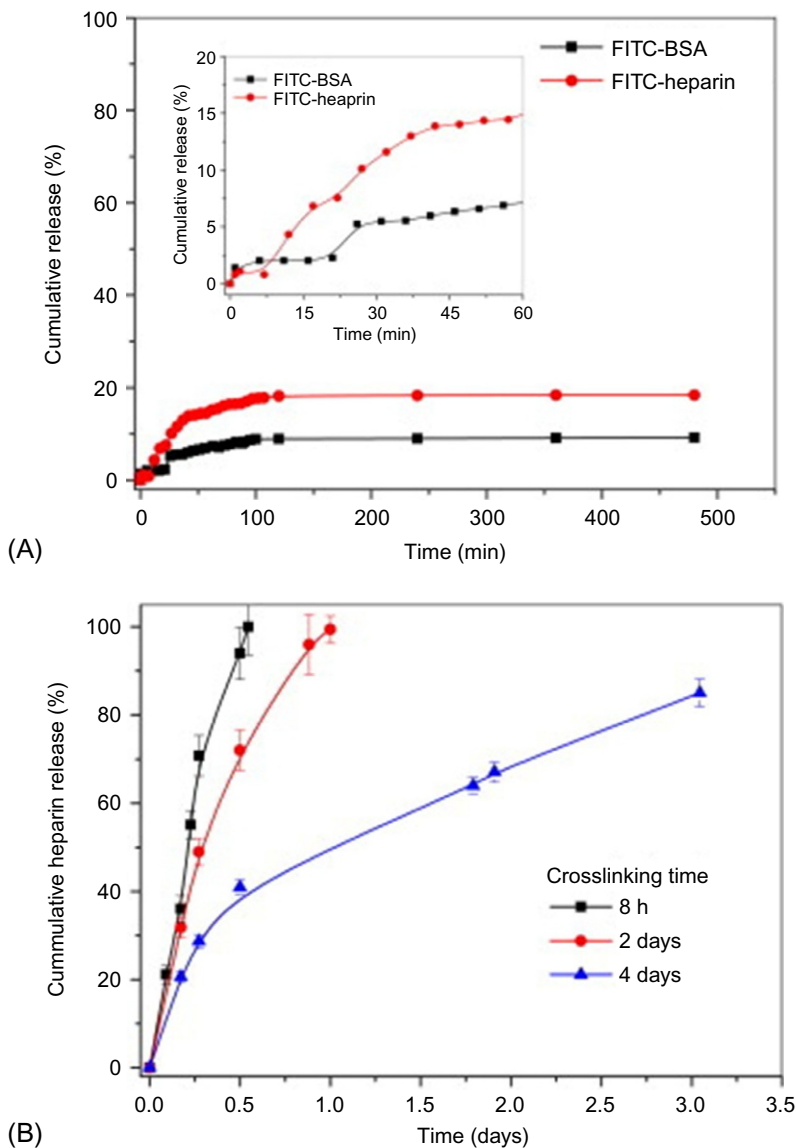


Fig. 7.2 (A) Release of FITC-BSA and FITC-heparin from gelatin-coated PCL fibers with the gelatin cross-linked for 4 days. (B) Release of heparin from gelatin-coated PCL. Reproduced from Lu Y, Jiang H, Tu K, Wang L. Mild immobilization of diverse macromolecular bioactive agents onto multifunctional fibrous membranes prepared by coaxial electrospinning. *Acta Biomater* 2009;5:1562–74 with permission from Elsevier.

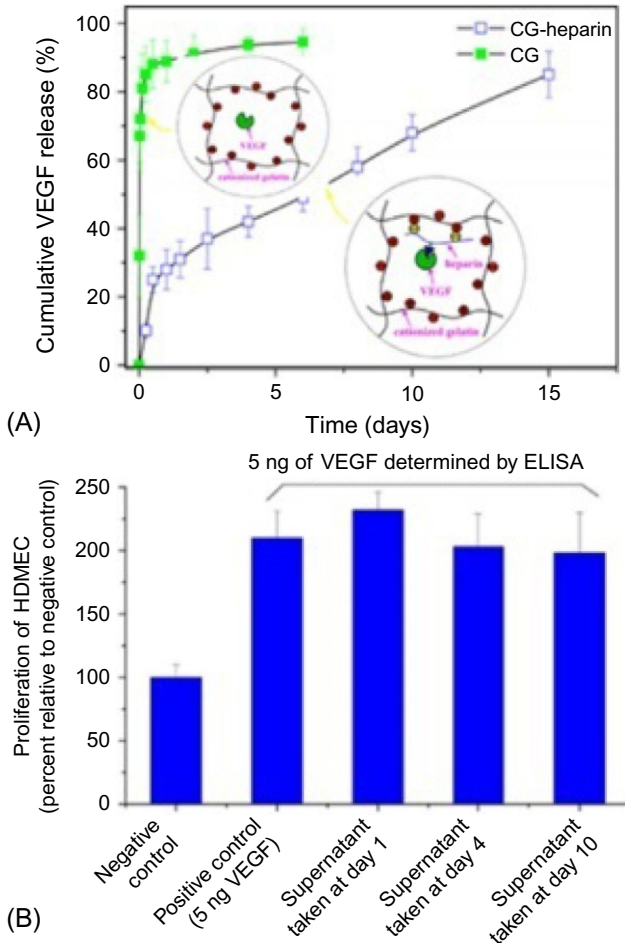


Fig. 7.3 (A) VEGF release from cationized gelatin membranes with and without heparin adsorbed at 23 $\mu\text{g}/\text{mg}$ ($n = 3$). (B) Proliferation of HDMECs in response to VEGF released from meshes.

Reproduced from Lu Y, Jiang H, Tu K, Wang L. Mild immobilization of diverse macromolecular bioactive agents onto multifunctional fibrous membranes prepared by coaxial electrospinning. *Acta Biomater* 2009;5:1562–74 with permission from Elsevier.

result of charge shielding by the buffer. To address this unwanted burst release profile, a perfluorosilane layer was deposited on the fibers via chemical vapor deposition (CVD). This layer provided a hydrophobic barrier that hindered the diffusion of methylene blue and also blocked fiber swelling. When placed in a solution of PBS at pH 7.4, these fibers showed sustained release over a period of 1200 min, around 100 times longer than the time period of the release from nonperfluorosilane coated fibers.

Due to the thermosensitive properties of the PNIPAAm polymer in the fiber coatings, the release rates from these electrospun fibers could also be modulated through varying the temperature of the fibers. In an aqueous solution, PNIPAAm undergoes reversible phase transition at 37°C from a well-hydrated, soluble form below 37°C to a dehydrated, insoluble form above 37°C. Below 37°C, it is thought that the PAA/PNIPAAm hydrogen bond network in the coating forms a barrier to the diffusion of the methylene blue molecules, while at temperatures above 37°C, the PNIPAAm forms intramolecular hydrogen bonds with itself, disrupting the PAA/PNIPAAm bond diffusion barrier. The thermoresponsive property leads to much faster release rates at 40°C than at 25°C. This example demonstrates the increased tailorability of release rates in LBL deposition as compared with simple adsorption. However, this method is not without its drawbacks. While payloads that are charged or polar (such as proteins) are easily incorporated into these layers, it is often more difficult to incorporate uncharged, hydrophobic drug molecules.

One way around this problem is to covalently link hydrophobic molecules to hydrophilic molecules with enough polar groups to allow their adsorption to the intended surface. As an example, Thierry et al. conjugated hydrophobic molecules of paclitaxel, a potent chemotherapeutic drug, to hyaluronan molecules through a succinate ester linkage. The polar hydroxyl groups on the hyaluronan molecules allowed the conjugated molecules to deposit via LBL assembly despite the bound hydrophobic paclitaxel molecules. Layers of hyaluronan/paclitaxel were alternated with layers of polyanionic chitosan. When measured using a quartz crystal microbalance, the results showed increasingly more pronounced frequency shifts as a function of layer number, indicating LBL deposition [15]. Samples were created using rhodamine-labeled chitosan molecules for the polyanion layer in order to measure the stability of the multilayer during release studies. As shown in Fig. 7.4, absorbance measurements of

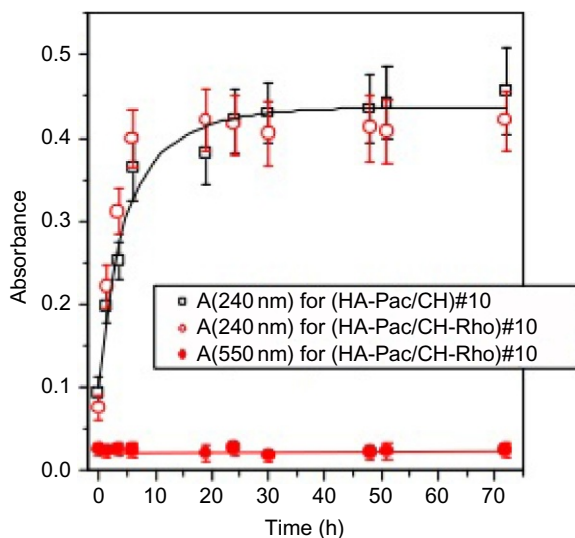


Fig. 7.4 Cumulative release of paclitaxel (*open symbols*) and rhodamine (*closed symbols*) from LBL depositions.

Reproduced from Thierry B, Kujawa P, Tkaczyk C, Winnik FM, Bilodeau L, Tabrizian M. Delivery platform for hydrophobic drugs: prodrug approach combined with self-assembled multilayers. *J Am Chem Soc* 2005;127:1626–7 with permission from The American Chemical Society.

releasate at 550 nm, a wavelength at which rhodamine absorbs but paclitaxel does not, show very low levels of released rhodamine over the time period measured. These low levels indicate that the rhodamine-labeled chitosan layers remain deposited, indicating stability of the multilayer complex. Absorbance measurements at 240 nm, a wavelength which paclitaxel absorbs, demonstrate a large initial burst release similar to the profiles of molecules loaded through simple adsorption.

As shown in the above examples, drugs incorporated in the LBL deposition strata often still exhibit a burst release within the first few hours or days. While this burst release can be advantageous in certain situations, such as preventing postsurgery infections, it is often desirable to have a flatter, more constant release profile over time [16].

7.2.3 Covalent bonding

Commonly used as a method to functionalize fibers or modify their surface properties, covalent modification involves immobilizing bioactive molecules onto the surface of the electrospun fibers via a chemical bond linkage. Often, a linkage is used that is enzymatically cleaved in the body, enabling release of the drug molecules to the target tissue. A typical example of this method of immobilization is described in a 2007 study by Choi and Yoo. In this study, electrospun PCL-polyethylene glycol (PEG) block copolymer fibers were covalently bonded to FITC-BSA molecules. After electrospinning, meshes were soaked first in ethanol and then in PBS to swell the fibers and expose amine groups. These amine groups were then covalently bonded to the carboxyl groups of BSA in order to immobilize the BSA on the fiber surface. The covalently bound FITC-BSA was released at a low rate over a period of 5 days with little-to-no burst release. As the ratio of PCL to PEG in the fibers increased, the release rate and overall cumulative release of the FITC-BSA decreased. In contrast, FITC-BSA blended into PCL fibers had much higher overall cumulative release, almost entirely a burst release within the first day. This burst release can be attributed to the high surface-area-to-volume ratio of the meshes and the lack of chemical bonds tethering the protein to the meshes [17]. In a subsequent study by the same group, this method was used to covalently bind recombinant human epidermal growth factor (rhEGF) by conjugating the carboxylic groups of the rhEGF molecules to exposed amine groups on PCL-PEG copolymers. Keratinocytes were cultured on these fibers, and reverse transcription polymerase chain reaction (RT-PCR) was performed to quantify expression of keratin 1, loricrin, and glyceraldehyde-3-phosphate dehydrogenase (GAPDH), a housekeeping gene used for normalization. Quantification of the band intensities, normalized to GAPDH levels, showed that both keratin 1 and loricrin were expressed at significantly higher levels in cells cultured on rhEGF-conjugated fibers than on other constructs (fibers soaked in rhEGF solution, on fibers without rhEGF present, on PCL fibers in rhEGF solution, on PCL fibers without rhEGF present, or on tissue culture plastic). When rhEGF-conjugated fibers were placed in a diabetic murine wound model, wound closure rates were significantly increased compared with rhEGF solution + fibers, just fibers, and nontreated wounds. While healing-related activities were significantly higher in wounds with rhEGF-conjugated fibers during the first 7 days of healing, the fibers alone had

little-to-no effect on wound repair after those first 7 days. However, EGFR expression after 14 days was confirmed by immunohistochemical staining, indicating that rhEGF was still being released from the fibers through this time point. The lack of significant impact on the healing process after day 7 is thus most likely due to EGF being required only at the initial stage of the wound-healing process, rather than the fibers becoming depleted of rhEGF. Thus, the controlled-release profile created by covalently linking the rhEGF to the fibers has a significant benefit during the early stage of wound healing.

In some applications of this method, the release of drug molecules is controlled by the rise and fall of enzyme levels within the target tissue. By choosing a covalent linkage which is cleaved by specific enzymes, drug release can be triggered and attenuated by biological events which up- or downregulate the expression of the enzyme cleaver. For instance, the cleavage rates of linkages susceptible to matrix metalloproteinase (MMP) activity rise and fall with the concentration of MMPs in the immediate area. It has been shown that MMP-9 concentrations in diabetic ulcers are inversely related to the healing rate of the ulcer; therefore, MMP-cleavable linkers would be an ideal way to deliver drugs to these wounds [18]. In a 2010 study, Kim and Yoo used an MMP-cleavable peptide to conjugate linear polyethylenimine (LPEI) to electrospun PCL-PEG meshes. The LPEI was then ionically complexed to their therapeutic payload, which in this case consisted of molecules of DNA intended to transfect cells within the wound site. Meshes immersed in MMP-2 solution showed significantly more release of LPEI and DNA over 72 h than those immersed in solution without MMP-2, as shown in Fig. 7.5. These results indicate successful cleavage of the polypeptide linker and subsequent release of the payload in response to the presence of MMP-2 [19].

This method is thus both a novel drug-attachment technique and a way to optimize the drug release kinetics to provide the highest dose of drug at the point when it will most benefit the wound. Because of the amount of variation in the wound environment over time as it progresses through the various stages of healing, the ability to temporally localize drug release has the potential to vastly benefit the wound-healing process.

7.3 Polymer/drug blend electrospinning

While there are many benefits to the postelectrospinning attachment methods detailed in the sections above, it is often easier and faster to simply incorporate the drug into the polymer solution and then electrospin the polymer/drug blend (Fig. 7.1). This method does have drawbacks. For instance, it exposes the drug to the harsh, organic solvents often used to dissolve the polymer and to the strong electric fields used to electrospin the fibers, which can often denature the drug [20]. The incorporation of drug molecules can also affect the viscosity or charge density of the electrospun solution, which can cause a change in elongation forces and a corresponding change in fiber diameter [21]. In addition, it does not necessarily allow for the localization of drug molecules to the surface of the fibers, meaning that drug release is often linked to the fiber degradation rate [22,23]. However, if the drug molecules can withstand the solvent and electrospinning process without losing their form and function and do not unduly

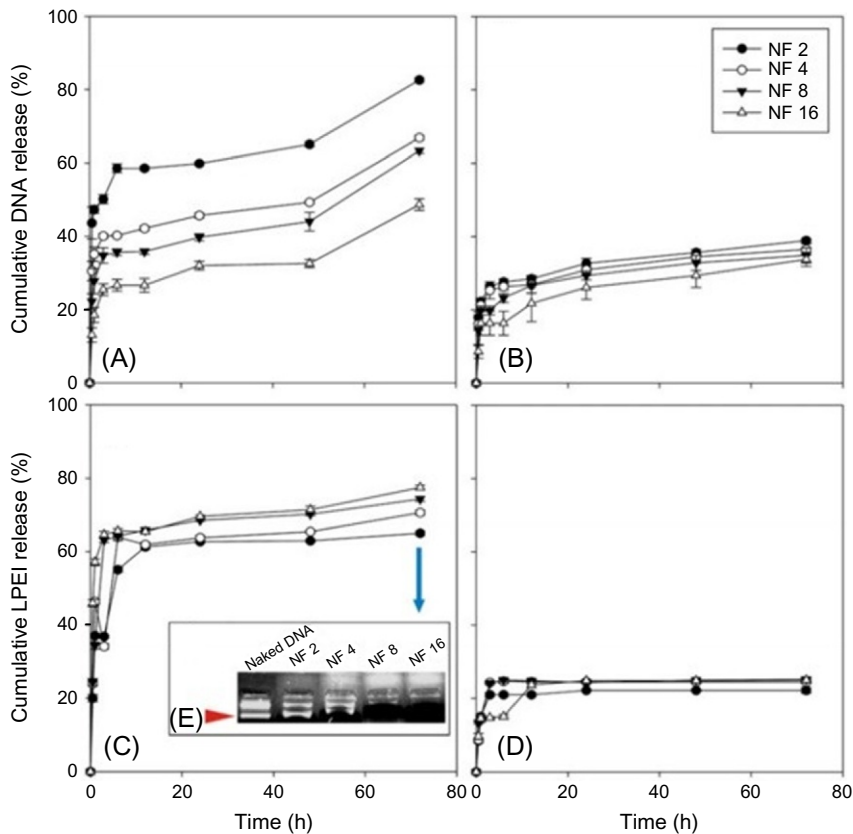


Fig. 7.5 Release of DNA (A and B) and LPEI (C and D) from electrospun meshes soaked in solution with 0.033 $\mu\text{g}/\text{mL}$ MMP-2 (A and C) or in the absence of MMP-2 (B and D). (E) An agarose gel retardation assay of DNA releasate from meshes incubated with MMP-2. NF (referring to fibrous meshes) 2 had 36.7 $\mu\text{g}/\text{mL}$ DNA initially incorporated, NF 4 had 18.3 $\mu\text{g}/\text{mL}$, NF 8 had 9.2 $\mu\text{g}/\text{mL}$, and NF 16 had 4.6 $\mu\text{g}/\text{mL}$ initially incorporated.

Reproduced from Kim HS, Yoo HS. MMPs-responsive release of DNA from electrospun nanofibrous matrix for local gene therapy: in vitro and in vivo evaluation. *J Control Release* 2010;145:264–71 with permission from Elsevier.

affect the electrospinning process, this method has some significant advantages. Namely, the drug incorporation is done in one step, without the reliance on covalent linkers or deposition aids, making it simple and relatively inexpensive. Additionally, it allows drug-laden fibers to be electrospun directly onto the surface where they are needed, such as a wound site [24].

In the first published use of an electrospun mesh for drug delivery, Kenawy et al. in 2002 electrospun blends of 5% (w/v) tetracycline hydrochloride with poly(lactic acid) (PLA), with poly(ethylene-co-vinyl acetate) (PEVA), and with a 50/50 combination of the two polymers into fibrous meshes. Release experiment showed a high burst release from the tetracycline/PLA fibers, likely from the tetracycline present on the

fiber surface, with negligible release after the first hour. This lack of prolonged release is most likely due to the partial crystallinity of PLA, which limits the diffusion of the aqueous environment into the inner regions of the fibers. In contrast, the PEVA fibers had a much more prolonged release profile, with a relatively constant release rate through the first 80 h and a release peak at 60% after 120 h. The 50/50 PLA/PEVA blend likewise had a smooth, prolonged release throughout the first 120 h, with negligible initial burst release. However, when the tetracycline concentration was increased to 25% (w/v), a burst release of 40% was seen, possibly due to a higher amount of surface-segregated tetracycline. All electrospun meshes showed higher total percent release than equivalent cast films formed from the same solutions, which is a result of the higher surface area of the electrospun meshes [25].

One of the most important factors determining the release kinetics of a drug molecule electrospun into fibers from a blend is the degree of hydrophilicity of the drug. This principle is demonstrated in a study by Zeng et al. in which the hydrophobic chemotherapy drug doxorubicin, in its water-soluble salt form doxorubicin hydrochloride, was incorporated into poly-L-lactide (PLLA) solutions and then electrospun. The release profile of the resulting meshes was compared with that of meshes electrospun using doxorubicin in its nonwater-soluble, nonsalt form and the release of meshes electrospun with paclitaxel, another hydrophobic cancer drug. Drug release was analyzed with and without the presence of proteinase K, an enzyme that degrades PLLA. Paclitaxel had a linear, zero-order release in the presence of proteinase K but no release in the absence of the enzyme. These profiles indicate that all of the release was due to the enzymatic degradation of the fibers, as there was no paclitaxel release in the absence of proteinase K, indicating negligible surface sequestration and good distribution of the drug throughout the fiber interior. This distribution is typical of a hydrophobic drug, which solubilizes easily in the organic solvents used in electrospinning but not in aqueous solutions.

In contrast, the hydrophilic doxorubicin hydrochloride salt exhibited a burst release in the first 2 h, with the profiles in the presence and absence of proteinase K only diverging after 150 min. These profiles indicate a high level of surface sequestration, with only around 13% of the doxorubicin salt encapsulated in the fiber interior. This surface sequestration is typical of hydrophilic drugs incorporated into an organic polymer solution, as their low solubility limits their distribution into the fiber interior. The meshes incorporating the nonsalt, lipophilic form of doxorubicin, however, had linear, zero-order kinetics in the presence of proteinase K similar to the paclitaxel release seen above, indicating good distribution within the fibers. While the profile in the absence of proteinase K showed a burst release of roughly 20%, this is much less than the burst release seen from the hydrophilic form of the drug. Thus, while there was some surface sequestration, the majority of this drug was incorporated throughout the fiber interior. This study thus demonstrates the importance of matching the hydrophilicity of the drug to the polymer/solvent blend during electrospinning in order to achieve maximal encapsulation by the fibers and a sustained release of the drug [26].

While release from drug-laden fibers is often linked to the polymer degradation rate, there are several ways to modify this rate to allow for greater control over the release profile. In a study by Maretschek, Greiner, and Kissel, the hydrophilic protein

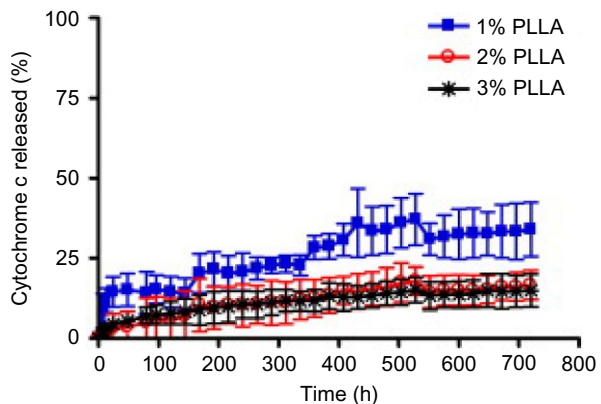
cytochrome c was incorporated into hydrophobic PLLA electrospun meshes. Because of the mismatch between the hydrophilic protein and the hydrophobic polymer, a high degree of surface sequestration was observed, with crystallite cytochrome c structures forming on the outsides of the fibers. While this morphology would typically result in a high burst release, these constructs showed a very slow, controlled release of the cytochrome c (Fig. 7.6).

This unusually attenuated release profile was due to the extremely high degree of hydrophobicity exhibited by the surface of the meshes, which limited the wetting of the mesh by the aqueous environment. When the emulsifier Tween 20 was added to the release media in order to improve mesh wettability, a burst release of almost 100% was seen, indicating that the cytochrome c was present almost exclusively on the outside of the fibers. In order to better control this release profile, new meshes were electrospun from hydrophilic poly(ethyleneimine) (PEI) and poly-L-lactide (PLL), blended with the hydrophobic PLLA used in the original meshes, with cytochrome c incorporated into the electrospinning solution as before. While the meshes electrospun from this polymer blend still had a high degree of surface sequestration of the cytochrome c, wettability was significantly increased. In addition, overall cytochrome c release was increased in proportion to the amount of hydrophilic polymer incorporated (Fig. 7.7). However, this release was almost entirely as an initial burst, with little subsequent sustained release.

Thus, the overall level of protein release was able to be controlled by varying the hydrophilicity and corresponding surface wettability of the polymer blend. However, due to the high degree of surface sequestration, the burst release of these proteins was unable to be attenuated, which is a significant drawback of this method of release control [27].

One intriguing method of reducing burst release is to add a coating to electrospun fibers, which changes their hydrophilicity and surface wetness. In a 2005 study, Zeng et al. used CVD to coat protein-loaded poly(vinyl alcohol) (PVA) fibers in order to tailor protein release rate. FITC-BSA was added to aqueous solutions of PVA and then electrospun, and the resultant meshes were coated by CVD with hydrophobic layer of poly(p-xylylene) (PPX) of various thicknesses. Release studies showed that increased

Fig. 7.6 Release of cytochrome c from meshes electrospun from various concentrations of PLLA. Reproduced from Mareschek S, Greiner A, Kissel T. Electrospun biodegradable nanofiber nonwovens for controlled release of proteins. *J Control Release* 2008;127:180–7 with permission from Elsevier.



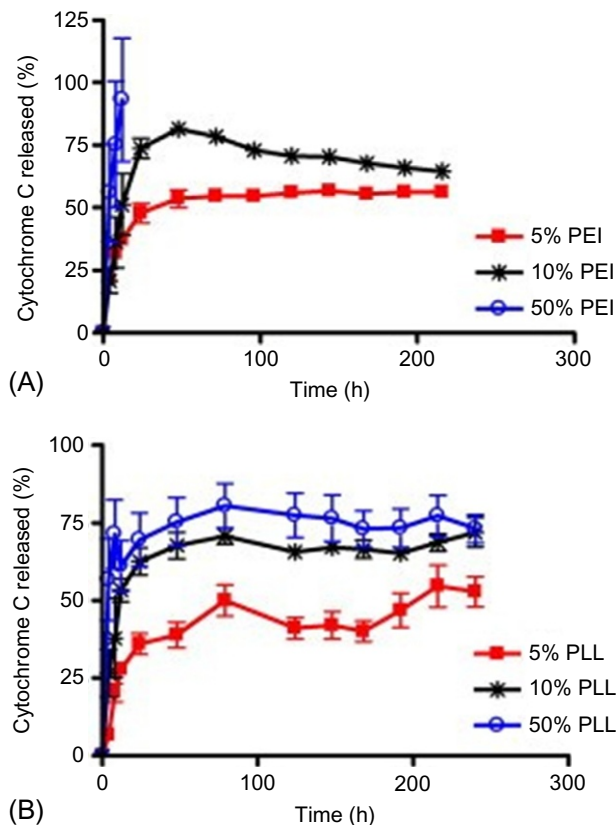


Fig. 7.7 Release of cytochrome c from meshes electrospun from hydrophobic PLLA blended with (A) PEI and (B) PLL.

Reproduced from Maretschek S, Greiner A, Kissel T. Electrospun biodegradable nanofiber nonwovens for controlled release of proteins. *J Control Release* 2008;127:180–7 with permission from Elsevier.

thickness of the PPX layer led to a flatter release profile, with a lower initial release rate and lower overall cumulative release, as shown in Fig. 7.8.

In order to establish the preservation of enzyme activity when incorporated in electrospun fibers by this procedure, luciferase, a bioluminescent enzyme, was incorporated in electrospun PVA meshes, which were then coated using the same CVD procedure. Mesh samples were then immersed in luciferase lysis buffer with 1% BSA and 250 mM β -mercaptoethanol, and luciferase activity was recorded over time. The results show significant luciferase activity beginning after 30 min, with activity increasing over time. This profile indicates that the enzyme retains its activity and is able to escape the hydrophobic PPX layer to react with substrate in the solution [28].

One way of addressing the difficulty in incorporating hydrophilic drugs into the interior of hydrophobic polymer fibers is to covalently couple the drug to a polymer with both hydrophobic and hydrophilic regions, which is then blended with a hydrophobic polymer and electrospun. One such hydrophilic/hydrophobic polymer is

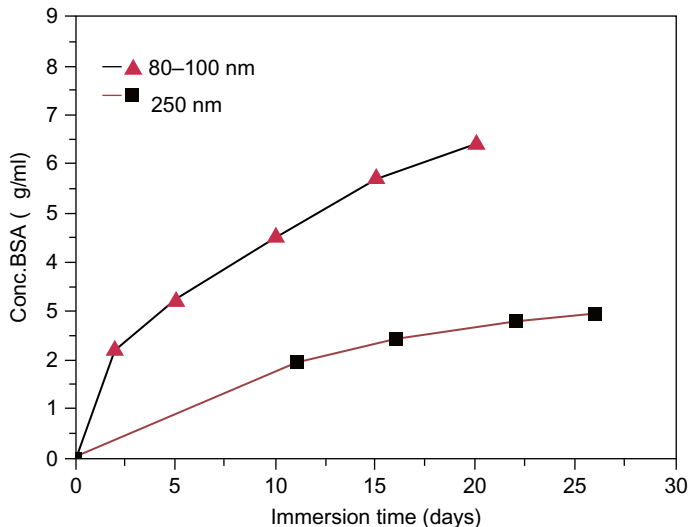


Fig. 7.8 Release of FITC-BSA from PVA fibers coated with PPX layers of different thicknesses.

Reproduced from Zeng J, Aigner A, Czubyko F, Kissel T, Wendorff JH, Greiner A. Poly(vinyl alcohol) nanofibers by electrospinning as a protein delivery system and the retardation of enzyme release by additional polymer coatings. *Biomacromolecules* 2005;6:1484–8 with permission from The American Chemical Society.

poly(ethylene glycol)-grafted chitosan (PEG-*g*-chitosan), which combines the hydrophilic properties of PEG with the hydrophobic nature of chitosan [29]. Drugs with anionic groups can be electrostatically complexed to the NH_2 residues, and drugs with or without these groups can be covalently bound to the polymer side chains. In a 2004 study by Jiang et al., ibuprofen was incorporated either by electrostatic conjugation or by covalent binding to PEG-*g*-chitosan chains, which were then blended with poly(lactic-*co*-glycolic acid) (PLGA) and electrospun into fibrous meshes. Release was compared between ibuprofen electrospun into PLGA fibers, ibuprofen electrostatically complexed to PEG-*g*-chitosan chains within blended PLGA/PEG-*g*-chitosan electrospun fibers, and ibuprofen covalently bound to PEG-*g*-chitosan side chains within blended PLGA/PEG-*g*-chitosan fibers, and it was shown that both the anionically complexed and covalently bound ibuprofen had a much more sustained, prolonged release profile as compared with release from the PLGA fibers. Furthermore, release of the covalently bound ibuprofen was even more sustained than the anionically complexed drug. This study thus demonstrates the ability to use several methods to create three distinct release profiles: one with a large (85%) burst release within the first 4 days followed by little sustained release, one with a medium burst release (45%) within the first 4 days followed by a medium sustained release (a further 25% over 12 more days), and one with a small (20%) burst release in the first 4 days followed by a medium sustained release (a further 20% over 12 more days). This

method thus allows a great deal of control over the release rate of a drug by modulating the strength of the interaction between the drug and the polymer [30].

7.4 Coaxial electrospinning

In order to attain a higher level of control over the release kinetics of a drug, coaxial electrospinning is often used to embed the drugs in either the core or the outer shell of electrospun fibers. In this method, one polymer solution is pushed through an inner capillary tube that is surrounded by an outer tube through which a second polymer solution is pushed. When voltage is applied, fibers are created which have an inner core of the first polymer and an outer shell of the second polymer (Fig. 7.1). This technique is commonly used to embed a drug within the core section of the fibers surrounded by a shell that is not only impermeable to diffusion of the drug but also degradable. The shell reduces initial burst release of the drug and can be used to delay drug release until shell degradation [31,32]. Wang et al. successfully demonstrated a significant reduction in burst release by incorporating dimethyloxalylglycine (DMOG), a proangiogenic compound, into the core of poly(DL-lactic acid) (PDLLA)/poly(3-hydroxybutyrate) (PHB) and PDLLA/PHB core-shell electrospun fibers, as compared with the release of DMOG from conventionally electrospun PHB and PDLLA fibers [33]. As seen in Fig. 7.9, burst release was most effectively attenuated when the DMOG was incorporated in a PDLLA core surrounded by a PHB shell (samples D and E). These samples showed a two-stage release profile with an initial fast release of around 25% of the incorporated drug, followed by a prolonged, constant release of up to 70% of the total payload. While the initial release was irrespective of the thickness of the PHB shell, the following prolonged linear release rate was higher in sample E, which had a thinner shell thickness of 120 nm, as compared with sample D with a

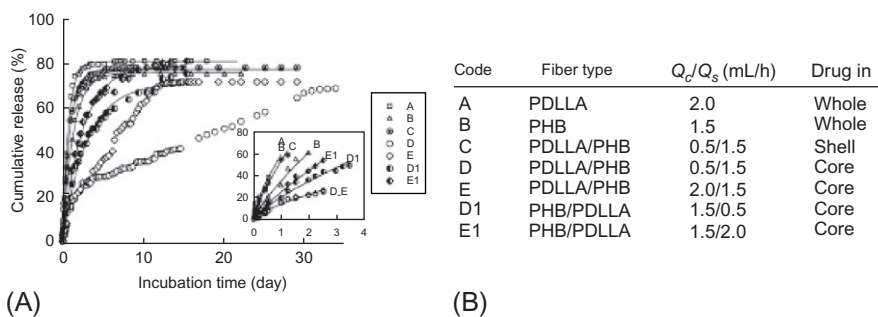


Fig. 7.9 (A) Release of DMOG from conventionally electrospun and core/shell fibers. (B) Fiber type, polymer flow rate, and drug location. The Q_c/Q_s values indicate the flow rate of the polymer electrospun for the core and for the shell, respectively.

Reproduced from Wang C, Yan K-W, Lin Y-D, Hsieh PC. Biodegradable core/shell fibers by coaxial electrospinning: processing, fiber characterization, and its application in sustained drug release. *Macromolecules* 2010;43:6389–97 with permission from The American Chemical Society.

shell thickness of 230 nm. These results demonstrate the ability to tailor the release rate by controlling the thickness of the outer shell in this morphology.

Another benefit of encapsulating drugs via coaxial electrospinning is that molecules such as enzymes or growth factors, which are prone to denaturation by organic solvents, can be incorporated in aqueous, low-viscosity solutions that would not normally be able to be electrospun. By extruding the aqueous solution through the inner capillary tube and the organic solution through the outer capillary tube, fibers are formed without mixing the aqueous and organic solutions, meaning that the labile molecules in the aqueous solution are entrapped within the fibers without ever being exposed to the harsh organic solvents. Jiang et al. used this method to encapsulate luciferase, which is normally denatured by organic solvents, within a core of water-soluble PEG surrounded by a shell electrospun from PCL in the organic solvent *N,N*-dimethylformamide (DMF) and showed that the enzyme retained its activity during the electrospinning process and after its release [34]. Similar procedures have replicated these results with a variety of polymer combinations and bioactive compounds [32,35,36]. Furthermore, Chen et al. used coaxial electrospinning to fabricate PCL/poly(*N*-isopropylacrylamide) (PNIPAAm) core/shell fibers with a thermoresponsive outer shell. Due to the unique properties of the PNIPAAm, the wettability of the surface increased dramatically when the fibers were heated past 32°C. These fibers have great potential as drug delivery vehicles, as body temperature would heat the fibers and allow for drug release upon implantation, and the low wettability below this point would prevent any loss of the drug before implantation [37].

7.5 Electrospinning drug-loaded micro/nanoparticles

An alternative method that offers many of the same benefits as coaxial electrospinning, electrospun meshes that incorporate drug-loaded micro- or nanoparticles (Fig. 7.1) allow fine control over drug release rates without necessarily compromising mesh mechanical integrity. With this morphology, the degradation rates of both the drug-loaded particle and the fiber material surrounding or holding the particle can be tailored, allowing many different types of release profiles to be achieved, and the particles can be used to entrap and protect labile molecules in a similar fashion to the coaxially electrospun fibers described in the previous section.

These meshes typically have two different types of morphologies: fibers with particles entrapped between them or fibers with particles placed within them. While the first type enables the preservation of fiber mechanical integrity, the second type enables more control over the drug release profile. In a good example of this first type of morphology, Ionescu et al. used sacrificial poly(ethylene oxide) (PEO) fibers to hold PLGA microspheres within an electrospun PCL fibrous mesh. A washing step then dissolved the PEO fibers, leaving the PLGA microspheres entrapped within the mesh. BSA and chondroitin sulfate (CS) were preloaded into the microspheres, and then their release profiles were compared with those of free microspheres. Fig. 7.10(A) shows BSA-laden microspheres in *red* and CS-laden microspheres in *black*, incorporated into the PCL electrospun mesh. As shown in Fig. 7.10(B), the free microspheres exhibited an

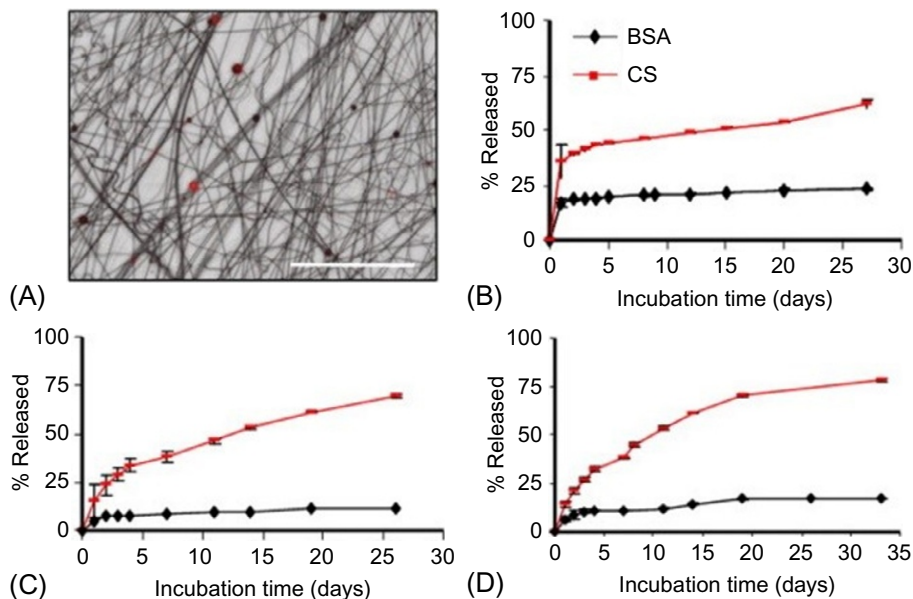


Fig. 7.10 Release of BSA and CS from PLGA microsphere-laden meshes. (A) Fluorescent micrograph showing BSA-laden microspheres in *red* and CS-laden microspheres in *black*, scale bar = 250 μm . (B) Release profile of BSA and CS from free PLGA microspheres. (C) Release profiles of BSA and CS from PLGA microspheres entrapped within PCL meshes, separate meshes for BSA and CS. (D) Release profile of BSA and CS from PLGA microspheres entrapped within PCL meshes, with both BSA- and CS-laden particles in the same mesh. Reproduced from Ionescu LC, Lee GC, Sennett BJ, Burdick JA, Mauck RL. An anisotropic nanofiber/microsphere composite with controlled release of biomolecules for fibrous tissue engineering. *Biomaterials* 2010;31:4113–20 with permission from Elsevier.

initial burst release followed by a slight prolonged release after the first day. The microspheres entrapped within the meshes (Fig. 7.10C and D) had slightly less of a burst release and slightly more prolonged release over 26 days, perhaps due to the limited diffusion throughout the fibrous architecture of the mesh, but this effect was almost negligible. In addition, the mechanical properties of the PCL mesh were not adversely affected by microparticle incorporation [38].

In contrast, Beck-Broichsitter et al. electrospun PVA and PEO fibers with PLGA nanoparticles encapsulated within the fibers. Coumarin 6 dye was used to model drug release, and fiber encapsulation of the nanoparticles was shown to significantly decrease the burst release and prolong the sustained release as compared with free nanoparticles. This morphology thus provides additional attenuation of burst release as compared with the nanoparticle entrapment morphology but at the expense of the structural integrity of the mesh [39].

One type of drug-encapsulating nanoparticle whose incorporation into electrospun meshes has yet to be fully explored is a polymeric micelle. An increasingly popular method of delivering bioactive agents, micelle encapsulation involves incorporating

the drug molecules in the center of spheres or cylindrical structures of amphiphilic block copolymers self-assembled through hydrophobic/hydrophilic interactions, called micelles. These structures protect the drug molecules from the outside environment and enable dispersion of drugs whose hydrophobicity would otherwise cause them to aggregate [40]. In addition, polymeric conjugation with ligands such as antibodies, growth factors, glycoproteins, and folate allow the drug-laden micelles to target and be taken up by specific cell types and tissues, like tumors [41].

Micellar structures have been incorporated in electrospun meshes in several ways. McKee et al. electrospun aqueous solutions of lecithin, a mixture of phospholipids and neutral lipids, and found that fibers were formed from entangled cylindrical micelles [42]. Kriegel et al. electrospun chitosan and PEO in solution with dodecyltrimethylammonium bromide (DTAB), an ionic surfactant, into fibers with encapsulated micelles in a bead-on-a-string morphology, while Nagarajan, Drew, and Mello achieved a similar morphology by electrospinning silk-elastin protein polymer chains [43,44]. However, to date, no significant studies have investigated the ability of these electrospun micelles to encapsulate and release bioactive compounds.

7.6 Commercialization prospects

The simplest application of electrospun systems for drug delivery is the delivery of antibiotics to prevent bacterial infection. In this application, it is often desirable to have a large initial burst release in order to bring antibiotic concentrations to the level at which bacteria are eliminated. This is achieved by electrospinning a blend of antibiotic and polymer into fibers which encapsulate the antibiotic within them. For example, in a 2004 study, Kim et al. incorporated the hydrophilic antibiotic cefoxitin sodium into separate electrospun meshes of PLGA and PLGA/PLA/PEG-*b*-PLA copolymers for the prevention of postsurgical abdominal adhesions. As expected, all mesh types exhibited a large burst release of at least 50% during the first several hours, but the faster degrading PLGA fibers had a higher burst release of 70% followed by negligible sustained release, while the slower degrading PLGA/PLA/PEG-*b*-PLA copolymers had a 50% burst release followed by 20% sustained release over the following 150 h [45]. Another method of achieving this high initial burst release is to adsorb the antibiotic onto the fiber surface. As described above, Bölgen et al. adsorbed the antibiotic ornidazole onto the surface of PCL electrospun fibers for the treatment of postsurgical abdominal adhesions and attained a similarly high burst release of 80% within the first several hours. When implanted into the abdominal wall of rats, these meshes successfully reduced abdominal adhesions [10].

These antibiotic-loaded meshes have many applications in the fields of wound care and surgery. They can be placed in surgical sites to prevent postsurgical infection and adhesion, as described above. Alternatively, the fibers can be electrospun as a coating directly onto an implant in order to prevent biofilm formation and implant rejection [46]. Antibiotic-laden meshes have been designed for use in preventing and treating oral infections and various types of wound infections [47–50]. Additionally, meshes have been fabricated to release other antibacterial substances like Manuka honey [51]. While patents have been filed on a variety of types of electrospun meshes for wound

and postsurgical treatment, as of yet, no major company has brought any of these products to market [52,53].

Another potential area of commercialization for electrospun meshes is in establishing hemostasis. Such a mesh would have the ability to aid in clotting and in the early stages of wound healing. In an early example of this application, Wnek et al. electrospun fibers from fibrinogen to create a wound-healing mesh. Upon placement in a wound, these fibers have the ability to react with thrombin to produce a fibrous clot structure, which blocks the loss of blood from the wound site and creates a mesh architecture to enable healing [54]. Sell et al. found that by cross-linking these fibrinogen meshes, their degradation was slowed and their mechanical strength was significantly improved. However, this cross-linking did decrease cell migration into the mesh interior, indicating a negative effect on host incorporation and bioactivity [55]. In another study, Spasova et al. electrospun meshes from high-molecular-weight poly(D- or L-)lactide (HMPDLA or HMPLLA), diblock copolymers of poly(D- or L-) lactide, and poly(*N,N*-dimethylamino-2-ethyl methacrylate) (PDMAEMA) blocks. X-ray photoelectron spectroscopy demonstrated that the PDMAEMA blocks had tertiary amino groups, which imbued the fibrous mesh with hemostatic and antibacterial properties. When placed in fresh human blood, these meshes caused a significant decrease in red blood cell count and thrombocyte number, indicating hemostatic activity [56].

Rather than just delivering one specific clotting factor, many groups are investigating the ability to deliver a whole collection of them, in the form of preparation rich in growth factors (PRGF). PRGF is a mix of clotting factors and growth factors released by lysing platelets at a wound site and is ideally suited for stimulating clotting and wound healing. Sell et al. successfully incorporated PRGF into electrospun meshes and demonstrated protein release from these meshes for up to 35 days in culture. Additionally, adipose-derived stem cell (ADSC) culture showed that these meshes increased cell proliferation and chemotaxis [57].

A similar application involves the delivery of plasma factor VIII (FVIII), a clotting factor in which people with hemophilia are deficient. Rather than delivering this factor to an immediate wound site, a more long-term approach involves releasing it systemically to treat this deficiency throughout the body. Liao and Leong addressed this by culturing myoblasts on aligned core/shell electrospun fibers to produce FVIII-producing skeletal myotubes. These core/shell fibers released angiogenic and lymphogenic factors to stimulate growth in the surrounding vasculature and lymphatic system in order to increase the uptake of FVIII. Upon implantation in hemophilic mice, these constructs integrated with the host tissue and successfully induced vascular and lymphatic growth and infiltration. In addition, sustained elevation of FVIII levels was seen in the mice over the following 2-month period, with a significant decrease in blood coagulation time [58].

There are several commercialized electrospun products designed to aid in hemostasis, which are in various stages of development. One prime example is the FASTCLOT line of products, developed by St. Teresa Medical, Inc. These products are electrospun meshes of dextran, which are layered with a proprietary mixture of lyophilized thrombin and fibrinogen. In a study by Bowlin et al., these electrospun meshes were shown to form a fibrin sealant over wound sites, achieving hemostasis

and allowing reestablishment of antegrade blood flow in an injured limb, preserving the limb [59]. A specific variation on the FASTCLOT line developed for the treatment of surgical wounds, called SURGICLOT, has currently finished clinical trials and is awaiting CE marking. If this approval is granted, SURGICLOT will be the first fully electrospun medical implant and drug delivery system on the market for use in humans. Another variation on this technology for use in animals, called ANIMALCLOT, is already on the market for use in animals. A similar product is under development by BioSurfaces Inc. In this product, clotting factors are embedded within electrospun fibers, rather than coating the surface. While the exact polymer/drug composition of this product has not been reported, initial animal trials have shown much quicker clot formation than combat gauze, the current industry standard [60].

Another potential area for the commercialization of electrospun drug delivery systems is the delivery of growth factors to target tissues. This function is often a component of tissue engineering meshes which integrate themselves with host tissue to promote cell adhesion, migration, proliferation, and differentiation in order to mimic natural tissue. Growth factor release enables tissue engineering meshes to promote these cellular activities in order to better integrate and stimulate tissue repair. As such, the release profiles of these meshes should ideally be tuned to maximize cellular response, which is usually best achieved by a flatter, sustained release over a period of days or weeks. For example, as described in an earlier section, Phipps et al. designed bone-mimetic electrospun meshes of blended PCL and collagen type I with embedded HA nanoparticles and adsorbed PDGF onto the surface of the fibers. Although the adsorbed PDGF exhibited a burst release in the first 4 days, this was followed by a period of sustained release over the next 20 days. The meshes were shown to significantly increase cellular chemotaxis and proliferation of mesenchymal stem cells into the mesh as compared with non-PDGF control meshes [9]. These results thus indicate the great potential of the PDGF-releasing meshes in bone regenerative therapy.

These growth factor-releasing meshes can also be used to treat chronic wounds, including diabetic ulcers. Choi, Leong, and Yoo developed an electrospun mesh of PCL/PEG block copolymers and PCL polymer chains with exposed functional amine groups. Epidermal growth factor (EGF) was then covalently bound to these amine groups. During release studies, it was shown that the EGF release from the mesh had very little initial burst and maintained consistent prolonged release throughout the 14-day period. When placed in a diabetic mouse model, the EGF-conjugated meshes induced significantly faster wound closure as compared with animals treated with EGF solutions and unconjugated fibers, just fibers, and no treatment controls [61]. Yang et al. did a similar study using coaxial electrospinning to embed fibroblast growth factor (FGF) in core/shell fibers with an FGF core and a poly(ethylene glycol)-poly(DL-lactide) (PELA) shell. These fibers had a small FGF burst release of around 18% within the first 12 h but then exhibited a constant prolonged release over the next 25 days. This release was shown to significantly improve the proliferation and collagen production in mouse embryo fibroblasts relative to non-FGF control meshes. In vivo testing in a mouse wound model showed significantly faster wound closure and less scar formation in the wounds treated with FGF-containing meshes as compared with the non-FGF controls [62]. This result demonstrates the benefit of

long-term release in maintaining consistent therapeutic drug levels in the local area despite constant clearance by the body.

In addition to wound treatment applications, growth factor-releasing meshes also show promise in several different areas. In the area of nerve regeneration, Cho et al. conjugated nerve growth factor (NGF) to exposed amine groups on electrospun PCL-PEG block copolymer fibers and then showed that the combination of NGF release and topographical cues promoted neuronal differentiation of mesenchymal stem cells [63]. In the area of cardiac tissue engineering, Tian et al. encapsulated VEGF into dextran or BSA cores surrounded by a poly(L-lactic acid-*co*- ϵ -caprolactone) (PLCL) shell to create core/shell fibers. These fibers showed a consistent release of VEGF over 672 h, with the BSA cores exhibiting a 10% initial burst release prior to the prolonged release. These meshes were shown to significantly induce mesenchymal stem cell proliferation as compared with non-VEGF-containing fibers [64]. In the area of cartilage engineering, Li et al. adsorbed TGF- β onto the fiber surfaces of PCL electrospun meshes. When cultured on these meshes, mesenchymal stem cells differentiated into a chondrocytic phenotype and produced significantly more glycosaminoglycans and collagen as compared with meshes without TGF- β adsorbed to them [65].

While the delivery of growth factors via electrospun meshes has a wide variety of applications in tissue engineering, the most promising avenue for near-term commercialization is in the treatment of chronic wounds. As detailed above, numerous electrospun products have been tested in animal models of chronic wounds, with encouraging results. Unfortunately, no major company has brought any of these products to market yet.

The delivery of anticancer drugs via electrospun meshes is likewise a promising avenue for commercialization. Due to the deleterious effects of anticancer drugs on quickly dividing cells, localization of their release within the body is extremely important in maximizing the therapeutic dose while minimizing side effects. In one application, Yohe et al. developed a superhydrophobic PCL/poly(glycerol monostearate-*co*- ϵ -caprolactone) (PGC-C18) mesh with the anticancer drugs SN-38 or CPT-11 incorporated by blend electrospinning for treatment of colorectal cancer. Due to the hydrophobicity of the meshes, there was negligible burst release from these constructs, with the most consistent release coming from a 90:10 mixture of PCL/PGC-C18 for SN-38 over a 70-day period. These 90:10 PCL/PGC-C18 SN-38-loaded meshes demonstrated extended tumor cell cytotoxicity over a 60-day time period, as compared with a 5-day time period for PCL/SN-38 meshes and a max 5-day period for CPT-11-loaded meshes. These results indicate the efficacy of these superhydrophobic electrospun meshes in preventing colorectal cancer resurgence following surgical tumor resection [66]. In a similar study, Qui et al. used mesoporous silica nanoparticles to load the anticancer drug doxorubicin into PLLA electrospun fibers. The resulting meshes had a sustained, prolonged release of doxorubicin and exhibited higher in vitro antitumor efficacy than doxorubicin directly loaded into the fibers without the nanoparticle carriers [67].

In order to optimize effective drug release rates for the treatment of malignant gliomata, Ranganath and Wang electrospun a blend of paclitaxel and PLGA copolymer that was composed of an 85:15 lactic-to-glycolic acid ratio into microfiber disks (MFD) and microfiber sheets (MFS) and a 50:50 lactide to glycolide ratio into

submicrofiber disks (SFD) and submicrofiber sheets (SFS). Disks were obtained via 3 mm diameter biopsy punches of electrospun mats, while sheets were obtained by slicing the mats into 5 mm \times 5 mm squares. SEM imaging showed that the microfiber meshes had fiber diameters of $3.5 \pm 0.32 \mu\text{m}$ while the submicrofiber meshes had fiber diameters of $0.930 \pm 0.035 \mu\text{m}$. Both mesh types had comparable paclitaxel payload, but the small fiber constructs had faster bulk degradation due to the higher glycolic acid content, and thus a higher release rate. The disk structures of both fiber types had lower initial burst release due to their compact structure, while the sheets exhibited burst release of 5%–10%. Nonetheless, all constructs had consistent, prolonged release throughout the 80-day release period. When placed in culture with C6 glioma cells, all paclitaxel-treated fibers caused significantly higher levels of apoptosis than control, nonpaclitaxel-treated blank fibers, and apoptotic activity continued to increase after days 8 and 12. At the furthest time point, day 12, the SFS-treated group had the most apoptosis, while the MFD had the least amount among treatment groups. Control wells in which free paclitaxel was placed had higher initial levels of apoptosis than fiber-treated groups, but after the paclitaxel was washed off and media was replaced on day 3 to simulate clearance by the body, the cell density began to rise again. When placed in a mouse glioma model, all paclitaxel-containing constructs were more effective at reducing tumor volume than treatment by paclitaxel solution, and the SFS and SFD groups were most effective of the constructs [23]. These results thus demonstrate the benefits of using electrospun carriers to maintain high concentrations of anticancer drugs in the local area of the tumor, rather than systemic treatments.

In addition to the colorectal cancer and glioma targets already discussed, drug-laden electrospun meshes have been fabricated to target ovarian cancer [68], lung cancer [22], hepatoma [69], liver carcinoma [70], cervical carcinoma [71], and gastric cancer [72]. Given the *in vitro* and *in vivo* efficacy of electrospun meshes as delivery vehicles for anticancer drugs, this application is a promising avenue for commercialization. However, no major company has brought electrospun drug-laden products to market.

7.7 Outlook, problems to be overcome

Despite the numerous advantages electrospun meshes have as drug delivery constructs, the process entails its own challenges and potential concerns with regard to polymer choice, solvent choice, drug interaction with both polymer and solvent, degradation rate, and the loss of mechanical integrity of meshes due to the incorporation of drugs within the fibers. Fortunately, many of these probable issues can be mitigated through appropriate polymer and drug combinations for the given application and desired degradation time line. Unfortunately, there are still many factors to address in order to create a stable and effective electrospun drug delivery system, and these include composition, modifying the fabrication process and long-term upscale production of such substrates. To outline these obstacles, it is logical to begin with composition in terms of drug, polymer, and solvent choices.

Choice of drug is highly dependent on the required action at the site; however, what is most important is matching the chosen drug type, whether it is hydrophobic or hydrophilic, with a similarly behaving polymer [73]. While both types are easily

encapsulated in electrospun fibers, it is logical that a hydrophobic drug should be combined with a hydrophobic polymer such as the drug paclitaxel combined with hydrophobic polymer PCL. The same goes for matching a hydrophilic drug with a hydrophilic polymer, such as tetracycline hydrochloride with PLGA. This is necessary for electrospun polymer/drug blends in order to ensure complete mixing and dissolution of the drug within the polymer solution and full encapsulation within the resulting fibers. If there is poor dissolution, the drug will simply become dispersed and possibly aggregated within the solution, which may result in fiber formation with drug particles on the outer surfaces of fibers, consequently causing a significant burst effect, nonideal for sustained drug delivery systems [73].

Solvent choice is yet another hurdle to be overcome as commonly used polymers are often best soluble in harsh organic solvents. While the electrospinning fabrication process involves the evaporation of the solvent as the fibers are formed, there is still concern with the initial drug-solvent interaction as potentially harmful to the drug or the overall function, potency, and efficacy of the system [74]. A study by Nie et al. evaluated the denaturation of the bone morphogenetic protein-2 (BMP-2) when in contact with the organic, hydrophobic solvent dichloromethane (DCM) [20]. When BMP-2 alone was added to DCM, the denaturation of the protein was greater than when a combination of BMP-2 and HA was added to the DCM. Concentration of HA, a hydrophilic mineral, was inversely related to levels of BMP-2 denaturation, indicating that a greater presence of a hydrophilic molecule allowed for BMP-2 attachment and shielding from interaction with the DCM [20]. However, in a 2011 study, Madurantakam et al. tested the biological activity of BMP-2 in the common electrospinning solvents hexafluoroisopropanol (HFP) and tetrafluoroethylene (TFE) and found no evidence of BMP-2 denaturation. These findings demonstrate that the effects of organic solvents on labile molecules can vary from solvent to solvent, and thus, solvent choice is extremely important when creating a drug-laden mesh [75]. In order to more fully address issues with denaturation of therapeutic agents, processing of materials without organic solvents must be further explored. Additionally, continued development of particles for drug encapsulation could help prevent denaturation of components [20,74]. Subsequent studies and adequate understanding of drug-polymer-solvent interactions will, in turn, facilitate the development of meshes that better incorporate labile biomacromolecules.

Electrospun meshes are highly controlled in terms of surface-area-to-volume ratio, fiber diameter, overall porosity, and mechanical integrity in terms of modulus of elasticity and maximum tensile strength. Further optimization of the fabrication process, including large-scale production, is needed to improve fiber morphology and drug encapsulation and arrangement for optimal release kinetics. The mechanical integrity of the mesh is usually critical to the template's efficacy when used as a tissue regeneration construct. The incorporation of drugs within the electrospun fibers can result in a decline of these properties, which affects the template's performance in a given application. While this is a major concern of many researchers in terms of tissue regeneration, it is only a minor concern for drug delivery systems because their intended function is to release the drug locally and not necessarily to cause new tissue formation. While one study reported that mechanical properties were maintained as the electrospinning process was scaled up, they limited the mechanical evaluation

of the meshes to fiber morphology and drug encapsulation, rather than Young's modulus and tensile strength [76]. However, a separate group produced meshes on a large-scale commercial instrument, the NANOSPIDER, mechanically tested for Young's modulus and tensile strength and found that the meshes exhibited maintenance of mechanical integrity when one particular drug, tenofovir (TFV), was incorporated with PVA yet experienced a threefold decline in the same properties when a different drug, levonorgestrel, was incorporated within the PVA [77]. The data suggest that these properties are not necessarily structure- or fabrication scale-dependent but merely a function of composition of the mesh [77].

Perhaps the most important obstacle to overcome is tailoring the degradation rate of the mesh to meet the needs of the host tissue regeneration. Ideally, the bulk of the mesh remains implanted for an adequate period of time such that the drug dissolution is local and steady, lasting long enough for either new tissue growth or to rid the area of any existing or potential infections. While composition and electrospinning technique for fabrication of the template are factors of degradation rate, the breakdown mechanisms and hydrophilicity of the mesh also play a role. The release of drug molecules can be influenced by their hydrophilicity, encapsulation within the fiber interior or within micro/nanoparticles, and by fiber hydrophilicity.

Electrospun drug delivery systems can only remain a promising endeavor if the capacity to scale-up is realized. It is often said that the scale-up potential of the electrospinning fabrication process is one of its greatest attributes [73]. However, there is very little evidence in mass scale production of electrospun meshes as drug delivery systems. In a recent study to develop vaginal drug delivery systems, Krogstad and Woodrow successfully fabricated their hydrophilic TFV and PVA meshes on both laboratory and mass production scale while maintaining the mechanical characteristics, drug-loading capabilities, and release kinetics despite the differences in manufacturing processes [76]. Blakney et al. used an industrial electrospinner, the NANOSPIDER, for production of TFA-PVA meshes, which also exhibited appropriate mechanical properties, high drug loading, and drug release [77]. The applications of both of these products necessitated an initial burst release of the drug, which was verified via release studies. Many other applications necessitate a more sustained release, and products with these release profiles have yet to be successfully produced on an industrial scale.

The presented obstacles described in this section are intertwined, and efforts to address one obstacle often alter the available options for addressing other obstacles. Despite these hurdles, it is reasonable to conclude that upon successful upscale production and clinical performance studies, this underutilized technology can and will produce advantageous drug delivery systems.

7.8 Conclusion

Over the past twenty years, there has been increasing interest in mechanisms for targeting drug delivery in order to increase drug levels in the target tissue while decreasing levels in untargeted tissues so as to maximize therapeutic effect and minimize side effects. Due to their high surface-area-to-volume ratio, tailorability of

release rates and degradation, and versatility of drug-loading methods, electrospun fibrous meshes are ideal drug delivery vehicles for many applications. Numerous advancements in postelectrospinning attachment, covalent linking, polymer chemistry, coaxial electrospinning, and micro/nanoparticle encapsulation have enabled labile drugs to be successfully loaded and released without denaturation. New methods of reducing burst release have enabled the use of these systems in applications requiring long-term, sustained release, such as tissue growth and tumor reduction. While many of the studies outlined in this chapter are exploratory in nature and rely on *in vitro* experiments, there are a significant number that include encouraging *in vivo* results in a variety of applications. Nevertheless, advancements in industrial scale-up and clinical studies will be necessary to bridge the gap between exploratory research and commercialization.

References

- [1] Bae YH, Park K. Targeted drug delivery to tumors: myths, reality and possibility. *J Control Release* 2011;153:198.
- [2] Qian ZM, Li H, Sun H, Ho K. Targeted drug delivery via the transferrin receptor-mediated endocytosis pathway. *Pharmacol Rev* 2002;54:561–87.
- [3] Sudimack J, Lee RJ. Targeted drug delivery via the folate receptor. *Adv Drug Deliv Rev* 2000;41:147–62.
- [4] Torchilin VP. Drug targeting. *Eur J Pharm Sci* 2000;11:S81–91.
- [5] Wang Y, Qiao W, Yin T. A novel controlled release drug delivery system for multiple drugs based on electrospun nanofibers containing nanoparticles. *J Pharm Sci* 2010;99:4805–11.
- [6] Chen C, Lv G, Pan C, Song M, Wu C, Guo D, et al. Poly (lactic acid)(PLA) based nanocomposites—a novel way of drug-releasing. *Biomed Mater* 2007;2:L1.
- [7] Roth CM, Lenhoff AM. Electrostatic and van der Waals contributions to protein adsorption: comparison of theory and experiment. *Langmuir* 1995;11:3500–9.
- [8] Li L, Li H, Qian Y, Li X, Singh GK, Zhong L, et al. Electrospun poly (ϵ -caprolactone)/silk fibroin core-sheath nanofibers and their potential applications in tissue engineering and drug release. *Int J Biol Macromol* 2011;49:223–32.
- [9] Phipps MC, Xu Y, Bellis SL. Delivery of platelet-derived growth factor as a chemotactic factor for mesenchymal stem cells by bone-mimetic electrospun scaffolds. *PLoS One* 2012;7:e40831.
- [10] Bölgen N, Vargel I, Korkusuz P, Menceloğlu YZ, Pişkin E. *In vivo* performance of antibiotic embedded electrospun PCL membranes for prevention of abdominal adhesions. *J Biomed Mater Res B Appl Biomater* 2007;81:530–43.
- [11] Casper CL, Yang W, Farach-Carson MC, Rabolt JF. Coating electrospun collagen and gelatin fibers with perlecan domain I for increased growth factor binding. *Biomacromolecules* 2007;8:1116–23.
- [12] Lu Y, Jiang H, Tu K, Wang L. Mild immobilization of diverse macromolecular bioactive agents onto multifunctional fibrous membranes prepared by coaxial electrospinning. *Acta Biomater* 2009;5:1562–74.
- [13] Delcorte A, Bertrand P, Wischerhoff E, Laschewsky A. Adsorption of polyelectrolyte multilayers on polymer surfaces. *Langmuir* 1997;13:5125–36.

- [14] Chunder A, Sarkar S, Yu Y, Zhai L. Fabrication of ultrathin polyelectrolyte fibers and their controlled release properties. *Colloids Surf B: Biointerfaces* 2007;58:172–9.
- [15] Thierry B, Kujawa P, Tkaczyk C, Winnik FM, Bilodeau L, Tabrizian M. Delivery platform for hydrophobic drugs: prodrug approach combined with self-assembled multilayers. *J Am Chem Soc* 2005;127:1626–7.
- [16] Yoo HS, Kim TG, Park TG. Surface-functionalized electrospun nanofibers for tissue engineering and drug delivery. *Adv Drug Deliv Rev* 2009;61:1033–42.
- [17] Choi JS, Yoo HS. Electrospun nanofibers surface-modified with fluorescent proteins. *J Bioact Compat Polym* 2007;22:508–24.
- [18] Liu Y, Min D, Bolton T, Nubé V, Twigg SM, Yue DK, et al. Increased matrix metalloproteinase-9 predicts poor wound healing in diabetic foot ulcers. *Diabetes Care* 2009;32:117–9.
- [19] Kim HS, Yoo HS. MMPs-responsive release of DNA from electrospun nanofibrous matrix for local gene therapy: in vitro and in vivo evaluation. *J Control Release* 2010;145:264–71.
- [20] Nie H, Soh BW, Fu YC, Wang CH. Three-dimensional fibrous PLGA/HAp composite scaffold for BMP-2 delivery. *Biotechnol Bioeng* 2008;99:223–34.
- [21] Piras A, Nikkola L, Chiellini F, Ashammakhi N, Chiellini E. Development of diclofenac sodium releasing bio-erodible polymeric nanomats. *J Nanosci Nanotechnol* 2006;6:3310–20.
- [22] Chen P, Wu Q-S, Ding Y-P, Chu M, Huang Z-M, Hu W. A controlled release system of titanocene dichloride by electrospun fiber and its antitumor activity in vitro. *Eur J Pharm Biopharm* 2010;76:413–20.
- [23] Ranganath SH, Wang C-H. Biodegradable microfiber implants delivering paclitaxel for post-surgical chemotherapy against malignant glioma. *Biomaterials* 2008;29:2996–3003.
- [24] Kataphinan W, Dabney S, Reneker D, Smith D, Akron U. Electrospun skin masks and uses thereof. Patent WO0126610, University of Akron; 2001.
- [25] Kenawy E-R, Bowlin GL, Mansfield K, Layman J, Simpson DG, Sanders EH, et al. Release of tetracycline hydrochloride from electrospun poly(ethylene-co-vinyl acetate), poly(lactic acid), and a blend. *J Control Release* 2002;81:57–64.
- [26] Zeng J, Yang L, Liang Q, Zhang X, Guan H, Xu X, et al. Influence of the drug compatibility with polymer solution on the release kinetics of electrospun fiber formulation. *J Control Release* 2005;105:43–51.
- [27] Maretschek S, Greiner A, Kissel T. Electrospun biodegradable nanofiber nonwovens for controlled release of proteins. *J Control Release* 2008;127:180–7.
- [28] Zeng J, Aigner A, Czubayko F, Kissel T, Wendorff JH, Greiner A. Poly(vinyl alcohol) nanofibers by electrospinning as a protein delivery system and the retardation of enzyme release by additional polymer coatings. *Biomacromolecules* 2005;6:1484–8.
- [29] Ouchi T, Nishizawa H, Ohya Y. Aggregation phenomenon of PEG-grafted chitosan in aqueous solution. *Polymer* 1998;39:5171–5.
- [30] Jiang H, Fang D, Hsiao B, Chu B, Chen W. Preparation and characterization of ibuprofen-loaded poly(lactide-co-glycolide)/poly(ethylene glycol)-g-chitosan electrospun membranes. *J Biomater Sci Polym Ed* 2004;15:279–96.
- [31] Tiwari SK, Tzezana R, Zussman E, Venkatraman SS. Optimizing partition-controlled drug release from electrospun core-shell fibers. *Int J Pharm* 2010;392:209–17.
- [32] Zhang Y, Wang X, Feng Y, Li J, Lim C, Ramakrishna S. Coaxial electrospinning of (fluorescein isothiocyanate-conjugated bovine serum albumin)-encapsulated poly(ϵ -caprolactone) nanofibers for sustained release. *Biomacromolecules* 2006;7:1049–57.
- [33] Wang C, Yan K-W, Lin Y-D, Hsieh PC. Biodegradable core/shell fibers by coaxial electrospinning: processing, fiber characterization, and its application in sustained drug release. *Macromolecules* 2010;43:6389–97.

- [34] Jiang H, Hu Y, Li Y, Zhao P, Zhu K, Chen W. A facile technique to prepare biodegradable coaxial electrospun nanofibers for controlled release of bioactive agents. *J Control Release* 2005;108:237–43.
- [35] Greiner A, Wendorff J, Yarin A, Zussman E. Biohybrid nanosystems with polymer nanofibers and nanotubes. *Appl Microbiol Biotechnol* 2006;71:387–93.
- [36] Liao I, Chew S, Leong K. Aligned core-shell nanofibers delivering bioactive proteins. *Nanomedicine (Lond)* 2006;1:465–71.
- [37] Chen M, Dong M, Havelund R, Regina VR, Meyer RL, Besenbacher F, et al. Thermo-responsive core–sheath electrospun nanofibers from poly(*N*-isopropylacrylamide)/polycaprolactone blends. *Chem Mater* 2010;22:4214–21.
- [38] Ionescu LC, Lee GC, Sennett BJ, Burdick JA, Mauck RL. An anisotropic nanofiber/microsphere composite with controlled release of biomolecules for fibrous tissue engineering. *Biomaterials* 2010;31:4113–20.
- [39] Beck-Broichsitter M, Thieme M, Nguyen J, Schmehl T, Gessler T, Seeger W, et al. Novel ‘nano in nano’ composites for sustained drug delivery: biodegradable nanoparticles encapsulated into nanofiber non-wovens. *Macromol Biosci* 2010;10:1527–35.
- [40] Kim B-S, Park SW, Hammond PT. Hydrogen-bonding layer-by-layer-assembled biodegradable polymeric micelles as drug delivery vehicles from surfaces. *ACS Nano* 2008;2:386–92.
- [41] Kedar U, Phutane P, Shidhaye S, Kadam V. Advances in polymeric micelles for drug delivery and tumor targeting. *Nanomed Nanotechnol Biol Med* 2010;6:714–29.
- [42] McKee MG, Layman JM, Cashion MP, Long TE. Phospholipid nonwoven electrospun membranes. *Science* 2006;311:353–5.
- [43] Kriegel C, Kit K, McClements DJ, Weiss J. Electrospinning of chitosan–poly(ethylene oxide) blend nanofibers in the presence of micellar surfactant solutions. *Polymer* 2009;50:189–200.
- [44] Nagarajan R, Drew C, Mello CM. Polymer-micelle complex as an aid to electrospinning nanofibers from aqueous solutions. *J Phys Chem C* 2007;111:16105–8.
- [45] Kim K, Luu YK, Chang C, Fang D, Hsiao BS, Chu B, et al. Incorporation and controlled release of a hydrophilic antibiotic using poly(lactide-co-glycolide)-based electrospun nanofibrous scaffolds. *J Control Release* 2004;98:47–56.
- [46] Zhang L, Yan J, Yin Z, Tang C, Guo Y, Li D, et al. Electrospun vancomycin-loaded coating on titanium implants for the prevention of implant-associated infections. *Int J Nanomedicine* 2014;9:3027.
- [47] Abrigo M, McArthur SL, Kingshott P. Electrospun nanofibers as dressings for chronic wound care: advances, challenges, and future prospects. *Macromol Biosci* 2014;14:772–92.
- [48] De Jager Heunis T. Development of an antimicrobial wound dressing by co-electrospinning bacteriocins of lactic acid bacteria into polymeric nanofibers. PhD Thesis, University of Stellenbosch.
- [49] Liu H, Leonas KK, Zhao Y. Antimicrobial properties and release profile of ampicillin from electrospun poly(ϵ -caprolactone) nanofiber yarns. *J Eng Fibers Fabr* 2010;5:10–9.
- [50] Liu X, Lin T, Gao Y, Xu Z, Huang C, Yao G, et al. Antimicrobial electrospun nanofibers of cellulose acetate and polyester urethane composite for wound dressing. *J Biomed Mater Res B Appl Biomater* 2012;100:1556–65.
- [51] Minden-Birkenmaier B. Preliminary investigation and characterization of electrospun polycaprolactone and Manuka honey scaffolds for dermal repair. *J Eng Fibers Fabr* 2015;10:126–38.
- [52] Sell SA, Minden-Birkenmaier BA. Honey and growth factor eluting scaffold for wound healing and tissue engineering. Google Patents; 2014.

- [53] Smith DJ, Reneker DH, McManus AT, Schreuder-Gibson HL, Mello C, Sennett MS. Electrospun fibers and an apparatus therefore. Google Patents; 2004.
- [54] Wnek GE, Carr ME, Simpson DG, Bowlin GL. Electrospinning of nanofiber fibrinogen structures. *Nano Lett* 2003;3:213–6.
- [55] Sell SA, Francis MP, Garg K, McClure MJ, Simpson DG, Bowlin GL. Cross-linking methods of electrospun fibrinogen scaffolds for tissue engineering applications. *Biomed Mater* 2008;3:045001.
- [56] Spasova M, Manolova N, Paneva D, Mincheva R, Dubois P, Rashkov I, et al. Polylactide stereocomplex-based electrospun materials possessing surface with antibacterial and hemostatic properties. *Biomacromolecules* 2009;11:151–9.
- [57] Sell SA, Wolfe PS, Ericksen JJ, Simpson DG, Bowlin GL. Incorporating platelet-rich plasma into electrospun scaffolds for tissue engineering applications. *Tissue Eng A* 2011;17:2723–37.
- [58] Liao I-C, Leong KW. Efficacy of engineered FVIII-producing skeletal muscle enhanced by growth factor-releasing co-axial electrospun fibers. *Biomaterials* 2011;32:1669–77.
- [59] Bowlin GL, Simpson DG, Bowman JR, Rothwell SW. Electrospun dextran fibers and devices formed therefrom. Google Patents; 2009.
- [60] Biosurfaces Inc. Drug Loading of Electrospun Materials, <<http://www.biosurfaces.us/drug-loading>>; 2015 [accessed 3.10.2016].
- [61] Choi JS, Leong KW, Yoo HS. In vivo wound healing of diabetic ulcers using electrospun nanofibers immobilized with human epidermal growth factor (EGF). *Biomaterials* 2008;29:587–96.
- [62] Yang Y, Xia T, Zhi W, Wei L, Weng J, Zhang C, et al. Promotion of skin regeneration in diabetic rats by electrospun core-sheath fibers loaded with basic fibroblast growth factor. *Biomaterials* 2011;32:4243–54.
- [63] Cho YI, Choi JS, Jeong SY, Yoo HS. Nerve growth factor (NGF)-conjugated electrospun nanostructures with topographical cues for neuronal differentiation of mesenchymal stem cells. *Acta Biomater* 2010;6:4725–33.
- [64] Tian L, Prabhakaran MP, Ding X, Kai D, Ramakrishna S. Emulsion electrospun vascular endothelial growth factor encapsulated poly(l-lactic acid-co-ε-caprolactone) nanofibers for sustained release in cardiac tissue engineering. *J Mater Sci* 2012;47:3272–81.
- [65] Li WJ, Laurencin CT, Catterson EJ, Tuan RS, Ko FK. Electrospun nanofibrous structure: a novel scaffold for tissue engineering. *J Biomed Mater Res* 2002;60:613–21.
- [66] Yohe ST, Herrera VL, Colson YL, Grinstaff MW. 3D superhydrophobic electrospun meshes as reinforcement materials for sustained local drug delivery against colorectal cancer cells. *J Control Release* 2012;162:92–101.
- [67] Qiu K, He C, Feng W, Wang W, Zhou X, Yin Z, et al. Doxorubicin-loaded electrospun poly(L-lactic acid)/mesoporous silica nanoparticles composite nanofibers for potential postsurgical cancer treatment. *J Mater Chem B* 2013;1:4601–11.
- [68] Yan E, Fan Y, Sun Z, Gao J, Hao X, Pei S, et al. Biocompatible core-shell electrospun nanofibers as potential application for chemotherapy against ovary cancer. *Mater Sci Eng C* 2014;41:217–23.
- [69] Luo X, Xie C, Wang H, Liu C, Yan S, Li X. Antitumor activities of emulsion electrospun fibers with core loading of hydroxycamptothecin via intratumoral implantation. *Int J Pharm* 2012;425:19–28.
- [70] Liu W, Wei J, Huo P, Lu Y, Chen Y, Wei Y. Controlled release of brefeldin A from electrospun PEG-PLLA nanofibers and their in vitro antitumor activity against HepG2 cells. *Mater Sci Eng C* 2013;33:2513–8.

-
- [71] Liu D, Liu S, Jing X, Li X, Li W, Huang Y. Necrosis of cervical carcinoma by dichloroacetate released from electrospun polylactide mats. *Biomaterials* 2012;33:4362–9.
 - [72] Kim Y-J, Park MR, Kim MS, Kwon OH. Polyphenol-loaded polycaprolactone nanofibers for effective growth inhibition of human cancer cells. *Mater Chem Phys* 2012;133:674–80.
 - [73] Zamani M, Prabhakaran MP, Ramakrishna S. Advances in drug delivery via electrospun and electrospayed nanomaterials. *Int J Nanomedicine* 2013;8:2997–3017.
 - [74] Iwase M, Kurata N, Ehana R, Nishimura Y, Masamoto T, Yasuhara H. Evaluation of the effects of hydrophilic organic solvents on CYP3A-mediated drug-drug interaction in vitro. *Hum Exp Toxicol* 2006;25:715–21.
 - [75] Madurantakam PA, Rodriguez IA, Beckman MJ, Simpson DG, Bowlin GL. Evaluation of biological activity of bone morphogenetic proteins on exposure to commonly used electrospinning solvents. *J Bioact Compat Polym* 2011;26:578–89.
 - [76] Krogstad EA, Woodrow KA. Manufacturing scale-up of electrospun poly(vinyl alcohol) fibers containing tenofovir for vaginal drug delivery. *Int J Pharm* 2014;475:282–91.
 - [77] Blakney AK, Krogstad EA, Jiang YH, Woodrow KA. Delivery of multipurpose prevention drug combinations from electrospun nanofibers using composite microarchitectures. *Int J Nanomedicine* 2014;9:2967.

This page intentionally left blank

Electrospun nanofibrous materials for wound healing applications

8

B. Balusamy, A. Senthamizhan, T. Uyar
Bilkent University, Ankara, Turkey

8.1 Introduction

Developments in regenerative medicine and tissue engineering over the decades advanced wound healing methods for enhancing healing process and also overcome existing complications. Archetypically, wound is defined as a disruption of cellular community that consequences in separation of normally connected tissues or a type of injury resulted from the skin that is torn, cut, or punctured [1]. The breach occurred by skin damage leads to bacterial infection that causes inflammation and infection locally or systemically. The wound healing is not a simple linear process, which is one of the most complex and dynamic processes that involved with multiple biological pathways, blood elements, cells, growth factors, and extracellular matrix (ECM) [2–4].

Eventually, wound healing occurs through three stages, namely, (a) inflammation, (b) new tissue formation, and (c) remodeling. The inflammation stage of wound healing process happens immediately following the tissue damage and lasts about 48 h. During this stage, multiple biological pathways are initiated to prevent blood and fluid losses and infection and remove dead and devitalized (dying) tissues. The second stage of the wound healing process occurs between 2 and 10 days after injury and which is characterized by cellular proliferation and migration of different cell types. The third stage of the wound healing is remodeling, and it begins after 2–3 years following the injury and lasts for a year or more in which all the process activated after injury wind down and cease. The detailed information on different stages of the wound repair process is depicted in Fig. 8.1 [4]. Based on the wound repair process, wounds are classified into acute and chronic wounds. Acute wounds are generally healing completely within 8–12 weeks time frame, whereas the chronic wounds take more than 12 weeks for healing process [5,6]. Wound management complications are always having significant impacts in clinical burden; thus, the wound dressing market has great economic potential worldwide [7]. Therefore, recent decades witnessed that a variety of wound dressing materials resulted from numerous approaches have been introduced at different aspects of wound healing process [8].

Development of wound dressing can be tracked back since ancient era from application of medicinal plant, animal fat, and honey to tissue engineering scaffolds. An

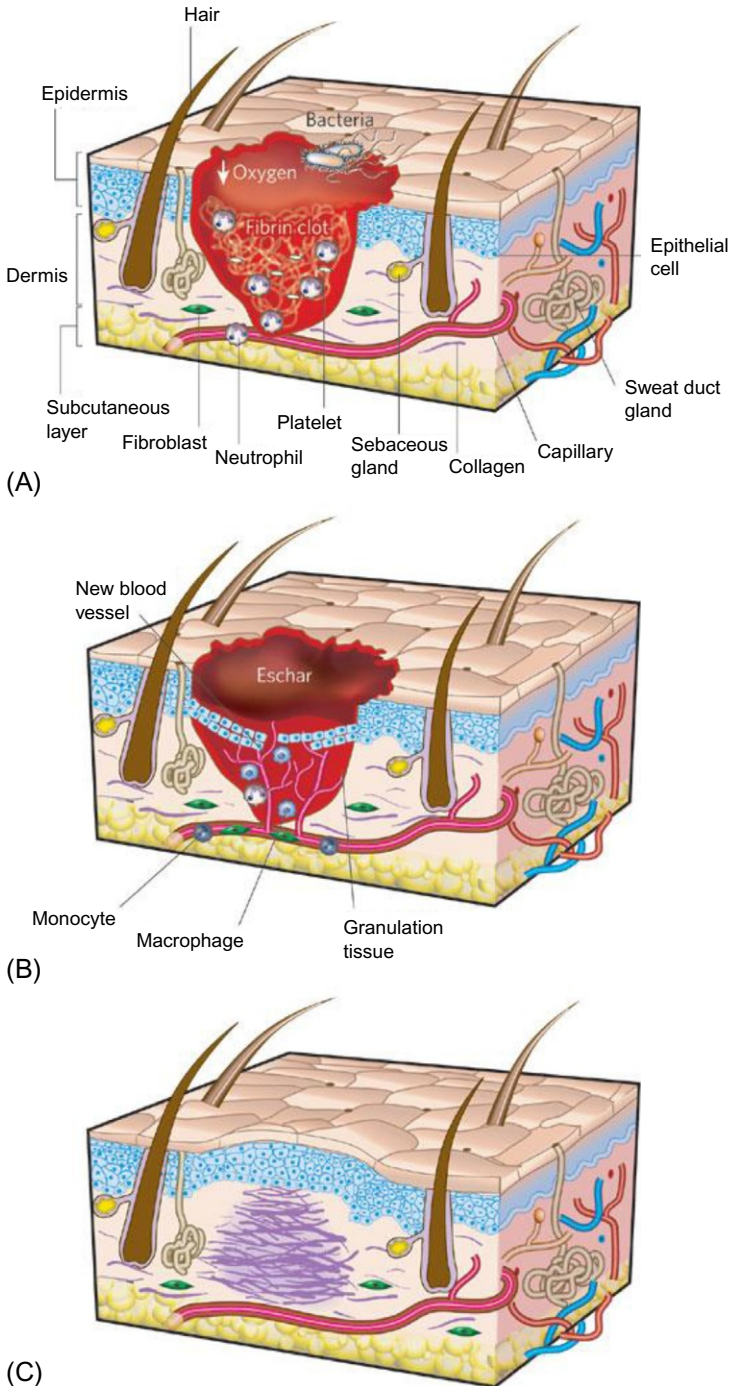


Fig. 8.1 See legend on opposite page.

ideal wound dressing is expected to possess the characteristics including provide or maintain a moist wound environment, removal of blood and excess exudates, gaseous exchange, protect the wound from microorganism invasion, protect the wound from trauma, thermal insulation provision, and most importantly cost-effective and less frequency of dressing change [8,9]. Clinical practice has been widely adopted plain gauze for wound care owing to their inexpensive and readily available nature, but still, it has many shortcomings that has inspired to develop variety of other materials including foams, adhesive films, hydrogels, alginates, hydrocolloids, and biological dressings possessing remarkable features [8,10]. In the recent past, nanotechnology-based therapy has significantly revolutionized the management of wound care and also recognized as possible next-generation therapy. To date, a wide range of nanomaterials composed of carbon, lipid, ceramic, metal, and metal oxide nanoparticles have been reported for their beneficial role in wound healing [11].

Electrospun nanofibers have received tremendous attention toward energy, environmental, and biomedical applications due to their exceptional characteristic features [12–16]. Electrospun nanofiber scaffolds offer ideal characteristics of wound dressings, that is, high surface area to volume ratio, adsorption of exudates, interconnected nanoporosity, controlled drug or biomolecules release, cell respiration, flexibility, and better sorption of proteins; thus, the electrospun nanofibers produced from different electrospinning approaches including blend, coaxial, emulsion electrospinning, and also postspinning modifications have been extensively used in wound healing applications [17–22]. Different biomolecules involved wound healing, fabrication of nanofibers, and current strategies used in electrospinning to produce wound dressing material were reviewed by Abrigo et al. [17]. Furthermore, the architectural feature of electrospun nanofibers mimics the ECM structure, which is the most important characteristic of any scaffold intended to use in tissue engineering applications since it influences the cell binding. Stevens and George [23] reported that the scaffolds with

Fig. 8.1 Classic stages of wound repair. There are three classic stages of wound repair: (A) inflammation, (B) new tissue formation, and (C) remodeling. (A) Inflammation. This stage lasts until about 48 h after injury. Depicted is a skin wound at about 24–48 h after injury. The wound is characterized by a hypoxic (ischaemic) environment in which a fibrin clot has formed. Bacteria, neutrophils, and platelets are abundant in the wound. Normal skin appendages (such as hair follicles and sweat duct glands) are still present in the skin outside the wound. (B) New tissue formation. This stage occurs about 2–10 days after injury. Depicted is a skin wound at about 5–10 days after injury. An eschar (scab) has formed on the surface of the wound. Most cells from the previous stage of repair have migrated from the wound, and new blood vessels now populate the area. The migration of epithelial cells can be observed under the eschar. (C) Remodeling. This stage lasts for a year or longer. Depicted is a skin wound about 1–12 months after repair. Disorganized collagen has been laid down by fibroblasts that have migrated into the wound. The wound has contracted near its surface, and the widest portion is now the deepest. The reepithelialized wound is slightly higher than the surrounding surface, and the healed region does not contain normal skin appendages. Reproduced with permission from Gurtner GC, Werner S, Barrandon Y, Longaker MT. Wound repair and regeneration. *Nature* 2008;453:314–21 with permission from Nature Publishing Group.

nanoscale architecture possess more binding sites due to higher surface area than the microscale architecture scaffold.

This chapter highlights wide range of polymeric electrospun nanofibers and incorporated active agents intended for wound healing applications rather than discussing various adopted electrospinning approaches for preparing nanofibrous wound dressing materials. A well-demonstrated example of such scaffolds has been discussed briefly under each section. In addition, current challenges associated with development of wound care materials and electrospun nanofibrous scaffolds in the market for wound healing are also presented.

8.2 Electrospun nanofibrous scaffolds in wound healing

Electrospun nanofibrous scaffolds in wound healing applications have been well demonstrated using a variety of natural, synthetic, and composite polymers and functionalization of fibers with active agents and herbal molecules [24–26]. A well-demonstrated example of each material is discussed under respective section of the chapter.

8.2.1 Natural polymer nanofibers as wound healing scaffolds

The electrospun nanofibrous scaffolds prepared using natural polymers possess excellent biodegradability, biocompatibility, and other biological properties recognized by cells for physiological process. To date, numerous nanofibrous scaffolds prepared from variety of natural polymers demonstrated their potency in enhanced wound healing including collagen, gelatin, hyaluronic acid, chitosan, and silk fibroin [27]. Collagen is an insoluble fibrous protein, is abundant in the animal kingdom, and is the main component of ECM, providing tensile strength and structural integrity to tissues. Powell et al. [28] prepared freeze-dried (FD) and electrospun (ES) collagen scaffolds further populated with human dermal fibroblasts (HF) and epidermal keratinocytes (HK), which have been isolated from surgical discard tissue to prepare freeze-dried collagen skin substitutes (FCSS) and electrospun collagen skin substitutes (ECSS), and then studied their potency in wound healing. In vitro studies indicated that both FCSS and ECSS did not reveal any significant differences in cell proliferation, surface hydration, or cellular organization and exhibited excellent stratification with a continuous layer of basal keratinocytes present at the dermal-epidermal junction. Immunostaining for involucrin showed positive staining in all the epidermal layers except for the basal cell layer in both the FDSS and ECSS as shown in Fig. 8.2. Basement membrane formation was evident in both the FDSS and ECSS as indicated by the continuous layer of collagen IV at the dermal-epidermal junction in the skin substitutes in vitro.

The wound healing study in athymic mice demonstrated that prepared grafts prepared with FD and ES scaffolds were well integrated into surrounding murine skin and possessed a uniformly dry epidermis (Fig. 8.3A and B). The FCSS and ECSS grafts were visibly smaller with a majority of the ECSS maintaining their original shape as shown in Fig. 8.3C and D upon 8 weeks exposure, but differences in surface area

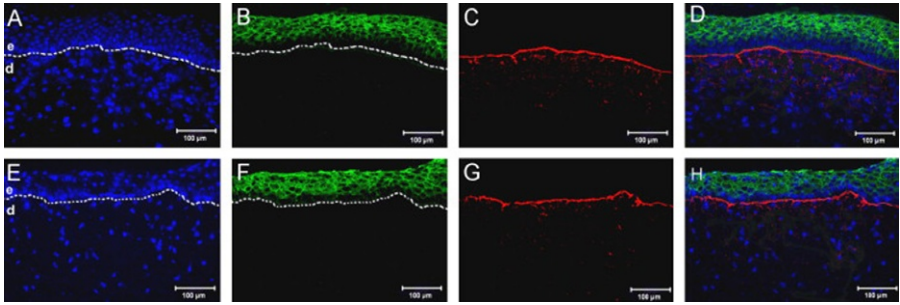


Fig. 8.2 Immunohistological images of FCSS (A–D) and ECSS (E–H) showing cell nuclei (A and E), human involucrin (B and F), human collagen type IV (C and G), and merged images (D and H). The epidermis and dermis are denoted by e and d, respectively. The dashed line indicates the dermal-epidermal junction. Scale bar = 100 µm.

Reproduced with permission from Powell HM, Supp DM, Boyce ST. Influence of electrospun collagen on wound contraction of engineered skin substitutes. *Biomaterials* 2008;29:834–43 with permission from Elsevier.

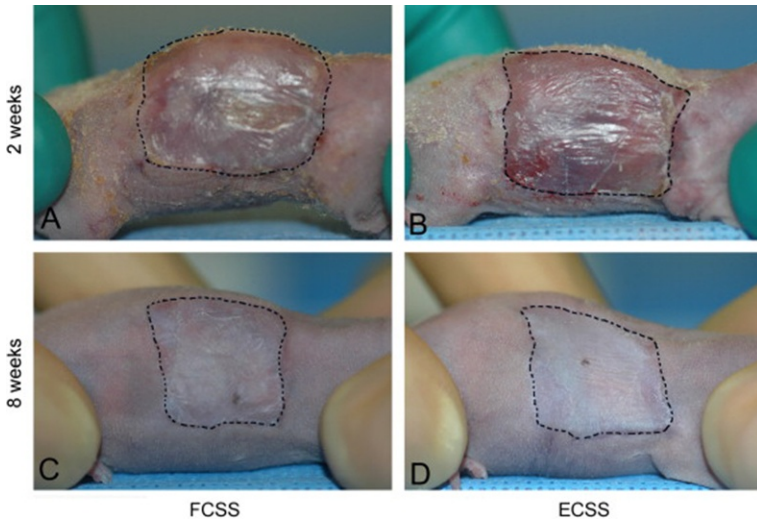


Fig. 8.3 Appearance of grafts on athymic mice 2 and 8 weeks after grafting. Skin substitutes fabricated using freeze-dried (FCSS; A and C) or electrospun collagen (ECSS; B and D) at 2 weeks (A and B) or 8 weeks (C and D), respectively. Wound areas are traced with a dashed black line.

Reproduced with permission from Powell HM, Supp DM, Boyce ST. Influence of electrospun collagen on wound contraction of engineered skin substitutes. *Biomaterials* 2008;29:834–43 with permission from Elsevier.

between the FCSS and ECSS groups were observed with the ECSS grafts on average larger than the FCSS. Further, the microscopic evaluation of skin biopsy collected from each animal showed excellent cell migration into the dermal component of both graft types. However, undigested bovine collagen sponge was visible in within the graft on animals from the FCSS group, whereas no residual ES collagen was found in any of the ECSS animals at week 8 and the dermal component of the grafted ECSS and the murine skin. And also, it was found that after grafting to full-thickness wounds in athymic mice, both skin substitutes had high rates of engraftment, 87.5% in the FCSS group and 100% in the ECSS group.

Similarly, in a recent study, tilapia skin collagen electrospun nanofibers have showed rapid and effective wound healing property [29]. The wound healing efficiency of tilapia collagen nanofibers was investigated using Sprague-Dawley (SD) rat models with dorsal full-thickness skin defects. The wound healing study results demonstrated that the significant rate of healing in animal treated with tilapia collagen nanofibers started to disappear at day 7, and most of the wound area were covered with a continuous epidermis at day 14 as compared with untreated control and the animals treated with Kaltostat, a commonly used wound dressing. Further, the histopathologic results confirmed that the collagen nanofibers caused lowest degree of inflammatory response and induced the best growth status of new epidermis throughout wound healing process (Fig. 8.4). The inflammatory response was significantly reduced at day 7, and new epidermis with intact structure and good continuity could also been found at day 14. The epidermal cells were fully differentiated, basal cells were closely arranged, the horny layer could be observed, and layers of keratinocytes were evident.

Gelatin (GE) is a derivative of native collagen obtained by partial hydrolysis and has lesser immunogenicity than collagen. The wound healing applications of pure GE nanofibers are limited due to complication in mechanical properties and degradation profile. Powell and Boyce [30] fabricated porous nonwoven fibrous GE scaffolds using electrospinning technique with various solution concentrations and further investigated their influence in dermal and epidermal tissue regeneration. The study results revealed that the nanofibrous scaffolds with interfiber distance of $>5\ \mu\text{m}$ offered deeper penetration of HF and also interfiber distances $\leq 10\ \mu\text{m}$ exhibited well-stratified dermal and epidermal layers. Therefore, the GE nanofibrous scaffolds with $5\text{--}10\ \mu\text{m}$ favored the formation of skin substitutes in vitro. Another study demonstrated the preparation of GE and PCL nanofibers using needleless electrospinning technique and further characterized their biocompatibility and therapeutic efficiency using in vitro cell cultures and in an experimental rat model with wound [31]. Cell proliferations of human mesenchymal stem cells (hMSCs), HF, and keratinocytes on the nanofibers were examined by staining the actin cytoskeleton with phalloidin and visualized by fluorescent microscopy. The in vitro study outcome indicated that significantly higher cell proliferation was observed on GE rather than the PCL nanofibers. Likewise, significantly faster wound closure was found for GE nanofibers on days 5 and 10 compared with the control group treated with gauze as shown in Fig. 8.5. No significant differences in wound closure were observed between the PCL-treated and control groups. Further, the presence of myofibroblasts was assessed at day 10 by quantifying the α -smooth muscle actin (SMA) immunofluorescent staining (Fig. 8.6). The myofibroblast distribution in the wound area corresponded to the degree

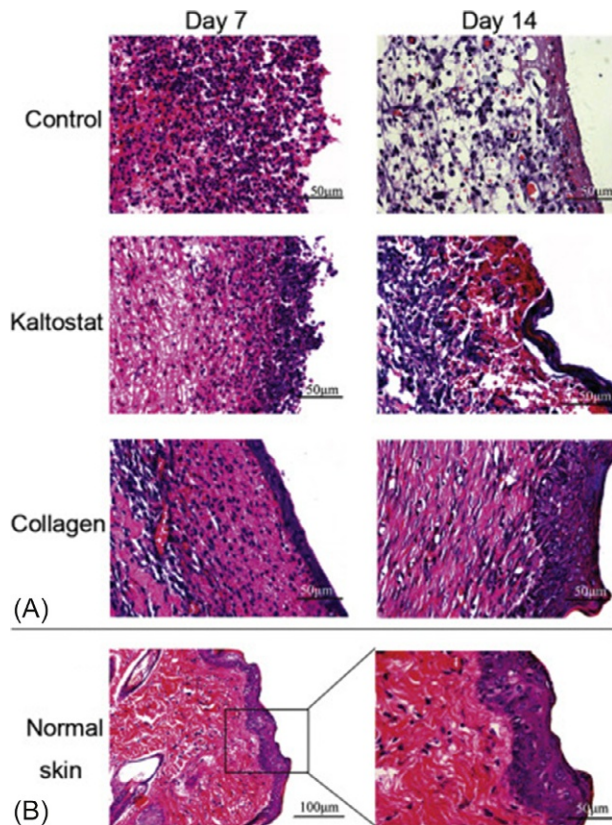


Fig. 8.4 Representative images of hematoxylin and eosin (H and E) staining. (A) Wound sections treated with tilapia collagen nanofibers or Kaltostat, with untreated wounds as control group, at days 7 and 14. (B) Normal skin.

Reproduced with permission from Zhou T, Wang N, Xue Y, Ding T, Liu X, Mo X, et al. Electrospun tilapia collagen nanofibers accelerating wound healing via inducing keratinocytes proliferation and differentiation. *Colloids Surf B* 2016;143:415–22 with permission from Elsevier.

of wound contraction at day 10, and the results demonstrated significantly higher area fraction of α -SMA staining, which was found for GE and which clearly indicates that GE-treated group wounds were more contracted than other groups.

Hyaluronic acid (HA) is a naturally occurring polysaccharide and one of the chief components of ECM. The HA is proved to be beneficial in wound healing applications since it plays major role in facilitating keratinocyte migration and proliferation, activating and moderating the inflammatory response, and reducing scar formation. A preclinical study was conducted to compare healing of wounds covered by an adhesive bandage, a sterilized solid HA, a gauze with Vaseline, an antibiotic dressing, and a sterilized HA nanofiber wound dressing on crossbred pigs as an experimental model [32]. The study results showed that the sterilized HA nanofiber wound dressing exhibited better

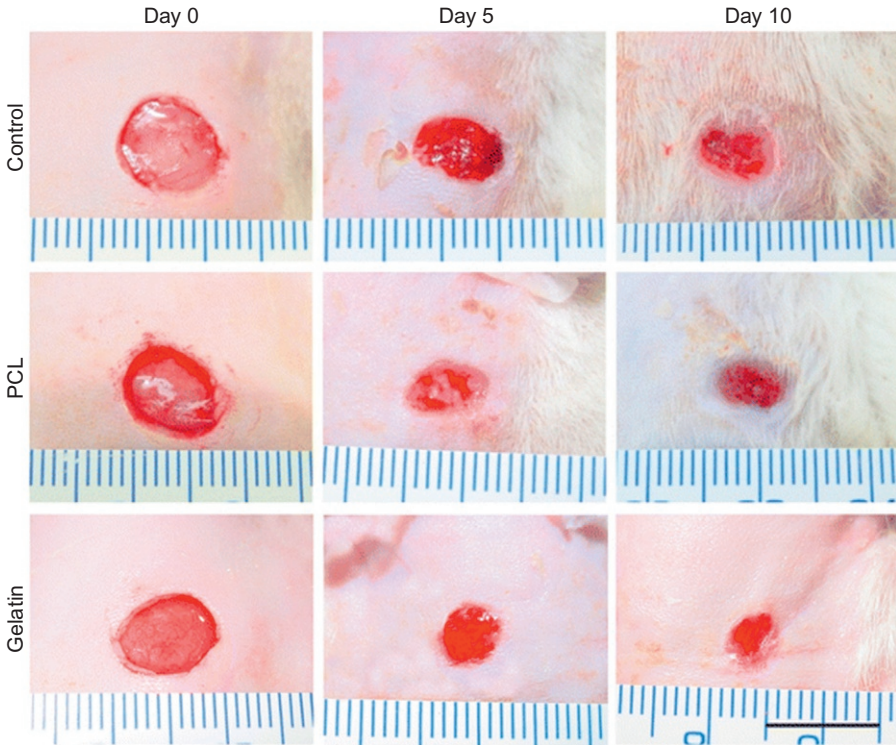


Fig. 8.5 Photographs of full-thickness skin wounds and subsequent wound contraction on days 5 and 10 after treatment with gauze (control), PCL, and gelatin nanofibers. Scale bar = 1 cm. Reproduced with permission from Dubský M, Kubinová Š, Širc J, Voska L, Zajícěk R, Zajícová A, et al. Nanofibers prepared by needleless electrospinning technology as scaffolds for wound healing. *J Mater Sci Mater Med* 2012;23:931–41 with permission from Springer.

healing efficiency than adhesive bandage, sterilized solid HA, and gauze with Vaseline dressing, but it was not statistically better than the antibiotic dressing. It was reported that the enhanced wound healing performance is due to HA aids in cell migration, cell proliferation, angiogenesis, and phagocytosis, and also nanofibers can pick up the exudates from the wound to a greater extent. Another study by Ji et al. [33] reported the preparation of a cross-linked HA hydrogel nanofibers by a reactive electrospinning method. A thiolated HA derivative, 3,3'-dithiobis(propanoic dihydrazide)-modified HA (HA-DTPH), and poly(ethylene glycol) diacrylate (PEGDA) were adopted as cross-linking agents, and the cross-linking reaction was occurred simultaneously during the electrospinning process. A cell morphology study on fibronectin (FN)-adsorbed HA nanofibrous scaffolds showed that the migration of NIH 3T3 fibroblasts into the scaffold through the nanofibrous network occurred, and a three-dimensional dendritic morphology has been demonstrated. Since the high molecular weight and hygroscopic nature of the HA lead to complications in successful preparation of nanofibers, the HA is often blended with other polymers for electrospinning process.

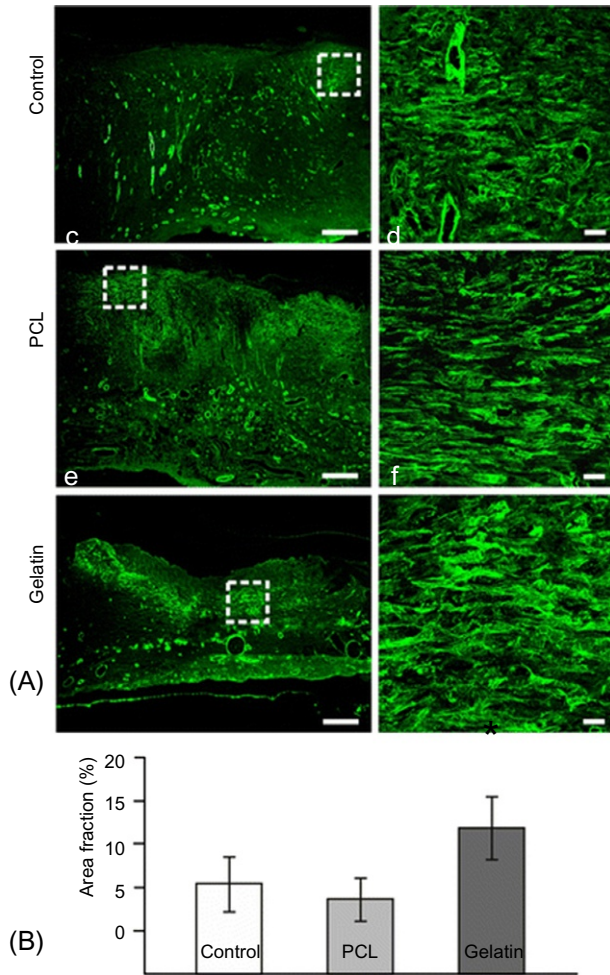


Fig. 8.6 (A) Representative micrographs of α -SMA staining for myofibroblasts and blood vessels in wounds 10 days after treatment with control (a and b), PCL (c and d), and gelatin (e and f). The right micrographs (b, d, and f) represent a higher magnification view of the marked areas in the left micrographs. Scale bar, 200 μ m (a, c, and e) and 20 μ m (b, d, and f). (B) Quantification of α -SMA immunostaining on day 10 after control treatment, PCL, and gelatin nanofibers. α -SMA expression was significantly increased for gelatin compared with control treatment. Mann–Whitney test, $*P < .05$, $**P < .01$.

Reproduced with permission from Dubský M, Kubinová Š, Širc J, Voska L, Zajícěk R, Zajícová A, et al. Nanofibers prepared by needleless electrospinning technology as scaffolds for wound healing. *J Mater Sci Mater Med* 2012;23:931–41 with permission from Springer.

Chitosan, a second most abundant polysaccharide in nature and is a derivative of deacetylated chitin. The chitosan has demonstrated to have great role in wound and burn treatments owing to their hemostatic, antifungal, antibacterial, and wound healing properties. Tchemtchoua et al. [34] compared the biological property of chitosan nanofibrous scaffolds with chitosan films and FD sponges. An initial cell adhesion property of chitosan nanofibers with human fibroblasts, microvascular endothelial cells, and keratinocytes resulted in attachment of cells on day 1 and followed by well spread of cells at day 3 (Fig. 8.7). Further, it has been noted that the keratinocytes formed clusters of flat cells by tightly joining together at day 7, which is a physiological and essential property of keratinocytes in vivo for forming a physical tight barrier.

The electrospun chitosan nanofibrous scaffold also demonstrated good biocompatibility than the FD sponges during implantation study. Further, the wound healing study on mice with full-thickness wounds (8 mm in diameter) in the back skin showed that the chitosan nanofibrous scaffolds were found to adhere uniformly to freshly

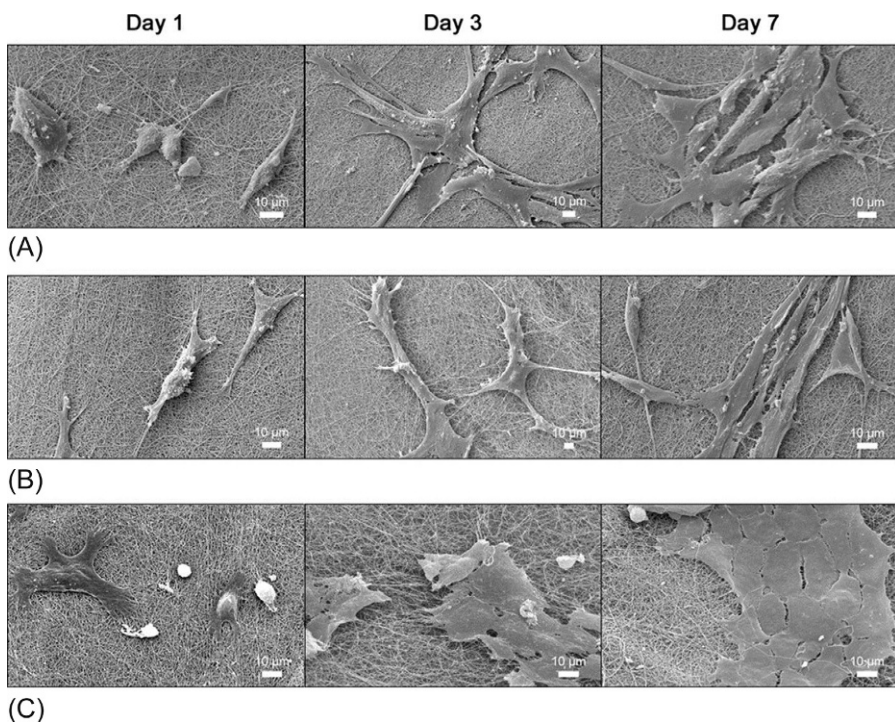


Fig. 8.7 Scanning electron microscopy observation of human fibroblasts (A), microvascular endothelial cells (B), and keratinocytes (C) cultured on electrospun chitosan nanofibers for 1, 3, or 7 days.

Reproduced with permission from Tchemtchoua VT, Atanasova G, Aqil A, Filée P, Garbacki N, Vanhooteghem O, et al. Development of a chitosan nanofibrillar scaffold for skin repair and regeneration. *Biomacromolecules* 2011;12:3194–204 with permission from American Chemical Society.

excised wound surface, to absorb the exudates, and to be fully biocompatible. The control wound beds exhibited the presence of inflammatory cells in a poorly organized tissue; in contrast, a progressive remodeling of the granulation tissue could already be observed in chitosan-treated wounds. At day 14, a well-developed vascular network was also present in the chitosan-treated wounds, and on day 21, most of the initial wound bed is replaced by a well-vascularized newly formed skin that has been not observed with control animals.

Silk fibroin (SF) is a typical fibrous protein, mainly produced by silkworm. Recently, significant attention has been turned toward SF in wound healing applications since fibroin has the unique properties of skin regeneration including excellent biocompatibility, enhanced collagen biosynthesis, minimal immunogenicity, anti-inflammatory activity, hemostatic activity reepithelialization, and elimination of scarring. Till now, few attempts have been made on the electrospun SF scaffolds in wound healing applications. Sheikh et al. [35] prepared 3-D SF nanofibrous scaffolds using cold-plate electrospinning (CPE) to overcome the limitations of the traditional electrospinning (TE) and salt leaching electrospinning (SLE). The prepared 3-D SF nanofibrous scaffolds were used to develop the skin substitute by coculturing two different cell lines in air-liquid culture system. Fig. 8.8A shows the schematic illustration of air-liquid culture system, consisting of keratinocytes cocultured with fibroblasts in the presence of 3-D nanofiber scaffolds produced by 50% of humidity during CPE. The results of incubation period 6, 7, and 8 weeks in the presence of 3-D nanofibers are presented in Fig. 8.8B–D, which demonstrated as the time of incubation passes; a number of fibroblasts and keratinocytes that are infiltrating into 3-D nanofiber scaffolds were increased. And also, the fibroblasts were observed in deep layers whereas keratinocytes at superficial layer, and it resembles the artificial dermis. And also, collagen-like ECM is predominately present in deeper layer of 3-D nanofiber scaffolds at 8 weeks by Masson's trichrome (MT) stain (Fig. 8.8E).

A recent study by Ju et al. [36] reported fabrication of SF nanomatrix by electrospinning and evaluated as wound dressing material in a burn rat model. In brief, the SF solution was mixed with polyethylene oxide (PEO) to obtain desirable viscosity and spinnability. A detailed description of the preparation procedure is illustrated in Fig. 8.9. The prepared SF electrospun nanomatrix was applied on the burned wound created on the back of SD rats to study the effect of SF nanomatrix in wound healing process as compared with medical gauze and MEDIFOAM (polyurethane hydrocellular dressing foam). The wound size reduction, histological examination, and the quantification of transforming growth factor (TGF)- β 1 and interleukin (IL)-1 α , 6, and 10 were considered as parameters in evaluating healing effects. Fig. 8.10 indicated that at day 28, the areas of wounds treated with SF nanomatrix and MEDIFOAM decreased to 4% and 8%, respectively, whereas the wound size of the medical gauze-treated group remains 18%.

Further, the histological analysis indicated that the deposition of collagen in the dermis was organized by covering the wound area in the SF nanomatrix-treated group. And also, the expression level of proinflammatory cytokine (IL-1 α) was significantly reduced on day 7 and increased expression of TGF- β 1 in the wound treated with SF nanomatrix noted on 21 days posttreatment as compared with gauze-treated group

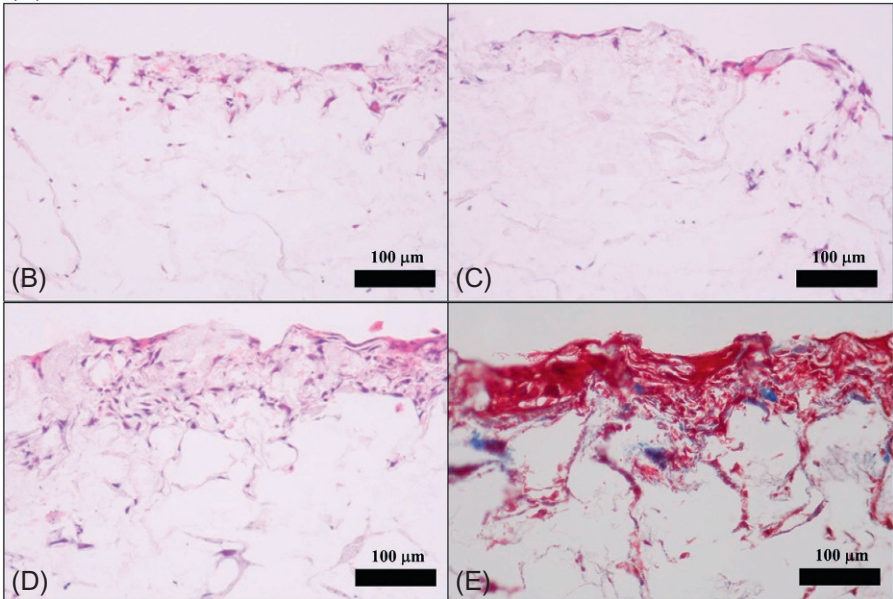
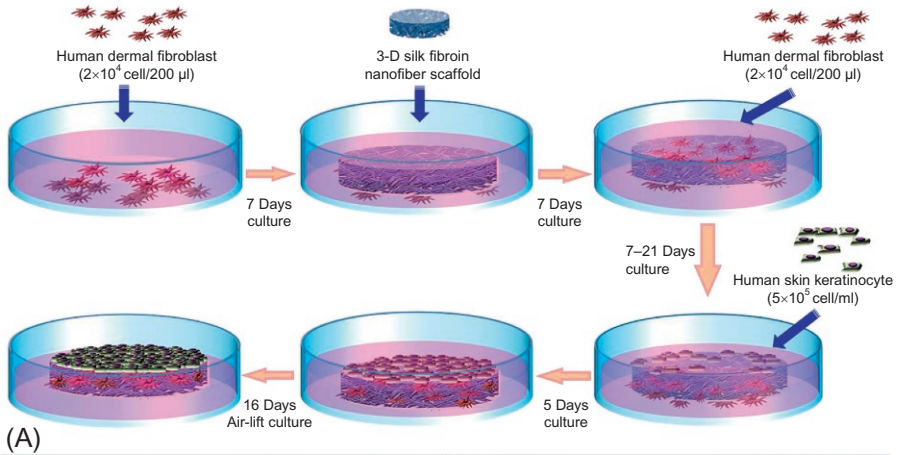


Fig. 8.8 Schematic illustration for cocultured method (fibroblasts and keratinocytes) using air-liquid culture system (A). Histological appearance after coculturing of 3-D nanofibers scaffolds prepared via 50% humidity by CPE technique. The H&E staining results after coculturing for 6 weeks (B), H&E staining results after coculturing 7 weeks (C), and H&E staining results after coculturing 8 weeks (D). The results of MT staining after coculturing of fibroblasts and keratinocytes for 8 weeks (E).

Reproduced with permission from Sheikh FA, Ju HW, Lee JM, Moon BM, Park HJ, Lee OJ, et al. 3D electrospun silk fibroin nanofibers for fabrication of artificial skin. *Nanomedicine* 2015;11:681–91 with permission from Elsevier.

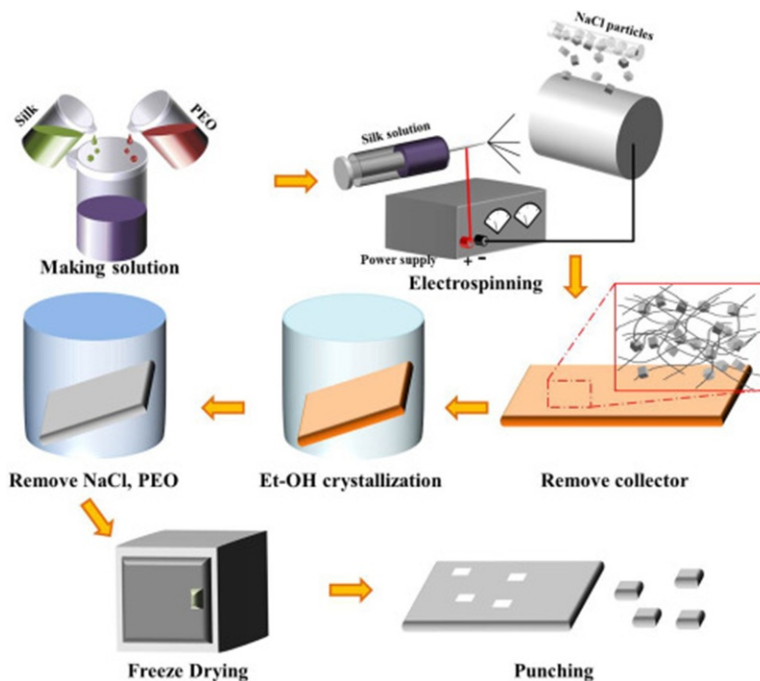


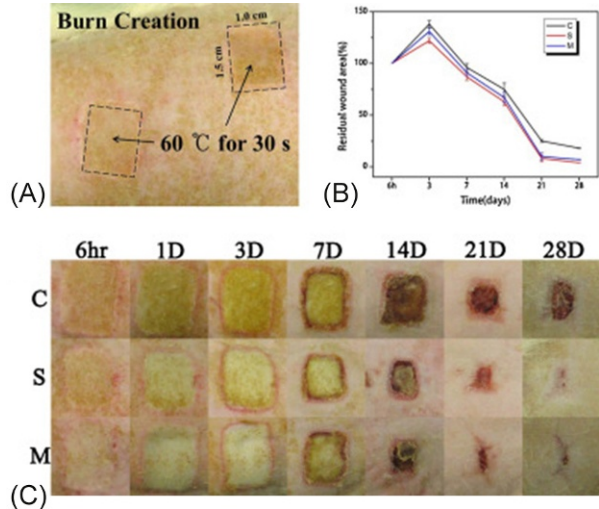
Fig. 8.9 Fabrication of the SF electrospun nanomatrix. A schematic depiction of the NaCl addition during electrospinning and crystallization.

Reproduced with permission from Ju HW, Lee OJ, Lee JM, Moon BM, Park HJ, Park YR, et al. Wound healing effect of electrospun silk fibroin nanomatrix in burn-model. *Int J Biol Macromol* 2016;85:29–39 with permission from Elsevier.

that revealed the enhanced wound healing property of SF nanomatrix. Likewise, many other nanofibers produced from natural polymers were used in wound healing applications.

Incorporation of active agents into polymeric nanofibers is always of great interest in improved biomedical applications. To date, a variety of bioactive agents including antimicrobial agents, growth factors, genes, vitamins, metal, and metal oxide nanoparticles have been introduced into polymeric nanofibers for enhanced wound healing [12,21,22,26]. A recent study by Li et al. [37] demonstrated the incorporation of vitamin A palmitate (VA) and vitamin E TPGS (VE), common derivatives of the unstable vitamins A and E into biodegradable GE nanofibers using electrospinning. The prepared nanofibers were studied for their sustained release behavior, antibacterial activity, cell proliferation, and in vivo wound healing performances. Both VA and VE were mixed with GE solution further electrospun to obtain nanofibers. The in vitro study results indicated that both vitamins have similar release profile, addition of VE showed improved antibacterial efficiency, and VA supports

Fig. 8.10 (A) Burn wound area on rat skin right after the creation. (B) Residual wound area change with healing time (28 days). (C) Gross findings of wound area treated with different wound dressing materials (C, medical gauze; S, SF nanomatrix; and M, MEDIFOAM). Reproduced with permission from Ju HW, Lee OJ, Lee JM, Moon BM, Park HJ, Park YR, et al. Wound healing effect of electrospun silk fibroin nanomatrix in burn-model. *Int J Biol Macromol* 2016;85:29–39 with permission from Elsevier.



better fibroblast cell proliferation. The in vivo wound healing study was performed in SD rats, and the efficiency of wound healing property was compared with commercial antiseptic gauze loaded with ampicillin, gauze soaked with a vitamin solution, GE fibers, and GE films loaded with VA and VE. Fig. 8.11 depicts representative images of wounds made to the skin of male rats at various times after infliction. Throughout the healing time, the areas of wounds treated by the commercial gauze or the gauze immersed in vitamin solution were larger than those treated with the fibers or the film. Compared with the GE fibers and gelatin/VA/VE (G/A+E) film, the wound areas of the G/A+E fiber-treated rats were smaller, indicating a better healing performance. The histological studies were also in agreement with the above findings, which illustrate the incorporation of vitamin in GE nanofibers enhanced the wound healing performances.

Silver nanoparticles (AgNPs) have been well recognized for their excellent antimicrobial efficiencies against wide range of pathogens. A considerable effort has been made to incorporate AgNPs in electrospun nanofibers for wound healing applications. Rath et al. [38] prepared AgNPs-incorporated collagen nanofibers and further investigated their antibacterial activity against potential pathogens and in vivo wound healing performance using Wistar rats. The antibacterial study suggested that AgNP composite nanofibers showed excellent activity against *Staphylococcus aureus* and *Pseudomonas aeruginosa*. In contrast, no inhibition potential against pathogens was noted with plain collagen nanofibers. The antibacterial study result clearly reveals that the AgNP composite nanofibers are capable of providing an aseptic environment at the wound site. The wound healing study also resulted

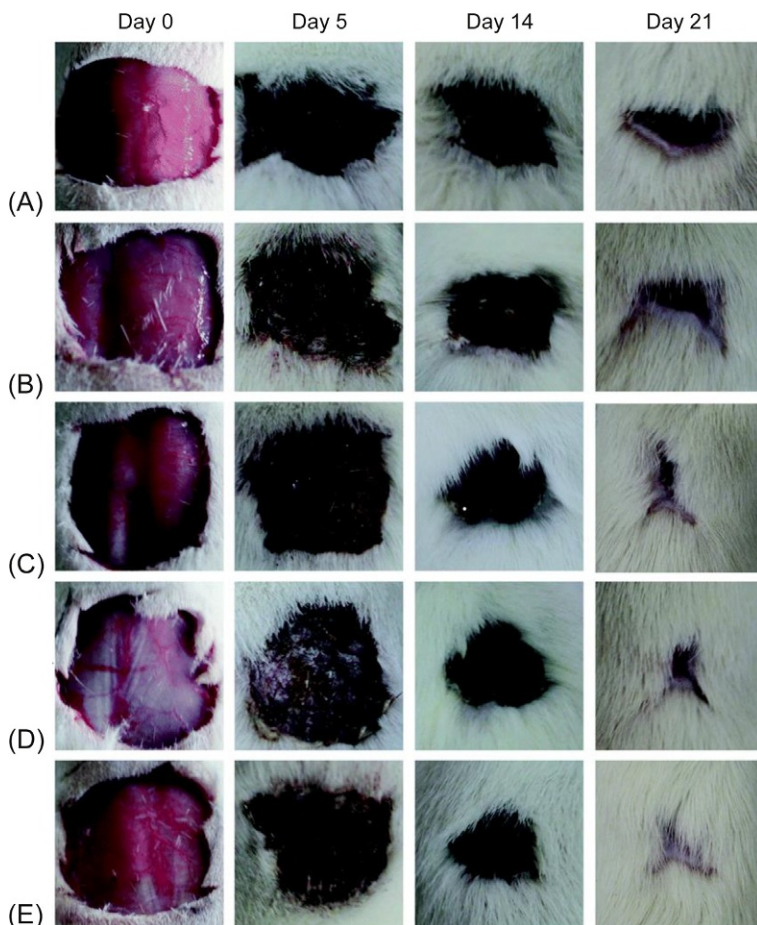


Fig. 8.11 Representative images of the skin wound recovery process after 0, 5, 14, and 21 days. The wound surfaces were treated with (A) commercial gauze, (B) the same type of gauze soaked with a vitamin solution (1.4% w/v VE and 0.14% w/v VA), (C) cross-linked gelatin (G) fibers (D) cross-linked gelatin films loaded with VA and VE, and (E) cross-linked gelatin fibers loaded with VA and VE (G/A+E).

Reproduced with permission from Li H, Wang M, Williams GR, Wu J, Sun X, Lv Y.

Electrospun gelatin nanofibers loaded with vitamins A and E as antibacterial wound dressing materials. *RSC Adv* 2016;6:50267–77 with permission from Royal Society of Chemistry.

in faster wound contraction than plain collagen nanofibers. Similarly, titanium dioxide (TiO_2) nanoparticles were incorporated into SF nanofibers. The nanofibers were studied for their hemocompatibility, cytocompatibility, cell spreading, and antibacterial activity. The altogether results showed that the prepared nanofibrous membrane TiO_2 nanoparticles possess good biocompatibility, cell adhesion, and antimicrobial potential, which further suggest the possible utilization for wound dressing [39].

In recent years, a significant attention has been paid toward antimicrobial peptides (AMPs) as alternative antimicrobial materials. In another study, antimicrobial peptide motif (Cys-KR12) originating from human cathelicidin peptide (LL37) was immobilized onto electrospun SF nanofiber membranes for wound care purposes. The study reported that Cys-KR12-immobilized SF nanofiber membrane exhibited antibacterial potential against *S. aureus*, *S. epidermidis*, *Escherichia coli*, and *P. aeruginosa*. The fibrous membrane also facilitated proliferation of keratinocytes and fibroblasts. Further, it suppressed the lipopolysaccharides (LPS)-induced TNF- α expression of monocytes, suggesting as a promising candidate in wound dressing application [40].

8.2.2 Synthetic polymer nanofibers as wound healing scaffolds

Synthetic polymers provide many advantages over natural polymers, most importantly ability to tailor for better mechanical and degradation properties by altering chemical composition, molecular weight, copolymerization, crystallinity, etc. Aliphatic polyesters are common biodegradable synthetic polymers that offer biomedical applications because of their mechanical strength, adjustable properties, their non-toxic degradation products and processability. There are many synthetic polymers including polyglycolic acid (PGA), poly(lactic acid) (PLA), and polycaprolactone (PCL) that have been approved by US Food and Drug Administration (FDA) for their applications in tissue engineering [41]. The polymers including PLA, PCL, poly(lactic-co-glycolic acid) (PLGA), PEO, polyurethane (PU), and poly(vinyl alcohol) (PVA) have been widely used in wound healing applications [17,21,26].

Synthetic polymeric nanofibers are generally used in wound healing applications by functionalizing with bioactive agents [42]. PCL is a hydrophobic polyester and widely used in tissue engineering applications upon incorporating various bioactive agents. Bahrami et al. [43] prepared unrestricted somatic stem cells (USSCs) loaded in PCL nanofibrous scaffolds and used for skin regeneration on full-thickness skin defects of rats. The wound healing study in animal model exhibited noticeable effect on wound closure on 21 days of treatment. The reconstructed skin area treated with nanofibrous scaffold loaded with USSCs has shown an intact epithelium together with the formation of hair follicles and sebaceous glands. Similarly, zinc oxide (ZnO) nanoparticles have been incorporated into PCL nanofibers using electrospun nanofibers, and further, their ability to perform as skin substitute materials was tested using American satin guinea pigs [44]. The in vivo fibroblast cell proliferation was analyzed during 20 days of subcutaneous implantation of neat PCL membranes and PCL membranes containing 1 wt% ZnO nanoparticles. The histological image indicated that the ZnO nanoparticle-impregnated PCL nanofibrous scaffolds enhanced the cell proliferation as shown in Fig. 8.12. Further, the wound healing study is also following a 30-day observation period; the wounds were completely closed without any sign of scar formation for nanoparticle incorporated membranes. Conversely, hair formation on healed area was significantly less for the animals treated with neat PCL membranes. The overall results indicated that the incorporation of ZnO nanoparticles notably enhanced the wound healing effects. And also, in another

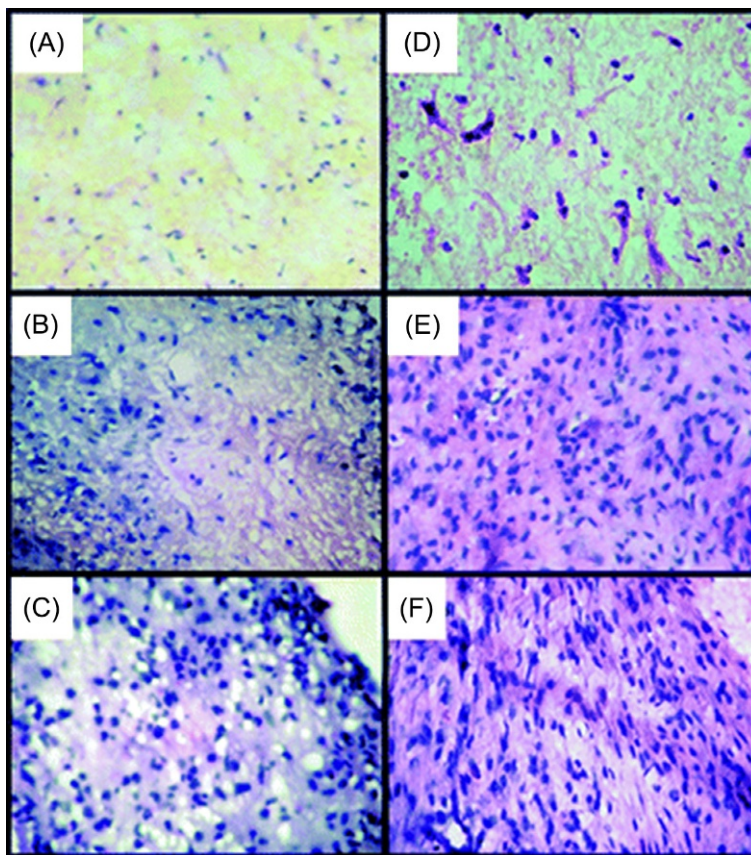


Fig. 8.12 Histological images (H&E staining) of neat PCL membranes (A–C) and PCL membranes containing 1 wt% ZnO nanoparticles (D–F) after 5 days (A and D), 10 days (B and E), and 20 days (C and F) of subcutaneous implantation in guinea pigs.

Reproduced with permission from Augustine R, Dominic EA, Reju I, Kaimal B, Kalarikkal N, Thomas S. Electrospun polycaprolactone membranes incorporated with ZnO nanoparticles as skin substitutes with enhanced fibroblast proliferation and wound healing. *RSC Adv* 2014;4:24777–85 with permission from The Royal Society of Chemistry.

recent study reported by Pinzón-García et al. [45], Bixin (Bix), an antioxidant carotenoid pigment, was loaded to PCL nanofibers, and the *in vivo* wound healing study in diabetic mice resulted in accelerated wound healing and in reduced scar formation as compared with pure PCL nanofibers.

PLA is an aliphatic biodegradable and compostable thermoplastic polymer derived from renewable plant sources and has generated considerable interest in wide range of biomedical applications. Nguyen et al. [46] incorporated curcumin (Cur) into PLA nanofibers for wound healing applications because of their multibiological functions including antiinflammatory, antioxidant, antitumor, and wound healing properties.

Cell attachment study showed the improved cell proliferation and attachment for Cur-loaded PLA nanofibers. Similarly, the wound healing study in C57BL/6 mice demonstrated enhanced wound healing property for Cur-loaded PLA nanofibers (99%) on day 15, which is significantly higher than the wound treated with gauze and PLA nanofibers as shown in Fig. 8.13.

PLGA is the most extensively used biodegradable and biocompatible polymer in therapeutic delivery and tissue engineering. Further, PLGA forms nontoxic end products, increases wettability, and promotes cell proliferation. Lee et al. [47] used PLGA polymer for incorporating metformin, an antihyperglycemic agent usually prescribed for treating type 2 diabetes. The prepared metformin-incorporated PLGA nanofiber was investigated to treat wounds in diabetic SD rat model. The biodegradable nanofibers were shown to release high concentration of metformin over three weeks' time and had more water-containing capacity than virgin PLGA fibers. The wound healing study outcome clearly demonstrated the enhanced wound healing and reepithelialization for the PLGA fibers incorporated with metformin than the animals

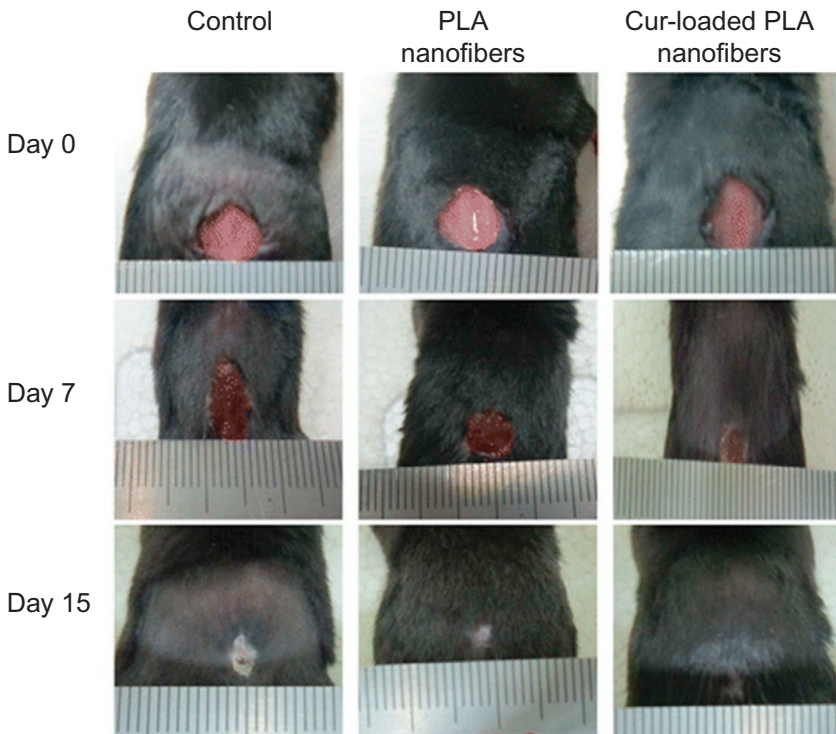


Fig. 8.13 Photographs of the closure of control, PLA nanofiber-treated and Cur-loaded PLA nanofiber-treated mouse back wounds on days 0, 7, and 15.

Reproduced with permission from Nguyen TTT, Ghosh C, Hwang SG, Tran LD, Park JS. Characteristics of curcumin-loaded poly(lactic acid) nanofibers for wound healing. *J Mater Sci* 2013;48:7125–33 with permission from Springer.

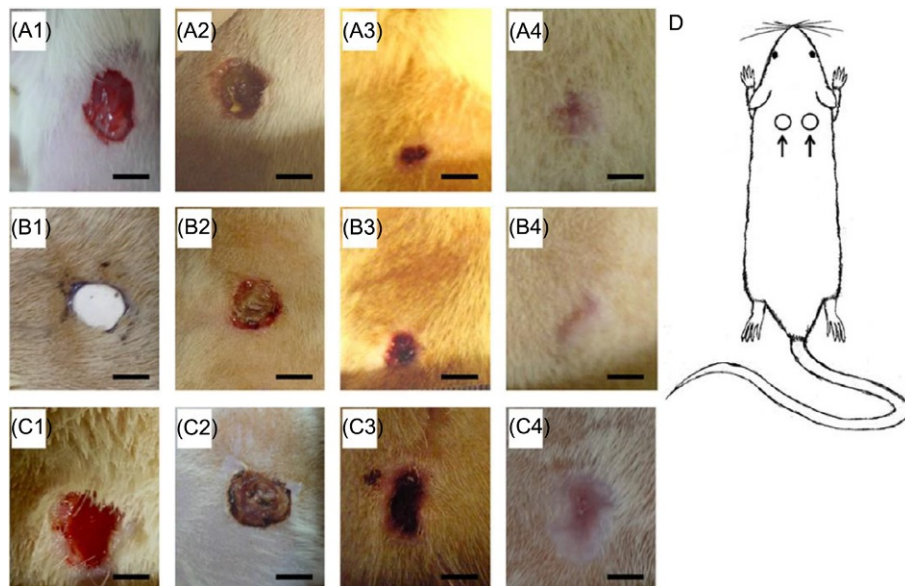


Fig. 8.14 Appearance of healing wound on days 0 (1), 3 (2), 7 (3), and 14 (4) after treatment: (A) PLGA with metformin group and (B) virgin PLGA (C) conventional gauze sponge group (two circular wounds with diameter of 8 mm were prepared on back of each rat, as shown in (D)) (scale bar = 5 mm). Group A exhibited faster healing than group B and group C (post hoc $P < .05$).

Reproduced with permission from Lee CH, Hsieh MJ, Chang SH, Lin YH, Liu SJ, Lin TY, et al. Enhancement of diabetic wound repair using biodegradable nanofibrous metformin-eluting membranes: *in vitro* and *in vivo*. ACS Appl Mater Interfaces 2014;6:3979–86 with permission from American Chemical Society.

treated with virgin PLGA nanofibrous membrane and conventional gauze as shown in Fig. 8.14. Similarly, fusidic acid (FA) is an antibiotic that belongs to a group of fusidanes, which has been incorporated into PLGA nanofiber to study the wound healing efficiency in lightly contaminated or *S. aureus* heavily infected wounds of rat. In either case, FA-loaded fibers have shown speed, quality (minimal scarring), reduced infection dissemination, and fatalities in wound healing than untreated sites [48].

PU is a block of copolymers, widely used in wound dressings because of their good barrier and oxygen permeability properties. Khil et al. [49] produced PU electrospun nanofibers and investigated their wound healing performance in guinea pigs. The PU nanofibers found to have good and immediate adherence property to wet wound surface. The wound treated with PU nanofibers had several characteristic findings compared with control animals in which severe infiltration of inflammatory cells and thick scab were observed. The PU nanofibrous membrane was uniformly adhered on the wound surface without any fluid accumulation. At the end of the study, the wounds covered with PU electrospun nanofibers showed increased rate of epithelialization and

well-organized dermis as compared with TEGADERM, a commercial wound healing material. Another study reported the preparation of PU nanofibers by blending emu oil that is composed of fatty acids and possesses analgesic and antiinflammatory effects. The results indicated that the emu oil contained PU nanofibers that enhanced cell viability and proliferation of 3T3-L1 fibroblasts cells. The membrane as well showed good bacteriostatic activity against both Gram-positive and Gram-negative pathogens and expected to have application in wound skin tissue engineering [50]. Similarly, ampicillin-loaded PU (A-PU) nanofibers were electrospun and have shown to maintain good viability in human keratinocyte (HaCaT) cells and exhibit good antibacterial activity against Gram-positive *S. aureus* and Gram-negative *K. pneumonia*. The overall outcome suggests that A-PU scaffolds can be used in wound healing and infection control applications [51]. Likewise, incorporation of AgNPs in PU nanofibers were also reported to show enhanced performances and suggesting for their use in wound healing applications [52,53].

PVA is a good biocompatible polymer used in variety of advanced biomedical applications. Nguyen et al. [54] reported the preparation of AgNPs-loaded PVA electrospun fibers by coupling microwave and electrospinning methods and further studied their antibacterial activity against *E. coli* (Gram-negative) and *S. aureus* (Gram-positive) bacteria for intended use in wound healing applications. The silver nitrate containing PVA solution was microwave irradiated and then electrospun for obtaining AgNPs-loaded PVA electrospun fibers. The antibacterial study revealed no obvious zones of inhibition observed for pure PVA membrane, whereas AgNPs-loaded PVA electrospun membrane heated 150°C showed strongest antimicrobial activities against both Gram-positive *S. aureus* and Gram-negative *E. coli*; however, *S. aureus* is more sensitive than the *E. coli* bacteria. The fabricated mat that had a high tensile stress and antimicrobial potential has beneficial for skin applications.

Poly-L-lactic acid (PLLA) is a biodegradable poly(α -hydroxy acids) and has been widely investigated for their use in treatment of musculoskeletal injuries, controlled-release systems, and tissue engineering. A recent study by Li et al. [55] reported recombinant silkworm AMP Bmattacin2-incorporated PLLA exhibited broad spectrum of antibacterial activity and selective killing ability toward skin and colon cancer cells over their normal cell counterparts. The antibacterial study using AATCC100 against *E. coli* and *S. aureus* indicated that PLLA/Bmattacin2 had 26.2% inhibition on *E. coli* while it had 32.3% inhibitive activity on *S. aureus* as shown in Fig. 8.15A. Further, live/dead assay by SYTO 9 and propidium iodide indicated the live (green) and dead bacteria (red) on fabricated membranes (Fig. 8.15b1 and b3). Further, SEM observations of both bacteria showed the morphology of bacteria has been destroyed with PLLA/Bmattacin2 treatment as shown in Fig. 8.15b6 and c6, respectively. Further, cell proliferation assay with human skin cell HFF1 demonstrated the increased cell proliferation rate on both PLLA and PLLA/Bmattacin2 at day 1, day 3, and day 7 showing their cell compatibility nature. The SEM and fluorescent staining also confirmed the cell spreading over the surface of the membranes. Therefore, the prepared PLLA/Bmattacin2 can be used in skin reconstruction, wound dressing, and healing.

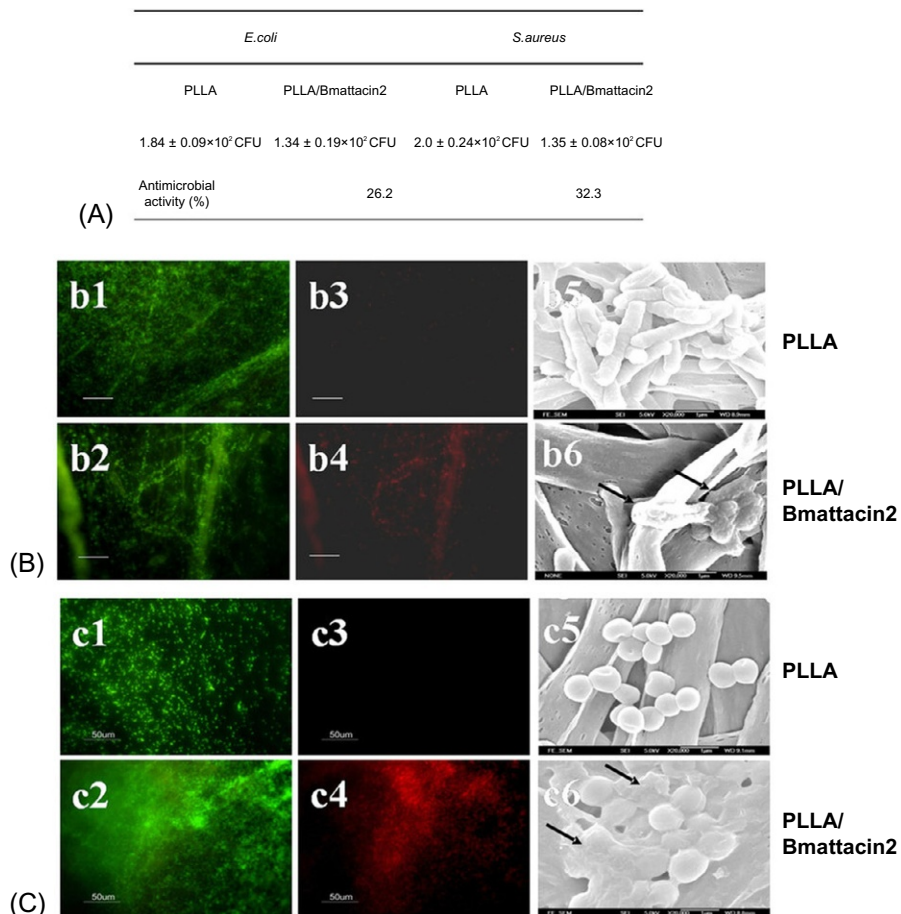


Fig. 8.15 Antibacterial effect of electrospun composite membranes. (A) Investigating antibacterial effect of electrospun composite membranes on *E. coli* and *S. aureus* by AATCC100 method. (B) Observation of *E. coli* cultured on the surface of PLLA or PLLA/Bmattacin2 membranes. (b1–b4) Live/dead bacterial staining. (b5 and b6) SEM observation. (C) Observation of *S. aureus* cultured on the surface of PLLA or PLLA/Bmattacin2 membranes. (c1–c4) Live/dead bacterial staining. (c5 and c6) SEM observation. Reproduced with permission from Li Z, Liu X, Li Y, Lan X, Leung PH, Li J, et al. Composite membranes of recombinant silkworm antimicrobial peptide and poly(L-lactic acid) (PLLA) for biomedical application. *Sci Rep* 2016;6:31149 with permission from Nature Publishing Group.

8.2.3 Composite polymer nanofibers as wound healing scaffolds

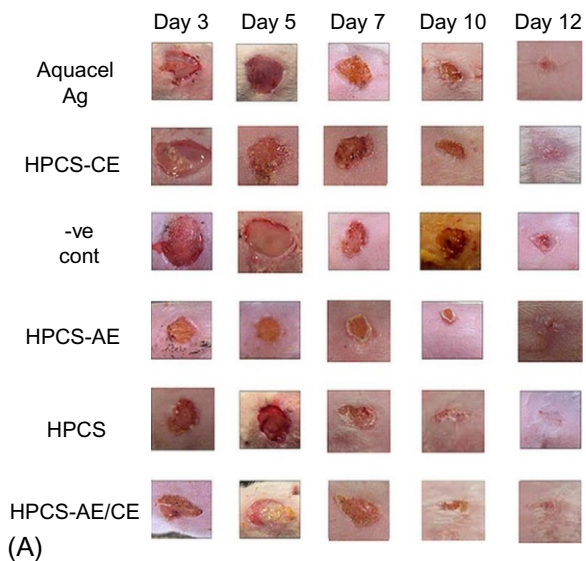
Composite polymeric nanofibers are produced by the combination of natural and/or synthetic polymers that possess advantages of each polymer to overcome the limitations and aiming wound healing applications. There have been a number of studies reported for the preparation of different polymeric nanofibers and incorporation of

active agents for improved wound healing performances. Ebrahimi-Hosseinzadeh et al. [56] reported preparation of nanofibrous scaffold by blending two natural polymers, namely, GE and HA. In vivo wound healing study in Wistar rats with deep second-degree burns has been investigated in comparison with ChitoHeal gel (a commercial wound dressing). Following 14 days of treatments with GE/HA, composite nanofibrous membranes and ChitoHeal gel reached up to wound closure of 81.9% and 77.8%, respectively, while untreated control has shown 65% wound closure efficiency. The histopathologic study conducted on postoperative days of 7 and 14 exhibited more epidermis formation in the gel and scaffold groups. And also, a number of inflammatory cells observed in these groups were significantly lesser than the control group.

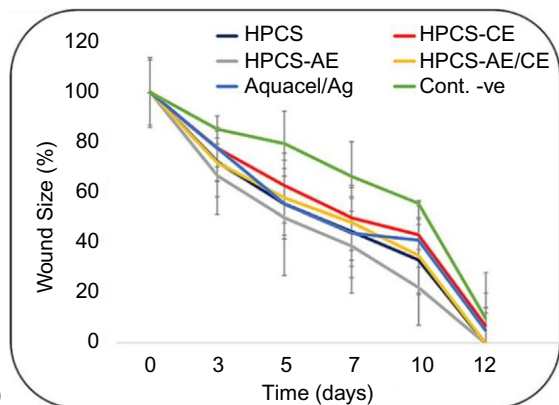
Application of herbal extracts is familiar in treating burns and wounds since ancient times. Recently, extracts of *Cleome droserifolia* (CE) and *Allium sativum* (AE) have been incorporated into honey, poly(vinyl alcohol), chitosan nanofibers (HPCS) to develop biocompatible antimicrobial nanofibrous wound dressing [57]. The extracts were incorporated into HPCS separately, HPCS-CE and HPCS-AE, or in combination, HPCS-CE/AE. The in vitro antibacterial study against *S. aureus*, *E. coli*, methicillin-resistant *S. aureus* (MRSA), and multidrug-resistant *P. aeruginosa* was carried out in comparison with AquacelAg, a commercial wound dressing, and the study revealed HPCS-AE and HPCS-AE/CE nanofiber mats have shown complete inhibition of *S. aureus*, and the HPCS-AE/CE exhibited mild antibacterial activity against MRSA. Further, the developed nanofiber dressings and the AquacelAg commercial dressing were used in wound healing study on experimental mice having an excisional 9 mm wound on the dorsal back.

Photographs of the wound region were recorded on days 3, 5, 7, 10, and 12 to determine the change in the wound size over time (Fig. 8.16). It was observed that the wound closure was greatly enhanced with the HPCS nanofiber mats, and upon addition of AE in the HPCS-AE mats, the wound closure rate increased. On the other hand, the wound closure rate was reduced upon addition of the CE to the HPCS-CE nanofibrous mats, whereas the combination of both extracts within the HPCS-AE/CE nanofiber dressings showed wound closure rates similar to those of the HPCS dressing. Upon comparing the wound closure rate of the developed nanofibrous dressings to the commercial AquacelAg, it was observed that the HPCS and the HPCS-AE/CE showed similar effects, whereas the HPCS-AE showed enhanced wound closure rates. Therefore, the antibacterial and wound healing properties of the developed nanofiber mats and their minimal side effects make them competitive candidates for use as effective wound dressings.

Hajiali et al. [58] incorporated lavender oil (LO) into sodium alginate and PEO (SA-PEO/LO) nanofibers and demonstrated their efficiency in antibacterial and treatment of skin burns induced by midrange ultraviolet radiation (UVB). The LO release measurement indicated that therefore, the produced alginate-based nanofibers were active for more than 2 days and able to release the antibacterial and antiinflammatory agent. The antibacterial study against *S. aureus* revealed SA-PEO/LO nanofibers inhibited the proliferation of the microorganisms and inhibition zones with an average diameter of (21.7 ± 1.6) mm. A desired portion of C57BL/6J mice skin was exposed to



(A)



(B)

Fig. 8.16 Photographic images of the extent of wound healing: (A) graphical illustration of the changes in wound size (B) on days 3, 5, 7, 10, and 12 for the developed nanofibrous dressings HPCS, HPCS-AE, HPCS-CE, and HPCS-AE/CE and the untreated negative control (-ve control) and the treated positive control with the commercial dressing AquacelAg. Reproduced with permission from Sarhan WA, Azzazy HME, El-Sherbiny IM. Honey/chitosan nanofiber wound dressing enriched with *Allium sativum* and *Cleome droserifolia*: enhanced antimicrobial and wound healing activity. ACS Appl Mater Interfaces 2016;8:6379–90 with permission from American Chemical Society.

narrowband UVB light source and immediately covered with SA-PEO or SA-PEO/LO nanofibers or a commercial alginate product used as standard of care (3M Tegaderm Alginate). The wound healing and cytokine expression studies have shown that alginate-based nanofibers controlled UVB-induced inflammation; therefore, the electrospun dressings were proved appropriate for the management of burn wounds.

In another study, curcumin-loaded poly(ϵ -caprolactone) (PCL)/gum tragacanth (GT) (PCL/GT/Cur) nanofibers were investigate for their wound healing potential in diabetic rats. The antibacterial study of the resultant membrane against MRSA and extended spectrum β -lactamase (ESBL) has shown PCL/GT/Cur nanofibers were 99.9% antibacterial against MRSA and 85.14% against ESBL as depicted in Fig. 8.17. Similarly, wound healing study resulted in curcumin-eluting


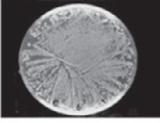
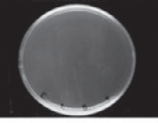
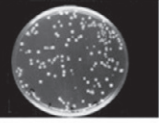


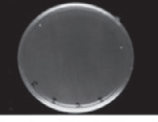
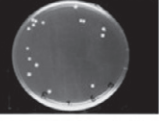
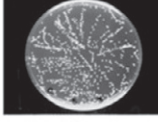
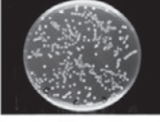
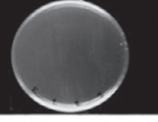
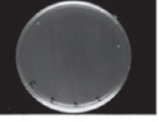
Bacteria	Control		GT/PVA/cur samples	
	MRSA	ESBL	MRSA	ESBL
First dilution				
Amount	Uncountable	Uncountable	No growth	6.1×10^5 (CFU/ml)
Second dilution				
Amount	Uncountable	Uncountable	No growth	7.5×10^5 (CFU/ml)
Third dilution				
Amount	3.2×10^7 (CFU/ml)	2.8×10^7 (CFU/ml)	No growth	No growth
Average				6.8×10^5 (CFU/ml)
Antibacterial (%)			99.9%	85.14

Fig. 8.17 Antibacterial activity against MRSA and ESBL for samples containing Cur (average CFU/ml).

Reproduced with permission from Mohammadi MR, Rabbani S, Bahrami SH, Joghataei MT, Moayer F. Antibacterial performance and *in vivo* diabetic wound healing of curcumin loaded gum tragacanth/poly(ϵ -caprolactone) electrospun nanofibers. *Mater Sci Eng C* 2016;69:1183–91 with permission from Elsevier.

nanofibers improved the wound healing compared with control samples significantly, and they showed complete healing at the surface with well-formed granulation tissue dominated by fibroblast proliferation, collagen deposition, complete early regenerated epithelial layer, and formation of sweat glands and hair follicles. No such appendage formation was observed in the untreated controls during this duration. Further, MT staining confirmed the increased presence of collagen in the dermis of the nanofiber-treated wounds on days 5 and 15, while the control wounds were largely devoid of collagen on day 5 and exhibited less collagen amount on day 15 [59].

Recently, Ganesh et al. [60] demonstrated enhanced wound healing effects of AgNPs-decorated chitosan (CS)-polyvinyl alcohol (PVA) composite electrospun nanofibers, loaded with sulfanilamide. The prepared electrospun nanofibers were systematically studied for *in vitro* release, antimicrobial, and *in vivo* wound healing activity. The release profile of drug and AgNPs was fast during initial hours and became relatively slow at later time period as the mean percentage of 99% in the formulations after 24 h. Further, the composite fibers incorporated with both sulfanilamide and AgNPs revealed enhanced antibacterial performance than the composite fibers incorporated with only sulfanilamide or AgNPs. The *in vivo* wound healing study in Wistar

rats demonstrated the enhanced wound healing effects at 14 days for the composite fibers incorporated with sulfanilamide and AgNPs, while control composite nanofiber without active agents and conventional sulfonamide formulation took more than 20 days to recover the wound due to enhanced cell attachment owing to high wettability and positive charge of the composite polymeric system.

Coaxial electrospinning technique has been adopted to prepare asiaticoside mixed chitosan as a core while alginate and PVA as shell nanofibers. Asiaticoside is a major triterpenoid component derived from *Centella asiatica* (L.) and widely used in antioxidant, antiinflammatory, immunomodulatory, and wound healing applications. In vitro drug release profile showed that alginate/PVA/chitosan coaxial nanofibers are faster and have more drug release rates. A complete burn wound healing performance noted for the alginate/PVA/chitosan coaxial nanofibers is incorporated with 5% asiaticoside (~99.2%) similar to positive control animal treated with asiaticoside cream. The histopathologic investigation also revealed that drug-loaded nanofibers demonstrated extended reepithelialization of desquamated epithelial regions, less inflammatory cell infiltrations, and numerous collagen proliferations and neovasculations as compared with control group. Also, positive expression of vascular endothelial growth factor (VEGF), cluster of differentiation 31 (CD31), proliferating cell nuclear antigen (PCNA), and down-regulation of tumor necrosis factor (TNF) and interleukin-6 (IL-6) also validated the improved effect of wound healing [61].

A recombinant platelet-derived growth factor, recombinant human PDGF-BB (rhPDGF-BB)-eluting PLGA-collagen hybrid scaffolds, has been reported to treat diabetic wounds in SD rats [62]. The in vivo and in vitro release of growth factors from the scaffolds was measured using an enzyme-linked immunosorbent assay kit and an elution method. The release profile demonstrated that the nanofibrous scaffold released growth factor for a time period of 21 days. The wound areas treated with rhPDGF-BB-eluting PLGA-collagen hybrid scaffolds (group A), PLGA-collagen hybrid scaffold (group B), and virgin PLGA scaffolds (group C) resulted in the proportions of the wound areas that were treated by group B and C fell slowly to $8.3\% \pm 1.6\%$ and $9.2\% \pm 0.9\%$, respectively, by day 14, whereas rhPDGF-BB-eluting membranes decreased to about $3.6\% \pm 0.5\%$ demonstrating promoted wound healing effect as shown in Fig. 8.18. Histopathologic study indicated that after 14 days, rhPDGF-BB-eluting PLGA-collagen hybrid scaffolds exhibited full reepithelialization and the highest proliferation of keratinocytes in the epidermis layer. Also the expression of collagen contents in PLGA-collagen hybrid scaffolds with rhPDGF-BB-eluting group or without rhPDGF-BB-eluting group was considerably higher than that in PLGA-only group with noted indication of collagen content in rhPDGF-BB-eluting PLGA-collagen hybrid scaffolds group, which was remarkably exceeded than that in PLGA-collagen hybrid scaffolds group on day 7 as can be seen from Fig. 8.19.

The electrospun nanofiber-based hydrocolloids and hydrogels are of significant interest in recent years for wound healing applications. Kim et al. [63] recently prepared nanofiber-based hydrocolloid scaffold using thermoplastic polyurethane (TPU)/sodium carboxymethyl cellulose (SCMC). A wound healing study on the prepared

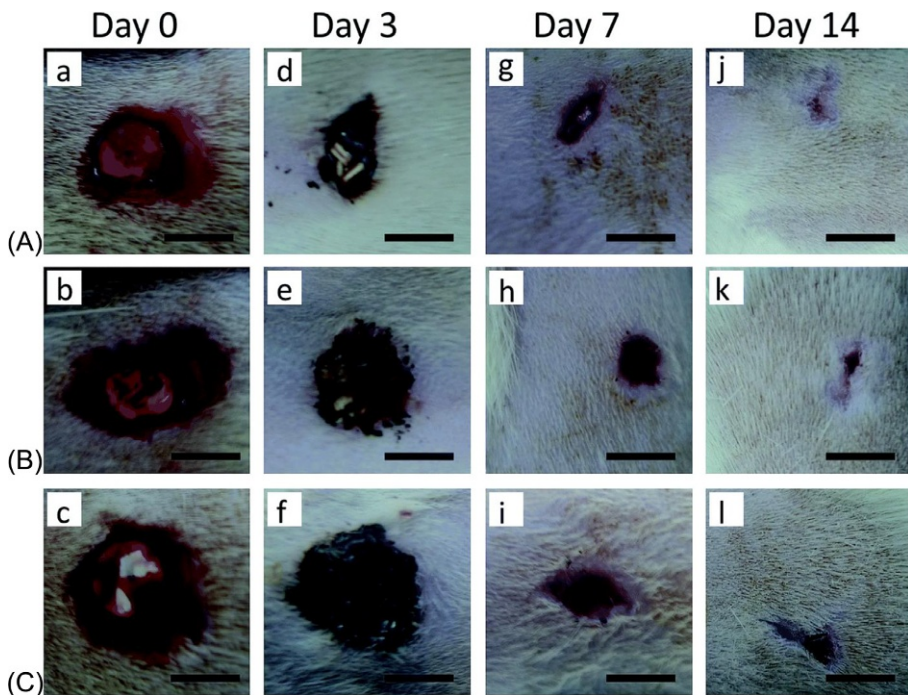


Fig. 8.18 The process of wound repair on different days. Days 0 (a–c), 3 (d–f), 7 (g–i), and 14 (j–l) following treatment with groups (A–C) (scale bar = 5 mm).

Reproduced with permission from Lee CH, Hsieh MJ, Chang SH, Lin YH, Liu SJ, Lin TY, et al. Enhancement of diabetic wound repair using biodegradable nanofibrous metformin-eluting membranes: *in vitro* and *in vivo*. *ACS Appl Mater Interfaces* 2016;6:3979–86 with permission from The Royal Society of Chemistry.

hydrocolloids has been demonstrated using Institute of Cancer Research (ICR) mice with full-thickness wound for a time period of 21 days. The wound size was observed on days 3, 7, 14, and 21 to evaluate the wound healing process. Wound healing in the hydrocolloid fiber-treated group was similar to that of the dried gauze and commercial wound dressing group. However, severe inflammatory reactions were noted in the dried gauze-treated group with reddening and swollen of wounds till 14 days. Conversely, the wound treated with hydrocolloid fibers was found to be neat and moist, without inflammatory exudates, and newly formed epidermis has been noted as similar to commercial wound dressing treatment. The histological evaluation demonstrated enhanced reformation of granulation tissue and reepithelialization over treatment time in all groups. But, a well-organized newly formed epithelium was observed in both commercial dressing and hydrocolloid fiber-treated groups, whereas this is not the case with gauze treatment. Similarly, Xu et al. [64] reported the preparation of chitosan/PLA/PEG hydrogel nanofibers for wound dressing application. The hydrogel nanofibers found to have quick absorption behavior, high equilibrate water absorption, and good air permeability, which may result in absorbing excess exudates,

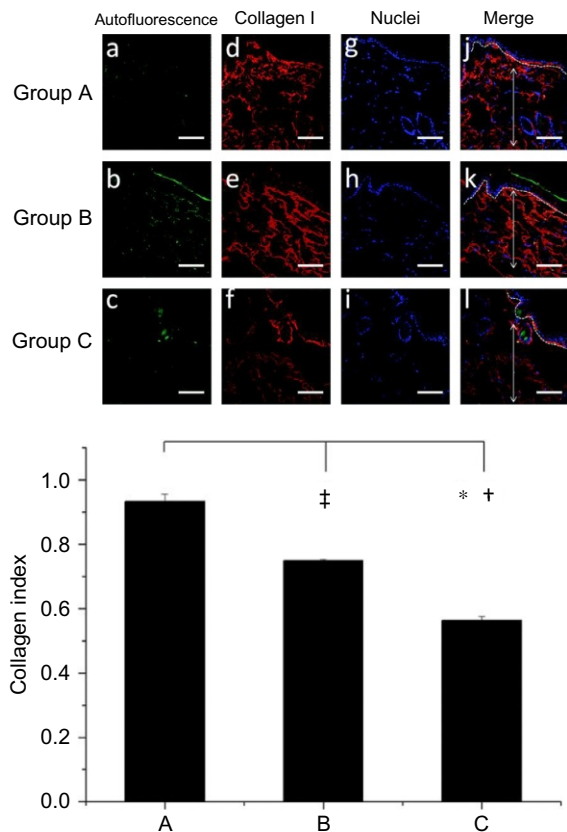


Fig. 8.19 Expression of collagen on day 7. DAPI-labeled nuclei (*blue*) (d–f). Cy3-conjugated secondary antibody (*orange*) (g–i). RhPDGF-BB-eluting PLGA-collagen hybrid scaffold increases collagen I in the dermis (*double arrow*). Dashed lines indicate dermal-epidermal junction. Scale bar = 75 μ m. Autofluorescence (a–c). Reproduced with permission from Lee CH, Hsieh MJ, Chang SH, Lin YH, Liu SJ, Lin TY, et al. Enhancement of diabetic wound repair using biodegradable nanofibrous metformin-eluting membranes: *in vitro* and *in vivo*. ACS Appl Mater Interfaces 2016;6:3979–86 with permission from The Royal Society of Chemistry.

creating a moist wound healing environment and oxygen exchanging in wound healing process. Also, the hydrogel exhibited a good antibacterial activity against *E. coli* bacteria indicating their possible application in wound dressing.

8.3 Current challenges and future directions

The future of wound dressing is a multifunctional device that could enhance the healing process, prevent infection, or effectively treat an infection when it occurs, with simultaneous monitoring of the wound status. To date, a few electrospun-based scaffolds are available in the market with intended application in tissue engineering from different companies including Ahlstrom Corporation (Finland), Espin Technologies (the United States), Hemcon Medical Technologies, Inc. (the United States), Nanofiber Solutions (the United States), and Neotherix (the United Kingdom). Although electrospinning is a well-established technology in wide range of applications, fabrication of ECM

mimicking scaffolds are considered to be a primary challenge till now. A significant attention needs to be paid for creating ECM analog structures to promote better cellular penetration and scaffold remodeling since if cells cannot penetrate into nanofibrous structure, then it will be of little use especially in wound healing applications. As discussed earlier, electrospun fibrous mats offer all essential requirements for effective wound care; still, more significant insights are needed on some elementary aspects of fabrication process including various parameters, polymer selection, and active agents to be loaded to scale-up in cost-effective industrial scale and to possess excellent wound care properties.

Acknowledgments

B. B. acknowledges TUBITAK-BIDEB 2216, Research Fellowship Programme for Foreign Citizens for postdoctoral fellowship. A. S. acknowledges the Scientific and Technological Research Council of Turkey (TUBITAK), BIDEB 2221-Fellowships for Visiting Scientists, and Scientists on Sabbatical for the fellowship. T. U. acknowledges the Turkish Academy of Sciences-Outstanding Young Scientists Award Program (TUBA-GEBIP).

References

- [1] Orsted H, Keast D, Forest-Lalande L, Mégie MF. Basic principles of wound healing. *Wound Care Canada* 2011;9:4–12.
- [2] Barrientos S, Stojadinovic O, Golinko MS, Brem H, Tomic-Canic M. Growth factors and cytokines in wound healing. *Wound Repair Regen* 2008;16:585–601.
- [3] Clark RAF. The molecular and cellular biology of wound repair. 2nd ed. New York: Plenum Press; 1995 [chapter 1].
- [4] Gurtner GC, Werner S, Barrandon Y, Longaker MT. Wound repair and regeneration. *Nature* 2008;453:314–21.
- [5] Harding KG, Morris HL, Patel GK. Science, medicine and the future: healing chronic wounds. *Br Med J* 2002;324:160–3.
- [6] Percival NJ. Classification of wounds and their management. *Surgery* 2002;20:114–7.
- [7] Sen CK, Gordillo GM, Roy S, Kirsner R, Lambert L, Hunt TK, et al. Human skin wounds: a major and snowballing threat to public health and the economy. *Wound Repair Regen* 2009;17:763–71.
- [8] Boateng JS, Matthews KH, Stevens HNE, Eccleston GM. Wound healing dressings and drug delivery systems: a review. *J Pharm Sci* 2008;97:2892–923.
- [9] Eccleston GM. Wound dressings. In: Aulton ME, editor. *Pharmaceutics: the science of dosage form design*. New York: Churchill Livingstone; 2007. p. 264–71.
- [10] Murphy PS, Evans GRD. Advances in wound healing: a review of current wound healing products. *Plast Surg Int* 2012;2012:190436.
- [11] Kalashnikova I, Das S, Seal S. Nanomaterials for wound healing: scope and advancement. *Nanomedicine* 2015;10:2593–612.
- [12] Agarwal S, Wendorff JH, Greiner A. Use of electrospinning technique for biomedical applications. *Polymer* 2008;49:5603–21.

- [13] Kanani AG, Bahrami SH. Review on electrospun nanofibers scaffold and biomedical applications. *Trends Biomater Artif Organs* 2010;24:93–115.
- [14] Leung V, Ko F. Biomedical applications of nanofibers. *Polym Adv Technol* 2011;22:350–65.
- [15] Senthamizhan A, Balusamy B, Uyar T. Glucose sensors based on electrospun nanofibers: a review. *Anal Bioanal Chem* 2016;408:1285–306.
- [16] Thavasi V, Singh G, Ramakrishna S. Electrospun nanofibers in energy and environmental applications. *Energy Environ Sci* 2008;1:205–21.
- [17] Abrigo M, McArthur SL, Kingshott P. Electrospun nanofibers as dressings for chronic wound care: advances, challenges, and future prospects. *Macromol Biosci* 2014;14:772–92.
- [18] Chen H, Peng Y, Wu S, Tan LP. Electrospun 3D fibrous scaffolds for chronic wound repair. *Materials* 2016;9:272.
- [19] Choi JS, Kim HS, Yoo HS. Electrospinning strategies of drug-incorporated nanofibrous mats for wound recovery. *Drug Deliv Transl Res* 2015;5:137–45.
- [20] El-Sherbiny IM, Ali IH. Eco-friendly electrospun polymeric nanofibers-based nanocomposites for wound healing and tissue engineering. In: Thakur MK, editor. *Eco-friendly polymer nanocomposites*. India: Springer; 2015. p. 399–431.
- [21] Hassiba AJ, Zowalaty MEE, Nasrallah GK, Webster TJ, Luyt AS, Abdullah AM, et al. Review of recent research on biomedical applications of electrospun polymer nanofibers for improved wound healing. *Nanomedicine (Lond)* 2016;11:715–37.
- [22] Rieger KA, Birch NP, Schiffman JD. Designing electrospun nanofiber mats to promote wound healing – a review. *J Mater Chem B* 2013;1:4531–41.
- [23] Stevens MM, George JH. Exploring and engineering the cell surface interface. *Science* 2005;310:1135–8.
- [24] Manoukian OS, Ahmad A, Marin C, James R, Mazzocca AD, Kumbar SG. Bioactive nanofiber dressings for wound healing. In: Ågren M, editor. *Wound healing biomaterials. Functional biomaterials, vol. 2*. Elsevier, UK: Woodhead Publishing; 2016. p. 451–81.
- [25] Mohiti-Asli M, Loba EG. Nanofibrous smart bandages for wound care. In: Ågren M, editor. *Wound healing biomaterials. Functional biomaterials, vol. 2*. Elsevier, UK: Woodhead Publishing; 2016. p. 483–99.
- [26] Norouzi M, Boroujeni SM, Omidvarkordshouli N, Soleimani Masoud. Advances in skin regeneration: application of electrospun scaffolds. *Adv Healthcare Mater* 2015; 4:1114–33.
- [27] Mele E. Electrospinning of natural polymers for advanced wound care: towards responsive and adaptive dressings. *J Mater Chem B* 2016;4:4801–12.
- [28] Powell HM, Supp DM, Boyce ST. Influence of electrospun collagen on wound contraction of engineered skin substitutes. *Biomaterials* 2008;29:834–43.
- [29] Zhou T, Wang N, Xue Y, Ding T, Liu X, Mo X, et al. Electrospun tilapia collagen nanofibers accelerating wound healing via inducing keratinocytes proliferation and differentiation. *Colloids Surf B* 2016;143:415–22.
- [30] Powell HM, Boyce ST. Fiber density of electrospun gelatin scaffolds regulates morphogenesis of dermal–epidermal skin substitutes. *J Biomed Mater Res* 2008;84A:1078–86.
- [31] Dubský M, Kubínová Š, Širc J, Voska L, Zajícěk R, Zajícová A, et al. Nanofibers prepared by needleless electrospinning technology as scaffolds for wound healing. *J Mater Sci Mater Med* 2012;23:931–41.
- [32] Uppal R, Ramaswamy GN, Arnold C, Goodband R, Wang Y. Hyaluronic acid nanofiber wound dressing—production, characterization, and *in vivo* behavior. *J Biomed Mater Res Part B Appl Biomater* 2011;97B:20–9.

- [33] Ji Y, Ghosh K, Li B, Sokolov JC, Clark RAF, Rafailovich MH. Dual-syringe reactive electrospinning of cross-linked hyaluronic acid hydrogel nanofibers for tissue engineering applications. *Macromol Biosci* 2006;6:811–7.
- [34] Tchemtchoua VT, Atanasova G, Aqil A, Filée P, Garbacki N, Vanhooteghem O, et al. Development of a chitosan nanofibrillar scaffold for skin repair and regeneration. *Biomacromolecules* 2011;12:3194–204.
- [35] Sheikh FA, Ju HW, Lee JM, Moon BM, Park HJ, Lee OJ, et al. 3D electrospun silk fibroin nanofibers for fabrication of artificial skin. *Nanomedicine* 2015;11:681–91.
- [36] Ju HW, Lee OJ, Lee JM, Moon BM, Park HJ, Park YR, et al. Wound healing effect of electrospun silk fibroin nanomatrix in burn-model. *Int J Biol Macromolec* 2016;85:29–39.
- [37] Li H, Wang M, Williams GR, Wu J, Sun X, Lv Y, et al. Electrospun gelatin nanofibers loaded with vitamins A and E as antibacterial wound dressing materials. *RSC Adv* 2016;6:50267–77.
- [38] Rath G, Hussain T, Chauhan G, Garg T, Goyal AK. Collagen nanofiber containing silver nanoparticles for improved wound-healing applications. *J Drug Target* 2016;24:520–9.
- [39] Jao WC, Yang MC, Lin CH, Hsu CC. Fabrication and characterization of electrospun silk fibroin/TiO₂ nanofibrous mats for wound dressings. *Polym Adv Technol* 2012;23:1066–76.
- [40] Song DW, Kim SH, Kim HH, Lee KH, Ki CS, Park YH. Multi-biofunction of antimicrobial peptide-immobilized silk fibroin nanofiber membrane: implications for wound healing. *Acta Biomater* 2016;39:146–55.
- [41] Murugan R, Ramakrishna S. Nano-featured scaffolds for tissue engineering: a review of spinning methodologies. *Tissue Eng* 2006;12:435–47.
- [42] Zahedi P, Rezaeian I, Ranaei-Siadat SO, Jafari SH, Supaphol P. A review on wound dressings with an emphasis on electrospun nanofibrous polymeric bandages. *Polym Adv Technol* 2010;21:77–95.
- [43] Bahrami H, Keshel SH, Chari AJ, Biazar E. Human unrestricted somatic stem cells loaded in nanofibrous PCL scaffold and their healing effect on skin defects. *Artif Cells Nanomed Biotechnol* 2016;44:1556–60.
- [44] Augustine R, Dominic EA, Reju I, Kaimal B, Kalarikkal N, Thomas S. Electrospun polycaprolactone membranes incorporated with ZnO nanoparticles as skin substitutes with enhanced fibroblast proliferation and wound healing. *RSC Adv* 2014;4:24777–85.
- [45] Pinzón-García AD, Cassini-Vieira P, Ribeiro CC, de Matos JCE, Barcelos LS, Cortes ME, et al. Efficient cutaneous wound healing using bixin-loaded PCL nanofibers in diabetic mice. *J Biomed Mater Res B Appl Biomater* 2016. <http://dx.doi.org/10.1002/jbm.b.33724>.
- [46] Nguyen TTT, Ghosh C, Hwang SG, Tran LD, Park JS. Characteristics of curcumin-loaded poly(lactic acid) nanofibers for wound healing. *J Mater Sci* 2013;48:7125–33.
- [47] Lee CH, Hsieh MJ, Chang SH, Lin YH, Liu SJ, Lin TY, et al. Enhancement of diabetic wound repair using biodegradable nanofibrous metformin-eluting membranes: *in vitro* and *in vivo*. *ACS Appl Mater Interfaces* 2014;6:3979–86.
- [48] Said SS, El-Halfawy OM, El-Gowelli HM, Aloufy AK, Boraei NA, El-Khordagui LK. Bioburden-responsive antimicrobial PLGA ultrafine fibers for wound healing. *Eur J Pharm Biopharm* 2012;80:85–94.
- [49] Khil MS, Cha DI, Kim HY, Kim IS, Bhattara N. Electrospun nanofibrous polyurethane membrane as wound dressing. *J Biomed Mater Res Part B Appl Biomater* 2003;67B:675–9.
- [50] Unnithan AR, Pichiah PBT, Gnanasekaran G, Seenivasan K, Barakat NAM, Cha YS, et al. Emu oil-based electrospun nanofibrous scaffolds for wound skin tissue engineering. *Colloids Surf A Physicochem Eng Asp* 2012;415:454–60.

- [51] Sabitha M, Rajiv S. Preparation and characterization of ampicillin-incorporated electrospun polyurethane scaffolds for wound healing and infection control. *Polym Eng Sci* 2015;55:541–8.
- [52] Chen JP, Chiang Y. Bioactive electrospun silver nanoparticles-containing polyurethane nanofibers as wound dressings. *J Nanosci Nanotechnol* 2010;10:7560–4.
- [53] Lakshman LR, Shalumon KT, Nair SV, Jayakumar R, Nair SV. Preparation of silver nanoparticles incorporated electrospun polyurethane nano-fibrous mat for wound dressing. *J Macromol Sci Pure Appl Chem* 2010;47:1012–8.
- [54] Nguyen TH, Kim YH, Song HY, Lee BT. Nano Ag loaded PVA nano-fibrous mats for skin applications. *J Biomed Mater Res Part B Appl Biomater* 2011;96B:225–33.
- [55] Li Z, Liu X, Li Y, Lan X, Leung PH, Li J, et al. Composite membranes of recombinant silkworm antimicrobial peptide and poly (L-lactic acid) (PLLA) for biomedical application. *Sci Rep* 2016;6:31149.
- [56] Ebrahimi-Hosseinzadeh B, Pedram M, Hatamian-Zarmi A, Salahshour-Kordestani S, Rasti M, Mokhtari-Hosseini ZB, et al. *In vivo* evaluation of gelatin/hyaluronic acid nanofiber as burn-wound healing and its comparison with ChitoHeal gel. *Fibers Polym* 2016;17:820–6.
- [57] Sarhan WA, Azzazy HME, El-Sherbiny IM. Honey/chitosan nanofiber wound dressing enriched with *Allium sativum* and *Cleome droserifolia*: enhanced antimicrobial and wound healing activity. *ACS Appl Mater Interfaces* 2016;8:6379–90.
- [58] Hajiali H, Summa M, Russo D, Armirotti A, Brunetti V, Bertorelli R, et al. Alginate–lavender nanofibers with antibacterial and anti-inflammatory activity to effectively promote burn healing. *J Mater Chem B* 2016;4:1686–95.
- [59] Mohammadi MR, Rabbani S, Bahrami SH, Joghataei MT, Moayer F. Antibacterial performance and *in vivo* diabetic wound healing of curcumin loaded gum tragacanth/poly (ϵ -caprolactone) electrospun nanofibers. *Mater Sci Eng C* 2016;69:1183–91.
- [60] Ganesh M, Aziz AS, Ubaidulla U, Hemalatha P, Saravanakumar A, Ravikumar R, et al. Sulfanilamide and silver nanoparticles-loaded polyvinyl alcohol-chitosan composite electrospun nanofibers: synthesis and evaluation on synergism in wound healing. *J Ind Eng Chem* 2016;39:127–35.
- [61] Zhu L, Liu X, Du L, Jin Y. Preparation of asiaticoside-loaded coaxially electrospinning nanofibers and their effect on deep partial-thickness burn injury. *Biomed Pharmacother* 2016;83:33–40.
- [62] Lee CH, Chao YK, Chang SH, Chen WJ, Hung KC, Liu SJ, et al. Nanofibrous rhPDGF-eluting PLGA–collagen hybrid scaffolds enhance healing of diabetic wounds. *RSC Adv* 2016;6:6276–84.
- [63] Kim S, Park SG, Kang SW, Lee KJ. Nanofiber-based hydrocolloid from colloid electrospinning toward next generation wound dressing. *Macromol Mater Eng* 2016;301:818–26.
- [64] Xu X, Zhou G, Li X, Zhuang X, Wang W, Cai Z, et al. Solution blowing of chitosan/PLA/PEG hydrogel nanofibers for wound dressing. *Fibers Polym* 2016;17:205–11.

This page intentionally left blank

Electrospun biomaterials for dermal regeneration

9

E.A. Growney Kalaf^a, K.R. Hixon^a, P.U. Kadakia, A.J. Dunn, S.A. Sell
Saint Louis University, St. Louis, MO, United States

9.1 Overview

9.1.1 Skin anatomy and physiology

The skin is the largest organ in the body and primarily functions as a barrier to the outside environment. This protective organ prevents against invasion from microorganisms, chemical infiltration into the body, and the mutation of cells exposed to UV light. The skin also prevents rapid evaporation of water from the body by essentially waterproofing the most superficial layers of cells. The skin acts as the largest sensory organ in the body and is able to react to external physical stimuli such as cold, heat, touch, and pressure. Sensory cells are located throughout the skin but are highly concentrated in the face, feet, and hands. The skin is also critical for regulating temperature in the body where subcutaneous adipose tissue insulates the body from heat loss. Receptors in the skin monitor temperature and send a response to the hypothalamus that regulates body function, including body temperature. If body temperature rises above 37°C, eccrine glands in the skin produce and release sweat onto the most superficial layer of the skin. The sweat then evaporates off of the skin leaving behind a cooler body. Vasodilation, another means of cooling the body, can also occur where the blood radiates out through the skin. Vasoconstriction routes blood away from superficial layers of the skin reducing heat loss at times of hypothermia [1]. The skin also functions to produce vitamin D for the rest of the body; UVB radiation causes epidermal cells to produce vitamin D3 from 7-dehydrocholesterol [2]. Vitamin D3 enters the circulation, and through a series of hydroxylation and catalysis in the liver and kidneys, vitamin D is produced [3]. This vitamin is broken down to 1,25-dihydroxyvitamin D3 that can regulate epidermal proliferation and differentiation, thus able to affect protection from light and wound healing [2–4].

There are two distinct layers of the skin: the superficial epidermis and the deeper dermis (Fig. 9.1). The epidermis is composed of four main cell types: keratinocytes, melanocytes, Langerhans cells, and Merkel cells. Keratinocytes make up the vast majority of cells in this tissue, and melanocytes produce melanin, a pigment for protecting against ultraviolet (UV) light. Langerhans cells coordinate with the immune system to fight infection. Merkel cells function as the sensory receptors in the skin and make direct contact with Merkel disks, sensory neurons of the dermis, which provide the

^a Authors contributed equally.

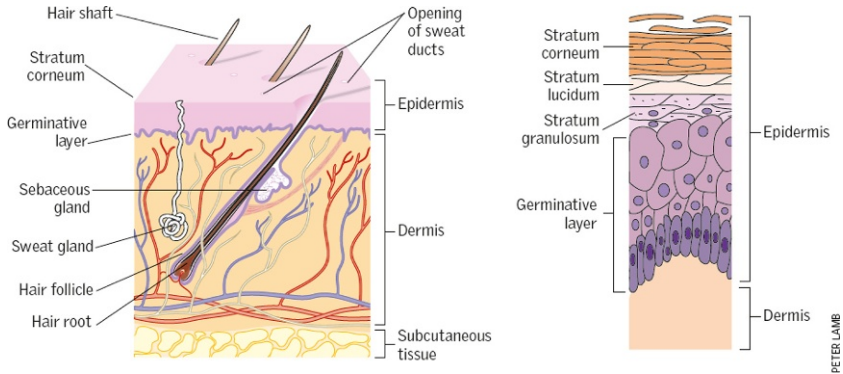


Fig. 9.1 The skin showing the layers of the epidermis and the main structures of the dermis. Reproduced with permission from McLafferty. The integumentary system: anatomy, physiology and function of skin. *Nurs Stand* 2012;27:35–42, with permission from RCN Publishing.

sensation of touch. This layer of the skin is completely avascular, relying on the dermis to provide oxygenation [1]. Epidermal cells grow from the basal layer distally from the dermis to produce the protective barrier the skin provides. There are four distinct layers, which represent the stages of maturation in the epidermis.

The stratum basale or stratum germinativum is the deepest layer and contains a single layer of columnar keratinocytes with interspersed melanocytes and Merkel cells. This row of cells is the only keratinocytes capable of cell division. Following cell division, one of the two daughter cells migrates upward through the layers while the other remains in the stratum basale for further expansion. Melanocytes make up one in six cells in this layer and have long projections that extend into the more superficial layers. Each of these projections contains melanin granules that can be transferred to surrounding keratinocytes. Once melanin granules have infiltrated a keratinocyte, they surround the nucleus, protecting the DNA from UV radiation. Blood vessels in the dermis extend to the cells in this layer exclusively leaving the remaining layers malnourished, preventing further cell division. These cells, instead, opt for increased keratin content and more cell organization [1].

The second deepest layer, the stratum spinosum or prickle cell layer gets its name from the cells that are prevalent in this region. Langerhans cells appear prickly or spiny under a microscope because of the projections extending out of the cell. These specialized dendritic cells act as antigen presenting cells to T cells in the tissue. The T cells then mount an appropriate response to defend against pathogens [1]. This layer is composed of 5–12 rows of cells stacked upon one another. Adjacent keratinocytes are joined by desmosomes that attract neighboring cells to connect together. These connections provide tensile strength and flexibility to the epidermis [1].

The next layer of cells, the stratum granulosum, contains 3–5 layers of flattened keratinocytes. These skin cells lose their nucleus and all metabolic function to further increase keratin and keratinocytes and flattened to maximize the density of

keratinocytes in the epidermis. Keratin acts to protect cells from heat, chemical exposure, and microorganisms. There are also Odland's bodies throughout this layer, which provide lipids to increase cell adhesion [1].

The stratum corneum is composed of dozens of layers of flattened keratinocytes. At this point, these cells have maximized their keratin content and will eventually be exposed to the outside world. These cells readily slough off in clumps and are continuously lost and replaced. If an area such as the heel or palm is exposed to consistent friction, a callus can form at the area [1].

The stratum lucidum is another layer that is only found in areas where the skin needs to be thicker such as the fingertips, soles of the feet, and palms of the hand. There are additional layers of flattened keratinocytes between the stratum granulosum and the stratum corneum. This additional buffer of cells helps waterproof the skin in areas where water can quickly be lost from the body, increasing water retention [1].

The dermis lies below the epidermis and provides the nutrients and physical support to the epidermis. Blood and lymph vessels, nerve endings, hair follicles, and oil- and sweat-producing glands reside in this layer of the skin. Collagen and elastin are also interwoven in the dermis providing the tensile and elastic properties of the skin [1]. In the skin, collagen I fibers have approximately 50–500 nm diameter [5]. Collagen III fibers range from 30 to 130 nm in diameter [5]. Each fibril unit of elastin is between 100 and 200 nm [6]. Between the epidermis and dermis, a unique structure forms called rete ridges. Hundreds of small projections of the dermis protrude into the epidermis much like the villi in the intestine. These projections increase the surface area between the two layers, providing more physical stability and nutrient exchange between the dermis and epidermis. When the skin is exposed to shear force, these ridges can separate the layers and fluid collects between the two forming a blister on the skin [1].

There are two distinct layers of the dermis: the superficial papillary dermis and the deep reticular dermis. The papillary dermis is a matrix of loosely packed collagen fibers with nerve and capillaries dispersed throughout. This provides the nutrient exchange and sensory function to the epidermis. The reticular dermis is composed of an interwoven collagen and elastin matrix that provide the physical strength of the skin. Collagen, with its high tensile strength, prevents tearing of the skin when it is stretched. In contrast, elastin contributes its elastic properties to the skin, allowing it to return to its normal shape and size after stretching. Both fibers are produced by fibroblasts, but elastin is much finer and comprises a much smaller concentration compared with collagen. Elastin fibers are found interwoven between larger collagen bundles [1]. This collagen matrix is rich with proteoglycans, which provide the viscous nature of the skin. Proteoglycans are composed of a protein with glycosylated branches. These glycosaminoglycan (GAG) chains trap and bind water and other cations, directing the flow of nutrients through the extracellular matrix (ECM). The addition of water to the matrix gives the skin its viscoelastic properties [7].

Understanding the physical and mechanical properties of the skin can be relatively difficult due to the complex nature of the tissue. This highly heterogeneous, anisotropic, viscoelastic tissue shows a nonlinear stress-strain relationship. This is due to a composition of a nearly random collagen framework. Initially when at rest, collagen

and elastin fibers appear randomly oriented. As load increases, the fibers stretch in parallel with the direction of the load. Elastin fibers take the brunt of the initial load, which stretches in a linear fashion. During this time, collagen fibers align in the parallel direction and carry more of the load. This appears as the toe region of the stress-strain curve. Collagen fibers also increase stiffness as the load increases, leaving the fibers more susceptible to rupture [8].

Physical properties of the skin are very dependent on the location, orientation, and strain rate of an applied load. Throughout the skin, there are natural lines of tension called Langer's lines. These lines are very important in understanding the wound healing process and must be factored in during surgical procedures to reduce scarring. If load is applied in the orientation of Langer's lines, there are significant differences in mechanical properties compared with an orthogonal loading [8]. Depending on the area of the body in which skin is tested, a highly variable range of values can be found as well. Ultimate tensile strength varies from 27 MPa on the back to 8.5 MPa on the abdomen [8]. Comparing this with the elastic modulus of the back, 99 MPa, and 18.8 MPa on the abdomen, values vary significantly depending on the location and orientation of load bearing [8].

Age of the skin must also be factored in when understanding mechanical properties of the skin. The aging process causes the skin to become thinner, stiffer, less tense, and less flexible [9]. Elderly skin is 0.7–0.8 mm thinner than normal skin [9]. Decreased synthesis of collagen leads to decreased thickness and strength. As collagen ages, it becomes stiffer and less flexible, leaving a much weaker tissue that is susceptible to skin tears [9].

9.1.2 Typical and atypical dermal wound healing

The skin is a dynamic organ in that there is constant turnover of cells to renew the tissue. When injured, healing follows three distinctive phases composed of various wound healing processes that overlap one another (Fig. 9.2) [10].

Inflammation is initiated by the formation of a blood clot to stop any hemorrhaging. The presence of the hematoma is important for providing both the framework for regrowth and numerous factors critical for regeneration [11]. These inflammatory cytokines specifically assist in the regulation of blood flow and the recruitment of inflammatory cells, lymphocytes, and macrophages to the tissue [10]. Additionally, the presence of platelets assists in the formation of the clot and provides signaling to further attract both macrophages and leukocytes [12]. Neutrophils are the first to arrive at the site of tissue damage where they work to rid the area of foreign pathogens. Monocytes arrive next, differentiating into macrophages, which release growth factors (i.e. platelet-derived growth factor (PDGF), vascular endothelial growth factor (VEGF), etc.) to encourage granulation tissue formation. Monocytes adhering to the ECM also transition into macrophages, expressing transforming growth factor- α (TGF- α), interleukin-1 (IL-1), transforming growth factor- β (TGF- β), and insulin-like growth factor 1 (IGF-1) [11,13].

Another component of the healing process is the regrowth of epithelial tissue. This process begins within a few hours post injury when the clotted blood and damaged

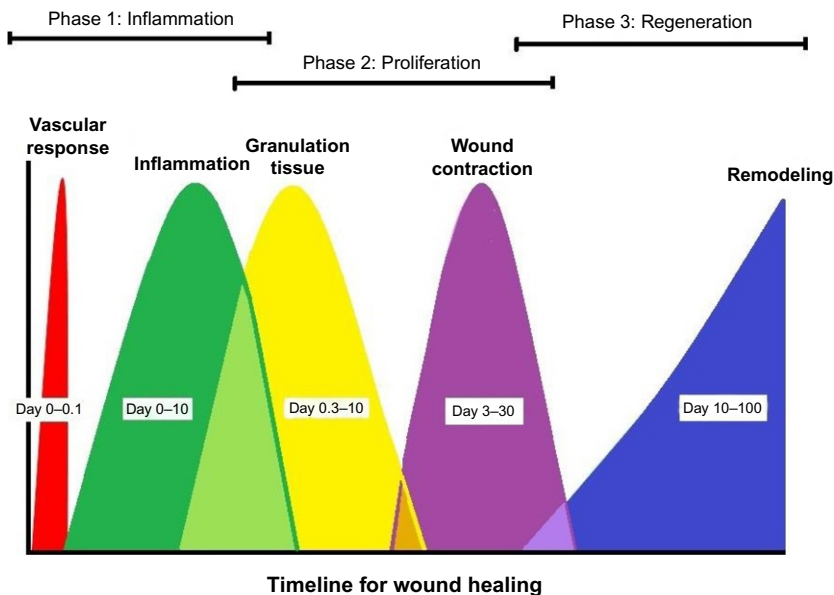


Fig. 9.2 Timeline and phases for wound healing.

Modified from Elia Ranzato SM. Cellular and molecular mechanisms of honey wound healing. New York: Nova Science Publishers, Incorporated; 2014.

stroma are removed. The cells themselves change in phenotype so they are able to migrate throughout, separating damaged from salvageable tissue [11,14]. This movement is determined by integrins expressed on the cell membranes. The migration itself is dependent on the degradation of the ECM. This is mediated by the activation of both plasmin and collagenase by plasminogen, which assists in this degradation [15]. After a few days, the cells begin to proliferate behind these migrating cells, and a basement membrane is formed from the wound edge. Once formed, the epithelial cells return back to their original phenotype and resume attachment [11].

The end of the inflammatory phase supports angiogenesis, proliferation of fibroblasts, and collagen accumulation, marking the start of the proliferation phase [10]. After about four days into the healing process, vascular ingrowth occurs along with the migration of macrophages and fibroblasts [16]. These three components work together where the fibroblasts encourage angiogenesis and create scaffolding for new tissue deposition. The new blood vessels provide the nutrients and oxygen for the tissue to survive, while macrophages deliver the growth factors necessary for these processes to occur [11]. Factors such as PDGF and TGF- β play integral roles in the recruitment and proliferation of the fibroblasts. This leads to granulation tissue formation, where fibrin and fibronectin provide the matrix for cellular infiltration. The matrix and fibroblasts work together to create and remodel the ECM, producing a vascularized connective tissue [10].

The final stage of wound healing, the remodeling phase, occurs during the second and third week of healing and can continue on for a year [11]. Fibroblasts assume a myofibroblast phenotype, leading to the compression of connective tissue and overall contraction of the wound [15]. A combination of the factors TGF- β 1 or 2 and PDGF, along with fibroblast adherence and the cross-linking of collagen bundles, plays a large role in the stimulation of this contraction [11,17]. Type III collagen is converted to type I and aligned parallel to the stress lines rather than in the typical basket weave pattern. The physical remodeling is characterized by the synthesis and subsequent degradation of the ECM [18]. Table 9.1 provides a summary of the typical factors present during the three stages of skin healing.

During this three-week period of wound healing, the site of injury only regains about 20% of what will be its final strength. From here on out, collagen accumulation is much slower, likewise reflecting a slow progression of increasing tensile strength. This increasing strength is primarily dependent on the remodeling of collagen into larger bundles and increasing intermolecular cross-links. Despite this, a fully healed wound containing scar tissue will only exhibit strength at 70% that of normal skin [10].

There are cases in which skin healing does not follow this characteristic pattern, and atypical healing occurs. This is most often caused by asynchrony of the overall repair process. In cases such as these, the phases listed previously will often occur simultaneously or out of order [10]. A common example of this is the development of diabetic ulcers or pressure ulcers in patients suffering from spinal cord injury [11,19]. In these situations, the tissue becomes ischemic, and consequently, the oxygen and nutrients necessary for healing are decreased [11]. Additionally, the tissue is often stuck in a phase of chronic inflammation with decreased synthesis of collagen, increased presence of proteinases, and an inappropriate macrophage response [19,20].

Table 9.1 Typical factors present during the three stages (inflammation, proliferation, and remodeling) of skin healing [3,5]

Phase	Factor
Inflammation	Platelet-derived growth factor (PDGF)
	Vascular endothelial growth factor (VEGF)
	Transforming growth factor- α (TGF- α)
	Interleukin-1 (IL-1)
	Transforming growth factor- β (TGF- β)
Proliferation	Insulin-like growth factor 1 (IGF-1)
	Vascular endothelial growth factor (VEGF)
	Transforming growth factor- β (TGF- β)
	Angiogenin
	Angiotropin
Remodeling	Angiopoietin
	Transforming growth factor- β (TGF- β)
	Platelet-derived growth factor (PDGF)

In the case of hypertrophic scarring, excess collagen is present leading to abnormal cell migration/proliferation, inflammation, cytokine production (i.e., TGF- β), and wound remodeling [11,21].

9.1.3 Treatment of dermal wounds

9.1.3.1 Gold standards in the treatment of dermal wounds

Wound healing, as mentioned previously, is a dynamic process with multiple overlapping phases; these phases are characteristics of the skin in all wounds, with the exception of atypical wound healing. Atypical healing, such as in the cases of large burn wounds and chronic diabetic ulcers, is linked to aberrations in the inflammatory pathway [22–25]. These aberrations cause abnormal myofibroblast contraction, prolonged edema, and an increased risk of infection [22]. The three main principles of wound care are proper maintenance of moisture, adequate debridement, and allowing bacterial colonization without infection [26]. Negligence of any of the three wound care principles can prolong or prevent adequate healing of the wound.

Noncellularized wound dressings and wound care adjuncts

According to an extensive product study by researchers at John Hopkins, the ideal wound dressing removes exudate, maintains a moist environment, protects against contaminants, causes no trauma on removal, leaves no debris in the wound bed, relieves pain, provides thermal insulation, and induces no allergic reactions [26,27]. There are an immense number of wound care products on the market, which can cause some clinical confusion when deciding which product is the ideal product for any given situation.

Wound dressings have been around since at least 1550 BC, when vegetable fibers were combined with animal fat and honey to create an antibacterial absorbent barrier to aid in healing [28–31]. Modern dressing products today are still similar in theory to those ancient techniques. Basic gauzes are the most popular products to prevent infection and absorb fluids but are often too absorbent and adherent to the wound; barrier products such as petroleum jelly and zinc oxide pastes are useful for periwound maintenance while the wounded tissue heals [32–35]. Combinations of gauze with petrolatum have lessened gauze adhesion but also lessened fluid absorption, and sodium-chloride-infused gauze has proved to be hostile to bacteria and highly absorbent but causes adhesion and desiccation of the wound surface [26].

Foams, films, hydrogels, and hydrocolloids act to maintain a moist healing environment and are used for wounds with low to moderate exudate. Foam and film bandages are adhesive and semiocclusive, allowing oxygen exchange while preventing fluid loss [31]. While foams provide thermal insulation and are moderately absorbent, films are nonabsorbent but clear to visualize wound healing. These thin films also adhere only to dry skin, which works to minimize adherence damage to the moist wound bed [36]. Water-based hydrogels are indicated for autolytic debridement cases and wounds with very low exudate, as they donate fluid to the wound site [37–39]. Hydrogels also provide a cooling, pain-relieving effect to the wound site [40–42].

Hydrocolloids are absorbent materials that form a gel by absorbing wound exudate, but can adversely affect the dry periwound area and cause injury unless used in conjunction with a barrier product [43].

Alginate dressings are used for moderate to heavy exuding wounds, as they can hold fluid up to 20 times dry weight [38,44,45]. As alginate is packed into the moist wound, a calcium-sodium ion-exchange reaction causes the alginate fibers to become soluble and form a gelatinous mass of exudate. Since alginate is highly absorbent, care must be taken not to desiccate the wound and delay wound healing [46]. Alginate gels lack the ability to thermoregulate and must be cut to the wound size to prevent periwound injury [47]. They are also nonadhesive so therefore require an additional dressing to secure them [44]. Collagen dressings also absorb exudate to create a gel and are useful for recalcitrant wounds [48]. The collagen chemically binds to and subsequently reduces the levels of matrix metalloproteases, which are present in high amounts in a chronic wound bed [49]. Such collagen products are typically xenogenic and require a secondary bandage to secure. Bioactive borate glass nanofibrous dressings have also been designed to enhance wound healing and angiogenesis (Dermafuse, Mo-Sci, and Rolla MO), and Integra Wound Matrix (Integra LifeSciences) is a nanofibrous bandage clinically available. However, none of the currently marketed wound dressings meet the ideal standards and are often used with adjuncts to aid in healing. Addition of honey and other antimicrobial products, compression therapy, and topical negative pressure devices have been shown to increase the healing rate of chronic wounds and venous ulcers [26].

Autografts and allografts

The standard of care for burn wounds is a split-thickness autograft from an uninjured part of the patient (Fig. 9.3) [50]. Early excision and grafting of the wound within 48 hours of injury have shown to decrease infection, blood loss, and hospital stay



Fig. 9.3 Illustration of a split-thickness autograft.

Reproduced with permission from Whitfield RM, Rinard J, King D. Coverage of megaprosthesis with human acellular dermal matrix after Ewing's sarcoma resection: a case report. *Sarcoma* 2011;2011:978617, doi: 10.1155/2011/978617 (2011).

while increasing the likelihood of proper graft acceptance [22,51,52]. Full-thickness autografts that contain fat tissue are typically only utilized on the facial area to preserve aesthetics; although the full-thickness grafts prevent contraction and retain a better cosmetic appearance, they have a higher risk of graft failure and have a higher incidence of donor site complications [53,54]. Autografting avoids any immune response and has a high success rate, but many complications can occur, both at the donor site and the graft site. Allogenic and xenogenic grafts have also been used for patients with more extensive burns and promote increased healing over traditional dressings [55,56]. These grafts are fully cellularized and vascularized, which contribute to the success of the graft implantation. Autografts can also be cultured in the lab from a small sample of healthy skin such as in the case of Epicel grafts, which is utilized both alone and in conjunction with split-thickness autografts.

9.1.3.2 *Current tissue engineered products for dermal wound treatment*

Atypical healing of the dermis can manifest in two main pathologies: delayed wound healing as seen in diabetic patients or excessive healing, as in the case of keloid formation or hypertrophic scars [57]. Both pathologies are due to abnormal ECM deposition by either a deficit of healing factors and vascularization or an overabundance of TGF- β and other proinflammatory markers [58,59]. Many strategies have been employed to aid in complete wound healing, and aspects of under and over healing must be taken into account when designing a product. Questions arise, then, about how to accelerate wound healing while simultaneously titrating the effects of “too much” healing.

Biological signaling is an inherent process and can benefit or detract from typical remodeling processes depending on the environment and specific environmental cues. The most useful repair strategy to prevent atypical healing of wound sites would be to use both biological signaling and environmental cues, an approach most utilized in cellularized tissue-engineered products. Until 2008, incorporating both cells and scaffold into a wound bed had not been a viable therapy; however, the current market climate shows that these tissue-engineered alternatives to the gold standard of treatment are viable and often more therapeutic substitutes [57]. It has been shown that bioactive molecules given in a single-agent strategy only partially impact wound repair.

Regeneration templates

Both epidermal and dermal skin substitutes are commercially available to treat varying thickness of wound sites, and cell-based templates are being produced for a more permanent wound dressing. Epidermal skin substitutes include autografted keratinocytes such as Epicel (Genzyme, Cambridge, MA) for full-thickness burn wounds cover more than 30% of the total body surface area. The downside for these 2–8 cell thick graft include the lack of long-term strength, along with an extended wait time to culture the autologous cells. Sprayable and thrombin suspensions such as CellSpray (Cambridge, the United Kingdom) and Bioseed-S (BioTissue, Freiberg, Germany) are not yet commercially available in the United States, with the exception

of ReCell (Avita, Northridge, CA), an autologous cell suspension of multiple phenotypes and beneficial cytokines. Keratinocyte-seeded and nonseeded dermal regeneration templates (DRTs) are designed to provide immediate wound closure and permanent regeneration of dermis tissue. Typically, DRTs are created from three-dimensional porous matrices of varying constituents. Allogenic and xenographic acellular constructs include Alloderm (LifeCell, Bridgewater, NJ), GraftJacket (KCI, San Antonio, TX), Integra (Integra, Plainsboro, NJ), GammaGraft (Promethean LifeSciences, Pittsburgh, PA), and Biobrane (Smith & Nephew, UK); a higher number of acellular skin substitutes are clinically available in the United States due to the stringent FDA requirements for cellularized products. These cellularized substitutes include Epicel, ReCell, and Dermagraft (Organogenesis, Canton, MA); ReCell wound healing is shown in Fig. 9.4 [60].

Tissue-engineered nanofibrous scaffolds are artificially created, as opposed to natural ECM such as autografts or decellularized matrix products. These artificially developed nanofibrous scaffolds include xenogenic ECM products such as Integra scaffolds, neonatal foreskin fibroblasts cultured on synthetic scaffolds such as Dermagraft and TransCyte (Advanced Biohealing, Westport, CT), and xenogenic skin equivalent scaffolds such as Apligraf (Organogenesis, Canton, MA) and Orcel (Forticell Bioscience, New York, NY). Very recently, researchers have also attempted to incorporate electrospun fibers onto market products as a support structure for the electrospun scaffold; addition of PCL/gelatin nanofibers onto a Tegaderm™ has shown significantly higher reepithelization over Tegaderm™ and control, with higher collagen coverage in the resulting granulation tissues (Table 9.2) [61].

9.1.4 Electrospinning

In order to match the fibrous nature of native skin ECM, an appropriate dermal regeneration template must be utilized. Collagen fibrils, the most abundant constituent of the ECM, provide both mechanical and structural stability in the skin [62]. These fibrillar structures have diameters that range from 50 to 500 nm [5,63,64]. Thus, any tissue-engineered scaffold for a skin application must be mechanically sound with a fiber diameter in the nanometer range. Currently, there are several fabrication methods that satisfy these constraints, including fiber drawing, molecular self-assembly, template synthesis, and temperature-dependent phase separation. Nonetheless, a process known as electrospinning has become the dominant approach in creating polymeric, nonwoven meshes [62].

The setup for electrospinning incorporates three main components: (1) a high voltage source, (2) a syringe or pipette, and (3) a grounded collecting target/mandrel. Polymers are typically dissolved in a highly volatile solvent; however, solvents like water have been previously used as well. Following dissolution, polymer solutions or melts are then added to a syringe affixed with a blunt-tip, conductive needle. Next, this syringe is placed onto a syringe pump and a high voltage is applied to the needle. While the syringe pump is running at a certain flow rate, repulsive electrostatic forces in the solution will overcome a critical surface tension limit and a fluid jet will be whipped from the needle tip through a Taylor cone formation. As the jet whips across a working

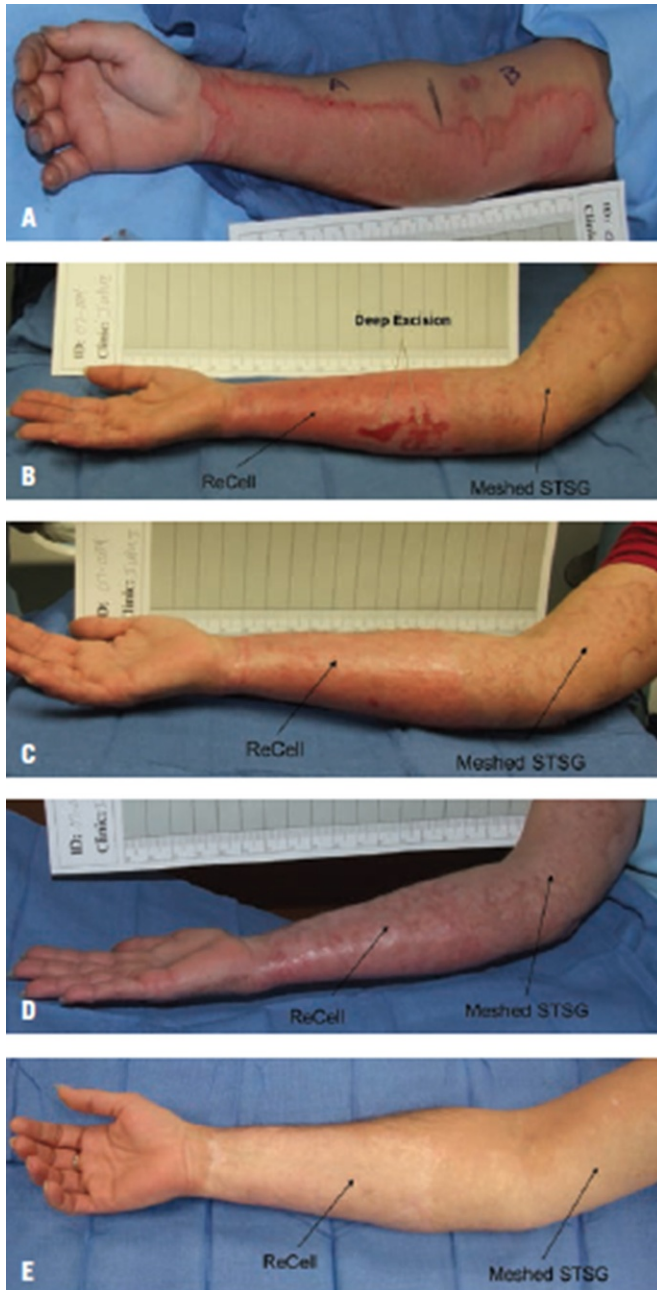


Fig. 9.4 Comparison of ReCell and split-thickness skin graft (STSG): (A) Predebridement and treatment, and healing at (B) week 3, (C) week 6, (D) week 12, and (E) week 52 postoperation. Reproduced with permission from Sood R, et al. A comparative study of spray keratinocytes and autologous meshed split-thickness skin graft in the treatment of acute burn injuries. *Wounds* 2015;27:31–40.

Table 9.2 Tissue-engineered products currently on the market for epidermal and dermal regeneration (all information from company websites)

Product	Company	Classification	Characteristics	Intended use
Epicel	Genzyme	Autograft	Sheets of skin cells from 2–8 cell layers thick	Burns
ReCell	Avita	Autologous cell spray	Suspension of cultured fibroblasts, Langerhans cells, keratinocytes, and melanocytes	Burns
Alloderm	LifeCell	Acellular (cadaveric)	Freeze-dried dermal matrix with intact collagen, elastic, and proteoglycans for cell infiltration	Burns, hernia repairs
GraftJacket	KCI	Acellular (cadaveric)	Meshed and nonmeshed dermal matrix	Chronic ulcers, ligament and tendon repair
Integra	Integra	Acellular (biosynthetic)	Bilayer matrix of semipermeable silicone and bovine/shark ECM scaffold	Burns, complex reconstruction, contracture release
GammaGraft	Promethian	Acellular (irradiated cadaveric)	Remains in place while host skin grows beneath	Chronic wounds, burns
Biobrane	UDL	Acellular (biosynthetic)	Semipermeable silicone bonded with collagen-coated nylon fibers	Burns, skin graft donor sites, superficial wounds, and chronic wounds
Dermagraft	Advanced Biohealing	Allogeneic (neonatal + biosynthetic)	Cryopreserved fibroblasts on bioabsorbable polyglactin mesh	Full-thickness diabetic foot ulcers
TransCyte	Advanced Biohealing	Acellular (biosynthetic)	Collagen-coated nylon mesh with incorporated ECM proteins and growth factors	Temporary coverage of full-thickness burns, primary treatment of superficial burns
Apligraf	Organogenesis	Allogenic bilayered	Cryopreserved bilayered bovine collagen and hyaluronic acid gel seeded with fibroblasts and keratinocytes	Chronic diabetic and venous ulcers
Orcel	Forticell Bioscience	Allogenic bilayered	Cryopreserved or fresh bovine collagen sponge seeded with keratinocytes and fibroblasts	Graft donor sites, surgical wounds

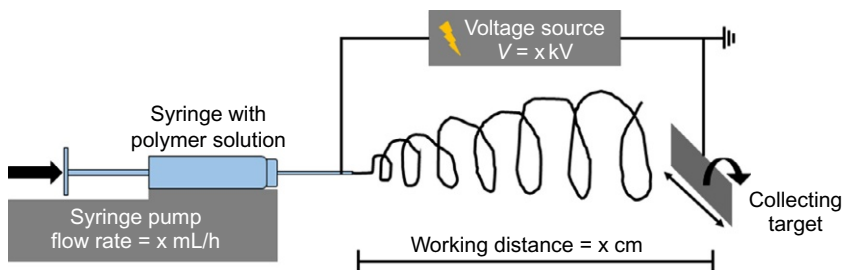


Fig. 9.5 Example setup for the horizontal electrospinning process.

distance between the needle tip and grounded collecting mandrel, the solvent will evaporate off. In the end, polymeric nanofibers land on the collecting target due to the presence of chain entanglements, forming a porous nonwoven mesh network. Uniquely, electrospinning can be accomplished in both the horizontal (Fig. 9.5) and vertical directions and sometimes even in both directions simultaneously [65–67].

Besides adequately meeting the constraints of an appropriate skin substitute, a few other benefits of electrospinning include ease of setup and inexpensive cost of operation [62,65]. In addition, this fabrication method produces nanofibrous scaffolds with large surface area to volume ratios, high porosities, and high pore interconnectivities. These characteristics, in turn, allow electrospun matrices to stimulate nutrient, gas, and waste exchange and control water loss via evaporation. With regard to dermal regeneration, oxygen permeability and fluid accumulation are vitally important for the proper course of wound healing [62,65,68]. Furthermore, as pore sizes in electrospinning normally range from 1 to 10 μm , the possibility of bacterial infections is significantly reduced [62]. Overall, the inherent features of electrospun scaffolds promote an ideal environment for cellular attachment, infiltration, and proliferation *in vivo*.

Another advantage of electrospinning involves the variety of polymers than can be electrospun. Synthetic polymers like polycaprolactone (PCL) and polylactide (PLA) lead to enhanced batch to batch consistency and can sufficiently mimic native ECM. On the other hand, natural polymers like collagen and silk fibroin improve scaffold biocompatibility and offer cells a recognizable environment to proliferate and remodel [64,69,70]. Along similar lines, electrospinning can also support the addition of numerous polymer/protein doping agents. For bioengineered skin, a few effective additives include bioglass, Manuka honey, and platelet-rich plasma (PRP).

The tunable and controllable nature of electrospinning renders it a tremendously valuable scaffold fabrication technique. Adjustable parameters can be separated into three main categories: 1) solution, 2) process, and 3) ambient conditions. Solution parameters, such as concentration, viscosity, molecular weight, surface tension, and conductivity, and processing parameters, such as applied voltage, syringe pump flow rate, distance from needle tip to collecting target (working distance), can all be altered to obtain desirable fiber diameters, fiber alignments, and fiber morphologies. For example, increasing the polymer concentration or decreasing the applied voltage will increase the resulting fiber diameters. Moreover, ambient conditions that may

Table 9.3 Effect of solution, processing, and ambient parameters on resulting electrospun fiber morphology

Parameter type	Parameters	Resulting fiber morphology (parameter: effect)
Solution parameters	Concentration/viscosity	↑ Concentration/viscosity: ↑ fiber diameter
	Molecular weight	↑ Molecular weight: ↓ bead formation
	Surface tension	↑ Surface tension: ↓ fluid jet stability
	Conductivity	↑ Conductivity: ↓ fiber diameter
Processing parameters	Applied voltage	↑ Applied voltage: ↓ fiber diameter
	Flow rate	↑ Flow rate: ↑ bead formation ↓ Flow rate: ↓ fiber diameter
	Working distance	Too high/low working distance: ↑ bead formation
Ambient parameters	Humidity	↑ Humidity: ↑ circular pores on fibers
	Temperature	↑ Temperature: ↓ fiber diameter

Reproduced with permission from Seaman S. Dressing selection in chronic wound management. *J Am Podiatr Med Assoc* 2002;92:24–33; Majno G. *The healing hand: man and wound in the ancient world*. Cambridge, MA: Harvard University Press; 1991.

influence the final results include humidity and temperature [65,66,71]. Table 9.3 describes how each of these parameters affect fiber morphology (Note: These effects are generalities and may not apply to all polymers).

9.2 Electrospun scaffolds for dermal wound healing

9.2.1 Natural biopolymers

Several naturally occurring polymers have been electrospun for tissue-engineered skin applications. Natural polymers are typically biodegradable and possess bioactive characteristics, such as enhanced cellular adhesion and proliferation [69,70]. These inherent properties allow scaffolds composed of natural materials to promote a physiologically appropriate environment for remodeling and regeneration [64]. Even with excellent biological features, natural polymers often exhibit low mechanical properties and can lead to the formation of inconsistent structures [70]. Thus, both the scaffold fabrication method and postprocessing techniques (i.e., physical or chemical cross-linking) are vitally important. Mechanical strength in electrospun scaffolds can be increased by utilizing a combination of natural and synthetic materials [64,70]. With regard to skin tissue, the ECM is primarily composed of collagen fiber networks [72]. Therefore, the electrospinning of collagen for dermal regeneration was an expected choice. Other natural polymers that have been electrospun for bioengineered skin include silk fibroin, gelatin, and chitosan/chitin [73]. This section will review these listed natural biopolymers in relation to electrospun scaffolds for skin tissue engineering.

9.2.1.1 Collagen

As previously stated, collagen is an abundant constituent of natural human skin ECM. For the purposes of this review, only scaffolds containing type I collagen will be discussed. This particular subset represents the main structural/functional protein of ECM throughout the body [63]. At a molecular level, type I collagen consists of two $\alpha 1$ and one $\alpha 2$ polymer chain arranged into coiled triple helical structures of 50–500 nm in diameter [5,63,64]. The fibrillar structure of native collagen has been demonstrated to be crucial for cellular function and response. In fact, this ECM protein contains arginine-glycine-aspartic acid (RGD) binding sites that promote both cellular adhesion and spreading [63]. Other benefits of using collagen in a tissue engineering application include biodegradability, biocompatibility, and no immunogenic or cytotoxic response [64,74]. Additionally, collagen can be obtained from several different sources using a variety of isolation methods [63,64]. Collagen type I has been previously electrospun from 1,1,1,3,3,3-hexafluoro-2-propanol (HFIP), a highly volatile organic solvent. Resultant fiber diameters ranged from 100 to 1200 nm and were considered both concentration- and source-dependent [5,63]. The lower end of these measurements falls within the fibrillar diameter range of native type I collagen. With an absence of mechanical stability in an aqueous environment, electrospun collagen scaffolds require either physical or chemical cross-linking, often in the form of glutaraldehyde vapor [64]. Porosity was shown to decrease from 89% to 71% following such cross-linking [63]. Mechanically, glutaraldehyde cross-linked collagen type I matrices exhibited an average tensile modulus of 11–26 MPa, which is comparable to commercially available tissue regenerative membranes and wound dressings [5,63]. It was also demonstrated that type I collagen-coated collagen electrospun scaffolds supported normal human keratinocyte adhesion and spreading. Furthermore, in a Sprague-Dawley rat animal model with full-thickness wounds of the back, noncoated electrospun collagen matrices promoted faster early-stage wound healing as compared with the control group (gauze). The later-stage wound healing process remained similar for both test conditions (Fig. 9.6) [63].

Another study compared the viability of electrospun and freeze-dried collagen scaffolds for wound contraction. After coculturing of fibroblasts and keratinocytes, it was observed that both templates displayed stratified epidermal and dermal cellular layers, along with a continuous basal layer. These scaffolds were then grafted onto full-thickness wounds in athymic mice, each presenting high rates of engraftment. The electrospun collagen scaffold, however, significantly reduced the amount of wound contraction 8 weeks postsurgery as compared with the freeze-dried version, leading to overall reduced morbidity [75].

Finally, collagen type I has been electrospun with a blend of several synthetic and natural polymers, such as poly(ethylene oxide) (PEO) and chondroitin 6-sulfate, respectively. The collagen-PEO scaffolds presented an elastic modulus of 12 MPa, while the collagen-chondroitin sulfate scaffolds showed enhanced rabbit conjunctival fibroblast (RCF) proliferation as compared with collagen controls [74,76]. More information regarding composite electrospun materials for skin tissue engineering can be found in Section 9.2.3.

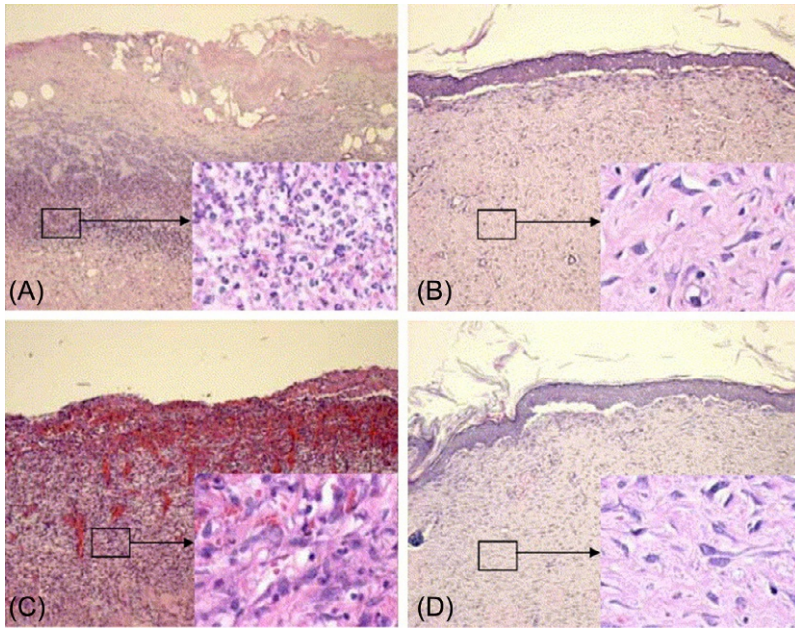


Fig. 9.6 H&E images ($100\times$) of full-thickness wound healing for a Sprague-Dawley rat model. (A) gauze at 1 week, (B) gauze at 4 weeks, (C) electrospun collagen matrix at 1 week, and (D) electrospun collagen matrix at 4 weeks. Zoomed regions are $400\times$.

Reproduced with permission from Rho KS, et al. Electrospinning of collagen nanofibers: effects on the behavior of normal human keratinocytes and early-stage wound healing. *Biomaterials* 2006;27:1452–1461, doi: <http://dx.doi.org/10.1016/j.biomaterials.2005.08.004>, with permission from Elsevier.

9.2.1.2 Silk fibroin

Silk from *Bombyx mori* (silkworm) is a natural material that consists of an outer coating of sericin protein and a central core of fibroin protein [77]. Silk fibroin (SF), which can be extracted from silkworm cocoons (Fig. 9.7), consists of random hydrophobic and hydrophilic coblocks of amino acids. The hydrophobic regions allow for the formation of high strength structures via β -sheet formation, while the hydrophilic regions allow for aqueous solubility [78]. As a biomaterial, this polymer has been studied for a multitude of applications ranging from soft-tissue engineering to high strength tissues and has been fabricated into a variety of formats, including fibers, gels, sponges, and macroporous scaffolds [78,79]. For tissue engineering purposes, SF is known for its excellent biocompatibility, high strength, slow degradation rate, and minimal inflammatory response [78–80]. The degradation of SF is highly unique as it is tunable and can take up to two years in vivo for complete resorption [64]. Like collagen, SF contains RGD binding sites, which allow for enhanced cellular attachment and spreading [81].

Processing and solution parameters play a large role in SF electrospinning. For instance, SF can be electrospun out of a variety of solutions, including formic acid, HFIP, and water [64,80,82]. However, the most influential parameter on final fiber

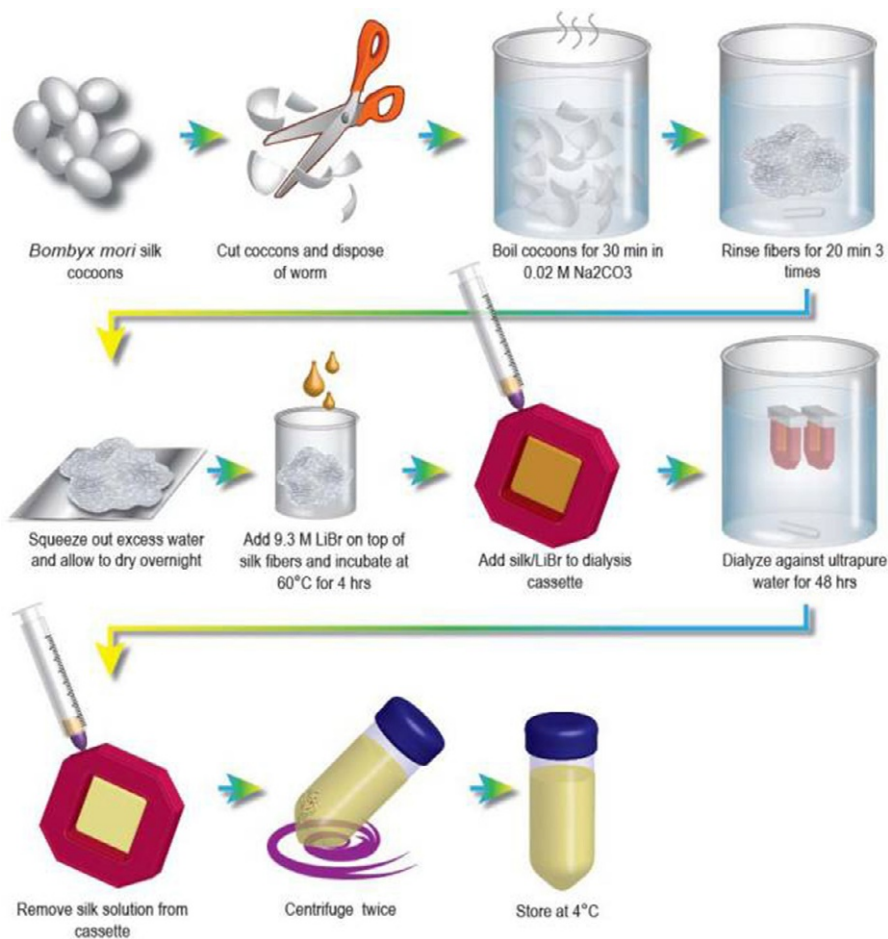


Fig. 9.7 Protocol for extracting silk fibroin from *B. mori* silkworm cocoons.

Reproduced with permission from Rockwood DN, et al. Materials fabrication from *Bombyx mori* silk fibroin. Nat Protoc 2011;6:1612–31, doi: 10.1038/nprot.2011.379, with permission from Macmillan Publishers Ltd: Nature Protocols.

formation and diameter is SF concentration. An increase in polymer concentration typically leads to an increase in fiber diameter [82]. Fiber diameters can range anywhere from 15 to 500 nm [82,83]. Similar to collagen, SF can be cross-linked to improve its strength, which is typically accomplished with methanol or ethanol. This cross-linking induces β -sheet formation, creating high-strength structures with tensile strengths of up to 740 MPa [78].

Aqueous SF blended with PEO and spun against depositing NaCl demonstrated a porosity of 84% and supported the adhesion and infiltration of 3T3 fibroblasts. In a full-thickness wound Sprague-Dawley rat study, these SF electrospun scaffolds closed the wound more rapidly and degraded more efficiently than an engineered dermal

substitute, Matriderm. Additionally, unlike Matriderm, the SF scaffolds did not induce any wound contraction, once again reducing chances of morbidity [84]. SF spun from formic acid also illustrated a high porosity of 76% and supported normal human oral keratinocytes (NHOK), normal human epidermal keratinocytes (NHEK), and normal human gingival fibroblasts (NHGF) adhesion and spreading on SF scaffolds coated with type I collagen and laminin [80].

9.2.1.3 Gelatin

Gelatin is a naturally occurring polymer derivative of collagen. Essentially, gelatin is the denatured form of a collagen triple helix. This denaturing process occurs through partial acid (type A) or alkaline (type B) hydrolysis [85]. For centuries, gelatin has been used for both drug delivery and wound dressings [64]. With regard to scaffold fabrication, gelatin is favorable due to its low cost, biocompatibility, nonantigenicity, and biodegradability [86]. Other benefits include the ability to activate macrophages and to have a hemostatic effect [87]. One of the chief shortcomings of this polymer is that upon hydration, the fibers transition into a colloidal sol (temperature $\geq 37^\circ\text{C}$). Thus, gelatin requires either cross-linking or combination with another polymer to be relevant for tissue engineering applications [64,88].

Altogether, gelatin electrospun fibers have exhibited fiber diameters as low as 200–500 nm and tensile moduli ranging from 8 to 12 MPa [64]. In terms of bio-engineered skin, one study electrospun gelatin type B from 2,2,2-trifluoroethanol (TFE) at several wt/vol percentages. Following fiber collection, these scaffolds were first cross-linked with vacuum dehydration (-100 kPa at 140°C) and were then chemically cross-linked in 1-ethyl-3-(3-dimethyl-aminopropyl)carbodiimide hydrochloride (EDC). Both fiber diameter and hydrated porosity increased with higher gelatin concentrations. The values for these measurements ranged from 0.6 to 3.0 μm and from 40% to 63%, respectively. After 14 days in coculture of human keratinocytes and fibroblasts from adult female breast or abdominal skin, the gelatin scaffolds at lower wt/vol percentages showed clear stratification of the epidermal and dermal layers, along with a continuous basal keratinocyte layer in between (Fig. 9.8). These results justified the potential use of gelatin electrospun scaffolds in full-thickness skin wounds [89].

A separate study utilized a combination of gelatin and chitosan (Section 2.1.4), another natural polymer, to electrospin nanofibers for skin tissue engineering. Both polymers were dissolved at various weight ratios in a combination of trifluoroacetic acid (TFA) and dichloromethane (DCM). The resulting fiber diameters of the gelatin-chitosan blend ranged from 120 to 220 nm, while the tensile strength was recorded to be 26 MPa. In relation to pure gelatin and pure chitosan electrospun scaffolds, the fiber diameters of the copolymer blend were similar, but the tensile strength was significantly higher. As this tensile strength landed within the range of normal human skin, a dermal regeneration application was deemed appropriate. High tensile strength was partially attributed to hydrogen bonding between the gelatin and chitosan [87].

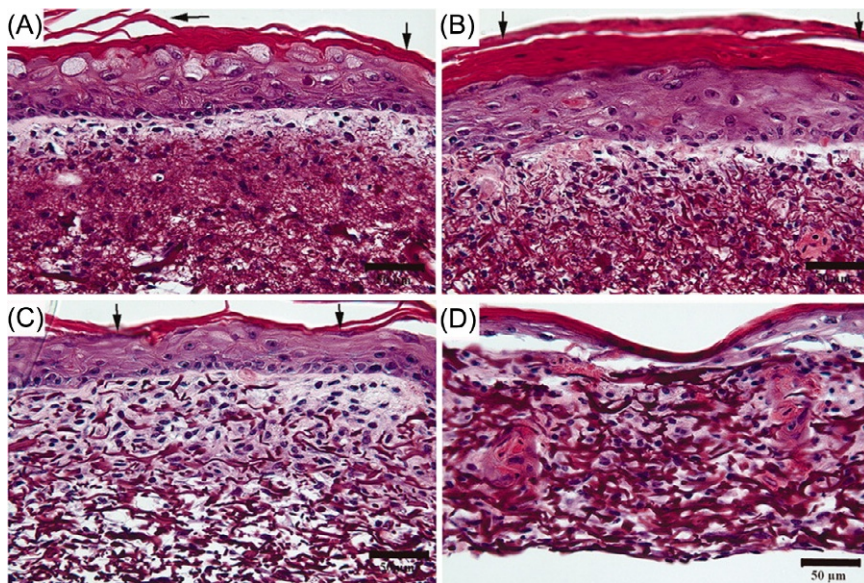


Fig. 9.8 H&E images of gelatin electrospun scaffolds after 14 days of coculture. (A) 10, (B) 12, and (C) 14 wt/vol% scaffolds demonstrated stratified epidermal and dermal cell layers. (D) 16 wt/vol% gelatin scaffolds did not show well-formed epidermis. All scale bars are 50 μm . Reproduced with permission from Powell HM, Boyce ST. Fiber density of electrospun gelatin scaffolds regulates morphogenesis of dermal-epidermal skin substitutes. *J Biomed Mater Res A* 2008;84:1078–86, doi: 10.1002/jbm.a.31498, with permission from John Wiley and Sons.

9.2.1.4 Chitin/chitosan

Chitin is the main structural amino polysaccharide found in the exoskeleton of invertebrates, crustaceans, and insects [90,91]. Chitosan, a natural poly-*N*-acetyl-glucosamine, is derived from chitin via alkaline deacetylation [91]. Both of these polymers are appropriate for skin tissue engineering due to their inherent biocompatibility, biodegradability, bioactivity, antibacterial, and wound healing properties [87,90,91]. Additionally, chitin/chitosan can also exhibit local hemostatic effects [91]. One study compared electrospun chitin nanofibers (Chi-N) with commercially available chitin microfibers (Chi-M). The Chi-N matrices, which were spun out of HFIP, demonstrated fiber diameters of 50–460 nm, while the Chi-M matrices had a fiber diameter of 8.77 μm . To continue, the nanofibers began to enzymatically degrade after approximately 14 days both *in vitro* and *in vivo*, a suitable time frame for dermal regeneration. After culture with NHOK, NHEK, and NHGF, it was observed that the Chi-N matrices allowed for more cellular attachment and spreading than the Chi-M matrices; however, the degree of each for both scaffolds was much less than the polystyrene (PS) control. Following a coating of type I collagen, the chitin nanofibers exhibited more cellular attachment than the microfibers and the PS control (cell spreading was similar between Chi-N and Chi-M matrices) [90].

Chitosan nanofibers blended with PEO have been previously electrospun from acetic acid for a third-degree burn wound dressing application (type IIIa and IIIb degree burns). Post implantation, these scaffolds demonstrated high antibacterial properties due to the presence of chitosan and excellent exudate absorption. Resultantly, the electrospun sheets were able to promote wound ventilation and stimulate skin tissue regeneration. Biodegradation of these scaffolds allowed for less mechanical damage to the wound and less pain upon dressing replacements. Finally, the chitosan nanofiber dressing supported a highly desirable healing time of approximately 14 days (Table 9.4) [92,93].

9.2.2 Synthetic polymers

Synthetic polymers used for skin applications, including wound and burn dressings, are commonly fabricated via electrospinning. Common synthetic polymers include polyglycolide (PGA), PLA, poloxamer, PCL, PS, and polyvinylpyrrolidone (PVP). It has been found in vitro and in vivo that many possess properties appropriate for wound healing and improve reepithelization. Due to their biocompatibility, biodegradability, structure, and mechanical properties, synthetic polymers can provide a good environment for cell proliferation, migration, and differentiation, making them an acceptable choice for tissue-engineered skin applications [91].

9.2.2.1 Polycaprolactone

PCL is a synthetic, biodegradable polymer that has been widely used in biomedical applications, especially drug delivery. This semicrystalline polymer is somewhat hydrophobic and can be utilized both as a homopolymer and in combination with other polymers, such as PLA or PGA, to create a copolymer (Fig. 9.9). With a fairly slow resorption time of 24 months and a nonacidic degradation environment, PCL is an ideal material for extended drug delivery [94]. Additionally, the degradation of PCL is enhanced by lipases and can occur by bulk or surface degradation [95].

The degradation of PCL in vivo is broken up into two stages. During the first stage, the longer of the two, the ester group, is cleaved via a hydrolytic reaction. Following this cleavage, the polymer is rapidly broken down through intracellular degradation in the phagosomes of macrophages and giant cells, and the molecular weight is decreased to 3000 or less [96].

Typical parameters under which PCL (6–12% w/v) is electrospun include flow rates between 0.1 and 1 mL/min and high applied voltages ranging from 22.5 to 36.76 kV. A working distance of approximately 35 cm is commonly used for all other parameters [96–98].

Previous studies have examined these electrospun PCL scaffolds for a dermal application. The average fiber diameter has been created to range from 284 ± 48 to 8320 ± 720 nm, and all studies found the electrospun scaffold porosity to be around 85% [96–98]. This falls within the desired range of 60–90% for optimal cellular infiltration [98]. The elastic modulus of these scaffolds can range anywhere from 6.7 ± 0.4 to 21.42 ± 0.04 MPa, depending on the combination of parameter values [96,98].

Table 9.4 Summary of natural biopolymers for bioengineered, electrospun skin

Material	Composition characteristics	Inherent properties	Advantages	References
Collagen type I	<ul style="list-style-type: none"> – Two $\alpha 1$ and one $\alpha 2$ chains – 50–500 nm in diameter – Triple helical structure 	<ul style="list-style-type: none"> – Naturally occurring – RGD binding sites – Can be obtained from a variety of sources 	<ul style="list-style-type: none"> – Biocompatible – Biodegradable – No immunogenic or cytotoxic response 	[5,63,64,74]
Silk fibroin (<i>B. mori</i>)	<ul style="list-style-type: none"> – Hydrophilic and hydrophobic coblock polymer – Light and heavy chain 	<ul style="list-style-type: none"> – Naturally occurring – RGD binding sites – Slow degradation rate 	<ul style="list-style-type: none"> – Biocompatible – High strength – No toxic degradation products 	[78–81]
Gelatin	<ul style="list-style-type: none"> – Derivative of collagen – Denatured form of collagen triple helix 	<ul style="list-style-type: none"> – Naturally occurring – Local hemostatic effect – Activates macrophages 	<ul style="list-style-type: none"> – Biocompatible – Nonantigenic – Low cost 	[64,85–87]
Chitin/chitosan	<ul style="list-style-type: none"> – Chitin: amino polysaccharide – Chitosan: poly-<i>N</i>-acetyl-glycosaminoglycan 	<ul style="list-style-type: none"> – Naturally occurring – Local hemostatic effect – Chitosan is obtain via alkaline deacetylation of chitin 	<ul style="list-style-type: none"> – Biocompatible – Biodegradable – Bioactive – Antibacterial – Wound healing properties 	[87,90,91]

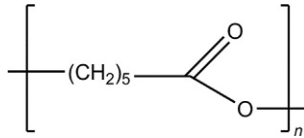


Fig. 9.9 Chemical structure of PCL.

A separate study seeded PCL scaffolds with human fetal fibroblasts and also applied them as skin substitutes within *in vivo* rat wound models. Overall, the fibroblasts had poor proliferation and adhesion. Due to its slow degradation, the scaffold delayed wound contraction but did not prevent it completely. Additionally, it elicited a foreign body response including the presence of many multinucleated macrophages [96].

9.2.2.2 Polyglycolide

PGA is a linear, aliphatic polyester (Fig. 9.10) [95]. While it possesses low solubility in organic solvents, PGA hydrolytically degrades very quickly *in vivo*, commonly taking around 2–4 weeks. The original mechanical properties of PGA steadily decrease upon implantation, often followed by an increase in localized pH and fibrous capsule formation [99].

PGA is primarily degraded hydrolytically through the breakdown of the ester backbone. However, *in vivo* PGA can also be broken down enzymatically. The by-product of this is nontoxic and will be excreted as water or carbon dioxide [100].

Copolymers of glycolic acid have commonly been combined with other components to reduce the degradation rate for skin applications. A common example of this is PLA that will be expanded on in Section 9.2.3 [95].

Standard electrospinning parameters include an applied voltage of around 17–22 kV, a working distance of 10–11 inches, and a flow rate of 2–10 mL/hr. This produces PGA (6–14% w/v) fibers with a diameter of 1.2–2.3 μm and a porosity of approximately 90%, falling within the desired range of 60–90% for optimal cellular infiltration [98,101,102]. The tensile strength was found to be approximately 8 MPa, depending on the variation of the parameters, where human skin is around 27.2 M [8,102]. Additionally, the elastic modulus was found to be 55–105 MPa [101].

A previous study seeded the scaffolds with PSMCs, and it was found that initially, there was high cell proliferation. However, due to the fast degradation of PGA, the scaffolds were only able to support cell growth until day five [103].

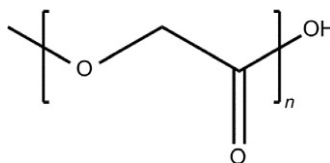


Fig. 9.10 Chemical structure of PGA.

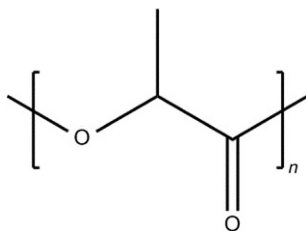


Fig. 9.11 Chemical structure of PLA.

9.2.2.3 Polylactide

PLA (Fig. 9.11) is an aliphatic polyester occurring in two forms: poly(L-lactide) PLLA and poly(D-lactide) PDLA. In vivo, PLA is both biodegradable and bioabsorbable [104].

However, due to its hydrophobic nature, degradation occurs slowly, taking anywhere from two to five years [104]. Hydrolysis of the polymer begins in the amorphous region, with the breaking of the ester bond of the polymeric chain. Following this, the crystalline region is also broken down by hydrolysis. This breakdown can occur through either surface or bulk degradation. While the degradation of PLA can highly affect cell proliferation, it has been shown that the by-products can be broken down through normal metabolic processes without initiating an inflammatory response [105].

Standard parameters under which PLA (5–10% w/v) is electrospun utilize an applied voltage of 10–20 kV, a working distance of 15 cm, and a flow rate of 0.5–1 mL/h. This provides an average fiber diameter ranging anywhere from 650–1140 nm, depending on the combination of parameters [106–109].

PLA is known to possess high mechanical strength [104]. Tensile strength of electrospun PLA is typically around 0.35 MPa, where characteristic human skin is around 27.2 MPa [8,108].

A previous study seeded human skin fibroblasts on PLA scaffolds to assess any potential cytotoxicity. The fibroblasts remained viable, exhibited normal morphology, and infiltrated the electrospun scaffold [107]. Another study similarly seeded human embryonic fibroblasts on PLA scaffolds and also found that cellular proliferation increased with time [109].

9.2.2.4 Polystyrene

PS is a synthetic, hydrophobic, thermoplastic polymer (Fig. 9.12). Most commonly utilized as a film, this form is not ideal due to its fragility. Additionally, it is often accompanied by volatile organic compound (VOC) emission that is dangerous for both the environment and humans. Both physical and chemical modifications have been explored to overcome these limitations; however, to do so is limiting, complex, and expensive. To date, there is no ideal PS form commercially available [110].

Electrospinning provides an advantageous route for creating PS sheets as the different parameters are tunable to the application. For example, when the concentration

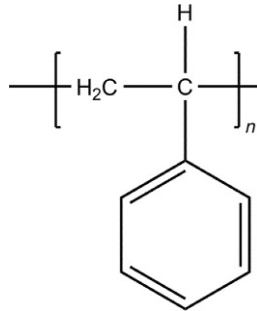


Fig. 9.12 Chemical structure of PS.

of PS is increased from 7 to 17 wt%, the diameter likewise increases from 340 to 3610 nm, decreasing the presence of beads [111]. Typical parameters for electrospinning include an applied voltage of 10–15 kV, a working distance of 10–35 cm, and a flow rate of 0.0625–0.07 mL/min. [110–112]

A standard PS electrospun scaffold possesses fiber diameters of approximately 10 μm and pore sizes ranging from 50 to 150 μm [113]. The ideal pore size for a skin application is between 200 and 250 μm [114]. A previous study found a tensile strength with double strand fibers of 1.5 MPa, where human skin is around 27.2 MPa [8,110].

Another study seeded fibroblasts, keratinocytes, and endothelial cells on electrospun PS scaffolds. Here, the cells were able to self-organize with few biochemical signals present. While the cells infiltrated the scaffold, PS will not degrade, which could prove problematic for *in vivo* applications [113].

9.2.2.5 Other

Poloxamer

Poloxamer is composed of triblock copolymers of polyethylene oxide (PEO)-polypropylene oxide (PPO)-polyethylene oxide (PEO), shown in Fig. 9.13 [115]. As a nonionic surfactant, the synthetic polymer has been previously used in drug delivery and medical imaging applications. Various poloxamer types are dissolvable in water and ethanol and are thermoreversible. Previous studies have briefly examined this polymer in electrospinning [116].

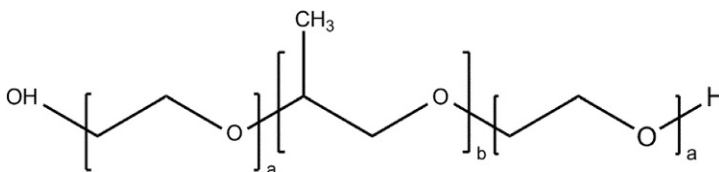


Fig. 9.13 Chemical structure of poloxamer.

Poloxamer is often used in conjunction with a material such as poly(lactide-*co*-epsilon-caprolactone) (PLCL) in order to neutralize the otherwise acidic microenvironment created by the lactic acid. Additionally, when electrospun in this combination, the fibers can reach average diameters as large as 1426.92 ± 456.32 nm. Increasing amounts of poloxamer likewise increase the fiber diameter and improve the fiber uniformity and homogeneity [116].

Furthermore, the presence of poloxamer in electrospun scaffolds improves the tensile strength and ultimate strain. With its addition, these mechanical properties are able to reach an average of 9.37 ± 0.38 and $187.43 \pm 10.66\%$ MPa, respectively. The material can also support cellular proliferation over 10 days, with these properties showing promise for a future application in an electrospun skin application [116].

Polyvinylpyrrolidone

PVP is a synthetic, water-soluble polymer (Fig. 9.14). It possesses low toxicity and is biocompatible [117]. PVP is commonly used in electrospinning, especially in combination with other harder to spin materials acting as a polymer carrier [118].

Typical parameters for electrospinning include a working distance of 12–15 cm, applied voltage of 8–15 kV, and flow rate of 1 mL/h [118–120]. The combination of these parameters produces PVP (4–10% w/v) fibers of 0.02–0.3 μ m in diameter [121].

As noted previously, PVP is most commonly used in combination with other natural/synthetic polymers for electrospun skin applications. *in vitro* and *in vivo* studies will be expanded upon with these composite scaffolds in Section 9.2.3 (Table 9.5).

9.2.3 Composite scaffolds

Methods of incorporating dual polymers into scaffolds have been developed to adjust parameters, such as degradation and pore size, in order to create more finely tuned scaffolds. These composite scaffolds include multipolymer constituents, simultaneous natural and synthetic fibers, and dual-layered and multisyringe techniques, with the goal of creating either homologous or layered scaffolds with varying mechanical properties.

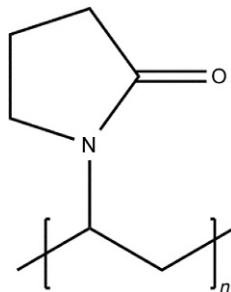


Fig. 9.14 Chemical structure of PVP.

Table 9.5 Summary table of common synthetic polymers used for electrospinning scaffolds for tissue engineering skin applications

Material	Composition characteristics	Inherent properties	Advantages	References
Polycaprolactone (PCL)	Hydrophobic semicrystalline polymer (homopolymer or copolymer)	<ul style="list-style-type: none"> – Synthetic – Biodegradable – High plasticity 	<ul style="list-style-type: none"> – Cheap – Slow degradation rate – Bioresorbable 	[94,122,123]
Poly(glycolic acid) (PGA)	Linear, aliphatic polyester	<ul style="list-style-type: none"> – Synthetic – Biocompatible – Highly crystalline 	<ul style="list-style-type: none"> – Excellent mechanical properties – Fast degradation rate – Bioresorbable 	[95,99]
Polylactide (PLA)	Hydrophobic aliphatic polyester	<ul style="list-style-type: none"> – Synthetic – Biodegradable – Biocompatible 	<ul style="list-style-type: none"> – Good mechanical properties – Bioabsorbable – Slow degradation rate 	[104,107]
Polystyrene (PS)	Thermoplastic amorphous polymer	<ul style="list-style-type: none"> – Synthetic – Hydrophobic – Thermoplastic 	<ul style="list-style-type: none"> – Cheap – High strength – Allows for cellular infiltration 	[110,113,124]
Ploxamer	Triblock copolymers	<ul style="list-style-type: none"> – Synthetic – Nonionic 	<ul style="list-style-type: none"> – Degradable – Thermoreversible – Allows cell proliferation 	[115,116]
Polyvinylpyrrolidone (PVP)	Hydrophilic linear polymer	<ul style="list-style-type: none"> – Synthetic – Biocompatible 	<ul style="list-style-type: none"> – Cheap – Low toxicity – Water-soluble 	[117]

Common composite electrospun scaffolds include collagen/chitosan, collagen/SF, chitosan/collagen, chitosan/SF, chitosan/PEG, chitosan/PVA, PCL/chitosan, PCL/gelatin, PCL/gelatin/collagen, PLA/gelatin, PLA/collagen, PLGA, PLGA/collagen, and PLGA/SF [125].

Electrospun collagen/chitosan scaffolds were shown to promote cell migration and proliferation. When applied to a full-thickness wound in an SD rat, it proved superior to the commercially available collagen sponge with respect to overall wound healing [126]. When collagen was, instead, combined with SF and electrospun from two separate syringes, there was improved attachment and infiltration of human keratinocytes and good human fibroblast activity [127].

Electrospun chitosan/collagen composite scaffolds seeded with 3T3 fibroblasts and HaCaT keratinocytes demonstrated improved cellular response over plain collagen scaffolds. When tested in an *ex vivo* human skin equivalent model, the composite scaffold promoted keratinocyte migration and overall reepithelization of full-thickness wounds [128]. When chitosan was electrospun with SF, there was antibacterial activity that would prove beneficial for a wound dressing application. Additionally, these scaffolds still allowed for cell attachment and proliferation [129]. Chitosan has also been electrospun in combination with PEG. When applied to full-thickness wounds *in vivo*, this composite scaffold led to reepithelialization, vascularization, and granulation tissue remodeling [130]. An electrospun chitosan/PVA scaffold was found to possess appropriate mechanical and swelling properties. Additionally, these scaffolds were applied to a rat wound model and found to encourage antibacterial activity and decrease the wound size [131].

PCL/chitosan composite electrospun scaffolds showed overall improved bioactivity and protein adsorption. When seeded with MG-63, L929, and NIH3T3 cells, the scaffolds possessed good adhesion and integration into the scaffolds [132]. When PCL was combined with gelatin, there was increased mechanical properties and stiffness of the scaffolds [133]. With the addition of collagen, making this a PCL/gelatin/collagen composite scaffold, there was high cell proliferation of L929 mouse fibroblasts. The cells showed characteristic morphology and good adhesion on the electrospun scaffolds [134].

PLA can be electrospun with gelatin leading to fiber sizes mimicking those of natural ECM. When fibroblasts were cultured on these scaffolds, there was improved adhesion and proliferation. When applied to an *in vivo* rat model, there was evidence of new tissue (both the dermis and epidermis) formation after 21 days [109]. In comparison, a PLA/chitosan composite electrospun scaffold promoted cell proliferation and attachment when seeded with mouse fibroblasts (L929) [135].

As was alluded previously, PLA and PGA are commonly combined to create PLGA scaffolds. By using both solution and melt electrospinning, the mechanical properties of these scaffolds can be improved while promoting human keratinocyte adhesion and infiltration [136]. Another study seeded human fibroblasts on PLGA electrospun scaffolds, which yielded high proliferation and good dispersion onto the scaffolds [137]. PLGA can be further combined with other materials to produce a PLGA/collagen composite scaffold showing improved closure in an *in vivo* rat full-thickness wound model as compared with commercially available dressings [138]. Similarly, when PLGA/SF electrospun composite scaffolds are used, mouse fibroblasts (L929) showed excellent

adhesion and proliferation. Furthermore, when applied to a diabetic rat wound model, the scaffolds led to decreased wound area [139].

There are various ways in which composite electrospun scaffolds can be obtained. Blend electrospinning premixes all polymers together into one solution prior to expulsion from the syringe [140]. In contrast, coaxial electrospinning utilizes two separate syringes such that the polymer solutions are kept separate but spin onto a concentric target [125,141]. Lastly, emulsion electrospinning uses a suspension of both a biomolecule and polymer, where the bioactive agent becomes embedded within the electrospun fibers [125,142]. The electrospinning of polymers provides an excellent technique for creating skin substitutes in tissue engineering. By combining the biocompatibility, biodegradability, and biological characteristics of natural polymers with the advantageous mechanical and physical properties of synthetic materials, these scaffolds can be optimally tailored for their desired application [125].

9.2.4 Addition of dopants to polymers

From a tissue engineering perspective, there is a missing piece of the triad in wound healing. Electrospun scaffolds provide the three-dimensional environment for cells to infiltrate, and the surrounding skin and wound bed provide the necessary cells for dermal regeneration. However, natural and synthetic polymer scaffolds lack signaling molecules to promote migration, proliferation, differentiation, and activation of cells throughout the scaffold. These structures need to be able to attenuate the inflammatory response, close the wound, and prevent infection by invading pathogens to promote proper wound regeneration. Scaffolds can incorporate various molecules to achieve these goals. These molecules can be added to the broken-down polymer solution. As the solution is electrospun, these dopant molecules are incorporated into the nanofibers, effectively creating a scaffold with these chemoattractants or morphogens dispersed throughout the scaffold.

9.2.4.1 Manuka honey

For centuries, honey has been used as a treatment by a variety of cultures to promote wound healing. With the flourishing antibiotic-resistant bacterial strain overwhelming hospitals, researchers have begun to look back to honey for its antibacterial and healing properties in wound healing. Honey comes from the nectar of flowers that is collected and transformed into honey by honey bees. The solution is primarily composed of sugar and water, and B vitamins, minerals, organic acids, flavonoids, proteins, and enzymes make up the remainder of the solution. Hydrogen peroxide produced by glucose oxidase in honey can be used to activate neutrophils through NF- κ B. This strengthens the local immune response and helps recruit and activate other leukocytes. Hydrogen peroxide also acts as an antiseptic, killing a wide variety of bacteria. Hydrogen peroxide in the wound bed also stimulates macrophage VEGF production and in turn angiogenesis to the tissue [143]. Flavonoids act as antioxidants to protect the surrounding tissue from damage [144]. Reactive oxygen species left behind in the wound are neutralized by flavonoids. This prevents chronic inflammation at the wound by decreasing NF- κ B activation. [145] The acidity of honey,

pH between 3.2 and 4.5, provides another level of antibacterial effects due to the hyperacidic environment [146]. The supersaturation of sugars in honey creates a negative osmotic pressure in the wound, flushing the necrotic tissue and debris from the area. [145] This osmotic gradient also supplies nutrients to the wounded tissue and removes water that is vital to bacterial survival in the wound [147].

Specific compositions of each honey batch depend on the plant, geographic location, and season in which the honey was harvested. In recent years, Manuka honey has begun to be used in clinical wound healing studies. Manuka honey comes from flowers of the *Leptospermum scoparium* tree in New Zealand and Australia. This honey has a particularly high acidity level that makes it the strongest antibacterial honey available [144].

Despite its antibacterial abilities, honey has been used in wound healing for a variety of reasons. Honey has been found to reduce inflammation, accelerate tissue regeneration in wound healing, and neutralize the smell of the wounds [144]. Recent studies have shown honey to increase the rate of wound closure and cleanse and reoxygenate the wound bed [146,148,149].

Manuka honey can be dispersed into a solution of HFIP and with the addition of a natural or synthetic polymer, such as polyethylene terephthalate (PET) or PCL, can be electrospun [150]. As the concentration of honey increases, the particles of honey begin to accumulate on top of electrospun fibers. With increasing concentrations of Manuka honey, PCL scaffolds have been found to have increased bacterial clearance of *E. coli* and group *B. Streptococcus*. [151] PET/honey nanofibrous scaffolds have been found to have no toxic effect on cells [152]. Because of the antibacterial and wound healing properties of honey, it could be a potential dopant for a skin dressing application.

9.2.4.2 Nanoparticles and ECM proteins

Nanoparticles have recently been functionalized to become dopants for electrospun materials. These particles have a range of functions from an antibacterial effect to modulating the environment to increase cell proliferation. Each elemental nanoparticle has specific properties and methods in which it can be incorporated into electrospun mats. The scope of applications for this process reaches much farther than the biological realm and could be used in multiple industries. Nanoparticles come from a variety of sources and can be recycled from waste materials. Laser impulses can reduce the element from bulk material to atoms and ions, and chemical methods break down bulk to metallic atoms. [153]

Silver has great potential as a possible dopant for wound healing. This metal has been found to have antibacterial, antifungal, and antiviral properties [153]. Silver salts can be added to polymer solutions and electrospun. Compared with silver particles, silver nanoparticles have a much greater surface area and can easily interact with bacteria and fungus. Although the exact mechanism is unknown at this time, it is believed that silver enters the cell and binds to the membrane of the cell preventing further respiration and transport into the cell and remains a viable option for further research [153]. Only select polymers, polyvinyl acetate (PVAc), polyvinylpyrrolidone (PVP), and polyacrylic acid (PAA), have been capable of successfully forming fibers with silver nanoparticles limiting the capabilities of this option [153].

Zinc oxide (ZnO) has been used as a nanoparticle for electrospinning. Much like silver, it is expected to have antibacterial effects, but unlike silver nanoparticles, ZnO has the ability to increase fibroblast proliferation [154]. This finding makes ZnO much more useful as a potential dopant for wound healing. ZnO produces hydrogen peroxide in a fashion that inhibits bacterial growth and promotes proliferation of fibroblasts [154]. ZnO nanoparticles were dispersed in acetone before PCL was added to the solution. The resulting solution was electrospun, and fibers were collected. These scaffolds were used in a guinea pig wound study. The resulting scaffolds at low concentrations were found to have no immunologic rejection or inflammatory response compared with a normal PCL scaffold [154]. Scaffolds containing ZnO were found to have increased healing and contraction compared with control scaffolds [154].

Chondroitin 6-sulfate and hyaluronan have been found to promote ECM secretion in porcine chondrocytes. The ECM is very important in the cellular environment. Not only does it provide support but also ECM directs and regulates cells function. Being able to mimic this function is critical for dermal wound healing. By incorporating sericin and GAGs into an electrospun scaffold, MSC differentiation toward epithelial cells was increased, and fibroblast, keratinocyte, and MSC proliferation were promoted [155]. These additions may prove valuable for promoting accelerated wound healing, thus creating a scaffold that can maintain high water content.

9.2.4.3 *Cytokines and chemokines*

In normal wound healing, specific growth factors are involved in stopping the inflammatory response. Interleukin-10 (IL-10) appears to limit and terminate the inflammatory response [156]. It also regulates the differentiation of T regulatory cells, B cells, natural killer cells (NK), and cytotoxic T cells and helper T cells [156]. Interleukin-13 (IL-13) inhibits the production of inflammatory cytokines [157].

PRP is a therapy that effectively concentrates autologous platelets to three- to five-fold increase over normal blood [158]. Platelets contain alpha and dense granules that contain a significant number of growth factors and cytokines that are relevant to wound healing [19]. With PRP, the concentrations of those growth factors are several times higher compared with normal blood [19]. These growth factors can be used effectively in wound healing to promote tissue regeneration, cellular recruitment, and mediation of the inflammatory response.

Promoting cell recruitment and tissue regeneration in a wound bed is necessary for a proper wound healing. Several of the growth factors in platelets act to achieve this process. PDGF is a powerful mitogen for fibroblasts and smooth muscle cells [159]. PDGF plays a role in angiogenesis, fibrous tissue formation, reepithelialization, and fibroblast chemotaxis and collagen synthesis [159]. TGF- β stimulates proliferation of undifferentiated mesenchymal stem cells and stimulates angiogenesis and endothelial cell chemotaxis [159]. VEGF much like its name suggests promotes angiogenesis and vascular permeability [159]. Epidermal growth factor (EGF) directly stimulates proliferation of epidermal cells and keratinization. [160] Fibroblast growth factor (FGF) promotes increased fibroblast, migration, and proliferation, as well as angiogenesis [161]. IGF-1 increases proliferation and affects differentiation of keratinocytes [162]. These growth factors could play an important role in chronic wound healing.

PRP can also affect the inflammatory process. Platelets play an important role in healthy wound healing. They provide signals that can promote and reduce inflammation. In a healthy well-vascularized wound, inflammatory cells and immune cells infiltrate the area and clean up and remove any debris left in the wound [19]. Interleukin-1 β (IL-1 β) induces adhesion molecules on endothelial cells, allowing infiltration of the tissue by inflammatory cells [163]. Tumor necrosis factor-alpha (TNF- α) facilitates apoptosis and removal of damaged cells [164]. Interferon gamma (IFN γ) promotes classical macrophage activation [165]. Granulocyte macrophage colony-stimulating factor (GM-CSF) influences the proliferation of granulocytes and monocytes [166]. A small case study of three spinal cord injury patients with stage IV pressure ulcers used PRP to attempt to stimulate healing [19]. In this study, wounds were injected with a patient's own PRP. The wound bed was also packed with PRP-alginate beads [19]. This provided immediate and sustained release of PRP growth factors into a wound site. The use of this therapy stimulated the wound healing response, but in each case, scarless dermal regeneration was not found. Each wound healed dysfunctionally with disorganized tissue [19]. The study concluded that the PRP growth factors and cytokines accelerate wound healing, but without a proper 3D structure, disorganized scarring inevitably occurs [19]. The growth factor milieu from PRP has been used to treat chronic osteomyelitis. However, disorganized scarring prevents full functioning skin from regenerating [167]. An electrospun fiber scaffold could provide the structure necessary for accelerated wound healing (Fig. 9.15).

By subjecting PRP to a freeze-dry-freeze cycle followed by lyophilization, a preparation rich in growth factors (PRGF) can be prepared [158]. Essentially, the platelets lyse during this process releasing the contents of the alpha and dense granules, the growth factors, and cytokines that can accelerate wound healing. This powder can be added to both natural and synthetic polymer solutions for electrospinning and becomes incorporated into the surrounding fibers [158]. This method has potential to provide a sustained release of growth factors and a 3D structure for cells to promote a healthy accelerated wound healing process.

As described above, EGF plays a role in epithelial regeneration and keratinization [160]. Incorporating EGF into an electrospun scaffold could lead to rapid reepithelialization and increase wound healing. EGF is able to elute into the surrounding wound bed and affects the surrounding cells to close the wound. These scaffolds are able to increase wound closure rate by threefold compared with nondoped silk scaffolds [168]. A burst effect was observed when the EGF/silk scaffolds were introduced to a wound. This effect showed rapid activation and migration of keratinocytes to reepithelialize the wound. The instantaneous burst release was matched by slow constant release of EGF as the study progressed [168]. Reepithelializing a wound bed is necessary for preventing water loss and pathogenic infiltration of the wound site.

9.2.4.4 Bioactive glass

Bioactive glass is normally used to produce a hydroxyapatite layer on a surface. This material is typically used in the bone because of its similar mineral content. This material bonds firmly with living bone strengthening the tissue; however, silicate bioactive glass 45S5 also has effects on soft tissues [169]. When this bioactive glass is broken



Fig. 9.15 Photograph of patient's chronic wound at the time of admission (top), two weeks after PRP treatment (middle), and 5 months after treatment.

Reproduced with permission from Yuan T, Zhang C, Zeng B. Treatment of chronic femoral osteomyelitis with platelet-rich plasma (PRP): a case report. *Transfus Apher Sci* 2008;38:167–173, doi: <http://dx.doi.org/10.1016/j.transci.2008.01.006>, with permission by Elsevier: Transfusion and Apheresis Science.

down, it leaves behind an SiO_2 glass network. This network is then infiltrated by Ca^{2+} and $(\text{PO}_4)_3$ -ions. The ions interact with the silicate layer and form an amorphous calcium phosphate layer on top of the SiO_2 layer. This layer incorporates hydroxide and carbonate ions from a solution to create a crystallized HCA layer [169].

When exposed to low concentrations of silicate 45S5 bioactive glass particles, human fibroblasts have been found to increase VEGF and FGF secretions [170]. Increasing vascularity and fibroblast concentrations is beneficial for wound healing. Ointments containing different compositions of bioglass healed wounds more quickly.

Fibroblasts proliferated more readily, and capillary angiogenesis occurred within seven days of placement at wound sites [171]. Bioactive glass has also been found to have an antibacterial effect on *S. aureus* due to bioactive glass' ability to change the environmental pH [172]. This change may not be reproducible in vivo due to the buffering of the wound bed. Bioactive glass is readily added and electrospun with PVA [173]. By creating a nanofibrous mat and incorporating bioactive glass, wound healing could be accelerated.

Specific borate glasses have been found to create cotton-like glass fibers that can mimic fibrin. These glasses also show antibacterial effects against several common microbes [169]. The 3D structure of this glass mat may trap platelets that can accelerate healing. In vivo, the bioglass scaffold has helped reduce scarring and alleviated the use of wound vacuums from the healing process in chronic wounds [169]. These glasses have also been found to increase microvessel density in mice, thus showing increased angiogenesis [174]. Borate glasses have also been found to close the wounded area faster than other bioactive glasses. This also allowed for increased collagen deposition into the wounded area. [175]

The merging of these two methods of incorporating bioactive glasses, silicate or borate, allows for the treatment of chronic wounds and could quickly be brought to market to be used in emergency situations or in chronic wound healing scenarios. The use of an electrospun-based material could help provide a better three-dimensional structure, while the addition of silicate and borate-based glasses could accelerate wound healing based on each of their own properties (i.e., antibacterial, angiogenic, increased wound closure, etc.).

9.2.4.5 Pharmaceuticals

Electrospinning allows for the ability of elution of man-made materials into the wound bed. By understanding the degradability of the polymer materials, drug release from the scaffold can be controlled. Various drug-loading methods can be used to affect the drug release rate from the scaffold. These include drug encapsulation, fiber coating, and drug embedding. This allows for the release of a range of drugs: anesthetics, analgesics, and antibiotics.

An ideal electrospun skin dressing would be able to limit pain at the wound. Anesthetics such as lidocaine can be incorporated into a scaffold [176]. The drug shows an initial burst release followed by sustained release over 72 h [176]. In total, over 90% of the anesthetic is eluted out of the scaffold [176].

Analgesics such as ibuprofen can be added into the fibers of a scaffold and eluted into the surrounding milieu. Shi et al. have designed a transdermal patch through which ibuprofen has been loaded onto fibers of cellulose/PVP [177]. Ibuprofen showed steadily increasing release from electrospun mats over 24 h in vitro [177]. An ex vitro skin study showed drug permeation into the surrounding skin, allowing for sustained release onto a wound site [177].

Antibiotic elution could be another potential capability of an electrospun skin application. Thakur et al. showed that mupirocin showed a burst release from a scaffold and a 36% total release of the antibiotic over 72 h. In a wound dressing,

antibiotics could prevent secondary infections, reducing hospital stay length and helping patients get home quicker [176]. Incorporation of cefoxitin sodium has shown increased clearance and antimicrobial effects on *S. aureus* up to 1 week after introduction [178]. Tetracycline hydrochloride has also been found to be incorporated into poly(lactic acid)/poly(ethylene-*co*-vinyl acetate) electrospun mats (Table 9.6) [179].

Table 9.6 Summary of dopants added to the electrospinning process

Dopant	Function		References
PRP/PRGF	Tissue regeneration, PDGF, TGF- β , VEGF, EGF, FGF, IGF-1	Angiogenesis, reepithelialization, fibroblast migration and proliferation, Keratinocyte proliferation, collagen synthesis, vascular permeability	[19,158–162]
	Pro-inflammatory, IL-1 β , TNF- α , IFN γ , GM-CSF	Leukocyte infiltration, apoptosis, classical macrophage activation, granulocyte and monocyte proliferation	[163–166]
	Antiinflammatory, IL-10, IL-13	Inhibit differentiation of immune cells, inhibit inflammatory cytokine production	[156,157]
Manuka honey	Inhibit bacterial growth, reduced inflammation, tissue regeneration, wound deodorization, neutrophil activation, VEGF production, ROS neutralization		[144,146,148,149]
Silver nanoparticles	Antibacterial, antifungal, and antiviral effects		[153]
Zinc oxide nanoparticles	Antibacterial, fibroblast proliferation		[154]
Chondroitin 6-sulfate/sericin	MSC differentiation, ECM production		[155]
EGF	Reepithelialization, wound closure		[168]
Bioactive glass	Increased VEGF and FGF production, antibacterial, scar reduction, angiogenesis, collagen deposition		[169–171,173–175]
Pharmaceuticals	Anesthetics, analgesics/antiinflammatory, antibiotics		[176–179]

9.2.5 Variations to the electrospinning process

In order to allow cells to rapidly invade the scaffold and align and distribute properly within the 3D environment, researchers have worked to develop scaffolding capable of functional regeneration. By adjusting these scaffolds to mimic the properties of skin tissue, it may be possible to create an ideal dermal substitute that promotes native intracellular response and duplicates intercellular reactions to conform to structural ECM standards of typical skin. General electrospinning parameters adjust the fiber size and deposition on the scaffold but often fail to adequately tailor pore sizes to increase the amount of cell infiltration. Variations to the electrospinning process primarily aim to tailor the pore size of the scaffold without significantly compromising mechanical integrity of the scaffold; for the skin, this entails a pore size of 70–200 μm , which is adequately large to allow optimal ingrowth of fibroblasts and endothelial cells [180]. Multiple techniques have been utilized to promote increased cell infiltration via pore size variation, from adding back pressure to the mandrel to directing the location of the fiber within microns of standard deviation.

9.2.5.1 Air impedance

Air-impedance electrospinning uses a hollow electrospinning mandrel (Fig. 9.16) with defined pores through which pressurized air flows [181]. These air jets disrupt fiber deposition and compaction, causing significantly higher cell penetration compared with scaffolds spun with the solid mandrel, with the amount dependent on the velocity of the air flow [181,182]. McClure et al. developed a perforated airflow impedance mandrel and tested the properties against a solid steel mandrel. Mechanical burst properties of scaffolds spun with air pressures from 50 to 400 kPa showed a gradual increase with increase in air pressure upon spinning. Maximum pore size of the scaffolds was shown in the 100 kPa air pressure mandrel, and cell penetration echoed the same results, whereas neither pressure nor static seeding of cells onto solid mandrel surfaces showed infiltration into the scaffold. However, these qualities only exist for the pore lumen, where the pressurized air is escaping the mandrel. Outside of the perforations, the scaffold is similar to the solid mandrel. These results were also reported from a study by Yin et al., using P(LLA-CL)/SF blended composite scaffolds [183].

9.2.5.2 Cryo-electrospinning

Cryogenic electrospinning involves typical fiber formation of a polymer onto either mandrels or solutions held at very low temperatures [184]. Higher porosities over standard procedures and topographical patterns can be formed by forming ice crystals on a supercooled hollow mandrel and electrospinning around the crystals, as in the case of Simonet et al. and two studies by Leong et al. [184–186] Leong in 2010 found that a bilayer cryogenic and standard electrospinning technique was able to create not only a porous structure that allows infiltration but also a physical barrier preventing cell infiltration where necessary, such as an artificial epidermal layer that allows vapor exchange [186]. Significantly, higher porosities and porous fibers of various polymers

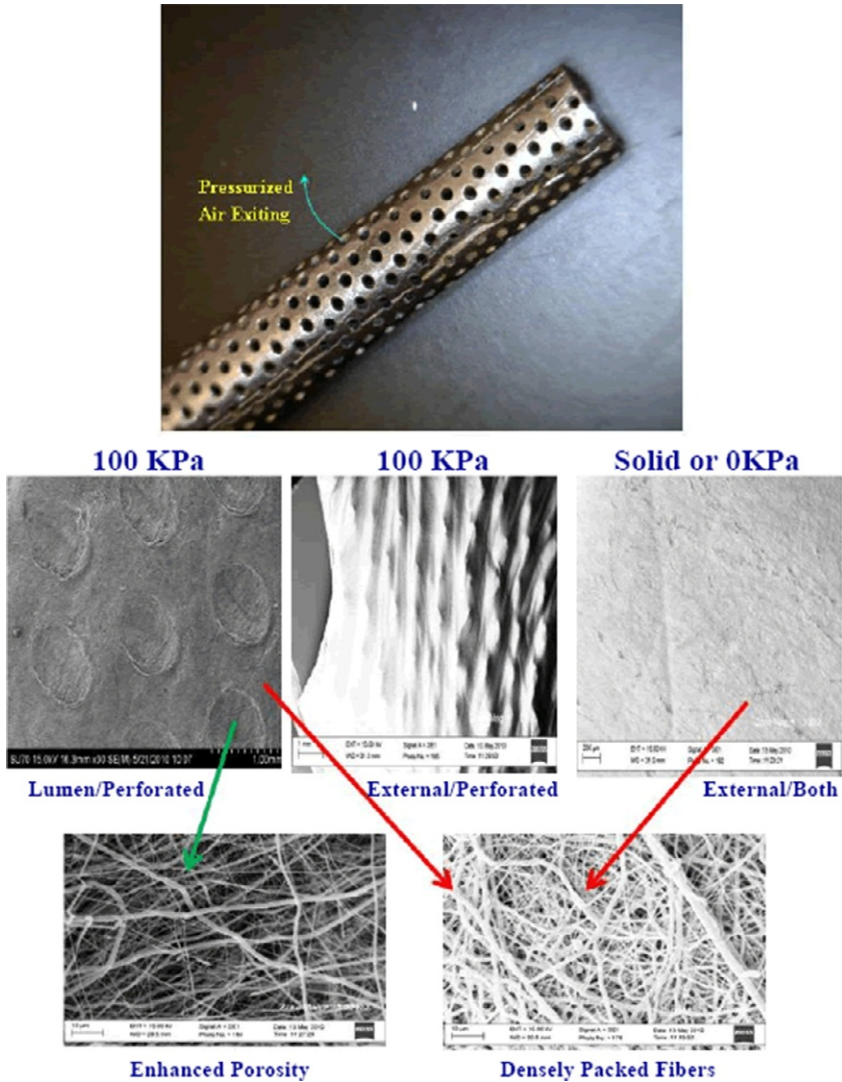


Fig. 9.16 Air impedance scaffold and SEM images showing the lumen and external scaffold topography.

Reproduced with permission from Bowlin GL. Enhanced porosity without compromising structural integrity: the nemesis of electrospun scaffolding. *J Tissue Sci Eng* 2011.

can be formed using a cryogenic bath, as McCann et al. determined (Fig. 9.17) [187]. Removing the fibers from the liquid nitrogen bath rapidly leads to nonporous fibers, whereas vacuum drying creates a porous fiber, removing the need for volatile solvents or selective dissolution of phase-separated polymers. Porous fibers increase surface area and can be used for encapsulation of active substances.

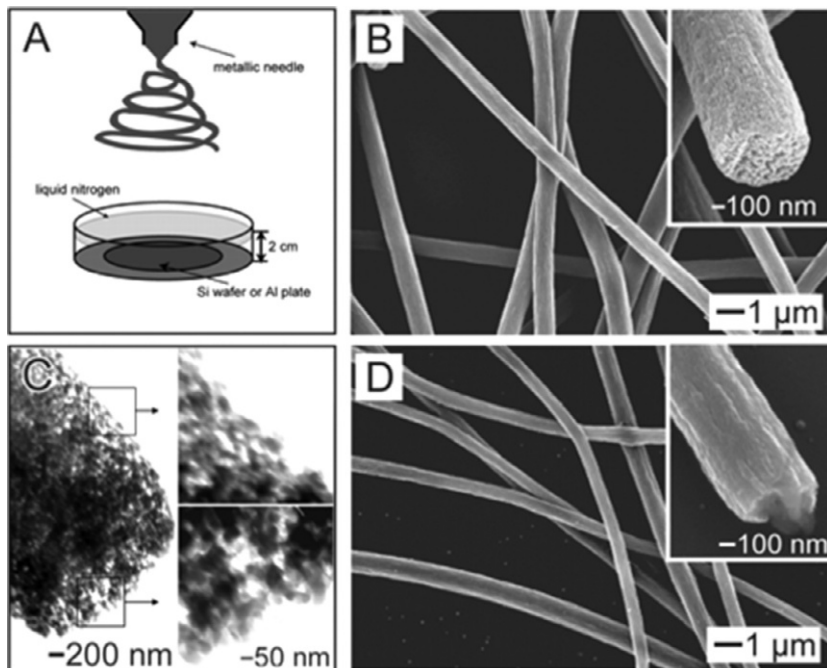


Fig. 9.17 (A) Cryo-electrospinning setup. Porous fibers from (B) vacuum drying and (D) rapid reheating after spinning. Note the high porosity in the vacuum-dried fibers (B and C). Reproduced with permission from McCann JT, Marquez M, Xia Y. Highly porous fibers by electrospinning into a cryogenic liquid. *J Am Chem Soc* 2006;128:1436–37; Rho KS, et al. Electrospinning of collagen nanofibers: effects on the behavior of normal human keratinocytes and early-stage wound healing. *Biomaterials* 2006;27:1452–61, doi: <http://dx.doi.org/10.1016/j.biomaterials.2005.08.004>, with permission. Copyright © 2006 American Chemical Society.

9.2.5.3 Sacrificial fiber and porogen incorporation

Porogens have been added in various ways to force pores within electrospun scaffolds. The addition of salt within an electrospun scaffold is a modified protocol of standard salt leaching, where salt is added to a polymer and dissolved once the polymer has cured to create a porous scaffold of porosities dependent on concentration and crystal size of the salt [188]. Nam et al., Kim et al., and Lee et al. used varying methods to create compressed layered nanofiber constructs interspersed with salt, and others have used water-soluble polymers to achieve a similar effect [189–192]. These scaffolds show significantly higher cellular infiltration over standard electrospun scaffolds.

Sacrificial fibers have also been shown to increase pore size and cell infiltration into electrospun scaffolds and even aid in alignment and ECM organization, as seen in the research of Baker et al., among others (Fig. 9.18) [193–195]. In this technique, two polymers are coelectrospun onto a central mandrel, typically one water-soluble polymer such as PEO and one insoluble polymer such as PCL. After spinning, the scaffold is then washed with water, dissolving the soluble polymer and leaving the insoluble polymer with a higher porosity than standard electrospun scaffolds.

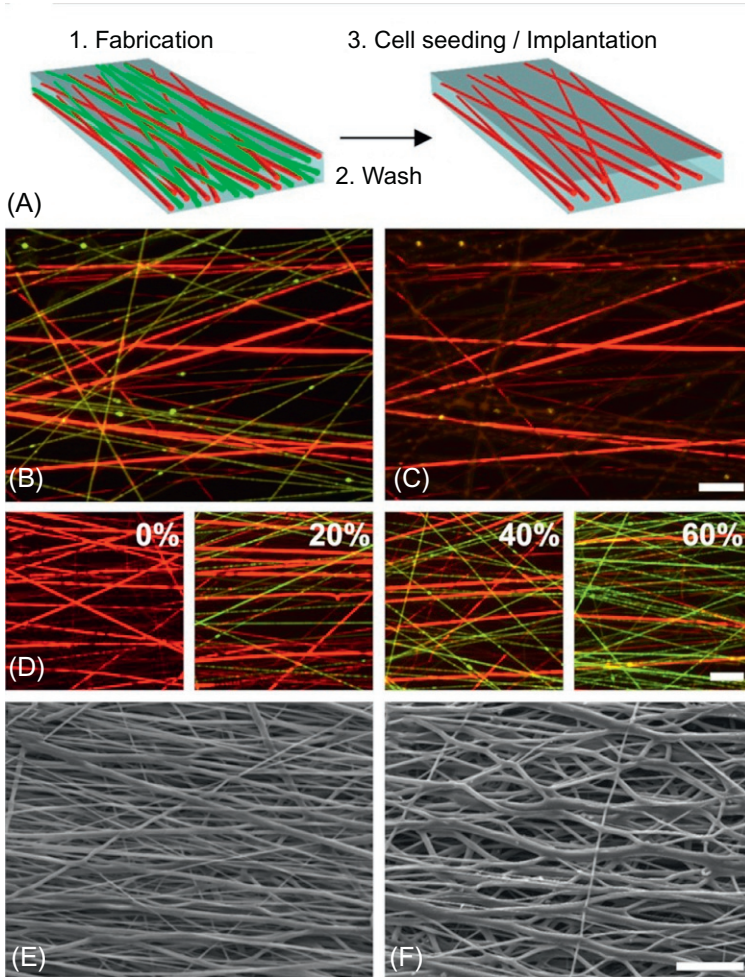


Fig. 9.18 (A) Sacrificial fiber incorporation, where PCL is shown in red and PEO is shown in green. (B) and (C) illustrate before and after washing, (D) demonstrates the % PEO content in PCL and PEO composite scaffolds, and (E) and (F) show SEM images of 0% (E) and 60% (F) PEO after hydration.

Reproduced with permission from Baker BM, et al. Sacrificial nanofibrous composites provide instruction without impediment and enable functional tissue formation. *Proc Natl Acad Sci U S A* 2012;109:14176–81, doi: 10.1073/pnas.1206962109. Copyright (C) 2012, National Academy of Sciences, USA.

9.2.5.4 Biased alternating current electrospinning

Deposition of fibers can be controlled by varying the electric field around the jet (Fig. 9.19) [196]. These fibers can be aligned singularly in very specific patterns, which can include forced aligned pores [197]. Multiple authors have experimented

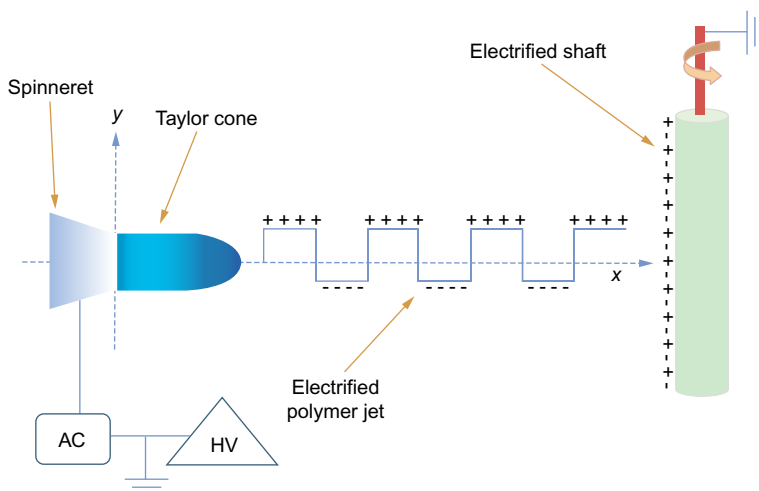


Fig. 9.19 Schematic of DC-biased AC-electrospinning.

Reproduced with permission from Ochanda FO, Samaha MA, Tafreshi HV, Tepper GC, Gad-el-Hak M. Fabrication of superhydrophobic fiber coatings by DC-biased AC-electrospinning. *J Appl Polym Sci* 2012;123:1112–9, doi: 10.1002/app.34583, with permission. Copyright © 2011 Wiley Periodicals, Inc.

with variations of electric fields, including electrostatic and magnetic forces, which can be tailored [198–202].

9.2.5.5 Alternative techniques to increase pore size

Various other techniques have been utilized to increase porosity, including inducing macroporosity via laser cutting and nanoyarn creation. [203,204] Laser cutting involves rapid, concise heating with intense laser energy to create controlled geometric patterns and voids in an electrospun scaffolds [205]. Controlling power, orientation, and pulse can create variations and patterns in the ablation of the scaffolds; these processing parameters can be optimized for cell growth and penetration (Fig. 9.20) [67,204,206,207]. Photopatterning and ultraviolet photolithography achieve a similar effect [208,209].

Using a technique known as dynamic liquid electrospinning, Wu et al. developed a scaffold with observed increased mechanical properties that promotes oriented cell growth and enhanced cell infiltration [210–212]. This “nanoyarn” (Fig. 9.21) is formed by a process that involves depositing fibers into a water vortex and then collecting the combined fibers onto a rotating mandrel within between a fiber collection chamber and a water-recycling chamber.

Blakeney et al. developed a method of removing the limitation of low cell infiltration through sheetlike scaffolds by electrospinning around a needle array (Fig. 9.22) [213]. This focused, low density, uncompressed three-dimensional

Fig. 9.20 Silk fibroin/ PLLA nanoyarn scaffolds. Reproduced with permission from Wu J, et al. Electrospun nanoyarn scaffold and its application in tissue engineering. *Mater Lett* 2012;89:146-9. Copyright © 2012, Elsevier Publishing.

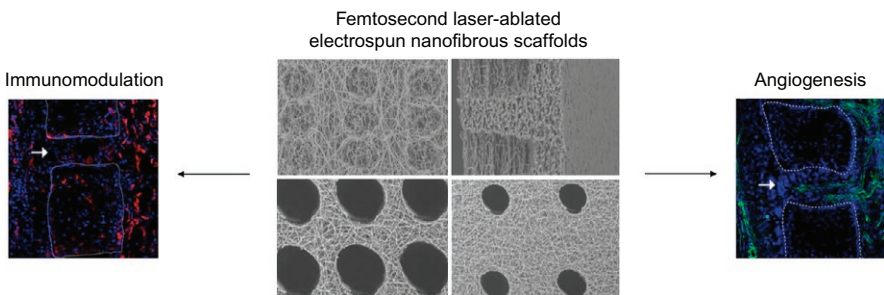
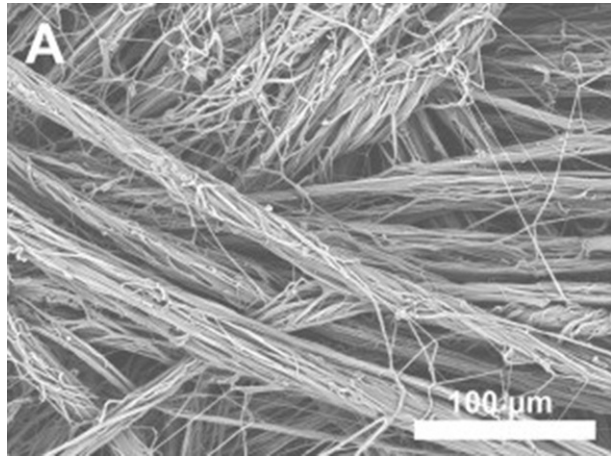


Fig. 9.21 Center top image depicts laser ablation of an 800 nm, 100 femtosecond laser with a 35 μJ energy at 5 pulses. Bottom center depicts spacing of 50 and 200 μm with a constant 100 μm diameter. Ablated scaffolds exhibit endothelial ingrowth and an increase in M2 macrophage infiltration over control.

Reproduced with permission from B.L. Lee, et al., Femtosecond laser ablation enhances cell infiltration into three-dimensional electrospun scaffolds, *Acta Biomater* **8**, 2012, 2648–2658. Copyright © 2013 Elsevier Publishing.

electrospun nanofibrous scaffold (FLUF), significantly increased cell ingrowth and proliferation over scaffolds spun with traditional electrospinning methods, as the FLUF simultaneously provides deep, interconnected pores and a stable, nanofibrous ECM [213].

9.3 Conclusions and outlook

The skin is a dynamic organ with unique healing properties. When the skin is damaged beyond traditional self-repair, it is vital to aid in the healing of the wound. Minor injuries may require only bandages or sutures to facilitate wound closure, but major wounds such as burns, pressure injuries, or diabetic ulcers can require a much more technical approach. Ideal dermal wound products will not only aid in wound closure

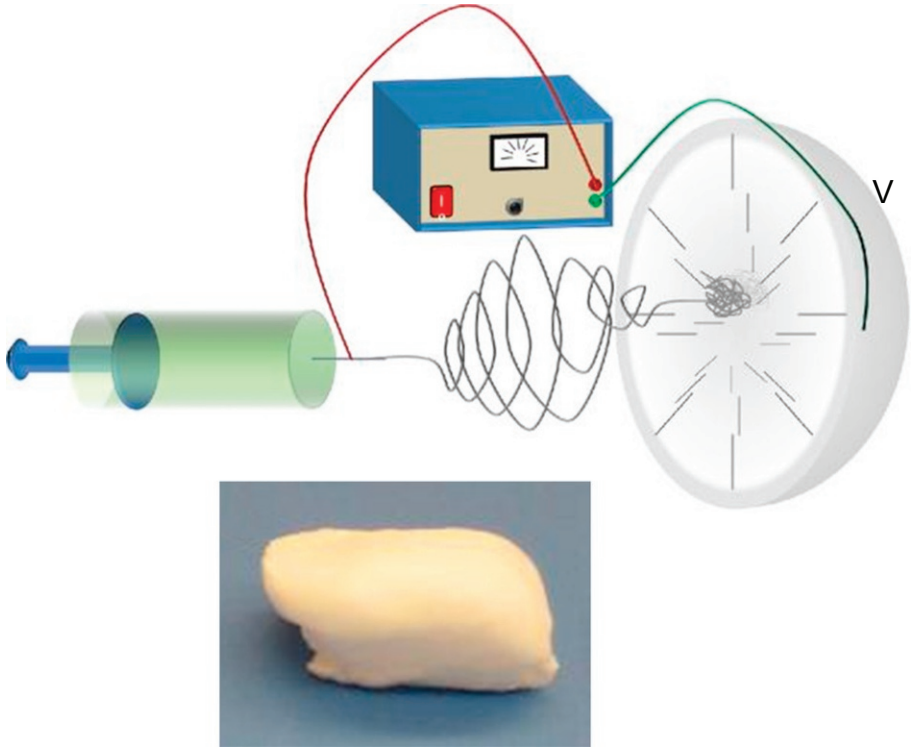


Fig. 9.22 Creation of the focused, low density, uncompressed nanofiber (FLUF). Modified from Blakeney BA, et al. Cell infiltration and growth in a low density, uncompressed three-dimensional electrospun nanofibrous scaffold. *Biomaterials* 2011;32:1583–90, doi: 10.1016/j.biomaterials.2010.10.056, with permission (Copyright © 2011 Elsevier Publishing).

but also facilitate skin regeneration through tissue-engineered constructs. In order to create such a construct, there are many considerations; the skin substitute must maintain proper moisture levels, allow for debridement either externally or physiologically, and prevent infection while allowing helpful bacteria to colonize [26]. Ideal products should leave no wound bed debris, relieve pain, provide thermal insulation while removing exudate, and cause no adverse reactions [26,27]. While there are many currently marketed products, they have yet to fit the ideal qualifications for a dermal wound healing product; researchers have attempted to fill in this ideal gap by using electrospun scaffolds for dermal regeneration and wound healing. Electrospinning is a highly versatile method of creating nanofibers that can incorporate natural and synthetic materials along with additives such as Manuka honey or PRP. The electrospun scaffold can be modified to allow cell infiltration and cell adhesion while attenuating the inflammatory response and minimizing bacterial infection. Scaffolds can also be doped with cytokines and chemokines to enhance and hasten the wound healing cascade. Creating a dermal regeneration template using bioresorbable materials creates a semipermanent bandage that allows the cells to replace degraded scaffold with newly

formed ECM, reducing scar formation. As the research in this chapter has shown, electrospinning is a highly applicable technique for dermal regeneration and can be tailored to provide all of the ideal properties of a wound healing and regenerative construct, both by a wound dressing and by a tissue engineering perspective.

Currently, there are no clinically available electrospun DRTs on the market; however, many researchers are attempting to create such a product in order to more adequately fulfill the qualifications of an ideal dermal wound healing product. Some considerations must be taken into account upon market approval including scale-up and cost recovery, but the existence of predicate wound healing devices and the low production and product cost creates an environment for monumental growth of electrospun scaffold in the wound healing market.

References

- [1] McLafferty. The integumentary system: anatomy, physiology and function of skin. *Nurs Stand* 2012;27:35–42.
- [2] Lehmann B, Sauter W, Knuschke P, Dressler S, Meurer M. Demonstration of UVB-induced synthesis of 1 alpha,25-dihydroxyvitamin D3 (calcitriol) in human skin by microdialysis. *Arch Dermatol Res* 2003;295:24–8. <http://dx.doi.org/10.1007/s00403-003-0387-6>.
- [3] Bikle DD, Nemanic MK, Gee E, Elias P. 1,25-Dihydroxyvitamin D3 production by human keratinocytes. Kinetics and regulation. *J Clin Invest* 1986;78:557–66. <http://dx.doi.org/10.1172/jci112609>.
- [4] Bikle DD, Nemanic MK, Whitney JO, Elias PW. Neonatal human foreskin keratinocytes produce 1,25-dihydroxyvitamin D3. *Biochemistry* 1986;25:1545–8.
- [5] Matthews JA, Wnek GE, Simpson DG, Bowlin GL. Electrospinning of collagen nanofibers. *Biomacromolecules* 2002;3:232–8.
- [6] Ushiki T. Collagen fibers, reticular fibers and elastic fibers. A comprehensive understanding from a morphological viewpoint. *Arch Histol Cytol* 2002;65:109–26.
- [7] Corr DT, Hart DA. Biomechanics of scar tissue and uninjured skin. *Adv Wound Care* 2013;2:37–43. <http://dx.doi.org/10.1089/wound.2011.0321>.
- [8] Gallagher AJ, Anniadh A, Bruyere K, Otténio M, Xie H, Gilchrist M. In: RCOBI conference 2012, Dublin, Ireland; 2012.
- [9] Pawlaczyk M, Lelonkiewicz M, Wieczorowski M. Age-dependent biomechanical properties of the skin. *Adv Dermatol Allergol* 2013;30:302–6. <http://dx.doi.org/10.5114/pdia.2013.38359>.
- [10] Lanza R, et al. *Principles of tissue engineering*. New York, NY: Elsevier; 2014.
- [11] Singer AJ, Clark RA. Cutaneous wound healing. *N Engl J Med* 1999;341:738–46. <http://dx.doi.org/10.1056/nejm199909023411006>.
- [12] Clark RAF. *The molecular and cellular biology of wound repair*. 2nd ed. Berlin: Plenum Press; 1996.
- [13] Rappolee DA, Mark D, Banda MJ, Werb Z. Wound macrophages express TGF-alpha and other growth factors in vivo: analysis by mRNA phenotyping. *Science* 1988;241:708–12.
- [14] Pilcher BK, et al. The activity of collagenase-1 is required for keratinocyte migration on a type I collagen matrix. *J Cell Biol* 1997;137:1445–57.
- [15] Mignatti P, Rifkin DB, Welgus HG, Parks WC. In: Clark RAF, editor. *The molecular and cellular biology of wound repair*. New York: Springer; 1988. p. 427–74.

- [16] Ellis H. Wound healing and wound infection: theory and surgical practice Thomas K. Hunt. 234 × 155 mm. Pp. 303+x. Illustrated. 1980. Hemel Hempstead: Prentice Hall £12.30. *Br J Surg* 1981;68:142. <http://dx.doi.org/10.1002/bjs.1800680227>.
- [17] Clark RA, Folkvord JM, Hart CE, Murray MJ, McPherson JM. Platelet isoforms of platelet-derived growth factor stimulate fibroblasts to contract collagen matrices. *J Clin Invest* 1989;84:1036–40. <http://dx.doi.org/10.1172/jci114227>.
- [18] Bryant RA. *Acute DPN. Chronic wounds: current management concepts*. 4th ed. New York: Elsevier; 2012. pp. 71–72.
- [19] Sell SA, et al. A case report on the use of sustained release platelet-rich plasma for the treatment of chronic pressure ulcers. *J Spinal Cord Med* 2011;34:122–7.
- [20] Loots MA, et al. Differences in cellular infiltrate and extracellular matrix of chronic diabetic and venous ulcers versus acute wounds. *J Invest Dermatol* 1998;111:850–7. <http://dx.doi.org/10.1046/j.1523-1747.1998.00381.x>.
- [21] Chiang RS, et al. Current concepts related to hypertrophic scarring in burn injuries. *Wound Repair Regen* 2016; <http://dx.doi.org/10.1111/wrr.12432>.
- [22] Rowan MP, et al. Burn wound healing and treatment: review and advancements. *Crit Care* 2015;19:243. <http://dx.doi.org/10.1186/s13054-015-0961-2>.
- [23] Farina Jr. JA, Rosique MJ, Rosique RG. Curbing inflammation in burn patients. *Int J Inflamm* 2013;2013:715645. <http://dx.doi.org/10.1155/2013/715645>.
- [24] Edgar DW, Fish JS, Gomez M, Wood FM. Local and systemic treatments for acute edema after burn injury: a systematic review of the literature. *J Burn Care Res* 2011;32:334–47. <http://dx.doi.org/10.1097/BCR.0b013e31820ab019>.
- [25] Sommer K, et al. Delayed wound repair in sepsis is associated with reduced local pro-inflammatory cytokine expression. *PLoS One* 2013;8:e73992. <http://dx.doi.org/10.1371/journal.pone.0073992>.
- [26] Fonder MA, et al. Treating the chronic wound: a practical approach to the care of non-healing wounds and wound care dressings. *J Am Acad Dermatol* 2008;58:185–206. <http://dx.doi.org/10.1016/j.jaad.2007.08.048>.
- [27] Seaman S. Dressing selection in chronic wound management. *J Am Podiatr Med Assoc* 2002;92:24–33.
- [28] Majno G. *The healing hand: man and wound in the ancient world*. Cambridge, MA: Harvard University Press; 1991.
- [29] Zahedi P, Rezaeian I, Ranaei-Siadat SO, Jafari SH, Supaphol P. A review on wound dressings with an emphasis on electrospun nanofibrous polymeric bandages. *Polym Adv Technol* 2010;21:77–95.
- [30] Ovington LG. The evolution of wound management: ancient origins and advances of the past 20 years. *Home Healthc Nurse* 2002;20:652–6.
- [31] Rovee DT. Evolution of wound dressings and their effects on the healing process. *Clin Mater* 1991;8:183–8.
- [32] Boateng JS, Matthews KH, Stevens HN, Eccleston GM. Wound healing dressings and drug delivery systems: a review. *J Pharm Sci* 2008;97:2892–923. <http://dx.doi.org/10.1002/jps.21210>.
- [33] Cameron J. Exudate and care of the peri-wound skin. *Nurs Stand* 2004;19. <http://dx.doi.org/10.7748/ns2004.10.19.7.62.c3737>. 62, 64, 66 passim.
- [34] Bishop SM, Walker M, Rogers AA, Chen WY. Importance of moisture balance at the wound-dressing interface. *J Wound Care* 2003;12:125–8. <http://dx.doi.org/10.12968/jowc.2003.12.4.26484>.
- [35] Cameron J, Hoffman D, Wilson J, Cherry G. Comparison of two peri-wound skin protectants in venous leg ulcers: a randomised controlled trial. *Journal of Wound Care* 2005;14:233–6.

- [36] Worley CA. So, what do I put on this wound? Making sense of the wound dressing puzzle: Part I. *Dermatol Nurs* 2005;17:143.
- [37] Jones V, Milton T. When and how to use hydrogels. *Nurs Times* 2000;96:3–4.
- [38] Baker PD. Creating the optimal environment. An overview of dressings for chronic wounds. *Adv Nurse Pract* 2005;13:37–8.
- [39] Lay-Flurrie K. The properties of hydrogel dressings and their impact on wound healing. *Prof Nurse* 2004;19:269–73.
- [40] Hampton S. A small study in healing rates and symptom control using a new sheet hydrogel dressing. *J Wound Care* 2004;13:297–300. <http://dx.doi.org/10.12968/jowc.2004.13.7.26639>.
- [41] Hollinworth H. Pain relief. *Nurs Times* 2001;97:63–6.
- [42] Eisenbud D, Hunter H, Kessler L, Zulkowski K. Hydrogel wound dressings: where do we stand in 2003? *Ostomy Wound Manage* 2003;49:52–7.
- [43] Szycher M, Lee SJ. Modern wound dressings: a systematic approach to wound healing. *J Biomater Appl* 1992;7:142–213.
- [44] Fletcher J. Understanding wound dressings: alginates. *Nurs Times* 2005;101:53–4.
- [45] Taylor BA. Selecting wound healing products. Choices for long-term care settings. *Adv Nurse Pract* 2003;11:63–6.
- [46] Pirone LA, Bolton LL, Monte KA, Shannon RJ. Effect of calcium alginate dressings on partial-thickness wounds in swine. *J Investig Surg* 1992;5:149–53.
- [47] Agren MS. Four alginate dressings in the treatment of partial thickness wounds: a comparative experimental study. *Br J Plast Surg* 1996;49:129–34.
- [48] Hess CT. *Wound care*. Philadelphia, PA: Lippincott Williams & Wilkins; 2005.
- [49] Cullen B. The role of oxidized regenerated cellulose/collagen in chronic wound repair. Part 2. *Ostomy Wound Manage* 2002;48:8–13.
- [50] Whitfield RM, Rinard J, King D. Coverage of megaprosthesis with human acellular dermal matrix after Ewing's sarcoma resection: a case report. *Sarcoma* 2011;2011: 978617. <http://dx.doi.org/10.1155/2011/978617>.
- [51] Janzekovic Z. A new concept in the early excision and immediate grafting of burns. *J Trauma* 1970;10:1103–8.
- [52] Orgill DP. Excision and skin grafting of thermal burns. *N Engl J Med* 2009;360:893–901. <http://dx.doi.org/10.1056/NEJMct0804451>.
- [53] Oh S-J, Kim SG, Cho JK, Sung CM. Palmar crease release and secondary full-thickness skin grafts for contractures in primary full-thickness skin grafts during growth spurts in pediatric palmar hand burns. *J Burn Care Res* 2014;35:e312–6.
- [54] Ray S, Rao K. Full thickness skin grafts. *INTECH Open Access*; 2011.
- [55] Hermans MH. Porcine xenografts vs. (cryopreserved) allografts in the management of partial thickness burns: is there a clinical difference? *Burns* 2014;40:408–15. <http://dx.doi.org/10.1016/j.burns.2013.08.020>.
- [56] Hermans MH. Preservation methods of allografts and their (lack of) influence on clinical results in partial thickness burns. *Burns* 2011;37:873–81. <http://dx.doi.org/10.1016/j.burns.2011.01.007>.
- [57] Gurtner GC, Werner S, Barrandon Y, Longaker MT. Wound repair and regeneration. *Nature* 2008;453:314–21. <http://dx.doi.org/10.1038/nature07039>.
- [58] Lin RY, et al. Exogenous transforming growth factor-beta amplifies its own expression and induces scar formation in a model of human fetal skin repair. *Ann Surg* 1995;222:146–54.
- [59] Ghahary A, Shen YJ, Scott PG, Gong Y, Tredget EE. Enhanced expression of mRNA for transforming growth factor-beta, type I and type III procollagen in human post-burn hypertrophic scar tissues. *J Lab Clin Med* 1993;122:465–73.

- [60] Sood R, et al. A comparative study of spray keratinocytes and autologous meshed split-thickness skin graft in the treatment of acute burn injuries. *Wounds* 2015;27:31–40.
- [61] Ong CT, et al. Preclinical evaluation of tegaderm supported nanofibrous wound matrix dressing on porcine wound healing model. *Adv Wound Care* 2015;4:110–8. <http://dx.doi.org/10.1089/wound.2014.0527>.
- [62] Zhong SP, Zhang YZ, Lim CT. Tissue scaffolds for skin wound healing and dermal reconstruction. *Wiley Interdiscip Rev Nanomed Nanobiotechnol* 2010;2:510–25. <http://dx.doi.org/10.1002/wnan.100>.
- [63] Rho KS, et al. Electrospinning of collagen nanofibers: effects on the behavior of normal human keratinocytes and early-stage wound healing. *Biomaterials* 2006;27:1452–61. <http://dx.doi.org/10.1016/j.biomaterials.2005.08.004>.
- [64] Sell SA, et al. The use of natural polymers in tissue engineering: a focus on electrospun extracellular matrix analogues. *Polymers* 2010;2:522.
- [65] Pham QP, Sharma U, Mikos AG. Electrospinning of polymeric nanofibers for tissue engineering applications: a review. *Tissue Eng* 2006;12:1197–211. <http://dx.doi.org/10.1089/ten.2006.12.1197>.
- [66] Bhardwaj N, Kundu SC. Electrospinning: a fascinating fiber fabrication technique. *Biotechnol Adv* 2010;28:325–47. <http://dx.doi.org/10.1016/j.biotechadv.2010.01.004>.
- [67] Lannutti J, Reneker D, Ma T, Tomasko D, Farson D. Electrospinning for tissue engineering scaffolds. *Mater Sci Eng C* 2007;27:504–9. <http://dx.doi.org/10.1016/j.msec.2006.05.019>.
- [68] Ingavle GC, Leach JK. Advancements in electrospinning of polymeric nanofibrous scaffolds for tissue engineering. *Tissue Eng Part B Rev* 2014;20:277–93. <http://dx.doi.org/10.1089/ten.TEB.2013.0276>.
- [69] Dhandayuthapani B, Yoshida Y, Maekawa T, Sakthi Kumar D. Polymeric scaffolds in tissue engineering application: a review. *Int J Polym Sci* 2011;2011:19p. <http://dx.doi.org/10.1155/2011/290602>.
- [70] O'Brien FJ. Biomaterials & scaffolds for tissue engineering. *Mater Today* 2011;14:88–95. [http://dx.doi.org/10.1016/S1369-7021\(11\)70058-X](http://dx.doi.org/10.1016/S1369-7021(11)70058-X).
- [71] Li Z, Wang C. One-dimensional nanostructures: electrospinning technique and unique nanofibers. Berlin Heidelberg: Springer; 2013, p. 15–28.
- [72] Pilehvar-Soltanahmadi Y, Akbarzadeh A, Moazzez-Lalaklo N, Zarghami N. An update on clinical applications of electrospun nanofibers for skin bioengineering. *Artif Cells Nanomed Biotechnol* 2015;1–15. <http://dx.doi.org/10.3109/21691401.2015.1036999>.
- [73] Vasita R, Katti DS. Nanofibers and their applications in tissue engineering. *Int J Nanomedicine* 2006;1:15–30.
- [74] Huang L, Nagapudi K, Apkarian RP, Chaikof EL. Engineered collagen-PEO nanofibers and fabrics. *J Biomater Sci Polym Ed* 2001;12:979–93.
- [75] Powell HM, Supp DM, Boyce ST. Influence of electrospun collagen on wound contraction of engineered skin substitutes. *Biomaterials* 2008;29:834–43. <http://dx.doi.org/10.1016/j.biomaterials.2007.10.036>.
- [76] Zhong, et al. Formation of collagen–glycosaminoglycan blended nanofibrous scaffolds and their biological properties. *Biomacromolecules* 2005;6:2998–3004. <http://dx.doi.org/10.1021/bm050318p>.
- [77] Suganya S, Venugopal J, Ramakrishna S, Lakshmi BS, Dev VR. Naturally derived biofunctional nanofibrous scaffold for skin tissue regeneration. *Int J Biol Macromol* 2014;68:135–43. <http://dx.doi.org/10.1016/j.ijbiomac.2014.04.031>.
- [78] Rockwood DN, et al. Materials fabrication from *Bombyx mori* silk fibroin. *Nat Protoc* 2011;6:1612–31. <http://dx.doi.org/10.1038/nprot.2011.379>.

- [79] Vepari C, Kaplan DL. Silk as a biomaterial. *Prog Polym Sci* 2007;32:991–1007. <http://dx.doi.org/10.1016/j.progpolymsci.2007.05.013>.
- [80] Min B-M, et al. Electrospinning of silk fibroin nanofibers and its effect on the adhesion and spreading of normal human keratinocytes and fibroblasts in vitro. *Biomaterials* 2004;25:1289–97. <http://dx.doi.org/10.1016/j.biomaterials.2003.08.045>.
- [81] Li L, et al. Electrospun poly (ϵ -caprolactone)/silk fibroin core-sheath nanofibers and their potential applications in tissue engineering and drug release. *Int J Biol Macromol* 2011;49:223–32. <http://dx.doi.org/10.1016/j.ijbiomac.2011.04.018>.
- [82] Sukigara S, Gandhi M, Ayutsede J, Micklus M, Ko F. Regeneration of *Bombyx mori* silk by electrospinning—part 1: processing parameters and geometric properties. *Polymer* 2003;44:5721–7. [http://dx.doi.org/10.1016/S0032-3861\(03\)00532-9](http://dx.doi.org/10.1016/S0032-3861(03)00532-9).
- [83] Sheikh FA, et al. 3D electrospun silk fibroin nanofibers for fabrication of artificial skin. *Nanomedicine* 2015;11:681–91. <http://dx.doi.org/10.1016/j.nano.2014.11.007>.
- [84] Lee OJ, et al. Development of artificial dermis using 3D electrospun silk fibroin nanofiber matrix. *J Biomed Nanotechnol* 2014;10:1294–303.
- [85] Elzoghby AO. Gelatin-based nanoparticles as drug and gene delivery systems: reviewing three decades of research. *J Control Release* 2013;172:1075–91. <http://dx.doi.org/10.1016/j.jconrel.2013.09.019>.
- [86] Barnes CP, Sell SA, Boland ED, Simpson DG, Bowlin GL. Nanofiber technology: designing the next generation of tissue engineering scaffolds. *Adv Drug Deliv Rev* 2007;59:1413–33. <http://dx.doi.org/10.1016/j.addr.2007.04.022>.
- [87] Dhandayuthapani B, Krishnan UM, Sethuraman S. Fabrication and characterization of chitosan-gelatin blend nanofibers for skin tissue engineering. *J Biomed Mater Res B Appl Biomater* 2010;94:264–72. <http://dx.doi.org/10.1002/jbm.b.31651>.
- [88] Huang Z-M, Zhang YZ, Ramakrishna S, Lim CT. Electrospinning and mechanical characterization of gelatin nanofibers. *Polymer* 2004;45:5361–8. <http://dx.doi.org/10.1016/j.polymer.2004.04.005>.
- [89] Powell HM, Boyce ST. Fiber density of electrospun gelatin scaffolds regulates morphogenesis of dermal-epidermal skin substitutes. *J Biomed Mater Res A* 2008;84:1078–86. <http://dx.doi.org/10.1002/jbm.a.31498>.
- [90] Noh HK, et al. Electrospinning of chitin nanofibers: degradation behavior and cellular response to normal human keratinocytes and fibroblasts. *Biomaterials* 2006;27:3934–44. <http://dx.doi.org/10.1016/j.biomaterials.2006.03.016>.
- [91] Mogosanu GD, Grumezescu AM. Natural and synthetic polymers for wounds and burns dressing. *Int J Pharm* 2014;463:127–36. <http://dx.doi.org/10.1016/j.ijpharm.2013.12.015>.
- [92] Kossovich LY, Salkovskiy Y, Kirillova IV. 6th World Congress of Biomechanics (WCB 2010). In: Lim CT, Goh JCH, editors. August 1–6, 2010 Singapore: In conjunction with 14th International Conference on Biomedical Engineering (ICBME) and 5th Asia Pacific Conference on Biomechanics (APBiomech) Heidelberg, Berlin: Springer; 2010. p. 1212–4.
- [93] Zhao Y, et al. Preparation of nanofibers with renewable polymers and their application in wound dressing. *Int J Polym Sci* 2016;2016:17. <http://dx.doi.org/10.1155/2016/4672839>.
- [94] Liao S, Chan CK, Ramakrishna S. Stem cells and biomimetic materials strategies for tissue engineering. *Mater Sci Eng C* 2008;28:1189–202. <http://dx.doi.org/10.1016/j.msec.2008.08.015>.
- [95] Hoffman Allan S, Frederick BR, Schoen J, Lemons Jack E. *Biomaterials science: an introduction to materials in medicine*. 3rd ed. New York: Elsevier; 2013.

- [96] Gomes SR, et al. In vitro and in vivo evaluation of electrospun nanofibers of PCL, chitosan and gelatin: a comparative study. *Mater Sci Eng, C* 2015;46:348–58. <http://dx.doi.org/10.1016/j.msec.2014.10.051>.
- [97] Lowery JL, Datta N, Rutledge GC. Effect of fiber diameter, pore size and seeding method on growth of human dermal fibroblasts in electrospun poly (epsilon-caprolactone) fibrous mats. *Biomaterials* 2010;31:491–504. <http://dx.doi.org/10.1016/j.biomaterials.2009.09.072>.
- [98] Gumusderelioglu M, Dalkiranoglu S, Aydin RS, Cakmak S. A novel dermal substitute based on biofunctionalized electrospun PCL nanofibrous matrix. *J Biomed Mater Res A* 2011;98:461–72. <http://dx.doi.org/10.1002/jbm.a.33143>.
- [99] Boland ED, Telemeco TA, Simpson DG, Wnek GE, Bowlin GL. Utilizing acid pretreatment and electrospinning to improve biocompatibility of poly(glycolic acid) for tissue engineering. *J Biomed Mater Res B Appl Biomater* 2004;71B:144–52. <http://dx.doi.org/10.1002/jbm.b.30105>.
- [100] Pillai CK, Sharma CP. Review paper: absorbable polymeric surgical sutures: chemistry, production, properties, biodegradability, and performance. *J Biomater Appl* 2010;25:291–366. <http://dx.doi.org/10.1177/0885328210384890>.
- [101] Boland ED, Wnek GE, Simpson DG, Pawlowski KJ, Bowlin GL. Tailoring tissue engineering scaffolds using electrostatic processing techniques: a study of poly(glycolic acid) electrospinning. *J Macromol Sci A* 2001;38:1231–43. <http://dx.doi.org/10.1081/MA-100108380>.
- [102] Aghdam RM, et al. Investigating the effect of PGA on physical and mechanical properties of electrospun PCL/PGA blend nanofibers. *J Appl Polym Sci* 2012;124:123–31. <http://dx.doi.org/10.1002/app.35071>.
- [103] Yixiang Dong TY, Susan L, Chan CK, Stevens MM, Ramakrishna S. Distinctive degradation behaviors of electrospun polyglycolide, poly(DL-lactide-co-glycolide), and poly(L-lactide-co-epsilon-caprolactone) nanofibers cultured with/without porcine smooth muscle cells. *Tissue Eng Part A* 2010;16:283–98.
- [104] Araque-Monrós MC, et al. Study of the degradation of a new PLA braided biomaterial in buffer phosphate saline, basic and acid media, intended for the regeneration of tendons and ligaments. *Polym Degrad Stab* 2013;98:1563–70. <http://dx.doi.org/10.1016/j.polymdegradstab.2013.06.031>.
- [105] Göpferich A. Mechanisms of polymer degradation and erosion. *Biomaterials* 1996;17:103–14. [http://dx.doi.org/10.1016/0142-9612\(96\)85755-3](http://dx.doi.org/10.1016/0142-9612(96)85755-3).
- [106] Casasola R, Thomas NL, Trybala A, Georgiadou S. Electrospun poly lactic acid (PLA) fibres: effect of different solvent systems on fibre morphology and diameter. *Polymer* 2014;55:4728–37. <http://dx.doi.org/10.1016/j.polymer.2014.06.032>.
- [107] Kurtycz P, et al. Electrospun poly(L-lactic)acid/nanoalumina (PLA/Al2O3) composite fiber mats with potential biomedical application — investigation of cytotoxicity. *Fibers Polym* 2013;14:578–83. <http://dx.doi.org/10.1007/s12221-013-0578-5>.
- [108] Kurtycz P, Karwowska E, Ciach T, Olszyna A, Kunicki A. Biodegradable polylactide (PLA) fiber mats containing Al2O3-Ag nanopowder prepared by electrospinning technique — antibacterial properties. *Fibers Polym* 2013;14:1248–53. <http://dx.doi.org/10.1007/s12221-013-1248-3>.
- [109] Hoveizi E, Nabiuni M, Parivar K, Rajabi-Zeleti S, Tavakol S. Functionalisation and surface modification of electrospun polylactic acid scaffold for tissue engineering. *Cell Biol Int* 2014;38:41–9. <http://dx.doi.org/10.1002/cbin.10178>.
- [110] Huan S, et al. Effect of experimental parameters on morphological, mechanical and hydrophobic properties of electrospun polystyrene fibers. *Materials* 2015;8:2718.

- [111] Kim G-T, et al. The morphology of electrospun polystyrene fibers. *Korean J Chem Eng* 2005;22:147–53. <http://dx.doi.org/10.1007/bf02701477>.
- [112] Casper CL, Stephens JS, Tassi NG, Chase DB, Rabolt JF. Controlling surface morphology of electrospun polystyrene fibers: effect of humidity and molecular weight in the electrospinning process. *Macromolecules* 2004;37:573–8. <http://dx.doi.org/10.1021/ma0351975>.
- [113] Sun T, et al. Self-organization of skin cells in three-dimensional electrospun polystyrene scaffolds. *Tissue Eng* 2005;11:1023–33. <http://dx.doi.org/10.1089/ten.2005.11.1023>.
- [114] Loh QL, Choong C. Three-dimensional scaffolds for tissue engineering applications: role of porosity and pore size. *Tissue Eng Part B Rev* 2013;19:485–502. <http://dx.doi.org/10.1089/ten.teb.2012.0437>.
- [115] Cespi M, Bonacucina G, Casettari L, Mencarelli G, Palmieri GF. Poloxamer thermogel systems as medium for crystallization. *Pharm Res* 2012;29:818–26. <http://dx.doi.org/10.1007/s11095-011-0606-3>.
- [116] Pan J-F, Liu N-H, Sun H, Xu F. Preparation and characterization of electrospun plcl/poloxamer nanofibers and dextran/gelatin hydrogels for skin tissue engineering. *PLoS One* 2014;9:e112885. <http://dx.doi.org/10.1371/journal.pone.0112885>.
- [117] Chaudhuri B, Mondal B, Ray SK, Sarkar SC. A novel biocompatible conducting poly(vinyl alcohol (PVA)-polyvinylpyrrolidone (PVP)-hydroxyapatite (HAP) composite scaffolds for probable biological application. *Colloids Surf B Biointerfaces* 2016;143:71–80. <http://dx.doi.org/10.1016/j.colsurfb.2016.03.027>.
- [118] Chuangchote S, Sagawa T, Yoshikawa S. Electrospinning of poly(vinyl pyrrolidone): Effects of solvents on electrospinnability for the fabrication of poly(p-phenylene vinylene) and TiO₂ nanofibers. *J Appl Polym Sci* 2009;114:2777–91. <http://dx.doi.org/10.1002/app.30637>.
- [119] Yang Q, et al. Influence of solvents on the formation of ultrathin uniform poly(vinyl pyrrolidone) nanofibers with electrospinning. *J Polym Sci B* 2004;42:3721–6. <http://dx.doi.org/10.1002/polb.20222>.
- [120] Li S, Sun B, Li X, Yuan X. Characterization of electrospun core/shell poly(vinyl pyrrolidone)/poly(L-lactide-co-epsilon-caprolactone) fibrous membranes and their cytocompatibility in vitro. *J Biomater Sci Polym Ed* 2008;19:245–58. <http://dx.doi.org/10.1163/156856208783432499>.
- [121] Heunis TDJ, Dicks LMT. Nanofibers offer alternative ways to the treatment of skin infections. *J Biomed Biotechnol* 2010;2010:10p. <http://dx.doi.org/10.1155/2010/510682>.
- [122] Hassan MI, Sultana N, Hamdan S. Bioactivity assessment of poly(epsilon-caprolactone)/hydroxyapatite electrospun fibers for bone tissue engineering application. *J Nanomater* 2014;2014:6. <http://dx.doi.org/10.1155/2014/573238>.
- [123] Yoshimoto H, Shin YM, Terai H, Vacanti JP. A biodegradable nanofiber scaffold by electrospinning and its potential for bone tissue engineering. *Biomaterials* 2003;24:2077–82. [http://dx.doi.org/10.1016/S0142-9612\(02\)00635-X](http://dx.doi.org/10.1016/S0142-9612(02)00635-X).
- [124] Asran AS, Seydewitz V, Michler GH. Micromechanical properties and ductile behavior of electrospun polystyrene nanofibers. *J Appl Polym Sci* 2012;125:1663–73. <http://dx.doi.org/10.1002/app.34847>.
- [125] Norouzi M, Boroujeni SM, Omidvarkordshouli N, Soleimani M. Advances in skin regeneration: application of electrospun scaffolds. *Adv Healthc Mater* 2015;4:1114–33. <http://dx.doi.org/10.1002/adhm.201500001>.
- [126] Chen J-P, Chang G-Y, Chen J-K. Electrospun collagen/chitosan nanofibrous membrane as wound dressing. *Colloids Surf A Physicochem Eng Asp* 2008;313–314:183–8. <http://dx.doi.org/10.1016/j.colsurfa.2007.04.129>.

- [127] Yeo I-S, et al. Collagen-based biomimetic nanofibrous scaffolds: preparation and characterization of collagen/silk fibroin bicomponent nanofibrous structures. *Biomacromolecules* 2008;9:1106–16. <http://dx.doi.org/10.1021/bm700875a>.
- [128] Sarkar SD, Farrugia BL, Dargaville TR, Dhara S. Chitosan–collagen scaffolds with nano/microfibrous architecture for skin tissue engineering. *J Biomed Mater Res A* 2013;101:3482–92. <http://dx.doi.org/10.1002/jbm.a.34660>.
- [129] Cai Z-X, et al. Fabrication of chitosan/silk fibroin composite nanofibers for wound-dressing applications. *Int J Mol Sci* 2010;11:3529.
- [130] Tchemtchoua VT, et al. Development of a chitosan nanofibrillar scaffold for skin repair and regeneration. *Biomacromolecules* 2011;12:3194–204. <http://dx.doi.org/10.1021/bm200680q>.
- [131] Charernsriwilaiwat N, Rojanarata T, Ngawhirunpat T, Opanasopit P. Electrospun chitosan/polyvinyl alcohol nanofibre mats for wound healing. *Int Wound J* 2014;11:215–22. <http://dx.doi.org/10.1111/j.1742-481X.2012.01077.x>.
- [132] Shalumon KT, et al. Fabrication of chitosan/poly(caprolactone) nanofibrous scaffold for bone and skin tissue engineering. *Int J Biol Macromol* 2011;48:571–6. <http://dx.doi.org/10.1016/j.ijbiomac.2011.01.020>.
- [133] Blackstone BN, Drexler JW, Powell HM. Tunable engineered skin mechanics via coaxial electrospun fiber core diameter. *Tissue Eng Part A* 2014;20:2746–55. <http://dx.doi.org/10.1089/ten.TEA.2013.0687>.
- [134] Gautam S, Chou CF, Dinda AK, Potdar PD, Mishra NC. Surface modification of nanofibrous polycaprolactone/gelatin composite scaffold by collagen type I grafting for skin tissue engineering. *Mater Sci Eng, C* 2014;34:402–9. <http://dx.doi.org/10.1016/j.msec.2013.09.043>.
- [135] Li Y, Chen F, Nie J, Yang D. Electrospun poly(lactic acid)/chitosan core–shell structure nanofibers from homogeneous solution. *Carbohydr Polym* 2012;90:1445–51. <http://dx.doi.org/10.1016/j.carbpol.2012.07.013>.
- [136] Kim SJ, Jang DH, Park WH, Min B-M. Fabrication and characterization of 3-dimensional PLGA nanofiber/microfiber composite scaffolds. *Polymer* 2010;51:1320–7. <http://dx.doi.org/10.1016/j.polymer.2010.01.025>.
- [137] Kumbhar SG, Nukavarapu SP, James R, Nair LS, Laurencin CT. Electrospun poly(lactic acid-co-glycolic acid) scaffolds for skin tissue engineering. *Biomaterials* 2008;29:4100–7. <http://dx.doi.org/10.1016/j.biomaterials.2008.06.028>.
- [138] Liu S-J, et al. Electrospun PLGA/collagen nanofibrous membrane as early-stage wound dressing. *J Membr Sci* 2010;355:53–9. <http://dx.doi.org/10.1016/j.memsci.2010.03.012>.
- [139] Shahverdi S, et al. Fabrication and structure analysis of poly(lactide-co-glycolic acid)/silk fibroin hybrid scaffold for wound dressing applications. *Int J Pharm* 2014;473:345–55. <http://dx.doi.org/10.1016/j.ijpharm.2014.07.021>.
- [140] Norouzi M, et al. Protein encapsulated in electrospun nanofibrous scaffolds for tissue engineering applications. *Polym Int* 2013;62:1250–6. <http://dx.doi.org/10.1002/pi.4416>.
- [141] Rieger KA, Birch NP, Schiffman JD. Designing electrospun nanofiber mats to promote wound healing - a review. *J Mater Chem B* 2013;1:4531–41. <http://dx.doi.org/10.1039/C3TB20795A>.
- [142] Sundaramurthi D, Krishnan UM, Sethuraman S. Electrospun nanofibers as scaffolds for skin tissue engineering. *Polym Rev* 2014;54:348–76. <http://dx.doi.org/10.1080/15583724.2014.881374>.
- [143] Cho M, Hunt TK, Hussain MZ. Hydrogen peroxide stimulates macrophage vascular endothelial growth factor release. *Am J Physiol Heart Circ Physiol* 2001;280:H2357–63.

- [144] Vandamme L, Heyneman A, Hoeksema H, Verbelen J, Monstrey S. Honey in modern wound care: a systematic review. *Burns* 2013;39:1514–25. <http://dx.doi.org/10.1016/j.burns.2013.06.014>.
- [145] Molan PC. Re-introducing honey in the management of wounds and ulcers - theory and practice. *Ostomy Wound Manage* 2002;48:28–40.
- [146] Molan P. Why honey works honey in modern wound management. *Wounds* 2009;9:36–7.
- [147] Chirife J, Scarmato G, Herszage L. Scientific basis for use of granulated sugar in treatment of infected wounds. *Lancet* 1982;1:560–1.
- [148] Gethin GT, Cowman S, Conroy RM. The impact of Manuka honey dressings on the surface pH of chronic wounds. *Int Wound J* 2008;5:185–94.
- [149] Ranzato E, Martinotti S, Burlando B. Epithelial mesenchymal transition traits in honey-driven keratinocyte wound healing: comparison among different honeys. *Wound Repair Regen* 2012;20:778–85. <http://dx.doi.org/10.1111/j.1524-475X.2012.00825.x>.
- [150] Sell SA, et al. A preliminary study on the potential of manuka honey and platelet-rich plasma in wound healing. *Int J Biomater* 2012;313781:2012. <http://dx.doi.org/10.1155/2012/313781>.
- [151] Minden-Birkenmaier BA, Neuhalfen RM, Janowiak BE, Sell SA. Preliminary investigation and characterization of electrospun polycaprolactone and Manuka honey scaffolds for dermal repair. *J Eng Fiber Fabr* 2015;10:126.
- [152] Arslan A, Simsek M, Aldemir SD, Kazaroglu NM, Gumusderelioglu M. Honey-based PET or PET/chitosan fibrous wound dressings: effect of honey on electrospinning process. *J Biomater Sci Polym Ed* 2014;25:999–1012. <http://dx.doi.org/10.1080/09205063.2014.918455>.
- [153] Zhang S, Tang Y, Vlahovic B. A review on preparation and applications of silver-containing nanofibers. *Nanoscale Res Lett* 2016;11:80. <http://dx.doi.org/10.1186/s11671-016-1286-z>.
- [154] Augustine R, Dominic EA, Reju I, Kaimal B, Kalarikkal N, Thomas S. Electrospun polycaprolactone membranes incorporated with ZnO nanoparticles as skin substitutes with enhanced fibroblast proliferation and wound healing. *RSC Adv* 2014;4:24777–85.
- [155] Bhowmick S, Scharnweber D, Koul V. Co-cultivation of keratinocyte-human mesenchymal stem cell (hMSC) on sericin loaded electrospun nanofibrous composite scaffold (cationic gelatin/hyaluronan/chondroitin sulfate) stimulates epithelial differentiation in hMSCs: In vitro study. *Biomaterials* 2016;88:83–96. <http://dx.doi.org/10.1016/j.biomaterials.2016.02.034>.
- [156] Moore KW, de Waal Malefyt R, Coffman RL, O'Garra A. Interleukin-10 and the interleukin-10 receptor. *Annu Rev Immunol* 2001;19:683–765. <http://dx.doi.org/10.1146/annurev.immunol.19.1.683>.
- [157] Wynn TA. IL-13 effector functions. *Annu Rev Immunol* 2003;21:425–56. <http://dx.doi.org/10.1146/annurev.immunol.21.120601.141142>.
- [158] Sell SA, Wolfe PS, Ericksen JJ, Simpson DG, Bowlin GL. Incorporating platelet-rich plasma into electrospun scaffolds for tissue engineering applications. *Tissue Eng Part A* 2011;17:2723–37.
- [159] Kushida S, et al. Platelet and growth factor concentrations in activated platelet-rich plasma: a comparison of seven commercial separation systems. *J Artif Organs* 2014;17:186–92. <http://dx.doi.org/10.1007/s10047-014-0761-5>.
- [160] Cohen S. The epidermal growth factor (EGF). *Cancer* 1983;51:1787–91.
- [161] Greenhalgh DG, Sprugel KH, Murray MJ, Ross R. PDGF and FGF stimulate wound healing in the genetically diabetic mouse. *Am J Pathol* 1990;136:1235–46.

- [162] Sadagurski M, et al. Insulin-like growth factor 1 receptor signaling regulates skin development and inhibits skin keratinocyte differentiation. *Mol Cell Biol* 2006;26:2675–87. <http://dx.doi.org/10.1128/mcb.26.7.2675-2687.2006>.
- [163] Contassot E, Beer HD, French LE. Interleukin-1, inflammasomes, autoinflammation and the skin. *Swiss Med Wkly* 2012;142:w13590. <http://dx.doi.org/10.4414/smw.2012.13590>.
- [164] Faurschou A. Role of tumor necrosis factor-alpha in the regulation of keratinocyte cell cycle and DNA repair after ultraviolet-B radiation. *Dan Med Bull* 2010;57:B4179.
- [165] McCabe A, MacNamara KC. Macrophages: key regulators of steady-state and demand-adapted hematopoiesis. *Exp Hematol* 2016;44:213–22. <http://dx.doi.org/10.1016/j.exphem.2016.01.003>.
- [166] Metcalf D. Hematopoietic cytokines. *Blood* 2008;111:485–91. <http://dx.doi.org/10.1182/blood-2007-03-079681>.
- [167] Yuan T, Zhang C, Zeng B. Treatment of chronic femoral osteomyelitis with platelet-rich plasma (PRP): A case report. *Transfus Apher Sci* 2008;38:167–73. <http://dx.doi.org/10.1016/j.transci.2008.01.006>.
- [168] Schneider A, Wang XY, Kaplan DL, Garlick JA, Egles C. Biofunctionalized electrospun silk mats as a topical bioactive dressing for accelerated wound healing. *Acta Biomater* 2009;5:2570–8. <http://dx.doi.org/10.1016/j.actbio.2008.12.013>.
- [169] Rahaman MN, et al. Bioactive glass in tissue engineering. *Acta Biomater* 2011;7:2355–73. <http://dx.doi.org/10.1016/j.actbio.2011.03.016>.
- [170] Day RM, et al. Assessment of polyglycolic acid mesh and bioactive glass for soft-tissue engineering scaffolds. *Biomaterials* 2004;25:5857–66. <http://dx.doi.org/10.1016/j.biomaterials.2004.01.043>.
- [171] Lin C, Mao C, Zhang J, Li Y, Chen X. Healing effect of bioactive glass ointment on full-thickness skin wounds. *Biomed Mater* 2012;7:045017. <http://dx.doi.org/10.1088/1748-6041/7/4/045017>.
- [172] Stoor P, Soderling E, Salonen JI. Antibacterial effects of a bioactive glass paste on oral microorganisms. *Acta Odontol Scand* 1998;56:161–5.
- [173] Lu H, Zhang T, Wang XP, Fang QF. Electrospun submicron bioactive glass fibers for bone tissue scaffold. *J Mater Sci Mater Med* 2009;20:793–8. <http://dx.doi.org/10.1007/s10856-008-3649-1>.
- [174] Watters RJ, Brown RF, Day DE. Angiogenic effect of bioactive borate glass microfibers and beads in the hairless mouse. *Biomed Glasses* 2015;1.
- [175] Zhou J, et al. In vivo and in vitro studies of borate based glass micro-fibers for dermal repairing. *Mater Sci Eng, C* 2016;60:437–45. <http://dx.doi.org/10.1016/j.msec.2015.11.068>.
- [176] Thakur RA, Florek CA, Kohn J, Michniak BB. Electrospun nanofibrous polymeric scaffold with targeted drug release profiles for potential application as wound dressing. *Int J Pharm* 2008;364:87–93. <http://dx.doi.org/10.1016/j.ijpharm.2008.07.033>.
- [177] Shi Y, Xu S, Dong A, Zhang J. Design and in vitro evaluation of transdermal patches based on ibuprofen-loaded electrospun fiber mats. *J Mater Sci Mater Med* 2013;24:333–41. <http://dx.doi.org/10.1007/s10856-012-4805-1>.
- [178] Kim K, et al. Incorporation and controlled release of a hydrophilic antibiotic using poly(lactide-co-glycolide)-based electrospun nanofibrous scaffolds. *J Control Release* 2004;98:47–56. <http://dx.doi.org/10.1016/j.jconrel.2004.04.009>.
- [179] Kenawy el R, et al. Release of tetracycline hydrochloride from electrospun poly(ethylene-co-vinylacetate), poly(lactic acid), and a blend. *J Control Release* 2002;81:57–64.

- [180] Shahrokhi S, Anna A, Jeschke MG. The use of dermal substitutes in burn surgery: acute phase. *Wound Repair Regen* 2014;22. <http://dx.doi.org/10.1111/wrr.12119>, doi:10.1111/wrr.12119.
- [181] Bowlin GL. Enhanced porosity without compromising structural integrity: the nemesis of electrospun scaffolding. *J Tissue Sci Eng* 2011;2.
- [182] McClure MJ, Wolfe PS, Simpson DG, Sell SA, Bowlin GL. The use of air-flow impedance to control fiber deposition patterns during electrospinning. *Biomaterials* 2012;33:771–9. <http://dx.doi.org/10.1016/j.biomaterials.2011.10.011>.
- [183] Yin A, et al. Fabrication of cell penetration enhanced poly (L-lactic acid-co-varepsilon-caprolactone)/silk vascular scaffolds utilizing air-impedance electrospinning. *Colloids Surf B Biointerfaces* 2014;120:47–54. <http://dx.doi.org/10.1016/j.colsurfb.2014.04.011>.
- [184] Simonet M, Schneider OD, Neuenschwander P, Stark WJ. Ultraporous 3D polymer meshes by low-temperature electrospinning: use of ice crystals as a removable void template. *Polym Eng Sci* 2007;47:2020–6.
- [185] Leong MF, Rasheed MZ, Lim TC, Chian KS. In vitro cell infiltration and in vivo cell infiltration and vascularization in a fibrous, highly porous poly (D, L-lactide) scaffold fabricated by cryogenic electrospinning technique. *J Biomed Mater Res A* 2009;91:231–40.
- [186] Leong MF, Chan WY, Chian KS, Rasheed MZ, Anderson JM. Fabrication and in vitro and in vivo cell infiltration study of a bilayered cryogenic electrospun poly(D, L-lactide) scaffold. *J Biomed Mater Res A* 2010;94:1141–9. <http://dx.doi.org/10.1002/jbm.a.32795>.
- [187] McCann JT, Marquez M, Xia Y. Highly porous fibers by electrospinning into a cryogenic liquid. *J Am Chem Soc* 2006;128:1436–7.
- [188] Suh SW, et al. Effect of different particles on cell proliferation in polymer scaffolds using a solvent-casting and particulate leaching technique. *ASAIO J* 2002;48:460–4.
- [189] Nam J, Huang Y, Agarwal S, Lannutti J. Improved cellular infiltration in electrospun fiber via engineered porosity. *Tissue Eng* 2007;13:2249–57. <http://dx.doi.org/10.1089/ten.2006.0306>.
- [190] Kim TG, Chung HJ, Park TG. Macroporous and nanofibrous hyaluronic acid/collagen hybrid scaffold fabricated by concurrent electrospinning and deposition/leaching of salt particles. *Acta Biomater* 2008;4:1611–9. <http://dx.doi.org/10.1016/j.actbio.2008.06.008>.
- [191] Lee YH, et al. Electrospun dual-porosity structure and biodegradation morphology of Montmorillonite reinforced PLLA nanocomposite scaffolds. *Biomaterials* 2005;26:3165–72. <http://dx.doi.org/10.1016/j.biomaterials.2004.08.018>.
- [192] Kidoaki S, Kwon IK, Matsuda T. Mesoscopic spatial designs of nano- and microfiber meshes for tissue-engineering matrix and scaffold based on newly devised multilayering and mixing electrospinning techniques. *Biomaterials* 2005;26:37–46. <http://dx.doi.org/10.1016/j.biomaterials.2004.01.063>.
- [193] Baker BM, et al. Sacrificial nanofibrous composites provide instruction without impediment and enable functional tissue formation. *Proc Natl Acad Sci U S A* 2012;109:14176–81. <http://dx.doi.org/10.1073/pnas.1206962109>.
- [194] Phipps MC, Clem WC, Grunda JM, Clines GA, Bellis SL. Increasing the pore sizes of bone-mimetic electrospun scaffolds comprised of polycaprolactone, collagen I and hydroxyapatite to enhance cell infiltration. *Biomaterials* 2012;33:524–34. <http://dx.doi.org/10.1016/j.biomaterials.2011.09.080>.
- [195] Ionescu LC, Lee GC, Sennett BJ, Burdick JA, Mauck RL. An anisotropic nanofiber/microsphere composite with controlled release of biomolecules for fibrous tissue engineering. *Biomaterials* 2010;31:4113–20. <http://dx.doi.org/10.1016/j.biomaterials.2010.01.098>.

- [196] Ochanda FO, Samaha MA, Tafreshi HV, Tepper GC, Gad-el-Hak M. Fabrication of superhydrophobic fiber coatings by DC-biased AC-electrospinning. *J Appl Polym Sci* 2012;123:1112–9. <http://dx.doi.org/10.1002/app.34583>.
- [197] Sarkar S, Deevi S, Tepper G. Biased AC electrospinning of aligned polymer nanofibers. *Macromol Rapid Commun* 2007;28:1034–9.
- [198] Deitzel J, Kleinmeyer J, Hirvonen J, Tan NB. Controlled deposition of electrospun poly (ethylene oxide) fibers. *Polymer* 2001;42:8163–70.
- [199] Zhang D, Chang J. Electrospinning of three-dimensional nanofibrous tubes with controllable architectures. *Nano Lett* 2008;8:3283–7.
- [200] Zhang K, Wang X, Jing D, Yang Y, Zhu M. Bionic electrospun ultrafine fibrous poly (L-lactic acid) scaffolds with a multi-scale structure. *Biomed Mater* 2009;4:035004. <http://dx.doi.org/10.1088/1748-6041/4/3/035004>.
- [201] Vaquette C, Cooper-White JJ. Increasing electrospun scaffold pore size with tailored collectors for improved cell penetration. *Acta Biomater* 2011;7:2544–57. <http://dx.doi.org/10.1016/j.actbio.2011.02.036>.
- [202] Liu W, Thomopoulos S, Xia Y. Electrospun nanofibers for regenerative medicine. *Adv Healthc Mater* 2012;1:10–25. <http://dx.doi.org/10.1002/adhm.201100021>.
- [203] Joshi VS, Lei NY, Walthers CM, Wu B, Dunn JC. Macroporosity enhances vascularization of electrospun scaffolds. *J Surg Res* 2013;183:18–26. <http://dx.doi.org/10.1016/j.jss.2013.01.005>.
- [204] Lee BL, et al. Femtosecond laser ablation enhances cell infiltration into three-dimensional electrospun scaffolds. *Acta Biomater* 2012;8:2648–58. <http://dx.doi.org/10.1016/j.actbio.2012.04.023>.
- [205] Huang H, Guo Z. Human dermis separation via ultra-short pulsed laser plasma-mediated ablation. *J Phys D Appl Phys* 2009;42:165204.
- [206] Zhong S, Zhang Y, Lim CT. Fabrication of large pores in electrospun nanofibrous scaffolds for cellular infiltration: a review. *Tissue Eng Part B Rev* 2012;18:77–87. <http://dx.doi.org/10.1089/ten.TEB.2011.0390>.
- [207] Woon Choi H, Johnson JK, Nam J, Farson DF, Lannutti J. Structuring electrospun polycaprolactone nanofiber tissue scaffolds by femtosecond laser ablation. *J Laser Appl* 2007;19:225–31.
- [208] Sundararaghavan HG, Metter RB, Burdick JA. Electrospun fibrous scaffolds with multi-scale and photopatterned porosity. *Macromol Biosci* 2010;10:265–70. <http://dx.doi.org/10.1002/mabi.200900363>.
- [209] Yixiang D, Yong T, Liao S, Chan CK, Ramakrishna S. Degradation of electrospun nanofiber scaffold by short wave length ultraviolet radiation treatment and its potential applications in tissue engineering. *Tissue Eng Part A* 2008;14:1321–9.
- [210] Wu J, et al. Electrospun nanoyarn scaffold and its application in tissue engineering. *Mater Lett* 2012;89:146–9.
- [211] Wu J, et al. Cell infiltration and vascularization in porous nanoyarn scaffolds prepared by dynamic liquid electrospinning. *J Biomed Nanotechnol* 2014;10:603–14.
- [212] Xu Y, et al. Fabrication of electrospun poly (L-lactide-co-ε-caprolactone)/collagen nanoyarn network as a novel, three-dimensional, macroporous, aligned scaffold for tendon tissue engineering. *Tissue Eng Part C Methods* 2013;19:925–36.
- [213] Blakeney BA, et al. Cell infiltration and growth in a low density, uncompressed three-dimensional electrospun nanofibrous scaffold. *Biomaterials* 2011;32:1583–90. <http://dx.doi.org/10.1016/j.biomaterials.2010.10.056>.

This page intentionally left blank

Electrospun materials for bone and tendon/ligament tissue engineering

10

N. Bölgün

Mersin University, Mersin, Turkey

10.1 Introduction

Tissue engineering approach has been developed in an effort to address current medical treatment limitations and proved to be very promising in the repair and reconstruction of varied tissues [1]. While extensive research was applied into repair of varied tissues, bone regeneration was one of the most heavily investigated areas in tissue engineering [2]. Along with significant advances in the development of bone tissue engineering, tendon/ligament regeneration has also gained focused interest in the last decade [3]. A variety of scaffolds that provide a suitable cell-supporting substrate for cells to proliferate and differentiate during the formation of new tissue have been illustrated with promising results [4], specifically, the nanofibrous scaffolds fabricated by electrospinning [5]. Nanofibers fabricated by electrospinning have been considered favorable owing to their structural similarity to the architecture of tissue extracellular matrix (ECM), thus promoting cell adhesion, growth, and differentiation in order to eventually obtain biologically functional tissue analogue [6]. Together with the ability to produce materials with nanoscale properties, the ease of processing tool setup, and the cost-effectiveness, the possibility to fabricate structures with a wide range of compositions has recently escalated interest in electrospinning.

In the bone repair research, electrospinning has gained momentum, as a method of producing nanofabricated polymeric and composite scaffolds, as the bone-associated cells' initial cell responses and further osteoblastic differentiation have been reported to facilitate on nanofibers, mainly due to the favorable condition provided by the nanofibrous substratum for cell adhesion and growth [7]. Focused attention has turned to combining the electrospun nanofibers with minerals, proteins, growth factors, drugs, and nanoparticles to further enhance their physical and chemical complexities and enhance bioactivity [8–10]. Recent reports involve the use of electrospun nanofibrous matrices with new compositions in combination with biological cues and some processing instruments to fabricate three-dimensional scaffolds, which highlight the *in vivo* feasibility of electrospun nanofibers in bone regeneration [11,12].

Tendons and ligaments are dense connective tissues composed of aligned and hierarchically structured collagen fibrils, which are responsible for joint movement and stability [13]. Tendons/ligaments are subjected to high physiological loads transmitted

between muscle to bone and bone to bone. Design of ligament/tendon scaffolds that mimic mechanical and structural properties of the original tissue presents the greatest challenges in regeneration of these connective tissues. Therefore, the mechanical properties of the material fabricated to as tendon/ligament scaffold should be sufficient to support healing tissue, and the structure of the scaffold should be capable of promoting cell activities, to improve the formation of new tissue [14]. Several studies demonstrated that electrospun nanofibers that mimic the structure of native collagen fibers support cell attachment and proliferation and are advantageous for tendon/ligament tissue engineering due to their ability to stimulate mechanobiological signals [15,16].

The design of scaffolds for bone and tendon/ligament injuries, which are able to maintain the tissues' structure, mechanical, and biological properties, lies at the forefront of material science. Most notably, electrospun nanoscaled fibers mimic the native collagen fibers, thus inducing key intracellular signaling pathways in an in vivo-like fashion. This chapter focuses on different approaches adopted to develop electrospun materials for use as scaffolds for bone and tendon/ligament regeneration.

10.2 Bone structure and bone tissue engineering

10.2.1 Bone structure

Bone is a connective tissue that derives its unique properties from a hierarchical architecture of nano-, micro-, and macrostructures, which is engineered with a tightly regulated, complex, and dynamic process. The organic compounds of natural bone are mainly type I collagen, a small quantity of type V collagen, a number of non-collagenous proteins such as osteocalcin, osteopontin, osteonectin, fibronectin, and thrombospondin, and the inorganic part is constituted by calcium phosphates, primarily hydroxyapatite [17,18]. There are three types of cells, osteoblasts, osteocytes, and osteoclasts, which play a role in the creation of ECM of bone and its mineralization, intracellular communication, calcium homeostasis, and bone resorption process [19–22]. The cells are activated by growth factors (such as insulin-like growth factors I and II and transforming growth factor β), cytokines, and proteins [23]. The remodeling and substantially the biological and biomechanical characteristic formation of bone are based on the synergic facilities of its constituent elements. In order to precisely engineer bone, the constituents of bone can be considered as three interfacing parts: the ECM, the cells, and the bioactive factors.

10.2.2 Tissue engineering of bone

Engineering of bone tissue involves the use of scaffold, cells, and biological factors. An advanced scaffold for bone tissue engineering must exhibit interconnected porosity, sufficient mechanical properties, controlled degradation rate, initial strength for safe sterilizing, reliability, and cost-effectiveness [24]. A range of scaffold fabrication methods including solid free-form fabrication, thermally induced phase separation, solvent casting/particle leaching, emulsion freeze-drying, gas foaming, and microsphere

sintering have been proposed for preparation of bone scaffolds [25–28]. A variety of materials have been used for regeneration of bone defects involving metals, ceramics, polymers, and their composites [29].

Until recent years, as bone tissue engineering strategy, the ECM/scaffold was viewed as providing mainly mechanical support during reconstruction of the defected bone. Since the bone ECM is composed of dynamic elements that are activated as in a synergistic orchestra fashion, researches on bone tissue engineering in the past decade focused on designing scaffolds with structure and composition that mimics the bone ECM. The bone ECM is a nanocomposite consisting of collagen fibers, inorganic nanocrystallites, and growth factors, which is considered in engineering of the bone. Therefore, many studies demonstrated new scaffold materials using advanced fabrication technologies and the design of the new materials with desired osteogenesis abilities. The biomimetic features and physicochemical properties of electrospun nanofibrous matrices are believed to play a key role in modulating the microenvironment to guide bone tissue regeneration [30].

10.3 Electrospun scaffolds for bone regeneration

Electrospun scaffolds provide an advantageous approach as bone substitutes by mimicking the native bone ECM. In addition, it is a promising method because of the ability of electrospinning process that enables to produce nanofibers from a wide range of materials including synthetic and natural polymers and their nanocomposites with calcium phosphates. Modulation of a polymeric electrospun nanofibrous scaffold with calcium phosphate minerals is an extensively used strategy to achieve bone-specific bioactivity. Electrospinning parameters such as polymer concentration and type, viscosity, conductivity, surface tension, flow rate, solvent type, applied voltage, distance between tip and collector, and ambient properties have been extensively studied as they affect the fiber morphology and the chemical and physical properties of the scaffold [31]. In regards to bone tissue engineering, it is important that the electrospun scaffold exhibits appropriate mechanical properties to provide structural support and desired fiber size, biomimicking the natural architecture of ECM of bone to create beneficial features for cell attachment, proliferation, and differentiation. The physical arrangement of fibers can also influence the cell adhesion, spreading, and elongation, which in turn influences cell differentiation and mineralization into bone tissues; therefore, the development of processing methods to fabricate aligned electrospun nanofibers has allowed to synthesize bone tissue engineering scaffolds that direct the cell behavior and tissue growth [32]. Research has been moving in the direction of designing bioactive, chemically modified, composite electrospun nanofibers suitable for the direction of differentiation of stem cells toward bone cells. The current landscape of bone regeneration via electrospun nanofibers has focused on incorporating of surface conjugating proteins, genes, and growth factors for enhanced cell function and directed cell differentiation for the reconstruction of bony tissues. Recent trials were carried out to fabricate three-dimensional electrospun constructs with macroporosity. In the following sections, progress in electrospinning approaches for bone reconstruction will be discussed.

10.3.1 *Polymeric nanofibers for bone regeneration*

A wide range of synthetic and natural polymers have been so far processed by electrospinning in the bone regeneration area. Among the synthetic polymers, poly(ϵ -caprolactone) (PCL), poly(lactic acid) (PLA), poly(glycolic acid) (PGA), poly(ethylene glycol) (PEG), poly(hydroxybutyrate) (PHB), and poly(hydroxybutyrate-co-hydroxyvalerate) (PHBV) have been the most extensively studied types.

PCL is one of the more significant polymers electrospun during the past decade, due to its rheological properties, very good blend compatibility, and FDA approval [33]. However, due to the hydrophobic nature of PCL, resulting in the lack of cell adhesion, modification methods such as plasma treatment [34] and coating with biologically active components [35] were applied after preparation of electrospun nanofibers. Some researchers have blended PCL with natural polymers such as gelatin and chitosan to alter the cell affinity to the electrospun scaffolds [36,37]. Combinations of PCL with other polymers such as PLA [38] and PEG [39] have also been electrospun to add different properties to the resulting scaffolds. PCL, first suggested biodegradable polymer for the fabrication of electrospun bone tissue engineering scaffold, which was cultured with osteogenic supplements under dynamic conditions with mesenchymal stem cells (MSCs), provided an appropriate environment for the formation of mineralized tissue [40]. The cell-scaffold constructs, implanted in the omenta of rats after culturing in a rotating bioreactor for 4 weeks, revealed a bone-like appearance and content [41].

Nanofibrous scaffolds of poly(L-lactide) (PLLA) and its combinations with hydroxyapatite (HA) or collagen/HA were fabricated, which were substantially incubated with human fetal osteoblasts. When collagen/HA was used with PLLA, a higher cell proliferation and increased mineralization were observed on the scaffold than on PLLA and PLLA/HA scaffolds, suggesting the positive influence of collagen and apatite on the osteoblastic responses to the nanofiber content [42]. Nanocomposites were fabricated by including cellulose nanocrystals to the electrospun maleic anhydride-grafted PLA nanofibers in order to enhance the mechanical properties of the scaffolds for bone tissue engineering applications [43]. Inclusion of 5 wt% cellulose nanocrystals increased the tensile strength more than 10 MPa compared with the plain nanofibers, which may contribute to the development of bone tissue engineering scaffolds with enhanced mechanical stability. Electrically conductive scaffolds were obtained by embedding multiwalled carbon nanotubes inside the poly-DL-lactide electrospun nanofibers [44]. Application of a direct current of 100 μ A on the conductive nanofibers resulted in growth of osteoblasts along the electric current direction, and in addition to cellular elongation, the proliferation was also affected by the electric stimulation, which may potentially contribute to the bone healing and fracture regeneration process (Figs. 10.1 and 10.2).

Electrospun scaffolds produced from natural polymers such as collagen, gelatin, silk fibroin, and their blends with synthetic polymers and inorganic minerals have attracted considerable attention in bone tissue engineering area, due to the presence of the components that facilitate and regulate cellular activities. Collagen is the most

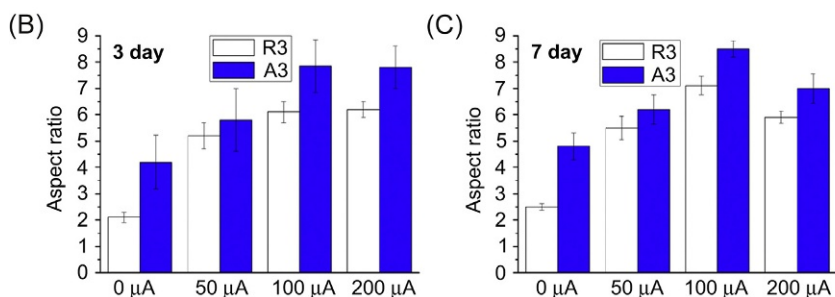
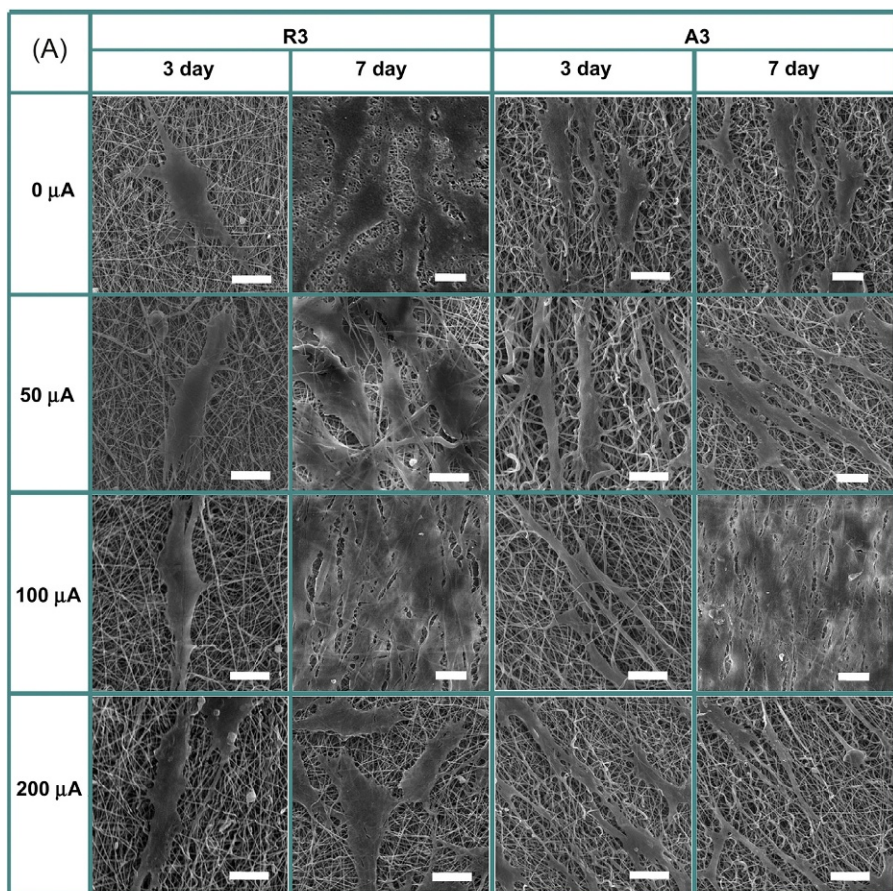


Fig. 10.1 Selected scanning electron microscope images of osteoblasts cultured on R3 and A3 nanofiber meshes for 3 and 7 days with electric stimulation of 0 μA , 50 μA , 100 μA , and 200 μA (A). All the scale bars mean 30 μm (B) and (C) represent the elongation of osteoblasts as measured by the aspect ratio after cultured for 3 and 7 days. Herein, the so-called name R3 corresponds to random-oriented composite fibers with weight ratio of multiwalled carbon nanotubes 3%, whereas A3 stands for aligned composite fibers with the same ratio of multiwalled carbon nanotubes as random composite fibers. Reused with permission from Shao S, Zhou S, Li L, Li J, Luo C, Wang J, et al. Osteoblast function on electrically conductive electrospun PLA/MWCNTs nanofibers. *Biomaterials* 2011;32(11):2821–33, copyright Elsevier.

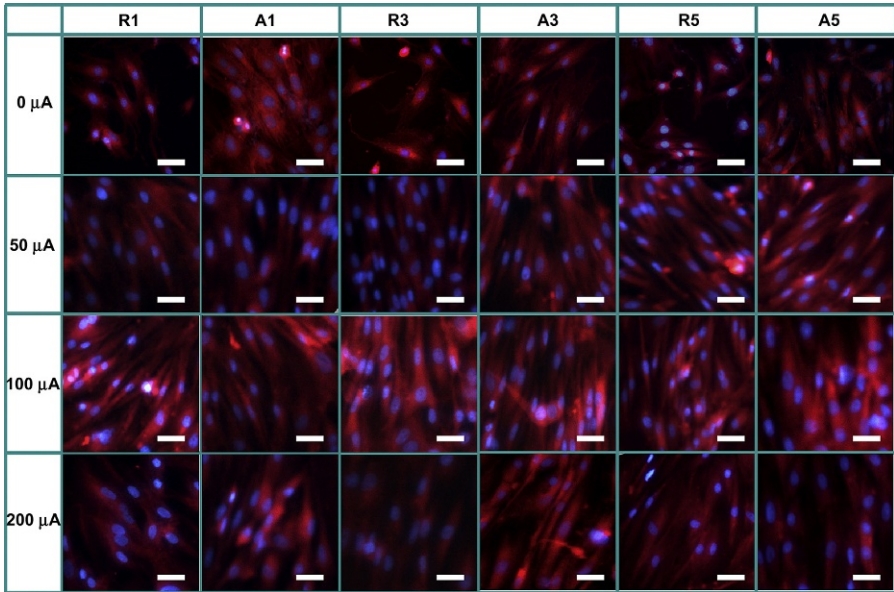


Fig. 10.2 Fluorescence microscope images of osteoblasts cultured on R1, R3, and R5 and A1, A3, and A5 for 5 days with DC electric stimulation of 0 μA , 50 μA , 100 μA , and 200 μA . The nucleus was stained by DAPI (blue), and the cytoplasm was stained by Rhodamine 123 (red). All the scale bars mean 50 μm . Herein, the so-called names R1, R3, and R5 correspond to random-oriented composite fibers with weight ratios of multiwalled carbon nanotubes, 1%, 3%, and 5%, respectively, whereas A1, A3, and A5 stand for aligned composite fibers with the same ratios of multiwalled carbon nanotubes as random composite fibers.

Reused with permission from Shao S, Zhou S, Li L, Li J, Luo C, Wang J, et al. Osteoblast function on electrically conductive electrospun PLA/MWCNTs nanofibers. *Biomaterials* 2011;32(11):2821–33, copyright Elsevier.

extensively used biopolymer in tissue engineering applications due to its key role in maintaining the biological and structural integrity of ECM. Thus, in the literature, a wide range of electrospun scaffolds prepared from collagen and its composites have been proposed for repair of bone tissue. Aligned PLGA/collagen blend [45], collagen-apatite-precipitated composite [46], triphasic PCL-collagen type I nanoHA [47], and PLA/poly-benzyl-L-glutamate/collagen [48] are examples of some of the hybrid scaffolds fabricated by electrospinning, which are proposed for bone tissue engineering applications. However, although electrospun collagen is believed to have strong potential as a biomimicking substrate for cell adhesion and proliferation, Zeugolis et al. reported that when collagen is electrospun into nanofibers out of fluoroalcohols, its unique biological structure is denatured and therefore proposed the method of collagen coating on electrospun nanofibers [49].

Due to its similar characteristics to collagen, nonantigenicity and cost-efficiency, gelatin-based electrospun scaffolds gained interest for bone regeneration. Gelatin nanofibers with small (110 ± 40 nm) and large (600 ± 110 nm) diameters were

obtained by electrospinning, and osteoblastic cell migration and differentiation were found to be directed by fiber diameter, which indicated that the cells can perceive the difference in diameter and convey this information through biological signals [50]. A bilayer scaffold including gelatin, PCL, calcium phosphate nanoparticles, and a drug (osteogenon) was prepared by electrospinning, and subsequently, polyaniline was deposited on the surface by inkjet printing in order to obtain a bioactive and conductive matrix for cells [51]. Gupta et al. prepared Poly(L-lactic acid)-co-poly(ϵ -caprolactone) (PLACL)/gelatin/HA nanofibrous scaffolds by blending HA to the polymer solution before electrospinning or simultaneously electro spraying HA on the PLACL/gelatin nanofibers. Electro spraying of HA nanoparticles on nanofibers offered a more favorable environment for growth of human fetal osteoblast cells and their mineralization compared with blending HA inside the polymeric nanofibers, which was attributed to the complete contact of cells with HA nanoparticles [52].

Silk fibroin has also been explored as a potential polymer for preparation of scaffolds for bone tissue engineering because of its ability to be electrospun out of water, which provides a way to introduce growth factors, which may not withstand organic solvents, into the nanofibers. Silk fibroin with bone morphogenetic protein-2 was successfully electrospun into nanofibers. The scaffold supported stem cell growth and differentiation toward osteogenic outcomes that indicated the maintenance of the bioactivity of bone morphogenetic protein-2 [8].

10.3.2 Nanocomposites of nanofibers with hydroxyapatite for bone tissue engineering

Combining inorganic substituents with organic materials during the course of electrospinning is common in bone tissue engineering, since the original bone comprises 70% (wt) inorganic crystals mainly hydroxyapatite and 30% (wt) organic proteins, which highlights the requirement for designing nanocomposites biomimicking bone architecture. Because of the ceramic nature of the incorporated HA, organic-inorganic nanocomposites provide adequate mechanical hardness to the scaffold. HA-enriched nanofibers due to the ability to alter adsorption of chemical species act to improve the biological properties of the scaffolds by enhancing the cell compatibility and inducing bone-forming process, involving cell proliferation and mineralization of bone matrix. Therefore, designing nanocomposites of nanofibers with HA is a reasonable way of generating scaffolds with appropriate properties targeted for bone repair.

The synergistic mechanical and biological properties of bioactive inorganics with natural or synthetic polymers provide a favorable environment for osteogenic differentiation and mineralization. However, electrospinning of the composite solutions requires special consideration in the preparation of fine crystalline nanoparticles and disperse them homogeneously within the polymer solution. In many cases, inorganic nanocrystals agglomerate, resulting in the formation of beaded and destroyed continuous nanofibrous morphology. In an approach applied to overcome this agglomeration, HA crystals of 35 nm were developed by a sol-gel process and

homogeneously dispersed in a PLA solution by using a surfactant, 12-hydroxysteric acid [53]. Bead-free electrospun fibrous morphology was achieved wherein the HA nanoparticles homogeneously dispersed within the fibers, which was attributed to the amphiphilic surfactant that acted as a mediator between the interface of hydrophilic HA and the hydrophobic PLA solution. In another approach, nanocomposites of HA and chitosan were fabricated by combining an in situ coprecipitation method with electrospinning [54]. HA/chitosan nanocomposites were synthesized by precipitating HA in situ from Ca and P precursors within the chitosan solution, which was then electrospun into continuous nanofibers with some aggregated HA nanoparticles. The nanocomposite was shown to promote the growth of human fetal osteoblasts to a significantly higher level than on pure chitosan nanofiber (Fig. 10.3). The approach of combining coprecipitation with electrospinning has been reported for nanocomposites such as gelatin/HA [55] and collagen/HA [46] systems, and the nanofibers demonstrated improvement in the cellular activities of bone cells. More studies focused on fabricating nanocomposite nanofibers with HA nanoparticles dispersed uniformly in the fibers with enhanced strength properties. PLA-grafted HA nanoparticles were synthesized, and PLA-grafted HA/PLA composite polymer was prepared. Uniform PLA-grafted HA/PLA composite nanofibers were generated by electrospinning [56]. Improved mechanical properties were achieved with the PLA-grafted HA/PLA nanofibers compared with the HA/PLA or PLA nanofibers. However, increasing the content of PLA-grafted HA nanoparticles more than 4% (wt) in the composite polymer caused aggregation of the nanoparticles, which resulted in decrease in the strength of the electrospun materials. Many researchers have investigated a number of characteristics of electrospun polymer/HA nanocomposites, because more promising results came out from the composite fibers with respect to the polymeric pristine component [57–60].

Significant interest has focused on investigating the interaction of stem cells with the composite nanofibers, because the nanocomposites provide an opportunity to modulate the physical, chemical, and biological properties of the scaffold, which in turn affect the fate of the stem cells. In an approach aiming to tune the stem cell fate by electrospun nanocomposite materials, Ca-deficient nanohydroxyapatite was used to fabricate nanocomposites of microfibrillar poly(L-lactic acid)-based fibers [61]. Electrospun plain poly(L-lactic acid) and poly(L-lactic acid)/Ca-deficient nanohydroxyapatite composites were cultured with multipotent (human bone marrow-derived mesenchymal stem cells) and pluripotent (murine-induced pluripotent stem cells and murine embryonic stem cells) stem cells in the absence of soluble osteogenic factors [62]. After 21 days of cell culture, it was demonstrated that nanocomposite scaffolds with respect to plain scaffold drove multipotent and pluripotent stem cells toward osteogenic differentiation. The expression of osteogenic markers, including high expression of alkaline phosphatase activity and bone matrix proteins, was only observed in stem cells cultured on composite scaffolds. Interestingly, when the cell culture experiments were conducted on a transwell system without a direct interaction of the cells with the biomaterial, the osteogenic differentiation was not obtained. The overall observations described the effect of chemical and topographical properties of the composite scaffold on the fate of the stem cells and

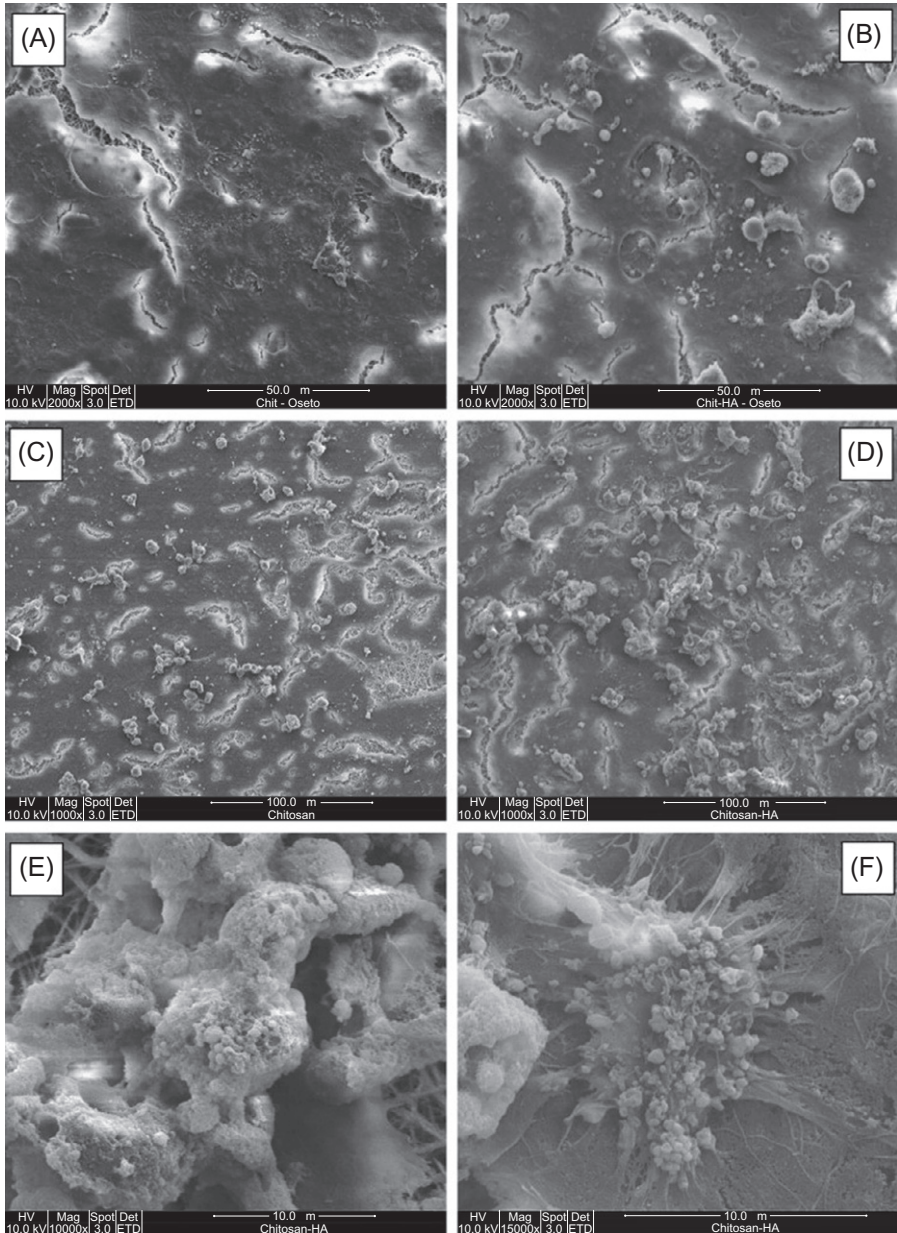


Fig. 10.3 Mineral depositions of human fetal osteoblast cells on the electrospun nanofibrous scaffolds: chitosan, day 10 (A) and day 15 (C), hydroxyapatite/chitosan, day 10 (B) and day 15 (D), apatite-like morphology of deposit at higher magnification (E), and visible tiny globular minerals and collagen bundles associated with a single human fetal osteoblast cell viewed at higher magnification (F).

Reused with permission from Zhang Y, Venugopal JR, El-Turki A, Ramakrishna S, Su B, Lim CT. Electrospun biomimetic nanocomposite nanofibers of hydroxyapatite/chitosan for bone tissue engineering. *Biomaterials* 2008;29(32):4314–22, copyright Elsevier.

highlighted the requirement of the direct interaction of stem cells with the polymeric nanocomposite as a key step for the differentiation process. In another approach, electrospun PCL/collagen type I/HA tricomponent scaffold was prepared, and mesenchymal stem cell responses to the composite material were evaluated. It was demonstrated that the tricomponent scaffold promoted the phosphorylation and activation of focal adhesion kinase, which is important for directing osteoblastic differentiation. The cell responses such as proliferation and spreading were more favorable on the tricomponent composite than on PCL or PCL/HA scaffolds [63]. PLGA/HA electrospun composites prepared for the delivery of BMP-2 plasmid DNA were cultured with human marrow stem cells. Encapsulation of HA nanoparticles in the nanofibers increased the release rate of DNA, without deleterious effects on cell viability. It was demonstrated that the fibers loaded with higher level of HA had a more rapid release rate of DNA; therefore, the HA could be used as an additive to modulate the release profile of the nanocomposite [64]. Although more promising results are coming out from the electrospun composite nanofibrous matrices prepared by loading HA nanoparticles in the fibers, the size of the particles, their agglomeration/dispersibility, the added amount, and optimizing mechanical properties have still been issues to explore for the successful electrospinning.

10.3.3 Surface mineralization of electrospun nanofibers

In addition to introducing calcium phosphate components directly into polymer solution before electrospinning to create composite nanofibers, modifying the surface of the nanofibers with bone mineral-like crystals is a fascinating approach. Calcium phosphates are considered to be more effective if exposed on the surface of nanofibers, providing a substrate favorable for the adhesion of bone cells. To expose minerals on the surface of nanofibers, calcium phosphates can be deposited directly on the surface by soaking the electrospun matrix in simulated body fluid (SBF) with ion concentrations similar to that of human blood plasma. Electrospun nanofibers made from various synthetic or natural polymers were incubated in SBF to produce apatite deposition on their surface. PHBV nanofibrous matrices were prepared by electrospinning and soaked in SBF to create HA deposition on their surface. Although the PHBV nanofibrous film was hydrophobic before SBF treatment, after HA deposition, the surface became hydrophilic. The degradation rate of HA-deposited films in the presence of polyhydroxybutyrate depolymerase was higher compared with the plain PHBV nanofibrous materials, which was attributed to the enhanced invasion of enzyme into the matrix due to increased surface hydrophilicity [65]. Since the synthetic polymers have fewer ionic molecular groups compared with natural polymers, surface treatment before SBF coating may be necessary to expose hydroxyl or carboxyl groups that induce mineralization [66]. Therefore, in an approach, the surface of electrospun PCL nanofibers was first activated by an alkaline solution and then mineralized in SBF solution [67]. The mineralized PCL nanofibers cultured with murine-derived preosteoblasts stimulated the expression of bone-associated genes when compared with the plain PCL nanofibers. Coating electrospun PLA fibers with the natural polymer, chitosan, before soaking the matrix in SBF accelerated the

mineralization of calcium phosphate [68]. Chitosan promoted more nucleation and growth of calcium phosphate crystals. Without chitosan coating, the Ca/P ratio was 1.35; however, as the chitosan content of the coated samples increased, a higher Ca/P ratio of 1.67 was achieved, which was attributed to the increased hydrophilicity of the chitosan-coated matrices. In another study aiming to fabricate nanofibrous scaffolds for tendon-to-bone insertion site repair, the surface of poly(lactic-co-glycolic acid) nanofibers was covalently immobilized with chitosan or chitosan/heparin after plasma treatment, and then, the matrix was mineralized in SBF solution [69]. The effect of positively or negatively charged surface on the nucleation of HA was demonstrated. Positively charged chitosan surface decreased the nucleation of HA, and therefore, the surface of the nanofibers was barely coated with minerals. However, negative charge of heparin attracted Ca^{2+} , resulting in enhanced nucleation of crystals leading to a more thick and dense coating. Meng et al. prepared poly(D,L lactide-co-glycolide)/gelatin nanofibers from a composite solution with the weight ratio of 9/1 and mineralized the matrix [70]. Addition of gelatin to the recipe favored more deposition of calcium phosphate on the surface of the composite nanofibers compared with pristine poly(D,L lactide-co-glycolide) nanofibers, which revealed the role of gelatin as nucleation-inducing center for mineralization.

Mineralization of electrospun nanofibers can also be achieved by electrodeposition. A rapid mineralization strategy of nanofibrous PLLA scaffolds within one hour was reported [71]. Using an electrochemical process with changing conditions such as voltage, temperature, and deposition time, the surface topography and chemical compositions could be controlled to provide a favorable interface for bone regeneration. Interestingly, flower-, flake-, fiber-, or needlelike mineral crystals were formed on the nanofibers, showing that the surface topography of calcium phosphate could be tailored, which could affect the cellular responses such as attachment, proliferation, and differentiation.

10.3.4 Functional nanomaterials combined electrospun nanofibers for bone repair

Compared with single-component nanofibers, combining nanomaterials such as nanoparticles or nanotubes within polymeric nanofibers makes the hybrid nanofibers more functional with promising mechanical, electric, biological, or magnetic properties. In order to introduce new functionalities to the fibers, nanomaterials with the size ranging from 1 to 100 nm have been doped into electrospun nanofibers by directly mixing them with a polymer solution for electrospinning. The simple mixing of polymer with the nanoparticle or nanotube in their plain form makes it possible to produce functional nanofibers promoting cell anchorage with improvements in mechanical properties [72].

10.3.5 Carbon nanotubes incorporated nanofibers

Carbon nanotubes have gained widespread attention for biomedical applications due to their excellent properties such as good mechanical properties and favorable biocompatibility [73–75]. It was reported that carbon nanotubes promoted osteoblast

attachment and proliferation by inducing osteogenic maturation of osteoblasts by adsorbing more specific proteins [76,77]. The incorporation of multiwalled carbon nanotubes (MWNTs) within electrospun nanofibers made it possible to produce functional fibers having improved properties for bone tissue engineering. Zhang prepared composites of MWNTs with poly(lactic-co-glycolic acid) for bone tissue regeneration [78]. The incorporation of MWNTs into poly(lactic-co-glycolic acid) nanofibers increased the thermal stability, tensile strength, and Young's modulus. The attachment and proliferation of rat bone marrow-derived mesenchymal stem cells were more favorable on the composite scaffold compared with neat poly(lactic-co-glycolic acid) scaffold, which demonstrated that carbon nanotubes enhanced the functions of the cells. In another approach, electrospun composite scaffold of PLA/MWNTs was cultured with adipose-derived human mesenchymal stem cells [79]. The composite scaffold played an important role in directing the stem cell behavior. Addition of MWNTs in the scaffold resulted in a preferential alignment and orientation of the cells on the nanofibers.

10.3.6 Magnetic nanoparticles incorporated nanofibers

Due to their biocompatible, nontoxic characteristics and unique feature of orientational movement in magnetic field, magnetic nanoparticles, especially iron oxides, attracted great attention in the biomedical field, such as drug delivery, hyperthermia, magnetic resonance imaging, cell targeting, and cell sheet construction [80–82]. Bone tissue is able to convert mechanical stress into biological events such as increased levels of expression of multiple genes and activity of proteins that play important roles in bone repair [83]. Manipulation of magnetic nanoparticles within a bone tissue engineering scaffold can provide artificial mechanical stresses on the bone cells. In this sense, a proper design of the magnetic nanoparticle combined bone scaffolds constitutes one of the most attractive research areas in bone tissue repair, since the incorporation of magnetic nanoparticles in the scaffold has effect on osteoinduction, leading to increased growth, proliferation, and differentiation of bone cells [84,85]. Regarding the beneficial effects of magnetic fields on regulating the orientation of matrix proteins and promoting new bone formation [86,87], introducing magnetic stimulation into electrospun nanofibers has been used as a strategy in bone repair [85]. Meng et al. prepared composite nanofibrous scaffolds with PLA, HA, and γ -Fe₂O₃ magnetic nanoparticles by electrospinning and cultured the scaffolds with preosteoblast cells under an applied static magnetic field [85]. The composite scaffold acted as a stimulating matrix for cells and providing magnetic activity accelerated proliferation and differentiation of the osteoblasts, compared with the nanofibrous scaffold without magnetic nanoparticles. Furthermore, an in vivo study for the new bone formation enhancement mediated by those magnetic responsive nanofibrous scaffolds were conducted [88]. The scaffolds were implanted in bone defects in a rabbit model and the magnets fixed on the cages provided a static magnetic field. The magnetic nanoparticle combined composite electrospun scaffolds accelerated new bone formation and remodeling under static magnetic field, which was attributed to the production of magnetic force in the scaffold under a magnetic field, which resulted in

stimulation of osteoblast cell proliferation. Interestingly, the degradation rate of the scaffolds under a magnetic field was higher than that without the magnetic field. It was reported that the underlying mechanism of faster degradation may be related to the more active macrophages due to the magnetic stimulation, which could provide a benefit in tuning the degradation rate of the scaffold for modulating bone repair. Inspired by the enhancement effect of magnetic stimulation on bone growth and operational flexibility of electrospinning for incorporating multiple components into nanofibers, more researchers fabricated magnetic nanofibrous composites by electrospinning and explored their potential use in bone tissue engineering. Wei et al. developed a magnetic fibrous composite scaffold with Fe_3O_4 , chitosan, and PVA by electrospinning, and ferrimagnetic behavior of this scaffold leads to good cell adhesion and proliferation of MG63 human osteoblast-like cells, suggesting its potential for bone repair applications [89]. Singh et al. fabricated magnetic nanoparticles that incorporated PCL nanofibers by electrospinning and characterized physicochemical, mechanical, and biological properties of the composite scaffolds and conducted an in vivo defect repair study [90]. The incorporation of magnetic nanoparticles in the formulation increased hydrophilicity, mechanical strength, degradation rate, and apatite-forming ability in SBF. Alkaline phosphatase activity and expression of bone-associated genes were enhanced when the composites were cultured with osteoblastic cells, compared with the plain PCL nanofibers. Bone regenerative ability of the composite scaffolds was demonstrated addressing the use of those scaffolds in bone tissue engineering applications. Increasing experimental data demonstrated in recent years clearly point out the positive synergistic effects of magnetic stimulation on bone cell activity and new bone formation in vivo. Although the underlying mechanism of the positive stimulation of the magnetic scaffold on bone formation is not clearly demonstrated yet, it is mainly hypothesized that the magnetic scaffolds generated microdeformation of the scaffold under a magnetic field, leading to a strain stimulation on growing cells, which results in the enhanced activation of the bone cells [91].

10.3.7 Nanodiamond incorporated nanofibers

Nanodiamonds demonstrated very high biocompatibility (no considerable cytotoxicity), excellent mechanical properties, and growth support for various cell types, particularly bone-associated cells [92–94]. Therefore, in recent years, their electrospun nanocomposite scaffolds were fabricated for bone tissue engineering applications. Serafim et al. loaded various ratios of carboxylated nanodiamond particles into electrospun gelatin hydrogel fibers [95]. Following Ca/P incubation of the nanocomposites, the nanoapatite crystals were preferentially formed on the fiber regions in the proximity of carboxylated nanodiamonds, and the MG63 osteoblast-like cells were stimulated by the presence of the nanodiamonds. In other approaches, nanodiamonds were incorporated in electrospun poly(lactide-co-glycolide) [96] and PCL [97] nanofibers as potential bone tissue engineering scaffolds. Although the nanodiamonds attracted great attention in the biomedical field due to the higher biocompatibility of those nanoparticles compared with the other

carbon-based species such as multiwalled carbon nanotubes, there are few recent studies related to their electrospun polymeric nanocomposites for bone regeneration. Future studies are needed to be performed to better explain the stimulation of bone-associated cells by electrospun nanodiamond composite scaffolds.

10.3.8 Therapeutic bone tissue engineering applications of nanofibers

An innovative approach to design a suitable bone tissue engineering electrospun scaffold for guided cell adhesion, proliferation, and directed differentiation is the incorporation of bioactive molecules such as growth factors or other chemicals and proteins that play a role in regulating bone cell behavior. The bioactive molecules can be coupled on to the surface of nanofibers or encapsulated within nanofibers. When administered on the surface of the nanofiber, the bioactive molecule will be recognized firstly by the cell and be able to regulate the initial cell response processes. On the other hand, when encapsulated within the nanofiber, the chemical stability and biological activity of the bioactive molecule will be protected for prolonged time course, because most osteogenic factors have rapid loss of biological activity *in vivo*. However, in this case, the encapsulation method needs to be designed carefully to protect incorporated bioactive molecule from being degraded. Drug release kinetics may be further regulated by altering fiber dimensions or degradation rate of the polymer and by chemically bounding or physically mixing the drug to the matrix. Scaffolds containing thin fibers or having faster degrading polymers may lead to loss in structural integrity before the tissue ingrowth is completed and may not withstand the mechanical load of the bone. Therefore, the design of the scaffold must be carefully investigated for suitable release kinetics and degradation rate.

A range of bioactive molecules have been combined with electrospun nanofibers including growth factors such as bone morphogenetic proteins and fibroblast and transforming and insulin-like growth factors. Bone morphogenetic protein-2 (BMP-2) is one of the most studied and promising of these molecules for regeneration of bone defects. Li et al. prepared silk fibroin/poly(ethylene oxide) scaffolds containing BMP-2 and/or hydroxyapatite nanoparticles via electrospinning and seeded the scaffolds with bone marrow-derived mesenchymal stem cells [8]. They added BMP-2 to the polymer-based solution and then electrospun. The aqueous-based process did not cause denaturation of the bioactive form of BMP-2. The addition of BMP-2 supported enhanced osteogenic response of human bone marrow-derived mesenchymal stem cells and higher cellular calcification. In another approach, a core-shell BMP-2-releasing electrospun scaffold was developed for repair of cranial bone defects [98]. To maintain the bioactivity of BMP-2, the aqueous core solution of the biomolecule was prepared with poly(ethylene oxide). The shell solution was composed of PCL/poly(ethylene glycol). Fast and slow BMP-2-releasing scaffolds were developed by altering the fiber's shell porosity, which was dependent on the relative amount of poly(ethylene glycol) in the shell. The scaffolds with slow release pattern increased the alkaline phosphatase activity *in vitro*, compared with the scaffolds with fast release pattern. The cranial bone defect repair study revealed significant bone regeneration efficiency of the implants

with slow release profile. Recently, Zhou's group encapsulated BMP-2 into bovine serum albumin nanoparticles to maintain bioactivity of BMP-2 and coelectrospun the solution composed of nanoparticles, dexamethasone, and poly(ϵ -caprolactone)-co-polyethylene glycol copolymer [99]. They evaluated the performance of the scaffold in the regeneration of critical-sized rat calvarial defect. The best bone repair efficacy was achieved with the dual drug-loaded nanofiber scaffold, thus showing the synergistic effect of BMP-2 and dexamethasone.

Adhesive proteins such as fibronectin, vitronectin, and laminin are utilized with polymeric nanofibers, because these proteins mediate the initial adhesion event and favor the subsequent differentiation of anchorage-dependent cells. However, the poor surface properties of synthetic polymers (PLA, PCL, and PGA and their copolymers) including their hydrophobicity and the lack of cell adhesive motifs limit the direct adsorption of proteins on their surface. Thus, the surface of the polymer needs to be activated to overcome these shortcomings. Preparation of hydrophilic compositions with natural polymers or poly(ethylene oxide) has been commonly applied to allow formation of bonds with the proteins. Recently, Lee et al. fabricated PCL-gelatin fibers via electrospinning and mineralized the surface of the matrice by SBF treatment [100]. The anchorage of a fusion protein of fibronectin 9–10 domain and osteocalcin to the hydroxyapatite-mineralized fiber was found to be highly specific, through a molecular recognition to the hydroxyapatite crystals. The initial mesenchymal stem cell adhesion levels, upregulations in the mRNA expressions of adhesion-signaling molecules, and expression of the osteogenic-related genes were enhanced with the fibers linked with protein. In vivo study in the rat calvarium model demonstrated a higher amount of new bone formation in the protein-linked fiber matrix.

Apart from proteins, nucleic acids may also be delivered by electrospun nanofibers. Recently, Zhao et al. adsorbed plasmid DNA transfection complexes onto PLLA/collagen type I electrospun scaffold for the delivery of recombinant human BMP-2 (rhBMP-2) [101]. In a mouse muscle pouch model, in vivo gene delivery efficacy and ectopic bone-inducing capability of the scaffold were evaluated, and the scaffold was found to be capable of cell transfection with strong transgene expression and formation of ectopic bone tissue.

In addition to biological molecules, some chemical drugs have been incorporated into electrospun nanofibers to improve their therapeutic activity. Our group prepared simvastatin-loaded and spiral-wounded 3D electrospun PCL scaffolds and evaluated their performance in the repair of cranial bone defects in a rat model [102]. We loaded simvastatin to the nanofibrous scaffolds by using two methods, either by adding simvastatin to the polymer solution before electrospinning or by embedding the drug to the scaffolds after electrospinning. X-ray microcomputed tomography and histological study results revealed the osseous tissue integration within the implant and mineralized bone restoration of the calvarium. The more successful results were obtained with the group in which simvastatin was incorporated into the scaffold during electrospinning.

The drug delivery application greatly enhances the capability of the electrospun nanofibrous scaffolds to guide new bone formation, and more extensive works are expected in bone tissue engineering with electrospun nanofibrous scaffolds with therapeutic design.

10.4 Tendon/ligament structure and tendon/ligament tissue engineering

10.4.1 Tendon/ligament structure

Tendons and ligaments transfer forces between musculoskeletal tissues. They obtain their tensile strength and elasticity from the hierarchically structured collagen fibrils of their structure. Tendon and ligament tissues contain collagen types I, III, IV, V, and VI; elastin; decorin; and cartilage oligomeric matrix protein. Tendon/ligament cells are oriented around collagen fibers and maintain the density and the composition of tendon/ligament tissues [103,104]. The fibroblastic cells in tendons are known as tenocytes and in ligament as ligament fibroblasts. These cells show very poor healing efficacy *in vivo*. Tendons and ligaments are responsible for joint movement and stability and subjected to high physiological loads transmitted between muscle to bone and bone to bone. When these loads exceed a critical threshold, a permanent tissue damage occurs, and because of the poor regenerative capacity of tendons and ligaments to heal due to their hypocellularity and hypovascularity, impaired function and mobility will result [105].

10.4.2 Tendon/ligament tissue engineering

For the repair of tendon and ligament tissues, current surgical treatment options are autografting and allografting; however, those options are limited by donor-site morbidity, healthy tissue availability, tissue compatibility, disease transmission, and graft failure. These problems have led researchers to focus on a more ideal solution, which is tissue engineering, to restore the tendon or ligament by developing functional scaffolds that resembles the original tissue [3,106]. An ideal engineered tendon/ligament would have mechanical properties that are sufficient to support healing tissues, should be capable of promoting cellular activities to improve the formation of new tissue, and would degrade at a rate comparable with that of developing tissue ingrowth. The requirement for fabrication of scaffolds with tendon-/ligament-like compositions, geometries, and mechanobiological properties has generated interest in the use of natural and synthetic polymeric materials for tendon/ligament tissue engineering. A wide variety of synthetic and natural polymers, such as PCL, PGA, polyurethane, collagen, and silk fibroin, and a variety of scaffold production methods have been used to develop functional matrices for tendon and ligament tissue engineering [107].

10.5 Electrospun scaffolds for tendon/ligament regeneration

Polymeric microfibers have been used for tendon/ligament tissue engineering applications; however, when nanofibers are used to culture cells, enhanced biological activity would be expected. Therefore, electrospun nanofibers that mimic the structure of native collagen fibers have been demonstrated to have many advantages over

micrometer-sized fibers to support cell attachment and proliferation for tendon/ligament tissue engineering due to their ability to stimulate mechanobiological signals.

Barber et al. fabricated scaffolds by braiding bundles of aligned electrospun PLLA nanofibers [108]. Braiding the nanofibrous aligned bundles introduced an additional degree of flexibility to the scaffolds, and in addition, braided nanofibers demonstrated similar mechanical behavior of original tendon's and ligament's normal triphasic mechanical behavior. The braided nanofibers were cultured with human mesenchymal stem cells. The cells adhered to the scaffolds, proliferated, and differentiated into tenogenic lineage in the presence of growth factors, which supported the potential of the braided and aligned nanofibrous scaffold for tendon/ligament tissue engineering.

Chainani et al. fabricated multilayered PCL scaffolds by sequentially collecting electrospun layers onto the surface of a grounded saline bath for rotator cuff tendon tissue engineering [109]. Seventy layers were collected from the surface of the bath to prepare the multilayered scaffolds. The dried multilayered electrospun scaffolds were coated with tendon-derived extracellular matrix, fibronectin, or phosphate-buffered saline (PBS) and seeded with human adipose stem cells. After 28 days in cell culture, immunofluorescence, biochemical assays, and histology results suggested that the electrospun scaffolds permitted tenogenic differentiation and the tendon-derived extracellular matrix coating promoted some aspects of this differentiation.

Sahoo et al. developed nanomicrofibrous scaffolds by electrospinning poly(D,L lactide-co-glycolide) solution onto a knitted poly(D,L lactide-co-glycolide) scaffold [110] for tendon/ligament tissue engineering and seeded porcine bone marrow stromal cells by pipetting cell-medium suspension onto the scaffolds. As a control group, knitted poly(D,L lactide-co-glycolide) scaffolds without nanofibers were seeded with cells suspended in fibrin gel. Cell attachment, proliferation, and expression of collagen type I, decorin, and biglycan genes were higher in the nanomicrofibrous scaffold compared with the knitted poly(D,L lactide-co-glycolide) scaffolds. Although this study demonstrated the differentiation of bone marrow stromal cells into tendon/ligament lineage, the limitation of the nanomicrofibrous scaffolds was their mechanical properties that were not comparable with the original value of tendon and ligament. In another study, Sahoo et al. coated bFGF-releasing poly(D,L lactide-co-glycolide) fibers over knitted degummed microfibrillar silk scaffolds by electrospinning (Figs. 10.4 and 10.5) [106]. The biohybrid scaffold system cultured with mesenchymal progenitor cells facilitated cell attachment, tenogenic differentiation, and synthesis of ligament and tendon major matrix. The collagen production enhanced the mechanical properties of the matrix, which had potential to be used as a tendon/ligament analogue for regeneration of injured tendon/ligament tissue.

The performance of electrospun 3D, 1 mm-thick scaffold prepared from poly(D,L lactide-co-glycolide) was compared with a 2D film scaffold prepared from the same polymer on cell proliferation and gene expression of primary rat adipose-derived stem cells [111]. Growth/differentiation factor 5, which modulates the repair process in tendons and ligament, was used in both of the scaffold groups. The electrospun scaffold mimicked the collagen fiber bundles present in natural tendon tissue, and the expression of the genes that encode the major tendon ECM protein was found to be higher in the electrospun scaffolds compared with the 2D film scaffold.

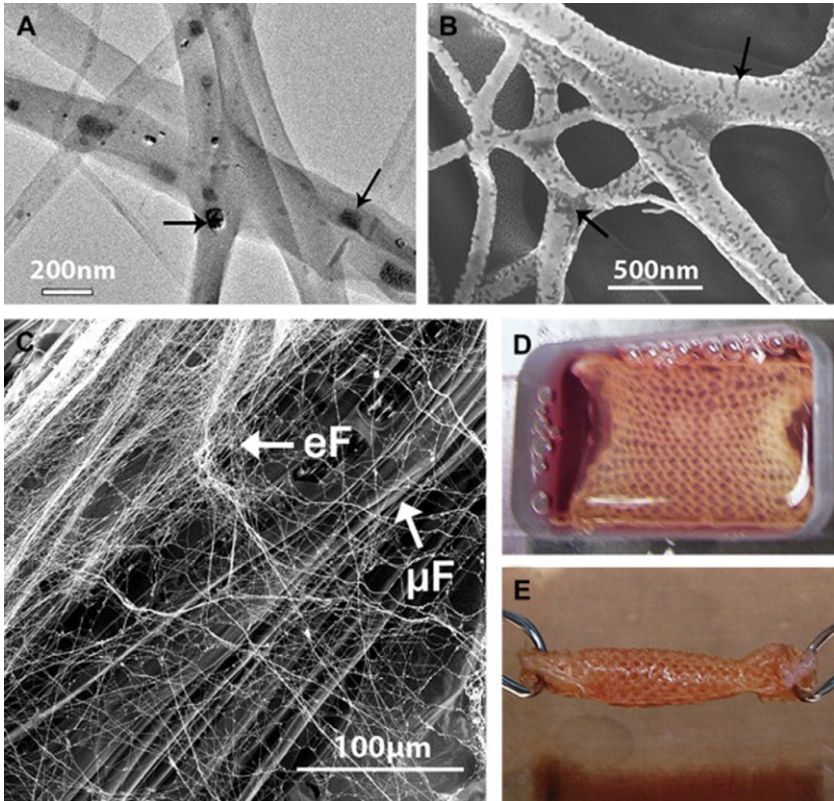


Fig. 10.4 (A) TEM and (B) backscattered SEM images of electrospun bFGF-containing poly(D,L lactide-co-glycolide) fibers showing the random distribution of proteins (indicated by black arrows) in the fibers, (C) SEM image of biohybrid scaffold developed by coating FGF(+) electrospun fibers (eF) on microfibrillar knitted silk scaffolds (μ F), and (D) and (E) BMSC-seeded biohybrid scaffold cultured in a custom-made chamber before being rolled up into cylindrical ligament/tendon analogues after 7 days of culture.

Reused with permission from Sahoo S, Toh SL, Goh JC. A bFGF silk/PLGA-based biohybrid scaffold for ligament/tendon tissue engineering using mesenchymal progenitor cells. *Biomaterials* 2010;3(11):2990–8, copyright Elsevier.

10.5.1 Aligned nanofibers for tendon/ligament tissue engineering

Tendons and ligaments are specific connective tissues composed of parallel collagen fibers; in terms of mimicking that structure, a variety of studies were performed to evaluate the effect of fiber alignment on the cell behavior in tendon/ligament tissue engineering area.

Poly(L-lactic-co- ϵ -caprolactone) was also used to coat knitted scaffolds of vicryl (PLGA, 10/90) and silk suture by electrospun nanofibers for possible ligament tissue

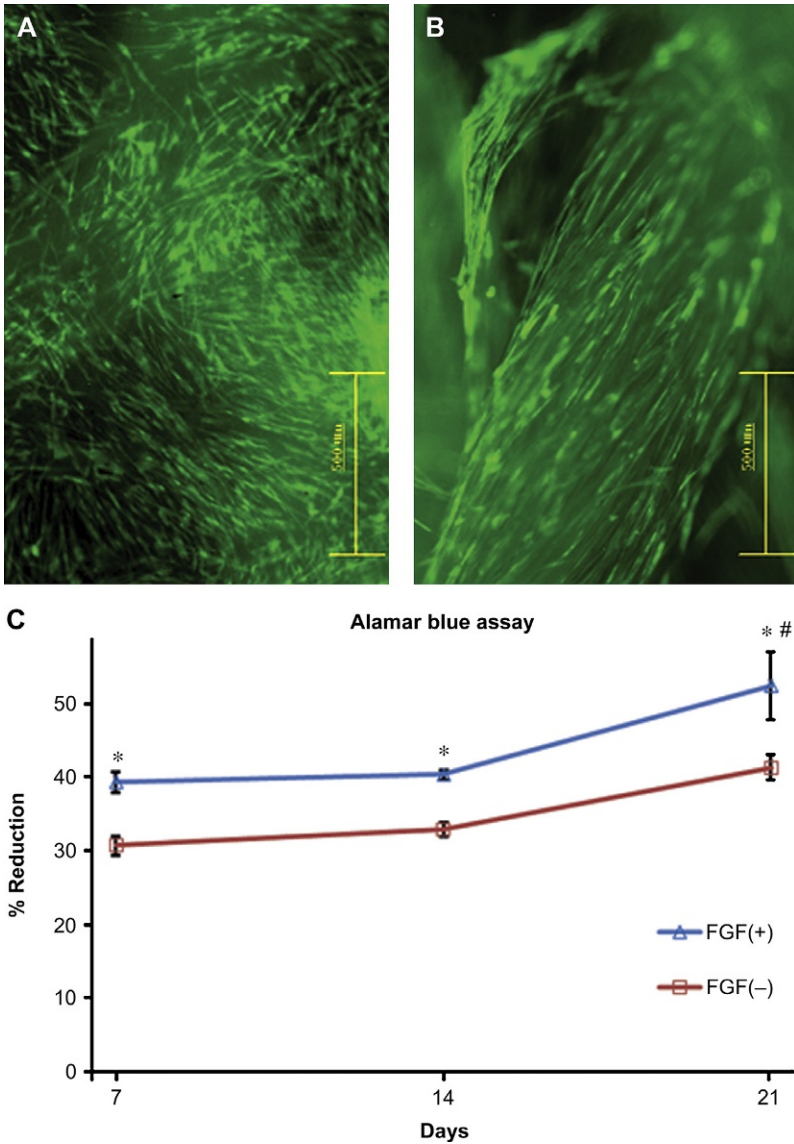


Fig. 10.5 Fluorescence microscopy showed FDA-stained cells proliferating on the electrospun fibrous surface (A) and the knitted microfibers (B) of the biohybrid scaffold. (C) Alamar Blue assay showing consistently and significantly higher cell viability on FGF(+) group ($*P < 0.05$, student's *t*-test), with cell proliferation increasing significantly (#, ANOVA and post hoc Tukey's tests) in both scaffold groups during the third week of culture.

Reused with permission from Sahoo S, Toh SL, Goh JC. A bFGF silk/PLGA-based biohybrid scaffold for ligament/tendon tissue engineering using mesenchymal progenitor cells. *Biomaterials* 2010;3(11):2990–8, copyright Elsevier.

engineering [112]. Highly aligned fibers covered the knitted scaffolds, and bone marrow mesenchymal stem cells oriented along the direction of fiber alignment with similar morphology to ligaments. On the other hand, Cardwell et al. studied the effect of fiber diameter and alignment on the mesenchymal stem cell differentiation into the tendon/ligament lineage [113] and demonstrated that fiber diameter affects cellular behavior more significantly than fiber alignment. Electrospun poly(esterurethane urea) matrices with small (less than 1 mm), medium (1-2 mm), or large (more than 2 mm) fiber diameters were fabricated and cultured with C3H10T1/2 model stem cells. They demonstrated that small-diameter electrospun fibers, regardless of orientation, enhanced the initial cell density on the scaffolds, while larger diameter scaffolds facilitated the gene expression levels. Yin et al. fabricated aligned or randomly oriented PLA nanofibers and seeded human tendon stem/progenitor cells onto the scaffolds [114] (Fig. 10.6). The expression of tendon-specific genes was found to be significantly higher on aligned nanofibers compared with the randomly oriented nanofibers, and the *in vivo* experiments showed that the aligned nanofibers induced the formation of tendon-like tissue.

10.6 Conclusions

Electrospun nanofibrous scaffolds have attracted great attention in the last fifteen years as promising materials in tissue regeneration, including bone and tendon/ligament repair. Nanofibers fabricated by electrospinning mimic very well the original extracellular matrix structure; therefore, the scaffolds prepared by electrospinning demonstrated great enhancements in the adhesion, proliferation, and differentiation of cells/stem cells. In addition, the electrospinning system enables to prepare aligned nanofibers, which can be preferentially used for the regeneration of tissues such as tendons and ligaments that have parallel-structured collagen fibers. Significant improvement has been achieved in the reconstruction of bone defects by using electrospun nanofibers. Electrospinning enabled to prepare combination of polymeric matrices with hydroxyapatite, growth factors, genes, and drugs that improved the functionality of the scaffolds and therefore supported formation of new bone tissue. In recent years, electrospun nanofibers and their composites with nanoparticles, carbon nanotubes, and nanodiamonds were developed to increase the functionality of the scaffolds for bone regeneration applications. Although the toxic effects of those nanoparticles are still being evaluated in the scientific area, the number of the studies related to the fabrication and *in vitro* and *in vivo* characterization of these nanofiber nanoparticle composites is expected to be increased. Nanofibrous electrospun scaffolds for tendon and ligament tissue engineering have attracted considerable interest in the last years, due to the electrospun nanofibers' desirable properties providing an adequate environment for cell differentiation, resulting in the expression of tendon-/ligament-specific genes and formation of tendon-/ligament-like tissues. Tendons and ligaments are tissues with very poor healing capacity. Although the number of studies related to the use of electrospun scaffolds in tendon/ligament regeneration is still limited, due to the promising results of the previous studies, more developments in this

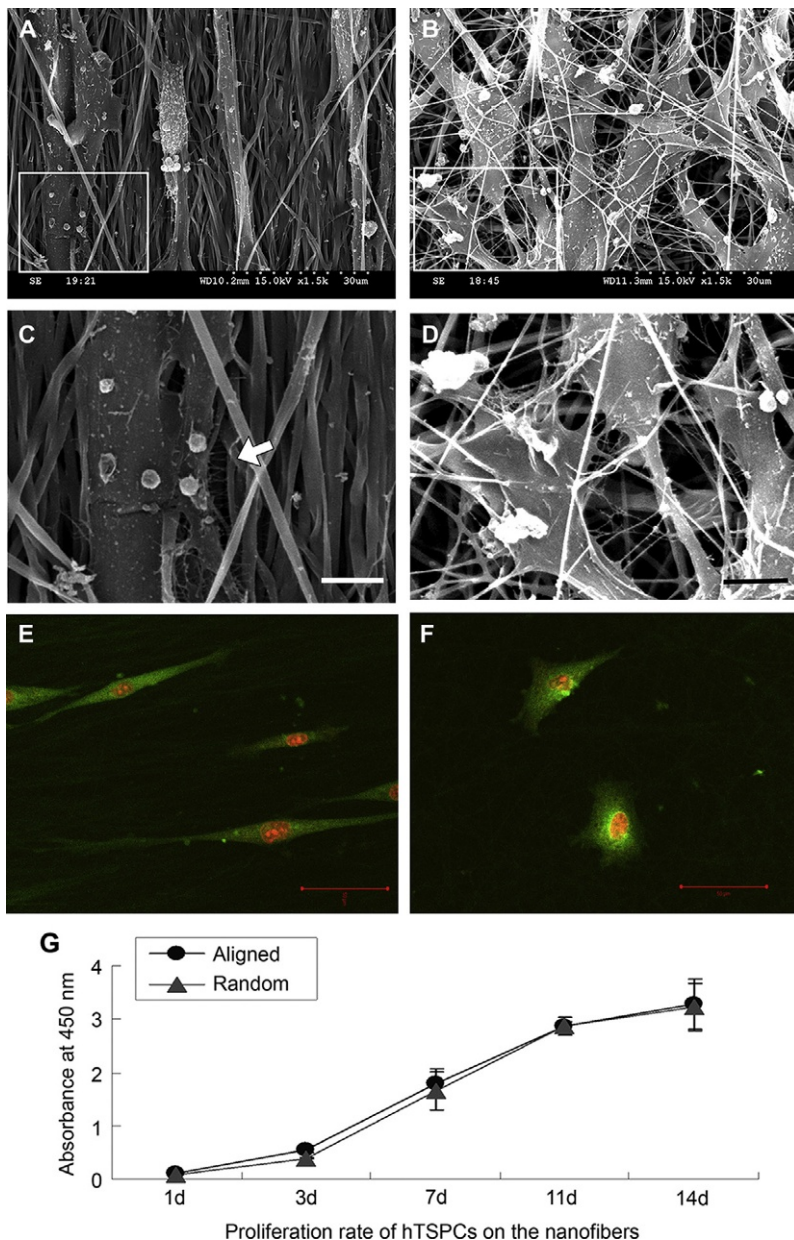


Fig. 10.6 Morphological changes of human tendon stem/progenitor cells (hTSPCs) growing on the scaffolds. (A) and (B) show hTSPCs cultured on the aligned and randomly oriented scaffold, respectively. (C) and (D) high magnification of boxed areas in (A) and (B) show the cell-matrix adhesion between hTSPCs and PLLA nanofibers. Arrow in (C) indicates filament-like structure on aligned scaffold. (E) Confocal micrograph of CFDA-stained elongated hTSPCs on the aligned scaffold. (F) Confocal micrograph showing the morphological change of CFDA-stained hTSPCs on the randomly oriented scaffold. (G) Cell proliferation on the aligned and randomly oriented scaffolds. Scale bars, 30 mm (A and B), 5 mm (C and D), and 50 mm (E and F). Reused with permission from Yin Z, Chen X, Chen JL, Shen WL, Nguyen TMH, Quayang HW, et al. The regulation of tendon stem cell differentiation by the alignment of nanofibers. *Biomaterials* 2010;31:2163–75, copyright Elsevier.

area are being expected in the future to contribute to the engineering of tendon and ligament tissues.

Although significant progress has been made to develop the desired kind of electrospun fibrous scaffolds for tissue engineering applications, the number of electrospun scaffolds in market is very few. Some of the electrospun products prepared and marketed by some companies are ReBOSSIS synthetic bone by ORTHOREBIRTH, ReDura™ Dural Patch by MEDPRIN, AVflo™ Vascular Access Graft by Nicast, HealSmart™ Personalized Antimicrobial Dressing by PolyRemedy, and Papyrus Coronary Balloon-Expandable Stent System by BIOTRONIK. The number of commercially already available products from electrospun nanofibers in the market for biomedical application is very low. The reasons are low mechanical properties of electrospun nanofibers, their limitation for 3D applications, their pore size that is smaller than a cellular diameter that cannot allow cell migration within the structure, and low yield of the electrospinning process. In order to overcome these issues, additive manufacturing techniques in combination with electrospinning and 3D electrospinning can be applied in achieving the desired 3D structured scaffolds with adequate mechanical properties and porosity.

Acknowledgment

The author declares that no conflict of interests exist in relation to the writing of this chapter.

References

- [1] Langer R, Vacanti JP. Tissue engineering. *Science* 1993;260(5110):920–6.
- [2] Huttmacher DW. Scaffolds in tissue engineering bone and cartilage. *Biomaterials* 2000;21(24):2529–43.
- [3] Laurencin CT, Freeman JW. Ligament tissue engineering: an evolutionary materials science approach. *Biomaterials* 2005;26(36):7530–6.
- [4] Stevens MM. Biomaterials for bone tissue engineering. *Mater Today* 2008;11(5):18–25.
- [5] Ma Z, Kotaki M, Inai R, Ramakrishna S. Potential of nanofiber matrix as tissue-engineering scaffolds. *Tissue Eng* 2005;11(1–2):101–9.
- [6] Smith LA, Ma PX. Nano-fibrous scaffolds for tissue engineering. *Colloid Surf B Biointerf* 2004;39(3):125–31.
- [7] Woo KM, Jun JH, Chen VJ, Seo J, Baek JH, Ryoo HM, et al. Nano-fibrous scaffolding promotes osteoblast differentiation and biomineralization. *Biomaterials* 2007;28(2):335–43.
- [8] Li C, Vepari C, Jin H-J, Kim HJ, Kaplan DL. Electrospun silk-BMP-2 scaffolds for bone tissue engineering. *Biomaterials* 2006;27(16):3115–24.
- [9] Kolambkar YM, Dupont KM, Boerckel JD, Huebsch N, Mooney DJ, Huttmacher DW, et al. An alginate-based hybrid system for growth factor delivery in the functional repair of large bone defects. *Biomaterials* 2011;32(1):65–74.
- [10] Sahoo S, Ang LT, Goh JC, Toh SL. Growth factor delivery through electrospun nanofibers in scaffolds for tissue engineering applications. *J Biomed Mater Res Part A* 2010;93(4):1539–50.
- [11] Kim G, Kim W. Highly porous 3D nanofiber scaffold using an electrospinning technique. *J Biomed Mater Res B Appl Biomater* 2007;81(1):104–10.

- [12] Wang J, Valmikinathan CM, Liu W, Laurencin CT, Yu X. Spiral-structured, nanofibrous, 3D scaffolds for bone tissue engineering. *J Biomed Mater Res A* 2010;93(2):753–62.
- [13] Wang JHC. Mechanobiology of tendon. *J Biomech* 2006;39(9):1563–82.
- [14] Goh JC, Ouyang H, Teoh S, Chan CKC, Lee E-H. Tissue-engineering approach to the repair and regeneration of tendons and ligaments. *Tissue Eng* 2003;9(suppl 1):S31–44.
- [15] Li WJ, Mauck RL, Cooper JA, Yuan X, Tuan RS. Engineering controllable anisotropy in electrospun biodegradable nanofibrous scaffolds for musculoskeletal tissue engineering. *J Biomech* 2007;40(8):1686–93.
- [16] Lee CH, Shin HJ, Cho IH, Kang YM, Kim IA, Park KD, et al. Nanofiber alignment and direction of mechanical strain affect the ECM production of human ACL fibroblast. *Biomaterials* 2005;26(11):1261–70.
- [17] Shi S, Kirk M, Kahn AJ. The role of type I collagen in the regulation of the osteoblast phenotype. *J Bone Miner Res* 1996;11(8):1139–45.
- [18] McKee MD, Glimcher MJ, Nanci A. High-resolution immunolocalization of osteopontin and osteocalcin in bone and cartilage during endochondral ossification in the chicken tibia. *Anat Rec* 1992;234(4):479–92.
- [19] Bab I, Ashton BA, Gazit D, Marx G, Williamson MC, Owen ME. Kinetics and differentiation of marrow stromal cells in diffusion chambers *in vivo*. *J Cell Sci* 1986;84:139–51.
- [20] Skerry TM, Bitensky L, Chayen J, Lanyon LE. Early strain-related changes in enzyme activity in osteocytes following bone loading *in vivo*. *J Bone Miner Res* 1989;4(5):783–8.
- [21] Vaes G. Cellular biology and biochemical mechanism of bone resorption. A review of recent developments on the formation, activation, and mode of action of osteoclasts. *Clin Orthop Relat Res* 1988;231:239–71.
- [22] Baron R. Molecular mechanisms of bone resorption by the osteoclast. *Anat Rec* 1989;224:317–24.
- [23] Trippel SB. Potential role of insulin like growth factors in fracture healing. *Clin Orthop Relat Res* 1998;355(suppl):S301–13.
- [24] Bose S, Roy M, Bandyopadhyay A. Recent advances in bone tissue engineering scaffolds. *Trends Biotechnol* 2012;30(10):546–54.
- [25] Hutmacher DW, Sittinger M, Risbud MV. Scaffold-based tissue engineering: rationale for computer-aided design and solid free-form fabrication systems. *Trends Biotechnol* 2004;22(7):354–62.
- [26] Mikos AG, Thorsen AJ, Czerwonka LA, Bao Y, Langer R, Winslow DN, et al. Preparation and characterization of poly(L-lactic acid) foams. *Polymer (Guildf)* 1994;35(5):1068–77.
- [27] Mooney DJ, Baldwin DF, Suh NP, Vacanti JP, Langer R. Novel approach to fabricate porous sponges of poly(D,L-lactic-co-glycolic acid) without the use of organic solvents. *Biomaterials* 1996;17(14):1417–22.
- [28] Nam YS, Park TG. Porous biodegradable polymeric scaffolds prepared by thermally induced phase separation. *J Biomed Mater Res* 1999;47(1):8–17.
- [29] Liu X, Ma PX. Polymeric scaffolds for bone tissue engineering. *Ann Biomed Eng* 2004;32(3):477–86.
- [30] Jang JH, Castano O, Kim HW. Electrospun materials as potential platforms for bone tissue engineering. *Adv Drug Deliv Rev* 2009;16(12):1065–83.
- [31] Pham QP, Sharma U, Mikos AG. Electrospinning of polymeric nanofibers for tissue engineering applications: a review. *Tissue Eng* 2006;12(5):1197–211.
- [32] Meng ZX, Wang YS, Ma C, Zheng W, Li L, Zheng YF. Electrospinning of PLGA/gelatin randomly-oriented and aligned nanofibers as potential scaffold in tissue engineering. *Mater Sci Eng C* 2010;30(8):1204–10.

- [33] Cipitria A, Skelton A, Dargaville TR, Dalton PD, Hutmacher DW. Design, fabrication and characterization of PCL electrospun scaffolds—a review. *J Mater Chem* 2011;93(ii):1539–50.
- [34] Prabhakaran MP, Venugopal J, Chan CK, Ramakrishna S. Surface modified electrospun nanofibrous scaffolds for nerve tissue engineering. *Nanotechnology* 2008;19:455102.
- [35] Ma Z, He W, Yong T, Ramakrishna S. Grafting of gelatin on electrospun poly(caprolactone) nanofibers to improve endothelial cell spreading and proliferation and to control cell orientation. *Tissue Eng* 2005;11(7–8):1149–58.
- [36] Chong EJ, Phan TT, Lim IJ, Zhang YZ, Bay BH, Ramakrishna S, et al. Evaluation of electrospun PCL/gelatin nanofibrous scaffold for wound healing and layered dermal reconstitution. *Acta Biomater* 2007;3(3 SPEC. ISS):321–30.
- [37] Prabhakaran MP, Venugopal JR, Ter Chyan T, Hai LB, Chan CK, Lim AY, et al. Electrospun biocomposite nanofibrous scaffolds for neural tissue engineering. *Tissue Eng Part A* 2008;14(11):1787–97.
- [38] Mo XM, Xu CY, Kotaki M, Ramakrishna S. Electrospun P(LLA-CL) nanofiber: a biomimetic extracellular matrix for smooth muscle cell and endothelial cell proliferation. *Biomaterials* 2004;25(10):1883–90.
- [39] Grafahrend D, Lleixa Calvet J, Salber J, Dalton PD, Moeller M, Klee D. Biofunctionalized poly(ethylene glycol)-block-poly(epsilon-caprolactone) nanofibers for tissue engineering. *J Mater Sci Mater Med* 2008;19(4):1479–84.
- [40] Yoshimoto H, Shin YM, Terai H, Vacanti JP. A biodegradable nanofiber scaffold by electrospinning and its potential for bone tissue engineering. *Biomaterials* 2003;24(12):2077–82.
- [41] Shin M, Yoshimoto H, Vacanti JP. In vivo bone tissue engineering using mesenchymal stem cells on a novel electrospun nanofibrous scaffold. *Tissue Eng* 2004;10(1–2):33–41.
- [42] Prabhakaran MP, Venugopal J, Ramakrishna S. Electrospun nanostructured scaffolds for bone tissue engineering. *Acta Biomater* 2009;5(8):2884–93.
- [43] Zhou C, Shi Q, Guo W, Terrell L, Qureshi AT, Hayes DJ, et al. Electrospun bio-nanocomposite scaffolds for bone tissue engineering by cellulose nanocrystals reinforcing maleic anhydride grafted PLA. *ACS Appl Mater Interf* 2013;5(9):3847–54.
- [44] Shao S, Zhou S, Li L, Li J, Luo C, Wang J, et al. Osteoblast function on electrically conductive electrospun PLA/MWCNTs nanofibers. *Biomaterials* 2011;32(11):2821–33.
- [45] Jose MV, Thomas V, Dean DR, Nyairo E. Fabrication and characterization of aligned nanofibrous PLGA/Collagen blends as bone tissue scaffolds. *Polymer* 2009;50(15):3778–85.
- [46] Song JH, Kim HE, Kim HW. Electrospun fibrous web of collagen-apatite precipitated nanocomposite for bone regeneration. *J Mater Sci Mater Med* 2008;19(8):2925–32.
- [47] Catledge SA, Clem WC, Shrikishen N, Chowdhury S, Stanishevsky AV, Koopman M, et al. An electrospun triphasic nanofibrous scaffold for bone tissue engineering. *Biomed Mater* 2007;2(2):142–50.
- [48] Ravichandran R, Venugopal JR, Sundararajan S, Mukherjee S, Ramakrishna S. Precipitation of nanohydroxyapatite on PLLA/PBLG/Collagen nanofibrous structures for the differentiation of adipose derived stem cells to osteogenic lineage. *Biomaterials* 2012;33(3):846–55.
- [49] Zeugolis DI, Khew ST, Yew ESY, Ekaputra AK, Tong YW, Yung LYL, et al. Electro-spinning of pure collagen nano-fibres—just an expensive way to make gelatin? *Biomaterials* 2008;29(15):2293–305.
- [50] Sisson K, Zhang C, Farach-Carson MC, Chase DB, Rabolt JF. Fiber diameters control osteoblastic cell migration and differentiation in electrospun gelatin. *J Biomed Mater Res A* 2010;94(4):1312–20.

- [51] Rajzer I, Rom M, Menaszek E, Pasierb P. Conductive PANI patterns on electrospun PCL/gelatin scaffolds modified with bioactive particles for bone tissue engineering. *Mater Lett* 2015;138:60–3.
- [52] Gupta D, Venugopal J, Mitra S, Giri Dev VR, Ramakrishna S. Nanostructured bio-composite substrates by electrospinning and electro spraying for the mineralization of osteoblasts. *Biomaterials* 2009;30(11):2085–94.
- [53] Kim H-W, Lee H-H, Knowles JC. Electrospinning biomedical nanocomposite fibers of hydroxyapatite/poly(lactic acid) for bone regeneration. *J Biomed Mater Res A* 2006;79(3):643–9.
- [54] Zhang Y, Venugopal JR, El-Turki A, Ramakrishna S, Su B, Lim CT. Electrospun biomimetic nanocomposite nanofibers of hydroxyapatite/chitosan for bone tissue engineering. *Biomaterials* 2008;29(32):4314–22.
- [55] Kim H-W, Song J-H, Kim H-E. Nanofiber generation of gelatin-hydroxyapatite biomimetics for guided tissue regeneration. *Adv Funct Mater* 2005;15(12):1988–94.
- [56] Xu X, Chen X, Liu A, Hong Z, Jing X. Electrospun poly(L-lactide)-grafted hydroxyapatite/ poly(L-lactide) nanocomposite fibers. *Eur Polym J* 2007;43(8):3187–96.
- [57] Thomas V, Dean DR, Jose MV, Mathew B, Chowdhury S, Vohra YK. Nanostructured bio-composite scaffolds based on collagen coelectrospun with nanohydroxyapatite. *Biomacromolecules* 2007;8(2):631–7.
- [58] Thomas V, Jagani S, Johnson K, Jose MV, Dean DR, Vohra YK, et al. Electrospun bio-active nanocomposite scaffolds of polycaprolactone and nanohydroxyapatite for bone tissue engineering. *J Nanosci Nanotechnol* 2006;6(2):487–93.
- [59] Deng X-L, Sui G, Zhao M-L, Chen G-Q, Yang X-P. Poly(L-lactic acid)/hydroxyapatite hybrid nanofibrous scaffolds prepared by electrospinning. *J Biomater Sci Polymer Edn* 2007;18(1):117–30.
- [60] Jose MV, Thomas V, Johnson KT, Dean DR, Nyairo E. Aligned PLGA/HA nanofibrous nanocomposite scaffolds for bone tissue engineering. *Acta Biomater* 2009;5(1):305–15.
- [61] Bianco A, Bozzo BM, Gaudio CD, Cacciotti I, Armentano I, Dottori M, et al. Poly (L-lactic acid)/calcium-deficient nanohydroxyapatite electrospun mats for bone marrow stem cell cultures. *J Bioact Compat Polym* 2011;26(3):225–41.
- [62] D'Angelo F, Armentano I, Cacciotti I, Tiribuzi R, Quattrocelli M, Fortunati E, et al. Tuning multi/pluri-potent stem cell fate by electrospun poly(L-lactic acid)-calcium-deficient hydroxyapatite nanocomposite mats. *Biomacromolecules* 2012;13(5):1350–60.
- [63] Phipps MC, Clem WC, Catledge SA, Jablonsky MJ, Hennessy KM, Thomas V, et al. Mesenchymal stem cell responses to bone-mimetic electrospun matrices composed of polycaprolactone, collagen I and nanoparticulate hydroxyapatite. *PLoS One* 2011;6(2), e16813.
- [64] Nie H, Wang C-H. Fabrication and characterization of PLGA/HAp compositescaffolds for delivery of BMP-2 plasmid DNA. *J Control Release* 2007;120(1–2):111–21.
- [65] Ito Y, Hasuda H, Kamitakahara M, Ohtsuki C, Tanihara M, Kang I-K, et al. A composite of hydroxyapatite with electrospun biodegradable nanofibers as a tissue engineering material. *J Biosci Bioeng* 2005;100(1):43–9.
- [66] Shin S-H, Purevdorj O, Castano O, Planell JA, Kim H-W. A short review: recent advances in electrospinning for bone tissue regeneration. *J Tissue Eng* 2012;3(1):1–11.
- [67] Yu H-S, Jang J-H, Kim T-I, Lee H-H, Kim H-W. Apatite-mineralized polycaprolactone nanofibrous web as a bone tissue regeneration substrate. *J Biomed Mater Res A* 2009;88(3):747–54.
- [68] Lin C-C, Fu S-J, Lin Y-C, Yang I-K, Gu Y. Chitosan-coated electrospun PLA fibers for rapid mineralization of calcium phosphate. *Int J Biol Macromol* 2014;68:39–47.

- [69] Liu W, Yeh Y-C, Lipner J, Xie J, Sung H-W, Thomopoulos S, et al. Enhancing the stiffness of electrospun nanofiber scaffolds with a controlled surface coating and mineralization. *Langmuir* 2011;27(15):9088–93.
- [70] Meng ZX, Li HF, Sun ZZ, Zheng W, Zheng YF. Fabrication of mineralized electrospun PLGA and PLGA/gelatin nanofibers and their potential in bone tissue engineering 2013;33(2):699–706.
- [71] He C, Xiao G, Jin X, Sun C, Ma PX. Electrodeposition on nanofibrous polymer scaffolds: Rapid mineralization, tunable calcium phosphate composition and topography. *Adv Funct Mater* 2010;20(20):3568–76.
- [72] Wang S, Zhao Y, Shen M, Shi X. Electrospun hybrid nanofibers doped with nanoparticles or nanotubes for biomedical applications. *Ther Deliv* 2012;3(10):1155–69.
- [73] Cao XD, Dong H, Li CM, Lucia LA. The enhanced mechanical properties of a covalently bound chitosan-multiwalled carbon nanotube nanocomposite. *J Appl Polym Sci* 2009;113(1):466–72.
- [74] Jeong JS, Moon JS, Jeon SY, Park JH, Alegaonkar PS, Yoo JB. Mechanical properties of electrospun PVA/MWNTs composite nanofibers. *Thin Solid Films* 2007;515(12):5136–41.
- [75] Volpato FZ, Ramos SLF, Motta A, Migliaresi C. Physical and in vitro biological evaluation of a PA 6/MWCNT electrospun composite for biomedical applications. *J Bioact Compat Polym* 2011;26(1):35–47.
- [76] Li X, Gao H, Uo M, Sato Y, Akasaka T, Abe S, et al. Maturation of osteoblast-like SaoS2 induced by carbon nanotubes. *Biomed Mater* 2009;4(1):015005.
- [77] Li X, Gao H, Uo M, Sato Y, Akasaka T, Feng Q, et al. Effect of carbon nanotubes on cellular functions in vitro. *J Biomed Mater Res A* 2009;91(1):132–9.
- [78] Zhang H. Electrospun poly (lactic-co-glycolic acid)/multiwalled carbon nanotubes composite scaffolds for guided bone tissue regeneration. *J Bioact Compat Polym* 2011;26(4):347–62.
- [79] McCullen SD, Stevens DR, Roberts WA, Clarke LI, Bernacki SH, Gorga RE. Characterization of electrospun nanocomposite scaffolds and biocompatibility with adipose-derived human mesenchymal stem cells. *Int J Nanomed* 2007;2(2):253–63.
- [80] Wilhelm C, Billotey C, Roger J, Pons JN, Bacri JC, Gazeau F. Intracellular uptake of anionic superparamagnetic nanoparticles as a function of their surface coating. *Biomaterials* 2003;24(6):1001–11.
- [81] Hadjipanayis CG, Bonder MJ, Balakrishnan S, Wang X, Mao H, Hadjipanayis GC. Metallic iron nanoparticles for MRI contrast enhancement and local hyperthermia. *Small* 2008;4(11):1925–9.
- [82] Shimizu K, Ito A, Arinobe M, Murase Y, Iwata Y, Narita Y, et al. Effective cell-seeding technique using magnetite nanoparticles and magnetic force onto decellularized blood vessels for vascular tissue engineering. *J Biosci Bioeng* 2007;103(5):472–8.
- [83] Nomura S, Takano-Yamamoto T. Molecular events caused by mechanical stress in bone. *Matrix Biol* 2000;19(2):91–6.
- [84] Wu Y, Jiang W, Wen X, He B, Zeng X, Wang G, et al. A novel calcium phosphate ceramic-magnetic nanoparticle composite as a potential bone substitute. *Biomed Mater* 2010;5(1):15001.
- [85] Meng J, Zhang Y, Qi X, Kong H, Wang C, Xu Z, et al. Paramagnetic nanofibrous composite films enhance the osteogenic responses of pre-osteoblast cells. *Nanoscale* 2010;2(12):2565–9.

- [86] Kotani H, Kawaguchi H, Shimoaka T, Iwasaka M, Ueno S, Ozawa H, et al. Strong static magnetic field stimulates bone formation to a definite orientation in vitro and in vivo. *J Bone Miner Res* 2002;17(10):1814–21.
- [87] Leesungbok R, Ahn S-J, Lee S-W, Choi J-J. The effects of a static magnetic field on bone formation around a SLA treated titanium implant. *J Oral Implantol* 2013;39:248–55.
- [88] Meng J, Xiao B, Zhang Y, Liu J, Xue H, Lei J, et al. Super-paramagnetic responsive nanofibrous scaffolds under static magnetic field enhance osteogenesis for bone repair in vivo. *Sci Rep* 2013;3:2655.
- [89] Wei Y, Zhang X, Song Y, Han B, Hu X, Wang X, et al. Magnetic biodegradable Fe₃O₄/CS/PVA nanofibrous membranes for bone regeneration. *Biomed Mater* 2011;6(5):055008.
- [90] Singh RK, Patel KD, Lee JH, Lee E-J, Kim J-H, Kim T-H, et al. Potential of magnetic nanofiber scaffolds with mechanical and biological properties applicable for bone regeneration. *PLoS One* 2014;9(4)e91584.
- [91] Xu H, Ning G. Magnetic responsive scaffolds and magnetic fields in bone repair and regeneration. *Front Mater Sci* 2014;8(1):20–31.
- [92] Amaral M, Dias AG, Gomes PS, Lopes MA, Silva RF, Santos JD, et al. Nanocrystalline diamond: in vitro biocompatibility assessment by MG 63 and human bone marrow cells cultures. *J Biomater Res A* 2008;87(1):91–9.
- [93] Grausova L, Kromka A, Burdikova Z, Eckhardt A, Rezek B, Vacik J, et al. Enhanced growth and osteogenic differentiation of human osteoblast-like cells on boron-doped nanocrystalline diamond thin films. *PLoS One* 2011;6(6)e20943.
- [94] Schrand AM, Dai L, Schlager JJ, Hussain SM, Osawa E. Differential biocompatibility of carbon nanotubes and nanodiamonds. *Diam Relat Mater* 2007;16(12):2118–23.
- [95] Serafim A, Cecoltan S, Lungu A, Vasile E, Iovuac H, Stancu IC. Electrospun fish gelatin fibrous scaffolds with improved biointeractions due to carboxylated nanodiamond loading. *RSC Adv* 2015;5:95467–77.
- [96] Parizek M, Douglas TE, Novotna K, Kromka A, Brady MA, Renzing A, et al. Nanofibrous poly(lactide-co-glycolide) membranes loaded with diamond nanoparticles as promising substrates for bone tissue engineering. *Int J Nanomed* 2012;7:1931–51.
- [97] Salaam AD, Dean D. Electrospun polycaprolactone-nanodiamond composite scaffolds for bone tissue engineering. In: *Proceedings of NEMB2010, 1st Global Congress on Nanoengineering for Medicine and Biology, 2010, USA; 2010.*
- [98] Srouji S, Ben-David D, Lotan R, Livne E, Avrahami R, Zussman E. Slow-release human recombinant bone morphogenetic protein-2 embedded within electrospun scaffolds for regeneration of bone defect: in vitro and in vivo evaluation. *Tissue Eng A* 2011;17(3–4):269–77.
- [99] Li L, Zhou G, Wang Y, Yang G, Ding S, Zhou S. Controlled dual delivery of BMP-2 and dexamethasone by nanoparticle-embedded electrospun nanofibers for the efficient repair of critical-sized rat calvarial defect. *Biomaterials* 2015;37:218–29.
- [100] Lee JH, Park J-H, El-Fiqi A, Kim J-H, Yun Y-R, Jang J-H, et al. Biointerface control of electrospun fiber scaffolds for bone regeneration: engineered protein link to mineralized surface. *Acta Biomater* 2014;10(6):2750–61.
- [101] Zhao X, Komatsu DE, Hadjiargyrou M. Delivery of rhBMP-2 plasmid DNA complexes via a PLLA/collagen electrospun scaffold induces ectopic bone formation. *J Biomed Nanotechnol* 2016;12(6):1285–96.
- [102] Pişkin E, Işoğlu IA, Bölgen N, Vargel I, Griffiths S, Cavuşoğlu T, et al. In vivo performance of simvastatin-loaded electrospun spiral-wound polycaprolactone scaffolds in reconstruction of cranial bone defects in the rat model. *J Biomed Mater Res A* 2009;90(4):1137–51.

- [103] Kjaer M. Role of extracellular matrix in adaptation of tendon and skeletal muscle to mechanical loading. *Physiol Rev* 2004;84(2):649–98.
- [104] Robinson PS, Huang TF, Kazam E, Iozzo RV, Birk DE, Soslowky LJ. Influence of decorin and biglycan on mechanical properties of multiple tendons in knockout mice. *J Biomech Eng* 2005;127(1):181–5.
- [105] Hsu S-L, Liang R, Woo SL. Functional tissue engineering of ligament healing. *Sports Med Arthrosc Rehab Ther Technol* 2010;2:12.
- [106] Sahoo S, Toh SL, Goh JC. A bFGF silk/PLGA-based biohybrid scaffold for ligament/tendon tissue engineering using mesenchymal progenitor cells. *Biomaterials* 2010;3(11):2990–8.
- [107] Kuo CK, Marturano JE, Tuan RS. Novel strategies in tendon and ligament tissue engineering: advanced biomaterials and regeneration motifs. *Sports Med Arthrosc Rehabil Ther Technol* 2010;2:20.
- [108] Barber JG, Handorf AM, Allee TJ, Li WJ. Braided nanofibrous scaffold for tendon and ligament tissue engineering. *Tissue Eng Part A* 2013;19(11–12):1265–74.
- [109] Chainani A, Hippensteel KJ, Kishan A, Garrigues NW, Ruch DS, Guilak F, et al. Multilayered electrospun scaffolds for tendon tissue engineering. *Tissue Eng Part A* 2013;19(23–24):2594–604.
- [110] Sahoo S, Ouyang H, Goh JC-H, Tay TE, Toh SL. Characterization of a novel polymeric scaffold for potential application in tendon/ligament tissue engineering. *Tissue Eng* 2006;12(1):91–9.
- [111] James R, Kumbar SG, Laurencin CT, Balian G, Chhabra AB. Tendon tissue engineering: adipose-derived stem cell and GDF-5 mediated regeneration using electrospun matrix systems. *Biomed Mater* 2011;6:1–13.
- [112] Vaquette C, Kahn C, Frochet C, Nouvel C, Six J-L, Luo L-H, et al. Aligned poly(L-lactic-co-ε-caprolactone) electrospun microfibers and knitted structure: a novel composite scaffold for ligament tissue engineering. *J Biomed Mater Res A* 2010;94(4):1270–82.
- [113] Cardwell RD, Dahlgren LA, Goldstein AS. Electrospun fibre diameter, not alignment, affects mesenchymal stem cell differentiation into the tendon/ligament lineage. *J Tissue Eng Regen Med* 2014;8(12):937–45.
- [114] Yin Z, Chen X, Chen JL, Shen WL, Nguyen TMH, Quyang HW, et al. The regulation of tendon stem cell differentiation by the alignment of nanofibers. *Biomaterials* 2010;31:2163–75.

Electrospun scaffolds for vascular tissue engineering

11

O. Karaman, M. Şen, E.A. Demirci
Izmir Katip Celebi University, Izmir, Turkey

11.1 Introduction

Coronary artery and peripheral vascular diseases are the primary causes of death in the world. The treatment of vascular diseases generally involves cardiac and peripheral bypass surgeries in which the damaged segment of blood vessels is replaced by appropriate prosthetic vascular grafts [1]. Vascular graft transplantation is currently being done by using autologous grafts, allografts, xenografts, and artificial prostheses. The lack of tissue donor and anatomical variability limits the use of autologous grafts and allografts. Besides, the use of detergents and decellularizing agents prior to transplantation raises concerns regarding long-term biofunctionality of these vascular grafts. Xenografts suffer from short life span as the tissues of animals, such as pigs, age at a quicker rate than humans. As a result, patients, especially pediatric patients, will need their implants to be replaced every 10–15 years. There are also other limitations in their clinical use of such grafts including immune response, donor-site morbidity, poor control over physical and mechanical properties, and lack of availability [2,3]. As an alternative, nowadays, synthetic vascular grafts are being fabricated from polyurethane (PU), poly(tetrafluoroethylene) (ePTFE), and polyethylene terephthalate (Dacron) [4–6]. Even though the development of synthetic prosthetic grafts yielded a technology that has saved the lives of many, developing such grafts for vessels with a diameter less than 6 mm remains elusive, owing to thrombus formation, aneurysm, and compliance mismatch [7–9]. Over the last few decades, vascular tissue engineering has emerged as an alternative approach to overcome the limitations of above mentioned vascular grafts. Basically, biodegradable polymers are used as scaffold materials for cell seeding or encapsulation in this approach, where the polymers are degraded as the cells grow and produce extracellular matrix (ECM) to give rise to the desired tissue.

Typical tissue-engineering models for vascular graft applications require a three-dimensional (3-D) cell-supporting scaffold for cells to function during the formation of vascular tissue. An ideal tissue-engineered vascular scaffold should completely integrate with the surrounding vessels, exhibit sufficient mechanical strength, and function as a 3-D framework for endothelial progenitor cells (EPCs) to fabricate vascular matrix. In order to provide adequate 3-D structure and enable full integration into the site of the damaged vessels, a biomimetic scaffold should fulfill the following requirements: (a) it should mimic the physical and chemical properties of the natural blood vessels, (b) it should be biocompatible, (c) it should be porous to allow vascular

formation, (d) it should have appropriate surface chemistry and mechanical strength characteristics to support cellular attachment, proliferation, and differentiation, and (e) it should degrade simultaneously with the newly growing tissue. To overcome the drawbacks of nondegradable vascular grafts currently used in clinic, vascular tissue engineering presents an alternative approach for regeneration of native vascular tissue [10–12].

Many research groups have focused on designing tissue-engineered vascular grafts that mimic the structure of natural blood vessels by using different scaffold fabrication techniques such as molecular self-assembly, solvent-casting/particulate-leaching technique, thermally induced phase separation, and electrospinning [13]. Among these techniques, electrospinning has a great potential to mimic the structure of ECM of vascular tissue, which is composed of 50–500 nm diameter structural protein and polysaccharide fibers. Therefore, in recent years, the interest on the electrospun scaffolds for development of tissue-engineered vascular grafts has increased tremendously [14–16]. Although studies on the *in vivo* feasibility of electrospun scaffolds for vascular tissue engineering are currently in the early stages, recent reports have highlighted the potential use of electrospun scaffolds due to their tunable mechanical and biological properties [17,18]. In the proposed chapter, we are planning to present a summary of the most recent *in vitro* and *in vivo* applications of electrospun scaffolds for the development of tissue-engineered vascular grafts. Moreover, the structure of the blood vessels, design parameters, and materials used for fabrication as well as biological and mechanical properties of electrospun scaffolds will be discussed throughout the proposed chapter.

11.2 Structure of blood vessels

Mesoderm, which is one of the three primary germ layers, is sandwiched between the two other germ layers known as ectoderm and endoderm. Mesoderm layer cells grow and diversify to give rise to body's connective tissue, blood vessel, blood cells, and many other cell types. All cells in the body including cancerous cells need a blood supply for survival, and the blood supply vastly depends on endothelial cells (ECs). ECs are the primary cells that form the inner lining of a blood vessel and act as an anticoagulant barrier between the vessel wall and blood [19]. These cells are quite efficient in controlling their number and adapting local requirements. They can migrate almost every region of the body and have a pivotal role in wound-repairing system [20]. Because cancerous cells also need blood supply, discovering new drugs that are efficient in blocking formation of new blood cells will have a substantial impact on blocking tumor growth.

Blood is circulated throughout the body via blood vessels, and in this circulation, the heart plays a central role. The blood vessels that carry blood away from the heart are known as arteries and those carrying blood into the heart as veins. Basically, the heart pumps blood low in oxygen (deoxygenated blood) to the lungs for oxygenation and blood rich in oxygen (oxygenated blood) to the rest of the body to provide cells with oxygen. Therefore, blood is transported by veins and arteries in two different

circulatory paths: pulmonary circulation and systematic circulation. Pulmonary circulation is the circuit where pulmonary arteries carry deoxygenated blood into the lungs for oxygenation, and then pulmonary veins collect and transport oxygenated blood into the heart. On the other hand, systematic circulation is the circuit where arteries carry oxygenated blood from the heart to cells for respiration, and veins transport deoxygenated blood rich in CO_2 in reverse direction from cells to the heart. Arteries and veins branch into smaller blood vessels called arterioles and venules, respectively. These two different small blood vessels are connected to each other for a complete blood circulation through further branching into capillaries where nutrients and wastes are exchanged.

Although arteries and veins have different roles and slightly differ in structure, they all have some general features in common (blood vessel wall, lumen, etc.). All of the blood vessels have blood vessel wall as a common feature, but the structure of the wall differs in different blood vessels. The pressure of blood is higher in arteries and arterioles, and for this reason, they have thicker walls than veins and venules. The wall of the blood vessels is composed of three layers: tunica intima, tunica media, and tunica adventitia (Fig. 11.1). Tunica intima known as inner layer is made up of a thin sheet of ECs known as endothelium and subendothelial connective tissue. Endothelium is surrounded by a basal lamina, which is a layer of ECM secreted by the epithelial cells. ECs that are in direct contact with blood are called vascular ECs. Tunica media that is separated from tunica intima by internal elastic lamina consists of bundles of smooth muscle cells (SMCs) and elastic tissue. While ECs are responsible of forming the structure of blood vessels, SMCs contract or relax to regulate the caliber of the blood vessels and provide shear strength. Tunica adventitia also known as tunica externa is the outermost layer of the blood vessel wall mainly composed of collagen (COL) and elastic connective tissue [21]. In the case of the finest branches of the blood vessels known as capillaries, the blood vessel wall is solely composed of ECs, basal lamina, and a small quantity of contractile cells known as pericytes that wrap around the ECs [22]. ECs line all the blood vessels and are responsible for passing all of the

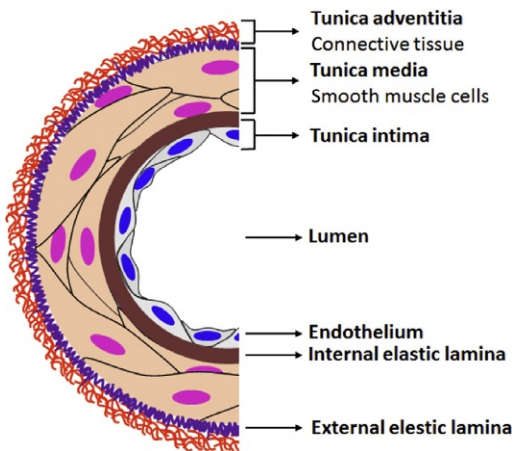


Fig. 11.1 Schematic cross-sectional view of a blood vessel structure. Both arteries and veins are composed of three layers: (i) tunica adventitia, (ii) tunica media, and (iii) tunica intima. ECs define the borders of the lumen, while smooth muscle and fibroblast cells cover the blood vessels on the exterior side.

molecules in and out of blood stream and transit of white blood cells. In the early development stages of embryo, small vessels made up of only ECs and basal lamina are formed first, and then based on the signals derived from ECs, these small vessels give rise to other blood vessels (arteries, veins, etc.) [23]. There are known to be three different mechanisms determining the fate of vessel growth: vascularization, angiogenesis, and arteriogenesis. Vascularization is defined as de novo EPC differentiation and assembly into capillary tubes, which involves six morphogenetic steps: (1) recruitment and differentiation of EPCs in a matrix that contains proper signaling factors (vascular endothelial growth factor (VEGF), placenta growth factor (PIGF), angiopoietin (Ang-1), cytokines, etc.); (2) EC quiescence; (3) EC activation, proliferation, and migration for vacuole and lumen formation; (4) EC differentiation for branching and sprouting and (5) formation of capillary tube networks; and lastly, (6) recruitment of SMCs for tube stabilization and maintenance through the use of some signaling factors (platelet-derived growth factor (PDGF), Ang-1, PDGF, protease inhibitors, etc.) [24]. All the vessels have a lumen through which blood flows. The lumen of arteries is smaller than the lumen of veins, a characteristic that contributes to the maintenance of the high blood pressure in arteries. Together, smaller diameter and thicker walls cause arteries to have a relatively round shape in cross section. Angiogenesis is the next process following vascularization and defined as sprouting of blood vessels from the existing vasculature. It starts in utero and occurs throughout life. Angiogenesis is essential to deliver nutrients and oxygen to metabolically active tissues. The last mechanism of vessel growth is arteriogenesis during which mural cells are recruited for stabilization of blood vessels. Arteriogenesis results in an increase in the diameter of existing arterial vessels.

11.2.1 Extracellular matrix

ECM architecture has a substantial impact on the formation of new blood capillaries. ECM serves not only as a structural support for vessel growth but also as an instrumental component that provides cues for guidance of new capillaries. The interaction of ECs with ECM and mural cells is essential for proper maturation and angiogenesis of the newly formed blood vessels [25]. Major components of ECM are glycosaminoglycans (GAGs) and fibrous proteins including COL, laminin, and fibronectin [26]. Basically, GAGs are carbohydrate polymers that are involved in the formation of heavily glycosylated proteins known as proteoglycans. Proteoglycans take part in regulating connective tissue structure and permeability along with trapping and storing growth factors that are essential for vessel growth and angiogenesis. During sprouting of the blood vessels, ECs release proteolytic enzymes, which play a central role in degradation of proteoglycans, thus releasing the growth factors incorporated into ECM such as VEGF [27,28]. Fibrous proteins serve as structural proteins and are among the major components of the connective tissue and blood vessel walls. Fibrous proteins and GAGs are organized in a highly ordered way to form a network that is closely associated with the ECs producing them. COL type IV and laminin are the main structural components of basal lamina providing support for ECs and separating them from adjacent perivascular cells. The fibrous protein elastin is known

to provide elasticity for tissues including the skin, lung, and blood vessels. It assembles as a cross-linked polymer on microfibrils to form elastic fibers and hardly undergoes remodeling [29]. A limited number of enzymes (elastase and matrix metalloproteinases) can catalyze the hydrolysis of elastin, which contributes to the longevity of elastin [30]. Elastic fibers basically modulate blood pressure through expansion and contraction.

11.2.2 Factors affecting vascularization

There are more than a dozen different proteins identified as factors influencing vascularization and angiogenesis. The most predominant factors are VEGF, angiogenin, hypoxia-inducible factor-1 α (HIF-1 α), basic fibroblast growth factor (bFGF), platelet-derived endothelial growth factor, transforming growth factor alpha (TGF- α) and beta (TGF- β), placental growth factor, hepatocyte growth factor, and epidermal growth factor (EGF). All the growth factors can bind ECM, which has profound therapeutic implications as ECM could be used for the delivery of these growth factors for proper vascularization [24]. Among these growth factors, VEGF (or VEGF-A) is known to be the most important proangiogenic factor that both regulates angiogenesis and modulates new blood vessel formation by stimulating proliferation, differentiation, migration, survival, and some other functions of ECs. Basically, VEGF is a 45 kDa heterodimeric heparin-binding protein that binds and activates tyrosine kinase receptors known as VEGF receptors (VEGFRs) located on the cell surface [31]. Signal transduction through VEGFRs upon VEGF binding leads to the formation of 3-D vascular tubes and regulation of the microvascular hyperpermeability, which characterizes the capacity of a blood vessel wall for diffusion of small molecules in and out of the blood vessels.

11.2.3 Required qualities of tissue-engineered blood vessels

The primary goal of engineering scaffolds for blood vessel formation is to fulfill all the requirements including elasticity, acellular porosity, controlled biodegradability, and other intrinsic properties of natural arteries to construct entirely biomimetic blood vessels [30]. To achieve this goal, a vigorous biotechnological process that will pave the way for clinical applications has to be developed. Considerable effort has been devoted to design biocompatible materials that do not only resemble the mechanical properties but also contain cues needed for regulation of cell growth and production of ECM. In this regard, artificial blood vessel scaffolds are required to have certain properties such as being resistant to thrombosis, a phenomenon referred to as the formation of blood clot inside a blood vessel, to be able to completely mimic natural blood vessels for regulation of cell behavior including cell adhesion, growth, and differentiation for the desired phenotype. Besides, scaffolds should also inhibit inflammation and formation of scar tissue, for which chemical, physical, and biological properties of the scaffold materials should be thoroughly investigated to comprehensively understand and modulate the interaction between cells and scaffold materials for proper vascularization. In this regard, many artificial and natural scaffolding materials have

been developed and modified with proangiogenic molecules capable of inducing capillary sprouting. However, guiding the growth of blood vessels for interconnectivity between capillary networks remains elusive, which could be addressed through the use of properly designed scaffolding materials [32]. Another issue that needs to be addressed is the high reproducibility and quality of tissue-engineered blood vessels for which it is important to design and use suitable bioreactors, where the external parameters including pH, temperature, and humidity can be precisely controlled. Bioreactors enable researchers to mimic the *in vivo* physiological conditions that are necessary for the production of vascular tissues with desired properties.

11.3 Biomaterials used for nanofiber fabrication in vascularization

There are a variety of natural and synthetic materials that have been used for fabrication of fibers in vascularization studies, and some of them are briefly described later.

11.3.1 Natural materials

The most common natural materials used for nanofiber fabrication can roughly be classified as proteins and polysaccharides. The most frequently used proteins include COL, fibronectin, fibrin, and decellularized ECM. As for the polysaccharides, chitosan (CS)/chitin and hyaluronic acid (HA) are the most commonly used natural scaffold materials. COL is a fibrous protein that serves as an extracellular structural protein in various connective tissues of animals. Because it is the most abundant protein in mammals forming 25%–30% of the whole body protein content, it has a pronounced biocompatibility property making its use in tissue-engineering studies advantageous. The protein can self-aggregate and cross-link to increase its strength, and its biodegradation can be tuned using enzymes like collagenase. Although there are known to be 19 different types of COL, mostly COL type I isolated from rat tail is used to create hydrogels. Incorporation of chemicals known to be influential for angiogenesis like VEGF into COL has been done to form functional 3-D tissues as it is illustrated in the following example. Hutmacher and his coworkers developed a hybrid mesh as a result of simultaneous deposition of poly(ϵ -caprolactone)-COL blend and HA using electrospinning, which enabled dual loading and controlled release of two potent angiogenic factors (VEGF₁₆₅ and PDGF) for the proper vascularization of the construct. Results show that fabrication of such hybrid scaffolds holds a great promise for attainment of 3-D vascularized tissue constructs [33]. The second most commonly used protein for vascular tissue-engineering scaffold materials is fibrin, which is converted from fibrinogen by the catalytic activity of thrombin. It has a pivotal role in blood clotting as it is the first scaffold formed by the body at the site of the wound. It has the property to bind to proteins including VEGF and fibronectin, which can affect the cell fate [34,35]. It has some advantages as opposed to other natural polymers as it can be retrieved from the patient's body, demonstrating better cell adhesion performance along with no immune response and toxicity. Its biodegradation can be tuned

using protease inhibitor apoptosis and cross-linking agents. Fibronectin, another commonly used protein in vascularization studies, is a major adhesive glycoprotein of ECM that binds to integrins known to be cell-membrane-spanning receptor proteins. Fibronectin plays a pivotal role in vascular morphogenesis during both normal development and angiogenesis as it is closely associated with angiogenesis sprouting [36]. It is mostly used to coat 2-D surfaces to enhance cell migration and endothelialization, an essential step for vascularization.

As it is stated above, there are some natural polysaccharides used in vascularization studies such as HA and chitin/CS. HA is a natural polysaccharide also referred to as a nonsulfated GAG composed of repeating disaccharides units of β -1,4-D-glucuronic acid- β -1,3-N-acetyl-D-glucosamine. HA is an essential ingredient of ECM and found abundantly in many parts of the body serving as a mediator in wound repair, cellular signal, matrix organization, and morphogenesis due to its biological and structural properties. Degradation of HA-based scaffolds and controlled release of their content are catalyzed by hyaluronidase in biological environments [37]. The stability of the HA gels can be tuned depending on the number of the cleavage sites and the amount of the enzymes available in the scaffold environment [38]. There are many research papers regarding the use of HA in developing new scaffold materials for vascularization [39–42]. Another frequently used polysaccharide in vascularization studies is CS known to be a linear polysaccharide composed of randomly distributed (1 \rightarrow 4)-2-acetamido-2-deoxy- β -D-glucan (N-acetyl-D-glucosamine) and (1 \rightarrow 4)-2-amino-2-deoxy- β -D-glucan (D-glucosamine) units. Basically, it is produced from chitin through sodium hydroxide treatment or enzymatic hydrolysis by enzymes capable of deacetylation of chitin such as chitin deacetylase [43]. Because CS has amino moieties, it can be chemically functionalized for tissue-engineering applications. It also can replace mucopolysaccharide, a major component of ECM, making it a suitable material for tissue-engineering scaffolds. Incorporation of CS into electrospun scaffolds enables angiogenesis and improves the blood compatibility of scaffolds [44].

11.3.2 Synthetic materials

Natural polymers have the biological properties needed for fine scaffolds such as biodegradation and cell adhesion; however, they exhibit poor mechanical properties and pose a risk for immunogenic reaction and infection. To address these drawbacks, synthetic polymers have emerged as an alternative to natural polymers for scaffolds in tissue-engineering studies. Poly-L-lactic acid, generally abbreviated as PLA or PLLA, is a biodegradable thermoplastic polyester known to be the most commonly used form of PLA in vascular tissue-engineered scaffolds. Poly(lactide-co-glycolide), also referred to as PLG, is a copolymer of PLA with another thermoplastic polyester polyglycolic acid (PGA). PLA and PLG are synthesized by ring-opening polymerization of glycolide and lactic acid, respectively, and they are by far the most frequently used synthetic materials to make scaffolds in tissue-engineering studies [45,46]. While *in vivo* degradation of PGA into water and carbon dioxide takes about 6 months, degradation of PLA takes a lot longer than that as it maintains its mechanical integrity for years. The two synthetic materials are approved by the Food and Drug

Administration (FDA) for clinical use. Polycaprolactone, also referred to as PCL, is another FDA-approved aliphatic polyester used in vascular tissue-engineering studies. Similar to PLG and PLLA, it is synthesized by ring-opening polymerization of ϵ -caprolactone. PCL is a biodegradable polymer with good mechanical and biocompatibility properties; all can be altered using a combination of techniques. Enzymatic degradation of this polymer through the hydrolysis of its ester linkage takes more than 1 year. Polyethylene glycol, also referred to as PEG, is basically a polyether compound with hydrophilic property. It can be used in a variety of medical applications including bioconjugation, surface modification, drug delivery, and tissue engineering due to its unique properties including, biocompatibility, nonimmunogenicity, and intrinsic resistance to protein adsorption. Although PEG is incapable of supporting cell growth as proteins cannot be adsorbed on it, it can be chemically modified to have the desired properties in tissue-engineering scaffolds [47,48]. Synthetic polymers have good mechanical and physical properties as they can be tuned; however, they are not as good as natural polymers in terms of biological performance. According to the results of a study performed by Walpoth and his coworkers [49], PCL vascular grafts did not show a good long-term performance in a rat abdominal aorta replacement model, despite the promising results they obtained in their previous report where PCL electrospun scaffolds demonstrated a good short-term performance inducing tissue regeneration as the scaffolds had high elongation and slow degradation. Upon infiltrating the scaffold wall, fibroblast cells differentiated into myoblast cells depositing a natural ECM and the macrophages secreting factors for angiogenic differentiation to induce neovascularization. In the latter study, the PCL electrospun scaffolds were used in a rat abdominal aorta replacement model for 18 months. Although the scaffolds showed promising results similar to the previous report for the first 6 months, the tissue regeneration showed a clear regression as a result of disappearance of macrophages and reduction of myofibroblast due to the lack of oxygen and nutrient. In order to overcome the drawbacks of both natural and synthetic polymers, hybrid materials made of natural and synthetic polymers could be designed, where the hybrid polymer possesses the good biological and mechanical properties of natural and synthetic polymers altogether.

11.4 Fabrication parameters for electrospun scaffolds

Scaffold properties and morphology are very important in tissue-engineering applications. There are mainly three fabrication parameters for electrospinning technique: solution parameters, processing parameters, and environmental parameters. All of these parameters have direct effect on fiber morphology and should be scrutinized carefully for correct application.

11.4.1 Solution parameters

There are several parameters that should be taken into account when preparing a polymer solution for fabrication of electrospun scaffolds such as polymer's concentration, molecular weight, viscosity, surface tension, and conductivity/surface charge density.

The concentration of polymer solution is directly associated with fiber characteristics. Low polymer concentration leads to the formation of nanobeads in electrospun scaffolds. Bead formation is not desired as it negatively affects the scaffold-cell interaction [50–52]. On the other hand, increasing the polymer concentration causes fiber diameter to increase, changing the characteristics of the scaffold such as porosity [52–54]. Porosity of the scaffold is important for cellular infiltration, especially for internal part of electrospun vascular scaffolds. Increasing the diameter of the fiber also increases the pore size. Therefore, the concentration of the polymer solution should be optimized for a desired case to fabricate uniform bead-free fibers. Molecular weight of the polymer determines rheological properties of the polymer solution [55]. At a constant concentration, lowering the molecular weight causes bead formation, whereas increasing the molecular weight increases the diameter of the fibers. In order to obtain continuous uniform fiber formation, high-molecular-weight polymers are preferred as they provide desired viscosity for the electrospinning process [56,57]. Viscosity is a crucial parameter in the formation of the desired fiber morphology. Concentration, molecular weight, and surface tension of the polymer directly affect the viscosity of the polymer solution [58]. The viscosity range for a continuous uniform fiber formation differs among different types of polymers. Generally, low viscosity is attributed to noncontinuous fiber formation with beads, while high viscosity contributes hard ejection of polymers jets from the polymer solution. Optimal viscosity for electrospinning should be determined beforehand for different polymer solutions [59,60]. Surface tension of the polymer solution is influenced by the solvent used for dissolving the polymer prior to electrospinning [61]. It is reported that on the one hand solvents with higher surface tension are not suitable for uniform fiber formation and, on the other hand, increasing the surface tension at a constant polymer concentration can help bead-free fiber formation in some cases [55,62]. Natural polymers generally have polyelectrolytic properties. It is important to have sufficient charged ions in polymer solution for efficient jet formation [63]. Solution conductivity is an important electrospinning parameter for controlling fiber diameter. Polymer solution should be conductive enough to be used in electrospinning for a continuous fiber formation. Increasing the conductivity of the solution between acceptable values does not only increase the charge but also reduces the fiber diameter. However, increasing the conductivity beyond the acceptable values creates strong electric fields leading to unstable electrospinning process and hereby poor fiber formation [58,64,65].

11.4.2 Processing parameters

There are a number of electrospinning process parameters that are quite influential for fabrication of uniform continuous fibers such as voltage, flow rate, collector material, needle-to-collector distance, and environmental factors (temperature, humidity, etc.). Voltage applied is one of the vital parameters of electrospinning process. The type of polymer and the solvent used in an electrospinning process determines the optimum voltage to obtain fiber with desired diameters; however, the influence of the voltage on the morphology is still under debate [66]. Several groups

demonstrated the positive influence of using higher voltages in order to increase fiber diameter [67,68]. In addition, increasing voltage amplitude dramatically could increase the risk for bead formation [50,67,69]. Flow rate is another important parameter for controlling fiber diameter. Because the polymer will have enough time for solidification, lower flow rate helps solidifying the polymer solution [69]. On the other hand, increasing the flow rate could cause beaded fiber formation due to insufficient drying time [58,69,70]. It should also be noted that high flow rate is attributed to the formation of fibers with larger diameters [63,71]. Collector in electrospinning process acts like a conductive substrate to collect formed fibers, and conductivity of the collector may alter fiber morphology. Wang et al. showed that collectors with less conductive areas could cause bead formation [72]. Aluminum foil is a commonly used collector material; however, it is comparably difficult to collect fibers from it at the end of the electrospinning process. Different types of collectors have been developed to solve this problem such as rotating rods or wheel [73], wire mesh [72], parallel or gridded bar [72], pin [74], and so on. The distance between tip and collector is another important process parameter that could be used to modulate the fiber polarization time. If the distance is too close, fibers cannot solidify before reaching the collector due to the limited time. On the other hand, longer distances might give rise to bead formation [54,75]. Environmental factors such as temperature and humidity can also affect fiber morphology during the electrospinning process [76]. Mit-Upatham et al. investigated the influence of temperature on fiber diameter, and according to their results, high temperature lowers the fiber diameter due to low viscosity [64]. Humidity is another environmental parameter that influences fiber morphology. Under low humidity conditions, polymer solution can dry and evaporate faster than usual, whereas fiber diameter conditions and the possibility of bead formation both increase under high humidity [77]. Therefore, all the electrospinning parameters should be diligently optimized for a desired case to minimize the risk of nanobead formation and hereby maximize the chance of continuously uniform fiber fabrication (Table 11.1).

11.5 Biological and mechanical properties of electrospun scaffolds for vascular tissue engineering

Vascular scaffolds should have proper biological and mechanical properties for long-term stability and able to support native vascular tissue formation. It is clear that many electrospun scaffolds developed by synthetic polymers have appropriate mechanical properties; however, they lack of biological cues that support cell adhesion and proliferation. Such limitations could be overcome with surface modification of synthetic polymers. In this section, surface modification techniques and their effects on mechanical properties of electrospun scaffolds are presented. In addition, cell sources used for growing in vitro 3-D vascular tissues with electrospun scaffolds are also discussed.

Table 11.1 A summary of fabrication parameters and conditions of electrospun vascular scaffolds

Electrospun materials				Mandrel			Process parameters				References
Material composition	Molecular weight (daltons)	Solvent (v/v)	Concentration (w/v) (%)	Material	Diameter	Speed (rpm)	Voltage (kV)	Flow rate (mL h ⁻¹)	Needle-mandrel distance (cm)	Needle size (gauge)	
PCL	70,000–90,000	TFE	14	SS	1.8 mm	2000	16	2	10	21	[78]
PCL-PCL-N ₃ (8:2)	80,000–2000	Methylene chloride/methanol (5:1)	25	SS	2 mm	N/A	11	8	11	N/A	[79]
PLLA	N/A	HFIP	19	Al	15 mm	15	12	1	12	N/A	[80]
P(LLA-CL) (1:1), COL/CS (9:1)	30,000–10,000	HFP/TFA (9:1)	8–6	SS	4 mm	300	14–20	0-1.6-0, 0.8-0-0.8	N/A	N/A	[81]
TPU-GO (%0.5, 1, 2)	N/A	DMF	10	Al	N/A	1500	20	0.5	20	18	[82]
PolyTHF	1000	HFP	6	PTFE	N/A	250	10	1.2	9	N/A	[83]
PCL-COL I (1:1)	N/A	HFP	18	SS	4.75 mm	5000	20	10	15	18	[84]
PCL, PVA-SA (1:1)	80,000	DCM-DMF (2:1), DIW	10–8	Copper	5 mm	300	15	1.2	15	20	[85]
CE-UPy-PLLCL + UPy-SDFα(R), CE-UPy-PLLCL + UPy-SDF1α(NR), CE-UPy-PLLCL	N/A	CHCl ₃ /HFIP (85:15)	15	N/A	18–2.1 mm	100	12–20	2–1.5	18–20	19	[86]
Pork gelatin type A	N/A	TFE	7–15	Al	N/A	95	22.5	2.5	20	18	[87]

Al, aluminum; CE-UPy-PLLCL, chain-extended UPy-poly(L-lactic acid caprolactone) diol; CHCl₃, chloroform; COL/CS, collagen/chitosan; DCM, dichloromethane; DIW, deionized water; DMF, N,N-dimethylformamide; GO, graphene oxide; HFIP, 1,1,1,3,3,3-hexafluoroisopropanol; HFP, 1,1,1,3,3,3-hexafluoro-2-propanol; PCL, polycaprolactone; PLLA, poly-L-lactic acid; PLLACL, poly-L-lactic acid-co-poly-ε-caprolactone; PolyTHF, polytetrahydrofuran; PTFE, ePTFE; PVA, polyvinylalcohol; SA, sodium alginate; SS, stainless steel; TFA, 2,2,2-trifluoroacetic acid; TFE, tetrafluoroethylene; TPU, Texin Rx85A.

11.5.1 Surface modification

Although synthetic polymers show extensive mechanical properties over natural polymers, they have major shortcomings such as thrombosis, intimal hyperplasia, calcification, chronic inflammation, and limited regeneration potential as mentioned above [88]. To overcome these limitations, mechanically durable synthetic nanofibers could be used to form the bulk structure of the vascular grafts. And to improve cell-scaffold interaction, biologically active peptides or natural polymers could be used for chemical modification of the scaffold surface [89]. Various surface modification techniques including wet-chemical modification, plasma treatment, coelectrospinning, and functional peptide grafting or coating with natural polymers are widely used to enhance the formation of the blood vessels [90]. Such surface-modified electrospun scaffolds can enhance anticoagulation, rapid endothelialization, and vascular regeneration. For instance, Zheng et al. developed small-diameter (2.2 mm) PCL-based electrospun vascular grafts functionalized with arginine-glycine-aspartic acid (RGD) peptide and implanted them in rabbit carotid arteries to investigate the healing characteristics of surface-modified scaffolds. It was shown that RGD-modified PCL grafts (PCL-RGD) were patent at 2- and 4-week time points, whereas 4 of the 10 nonmodified PCL grafts were occluded due to thrombus formation. Therefore, RGD functionalization of PCL scaffolds improved the vascular regeneration capacity of the grafts [91]. In another study, Gong et al. developed hybrid vascular grafts with PCL nanofibers to form natural decellularized small-diameter vessels with heparin-coated intimal surface. Mechanical characterization revealed that reinforcing the decellularized graft with PCL nanofibers significantly increases the tensile modulus. In addition, it was shown that all grafts after implantation in a rat abdominal aorta were patent for up to 6 weeks [88]. Similarly, Heo et al. immobilized COL type IV (COL-IV) to PLLA and developed vascular grafts to investigate the impact of surface modification on rapid endothelialization. It was shown that COL-IV immobilization significantly enhanced EC attachment, proliferation, and upregulation of endothelialization markers [92]. In addition to chemical surface coating of vascular grafts, there are some studies on coelectrospun of biologically active molecules with synthetic polymers. Chen et al. incorporated heparin and VEGF into the core of poly(L-lactic acid-co- ϵ -caprolactone) (P(LLA-CL)) core-shell nanofibers for anticoagulation and rapid endothelialization, respectively. The results confirmed that heparin released from the core-shell nanofibers acted as an anticoagulant, while VEGF enhanced EPC growth on fiber scaffolds [93].

Wet chemistry is another method that has been used for surface modification of synthetic nanofibers [94]. Wet-chemical modification is usually done by acidic or basic treatment of nanofiber surfaces, which leads to the hydrolysis of scaffold surface. Surface wetting properties that enhance cell attachment on the electrospun vascular grafts could be obtained by optimum modification conditions [95]. However, the hydrolysis process should carefully be optimized so that it doesn't affect bulk properties of nanofibers [17]. Zhu et al. demonstrated that wet-chemical surface

modification followed by grafting functional molecules on electrospun PCL nanofibers significantly increases human EC adhesion [96].

Treating nanofibers with plasma generates functional carboxyl or amine reactive groups on the surface that could potentially be used for conjugation of bioactive agents [97]. It should be noted that upon plasma treatment, reactive moieties remain on the surface for only few minutes, and for that conjugation, reaction must be done rapidly. Cheng et al. modified the surface of PLA fibrous nanofibers with plasma treatment for heparin conjugation. It was shown that plasma surface modification significantly improved heparin conjugation compared with wet-chemical technique. In vivo studies on Sprague-Dawley rats revealed that platelet attachment significantly decreased on heparin-immobilized scaffolds [97]. One of the major risks on artificial vascular grafts is thrombosis after implantation. Therefore, the surface properties of the vascular grafts should mimic the morphological and mechanical properties of vascular ECM. To this end, Savoji et al. modified the surface of electrospun poly(ethylene terephthalate) (PET) with amine-rich thin plasma. The results showed that modified PET scaffolds significantly improved the adhesion and growth of human umbilical vein endothelial cells (HUVEC) [98]. In another study, Guex et al. covalently conjugated VEGF on plasma surface-modified PCL electrospun nanofibers, which revealed that functionalizing PCL scaffolds with VEGF significantly improved EC proliferation compared with the unmodified scaffolds [99].

11.5.2 Mechanical properties

Electrospun vascular grafts developed by using natural polymers provide effective infiltration and adequate oxygen and nutrient supply. However, the major limitation of using decellularized and natural polymer-based vascular grafts is their inadequate mechanical properties, which is the main cause of failure [100,101]. The mechanical properties directly affect the success of electrospun vascular grafts and can be controlled by changing the fiber diameter, porosity, alignment, and natural-to-synthetic polymer ratio [17]. The studies in the recent literature mainly focus on fabricating electrospun vascular grafts having mechanical properties similar to native vessels [17]. Uniaxial tensile properties, burst strength, and compliance of vascular grafts should be critically characterized to be able to determine in vivo success of the vascular grafts [17,102–104].

Pore size of the electrospun vascular grafts is one of the main parameters that should be optimized during fabrication process. Small pore size could limit the infiltration of cells into the grafts and inhibit regeneration of the grafts into neoarteries [104]. Ju et al. fabricated PCL/COL bilayered scaffold that had larger pores in the outer layer to overcome the limited infiltration of SMC and smaller pores in the inner layer to enhance EC adhesion. They controlled the pore size of the grafts by changing the diameter of the electrospun fibers (diameter of the fibers: 0.27–4.45 μm). It was shown that increasing the fiber diameter increased the porosity of the grafts and decreased the Young's modulus from 2.03 MPa down to 0.26 MPa. The results demonstrated the positive impact

of bilayered scaffolds on the improved SMC infiltration throughout the outer layer and enhanced vascular regeneration of EC within the inner layer [105]. In another study, Wu et al. fabricated multilayered and blended poly(L-lactide-*co*-caprolactone) (P(LLA-CL)), COL, and CS-based electrospun tubular scaffold via bidirectional gradient electrospinning and regular electrospinning. P(LLA-CL), which is known to ensure mechanical integrity and slow degradation, was used to compose the middle layer of the multilayer scaffold. The outer and inner layer of the multilayer scaffold was composed of COL and CS in order to mimic the structure and components of natural ECM. The blended nanofibers were developed by electrospinning the mixture of P(LLA-CL)/COL/CS. The results revealed that the average pore size of the multilayered scaffold was larger than those of the blended scaffolds, mostly because of the middle layer of P(LLA-CL) fibers. It was also reported that the multilayered scaffold showed enhanced mechanical property and biocompatibility compared with the blended scaffolds. In addition, endothelialization of porcine iliac artery endothelial cells (PIECs) on the multilayered and blended scaffolds were investigated, respectively. Results demonstrated enhanced endothelialization of PIECs on the multilayered scaffolds due to bioactive inner layer [106].

Fiber orientation (aligned or random) is an important parameter that determines the mechanical properties of scaffolds [107,108]. For instance, McClure et al. developed tubular scaffolds composed of aligned and random PCL/polydioxanone (PDO)/silk fibroin. The results revealed that improving the alignment of the fibers by changing the mandrel rotation speed significantly increased the dynamic compliance, burst strength, and tensile modulus [109]. Additionally, not only the alignment of the fibers affects the mechanical properties, but also it influences the adhesion and proliferation of cells [110–113]. Wong et al. developed tubular scaffolds composed of aligned PU nanofibers. In order to mimic the viscoelastic properties of natural arteries, they blended PU with elastin and COL prior to nanofiber fabrication. In this study, unmodified PU scaffolds had an average Young's modulus of 27.26 ± 2.03 MPa. According to the results, COL and elastin blending had reverse effects on the Young's modulus of the scaffolds. Five percent COL and elastin blending resulted in an average Young's modulus of 57.32 ± 10.06 MPa and 20.24 ± 1.36 MPa, respectively. It was mentioned that the Young's modulus values became similar to those observed in the blood vessels by 5% elastin blending. Furthermore, the growth of SMCs when seeded on both COL-blended and elastin-blended scaffolds was significantly higher than that of PU. It was also observed that SMCs proliferated along the aligned nanofibers in a directional manner in each experimental group [112]. Similarly, Zhong et al. fabricated random and aligned PLGA/PCL hybrid electrospun scaffold and investigated how the alignment affects human vascular smooth muscle cells (HVSMCs) spreading on the nanofibers. They reported that HVSMCs spread along the direction of the electrospun nanofibrous scaffolds (Fig. 11.2A–F) [114]. In another study, Nezarati et al. fabricated nanofibrous PU vascular grafts with mechanical properties similar to native capillaries to prevent intimal hyperplasia. Here, researchers improved the mechanical properties of the scaffolds by increasing the alignment of the nanofibers [115].

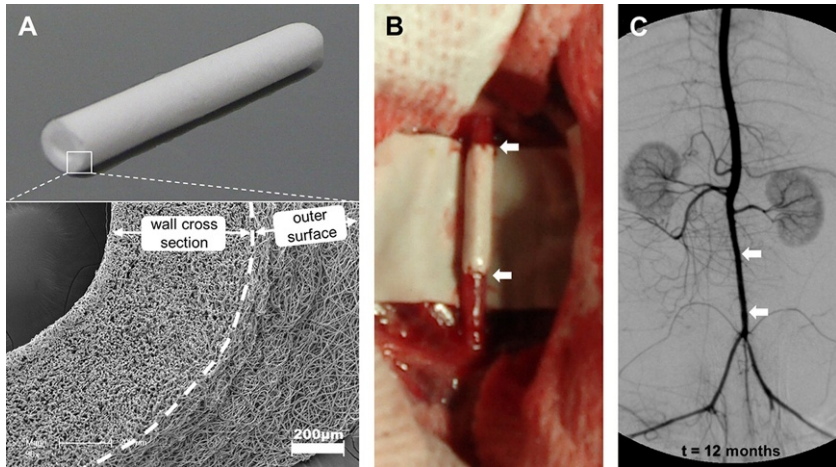


Fig. 11.2 Two millimeter inner diameter vascular grafts made of electrospun PCL micro- and nanofibers (A) were used for infrarenal abdominal aorta replacements in the rat model (B). Follow-up times were 1.5, 3, 6, 12, and 18 months (n 1/4 3 at each time point), and all grafts were patent by angiography and histology at all time points (C).

From De Valence S, Tille JC, Mugnai D, Mrowczynski W, Gurny R, Moller M, et al. Long term performance of polycaprolactone vascular grafts in a rat abdominal aorta replacement model. *Biomaterials* 2012;33:38–47, with permission from Elsevier.

11.5.3 Cell sources

Bone marrow mononuclear progenitor cells, HUVEC, mesenchymal stem cells (MSCs), SMCs, and EPCs are the cell sources that are commonly used in *in vitro* and *in vivo* vascular tissue-engineering applications [24,116]. Although using these cell lines individually or in cocultures showed promising results, the real impact of electrospun scaffolds remains elusive. Since physical and biological parameters directly affect adhesion, proliferation, and differentiation of the cells, more studies need to be performed to identify the ideal cell source combination when electrospun scaffolds are used as a vascular graft. Merkle et al. fabricated core-shell structure of tubular scaffolds by coaxial electrospinning. The core structure of the scaffold was composed of polyvinyl alcohol (PVA) for mechanical support, while the shell part composed of gelatin for biological cues. The results demonstrated that adhesion and spreading of HUVEC and rat SMC on this scaffold were significantly higher than those on PVA-based tubular scaffolds [117]. Similarly, Shalumon et al. fabricated aligned and random PLLA/gelatin hybrid electrospun scaffolds and investigated their potential to be used as vascular grafts. They reported that the viability and proliferation of seeded HUVECs and SMCs significantly increased by increasing the gelatin content. Moreover, the results showed that cellular orientation and elongation was controlled by the orientation of the fibers [118]. In another study, Ying et al. fabricated electrospun fibrous thermoplastic polyurethane (TPU)/graphene oxide (GO) scaffolds with different GO contents. They reported that the highest HUVEC attachment was

obtained at a 0.5 wt% GO loading. The results also showed that HUVEC-seeded electrospun scaffolds meet the mechanical requirements of vascular grafts [119]. In another study, Zhang et al. developed poly(propylene carbonate) electrospun tubular scaffolds and seeded bone marrow-derived MSCs. SEM imaging along with hematoxylin and eosin (H&E) staining was performed to characterize cell morphology and vascular tissue formation. The results revealed that cells completely integrated into the scaffolds and formed the 3-D cellular network at day 14 [120].

11.6 In vivo applications of tubular electrospun scaffolds in vascular tissue engineering

Here, only recent in vivo applications of electrospun vascular scaffolds were reviewed. Information about the previous in vivo applications of electrospun vascular scaffolds can be found in the following review chapters [17,18]. In some recent studies, the performance of cell-laden and acellular electrospun scaffolds has been evaluated in vivo. For instance, Zhu et al. developed a bilayered vascular scaffold and investigated the efficacy of the designed scaffold both in vitro and in vivo. The internal layer of the scaffold was composed of aligned PCL microfibers fabricated by wet spinning to provide guidance for the regeneration of aligned vascular smooth muscle cells (VSMCs), whereas the external layer of the scaffold was developed out of random PCL nanofibers to provide mechanical strength and prevent leakage of the blood. It was reported that elastic modulus and burst pressure of the tubular scaffolds were significantly enhanced after depositing the external layer. Microscopy images confirmed the cell infiltration inside the scaffolds and the alignment of the VSMCs along the aligned microfibers in a directional manner. Furthermore, the tubular scaffolds were implanted in a rat abdominal aorta, and the support of the scaffold on the vascular regeneration was evaluated. The results demonstrated that complete vascular regeneration was observed within three months with no thrombosis and intimal hyperplasia [121]. In another interesting study, Bergmeister et al. developed biodegradable TPU electrospun tubular scaffolds. The electrospinning conditions for scaffold fabrication were 9 cm needle-target distance, 2 cm target-back electrode distance, 0.02 mL min⁻¹ flow rate, 10 kV at the needle, and 250 rotations min⁻¹ of the mandrel. The in vitro and in vivo efficacy of the designed scaffold was determined by comparing commercially available ePTFE conduits. TPU tubular scaffolds were further characterized with scanning electron microscopy (SEM). It was observed that the scaffolds had an inner diameter of 1.6 mm and a mean wall thickness of $78 \pm 10 \mu\text{m}$ and composed of random fibers with the average diameter of $1.39 \pm 0.76 \mu\text{m}$ and a mean wall thickness of $78 \pm 10 \mu\text{m}$ (Fig. 11.2A). The in vitro biocompatibility results revealed that there was no EC adhesion on ePTFE after 24 h of incubation; however, TPU scaffolds significantly enhanced EC adhesion. Additionally, it was observed that TPU scaffolds had sufficient mechanical properties for in vivo implantation. Thereafter, the tubular scaffolds were implanted into the infrarenal aorta of inbred Sprague-Dawley rats. Upon the implantation, the implant showed reddened scaffold wall; however, no leakage was obtained (Fig. 11.3C). The results of the in vivo study

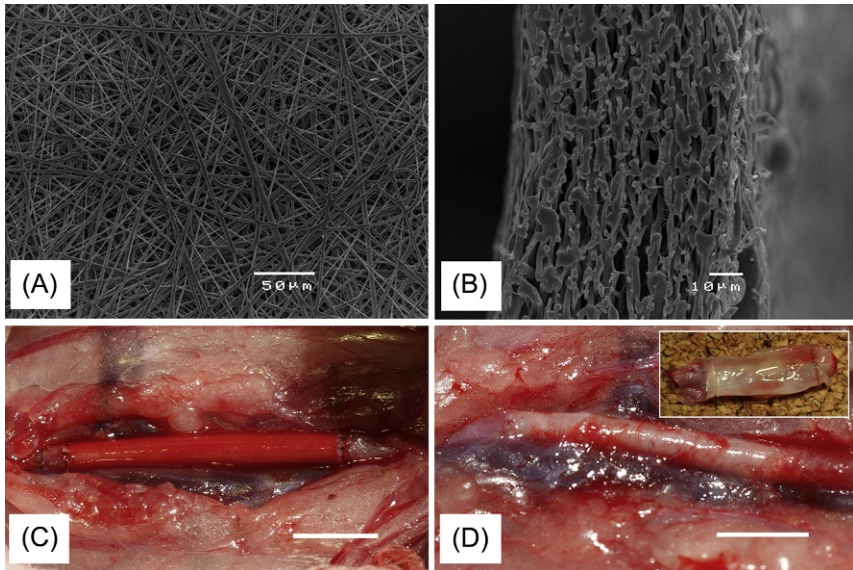


Fig. 11.3 Scanning electron microphotograph of the luminal surface (A) and wall thickness (B) of a TPU electrospun vascular scaffold. TPU scaffold immediately (C) and 12 months after implantation (D). Scale bars 6 mm.

Reproduced from Bergmeister H, Seyidova N, Schreiber C, Strobl M, Grasl C, Walter I, et al. Biodegradable, thermoplastic polyurethane grafts for small diameter vascular replacements. *Acta Biomater* 2015;11:104–13, with permission from Elsevier.

12 months after the implantation revealed that TPU scaffolds remained mechanically stable and showed complete integration in the surrounding tissue with no aneurysmal dilatation. In addition, the luminal surface was completely covered with neointima; therefore, no sign of thrombus formation appeared (Fig. 11.3D) [122].

Pu et al. also developed a bilayered PLA fibrous scaffolds consisting of a 30 μm thick aligned-fiber layer for mechanical support and 190 μm random fiber layer for cell infiltration and tissue growth (the schematic figure of designed scaffold is represented in Fig. 11.4A). They used two slowly rotating parallel disks as collectors with the following electrospinning parameters: gap between disks, 15 mm; voltage, 12 kV; and needle-tip-to-collector distance, 12 cm. The bilayered scaffold was characterized by scanning electron microscopy (Fig. 11.5B–C). Following the scaffold characterization, the biocompatibility and biological performance of the bilayer electrospun scaffolds were evaluated by in vivo experiments where scaffolds were implanted in Sprague-Dawley rats. In the study, significantly high (more than two times) cell infiltration was observed as compared with control scaffolds (single-layer scaffolds with random fibers) at 5- and 14-day samples (Fig. 11.4). Furthermore, besides the cell infiltration, the results also showed that COL fiber deposition, cell proliferation, and ingrowth of smooth muscles were significantly higher on the bilayered scaffolds

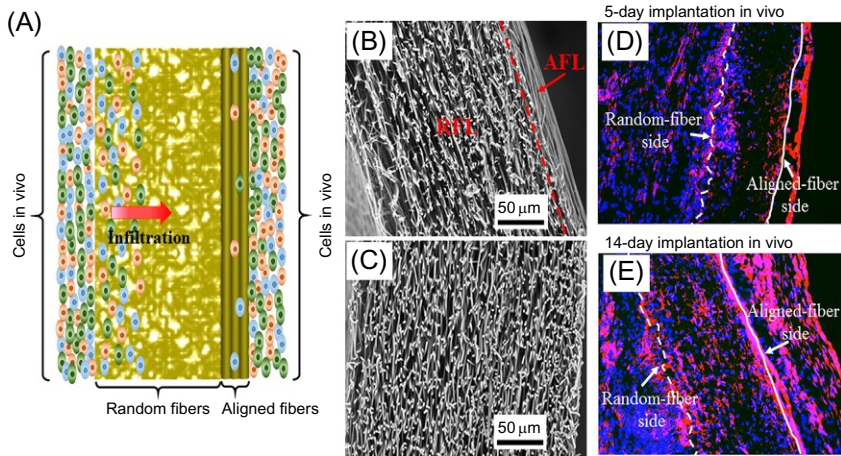


Fig. 11.4 Schematic figure of designed bilayer scaffold (A). Cross-sectional SEM images of electrospun bilayer (B) and control scaffolds (C) of thickness equal to 220 and 250 μm , respectively. The dashed line shown in (B) indicates the aligned-fiber layer and random fiber layer AFL/RFL interface in the bilayer scaffold. Representative cross-sectional images of bilayer scaffolds subcutaneously implanted in Sprague-Dawley rats for 5 days (D) and 14 days (E). Blue and red colors indicate staining of cell nuclei and α -actin, respectively. Dashed and solid lines indicate the boundaries between surrounding tissue and scaffold surfaces with random and aligned fibers, respectively. All images have the same magnification. Reproduced from Pu J, Yuan F, Li S, Komvopoulos K. Electrospun bilayer fibrous scaffolds for enhanced cell infiltration and vascularization in vivo. *Acta Biomater* 2015;13:131–41, with permission from Elsevier.

than control groups [80]. As it was shown in recently published studies, bilayer scaffolds with highly porous inner layer support cell infiltration, whereas those with lower external layer porosity provide long-term mechanical supports [80,101,105].

One other disadvantage of nondegradable vascular grafts is their lack of growth especially when applied to pediatric patients [17]. In majority of the cases, these patients have to go through secondary surgery, which increases the motility and morbidity rate of vascular graft implantation, whereas biodegradable vascular grafts that allow native vascular tissue regeneration have the potential to adapt to patients' natural growth and to overcome the limitations caused by nondegradable vascular scaffolds. Wang et al. fabricated macroporous biodegradable electrospun PCL scaffolds with thick fibers (5–6 μm) in order to form larger pores (30 μm). The developed electrospun scaffolds were implanted in rat abdominal aorta and evaluated for 7, 14, 28, and 100 days. The results revealed that macropore structure of the scaffold significantly increased cell infiltration and ECM formation. Endothelialization was completely occurred at day 100 samples where SMCs were aligned with ECM fibers similar to those in the native arteries [104].

Compared with acellular electrospun scaffolds, there are only few in vivo studies that used cell-laden electrospun scaffolds as a vascular graft. For instance, Hashi et al.

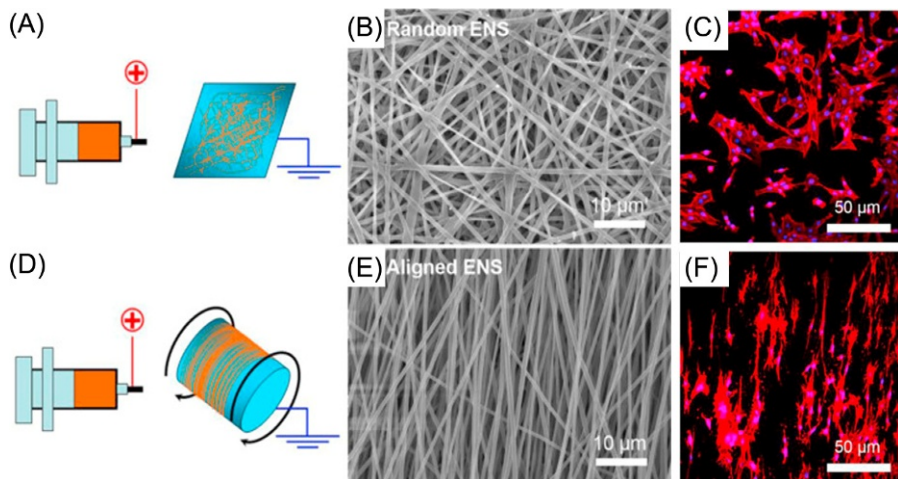


Fig. 11.5 Schematic of the experimental setup for preparing PLGA/PCL random electrospun nanofibrous scaffolds (ENS) (A) and aligned ENS (D), SEM micrograph of PLGA/PCL random ENS (B) and aligned ENS (E), and cell shape and distribution on PLGA/PCL random (C) and aligned (F) ENS. Blue colors indicate nuclei. Red colors indicate actins.

Reproduced from Zhong J, Zhang H, Yan J, Gong X. Effect of nanofiber orientation of electrospun nanofibrous scaffolds on cell growth and elastin expression of muscle cells. *Colloids Surf B: Biointerfaces* 2015;136:772–8, with permission from Elsevier.

fabricated porous PLLA electrospun scaffolds composed of micro- and nanofibers. They investigated the effect of initial bone marrow MSCs seeding on vascular regeneration. The results showed that the developed scaffolds allowed cell infiltration and vascular regeneration. Acellular grafts (without MSCs) showed significant intimal thickening compared with MSC-laden scaffolds, whereas cellular-laden scaffolds showed long-term patency and organization of ECs and SMCs as in native arteries [123].

11.7 Conclusions and future perspectives

Electrospun scaffolds, which provide sites for cell attachment, proliferation, differentiation, migration, and mechanical support during tissue formation, have become a strong alternative for many types of tissue-engineering applications. Although there are some available fibrous scaffolds on the market especially for wound-dressing and bone tissue-engineering applications, human implantable electrospun scaffold as a vascular graft is yet to be achieved. Even though recent advances in electrospinning technology and material science, as reviewed in the chapter, revealed promising results in *in vitro* studies, there are still few *in vivo* studies and no clinical trials where electrospun vascular grafts are used. Evaluation of scaffolds should be performed

thoroughly under dynamic conditions, prior to *in vivo* studies. To speed up the process, appropriate *in vitro* bioreactor systems could be designed, where actual blood flow is simulated.

All the reviewed articles in this chapter mention that the major reason for vascular electrospun scaffold application failure is their inadequate mechanical properties. In many studies, the scaffolds were characterized only with uniaxial tensile tests; however, the dynamic mechanical properties of scaffolds including burst strength and dynamic compliance should be analyzed to predict the conditions of the scaffolds in dynamic systems as well. It was also examined in the literature that changing the orientation of the fibers could influence the mechanical properties. Generally, scaffolds that are composed of aligned nanofibers showed not only similar mechanical properties with native vascular arteries but also enhanced *in vitro* cell adhesion, proliferation, and differentiation.

Mechanically durable synthetic polymers have been widely used to fabricate tubular scaffolds for vascular tissue engineering. The limitation caused by poor biological activity of synthetic polymer-based scaffolds was overcome by surface treatment techniques and coelectrospinning of synthetic polymers with natural polymers. More studies should be conducted to determine optimum biological and physical properties of vascular scaffolds. In order to start clinical applications of vascular electrospun scaffolds, the developed scaffolds should accelerate vascular regeneration and degradation properties with no toxic effect. Even though vascular electrospun scaffolds, especially recently reported bilayer scaffolds with different inner and external structures, have shown promising *in vitro* and *in vivo* results, further studies are required prior to clinical applications in order to develop mechanically durable and cell-supporting vascular grafts.

As reviewed in this chapter, there have been many promising studies to develop electrospun nanofibrous vascular grafts; however, to the best of our knowledge, no product in the market has been licensed. We strongly believe that the successfully developed such grafts are still in the process of clinical studies or FDA approval stage. Therefore, in the near future, they will be in the market as promising alternatives to teflon-based grafts especially for small-diameter vascular graft applications.

Acknowledgments

O. Karaman and M. Şen acknowledge funding from TÜBİTAK (the Scientific and Technological Research Council of Turkey) through the Research Projects 214 M268 and BAP (Research Projects Fund by Izmir Katip Celebi University Scientific) through the Research Projects 2015-GAP-MUMF-0013 and 2016-ONP-MUMF-0022.

References

- [1] Poh M, Boyer M, Solan A, Dahl SL, Pedrotty D, Banik SS, et al. Blood vessels engineered from human cells. *Lancet* 2005;365:2122–4.
- [2] McKee JA, Banik SS, Boyer MJ, Hamad NM, Lawson JH, Niklason LE, et al. Human arteries engineered *in vitro*. *EMBO Rep* 2003;4:633–8.

- [3] Verma S, Szmítok PE, Weisel RD, Bonneau D, Latter D, Errett L, et al. Should radial arteries be used routinely for coronary artery bypass grafting? *Circulation* 2004;110:e40–6.
- [4] Bastijanic JM, Marchant RE, Kligman F, Allemang MT, Lakin RO, Kendrick D, et al. In vivo evaluation of biomimetic fluorosurfactant polymer-coated expanded polytetrafluoroethylene vascular grafts in a porcine carotid artery bypass model. *J Vasc Surg* 2016;63:1620–1630.e4.
- [5] Kannan RY, Salacinski HJ, Butler PE, Hamilton G, Seifalian AM. Current status of prosthetic bypass grafts: a review. *J Biomed Mater Res B Appl Biomater* 2005;74:570–81.
- [6] Nabzdyk CS, Chun MC, Oliver-Allen HS, Pathan SG, Phaneuf MD, You JO, et al. Gene silencing in human aortic smooth muscle cells induced by PEI-siRNA complexes released from dip-coated electrospun poly(ethylene terephthalate) grafts. *Biomaterials* 2014;35:3071–9.
- [7] Klinkert P, Post PN, Breslau PJ, Van Bocke JH. Saphenous vein versus PTFE for above-knee femoropopliteal bypass: a review of the literature. *Eur J Vasc Endovasc Surg* 2004;27:357–62.
- [8] Whittemore AD, Kent KC, Donaldson MC, Couch NP, Mannick JA. What is the proper role of polytetrafluoroethylene grafts in infrainguinal reconstruction? *J Vasc Surg* 1989;10:299–305.
- [9] Wise SG, Byrom MJ, Waterhouse A, Bannon PG, Weiss AS, Ng MKC. A multilayered synthetic human elastin/polycaprolactone hybrid vascular graft with tailored mechanical properties. *Acta Biomater* 2011;7:1429.
- [10] He W, Nieponice A, Soletti L, Hong Y, Gharaibeh B, Crisan M, et al. Pericyte-based human tissue engineered vascular grafts: in vivo feasibility assessment. In: *Proceedings of the ASME summer bioengineering conference*; 2010. p. 515–6.
- [11] He W, Nieponice A, Soletti L, Hong Y, Gharaibeh B, Crisan M, et al. Pericyte-based human tissue engineered vascular grafts. *Biomaterials* 2010;31:8235–44.
- [12] L'Heureux N. Tissue engineering of a completely biological & autologous human blood vessel for adult arterial revascularization. *FASEB J* 2007;21:A141.
- [13] Barnes CP, Sell SA, Boland ED, Simpson DG, Bowlin GL. Nanofiber technology: designing the next generation of tissue engineering scaffolds. *Adv Drug Deliv Rev* 2007;59:1413–33.
- [14] Bhardwaj N, Kundu SC. Electrospinning: a fascinating fiber fabrication technique. *Bio-technol Adv* 2010;28:325–47.
- [15] Heydarkhan-Hagvall S, Schenke-Layland K, Dhanasopon AP, Rofail F, Smith H, Wu BM, et al. Three-dimensional electrospun ECM-based hybrid scaffolds for cardiovascular tissue engineering. *Biomaterials* 2008;29:2907–14.
- [16] Karaman O, Kumar A, Moeinzadeh S, He XZ, Cui T, Jabbari E. Effect of surface modification of nanofibres with glutamic acid peptide on calcium phosphate nucleation and osteogenic differentiation of marrow stromal cells. *J Tissue Eng Regen Med* 2016;10: E132–46.
- [17] Hasan A, Memic A, Annabi N, Hossain M, Paul A, Dokmeci MR, et al. Electrospun scaffolds for tissue engineering of vascular grafts. *Acta Biomater* 2014;10:11–25.
- [18] Rocco KA, Maxfield MW, Best CA, Dean EW, Breuer CK. In vivo applications of electrospun tissue-engineered vascular grafts: a review. *Tissue Eng Part B Rev* 2014;20:628–40.
- [19] Sumpio BE, Riley JT, Dardik A. Cells in focus: endothelial cell. *Int J Biochem Cell Biol* 2002;34:1508–12.
- [20] Conway EM, Collen D, Carmeliet P. Molecular mechanisms of blood vessel growth. *Cardiovasc Res* 2001;49:507–21.

- [21] Pugsley MK, Tabrizchi R. The vascular system – an overview of structure and function. *J Pharmacol Toxicol Methods* 2000;44:333–40.
- [22] Bergers G, Song S. The role of pericytes in blood-vessel formation and maintenance. *Neuro Oncol* 2005;7:452–64.
- [23] Wagenseil JE, Mecham RP. Vascular extracellular matrix and arterial mechanics. *Physiol Rev* 2009;89:957–89.
- [24] Lutolf MP, Hubbell JA. Synthetic biomaterials as instructive extracellular microenvironments for morphogenesis in tissue engineering. *Nat Biotechnol* 2005;23:47–55.
- [25] Garmy-Susini B, Jin H, Zhu Y, Sung RJ, Hwang R, Varner J. Integrin $\alpha_4\beta_1$ -VCAM-1-mediated adhesion between endothelial and mural cells is required for blood vessel maturation. *J Clin Invest* 2005;115:1542–51.
- [26] Frantz C, Stewart KM, Weaver VM. The extracellular matrix at a glance. *J Cell Sci* 2010;123:4195–200.
- [27] Hanahan D, Folkman J. Patterns and emerging mechanisms of the angiogenic switch during tumorigenesis. *Cell* 1996;86:353–64.
- [28] Van Hinsbergh VW, Koolwijk P. Endothelial sprouting and angiogenesis: matrix metalloproteinases in the lead. *Cardiovasc Res* 2008;78:203–12.
- [29] Fornieri C, Quaglini Jr. D, Mori G. Role of the extracellular matrix in age-related modifications of the rat aorta. Ultrastructural, morphometric, and enzymatic evaluations. *Arterioscler Thromb* 1992;12:1008–16.
- [30] Chuang TH, Stabler C, Simionescu A, Simionescu DT. Polyphenol-stabilized tubular elastin scaffolds for tissue engineered vascular grafts. *Tissue Eng Part A* 2009;15:2837–51.
- [31] Olsson AK, Dimberg A, Kreuger J, Claesson-Welsh L. VEGF receptor signalling – in control of vascular function. *Nat Rev Mol Cell Biol* 2006;7:359–71.
- [32] Gauvin R, Guillemette M, Dokmeci M, Khademhosseini A. Application of microtechnologies for the vascularization of engineered tissues. *Vasc Cell* 2011;3:24.
- [33] Ekaputra AK, Prestwich GD, Cool SM, Huttmacher DW. The three-dimensional vascularization of growth factor-releasing hybrid scaffold of poly(ϵ -caprolactone)/collagen fibers and hyaluronic acid hydrogel. *Biomaterials* 2011;32:8108–17.
- [34] Clark RAF. Fibrin glue for wound repair: facts and fancy. *Thromb Haemost* 2003;90:1003–6.
- [35] Ye Q, Zund G, Benedikt P, Jockenhoewel S, Hoerstrup SP, Sakyama S, et al. Fibrin gel as a three dimensional matrix in cardiovascular tissue engineering. *Eur J Cardiothorac Surg* 2000;17:587–91.
- [36] Van Obberghen-Schilling E, Tucker RP, Saupe F, Gasser I, Cseh B, Orend G. Fibronectin and tenascin-C: accomplices in vascular morphogenesis during development and tumor growth. *Int J Dev Biol* 2011;55:511–25.
- [37] Collins MN, Birkinshaw C. Hyaluronic acid based scaffolds for tissue engineering—a review. *Carbohydr Polym* 2013;92:1262–79.
- [38] Schante CE, Zuber G, Herlin C, Vandamme TF. Improvement of hyaluronic acid enzymatic stability by the grafting of amino-acids. *Carbohydr Polym* 2012;87:2211–6.
- [39] Joddar B, Ramamurthi A. Elastogenic effects of exogenous hyaluronan oligosaccharides on vascular smooth muscle cells. *Biomaterials* 2006;27:5698–707.
- [40] Lepidi S, Grego F, Vindigni V, Zavan B, Tonello C, Deriu GP, et al. Hyaluronan biodegradable scaffold for small-caliber artery grafting: preliminary results in an animal model. *Eur J Vasc Endovasc Surg* 2006;32:411–7.
- [41] Ruiz A, Flanagan CE, Masters KS. Differential support of cell adhesion and growth by copolymers of polyurethane with hyaluronic acid. *J Biomed Mater Res A* 2013; 101:2870–82.

- [42] Zhu C, Fan D, Wang Y. Human-like collagen/hyaluronic acid 3D scaffolds for vascular tissue engineering. *Mater Sci Eng C Mater Biol Appl* 2014;34:393–401.
- [43] Jayakumar R, Menon D, Manzoor K, Nair SV, Tamura H. Biomedical applications of chitin and chitosan based nanomaterials—a short review. *Carbohydr Polym* 2010;82:227–32.
- [44] Zhao J, Qiu H, Chen DL, Zhang WX, Zhang DC, Li M. Development of nanofibrous scaffolds for vascular tissue engineering. *Int J Biol Macromol* 2013;56:106–13.
- [45] Couet F, Rajan N, Mantovani D. Macromolecular biomaterials for scaffold-based vascular tissue engineering. *Macromol Biosci* 2007;7:701–18.
- [46] Pankajakshan D, Agrawal DK. Scaffolds in tissue engineering of blood vessels. *Can J Physiol Pharmacol* 2010;88:855–73.
- [47] Mann BK, Gobin AS, Tsai AT, Schmedlen RH, West JL. Smooth muscle cell growth in photopolymerized hydrogels with cell adhesive and proteolytically degradable domains: synthetic ECM analogs for tissue engineering. *Biomaterials* 2001;22:3045–51.
- [48] Miller JS, Shen CJ, Legant WR, Baranski JD, Blakely BL, Chen CS. Bioactive hydrogels made from step-growth derived PEG-peptide macromers. *Biomaterials* 2010;31:3736–43.
- [49] De Valence S, Tille JC, Mugnai D, Mrowczynski W, Gurny R, Moller M, et al. Long term performance of polycaprolactone vascular grafts in a rat abdominal aorta replacement model. *Biomaterials* 2012;33:38–47.
- [50] Deitzel J, Kleinmeyer J, Harris D, Tan NB. The effect of processing variables on the morphology of electrospun nanofibers and textiles. *Polymer* 2001;42:261–72.
- [51] Eda G, Shivkumar S. Bead-to-fiber transition in electrospun polystyrene. *J Appl Polym Sci* 2007;106:475–87.
- [52] Lee K, Kim H, Bang H, Jung Y, Lee S. The change of bead morphology formed on electrospun polystyrene fibers. *Polymer* 2003;44:4029–34.
- [53] Haider S, Al-Zeghayer Y, Ali FAA, Haider A, Mahmood A, Al-Masry WA, et al. Highly aligned narrow diameter chitosan electrospun nanofibers. *J Polym Res* 2013;20:1–11.
- [54] Ki CS, Baek DH, Gang KD, Lee KH, Um IC, Park YH. Characterization of gelatin nanofiber prepared from gelatin–formic acid solution. *Polymer* 2005;46:5094–102.
- [55] Haghi A, Akbari M. Trends in electrospinning of natural nanofibers. *Phys Status Solidi (A)* 2007;204:1830–4.
- [56] Koski A, Yim K, Shivkumar S. Effect of molecular weight on fibrous PVA produced by electrospinning. *Mater Lett* 2004;58:493–7.
- [57] Tan S, Inai R, Kotaki M, Ramakrishna S. Systematic parameter study for ultra-fine fiber fabrication via electrospinning process. *Polymer* 2005;46:6128–34.
- [58] Kim K-H, Jeong L, Park H-N, Shin S-Y, Park W-H, Lee S-C, et al. Biological efficacy of silk fibroin nanofiber membranes for guided bone regeneration. *J Biotechnol* 2005;120:327–39.
- [59] Ayutsede J, Gandhi M, Sukigara S, Ye H, Hsu C-M, Gogotsi Y, et al. Carbon nanotube reinforced Bombyx mori silk nanofibers by the electrospinning process. *Biomacromolecules* 2006;7:208–14.
- [60] Larrondo L, St John Manley R. Electrostatic fiber spinning from polymer melts. I. Experimental observations on fiber formation and properties. *J Polym Sci: Polym Phys Ed* 1981;19:909–20.
- [61] Yang Q, Li Z, Hong Y, Zhao Y, Qiu S, Wang C, et al. Influence of solvents on the formation of ultrathin uniform poly(vinyl pyrrolidone) nanofibers with electrospinning. *J Polym Sci B Polym Phys* 2004;42:3721–6.
- [62] Pham QP, Sharma U, Mikos AG. Electrospun poly(ϵ -caprolactone) microfiber and multilayer nanofiber/microfiber scaffolds: characterization of scaffolds and measurement of cellular infiltration. *Biomacromolecules* 2006;7:2796–805.

- [63] Zong X, Kim K, Fang D, Ran S, Hsiao BS, Chu B. Structure and process relationship of electrospun bioabsorbable nanofiber membranes. *Polymer* 2002;43:4403–12.
- [64] Mit-Uppatham C, Nithitanakul M, Supaphol P. Ultrafine electrospun polyamide-6 fibers: effect of solution conditions on morphology and average fiber diameter. *Macromol Chem Phys* 2004;205:2327–38.
- [65] Zuo W, Zhu M, Yang W, Yu H, Chen Y, Zhang Y. Experimental study on relationship between jet instability and formation of beaded fibers during electrospinning. *Polym Eng Sci* 2005;45:704–9.
- [66] Laudenslager MJ, Sigmund WM. Electrospinning. *Encyclopedia of nanotechnology*. New York: Springer; 2012.
- [67] Demir MM, Yilgor I, Yilgor E, Erman B. Electrospinning of polyurethane fibers. *Polymer* 2002;43:3303–9.
- [68] Zhang C, Yuan X, Wu L, Han Y, Sheng J. Study on morphology of electrospun poly(vinyl alcohol) mats. *Eur Polym J* 2005;41:423–32.
- [69] Yuan X, Zhang Y, Dong C, Sheng J. Morphology of ultrafine polysulfone fibers prepared by electrospinning. *Polym Int* 2004;53:1704–10.
- [70] Wannatong L, Sirivat A, Supaphol P. Effects of solvents on electrospun polymeric fibers: preliminary study on polystyrene. *Polym Int* 2004;53:1851–9.
- [71] Megelski S, Stephens JS, Chase DB, Rabolt JF. Micro- and nanostructured surface morphology on electrospun polymer fibers. *Macromolecules* 2002;35:8456–66.
- [72] Wang X, Um IC, Fang D, Okamoto A, Hsiao BS, Chu B. Formation of water-resistant hyaluronic acid nanofibers by blowing-assisted electro-spinning and non-toxic post treatments. *Polymer* 2005;46:4853–67.
- [73] Xu C, Inai R, Kotaki M, Ramakrishna S. Aligned biodegradable nanofibrous structure: a potential scaffold for blood vessel engineering. *Biomaterials* 2004;25:877–86.
- [74] Sundaray B, Subramanian V, Natarajan T, Xiang R-Z, Chang C-C, Fann W-S. Electrospinning of continuous aligned polymer fibers. *Appl Phys Lett* 2004;84:1222–4.
- [75] Geng X, Kwon O-H, Jang J. Electrospinning of chitosan dissolved in concentrated acetic acid solution. *Biomaterials* 2005;26:5427–32.
- [76] Huan S, Liu G, Han G, Cheng W, Fu Z, Wu Q, et al. Effect of experimental parameters on morphological, mechanical and hydrophobic properties of electrospun polystyrene fibers. *Materials* 2015;8:2718–34.
- [77] Casper CL, Stephens JS, Tassi NG, Chase DB, Rabolt JF. Controlling surface morphology of electrospun polystyrene fibers: effect of humidity and molecular weight in the electrospinning process. *Macromolecules* 2004;37:573–8.
- [78] Zhu M, Wang Z, Zhang J, Wang L, Yang X, Chen J, et al. Circumferentially aligned fibers guided functional neoartery regeneration in vivo. *Biomaterials* 2015;61:85–94.
- [79] Wang Z, Lu Y, Qin K, Wu Y, Tian Y, Wang J, et al. Enzyme-functionalized vascular grafts catalyze in-situ release of nitric oxide from exogenous NO prodrug. *J Control Release* 2015;210:179–88.
- [80] Pu J, Yuan F, Li S, Komvopoulos K. Electrospun bilayer fibrous scaffolds for enhanced cell infiltration and vascularization in vivo. *Acta Biomater* 2015;13:131–41.
- [81] Wu T, Huang C, Li D, Yin A, Liu W, Wang J, et al. A multi-layered vascular scaffold with symmetrical structure by bi-directional gradient electrospinning. *Colloids Surf B: Bio-interfaces* 2015;133:179–88.
- [82] Jing X, Mi H-Y, Salick MR, Cordie TM, Peng X-F, Turng L-S. Electrospinning thermo-plastic polyurethane/graphene oxide scaffolds for small diameter vascular graft applications. *Mater Sci Eng C* 2015;49:40–50.

- [83] Bergmeister H, Seyidova N, Schreiber C, Strobl M, Grasl C, Walter I, et al. Biodegradable, thermoplastic polyurethane grafts for small diameter vascular replacements. *Acta Biomater* 2015;11:104–13.
- [84] Ahn H, Ju YM, Takahashi H, Williams DF, Yoo JJ, Lee SJ, et al. Engineered small diameter vascular grafts by combining cell sheet engineering and electrospinning technology. *Acta Biomater* 2015;16:14–22.
- [85] Liu Y, Jiang C, Li S, Hu Q. Composite vascular scaffold combining electrospun fibers and physically-crosslinked hydrogel with copper wire-induced grooves structure. *J Mech Behav Biomed Mater* 2016;61:12–25.
- [86] Muylaert DE, Van Almen GC, Talacia H, Fledderus JO, Kluin J, Hendrikse SI, et al. Early in-situ cellularization of a supramolecular vascular graft is modified by synthetic stromal cell-derived factor-1 α derived peptides. *Biomaterials* 2016;76:187–95.
- [87] Elsayed Y, Lekakou C, Labeed F, Tomlins P. Fabrication and characterisation of biomimetic, electrospun gelatin fibre scaffolds for tunica media-equivalent, tissue engineered vascular grafts. *Mater Sci Eng C* 2016;61:473–83.
- [88] Gong WH, Lei D, Li S, Huang P, Qi Q, Sun YJ, et al. Hybrid small-diameter vascular grafts: anti-expansion effect of electrospun poly epsilon-caprolactone on heparin-coated decellularized matrices. *Biomaterials* 2016;76:359–70.
- [89] Pham QP, Sharma U, Mikos AG. Electrospinning of polymeric nanofibers for tissue engineering applications: a review. *Tissue Eng* 2006;12:1197–211.
- [90] Yoo HS, Kim TG, Park TG. Surface-functionalized electrospun nanofibers for tissue engineering and drug delivery. *Adv Drug Deliv Rev* 2009;61:1033–42.
- [91] Zheng WT, Wang ZH, Song LJ, Zhao Q, Zhang J, Li D, et al. Endothelialization and patency of RGD-functionalized vascular grafts in a rabbit carotid artery model. *Biomaterials* 2012;33:2880–91.
- [92] Heo Y, Shin YM, Bin Lee Y, Lim YM, Shin H. Effect of immobilized collagen type IV on biological properties of endothelial cells for the enhanced endothelialization of synthetic vascular graft materials. *Colloids Surf B: Biointerfaces* 2015;134:196–203.
- [93] Chen X, Wang J, An QZ, Li DW, Liu PX, Zhu W, et al. Electrospun poly(L-lactic acid-co-epsilon-caprolactone) fibers loaded with heparin and vascular endothelial growth factor to improve blood compatibility and endothelial progenitor cell proliferation. *Colloids Surf B: Biointerfaces* 2015;128:106–14.
- [94] Yuan XY, Mak AFT, Yao KD. Surface degradation of poly(L-lactic acid) fibres in a concentrated alkaline solution. *Polym Degrad Stab* 2003;79:45–52.
- [95] Croll TI, O'Connor AJ, Stevens GW, Cooper-White JJ. Controllable surface modification of poly(lactic-co-glycolic acid) (PLGA) by hydrolysis or aminolysis I: physical, chemical, and theoretical aspects. *Biomacromolecules* 2004;5:463–73.
- [96] Zhu YB, Gao CY, Liu XY, Shen JC. Surface modification of polycaprolactone membrane via aminolysis and biomacromolecule immobilization for promoting cytocompatibility of human endothelial cells. *Biomacromolecules* 2002;3:1312–9.
- [97] Cheng Q, Komvopoulos K, Li S. Plasma-assisted heparin conjugation on electrospun poly(L-lactide) fibrous scaffolds. *J Biomed Mater Res A* 2014;102:1408–14.
- [98] Savoji H, Hadjizadeh A, Maire M, Ajji A, Wertheimer MR, Lerouge S. Electrospun nanofiber scaffolds and plasma polymerization: a promising combination towards complete, stable endothelial lining for vascular grafts. *Macromol Biosci* 2014;14:1084–95.
- [99] Guex AG, Hegemann D, Giraud MN, Tevaearai HT, Popa AM, Rossi RM, et al. Covalent immobilisation of VEGF on plasma-coated electrospun scaffolds for tissue engineering applications. *Colloids Surf B: Biointerfaces* 2014;123:724–33.

- [100] Lee SJ, Yoo JJ, Lim GJ, Atala A, Stitzel J. In vitro evaluation of electrospun nanofiber scaffolds for vascular graft application. *J Biomed Mater Res A* 2007;83:999–1008.
- [101] Montini-Ballarín F, Calvo D, Caracciolo PC, Rojo F, Frontini PM, Abraham GA, et al. Mechanical behavior of bilayered small-diameter nanofibrous structures as biomimetic vascular grafts. *J Mech Behav Biomed Mater* 2016;60:220–33.
- [102] Lee SJ, Heo DN, Park JS, Kwon SK, Lee JH, Lee JH, et al. Characterization and preparation of bio-tubular scaffolds for fabricating artificial vascular grafts by combining electrospinning and a 3D printing system. *Phys Chem Chem Phys* 2015;17:2996–9.
- [103] McKenna KA, Hinds MT, Sarao RC, Wu PC, Maslen CL, Glanville RW, et al. Mechanical property characterization of electrospun recombinant human tropoelastin for vascular graft biomaterials. *Acta Biomater* 2012;8:225–33.
- [104] Wang Z, Cui Y, Wang J, Yang X, Wu Y, Wang K, et al. The effect of thick fibers and large pores of electrospun poly(ϵ -caprolactone) vascular grafts on macrophage polarization and arterial regeneration. *Biomaterials* 2014;35:5700–10.
- [105] Ju YM, Choi JS, Atala A, Yoo JJ, Lee SJ. Bilayered scaffold for engineering cellularized blood vessels. *Biomaterials* 2010;31:4313–21.
- [106] Wu T, Huang C, Li D, Yin A, Liu W, Wang J, et al. A multi-layered vascular scaffold with symmetrical structure by bi-directional gradient electrospinning. *Colloids Surf B: Biointerfaces* 2015;133:179–88.
- [107] Agarwal S, Wendorff JH, Greiner A. Use of electrospinning technique for biomedical applications. *Polymer* 2008;49:5603–21.
- [108] Boudriot U, Dersch R, Greiner A, Wendorff JH. Electrospinning approaches toward scaffold engineering – a brief overview. *Artif Organs* 2006;30:785–92.
- [109] McClure MJ, Sell SA, Ayres CE, Simpson DG, Bowlin GL. Electrospinning-aligned and random polydioxanone-polycaprolactone-silk fibroin-blended scaffolds: geometry for a vascular matrix. *Biomed Mater* 2009;4:055010.
- [110] Bashur CA, Shaffer RD, Dahlgren LA, Guelcher SA, Goldstein AS. Effect of fiber diameter and alignment of electrospun polyurethane meshes on mesenchymal progenitor cells. *Tissue Eng A* 2009;15:2435–45.
- [111] Sinclair KD, Webb K, Brown PJ. The effect of various denier capillary channel polymer fibers on the alignment of NHDF cells and type I collagen. *J Biomed Mater Res A* 2010;95A:1194–202.
- [112] Wong CS, Liu X, Xu ZG, Lin T, Wang XG. Elastin and collagen enhances electrospun aligned polyurethane as scaffolds for vascular graft. *J Mater Sci Mater Med* 2013;24:1865–74.
- [113] Zhu YB, Cao Y, Pan J, Liu YX. Macro-alignment of electrospun fibers for vascular tissue engineering. *J Biomed Mater Res Part B: Appl Biomater* 2010;92B:508–16.
- [114] Zhong J, Zhang H, Yan J, Gong X. Effect of nanofiber orientation of electrospun nanofibrous scaffolds on cell growth and elastin expression of muscle cells. *Colloids Surf B: Biointerfaces* 2015;136:772–8.
- [115] Nezarati RM, Eifert MB, Dempsey DK, Cosgriff-Hernandez E. Electrospun vascular grafts with improved compliance matching to native vessels. *J Biomed Mater Res B Appl Biomater* 2015;103:313–23.
- [116] Benrashed E, McCoy CC, Youngwirth LM, Kim J, Manson RJ, Otto JC, et al. Tissue engineered vascular grafts: origins, development, and current strategies for clinical application. *Methods* 2016;99:13–9.
- [117] Merkle VM, Tran PL, Hutchinson M, Ammann KR, Decook K, Wu X, et al. Core-shell PVA/gelatin electrospun nanofibers promote human umbilical vein endothelial cell and smooth muscle cell proliferation and migration. *Acta Biomater* 2015;27:77–87.

- [118] Shalumon KT, Deepthi S, Anupama MS, Nair SV, Jayakumar R, Chennazhi KP. Fabrication of poly(L-lactic acid)/gelatin composite tubular scaffolds for vascular tissue engineering. *Int J Biol Macromol* 2015;72:1048–55.
- [119] Jing X, Mi HY, Salick MR, Cordie TM, Peng XF, Turng LS. Electrospinning thermoplastic polyurethane/graphene oxide scaffolds for small diameter vascular graft applications. *Mater Sci Eng C Mater Biol Appl* 2015;49:40–50.
- [120] Zhang J, Qi H, Wang H, Hu P, Ou L, Guo S, et al. Engineering of vascular grafts with genetically modified bone marrow mesenchymal stem cells on poly(propylene carbonate) graft. *Artif Organs* 2006;30:898–905.
- [121] Zhu M, Wang Z, Zhang J, Wang L, Yang X, Chen J, et al. Circumferentially aligned fibers guided functional neoartery regeneration in vivo. *Biomaterials* 2015;61:85–94.
- [122] Bergmeister H, Seyidova N, Schreiber C, Strobl M, Grasl C, Walter I, et al. Biodegradable, thermoplastic polyurethane grafts for small diameter vascular replacements. *Acta Biomater* 2015;11:104–13.
- [123] Hashi CK, Zhu YQ, Yang GY, Young WL, Hsiao BS, Wang K, et al. Antithrombogenic property of bone marrow mesenchymal stem cells in nanofibrous vascular grafts. *Proc Natl Acad Sci U S A* 2007;104:11915–20.

This page intentionally left blank

Electrospun scaffolds for cardiac tissue engineering

12

A.H. Hekmati*, M. Norouzi[†]

*Islamic Azad University, South Tehran Branch, Tehran, Iran, [†]University of Manitoba, Winnipeg, MB, Canada

12.1 Introduction

Cardiovascular diseases (CVDs) have been considered as the leading cause of death worldwide since the past two decades. Myocardial infarction (MI) and heart failure caused by frequently occurred MI are the major causes of death among the CVDs. MI occurs by obstruction of one or more branches of the coronary arteries, which leads to myocardial necrosis and death of cardiomyocytes. Due to the limited regenerative capacity of the adult heart, MI causes permanent damage, and it transforms the infarcted area into a fibrous scar leading to a significant reduction of the cardiac function progressively [1–3].

Still, heart transplantation is the most effective method to restore heart functions for patients with end-stage heart failure; however, shortage of organ donors represents a major limitation. Therefore, the concept of tissue engineering and cell therapy has been recognized as an alternative therapeutic approach to stimulate the regeneration of the infarcted tissue, avoiding adverse remodeling and scar formation [2,4].

Nowadays, cell therapy is suggested as a candidate for MI treatment to replace the defective myocardial tissue with fetal or neonatal cardiomyocytes, skeletal myoblasts, embryonic stem cells, bone marrow-derived mesenchymal, hematopoietic stem cells, and adipose-derived stem cells [5]. Nevertheless, direct injection of the cells into the diseased myocardium reduces the efficiency of cell engraftment because most of the injected cells are lost in the blood circulation. Additionally, most of the successfully injected cells die within a week as a result of mechanical disruption, unfavorable environmental conditions, etc. Therefore, a variety of carriers such as hydrogels, self-assembling peptides, and nanofibrous scaffolds can be utilized to deliver cells into the myocardial tissue. Furthermore, three-dimensional scaffold implants containing cell can present some advantages over the direct cell injection through increasing the efficiency of cell engraftment, replacing temporarily the injured tissue, providing a substrate for cell proliferation and migration, and supplying a mechanical support to the regenerative process [2,6,7].

Furthermore, biomaterials mimicking the fibrillar architecture of the extracellular matrix (ECM) can provide the essential guidance for the functioning of cardiac cells. As the diameter of proteins in native ECM is at the nanoscale, the nanofibrous scaffolds have been increasingly explored for tissue engineering applications [1,2,8].

Electrospinning is a straightforward and versatile technique to produce fibers with the diameter in the range of nanometer to micrometer [1,9–14]. In addition, electrospun nanofibers provide high surface area to volume ratio and variable pore size, while their mechanical properties can be manipulated by controlling the electrospinning parameters. Moreover, various cells, biomacromolecules, and pharmacological agents can be incorporated into the electrospun scaffolds providing essential factors for cardiac tissue engineering [9,10,15–17]. In this chapter, applications of electrospun nanofibers for cardiac tissue engineering including cardiac patches, drug delivery systems, and heart valve scaffolds are reviewed.

12.2 Cardiac patch

Cardiac patches can support or replace the heart muscle function with the capability of delivering cellular and pharmacological therapies after MI. An ideal cardiac patch should be biocompatible, biodegradable, and biomimetic replicating cardiac ECM properties in terms of physical and biochemical cues. Interconnected porous structure with variable pore dimensions is required for cell colonization, migration, proliferation, vascularization, and nutrient and oxygen diffusion. Considering the myocardial and endothelial cell dimensions that are in the range of 10–100 and 8–12 μm , respectively, pore size ranging between tens and hundreds of micrometers are suitable, while too large pores may prevent vascularization by endothelial cells [2,10].

Furthermore, a cardiac patch needs to match the mechanical properties of the host tissue. Therefore, tensile stress, Young's modulus, and strain of 3–15 kPa, ≈ 0.5 MPa, and 22%–90%, respectively, are recommended for cardiac patches. Since the patches need to withstand both the contractile and expansive forces generated at each cardiac cycle, elastomeric properties are also essential to sustain the cyclic stresses. In addition, the myocardium bears mechanical forces along a specific direction resulting in the anisotropic structure. Therefore, cardiac patches with anisotropic properties can promote ECM deposition and cell organization similar to the native tissue. Moreover, not only appropriate conductivity of electrospun cardiac patches can reduce the chance of postimplantation arrhythmia, but also rhythmic contraction of cardiomyocytes enhances cell alignment and differentiation [1,2,18].

Both synthetic and natural polymers have been studied for fabrication of cardiac patches. Generally, natural polymers such as collagen, gelatin, silk fibroin, fibrinogen, chitosan, alginate, and hyaluronic acid show excellent biocompatibility, cell attachment, and proliferation while they are characterized by the poor mechanical properties and fast degradation kinetics. On the other hand, biocompatible synthetic polymers demonstrate desirable mechanical and physical features while they show poor capability of cell attachment due to the lack of cell recognition sites [5,10]. The biocompatible synthetic polymers mostly utilized for cardiac tissue engineering include polyglycerol sebacate, polyethylene glycol, polyglycolic acid, poly-L-lactide, polyvinyl alcohol, polycaprolactone, polyurethanes, and poly(*N*-isopropylacrylamide). Therefore, amalgamating the desired biological properties of natural polymers with

the good physical properties of synthetic polymers can provide ideal patches for cardiac tissue engineering applications [2].

A contractile cardiac patch made of cardiomyocytes seeded onto polycaprolactone nanofibrous meshes was fabricated by Shin et al. The cardiomyocytes started beating after 3 days and expressed cardiac-specific proteins 14 days post seeding [19]. In another study, poly(glycerol sebacate) (PGS)/fibrinogen (core/shell) nanofibers were fabricated by coaxial electrospinning with Young's modulus (3.28 ± 1.7 MPa) comparable with that of native myocardium. Neonatal cardiomyocytes cultured on the scaffolds demonstrated normal expression of cardiac marker proteins α -actinin, troponin T, β -myosin heavy chain, and connexin 43 [20].

Aligned electrospun scaffolds have shown some improvement in orientation and organization of cultured cells and the electrophysiological function of cardiac tissue [8]. For example, cell seeded on aligned polyurethane-based scaffolds exhibited a higher expression of cardiac markers compared with the nonaligned scaffolds [21]. Similarly, better synchronized beating of cardiac tissue was observed on aligned PGS/gelatin electrospun scaffolds compared with the random ones [22]. Both fiber alignment and higher gelatin content could facilitate differentiation of neonatal rat cardiac fibroblast cells and collagen deposition (Fig. 12.1). Generally, fiber alignment can be obtained through introduction of an insulating gap into the collector, which acts as a capacitor

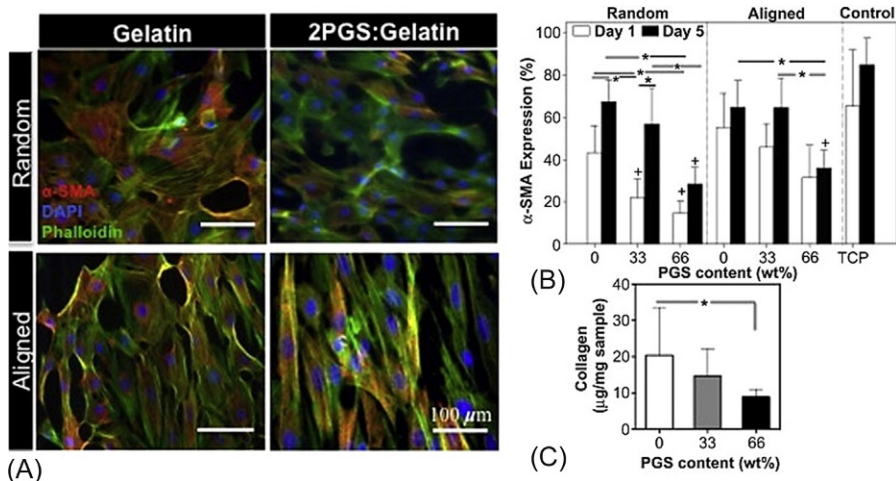


Fig. 12.1 Effects of physicochemical features of scaffolds on differentiation of neonatal rat cardiac fibroblast cells (CFs). (A) Overlaid images of CFs cultured on random and aligned scaffolds at fifth day, stained for α -SMA (red), F-actin (green), and DAPI (blue). (B) α -SMA expression on days 1 and 5 of CF culture. Both lower PGS content and fiber alignment could increase α -SMA expression. (C) Collagen deposition on fifth day indicating higher collagen deposition with lower PGS content (* and +, $P < .05$).

Reproduced with permission from Kharaziha M, Nikkhah M, Shin S, Annabi N, Masoumi N, Gaharwar AK, et al. PGS: gelatin nanofibrous scaffolds with tunable mechanical and structural properties for engineering cardiac tissues. *Biomaterials* 2013;34:6355–6366.

separating charge. Due to the opposite electrostatic forces formed by the gap, the charged fibers are stretched and aligned perpendicular to each edge of the gap [1,23].

Some conductive and biocompatible polymers such as polyaniline (PANi) and polypyrrole (PPy) have been employed to fabricate conductive cardiac patches [1,24]. For instance, an electrically active scaffold made of aligned composite nanofibers of PANi and poly(lactic-*co*-glycolic acid) (PLGA) was fabricated by Hsiao et al. [25]. The cultured cells formed clusters, and all of the cardiomyocytes within the clusters beat synchronously, which was mediated by the intercellular gap junction protein connexin 43, while the contractions of isolated clusters could be coupled together via an electric stimulation. Furthermore, functionalizing the electrospun nanofibers with conductive and biocompatible additives such as carbon nanotubes (CNTs) and gold nanoparticles (AuNPs) is another approach to produce conductive cardiac patches [24,26]. For example, upon electric stimulation, human mesenchymal stem cells (hMSCs) cultured on the electrospun scaffolds made of poly(lactic acid)/CNT reoriented perpendicular to the direction of the current and upregulated expression of Nkx2.5, GATA4, cardiac troponin T, cardiac myosin heavy chain, and connexin 43 were observed after the electric stimulation [27]. Similarly, incorporation of AuNPs into electrospun scaffolds could promote differentiation of mesenchymal stem cells (MSCs) to cardiomyogenic cells mainly due to the improved conductivity [28].

As mentioned earlier, cell therapy has been considered as a promising therapeutic approach for MI regeneration. Compared with the direct cell injection, cell-loaded nanofibrous cardiac patches can increase the efficiency of cell engraftment, stimulate cell proliferation, facilitate cell differentiation, and guide tissue regeneration. For instance, promoted differentiation of mouse embryonic stem cells cultured on nanofibrous scaffolds into functional cardiomyocytes was reported in comparison with the cell grown without the scaffold [29].

In another study, poly(ϵ -caprolactone)/gelatin nanofibrous scaffolds seeded with rat bone marrow MSCs were implanted on the epicardium of the infarcted region of Sprague-Dawley rats. The cells loaded in the scaffold could migrate toward the scar tissue and enhanced new blood vessel formation at the infarct site. Angiogenesis and the cardiac functions increased significantly 4 weeks post implantation [30]. Ehler et al. [31] also successfully fabricated cell-laden composite living fibers containing primary cardiomyocytes via cell electrospinning method for MI treatment (Fig. 12.2).

12.3 Bio-functionalized cardiac patch

Cardiac patches can be biofunctionalized with growth factors, cytokines, and drugs providing localized and sustained delivery of the biomolecules [32]. Furthermore, bio-functionalized cardiac patches can promote cell proliferation, migration, and differentiation. For example, Yu et al. [33] prepared YIGSR-incorporated and RGD (adhesive peptides derived from laminin)-incorporated PLGA nanofibers, and they reported higher expression of α -myosin heavy chain and β -tubulin and faster contraction of cardiomyocytes on YIGSR-PLGA compared with RGD-PLGA and PLGA nanofibers.

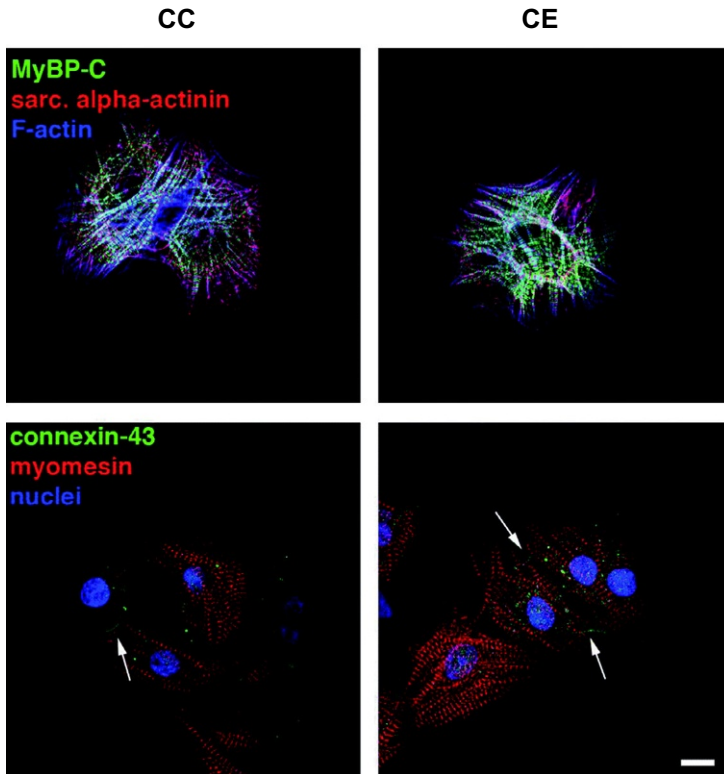


Fig. 12.2 Confocal images of neonatal rat cardiac myocytes. *CE*, cell electrospun cells; *CC*, culture cells as the control. A-band protein MyBP-C staining indicates well-structured myofibrils, while the Z-disk protein sarcomeric alpha-actinin and the M-band protein myomesin show that there is no difference between the two treatments. Moreover, gap junction between neighboring cardiac myocytes can be observed by connexin 43 staining. Also, filamentous actin cytoskeleton and the nuclei have been shown.

Reproduced with permission from Ehler E, Jayasinghe SN. Cell electrospinning cardiac patches for tissue engineering the heart. *Analyst* 2014;139:4449–4452.

Moreover, introducing angiogenic growth factors such as vascular endothelial growth factor (VEGF), basic fibroblast growth factor (bFGF), hepatocyte growth factor (HGF), and insulin-like growth factor-1 (IGF-1) in cardiac patches can provide controlled release of the growth factors and promote angiogenesis [9,34–36]. In one study, VEGF was encapsulated in poly(L-lactic acid-co-ε-caprolactone) (PLCL) nanofibers via emulsion electrospinning with the capability of releasing the growth factor [37]. In another work, granulocyte colony-stimulating factor (G-CSF)-incorporated poly(L-lactide) (PLA) nanofibers were fabricated by blend electrospinning, which promoted the differentiation of C2C12 murine skeletal myoblasts to cardiomyocyte phenotype through enhanced coexpression of cardiac troponin I and connexin 43 [38].

12.4 Heart valve scaffolds

Valvular heart disease is another major health problem that causes substantial mortality worldwide [39,40]. Polymeric scaffolds have some advantages over the decellularized biological scaffolds including less immunogenicity and thrombogenicity as well as controllable biodegradability and mechanical properties. To design a suitable scaffold for tissue engineering of the heart valve, specific structure and geometry are required. Utilizing appropriate shapes and arrangements of collectors allows fabrication of nanofibrous scaffolds with desired architecture. Furthermore, scaffolds designed for heart valve tissue engineering not only must withstand the hemodynamic pressures of the heart but also need to be resistant to calcification and thrombosis owing to their direct contact with blood [39,41].

A trileaflet electrospun PCL heart valve scaffold was produced by Del Gaudio et al. [42] The leaflets synchronously opened in the ejection phase while the proper apposition of the leaflets could prevent high leakage volumes in the diastolic phase. In another study, PGS/PCL electrospun scaffolds were fabricated demonstrating higher elastic modulus and ultimate tensile strength with higher PGS concentrations comparable with human aortic leaflets' mechanical characteristics (elastic modulus of 15.6 ± 6.4 MPa and ultimate tensile strength of 2.6 ± 1.2 MPa). Additionally, PGS/PCL scaffolds could improve attachment and proliferation of human umbilical vein endothelial cells (HUVECs) compared with PCL-only scaffolds [18].

A nanofiber coating on the surface of the scaffolds is proposed as another approach to improve physical and biological functions of the conventional scaffolds. In some cases, decellularized scaffolds were coated with electrospun nanofibers showing better mechanical properties and degradation kinetics than those of the original scaffolds [39]. For instance, Hong et al. [43] coated decellularized porcine aortic heart valve with nanofibers made of poly(3-hydroxybutyrate-co-4-hydroxybutyrate) that improved the mechanical strength of tissue engineered heart valves. In the next attempt, decellularized porcine aortic heart valve was coated with basic fibroblast growth factor/chitosan/poly-4-hydroxybutyrate via electrospinning and seeded with MSCs. The hybrid scaffolds demonstrated a significant increase in cell mass, 4-hydroxyproline and collagen formation, and mechanical strength compared with the original heart valve [44].

A composite scaffold made of an electrospun polyurethane and poly(ethylene glycol) hydrogel was fabricated for aortic valve tissue engineering. This multilayered construct could provide the desired mechanical properties while enabling 3D culture of cells. Valve interstitial cells encapsulated into the hydrogel portion of the composite demonstrated an activated phenotype in response to the stiffness of electrospun fibers that resulted in α -SMA expression and collagen secretion [41]. Similarly, the benefit of a combination of a knitted valvular scaffold and electrospun scaffold for valve tissue engineering was reported by Van Lieshout et al. [45].

12.5 Conclusion

Electrospun nanofibrous scaffolds can mimic the architecture of the protein fibers in the native ECM. Moreover, the versatility of the electrospinning can provide scaffolds with desired mechanical, electric, and degradation properties suitable for cardiac tissue engineering. Therefore, electrospun scaffolds have found applications to restore the cardiac function, provide a substrate for cell proliferation/differentiation, and guide tissue regeneration. Moreover, nanofibers can be incorporated with different biomolecules and drugs providing local drug delivery and improving cardiac tissue regeneration. As well, combination of other bioengineered constructs such as decellularized scaffolds and 3D-printed hydrogels with the electrospun scaffolds exhibited some more benefits. Although the application of electrospun scaffolds is widely being investigated by scientific community, further animal studies are still required to prove the efficacy of this kind of new materials in cardiac tissue engineering. This is a key step in going toward the commercialization of electrospun cardiac tissues, which need some more years to be completed.

References

- [1] Zhao G, Zhang X, Lu TJ, Xu F. Recent advances in electrospun nanofibrous scaffolds for cardiac tissue engineering. *Adv Funct Mater* 2015;25:5726–38.
- [2] Boffito M, Sartori S, Ciardelli G. Polymeric scaffolds for cardiac tissue engineering: requirements and fabrication technologies. *Polym Int* 2014;63:2–11.
- [3] Godin B, Sakamoto JH, Serda RE, Grattoni A, Bouamrani A, Ferrari M. Emerging applications of nanomedicine for the diagnosis and treatment of cardiovascular diseases. *Trends Pharmacol Sci* 2010;31:199–205.
- [4] Hwang H, Kloner RA. Improving regenerating potential of the heart after myocardial infarction: factor-based approach. *Life Sci* 2010;86:461–72.
- [5] Tallawi M, Rosellini E, Barbani N, Cascone MG, Rai R, Saint-Pierre G, et al. Strategies for the chemical and biological functionalization of scaffolds for cardiac tissue engineering: a review. *J R Soc Interface* 2015;12:1–24.
- [6] Jawad H, Ali N, Lyon A, Chen Q, Harding S, Boccaccini A. Myocardial tissue engineering: a review. *J Tissue Eng Regen Med* 2007;1:327–42.
- [7] Pavo N, Charwat S, Nyolczas N, Jakab A, Murlasits Z, Bergler-Klein J, et al. Cell therapy for human ischemic heart diseases: critical review and summary of the clinical experiences. *J Mol Cell Cardiol* 2014;75:12–24.
- [8] Orlova Y, Magome N, Liu L, Chen Y, Agladze K. Electrospun nanofibers as a tool for architecture control in engineered cardiac tissue. *Biomaterials* 2011;32:5615–24.
- [9] Prabhakaran MP, Venugopal J, Kai D, Ramakrishna S. Biomimetic material strategies for cardiac tissue engineering. *Mater Sci Eng C* 2011;31:503–13.
- [10] Norouzi M, Boroujeni SM, Omidvarkordshouli N, Soleimani M. Advances in skin regeneration: application of electrospun scaffolds. *Adv Healthc Mater* 2015;4:1114–33.

- [11] Mirdailami O, Soleimani M, Dinarvand R, Khoshayand MR, Norouzi M, Hajarizadeh A, et al. Controlled release of rhEGF and rhbFGF from electrospun scaffolds for skin regeneration. *J Biomed Mater Res A* 2015;103:3374–85.
- [12] Norouzi M, Shabani I, Atyabi F, Soleimani M. EGF-loaded nanofibrous scaffold for skin tissue engineering applications. *Fiber Polym* 2015;16:782–7.
- [13] Norouzi M, Shabani I, Ahvaz HH, Soleimani M. PLGA/gelatin hybrid nanofibrous scaffolds encapsulating EGF for skin regeneration. *J Biomed Mater Res A* 2015;103:2225–35.
- [14] Norouzi M, Soleimani M, Shabani I, Atyabi F, Ahvaz HH, Rashidi A. Protein encapsulated in electrospun nanofibrous scaffolds for tissue engineering applications. *Polym Int* 2013;62:1250–6.
- [15] Norouzi M, Nazari B, Miller DW. Injectable hydrogel-based drug delivery systems for local cancer therapy. *Drug Discov Today* 2016;21(11):1835–49.
- [16] Hekmati AH, Khenoussi N, Nouali H, Patarin J, Drean J. Effect of nanofiber diameter on water absorption properties and pore size of polyamide-6 electrospun nanoweb. *Text Res J* 2014;84(19):2045–55. <http://dx.doi.org/10.1177/0040517514532160>.
- [17] Hekmati AH, Rashidi A, Ghazisaeidi R, Drean J. Effect of needle length, electrospinning distance, and solution concentration on morphological properties of polyamide-6 electrospun nanowebs. *Text Res J* 2013;83(14):1452–66. <http://dx.doi.org/10.1177/0040517512471746>.
- [18] Sant S, Hwang CM, Lee S, Khademhosseini A. Hybrid PGS–PCL microfibrillar scaffolds with improved mechanical and biological properties. *J Tissue Eng Regen Med* 2011;5:283–91.
- [19] Shin M, Ishii O, Sueda T, Vacanti J. Contractile cardiac grafts using a novel nanofibrous mesh. *Biomaterials* 2004;25:3717–23.
- [20] Ravichandran R, Venugopal JR, Sundarajan S, Mukherjee S, Sridhar R, Ramakrishna S. Expression of cardiac proteins in neonatal cardiomyocytes on PGS/fibrinogen core/shell substrate for cardiac tissue engineering. *Int J Cardiol* 2013;167:1461–8.
- [21] Rockwood DN, Akins RE, Parrag IC, Woodhouse KA, Rabolt JF. Culture on electrospun polyurethane scaffolds decreases atrial natriuretic peptide expression by cardiomyocytes in vitro. *Biomaterials* 2008;29:4783–91.
- [22] Kharaziha M, Nikkhah M, Shin S, Annabi N, Masoumi N, Gaharwar AK, et al. PGS: Gelatin nanofibrous scaffolds with tunable mechanical and structural properties for engineering cardiac tissues. *Biomaterials* 2013;34:6355–66.
- [23] Jalili R, Morshed M, Ravandi SAH. Fundamental parameters affecting electrospinning of PAN nanofibers as uniaxially aligned fibers. *J Appl Polym Sci* 2006;101:4350–7.
- [24] Cicha I, Singh R, Garlich CD, Alexiou C. Nano-biomaterials for cardiovascular applications: clinical perspective. *J Control Release* 2016;229:23–36.
- [25] Hsiao C, Bai M, Chang Y, Chung M, Lee T, Wu C, et al. Electrical coupling of isolated cardiomyocyte clusters grown on aligned conductive nanofibrous meshes for their synchronized beating. *Biomaterials* 2013;34:1063–72.
- [26] Kharaziha M, Shin SR, Nikkhah M, Topkaya SN, Masoumi N, Annabi N, et al. Tough and flexible CNT–polymeric hybrid scaffolds for engineering cardiac constructs. *Biomaterials* 2014;35:7346–54.
- [27] Mooney E, Mackle JN, Blond DJ, O’Cearbhaill E, Shaw G, Blau WJ, et al. The electrical stimulation of carbon nanotubes to provide a cardiomimetic cue to MSCs. *Biomaterials* 2012;33:6132–9.
- [28] Kim S, Kim B. Control of adult stem cell behavior with biomaterials. *J Tissue Eng Regen Med* 2014;11:423–30.

- [29] Gupta MK, Walthall JM, Venkataraman R, Crowder SW, Jung DK, Shann SY, et al. Combinatorial polymer electrospun matrices promote physiologically-relevant cardiomyogenic stem cell differentiation. *PLoS One* 2011;6:1–12, e28935.
- [30] Jin J, Jeong SI, Shin YM, Lim KS, Lee YM, Koh HC, et al. Transplantation of mesenchymal stem cells within a poly (lactide-co-ε-caprolactone) scaffold improves cardiac function in a rat myocardial infarction model. *Eur J Heart Fail* 2009;11:147–53.
- [31] Ehler E, Jayasinghe SN. Cell electrospinning cardiac patches for tissue engineering the heart. *Analyst* 2014;139:4449–52.
- [32] Spadaccio C, Chachques E, Chello M, Covino E, Chachques JC, Genovese J. Predifferentiated adult stem cells and matrices for cardiac cell therapy. *Asian Cardiovasc Thorac Ann* 2010;18:79–87.
- [33] Yu J, Lee A, Lin W, Lin C, Wu Y, Tsai W. Electrospun PLGA fibers incorporated with functionalized biomolecules for cardiac tissue engineering. *Tissue Eng A* 2014;20:1896–907.
- [34] Tandon V, Zhang B, Radisic M, Murthy SK. Generation of tissue constructs for cardiovascular regenerative medicine: from cell procurement to scaffold design. *Biotechnol Adv* 2013;31:722–35.
- [35] Nelson DM, Baraniak PR, Ma Z, Guan J, Mason NS, Wagner WR. Controlled release of IGF-1 and HGF from a biodegradable polyurethane scaffold. *Pharm Res* 2011;28:1282–93.
- [36] Simón-Yarza T, Formiga FR, Tamayo E, Pelacho B, Prosper F, Blanco-Prieto MJ. Vascular endothelial growth factor-delivery systems for cardiac repair: an overview. *Theranostics* 2012;2(6):541–52.
- [37] Tian L, Prabhakaran MP, Ding X, Kai D, Ramakrishna S. Emulsion electrospun vascular endothelial growth factor encapsulated poly (l-lactic acid-co-ε-caprolactone) nanofibers for sustained release in cardiac tissue engineering. *J Mater Sci* 2012;47:3272–81.
- [38] Spadaccio C, Rainer A, Trombetta M, Centola M, Lusini M, Chello M, et al. AG-CSF functionalized scaffold for stem cells seeding: a differentiating device for cardiac purposes. *J Cell Mol Med* 2011;15:1096–108.
- [39] Jana S, Tefft B, Spoon D, Simari R. Scaffolds for tissue engineering of cardiac valves. *Acta Biomater* 2014;10:2877–93.
- [40] Cowie MR, Mosterd A, Wood DA, Deckers JW, Poole-Wilson PA, Sutton GC, et al. The epidemiology of heart failure. *Eur Heart J* 1997;18:208–25.
- [41] Puperi DS, Kishan A, Punske ZE, Wu Y, Cosgriff-Hernandez E, West JL, et al. Electrospun polyurethane and hydrogel composite scaffolds as biomechanical mimics for aortic valve tissue engineering. *ACS Biomater Sci Eng* 2016;2:1546–58.
- [42] Del Gaudio C, Bianco A, Grigioni M. Electrospun bioresorbable trileaflet heart valve prosthesis for tissue engineering: in vitro functional assessment of a pulmonary cardiac valve design. *Ann Ist Super Sanita* 2008;44:178–86.
- [43] Hong H, Dong N, Shi J, Chen S, Guo C, Hu P, et al. Fabrication of a novel hybrid scaffold for tissue engineered heart valve. *J Huazhong Univ Sci Technol Med Sci* 2009;29:599–603.
- [44] Hong H, Dong N, Shi J, Chen S, Guo C, Hu P, et al. Fabrication of a novel hybrid heart valve leaflet for tissue engineering: an in vitro study. *Artif Organs* 2009;33:554–8.
- [45] Van Lieshout M, Vaz C, Rutten M, Peters G, Baaijens F. Electrospinning versus knitting: two scaffolds for tissue engineering of the aortic valve. *J Biomater Sci Polym Ed* 2006;17:77–89.

This page intentionally left blank

Electrospun scaffolds for neural tissue engineering

13

P. Chen, A.E. Rodda, H.C. Parkington, J.S. Forsythe
Monash University, Melbourne, VIC, Australia

13.1 Introduction

13.1.1 Neuronal networking

During development, neurons extend processes (neurites) outward to make contact with other cells (targets such as neurons and muscle). Neurites possess receptors in the membranes of their extending growth cones and filopodia that are highly specialized in sensing adhesion molecules in the surrounding matrix and soluble agents secreted by target cells. Receptor activation sets in train the development of strong actin filament formation in the growth cone that, together with interactions with microtubules, “pushes” the neurite filopodia forward in the direction of the target. Thus, the growth cone responds to biochemical cues for receptor activation and uses biomechanical cues in the matrix to form the stable focal point contact adhesions necessary for neurite progression [1–3].

13.1.2 Challenges of repairing the injured brain

Death of neurons is a consequence of significant trauma, stroke, or in some neurological diseases. Neural stem cells (NSCs) are the source of cells during brain development in the embryo, but these are restricted mostly, though not exclusively, to the subventricular zone (SVZ) in the brains of adults. SVZ cells express the astrocyte marker, glial fibrillary acidic protein (GFAP), and give rise to neurons, astrocytes, and oligodendrocytes [4,5]. Trauma results in cell injury or death and often ischemia [6]. As a result, an inflammatory response is mounted, with the release of cytokines and chemokines, which, together with growth factors and neurotropic factors, induce proliferation, migration, and differentiation of NSC from the SVZ [7,8]. However, the ability of these cells to actually reach the site of damage and to network with surviving neurons in a meaningful way has not been established. NSCs traveling from the SVZ to the olfactory bulb in rodents use blood vessels as “highways” [9,10]. However, what occurs in other brain regions or in other species is not well understood, and so, the provision of guided pathways is a potential application for synthetic electrospun scaffolds.

In adulthood, traumatic injury or neurological disease can disrupt established connections, and reconnection can be slow, difficult, or even impossible. Among the difficulties include significant distances between neurons and their targets. For instance,

traumatic injury results in degeneration of the axon distally. Similarly, following stroke, a cavity forms as a result of cell death. The extracellular matrix (ECM) environment may also be changed at the site of the damage. As a consequence, the local environment may lack the appropriate physical cues required for the reconnection of neural networks. In addition, the cells that do not survive the trauma die and cytoplasmic components (e.g., ATP and potassium) are released, disrupting homeostasis. Damaged cells may release cytokines, chemokines, and other proinflammatory moieties, setting up a region of chemical cues inappropriate for repair. This region of trauma-induced disruption may become invaded by cells other than neurons and perhaps even extra brain-derived cells that “mop up” and form a fibrous scar at the core of the damage. Astrocytes form a barrier around this core in an attempt to shield surviving neurons, and this forms a glial scar [11]. Newly differentiated NSCs from the SVZ may contribute cells to this glial scar [12]. Astrocyte scar tissue formation protects nearby neurons from the inflammation of the core and restricts the area of damage, and prevention of its formation results in a greater area of damage in the longer term [13]. However, it is not conducive to axon repair and regeneration, possibly due to chondroitin sulfate proteoglycan secretion by the astrocytes of the glial scar that can actively repel neurite progress. However, it has recently been elegantly demonstrated that the glial and fibrotic scars contain a plethora of agents capable of both promoting and preventing neurite regrowth; these are secreted not only by astrocytes but also by many cell types [14]. This provides the impetus toward the development of artificial extracellular matrices with a view to providing a biophysical substrate on which axonal growth cones can project toward their target cells and reestablish network formation.

Scaffolds have been actively investigated to provide a more conducive regenerative environment within the injured brain. Of the myriad of neural scaffolds investigated, electrospun fibers have been highly successful as they can be engineered to provide both chemical and physical cues to assist repair and rewiring in the injured brain [15–19].

Electrospinning offers many advantages for the fabrication of a range of neural scaffolds that can be tuned, physically and chemically, to promote repair. Processing parameters can be tailored to meet specific requirements such as the type of polymer and molecular weight, and the incorporation and delivery methods of bioactive molecules. Similarly, the electrospun scaffold architecture can be tuned using variables such as fiber diameter, interfiber spacing, fiber alignment, and pore size. The highly porous characteristics of electrospun scaffolds allow exchange of nutrients and waste while also providing a three-dimensional (3D) microenvironment for cellular support and development.

Another important requirement for brain repair is the seamless integration of the implanted electrospun scaffold into the surrounding brain tissue. For this to occur, it is critical that the scaffold does not elicit an excessive inflammatory and foreign body response. This is inherently very difficult and is dependent on the scaffold architecture, chemistry, mechanical properties, and method of delivery. However, using appropriate designs, electrospun scaffolds can be integrated into the brain and enhance/augment regenerative abilities. This chapter will provide an overview of

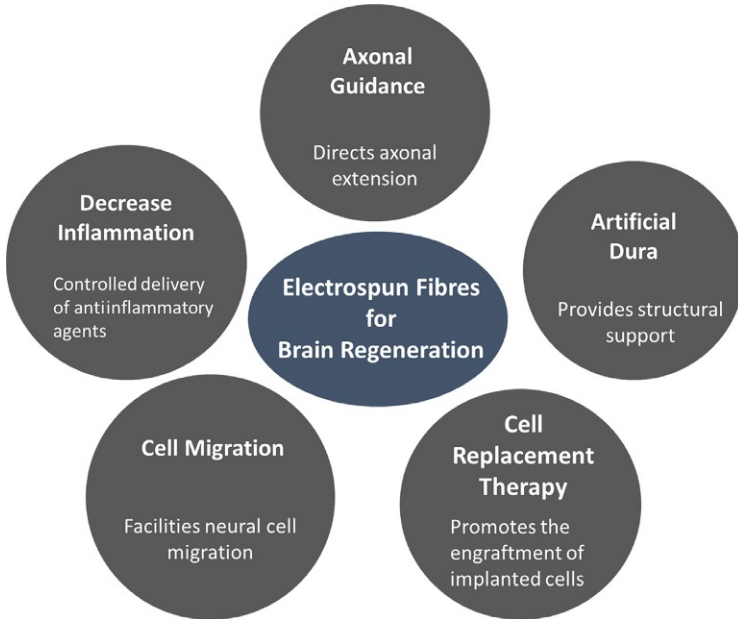


Fig. 13.1 Applications of electrospun scaffolds in brain regeneration.

the design principles of electrospun scaffolds for neural tissue engineering, with a particular focus on brain repair as outlined in [Fig. 13.1](#).

13.2 3D in vitro platforms to study neuronal physiology

The architecture of electrospun scaffolds, especially fiber diameter and alignment, directly affects the rate of cell proliferation, spreading, aggregation, and differentiation [20,21]. Investigating neural interactions in vitro allows an initial and rapid evaluation of the performance of electrospun scaffolds for brain repair. However, the unique in vitro platforms offered by electrospun fibers have also allowed the development of simplistic brain-in-a-dish tools, which can potentially be used for toxicologic and drug screening and answer fundamental questions around neuronal physiology [22].

13.2.1 Axonal extension—contact guidance and growth cone signalling

Neurons receive many physical and chemical cues relevant to axon extension via filopodia that emerge from the growth cone at the tip on the axon (described earlier and shown in [Fig. 13.2](#)). The strength of the traction force exhibited by a filopodium with its substrate influences the direction of neurite extension [1,3,23]. A uniform

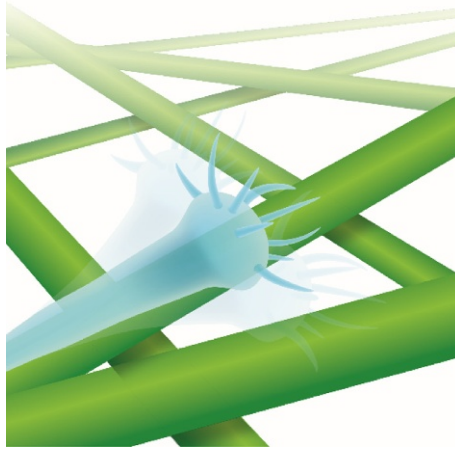


Fig. 13.2 The filopodia emerging from a growth cone at the tip of an axon. The strength of the traction force exhibited by a filopodium with the substrate influences the direction of neurite extension.

traction force in all directions provided by randomly orientated electrospun fibers results in neurite outgrowth in all directions [20]. To restore neural pathways, it may be important to guide axonal extension, which can potentially be achieved using aligned fibers produced using different types of collection devices during electrospinning [24,25]. Exploiting contact guidance provided by aligned fibers is beneficial as the physical cues are stable and can therefore be present throughout the regenerative process.

In the peripheral nervous system, the dorsal root ganglia (DRG) contain cell bodies of neurons that convey sensory information from the periphery to the spinal cord. These neurons do not possess dendrites, they do not form connections within the DRG, and their axons run in parallel [24]. This highly aligned parallel axon formation can be replicated *in vitro* by culturing DRGs on aligned electrospun fibers [20,26–28]. The length of DRG neurites cultured on aligned fibers is longer than that which occurs on randomly orientated fibers [20]. On the other hand, in the central nervous system (CNS), the axon extension behavior of neurons is distinctly different from DRG neurons, due to their different physiological roles in the brain where neural network formation is critical. Hippocampal neurites extend both parallel and perpendicular to aligned fibers leading to the formation of neural networks and fire action potentials signifying neurite-to-neurite communication as a result of functional sodium and potassium channels [26].

Apart from fiber alignment, the distance between adjacent fibers (interfiber spacing) in electrospun scaffolds also influences the direction of axon extension. There is a correlation between fiber diameter and interfiber spacing. The interfiber spacing between small diameter fibers tends to be smaller than for large diameter fibers [29],

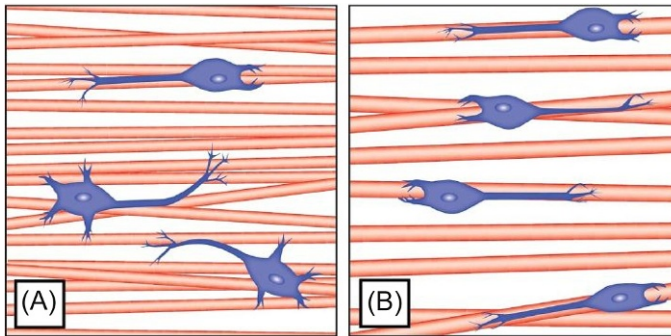


Fig. 13.3 The influence of fiber diameter and interfiber spacing on the direction of neurite extension on aligned fiber scaffolds. (A) Fiber diameter <300 nm (not to scale). Neurites are able to hop between fibers due to the small interfiber spacing distance. (B) Fiber diameter between 300 and 1325 nm. Neurites stay and extend their axons on a single fiber. The interfiber spacing is too large for neurites to hop to the neighboring fibers.

which impacts the ability of neurites to “hop” between fibers (Fig. 13.3). For aligned fibers with a diameter of ~ 300 nm, DRG neurites traverse from one fiber to another, and neurite extension is shorter [28,30]. In another study using randomly aligned fibers, axons from embryonic cortical neurons traverse fibers with an interfiber spacing in the range 2–15 μm [16,17]. Another factor that can limit the extension of neurites is the presence of crossed fibers, which can inhibit and divert the migration of Schwann cells and the extension of neurites away from the longitudinal axis [20,27].

13.2.2 Neural stem cell differentiation

Fiber orientation and diameter of electrospun scaffolds influence the differentiation behavior of stem cells. Both aligned and randomly aligned fiber scaffolds are capable of supporting the attachment, proliferation, and differentiation of NSCs into different types of neurons [18,20,31,32]. Aligned fibers were more proficient at guiding human endometrial stem cell differentiation into the neuronal lineage, such as neurons and oligodendrocytes, and hindered differentiation into the glial lineage [31]. Randomly orientated fibers resulted in clustering of mouse embryonic stem cells, which hindered cell differentiation [20]. In contrast, aligned fibers supported differentiation of mouse embryonic stem cells into neural progenitors while hindering the growth of astrocytes. Hence, a greater number of neurons and oligodendrocytes were detected on aligned fibers [20]. The differentiation of NSCs can be modulated by changing the diameter of randomly aligned fibers. Relatively larger diameter fibers (1452 nm) promoted differentiation toward neurons, while smaller fiber diameters (~ 300 nm) promoted differentiation toward glia [21].

13.2.3 Interaction of astrocytes on electrospun scaffolds

Astrocytes play important roles in both the healthy and damaged brain. In the healthy brain, astrocytes service the synapse, removing released neurotransmitter and recycling it back to the neurons, removing the potassium released during the repolarization of the action potential, providing metabolic substrates (glucose and lactate), and ensuring vasodilation in the region close to neurons that are active. Activation of astrocytes upon injury may lead to the formation of a glial scar, which is an attempt to “wall off a foreign object,” and this can prevent integration of the scaffold into the brain. Astrocytes can regulate cell homeostasis and prevent nerve regeneration at the injured site [33]. It is useful to explore the activity of astrocytes cultured on biomaterials as astrocytes are essential in nerve repair and regeneration.

Similar to neurons, astrocytes are capable of migrating on electrospun scaffolds. They are also able to penetrate into random and aligned fiber scaffolds both *in vitro* and *in vivo* [25,34–36]. However, astrocyte morphology differs when cultured on aligned versus randomly oriented fibers. Astrocytes cultured on aligned fibers follow the direction of fiber alignment [34,35] and exhibit a rectangular morphology, whereas those cultured on randomly orientated fibers form circular colonies [35]. Interestingly, both random and aligned electrospun scaffolds are able to direct the arrangement of astrocytes into a cytotropic phenotype [35]. Astrocytes cultured on scaffolds that display this phenotype were observed to be less stressed compared with those that were cultured on microgrooved substrates and patterned hydrogels [35,37,38].

It is still unclear whether the observed cytotropic- or cytotoxic-like phenotype can actually be used to predict the activity of astrocytes. Some astrocytes remain quiescent even when they do not exhibit a cytotropic phenotype [39]. Astrocytes cultured on two-dimensional (2D) and 3D substrates made from the same material exhibited the same morphology but had different activities [39]. 2-D materials induced the activation of astrocytes [39,40]. Even though the relationship between phenotype and activity is unclear, all of the previous studies reached the same conclusion that 3-D materials were a better platform for the culture of astrocytes. It was observed that 3-D astrocyte morphologies led to quiescent astrocytes with low expression of the stress marker, GFAP [35,37,39]. If astrocytes can be cultured on 3-D electrospun scaffolds without being activated, they will be able to support the outgrowth and repair mechanisms of neurons [34,39,40].

13.2.4 Neural cocultures

The aim of coculture is to study the interactions between different types of cells. There are many cellular regulations and mechanisms involved in the repair and regeneration of neurons, which involve the interplay between different cell types. Electrospun fibrous scaffolds have been used to create an environment not only for cell survival and development but also to support intercellular activities.

Selective cocultures can be performed for glia and neurons, which can be sourced separately, for example, primary Schwann and neuronal cells, or they can be sourced

collectively. The latter more closely resembles the physiological condition. The culture of DRG explants provides a useful means of colocalized primary neurons and Schwann cells. Fiber diameter plays an important role in cell migration and extension in this coculture environment with smaller fiber diameters leading to longer neurites and a longer migration of Schwann cells [29]. The coculture of primary Schwann and neuronal cells enhances the extension of neurites, which is attributed to the neurotropic factors and ECM proteins produced by Schwann cells [29].

13.3 Surface functionalization and drug release

Both topographic and biochemical cues are essential for neuronal development, as discussed previously. An electrospun scaffold is able to provide a range of physical and topographic support for cell attachment, neurite outgrowth, and axon extension. However, problems may be encountered, such as unsuitable fiber diameter or surface tension, which can result in poor cell adhesion [16,17,41]. The surface of the scaffold can be chemically modified or functionalized with biomolecules to make it more suitable for protein adsorption, which, in turn, improves cell receptor binding. Table 13.1 provides an overview of the types and methods of electrospun fiber biofunctionalization.

13.3.1 Functionalization using ECM molecules

The binding affinity of neural cells to electrospun scaffolds is improved significantly with the incorporation of ECM molecules [18,42,52], which enhances cell contact guidance [48]. Studies have shown that the number of NSCs, DRG, and Schwann cells attached on electrospun scaffolds increases when biofunctionalized with ECM molecules [18,53]. The common methods of incorporating ECM molecules to the scaffold include blending, adsorbing, and covalent bonding. As discussed in Section 13.2.1, neurite attachment to the substrate activates signaling cascades essential to cytoskeletal rearrangement and the forward progressing of neurite filopodia, and this explains why functionalization with ECM molecules enhances cellular interactions with the fibers resulting in increased cell spreading [15]. Functionalization using natural ECM molecules, such as collagen and laminin, leads to higher proliferation rates and longer neurite extensions than unfunctionalized substrates [15,44,53,54]. ECM molecules can be blended into the polymer solution and hence incorporated into the scaffold during electrospinning. In this case, ECM molecules are incorporated into the electrospun fibers with some of the molecules presented on the surface [15]. The blending of ECM molecules with the polymer solution may change fiber diameter and interfiber distance [15,46,52,54]. Nevertheless, the most important parameter for the fabrication of ECM functionalized fibers is an appropriate ratio of polymer and blended ECM molecules that will lead to improvements in cell attachment, differentiation, and axonal extension.

The extent of ECM molecule incorporation into the scaffold depends on the surface functionalization technique. A comparison between blending, covalent bonding, and physical adsorption of laminin with electrospun PLLA found that the highest amount

Table 13.1 Biofunctionalization strategies for electrospun fibers

Biomolecule/role	Immobilization technique	Type of polymer	Cell type	References
<i>ECM-derived factors</i>				
Gelatin—increased proliferation and differentiation rate	Blending	PCL	Neural stem cells (NSCs)	[15]
Collagen—axonal extension	Blending	PCL	DRG explants	[18]
Collagen—cell adhesion	Blending	PLLA- <i>co</i> -PCL	Mesenchymal stem cells (MSCs)	[42]
Collagen I/III—cell proliferation	Blending	PLLA- <i>co</i> -collagen	Neural stem cells	[19]
Laminin—axonal extension	Covalent bonding, adsorption, and blending	PLLA	PC12	[43]
Laminin—cell adhesion	Covalent bonding	PLLA	Schwann cells	[44]
Laminin—neurite extension	Covalent bonding	PCL	Dorsal root ganglia	[41]
Laminin (patterned)—guided cell growth	Covalent bonding	PA	Radial glial clones (neural precursors)	[45]
Fibronectin—cell adhesion	Blending	PLLA	In vivo	[46]
<i>Neurotropic factors</i>				
GDNF—neurite extension	Encapsulation	PCL	PC12	[47]
GDNF—increased cell survival	Covalent bonding, soluble	PCL	SN4741	[48]
BDNF—cell survival and neurite extension	Covalent bonding, adsorption, soluble	PCL LbL with heparin/PLL	Neural progenitor cells	[49]
BDNF mimetic—cell migration and neurite sprouting	Blending	PCL	Neuroblasts (in vivo)	[50]
NGF—cell differentiation	Covalent bonding	PCL	Mesenchymal stem cells (MSCs)	[51]

of laminin was detected on PLLA-/laminin-blended samples [43]. Since laminin improves cell-substrate binding, the amount of laminin incorporated in the scaffold will influence cell attachment and axon extension. PLLA/laminin blends resulted in longer axon extension compared with physical adsorption and covalent bonding techniques [43]. Regardless of the functionalization technique, the addition of laminin was shown to significantly improve cell attachment and neurite extension compared with a nonfunctionalized scaffold [41,45].

Type I and III collagen are ECM molecules that naturally occur in the peripheral nervous system [55] but are absent in the brain. Collagens bind to integrin receptors embedded in the plasma membrane, including growth cone regions, and hence, it is not surprising to find that collagen incorporation into electrospun scaffolds improves cell-substrate interactions [52]. The addition of both type I and III collagen into electrospun fibers resulted in the highest proliferation rate of NSCs compared with those that were only blended with a single type of collagen [52]. In another study, PCL/gelatin (gelatin is collagen fragment) blends improved adhesion, proliferation, and differentiation of NSCs compared to pure PCL scaffold. [15].

Core-shell electrospinning techniques can also be used to present ECM molecules on the surface of fibers. Core-shell electrospun scaffolds usually consist of two polymers in which one of them, most likely the outer shell, is blended with ECM molecules. The advantage of this system is the controlled release profile. As an example, scaffolds consisting of a PLLA core (which provides structural stability) were biofunctionalized by an outer shell consisting of gelatin blended with retinoic acid (RA) and purmorphamine, which activates the hedgehog signaling system involved in axon guidance [56]. The gelatin supported cell attachment, while RA and purmorphamine promoted neurite extension and the differentiation of NSCs into motor neurons.

13.3.2 Functionalization using neurotrophic factors

Neurotrophic factors such as nerve growth factor (NGF), brain-derived neurotrophic factor (BDNF), and glial cell-derived neurotrophic factor (GDNF) are key components in the development of the CNS, as they help to promote neural survival and proliferation [48,49,51]. A major hurdle using neurotrophins is that they typically have a short half-life in vivo and must therefore be continuously delivered in the brain. However, electrospun scaffolds have been used to provide sustained and localized delivery of neurotrophins.

Electrospun scaffolds can be functionalized with neurotrophic factors, which have been either immobilized or freely adsorbed onto the fiber surface. It should be noted that covalent immobilization of the protein may alter the ability of the factor to interact with its receptor embedded in the membrane of the neuron. However, the immobilized forms of neurotrophins can provide long-term support for cell survival because they are less prone to degradation. In contrast, adsorbed forms may have decreased effects as they can be washed off or may not be adsorbed onto the scaffold in the first place [43,48,49,51]. The growth factors may be released in response to cellular activity or circulating factors, and thus, production may be sporadic rather than continuous [51].

NGF immobilized on aligned fibrous scaffolds supported the differentiation of mesenchymal stem cells (MSCs) into cells expressing neural markers [51], whereas GDNF has been incorporated within electrospun fibers, which helped guide differentiation of human-induced PC12 cells into neurons. Encapsulated GDNF remained bioactive for 30 days [47]. Incorporation of immobilized GDNF onto electrospun PCL scaffolds increased the integration of exogenous neural stem/progenitor cells in the scaffold and enhanced topographic cues for migration of neural stem/progenitor cells and prevented the formation of an astroglial scar [36]. Layer-by-layer (LbL) deposition techniques have been used to provide greater control and reliability of scaffold bio-functionalization. Immobilization of BDNF onto polylysine-terminated LbL-coated fibers resulted in longer neurite extension of neural progenitor cells (NPCs) compared with scaffolds that contained soluble BDNF or adsorbed BDNF [49].

13.3.3 Gradient or patterned coatings

Micropatterning is another surface functionalization technique where biomolecules such as laminin [45] and collagen [54] are coated onto a substrate in different patterns, gradients, or shapes. The patterned coating can also be used to enhance the effectiveness of biomolecules and enhance topographic cues presented to cells. In the presence of gradient coatings of biomolecules, neurons can undergo chemotaxis where axonal outgrowth can be guided toward a higher concentration of the coated biomolecule [41]. The patterning of biomolecules on the scaffold can also allow controlled studies of cell processes such as migration pattern, biochemical cues, cell-to-substrate interactions, and differentiation patterns within a defined area [54]. Micropatterns of laminin strips on the surface of random fibers guide glial outgrowth along the printed striped patterns (Fig. 13.4) [57].

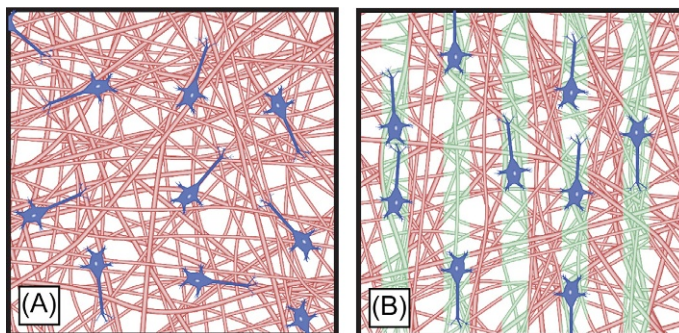


Fig. 13.4 The influence of patterned laminin coatings on neuron attachment and development. (A) Neurons attach and grow in a random direction in the absence of laminin coating. (B) Neurons grow along the stripes of laminin coating (shown in green).

13.4 Electrospun fibers for brain repair

13.4.1 Cellular responses of electrospun scaffolds in the brain

The ability of electrospun scaffolds to support cellular migration and axonal guidance has been investigated in the brain. Cells use physical contact guidance cues offered by electrospun fibers; however, the infiltration of neurites into the body of the scaffold varies depending on the architecture and location of the implant in the brain [50].

Neurites tend to grow on the surface of the scaffold in a direction perpendicular to the orientation of the aligned fibers at the surface of the implanted scaffold instead of penetrating into the scaffold [25,46,50]. In contrast, neurites are able to penetrate through randomly orientated fiber scaffolds [25]. This could be because the porosity and interfiber spacing between randomly oriented fibers are larger than for aligned fibers. Interestingly, neurite entry into the scaffold is likely to be mediated by the initial migration of astrocytes, which provide trophic cues.

13.4.2 Inflammatory responses of electrospun scaffolds in the brain

Tissue delamination, that is, separation of brain tissue from an implanted electrospun scaffold at the interface, constitutes a major problem for in vivo studies. The cause of the delamination is most likely a result of excessive inflammatory responses that occurs at the interface resulting in the formation of an astroglial scar [50]. Encapsulation by astroglia isolates the scaffold limiting integration with the penumbra [36]. This typical foreign body response also occurs at the interface of neural electrodes resulting in implant failure [58]. One strategy to improve scaffold integration is to bio-functionalize the fibers with neurotropic factors, which minimizes the inflammatory response and improves neural cell survival following implantation. Antiinflammatory agents have recently been incorporated into electrospun scaffolds for use in peripheral locations [59–61].

13.4.3 Using electrospun scaffolds to guide cell migration in the brain

When there is damage in the brain, NPCs from the SVZ region migrate toward the injured site in an attempt to repair and regenerate the damaged area [4]. However, loss of cells and ECM as a consequence of the damage will mean that a microenvironment capable of supporting NPCs is lacking. Migrating NPCs (neuroblasts) use the brain's vasculature as a physical and biochemical scaffold in their progress toward the site of injury [62]. However, neuroblasts have difficulty traversing discontinuity in the vasculature [63]. As a consequence, almost all neuroblasts remain in the SVZ and do not make it to the site of ischemic injury [63]. To address this problem, aligned electrospun scaffolds have been used to guide neuroblasts long distances [50,64]. Injection of electrospun fibers, which deliberately intersects with the SVZ, results in the neuroblasts migrating along the fibers. A mimetic of brain-derived neurotropic

factor was encapsulated and released from the electrospun aligned PCL scaffolds resulting in increased numbers of neuroblasts within the scaffold, which can be attributed to BDNF's role in modulating neuroblast migratory mechanisms [62] and its antiinflammatory properties [65]. Recently, coating aligned electrospun scaffolds with graphene increased the distance that neuroblasts travel from the SVZ along the scaffold, simulating neuroblast migration along blood vessels, an effect that could have been due to graphene's propensity to adsorb and retain certain proteins on the surface of the scaffold [64].

Electrospun PCL fibers have been investigated as a novel means of treating aggressive brain tumors. Aligned PCL scaffolds are able to guide glioblastoma multiform tumor cells from the tumor site to an extracortical location [66]. The extracortical location for this experiment was an apoptotic tumor sink made from hydrogel and cyclopamine. This migration was possible because the electrospun PCL scaffold mimicked white matter tracts and blood vessels [66]. Moreover, migration of tumor cells from the tumor site into a hydrogel demonstrated that electrospun scaffolds can be used to guide cell migration between different types of materials and tissues.

13.4.4 Delivering electrospun scaffolds in the brain

Delivery of implants into the brain poses problems such as the need for surgery and the bulkiness of the biomaterial [46,67]. The extent of the surgery required depends on the structure of the scaffold and on the location within the brain. A common approach for the implantation of electrospun scaffolds is to implant it as a tube and deliver via a syringe [50,68]. The limitation of this type of implantation is that the cells within the brain may not be able to infiltrate the scaffold, and exogenous cells cannot be delivered on the scaffold as they do not survive the rolling and injection process [36].

A potential solution to the problem with in vivo applications is to create a hybrid material consisting of an injectable hydrogel containing discontinuous or short electrospun fibers [46,67,69]. Short fibers provide the physical cues required for contact guidance, while the hydrogel matrix provides both support for the fibers and a tunable 3-D cellular microenvironment. It would be important to ensure the presence of sufficient levels of short PLLA fibers in the hybrid material in order to improve cell engraftment during migration. This suggests that the architecture of the scaffold plays an important role in neurite infiltration and cell guidance even when the hybrid material is decorated with surface-functionalized molecules such as fibronectin, BDNF mimetic, and GDNF [46,67].

13.4.5 Dura repair

The application of scaffolds as an implant for dura repair has recently been reported. The dura is a thick membrane that protects the brain and spinal cord. It also prevents cerebrospinal fluid from leaking out of the CNS [70]. Complicated neurosurgery is usually required to repair the dura following traumatic brain injury. There are many commercialized autografts that have been used to repair dura; however, the

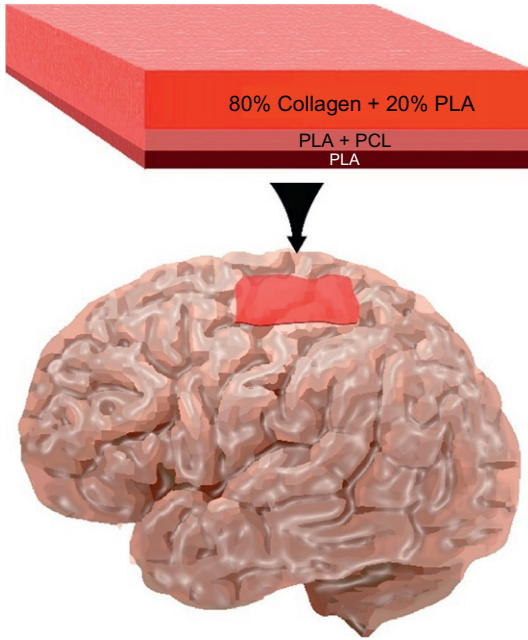


Fig. 13.5 Multilayered electrospun scaffold for dura repair. Each layer of the scaffold has its characteristics that contribute to the overall function of the scaffold.

functionality of these materials is limited. Tissue engineering strategies focusing on regeneration of the dura have utilized a multilayer electrospun PCL and PLA scaffold functionalized with type I collagen (Fig. 13.5) [71]. The material was able to repair the tissue in the damaged area without causing any inflammatory response. There was formation of collagenous fibers and fibroblast-like cells, which established the ability of the scaffold to support cell growth and tissue regeneration. Hence, an increase in the dura thickness and wound healing was observed [71].

13.5 Electroactive fibers for nerve stimulation

Neurons transmit information through synaptic and electric couplings. The firing pattern of the action potential is a key to the synaptic process [72]. The influx and efflux of ions including sodium (Na^+), potassium (K^+), and calcium (Ca^{2+}) through their voltage-gated channels lead to electric signals (action potentials) that travel along the axon. Neuronal signaling occurs both within and between neural cells. Since the synaptic process is a combination of electric and chemical events, growth and differentiation of neurons may be regulated as a result of electric stimulation [73]. Accordingly, the combination of a conductive substrate and electric stimulation may further enhance growth and differentiation of neurons and the formation of neuronal networks.

13.5.1 Passive versus active stimulation

Both passive and active electric stimulation can promote neurite outgrowth and formation of neuronal networks. Electric stimulation can be used to regulate cell function, enhance the formation of neural networks, and test for the excitability of the differentiated cells. Electrospun scaffolds can be imparted with electric properties by coating, doping, or blending with conductive materials, such as conductive polymers, carbon nanotubes, and graphene [74–77]. Polyaniline (PANI), poly(3,4-ethylenedioxythiophene) (PEDOT), and polypyrrole (PPy) are commonly used conductive polymers [78–81]. Table 13.2 shows the types of conductive materials used to coat electrospun scaffolds.

It is important to identify a process that preserves the architecture of the scaffold and its topographic cues when implementing conducting coatings [83]. Electric stimulation of conductive electrospun polymers often leads to an increase in cell proliferation and neurite outgrowth [75,80,81]. SH-SY5Y cells cultured on polyethylene terephthalate fibers coated with PEDOT exhibit increases in cytoplasmic calcium upon electric stimulation demonstrating the ability to support neural signaling [79].

Electrospinning of pure conductive polymers such as PANI is problematic due to the difficulty in achieving uniform and continuous fiber diameters [80,82]. The incorporation of conductive materials into non-conducting scaffolds will change the mechanical properties and surface chemistry of the electrospun scaffold, which will influence cell adhesion and cell-to-substrate interactions. Surface functionalization of the conducting fibers with ECM molecules may be necessary to enhance cell adhesion [80,82], which can be performed so as not to affect the electric communication with neurons [84].

Table 13.2 Types of conductive electrospun scaffolds

Base material	Conductive material	Cells	Mode of stimulation	References
PVC	Graphene (coated)	Primary motor neurons	Active—DC 100 mV pulse	[75]
PCL/gelatin	PANI (doped)	Nerve stem cells	Active—DC steady potential 1.5 V for 15, 30, 60 mins (24 h post seeding)	[80]
PET	PEDOT-doped tosylate	SH-SY5Y	1.5–3.0 V	[79]
PLLA	None	Schwann cells	Constant DC—1mA, 50 mV/mm for 8 h	[44]
PLLA	PANI (blended)	Nerve stem cells	100 mV/mm for 1 h	[82]

PANI, polyaniline; *PCL*, poly- ϵ -caprolactone; *PEDOT*, poly(3,4-ethylenedioxythiophene); *PET*, polyethylene terephthalate; *PLLA*, poly-L-lactic acid; *PVC*, polyvinyl chloride.

Electrospun scaffolds have been coated with carbon-based materials such as graphene and carbon nanotubes, which are well-known for their unique electric properties and to enhance charge transfer [78]. Graphene is biocompatible and promotes the growth and development of primary motor neurons without electric stimulation and further enhances the maturation and growth speed of neurons upon electric stimulation [75]. One advantage of using graphene is that it has a higher electric conductivity than conducting polymers, which leads to better electron transport properties [75]. Graphene-coated electrospun scaffolds require coatings with ECM molecules such as laminin to improve cell interactions. Graphene can be coated onto the scaffold via many techniques such as LbL deposition [64], coating [85], or filtration [75]. Filtration of graphene oxide produces a uniform coating on the fibers without changing the structure of the scaffold [75]. In the absence of electric stimulation, the growth and development of motor neurons on graphene-coated scaffolds showed no difference from tissue culture polystyrene plate and uncoated scaffold. In contrast, an electric stimulation of graphene-coated scaffolds significantly promoted the growth and development of primary motor neurons. The uniform coating of graphene oxide allows the electrons to transfer more freely along the fibers; hence, graphene provides a local electric conductivity, which may enhance spontaneous synaptic activity [75].

13.5.2 Electrospun coatings for neural electrodes

Electrodes are routinely used to electrically stimulate and/or record from regions of the brain for diagnostic or therapeutic purposes [78]. Current problems with electrodes are high impedance, poor long-term recording/stimulating properties, high fluctuations in recording, and tissue delamination [58,76,86]. These limitations can be overcome by using a material with high surface area, which will increase the charge transfer capacity. Moreover, the elastic modulus of the material should be similar to neural tissue, as a mismatch in the electrode-tissue stiffness activates a foreign body response and formation of a glial scar, which inhibits the stimulation-recording function of the electrode. Coating of 3-D electrospun fibers with conductive polymers, such as PEDOT and PPy, results in a decrease in the impedance compared with a 2-D film electrode [76,78]. Electrospun fibers can be coupled with hydrogels to further reduce the induction of an inflammatory response. The recording/stimulating property was enhanced when the electrospun PCL-hydrogel was loaded with neural growth factor, which encourages neurite extension toward the electrode surface [86].

13.6 Commercialization aspects

A number of commercial electrospun products are available for neural tissue engineering as outlined in Table 13.3. These electrospun products are mainly used as in vitro culture platforms for the study of neuronal physiology. Various formats are available including disks, hollow tubes, and sheets and manufactured from common biocompatible polymers or copolymers such as PCL, PLLA, PLGA, PC, and PCU. For the

Table 13.3 Commercialized electrospun products for neural tissue engineering

Product name/company	Material	Architecture and format	References
<i>In vitro: cell culture platforms to study neuronal physiology</i>			
Silk fibroin scaffold/SKE Research Equipment	Silk	Disk, sheet, tubular—freestanding scaffolds	—
Mimetix scaffold/Electrospinning company	PLLA/PLGA/ PCL/PLCL/ PAN	Disk—fixed in multiwell TCPS	—
NanoAligned, NanoECM, NanoHep/Nanofiber Solutions	PCL	Disk—freestanding	—
Corning Transwell, Snapwell/Corning Inc.	PC/PTFE collagen-coated PET	Disk—fixed to insert for multiwell TCPS	[87–91]
<i>In vivo</i>			
Redura/Medprin Regenerative Medical Technologies Co., Ltd.	PLLA	Sheet—freestanding	[92]

PAN, polyacrylonitrile; PC, Polycarbonate; PCU, polycarbonate urethane; PET, polyester; PTFE, polytetrafluoroethylene.

convenience of cell culture applications, the size of the electrospun inserts conforms to a variety of multiwell tissue culture plate or petri dish formats. The electrospun membranes can be either fixed to the culture plate or freestanding. A variety of fiber diameter, fiber orientation, scaffold thickness, and porosities are available, and many companies also offer custom-made electrospun scaffolds for specific applications.

Most electrospun scaffolds developed for brain repair have been used in preclinical settings. At present, the only commercial product available is limited to artificial dura (Table 13.3). However, more electrospun products will most likely be commercialized due to the increased amount of research activities targeting biomaterial strategies for brain repair.

13.7 Future challenges

Electrospun scaffolds have opened up new possibilities for neural repair in the brain. Appropriately designed electrospun scaffolds are able to provide physical support, enhance cell viability, and direct migration, proliferation, and differentiation

in vitro. This also facilitates the application of electrospun scaffolds as an in vitro model to interrogate brain physiology. Nevertheless, controlled guidance of axons over long distances in the brain and cellular stimulation with specific drugs/proteins remains a challenge. A better understanding of the inflammatory responses and regeneration mechanisms is required for the development of effective electrospun biomaterials. This understanding will also offer the possibility of creating a scaffold that can provide regenerative cues that match the dynamics of the brain regenerative processes. The combination of neural tissue engineering and electrodes increases the chance of monitoring or modulating the regeneration in real time. Further studies are required to find optimal delivery methods that avoid the need for complicated surgery. Advances in technology and better knowledge of cell-to-substrate interactions will improve researchers' ability to design scaffolds to be more efficient and target-specific.

References

- [1] Kerstein PC, Nichol RH, Gomez TM. Mechanochemical regulation of growth cone motility. *Front Cell Neurosci* 2015;7(9):244.
- [2] Kolodkin L, Tessier-Lavigne M. Mechanisms and molecules of neuronal wiring: a primer. *Cold Spring Harb Perspect Biol* 2011;3(6), a001727.
- [3] Short CA, Suarez-Zayas EA, Gomez TM. Cell adhesion and invasion mechanisms that guide developing axons. *Curr Opin Neurobiol* 2016;29(39):77–85.
- [4] Doetsch F, Alvarez-Buylla A. Network of tangential pathways for neuronal migration in adult mammalian brain. *Neurobiology* 1996;93:14895–900.
- [5] Doetsch F, Garcia-Verdugo JM, Alvarez-Buylla A. Cellular composition and three dimensional organisation of the subventricular germinal zone in the adult mammalian brain. *J Neurosci* 1997;17(13):5046–61.
- [6] Gregoire CA, Goldenstein BL, Floriddia EM, Barnabe-Heider F, Fernandes KJ. Endogenous neural stem cell responses to stroke and spinal cord injury. *Glia* 2015;63(8):1469–82.
- [7] Christie KJ, Turnley AM. Regulation of endogenous neural stem/progenitor cells for neural repair-factors that promote neurogenesis and gliogenesis in the normal and damaged brain. *Front Cell Neurosci* 2013;18(6):70.
- [8] Lois C, Alvarez-Buylla A. Long-distance neuronal migration in the adult mammalian brain. *Science* 1994;264:1145–8.
- [9] Thored P, Wood J, Arvidsson A, Cammenga J, Kokaia Z, Lindvall O. Long-term neuroblast migration along blood vessels in an area with transient angiogenesis and increased vascularization after stroke. *Stroke* 2007;38(11):3032–9.
- [10] Yamashita T, Ninomiya M, Acosta PH, Garcia-Verdugo J, Sunabori T, Sakaguchi M, et al. Subventricular zone-derived neuroblasts migrate and differentiate into mature neurons in the post-stroke adult striatum. *Neurobiol Dis* 2006;26(24):6627–36.
- [11] Burda JE, Sofroniew MV. Reactive gliosis and the multicellular response to CNS damage and disease. *Neuron* 2014;81(2):229–48.
- [12] Brenner EJ, Luciano D, Jo R, Abdi K, Paez-Gonzalez P, Sheng H, et al. Protective astrogenesis from the SVZ niche after injury is controlled by Notch modulator Thbs4. *Nature* 2013;497:369–73.

- [13] Bush TG, Puvanachandra N, Horner CH, Polito A, Ostenfeld T, Svendsen CN, et al. Leukocyte infiltration, neuronal degeneration, and neurite outgrowth after ablation of scar-forming, reactive astrocytes in adult transgenic mice. *Neuron* 1999;23(2):297–308.
- [14] Anderson MA, Burda JE, Ren Y, Ao Y, O'Shea TM, Kawaguchi R, et al. Astrocyte scar formation aids central nervous system axon regeneration. *Nature* 2016;14:195–200.
- [15] Ghasemi-Mobarakeh L, Prabhakaran M, Morshed M, Masr-Esfahani MH, Ramakrishna S. Electrospun poly(ϵ -caprolactone)/gelatin nanofibrous scaffolds for nerve tissue engineering. *Biomaterials* 2008;29:4532–9.
- [16] Nisbet DR, Pattanawong S, Ritchie NE, Shen W, Finkelstein DI, Horne MK, et al. Interaction of embryonic cortical neurons on nanofibrous scaffolds for neural tissue engineering. *J Neural Eng* 2007;4:35–41.
- [17] Nisbet DR, Rodda AR, Horne MK, Forsythe JS, Finkelstein DI. Neurite infiltration and cellular response to electrospun poly- ϵ -caprolactone scaffolds implanted into the brain. *Biomaterials* 2007;30(27):4573–80.
- [18] Schnell E, Klinkhammer K, Balzer S, Brook G, Klee D, Dalton P, et al. Guidance of glial cell migration and axonal growth on electrospun nanofibers of poly- ϵ -caprolactone and a collagen/poly- ϵ -caprolactone blend. *Biomaterials* 2007;28(19):3012–25.
- [19] Kijenska E, Prabhakaran MP, Swieszkowski W, Kurzydowski KJ, Ramakrishna S. Electrospun bio-composite P(LLA-CL)/collagen I/collagen III scaffolds for nerve tissue engineering. *J Biomed Mater Res B* 2012;100:1093–102.
- [20] Xie JW, Willerth SM, Li X, Matthew R, Rader MA, Sakiyama-Elbert SE, et al. The differentiation of embryonic stem cells seeded on electrospun nanofibers into neural lineages. *Biomaterials* 2009;30(3):354–62.
- [21] Christopherson GT, Song H, Mao HQ. The influence of fiber diameter of electrospun substrates on neural stem cell differentiation and proliferation. *Biomaterials* 2008;30:556–64.
- [22] Ramamoorthi K, Hara J, Ito C, Asuri P. Role of three-dimensional matrix stiffness in regulating the response of human neural cells to toxins. *Cell Mol Bioeng* 2014;7:278–84.
- [23] Athamneh AI, Suter DM. Quantifying mechanical force in axonal growth and guidance. *Front Cell Neurosci* 2015;9:359.
- [24] Corey JM, Lin DY, Mycek KB, Chen Q, Samuel S, Feldman EL, et al. Aligned electrospun nanofibers specify the direction of dorsal root ganglia neurite growth. *J Biomed Mater Res A* 2007;83(3):636–45.
- [25] Nisbet DR, Rodda AE, Horne MK, Forsythe JS, Finkelstein DI. Neurite infiltration and cellular response to electrospun polycaprolactone scaffolds implanted into the brain. *Biomaterials* 2009;30:4573–80.
- [26] Bourke JL, Coleman HA, Pham V, Forsythe JS, Parkington H. Neuronal electrophysiological function and control of neurite outgrowth on electrospun polymer nanofibers are cell type dependent. *Tissue Eng A* 2014;20(5–6):1089–95.
- [27] Wang HB, Mullins ME, Cregg JM, Hurtado A, Oudega M, Trombley MT, et al. Creation of highly aligned electrospun poly-L-lactic acid fibers for nerve regeneration applications. *J Neural Eng* 2009;6(1). 016001.
- [28] Wang HB, Mullins ME, Cregg JM, McCarthy W, Gilbert RJ. Varying the diameter of aligned electrospun fibers alters neurite outgrowth and Schwann cell migration. *Acta Biomater* 2010;6:2970–8.
- [29] Daud MFB, Pawar KC, Claeysens F, Ryan AJ, Haycock JW. An aligned 3D neuronal-glia co-culture model for peripheral nerve studies. *Biomaterials* 2012;33:5901–13.

- [30] Christopherson GT, Song H, Mao HQ. The influence of fiber diameter of electrospun substrates on neural stem cell differentiation and proliferation. *Biomaterials* 2009; 30:556–64.
- [31] Mirzaei E, Ai J, Ebrahimi-Barough S, Verdi J, Ghanbari H, Farifi-Majidi R. The differentiation of human endometrial stem cells into neuron-like cells on electrospun PAN-derived carbon nanofibers with random and aligned topographies. *Mol Neurobiol* 2015. <http://dx.doi.org/10.1007/s12035-015-9410-0>.
- [32] Yang F, Murugan R, Wang S, Ramakrishna S. Electrospinning of nano/micro scale poly(L-lactic acid) aligned fibers and their potential in neural tissue engineering. *Biomaterials* 2005;26(15):2603–10.
- [33] Maclean FL, Williams RJ, Horne MK, Nisbet DR. A Commentary on the Need for 3D-Biologically Relevant *In Vitro* Environments to Investigate Astrocytes and Their Role in Central Nervous System Inflammation. *Neural Chem Res* 2016;41:589–92.
- [34] Baiguera S, Del-Gaudio C, Fioravanzo L, Grigioni M, Folin M. *In vitro* astrocyte and cerebral endothelial cell response to electrospun poly(ϵ -caprolactone) mats of different architecture. *J Mater Sci Mater Med* 2010;21:1353–62.
- [35] Lau CL, Kovacevic M, Tingleff TS, Forsythe JS, Cate HS, Merlo D, et al. 3D Electrospun scaffolds promote a cytotropic phenotype of cultured primary astrocytes. *J Neurochem* 2014;130(2):215–26.
- [36] Wang TY, Forsythe JS, Nisbet DR, Parish CL. Promoting engraftment of transplanted neural stem cells/progenitors using biofunctionalised electrospun scaffolds. *Biomaterials* 2012;33:9188–97.
- [37] Ereifej ES, Matthew HW, Newaz G, Mukhopadhyay A, Auner G, Salakhutdinov I, et al. Nanopatterning effects on astrocyte reactivity. *J Biomed Mater Res A* 2013;101(6):1743–57.
- [38] Hsiao T, Tresco P, Hlady V. Astrocytes alignment and reactivity on collagen hydrogels patterned with ECM proteins. *Biomaterials* 2015;39:124–30.
- [39] Min SK, Kim SH, Kim CR, Paik SM, Jung SM, Shin HS. Effect of topography of an electrospun nanofiber on modulation of activity of primary rat astrocytes. *Neurosci Lett* 2012;534:80–4.
- [40] Maclean FL, Williams RJ, Horne MK, Nisbet DR. A commentary on the need for 3D-biologically relevant *in vitro* environments to investigate astrocytes and their role in central nervous system inflammation. *Neurochem Res* 2016;41:589–92.
- [41] Xie J, Liu W, MacEwan MR, Bridgeman PC, Xia Y. Neurite outgrowth on electrospun nanofibers with uniaxial alignment: the effects of fiber density, surface coating, and supporting substrate. *ASC Nano* 2014;8(2):1878–85.
- [42] Prabhakaran MP, Venugopal JR, Ramakrishna S. Mesenchymal stem cell differentiation to neuronal cells on electrospun nanofibrous substrates for nerve tissue engineering. *Biomaterials* 2009;30(28):4996–5003.
- [43] Koh HS, Yong T, Chan CK, Ramakrishna S. Enhancement of neurite outgrowth using nano-structured scaffolds coupled with laminin. *Biomaterials* 2008;29:3574–82.
- [44] Koppes AN, Zaccor NW, Rivet CJ, Williams LA, Piselli JM, Gilbert RJ, et al. Neurite outgrowth on electrospun PLLA fibers is enhanced by exogenous electrical stimulation. *J Neural Eng* 2014;11(4):046002.
- [45] Delgado-Rivera R, Griffin J, Ricuero CL, Grument M, Meiners S, Uhrich KE. Microscale Plasma-Initiated Patterning of Electrospun Polymer Scaffolds. *Col & Surf B: Biointer* 2011;84:591–6.
- [46] Rivet CJ, Zhou K, Gilbert RJ, Finkelstein DI, Forsythe JS. Cell infiltration into a 3D electrospun fiber and hydrogel hybrid scaffold implanted in the brain. *Biomatter* 2015;5(1). <http://dx.doi.org/10.1080/21592535.2015.1005527>.

- [47] Mohtaram NK, Ko J, Agbay A, Rattray D, Neil PO, Rajwani A, et al. Development of glial cell-derived neurotrophic factor-releasing artificial dura for neural tissue engineering applications. *J Mater Chem B* 2015;3:7974–85.
- [48] Wang TY, Bruggeman KAF, Sheean RKT, Turner, Bradley J, Nisbet DR, Parish CL. Characterisation of the stability and bio-functionality of tethered proteins on bio-engineered scaffolds: implications for stem cell biology and tissue repair. *J Biol Chem* 2014;289(21):15044–51.
- [49] Zhou K, Thouas GA, Bernard C, Forsythe JS. 3D presentation of a neurotrophic factor for the regulation of neural progenitor cells. *Nanomedicine* 2014;9(8):1239–51.
- [50] Fon D, Zhou K, Ercole F, Fehr F, Marchesan S, Minter MR, et al. Nanofibrous scaffolds releasing a small molecule BDNF-mimetic for the re-direction of endogenous neuroblast migration in the brain. *Biomaterials* 2014;35(9):2692–712.
- [51] Cho YI, Choi JS, Jeong SY, Yoo HS. Nerve growth factor (NGF)-conjugated electrospun nanostructures with topographical cues for neuronal differentiation of mesenchymal stem cells. *Acta Biomater* 2010;6:4725–33.
- [52] Kijenska E, Prabhakaran MP, Swieszkowski W, Kurzydowski KJ, Ramakrishna S. Electrospun bio-composite P(LLA-CL)/collagen I/collagen III scaffolds for nerve tissue engineering. *J Biomed Mater Res B Appl Biomater* 2012;100:1093–102.
- [53] Binan L, Tendev C, De-Crescenzo G, El-Ayoubi R, Ajji A, Jolicœur M. Differentiation of neuronal stem cells into motor neurons using electrospun poly-L-lactic acid/gelatin scaffold. *Biomaterials* 2014;35:664–74.
- [54] Malkoc V, Gallego-Perez D, Nelson T, Lannutti J, Hansford DJ. Controlled neuronal cell patterning and guided neurite growth on micropatterned nanofiber platforms. *J Micromech Microeng* 2015;25(12):125001.
- [55] Seyer JM, Kang AH, Whitaker JN. The characterisation of type I and type III collagen from human peripheral nerve. *Biochim Biophys Acta* 1977;492(2):415–25.
- [56] Binan L, Ajji A, De-Crescenzo G, Jolicœur M. Approaches for Neural Tissue Regeneration. *Stem Cell Rev and Rep* 2013;10(1):44–59.
- [57] Delgado-Rivera R, Griffin J, Ricuero CL, Grument M, Meiners S, Uhrich KE. Microscale plasma-initiated patterning of electrospun polymer scaffolds. *Colloids Surf B: Biointerfaces* 2011;84:591–6.
- [58] Abidian MR, Martin DC. Experimental and theoretical characterization of implantable neural microelectrodes modified with conducting polymer nanotubes. *Biomaterials* 2008;29(9):1273–83.
- [59] Kim C, Shores L, Guo Q, Aly A, Jeon OH, Kim DH, et al. Electrospun microfiber scaffolds with anti-inflammatory tributanoylated N-acetyl-d-glucosamine promote cartilage regeneration. *Tissue Eng A* 2016;22:689–97.
- [60] Li R, Pavuluri S, Bruggeman K, Long BM, Parnell AJ, Martel A, et al. Co-assembled nanostructured bioscaffold reduces the expression of proinflammatory cytokines to induce apoptosis in epithelial cancer cells. *Nanomedicine* 2016;12:1397–407.
- [61] Minardi S, Corradetti B, Taraballi F, Byun JH, Cabrera F, Liu X, et al. IL-4 release from a biomimetic scaffold for the temporally controlled modulation of macrophage response. *Ann Biomed Eng* 2016;44:2008–19.
- [62] Snapyan M, Lemasson M, Brill MS, Blais M, Massouh M, Ninkovic J, et al. Vasculature guides migrating neuronal precursors in the adult mammalian forebrain via brain-derived neurotrophic factor signaling. *J Neurosci* 2009;29(13):4172–88.
- [63] Kojima T, Hirota Y, Ema M, Takahashi S, Miyoshi I, Okano H, et al. Subventricular zone-derived neural progenitor cells migrate along a blood vessel scaffold toward the post-stroke stratum. *Stem Cells* 2010;31(28):545–54.

- [64] Zhou K, Motamed S, Thouas GA, Bernard CC, Li D, Parkinson HC, et al. Graphene functionalized scaffolds reduce the inflammatory response and supports endogenous neuroblast migration when implanted in the adult brain. *PLoS One* 2016;11(3a):e0151589.
- [65] Mizoguchi Y, Kato TA, Seki Y, Ohgidani M, Safata N, Horikawa H, et al. Brain-derived neurotrophic factor (BDNF) induces sustained intracellular Ca²⁺ elevation through the up-regulation of surface transient receptor potential 3 (TRPC3) channels in rodent microglia. *J Biol Chem* 2014;289(26):18549–55.
- [66] Jain A, Betancur M, Patel GD, Valmikinathan CM, Mukhatyar VJ, Vakharia S, et al. Guiding intracortical brain tumour cells to an extracortical cytotoxic hydrogel using aligned polymeric nanofibres. *Nat Mater* 2014;13(3):308.
- [67] Wang TY, Bruggeman KAF, Kauhausen JA, Rodriguez AL, Nisbet DR, Parish CL. Functionalised composite scaffold improve the engraftment of transplanted dopaminergic progenitors in a mouse model of Parkinson's disease. *Biomaterials* 2016;74:89–98.
- [68] Liu J, Fu TM, Cheng Z, Hong G, Zhou T, Jin L, et al. Syringe-injectable electronics. *Nat Nanotechnol* 2015;10. <http://dx.doi.org/10.1038/NNANO.2015.115>.
- [69] Hsieh A, Zahir T, Kapitsky Y, Amsden B, Wam WK, Shoichet MS. Hydrogel/electrospun fiber composites influence neural stem/progenitor cell fate. *Soft Matter* 2010;6:2227–37.
- [70] Dubrovsky B. Fundamental neuroscience and the classification of psychiatric disorders. *Neurosci Biobehav Rev* 1995;19(3):511–8.
- [71] Wang YF, Guo HF, Ying DJ. Multiplayer scaffold of electrospun PLA-PCL-collagen nanofibers as a dural substitute. *J Biomed Mater Res B Appl Biomater* 2013;101:1359–66.
- [72] Heo C, Yoo J, Lee S, Jo A, Jung S, Yoo H, et al. The control of neural cell-to-cell interactions through non-contact electrical field stimulation using graphene electrodes. *Biomaterials* 2011;32:19–27.
- [73] Meng S. Nerve cell differentiation using constant and programmed electrical stimulation through conductive non-functional graphene nanosheets film. *Tissue Eng Regen Med* 2014;11(4):274–83.
- [74] Fabbro A, Scaini D, Leon V, Vazquez E, Cellot G, Lombardi L, et al. Graphene-based interfaces do not alter target nerve cells. *ACS Nano* 2015;10(1):615–23.
- [75] Feng ZQ, Wang T, Zhao B, Li J, Jin L. Soft graphene nanofibers designed for the acceleration of nerve growth and development. *Adv Mater* 2015;27(41):6462–8.
- [76] Yang G, Kampstra KL, Abidian MR. High performance conducting polymer nanofiber biosensors for detection of biomolecules. *Adv Mater* 2011;26(29):4954–60.
- [77] Abidian MR, Martin DC. Experimental and theoretical characterization of implantable neural microelectrodes modified with conducting polymer nanotubes. *Biomaterials* 2008;29(9):1273–83.
- [78] Abidian MR, Corey J, Kipke DR, Martin DC. Conducting-polymer nanotubes improve electrical properties, mechanical adhesion, neural attachment, and neurite outgrowth of neural electrodes. *Small* 2010;6(3):421–9.
- [79] Bolin MH, Svennersten K, Chronakisc IS, Richter-Dahlfors A, Jager EWH, Berggren M. Nano-fiber scaffold electrodes based on PEDOT for cell stimulation. *Sens Actuators B* 2009;142:451–6.
- [80] Ghasemi-Mobarakeh L, Prabhakaran MP, Morshed M, Nars-Esfahani MH, Ramakrishna S. Electrical stimulation of nerve cells using conductive nanofibrous scaffolds for nerve tissue engineering. *Tissue Eng A* 2009;15(11):3605–19.
- [81] Lee JY, Bashur CA, Goldstein AS, Schmidt CE. Polypyrrole-coated electrospun PLGA nanofibers for neural tissue applications. *Biomaterials* 2009;30(26):4325–35.

- [82] Prabhakaran MP, Ghasemi-Mobarakeh L, Jin G, Ramakrishna S. Electrospun conducting polymer nanofibers and electrical stimulation of nerve stem cells. *J Biosci Bioeng* 2011;112(5):501–7.
- [83] Bolin MH, Svenersten K, Chronakisc IS, Richter-Dahlfors A, et al. Nano-fiber scaffold electrodes based on PEDOT for cell stimulation'. *Sens and Actua B* 2009;142:451–6.
- [84] Fabro A, Scaini D, Leon V, Vazquez E, Cellot G, Lombardi L, Torrisi F, et al. Graphene-based interfaces do not alter target nerve cells. *ACS Nano* 2016;10(1):615–23.
- [85] Shah S, Solanki A, Lee K. Nanotechnology-Based Approaches for Guiding Neural Regeneration. *Acc of Chem Res* 2014;49(1):17–26.
- [86] Han N, Rao SS, Johnson J, Parikh KS, Bradley PA, Lannitti J, et al. Hydrogel–electrospun fiber mat composite coatings for neural prostheses, *Front Neuroeng* 2011;4(2). <http://dx.doi.org/10.3389/fneng.2011.00002>.
- [87] Chen G, Sima J, Jin M, Wang KY, Xue XJ, Zheng W, et al. Semaphorin-3A guides radial migration of cortical neurons during development. *Nat Neurosci* 2008;11(1):36–44.
- [88] Freese C, Reinhardt S, Hefner G, Unger RE, Kirkpatrick CJ, Endres K. A novel blood-brain barrier co-culture system for drug targeting of Alzheimer's disease: establishment by using acitretin as a model drug. *PLoS One* 2014;9(3), e91003.
- [89] Ma L, Li XW, Zhang SJ, Yang F, Zhu GM, Yuan XB, et al. Interleukin-1 beta guides the migration of cortical neurons. *J Neuroinflammation* 2014;11(1):114.
- [90] Smit M, Leng J, Klemke RL. Assay for neurite outgrowth quantification. *Biotechniques* 2003;35:254–6.
- [91] Zheng W, Geng AQ, Li PF, Wang Y, Yuan XB. Robo4 regulates the radial migration of newborn neurons in developing neocortex. *Cereb Cortex* 2011;22(11):2587–601.
- [92] Zenga F, Tardivo V, Pacca P, Garzaro M, Garbossa D, Ducati A. Nanofibrous synthetic dural patch for skull base defects: preliminary experience for reconstruction after extended endonasal approaches. *J Neurol Surg Rep* 2016;77:e50–5.

Coaxial electrospun nanofibers for nanomedicine

14

K. Vodsed'álková, L. Vysloužilová, L. Berezkinová
Nanopharma, Pardubice, Czech Republic

14.1 Introduction

Nanofibers are unique structures with low area weight and a high specific surface area, that is, they are very fine fibers with diameters below 1 μm . They have high porosity and a very small diameter of interfiber pores that allow the nanofibrous structures to prevent microorganisms, bacteria, viruses, fine powders, and pollen particles from passing through, for instance, while keeping very good vapor permeability. Nanofibers are used for broad range of applications where their great specific properties excel. These materials can be used, for example, as wound dressing [1], materials for drug delivery system [2], blood vessel prosthesis and nervous tissue [3], bone and cartilage regeneration [4], electrically conductive nanofibers [5], membranes for batteries [6], nanofibers composites [7,8], or highly efficient materials for filtration [9]. They can be also used in optics, as special probes for detection systems or sound insulators [5]. Nanofibrous materials have great potential in tissue engineering as materials acceptable for cell life, cell proliferation, and differentiation, because their structure is similar to extracellular matrix (ECM) of natural tissue [10]. Currently, a few companies are engaged in the commercial production of scaffolds, for example, Nanopharma and its NanoMatrix3D. NanoMatrix3D products are primarily used for research of differentiation, in vitro expansion, and cultivation of cells.

Nanofibers can be produced by several methods such as drawing, template synthesis, phase separation, self-assembly, Forcespinning, AC spinning, and electrospinning.

Electrospinning is the most used method for production of nanofibers. This technology allows a formation of nanofibers from polymer solution or melt, respectively, by a high electric field. Polymeric solution is delivered through needle or needleless spinning electrode and is subjected to a strong electric field. Polymer solution is then drawn and elongated by external and internal electric forces, and nanofibers are created [11]. A needleless electrospinning is a technology for the increase of productivity of nanofibers introduced by Yarin and Zussman in 2003 [12]. Nanofibers are formed from a free surface of a polymeric layer using a strong electric field. Electrospun liquid is destabilized by this strong external electric field, and electrospinning starts from the fastest growing capillary wave as described by Lukas et al. [13]. Nanofibers, produced by electrospinning process, can be transmitted with various functional attributes. These functions are determined by their inner morphology or their complex chemical composition. Many functionalized composite nanofibers were produced

directly by electrospinning of polymer blends or by polymer solutions with various bioactive agents. Apart from the usage of blends, “core-shell electrospinning,” also called as “coaxial electrospinning” or “coelectrospinning,” is a very sophisticated method and an alternative route how to produce composite functionalized nanofibers with core-shell structure, as explained by Song et al. [14].

Another method used for production of nanofibers is Forcespinning. Forcespinning in contrast with electrospinning uses centrifugal forces to form fibers from polymer solution and ranks among production techniques for fibers ranging from nanometers to micrometers in size. It is also referred as centrifugal spinning, rotary jet spinning, and others. The technique of centrifugal spinning has very good potential for industrial production of fibers. The key part of the equipment is a spinning unit that consists of two parts—container and nozzles (taps)—and is connected to a drive unit. The polymer is inserted into the container as a polymer solution. Rotation leads to the polymer solution being ejected from the nozzles, and the concurrent effect of inertial (centrifugal) forces causes the fibers to extend and form. The fibers are caught in collectors of various shapes. This technique is able to cover more complicated shapes than classic electrospinning and is able to use a broader range of polymer materials compared with other techniques. Another advantage is much higher productivity when compared with the electrospinning method, while it is also much simpler.

A relatively new method for production of nanofibers is AC spinning [15]. This is a new experimental method used to produce nanofibers, which again utilizes an electrostatic field, but with an alternating current with a frequency of tens Hz. This idea allows for the most productive preparation of nanofibers among the methods using electrostatic field—involving spitting of a parallelized nanofibrous “cloud.” When using the alternating current, the created fibers are able to self-organize thanks to the carried alternating charge and to travel to some extent in a free space; thus, it is not necessary to use the collecting counterelectrode, which facilitates the production of fibers simpler. Another positive effect is the possibility to deposit the nanofiber flow in a more targeted manner. This method is currently being used with successful results to prepare core and coreless nanofibrous yarn, which present another interesting structural solution for carriers of active substances and others. Thus, the indisputable benefit of this method is relatively good productivity compared with electrostatic methods; however, this technique is still new, and thus, it is only being used within a limited group of polymers, such as polyamide (PA), polyvinyl butyral (PVB), and polylactic acid (PLA). Another benefit is the possibility to produce nanofibrous yarn and also randomly oriented nanofibrous layers, which display better porosity than other electrostatic methods.

14.2 Coaxial electrospinning

14.2.1 Background

Core-shell nanofibers, also called as core-sheath nanofibers, are bicomponent nanofibers with core-shell structure produced by a special technology known as coaxial electrospinning. Coaxial electrospinning is suitable for materials that are difficult to

spin in a common way, if at all. In the event that a well-electrospinnable polymer solution is used as a shell, fine fiber can even be produced from an otherwise electrostatically unspinnable fluid [14]. This technique can also be employed to encapsulate nanoparticles in higher concentration than by classical electrospinning. It is possible to prepare biodegradable core-shell nanofibers for controlled release of bioactive agents ranging from growth factors to antibiotics, immunosuppressives, anesthetics, and vitamins. This drug delivery system enables local controlled release while avoiding the negative aspects of nanoparticles as sole drug. This option is developing quickly. A new idea in the development of electrostatically prepared scaffolds for tissue engineering is to use nanofibers with the core-shell structure, composed of two different polymers that degrade at a different rate [16]. In this case, natural and synthetic polymers can be used. The main reason for using natural polymers is that they are inherently capable of binding cells since they carry specific protein sequences. On the other hand, synthetic biodegradable polymers provide the necessary mechanical properties, such as viscoelasticity and strength, and their degradation rate can be controlled as needed.

The best benefit of this method is the possibility to spin substances, which cannot be spun otherwise and [17,18], above all, the possibility to incorporate active substances into the nanofiber core in a scale of up to 10 wt%, which represents a great functional benefit against conventional carriers of active substances such as foils, in conjunction with the high specific surface area of nanofibers.

14.2.2 Physical principle

Like common electrospinning, its core-shell variant also occurs when electric forces at the surface of polymer solutions overcome the surface tension and cause an electrically charged jet to be ejected. Due to a bending instability, the jet is subsequently stretched to form ultrathin fibers. The necessary requirement in a wild jet motion is that its core-shell arrangement has to be preserved.

The core-shell electrospinning process is expected to be fast enough to prevent any mixing of the core and shell materials, as mentioned by Sun et al. [19]. The characteristic time τ_1 of a jet element passing the bending/whipping unstable zone of a jet must be shorter than a diffusion or mixing of two coaxially electrospun polymer solutions. Under these conditions, a sharp boundary inside a fiber can be formed, as reported by Song et al. [20]. It was found that the characteristic time, τ_1 , of bending instability in electrospinning is of the order of milliseconds, as claimed by Sun et al. [19]. One supposes that this time is nearly the same for the core-shell electrospinning too.

Characteristic time, τ_1 , of a jet passing through the bending instability has to be compared with characteristic times of two kinds of diffusions, τ_2 and τ_3 , to estimate sharpness of a wall between a core and a shell. Diffusive spreading in two identical polymers doped by dyeing agents can be described by a characteristic time $\tau_2 = d^2/D_d$, where d is a nanofiber cross-sectional diameter and D_d implies the diffusion coefficient of the dopant. The last characteristic time τ_3 describes a spreading of a sharp boundary between two different polymers due to mutual diffusion of polymeric chains. For τ_3 holds $\tau_3 = d^2/D_p$, where D_p is the polymer diffusion coefficient. More

information about characteristic diffusion times can be found in the work of Hiemenz and Lodge [21]. Characteristic diffusion times τ_2 and τ_3 are generally larger than τ_1 , and so all the boundaries survive in core-shell electrospun nanofibers as relatively sharp walls, which is in agreement with the experimental results of Sun's [19] work.

In the case of a pair of various polymers both solved in the same solvent, mutual diffusion during jet formation can be ruled out, since $\tau_1 < \tau_2 < \tau_3$. When core and shell polymers are dissolved in different solvents, these must be cautiously selected to avoid any precipitation at the solution-solution interface. The use of immiscible solvents in the core and shell usually contributes toward the internal stability of the jet. Critical physical properties of solutions that determine the stability of coaxial jets are not well understood, as has been mentioned by Andradý [22]. A bimodal distribution or a mix of thin and thick fibers is sometimes observed in coaxial electrospinning, as was done by Andradý [22]. This suggests multiple jets from a two-layered cone rather than the branching or splitting of the main jet with the subsequent separation of its components during core-shell electrospinning.

14.2.3 *Electrospinning setup—needle versus needleless coaxial electrospinning*

The critical component of the core-shell electrospinning setup is a composite spinneret comprising two separately fed chambers that culminate into a coaxial capillary orifice, that is, small capillary tubes with one inside the other. The polymer solutions, or other liquid components, are fed at carefully determinate flow rates, which are controlled by syringe pumps. The process has surprisingly deep historical roots. John F. Cooley submitted a visionary patent application in the year 1899, Cooley [23].

A needle coaxial electrospinning is usually used technology for production of core-shell nanofibers. The disadvantage is very low production in this case. Yarin and Zussman brought a revolutionary idea in 2003, and they represent needleless electrospinning from a free surface of the polymer liquid, which allowed increase of productivity of nanofibers [12]. Technology to mass production of nanofibers was developed in 2004 and patented under the brand name Nanospider [24]. The first equipment for the needleless coaxial electrospinning was developed at the Technical University of Liberec and was patented in 2009 under the name “Weir spinner” [25]. The polymeric two-layer is overflowing through the blade of a spinning electrode (Weir spinner), and electrospinning starts from its free surface, which is destabilized in a high external electric field. The instability on the liquid free surface is categorized as Larmor-Tonks-Frenkel one, which has its nature in the self-organization by the mechanism of the “fastest forming instability” [26–30].

A needle coaxial spinning electrode consists of two coaxially arranged capillaries (Fig. 14.1). The composite droplet created in an orifice of this spinning electrode forms a composite Taylor cone that pulls up both the shell polymer solution and the core polymer solution. Then, both polymer solutions together are drawn and elongated by the electrospinning jet and collected on the grounded collector [30].

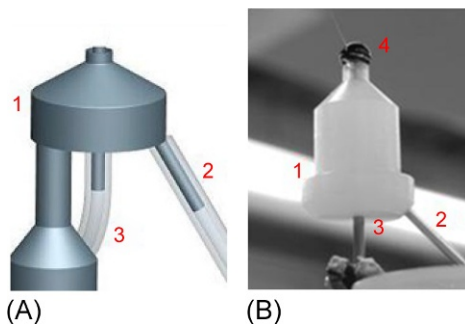


Fig. 14.1 (A) Model of the needle coaxial spinning electrode, (B) electrospinning from the needle coaxial spinning electrode, (1) spinning electrode, (2) feed of the core liquid, (3) feed of the shell polymer solution, and (4) bicomponent droplet.

Needleless coaxial electrospinning is the electrospinning variant using a principle of electrospinning from a free surface of the polymer two-layer. Fig. 14.2 shows the typical electrospinning setup with the Weir spinner as a spinning electrode. The Weir spinner (see Fig. 14.3A and B) consists of three chambers—two feeding chambers for dispensing of shell and core liquids and one outflow chamber for the waste material (nonelectrospun liquids). The middle part between chambers represents the plate electrode. This spinning electrode allows the increase of productivity of core-shell nanofibers. A large number of Taylor cones and polymeric jets are created by this needleless spinning electrode. In the next step, shell of Taylor cones pull up the core liquid, and both materials (core and shell) are drawn and elongated together by electric forces to produce core-shell nanofibers.

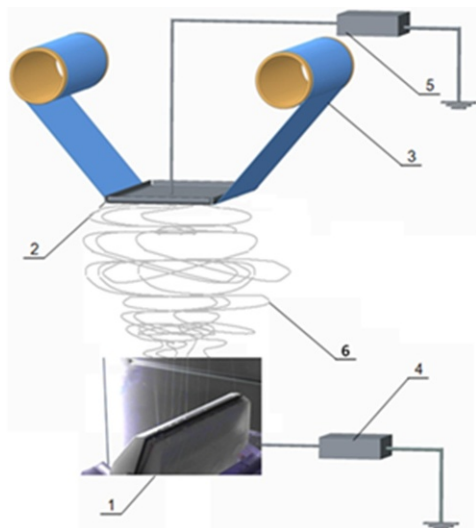


Fig. 14.2 The scheme of electrospinning setup: (1) spinning electrode (Weir spinner), (2) collector, (3) nanofibrous substrate for collecting nanofibers, (4) positive high-voltage source, (5) negative high-voltage source, and (6) polymeric jets/the zone of electrospinning [30].

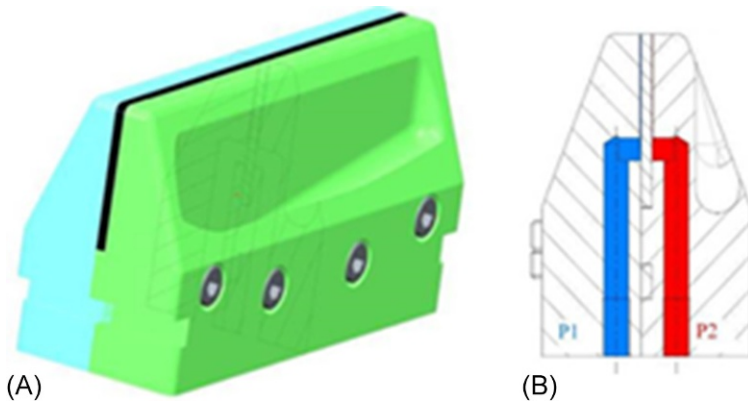


Fig. 14.3 (A) 3D model of the Weir spinning electrode. (B) cross section with highlighted polymer feeding chambers (*P1*, shell; *P2*, core) [30].

The cylindrical coaxial spinning electrode with a smooth surface is the next needleless spinning electrode for production of core-shell nanofibers (see Fig. 14.4) [30]. This spinning electrode is made of duraluminium. This consists of three cylindrical parts used for distributing polymers to the top layer. Two lateral chambers are supplied by the shell polymer solution, while the inner chamber feeds the spinning electrode with the core liquid. A bicomponent polymeric ring is created along an orifice of the cylindrical coaxial spinning electrode and core-shell nanofibers can be created [30].

Core-shell structured nanofibers can be also produced using a single-nozzle technique. The single-nozzle method was demonstrated by Bazilevsky [31] using blends

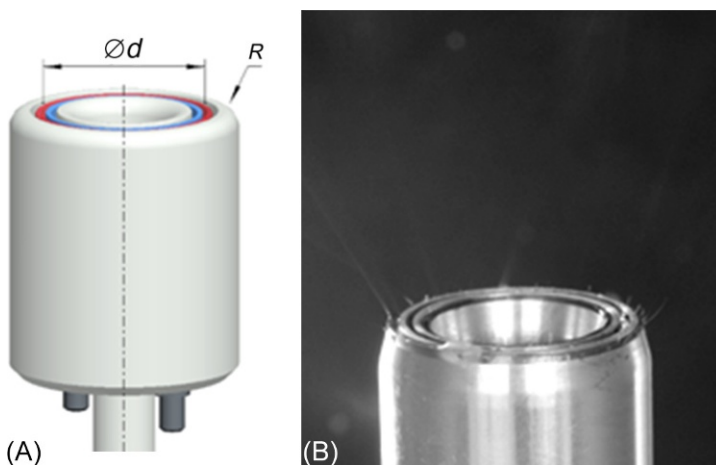


Fig. 14.4 (A) Model of cylindrical coaxial spinning electrode, optimized design for core-shell nanofibers. (B) Electrospinning from the cylindrical coaxial spinning electrode [30].

of immiscible polymers. Polymethylmethacrylate (PMMA) and polyacrylonitrile (PAN) were dissolved separately in dimethylformamide (DMF). It was proved that the outer shell flow is sufficiently strong to stretch the inner droplet into the Taylor cone, thus forming a core-shell jet.

Substantially, coaxial nanofibers can be divided into three basic types, core-shell, hollow, and porous. It is not easy to demonstrate experimentally that coaxial electrospinning really provides with the core-shell configuration of electrospun fibers. Different methods can be used in order to detect core-shell structure, for example, focused ion beam-scanning electron microscopy (FIB-SEM), transmission electron microscopy (TEM), and fluorescent confocal microscopy. Vodsed'áľková et al. [32] carried out a lot of experiments to prove core-shell structure of nanofibers. In one type of the experiment, two different polymers were dissolved in different solvents. In this case, PCL was used as a shell and gelatin as a core, and after sectioning through nanofibrous layer, core-shell structure was recognizable under SEM using backscattered electron imaging, as you can see in Fig. 14.5. Resulting core-shell structure is in agreement with the theory related to characteristic diffusion times that have been mentioned earlier.

The core-shell electrospinning can also be used to prepare hollow nanofibers. To obtain hollow fibers from core-shell fibers, the core part, used as a template, has to be selectively removed either by thermal decomposition or by choosing appropriate selective solvent. The requirement is that the shell material is stable either against the annealing temperature or against the applied selective solvent. The hollow nanofibers (Fig. 14.6) of polyvinylalcohol (PVA) as a shell were made by Vodsed'áľková et al. [32].

Coaxial electrospinning can be used to produce porous core-shell nanofibers by selecting a suitable solvent system for controlled release of bioactive agents. The porous nanofibers may be used in diverse applications given their larger specific

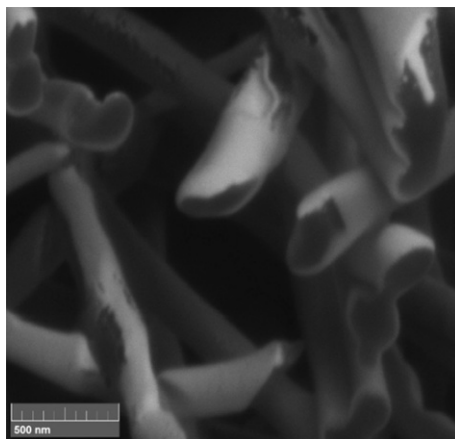


Fig. 14.5 Cross-sectional imaging of nanofibrous layer, PCL as a shell and gelatin as a core [32].

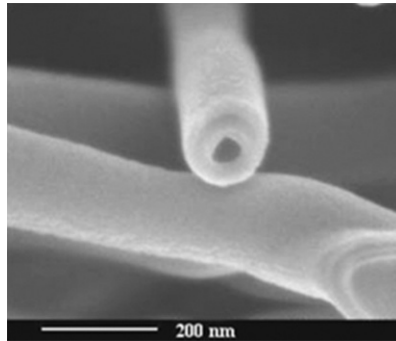


Fig. 14.6 Cross-sectional imaging of nanofibrous layer, PCL as a shell and PVA as a core [32].

surface area in comparison with the standard smooth nanofibers. Firstly, polycaprolactone (PCL) was dissolved in tetrahydrofuran (THF) and dimethylsulfoxide (DMSO) with a volume ratio of 7:3 to obtain a 16 wt% polymer solution. This polymer solution was used as a shell polymer. Secondly, PCL was dissolved in chloroform and ethanol with a volume ratio of 9:1 to obtain a 10 wt% polymer solution. This solution was used as the core polymer. It was determined that the morphology of porous core-shell nanofibers is influenced by the flow rate of the core polymer. SEM images in (Fig. 14.7) show porous and nonporous morphology of core-shell nanofibers. Flow rate of the core polymer influenced the density of pores on the surface of the core-shell

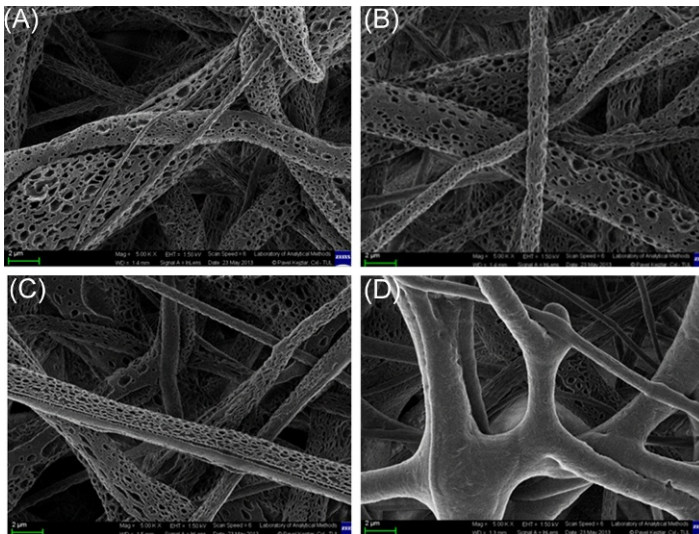


Fig. 14.7 Characterization of electrospun nanofibers. SEM (5,000 \times) morphology of coaxial nanofibers with various flow rates mL/h (A) flow rate of shell/core 50/10, (B) flow rate of shell/core 80/10, (C) flow rate of shell-core 80/20, and (D) flow rate of shell/core 80/50 mL/h [33].

nanofibers. Pores were observed on the core-shell nanofibers, wherein the core polymer was fed at 10 mL/h and shell polymer 50–80 mL/h. When the flow rate of the core polymer increased to 20 mL/h, only few pores appeared on the surface of the core-shell nanofibers. A greater volume of core polymer solution decreased the rate of evaporation of the solvents from nanofibers, and it noticeably slowed down the process of solidification of nanofibers. Pores on the surface of the core-shell nanofibers did not form due to the slow evaporation of solvents in the case of flow rate of core-shell polymer 80/50 mL/h [33].

14.2.4 Potential application of core-shell nanofibers

Core-shell nanofibers are preferably used in nanomedicine due to the possibility to encapsulate nanoparticles in higher concentration than by classic electrospinning; possibility to prepare biodegradable core-shell nanofibers for controlled release of bioactive agents ranging from growth factors to antibiotics, immunosuppressives, anesthetics, and vitamins; and possibility to electrospin materials that are difficult or impossible to process into nanofibers by conventional fiber-forming techniques or by classic electrospinning. Due to the characteristics and advantages that have been mentioned above, core-shell nanofibers are excellent candidates for application in wound healing, drug delivery, and tissue engineering.

Commercial wound dressings that exert their antimicrobial effect by eluting germicidal compounds have been developed to provide sustained release of therapeutic doses of silver ions to the wound. However, silver ions are highly toxic to keratinocytes and fibroblasts and may delay wound repair if applied indiscriminately to healing tissue areas. In addition to this, constant wound cleaning and redressing is needed, causing discomfort to patients and requiring substantial nursing input. A biodegradable drug-eluting wound dressing from an electrospun nanofibrous matrix potentially offers several advantages over conventional ones [34].

Depending on the wound type and its healing, the most suitable wound dressing system must be used. Because of unique properties of nanofibrous structures, the applications of these materials on various types of wounds are plentiful with respect to other modern wound dressing materials, such as hydrocolloids and hydrogels. The following properties are generally considered in all modern wound dressing materials: maintain the most suitable environment at the wound interface; absorb excess exudates without leakage to the surface of a wound; provide thermal insulation and mechanical and bacterial protections; allow gaseous and fluid exchanges; absorb wound odor; be nonadherent to the wound and easily removable without trauma; provide some debridement action (remove dead tissue and foreign particles); and be nontoxic, nonallergic, nonsensitizing (to both patient and medical staff), sterile, and nonscarring [35–37].

Electrospun drug-loaded nanofibrous membranes potentially offer advantages over conventional ones. Local antibiotics and anesthetic have the advantage of delivering high drug concentrations to the precise area required, and the total dose of antibiotic applied locally is not normally sufficient to produce toxic systemic effects [38]. Antibiotic-loaded wound dressings made out of biodegradable polymeric membranes boast a number of advantages. First, biodegradable membranes provide bactericidal

concentrations of antibiotics for the prolonged time needed to completely treat the particular infection. Second, the biodegradable nanofibrous membranes dissolve; thus, there is no need for removal. Third, the changeable biodegradability ranging from weeks to months is able to allow many types of infections to be treated. Lastly, the biodegradable membranes dissolve slowly resulting that the soft tissue or bone defect is slowly filled up with normal tissue and there is no need for reconstruction [38]. In one published study, a sandwich-structured nanofibrous membrane was produced via electrospinning to develop biodegradable and biomimetic drug-eluting dressings. The materials used to prepare the membranes included polylactide-polyglycolide (PLGA), collagen, vancomycin, gentamicin, and lidocaine [39]. The blended solutions were electrospun into sandwich-structured membranes, with PLGA/collagen used as a surface layer and PLGA/drugs used as a core layer. After electrospinning, an elution method and an HPLC assay were employed to characterize the *in vitro* release rates of the pharmaceuticals over a 30-day period. A bacterial inhibition test was carried out to determine the bioactivity of the released antibiotics. Furthermore, to assay the cytocompatibility and cell behavior of electrospun sandwich-structured nanofibers, the interaction between normal human fibroblasts and the nanofibrous matrix was studied. The experimental results showed that biodegradable membranes released high concentrations of vancomycin and gentamicin for 4 and 3 weeks, respectively, and lidocaine for 2 weeks. The bioactivity of vancomycin and gentamicin ranged from 30% to 100% and 37% to 100%. In addition, it was found that nanofibrous structures were functionally active in responses in human fibroblasts [39].

Another advantage of these nanofibrous wound dressings or patches is that relatively small drug molecules penetrate the skin, and this is how transdermal patches work. In contrast to drugs taken orally, patches have the advantage that the substance does not have to be digested first. This means that the substance remains chemically unchanged and directly accesses the part of the body where it needs to take effect via the bloodstream. As a result, this also avoids filtration and initial metabolism by the liver.

Other options for using nanofibrous materials from classic or core-shell nanofibers appear in tissue engineering and drug delivery. Core-shell nanofibers are preferably used in tissue engineering and drug delivery due to the possibility to prepare biodegradable core-shell nanofibers for controlled release of bioactive agents, to encapsulate nanoparticles in higher concentration than by classic electrospinning, and to prepare nanofibers with the core-shell structure composed of two different polymers that degrade at a different rate. The structure and functional properties of nanofibrous structures from classic or core-shell nanofibers closely resemble the ECM that forms the natural environment for cell proliferation. These nanofibrous structures are subsequently seeded with different types of cells that adhered to them to proliferate and regenerate the injured tissues. A common approach of tissue engineering is to construct a three-dimensional scaffold simulating the spatial arrangement of cells in the real organ. 3-D scaffolds can provide a better link between single cells and organs than traditional 2-D cultures. 3-D scaffold offers another direction for cell-cell interactions, cell migration, and cell morphogenesis, which are important aspects in regulation of the cell cycle and tissue functions. There are few methods of how to produce

voluminous 3-D scaffolds; for example, AC spinning, a combination of electrospinning/coaxial electrospinning method and linearized air in order to obtain voluminous structure with the required porosity, and a combination of electrospinning/coaxial electrospinning and melt blown technology, which enables the formation of a layer containing both microfibers and nanofibers while guaranteeing good mechanical properties of the 3-D scaffolds [40,41]. A series of experiments have been carried out in the field of tissue engineering and biomedicine. Experts have treated this area, and the results indicate possibilities for future utilization as artificial cartilage and artificial bone [42], skin implants [43], dental implants [44], vessels [45], and others.

Unique properties of electrospun fibers such as high loading, simultaneous delivery of diverse therapies, ease of operation, and cost-effectiveness have expanded their use in drug delivery. Drug delivery is the method used for administering a pharmaceutical compound to achieve a therapeutic effect. The main aspects for the development of core-shell delivery systems for tissue engineering are the bioactivity of the active substances that are incorporated within the core of scaffolds and the controlled release of this substances according to the time frame of tissue regeneration. In the study on applying electrospun nanofibers for the sustained release of a model drug, electrospun nanofibers have been successfully used to achieve different controlled drug release profiles, such as immediate, smooth, pulsatile, delayed, and biphasic releases. It is also possible to produce multidrug delivery systems with timed programmed release profile [46,47]. Drugs can be embedded in the fiber through dissolution or dispersion in the polymer solution. Many interesting biochemical factors for tissue development, for example, proteins or nucleic acid, do not dissolve in organic solvent and may suffer loss of bioactivity when dispersed in the polymer solution.

Core-shell electrospinning, where the drug is dissolved in an aqueous core solution and the polymer in an organic shell solution, is one approach to overcome this drawback by extruding the core and shell polymer solutions through two concentric nozzles [48]. The hydrophilic core polymer solution simplify the loading and preservation of protein bioactivity, whereas the hydrophobic shell polymer allows fiber formation. The same situation occurs also in the case of the incorporation of growth factors, enzymes, or liposomes. In the study published by Mičková et al. [49], coaxial electrospinning was successfully used for the incorporation of liposomes into nanofibers. Two methods were compared in this study. First, blend electrospinning was used for the incorporation of the liposomes into nanofibers, and the results showed that this method caused the liposomes to break and release encapsulated material. To overcome this problem, coaxial electrospinning was used. During coaxial electrospinning the hydrodynamic forces in the core of the jet are lowered compared with blend electrospinning and preventing the disruption of the liposomal membrane. The use of such coaxial nanofibers with incorporated liposomes as drug delivery systems can combine the unique properties and advantages of nanofibers and liposomes.

Core-shell nanofibers can be used in the case of incorporation of growth factors that are used as a biological stimulus to promote stem-cell proliferation and differentiation. The hydrophilic core polymer solution simplify the loading and preservation of growth factors, whereas the hydrophobic shell polymer allows fiber formation and

the degradation rate can be controlled as needed. The growth factors can be also supplied directly into the culture medium at regular intervals, but this is feasible only *in vitro* but not *in vivo*, because it is necessary to have a sustained release of bioactive growth factor from the scaffold. For example, Srouji et al. developed a core-shell scaffold for bone morphogenetic protein-2 (BMP-2) release to support bone regeneration. BMP-2 was incorporated in an aqueous solution of poly(ethylene oxide) (PEO) used as a core, whereas the shell solution was fabricated of a poly(caprolactone) blended with poly(ethylene glycol) (PEG). The blending of PEO and PEG influenced pores in the shell, which dramatically affected the diffusion of BMP-2 and other proteins out of the fiber core [50].

Scaffolds with persistent release of growth factors or other active substances are also often fabricated using different types of hydrogels. However, this type of hydrogel-based scaffolds have some limitations, such as cell death in the depths of the scaffolds and poor mechanical properties, and can be used in the case where mechanical properties or 3-D distribution of cells are not of major concern.

Core-shell nanofibers can be also used for the purpose to achieve linear drug release or prolong an initial burst release. In this case, the release kinetics depends on the time of degradation of the polymer material that is used as the shell. Preferably, it is also possible to use porous core-shell nanofibers for controlled release of bioactive agents incorporated in the core. Gradual release of bioactive agents from the porous core-shell nanofibers is a great advantage of this method. The porous shell allows the protection of the core against the ambient environment, and simultaneously, the sufficient size of the pores enables the gradual diffusion of the bioactive agents from the core.

Furthermore, there are plenty of areas where coaxial electrospinning can be preferably used in the case of the incorporation of nanoparticles, for example, artificial bone and dental implants. In the case of bone regeneration, coaxial electrospinning can be used for the incorporation of hydroxyapatite (HA) within the core. HA has been shown to increase osteoblasts and osteoblast-like cell proliferation [51]. Gradual controlled release of HA from the core during the disintegration of the shell material can also prevent problems with mild poisoning of cells with calcium and phosphate. Additionally, incorporation of nano-HA crystals not only increases the osteogenic potential of produced scaffolds but also has been suggested that these scaffolds have mechanical properties superior to those made without HA [52].

14.3 Conclusion

In this chapter, a large number of promising methods for the preparation of electrospun scaffolds for use in the field of nanomedicine were described. The main attention was paid to very sophisticated method of coaxial electrospinning, which offers substantial advantages over conventional methods, especially the possibility to electrospin materials that are difficult to spin in a common way, encapsulation of nanoparticles in higher concentration, preparation of biodegradable core-shell nanofibers for controlled release of bioactive agents, and preparation of scaffolds with the core-shell structure composed of two different polymers that degrade at a different

rate. Due to aforementioned advantages, core-shell nanofibers are excellent candidates for use in the field of wound healing, tissue engineering, and drug delivery.

For this reason, the introduction of core-shell nanofibers is rather slow compared with their monocomponent alternative. The technology is cautiously further explored mainly by SMEs in Europe, Asia, and North America in terms of production device optimization and collection of comprehensive *in vitro* and *in vivo* data to demonstrate the system's reproducibility and its ability to safely uniformly release drugs, among other features.

As new precedents of nanofiber-based medical devices are gradually introduced to clinical application, nanofibers become more mainstream, which implies other important circumstances such as easier capital raising for nanofiber technologies, a clearer vision on their regulatory classification, and, thus, commercialization horizons in terms of medical device- or drug-related scenarios.

Currently, there are no registered products or devices involving coaxial nanofibers on the market yet. Most developments are currently under preclinical investigation, meaning that it will still take a few years until finalized core-shell nanofiber-based medical products emerge and spread.

References

- [1] Jin HJ, Fridrikh SV, Rutledge GC, Kaplan DL. Electrospinning *Bombyx mori* silk with poly(ethylene oxide). *Biomacromolecules* 2002;3(6):1233–9.
- [2] Kenawy ER, Bowlin GL, Mansfield K, Layman J, Simpson DG, Sanders EH, et al. Release of tetracycline hydrochloride from electrospun poly(ethylenecovinylacetate), poly(lactic acid), and a blend. *J Control Release* 2002;81:5764.
- [3] Bornat A. Production of electrostatically spun products. Liverpool Patent US 4689186 A; 1987.
- [4] Martino Di, Liverani L, Rainer A, et al. Electrospun scaffolds for bone tissue engineering. *Musculoskelet Surg* 2011;95:69. <http://dx.doi.org/10.1007/s12306-011-0097-8>.
- [5] MacDiarmid AG, Jones WE, Norris ID, Gao J, Johnson Jr. AT, Pinto NJ, et al. Electrostatically generated nanofibers of electronic polymers. *Synth Met* 2001;119:2730.
- [6] Norris ID, Shaker MM, Ko FK, Macdiarmid AG. Electrostatic fabrication of ultrafine conducting fibers: polyaniline/polyethylene oxide blends. *Synth Met* 2000;114:10914.
- [7] Dai HQ, Gong J, Kim H, Lee D. A novel method for preparing ultrafine aluminoborate oxide fibers via an electrospinning technique. *Nanotechnology* 2002;13(5):6747.
- [8] Reneker DH, Yarin AL, Evans EA, Kataphinan W, Rangkupan R, Liu W, et al. Electrospinning and nanofibers. In: *New frontiers in fiber science*; 2001.
- [9] Rangarajan S, Mehta K, Chase GG. Nanofibers in coalescer filter media. In: Holcomb AG, Gebes PF, editors. *Fall topical conference of the American filtration and separations society, Minneapolis*; 1999. p. 177185.
- [10] Li WJ, Laurencin CT, Catterton EJ, Tuan RS, Ko FK. Electrospun nanofibrous structure: a novel scaffold for tissue engineering. *J Biomed Mater Res* 2002;60(Sv. (4)):613–21.
- [11] Moghe AK, Gupta B. Co-axial electrospinning for nanofiber structures: preparation and applications. *Polym Rev* 2008;48:353–77.
- [12] Yarin AL, Zussman E. Upward needleless electrospinning of multiple nanofibers. *Polymer* 2004;45:2977–80.

- [13] Lukas D, Sarkar A, Pokorny P. Self-organization of jets in electrospinning from free liquid surface: a generalized approach. *J Appl Phys* 2008;103(8):084309-1–084309-7.
- [14] Song T, Zhang Y, Zhou T, Lim Ch, Ramakrishna S, Liu B. Encapsulation of self-assembled FePt magnetic nanoparticles in PCL nanofibres by coaxial electrospinning. *Chem Phys Lett* 2005;415:317–22.
- [15] Pokorny P, Kostakova E, Sanetnik F, Mikes P, Chvojka J, Kalous T, et al. Effective AC needleless and collector less electrospinning for yarn production. *Phys Chem Chem Phys* 2014;16(48):26816–22.
- [16] Gupta BS, King MW, Hudson S, Hufenus R, Gluck J, Moghe A. Electrospun core-sheath fibres for soft tissue engineering. NTC Project, Project No.: F05-NS04; 2007.
- [17] Rutledge G, Yu JH, Fridrikh SV. Production of submicron diameter fibres by two-fluid electrospinning process. World Intellectual Property Organization, Patent No. WO09568; 2005.
- [18] Li LD, Wand Y, Xia Y. Electrospinning of polymeric and ceramic nanofibers as uniaxially aligned arrays. *Nano Lett* 2004;4:933–8.
- [19] Sun Z, Zussman E, Yarin AL, Wendorf JH, Greiner A. Compound core-shell polymer nanofibres by co-electrospinning. *Adv Mater* 2003;15:1921–32.
- [20] Song T, Zhang ZZ, Zhou TJ. Fabrication of magnetic composite nanofibres of poly(ϵ -caprolactone) with FePt nanoparticles by coaxial electrospinning. *J Magn Magn Mater* 2006;303:286–9.
- [21] Hiemenz PC, Lodge TP. *Polymer chemistry*. Boca Raton: Taylor & Francis Group; 2007.
- [22] Andradý AL. *Science and technology of polymer nanofibres*. New Jersey: Wiley; 2008.
- [23] Cooley JF. Apparatus for electrically dispersing fluids. U.S. Patent No. 692 631; 1902.
- [24] Jirsak O, Sanetnik F, Lukas D, Kotek V, Martinova L, Chaloupek J. A method of nanofibres production from a polymer solution using electrostatic spinning and a device for carrying out the method. Patent, WO2005024101; 2005.
- [25] Pokorny P. Fontanovy spinner. Patent PV 2009–425, Česká Republika; 2009.
- [26] Frenkel J. *Kinetic theory of liquids*. New York: Dover Publications; 1955.
- [27] Tonks LA. Theory of liquid surface rupture by a uniform electric field. *Phys Rev* 1935;48:562. <http://dx.doi.org/10.1103/PhysRev.48.562>.
- [28] Larmor J. On the influence of electrification on ripples. *Proc Camb Phil Soc Math Phys Sci* 1890;7:69–72.
- [29] Lukas D, Sarkar A, Pokorny P. Self-organization of jets in electrospinning from free liquid surface: a generalized approach. *J Appl Phys* 2008;103(8):20.
- [30] Vysloužilová L, Valtera J, Pejchar K, Beran J, Lukáš D. Design of coaxial needleless electrospinning electrode with respect to the distribution of electric field. *Appl Mech Mater* 2014;693:394–9. ISSN: 1660-9336. <http://dx.doi.org/10.4028/www.scientific.net/AMM.693.394>.
- [31] Bazilevsky A, Yarin AL, Megaridis CM. Co-electrospinning of core-shell fibres using a single-nozzle technique. *Langmuir* 2007;23:2311–4.
- [32] Vodsedalkova K, Cudlinova M, Berezkinova L. Application of core-shell nanofibers with controlled release of bioactive substances for topical treatments. *BioNanoMed*, 26–28 March, Krems, Austria; 2014.
- [33] Vodsedalkova K, Cudlinova M, Lubasova D. Porous core-shell nanofibers. In: *Fiber Society*, 21–23, May, Liberec, Czech Republic; 2014.
- [34] Sill TJ, von Recum HA. Electrospinning application in drug delivery and tissue engineering. *Biomaterials* 2008;29:1989–2006.

- [35] Zahedi P, Rezaeian I, Ranaei-Siadat S-O, Jafari S-H, Supaphol P. A review on wound dressings with an emphasis on electrospun nanofibrous polymeric bandages. *Polym Adv Technol* 2010;21:77–95. <http://dx.doi.org/10.1002/pat.1625>.
- [36] Abrigo M, McArthur SL, Kingshott P. Electrospun nanofibers as dressings for chronic wound care: advances, challenges, and future prospects. *Macromol Biosci* 2014;14:772–92. <http://dx.doi.org/10.1002/mabi.201300561>.
- [37] Norouzi M, Boroujeni SM, Omidvarkordshouli N, Soleimani M. Advances in skin regeneration: application of electrospun scaffolds. *Adv Healthcare Mater* 2015;4:1114–33. <http://dx.doi.org/10.1002/adhm.201500001>.
- [38] Zilberman M, Elsner JJ. Antibiotic-eluting medical devices for various applications. *J Control Release* 2008;130(3):202–15. <http://dx.doi.org/10.1016/j.jconrel.2008.05.020>.
- [39] Chen DW, Hsu YH, Liao JY, Liu SJ, Chen JK, Ueng SW. Sustainable release of vancomycin, gentamicin and lidocaine from novel electrospun sandwich-structured PLGA/collagen nanofibrous membranes. *Int J Pharm* 2012;430(1–2):335–41. <http://dx.doi.org/10.1016/j.ijpharm.2012.04.010>.
- [40] Erben J, Jencova V, Chvojka J, Blazkova L, Strnadova K, Modrak M, et al. The combination of meltblown technology and electrospinning – the influence of the ratio of micro and nanofibers on cell viability. *Mater Lett* 2016;173:153–7. <http://dx.doi.org/10.1016/j.matlet.2016.02.147>.
- [41] Erben J, Pilarova K, Sanetnik F, Chvojka J, Jencova V, Blazkova L, et al. The combination of meltblown and electrospinning for bone tissue engineering. *Mater Lett* 2015;143:172–6. <http://dx.doi.org/10.1016/j.matlet.2014.12.100>.
- [42] Holmes B, Castro NJ, Zhang LG, Zussman E. Electrospun fibrous scaffolds for bone and cartilage tissue generation: recent progress and future developments. *Tissue Eng Part B Rev* 2012;18(6):478–86. <http://dx.doi.org/10.1089/ten.teb.2012.0096>.
- [43] Bonvallet PP, Schultz MJ, Mitchell EH, Bain JL, Culpepper BK, Thomas SJ, et al. Microporous dermal-mimetic electrospun scaffolds pre-seeded with fibroblasts promote tissue regeneration in full-thickness skin wounds. *PLoS One* 2015;10(3):e0122359. <http://dx.doi.org/10.1371/journal.pone.0122359>.
- [44] Sheikh Z, Najeeb S, Khurshid Z, Verma V, Rashid H, Glogauer M. Biodegradable materials for bone repair and tissue engineering applications. *Materials* 2015;8:5744–94.
- [45] Ercolani E, Del Gaudio C, Bianco A. Vascular tissue engineering of small-diameter blood vessels: reviewing the electrospinning approach. *J Tissue Eng Regen Med* 2015 Aug;9(8):861–88. <http://dx.doi.org/10.1002/term.1697>.
- [46] Yu DG, Wang X, Li XY, Chian W, Li Y, Liao YZ. Electrospun biphasic drug release polyvinylpyrrolidone/ethyl cellulose core/sheath nanofibers. *Acta Biomater* 2013;9:5665–72.
- [47] Son YJ, Kim WJ, Yoo HS. Therapeutic applications of electrospun nanofibers for drug delivery systems. *Arch Pharm Res* 2014;37:69. <http://dx.doi.org/10.1007/s12272-013-0284-2>.
- [48] Chakraborty S, Liao IC, Adler A, Leong KW. Electrohydrodynamics: a facile technique to fabricate drug delivery systems. *Adv Drug Deliv Rev* 2009;61(12):1043–54. <http://dx.doi.org/10.1016/j.addr.2009.07.013>.
- [49] Mickova A, Buzgo M, Benada O, Rampichova M, Fisar Z, Filova E, et al. Core/shell nanofibers with embedded liposomes as a drug delivery system. *Biomacromolecules* 2012;13(4):952–62. <http://dx.doi.org/10.1021/bm2018118>. See comment in PubMed Commons below.
- [50] Srouji S, Ben-David D, Lotan R, Livne E, Avrahami R, Zussman E. Slow-release human recombinant bone morphogenetic protein-2 embedded within electrospun scaffolds for

regeneration of bone defect: in vitro and in vivo evaluation. *Tissue Eng Part A* 2011;17:269.

- [51] Phipps MC, Clem WC, Grunda JM, Clines GA, Bellis SL. Increasing the pore sizes of bone-mimetic electrospun scaffolds comprised of polycaprolactone, collagen I and hydroxyapatite to enhance cell infiltration. *Biomaterials* 2012;33:524.
- [52] Tyagi P, Catledge SA, Stanishevsky A, Thomas V, Vohra Y. Nanomechanical properties of electrospun composite scaffolds based on polycaprolactone and hydroxyapatite. *J Nanosci Nanotechnol* 2009;9:4839–45.

Electrospun-based systems in cancer therapy

15

M. Norouzi^{*,†}, B. Nazari[‡], D.W. Miller^{*}

^{*}University of Manitoba, Winnipeg, MB, Canada, [†]Kleysen Institute for Advanced Medicine, Winnipeg, MB, Canada, [‡]Tehran University of Medical Sciences, Tehran, Iran

15.1 Introduction

Cancer, which is defined as an uncontrolled growth of cells, is one of the leading causes of death. In 2012, approximately 14.1 million new cases and 8.2 million cancer-related deaths were reported worldwide. Also, it is estimated that the annual new cancer cases will increase to 22 million within the next two decades [1–3].

Available treatment regimens include surgery, radiation, chemotherapy, hormonal therapy, immunotherapy, and gene therapy adopted based on the type and stage of cancer [4,5]. Nowadays, chemo- and radiotherapy are the most common approaches for cancer treatment and inhibition of tumor recurrence. Nevertheless, they are often associated with serious side effects to normal tissue and cells due to the poor selectivity of most chemo- and radiotherapeutics toward cancer cells [6–8].

Compared with the conventional chemotherapy, localized drug delivery technique not only can decrease the toxicity in normal tissues through avoiding systemic circulation of the chemotherapeutics but also can provide a sustained release and high concentration of drugs at the tumor vicinity. Moreover, it can decrease the frequency of drug administration required [9,10].

Many local delivery systems such as nanofibers [11,12], hydrogels [10,13], nano-/microparticles [14,15], micelles [16,17], and liposomes [18,19] have been investigated for local drug delivery. Amidst the various drug delivery systems considered, biodegradable polymer electrospun nanofibers have attracted much attention due to their appealing characteristics such as large surface area to volume ratio associated with high loading capacity and high encapsulation efficiency. In addition, high interconnected porosity of electrospun nanofibrous-based systems can facilitate cell binding, which consequently can reduce metastasis of cancer cells. The nanofibrous scaffolds can be utilized as implantable devices in the tumor site or at the surgical resection margins for cancer chemo-, hyperthermia, or photothermal therapy of solid tumors [12,20–26].

Several anticancer agents including chemotherapeutics, magnetic nanoparticles, photothermal agents, and genes have been embedded into electrospun fibers, demonstrating enhanced tumor growth inhibition and anticancer efficacy. Various techniques have been utilized to incorporate anticancer agents into nanofibers including blend electrospinning, emulsion electrospinning, coaxial electrospinning, and postspinning modifications such as coating and layer-by-layer (LBL) self-assembly [12,21,27,28].

In this chapter, application of electrospun-based systems for local chemotherapy, magnetic hyperthermia therapy, photothermal-chemotherapy, gene therapy, and circulating tumor cell capturing are reviewed.

15.2 Chemotherapy

Various chemotherapeutic agents such as doxorubicin (DOX), paclitaxel (PTX), cisplatin (CDDP), and dichloroacetate (DCA) have been loaded into electrospun fibrous scaffolds to provide local drug delivery and cancer therapy [29–31]. Table 15.1 illustrates a summary of the prepared electrospun-based systems for local chemotherapy.

As an example, dichloroacetate (DCA)-loaded polylactide (PLA) electrospun nanofibers were fabricated and implanted to cover the solid tumors in mice. The nanofibers allowed controlled release and high concentrations of DCA at the tumor site, which could induce multiple ATP depletion in cervical carcinoma cells, resulting in necrosis of the tumor cells as the main process of cell death. Therefore, 96% tumor suppression degree was achieved by 19 days in tumor-bearing mice upon treatment with the DCA-loaded electrospun mats. Both tumor volume and tumor weight decreased significantly meanwhile tumors completely disappeared in half of the tumor-bearing mice [29].

To avoid local lung cancer recurrence after surgical resection that stems from microscopic disease remaining after surgery, Kaplan et al. [39] provided localized and sustained release of cisplatin using cisplatin-loaded superhydrophobic scaffolds of polycaprolactone and poly(glycerol monostearate-*co*-caprolactone) nanofibers. The superhydrophobic nature of the scaffolds prevented burst release of the drug while enabling a sustained release in a linear fashion over ~90 days. In vivo studies on murine model of lung cancer showed a significant increase in median recurrence-free survival to >23 days, in comparison with the standard intraperitoneal cisplatin therapy of equivalent dose.

To reduce burst release of the drugs from nanofibers, they can also be encapsulated in nanoscale carriers, such as mesoporous silica nanoparticles (MSNs), hydroxyapatite nanoparticles, and liposomes [55,61,62]. Such formulations also allow for multifunctional delivery systems. An example of such a system is the MSNs embedded in electrospun PLLA nanofibers reported by Yuan et al. [47]. The MSNs consisted of sodium bicarbonate and DOX encapsulated for long-term pH-sensitive DOX release and an ibuprofen (IBU) coating on the outside for an initial short-term release. The MSNs entrapped in the nanofibers provided an acid-responsive drug release profile with the increased CO₂ generated under acidic environmental conditions resulting in larger pores or channels in the polymer and accelerating DOX release from 79% (pH = 7.4) to 99% (pH = 5) at 120 days. The nanofibers embedded with MSNs showed tumor growth inhibition in liver-tumor-bearing mice, which was associated with increased Bax/Bcl-2 ratio, activation of caspase-3 levels, and attenuation of IL-6/STAT3/NF-κB signaling pathways in the tumor cells [47].

In another work, DOX-loaded MSNs and hydroxycamptothecin (CPT)-loaded hydroxyapatite nanoparticles were prepared and incorporated into PLGA nanofibers

Table 15.1 Electrospun-based systems for local chemotherapy

Polymer	Drug	Solvent	Method	Cancer cell (in vitro)	Cancer (in vivo)	Highlight	References
PVA, GE	DOX-FA-PCL-PEG micelles	AA, water	Coaxial electrospinning	4T1 (breast cancer)	Breast cancer	DOX was encapsulated in FA-conjugated PCL-PEG active-targeting micelles. Then, they were trapped in the core of the core-shell nanofibers of PVA-gelatin	[32]
PVA, CS	DOX	AA	Coaxial electrospinning	SKOV3 (ovary cancer)	–	The released DOX was delivered into SKOV3 cell nucleus	[33]
PEO, CS, GO	DOX	AA	Blend electrospinning	A549 (lung cancer)	–	Higher amount of DOX was released at pH 5.3 compared with 7.4 because of the reduced interaction between DOX and PEO/CS/GO nanofibers	[31]
PCL, MWCNTs	GTP	DMF/CH ₂ Cl ₂	Blend electrospinning	A549 (lung cancer), HepG2 (hepatocellular carcinoma)	–	GTP-loaded composite nanofibers exhibited low cytotoxicity to normal osteoblast cells but high inhibition effect to tumor cells especially to HepG2 cells	[34]
PCL, GE	DOX-UCNPS, INDO	TFE	Blend electrospinning	–	Hepatoma H22 tumor	DOX could be released from mesoporous silica, while NaGdF ₄ /Yb/Er@NaGdF ₄ /Yb provided upconversion fluorescence/magnetic resonance dual-model imaging	[35]
PCL, GE	SN-38	TFE	Blend electrospinning	U251, U87 (glioblastoma)	–	–	[36]

Continued

Table 15.1 Continued

Polymer	Drug	Solvent	Method	Cancer cell (in vitro)	Cancer (in vivo)	Highlight	References
PCL, PEO	NIC, Ag NPs	DCM/DMF	Blend electrospinning	A549 (lung cancer), MCF-7 (breast cancer)	–	Codelivery of NIC and Ag NPs from nanofibers exhibited superior anticancer potential compared with either NIC- or Ag NPs-loaded nanofibers	[37]
PCL-PEG-PCL (PCEC)	CUR	DCM/isopropanol	Blend electrospinning	9L (glioma)	–	Antitumor activity of the CUR-loaded fibers against the cells was maintained over the whole experiment process, while the antitumor activity of free CUR disappeared within 48 h	[38]
PCL, PGC-C18	CIS	DCM/DMF	Blend electrospinning	LLC (Lewis lung carcinoma)	Lung cancer	Local and sustained release of cisplatin could significantly inhibit lung cancer recurrence in comparison with intraperitoneal cisplatin therapy	[39]
PCL, PGC-C18	CPT-11, SN-38	CHCl ₃ /MetOH	Blend electrospinning	HT-29 (colon cancer)	–	PGC-C18 increased hydrophobicity of PCL, resulting in a slowed drug release via increasing the stability of the entrapped air layer	[40]
PLA	DCA	CHCl ₃ /MetOH	Blend electrospinning	U14 (cervical carcinoma)	Cervical carcinoma	Controlled release of DCA from the nanofibers resulted in necrosis of the tumor cells	[29]
PLA	CIS	CHCl ₃ /MetOH/DMSO	Blend electrospinning	–	Liver cancer	Multilayered CIS nanofibers were found better than single layer in terms of the retarded tumor recurrence, prolonged survival time and less systemic toxicity	[41]

PLA, PEO	CIS	TFE	Blend electrospinning	–	Cervical carcinoma	Vaginal implantation of the CIS/fiber resulted in the preferred partition of CIS in vaginal tract; reasonable distribution in the rectum, uterus, and tumor; and very low concentration in peripheral organs compared with intravenous injection of CIS	[42]
PLA, PEO	CIS, CUR	TFE/CHCl ₃	Blend electrospinning	HeLa (cervical carcinoma)	Cervical carcinoma	About 10 h after fiber implantation, the concentration ratio between curcumin and cisplatin decreased to 3:1, which probably allows the optimum synergetic effect to destroy the residual tumor cells	[43]
PLA, PEG	PTX, DOX	CHCl ₃	Emulsion electrospinning	C6 (glioma)	–	Due to the hydrophilicity, DOX could easily diffuse out from the fibers, resulting in a faster release rate than hydrophobic PTX	[44]
PLLA	DOX-loaded MSNs	MC/DMF	Blend electrospinning	HeLa (cervical carcinoma)	–	–	[45]
PLLA	DOX-loaded MSNs	DCM/ammonium fluoride/HFIP/EtOH	Blend electrospinning	HeLa (cervical carcinoma)	Liver cancer	A pH-triggered release system was fabricated using inorganic cap CaCO ₃ to control the opening of pore entrances of drug-loaded MSNs inside PLLA fibers	[46]
PLLA	IBU, DOX-loaded MSNs	DCM/DMF	Blend electrospinning	–	Hepatocellular carcinoma	MSNs containing sodium bicarbonate and DOX inside for a long-term pH-sensitive release of DOX and IBU outside for an initial short-term release were prepared	[47]
PLLA	IBU, DOX-loaded MSNs coated with PDA	DCM/HFIP/EtOH	Blend electrospinning	HeLa (cervical carcinoma)	–	The hybrid nanofibers showed short-term IBU release to inhibit inflammation at an early stage and long-term antitumor efficacy resulted from DOX	[48]

Continued

Table 15.1 Continued

Polymer	Drug	Solvent	Method	Cancer cell (in vitro)	Cancer (in vivo)	Highlight	References
PLLA	5-FU, oxaliplatin	CHCl ₃ /MetOH/DMSO	Blend electrospinning	HCT-8 (colon cancer)	Colon cancer	Larger necrotic region was seen in tumors treated with nanofibers than the groups treated with a combination of free drugs	[49]
PLLA	TB-II	CHCl ₃ /acetone	Blend electrospinning	SMMC-7721 (hepatocellular Carcinoma)	Hepatocellular carcinoma	–	[50]
PELA	HCPT	MC	Emulsion electrospinning	HepG2 (hepatocellular carcinoma)	Hepatoma H22 tumor	The nanofibrous system showed over 20 times higher inhibitory effect than free HCPT after 72 in vitro	[51]
PLDLA, QCS	DOX	DMF/DMSO	Blend electrospinning	HeLa (cervical carcinoma)	–	Positively charged tertiary amino groups of QCS probably led to destruction of cell membrane facilitating DOX penetration into cells	[52]
PLDLA, PEO coated with QCS	GOS	DMF/DMSO	Blend electrospinning, coating	Graffi cells (myeloid sarcoma)	Myeloid sarcoma	The GOS-containing nanofibers induced apoptosis in Graffi cells	[53]
PLGA	PTX	DCM	Blend electrospinning	C6 (glioma)	–	IC50 of the PTX-PLGA nanofibers was 36 mg/mL, which was comparable with commercial paclitaxel formulation Taxol (ca. 30 mg/mL)	[54]
PLGA	PTX	DCM/DMF	Blend electrospinning	C6 (glioma)	Glioma	Animal treated with PLGA-PTX showed much smaller tumors compared with Taxol, indicating sustained release of paclitaxel	[30]
PLGA	DOX-MSNs, HCPT-HANPs	HFIP	Blend electrospinning	HeLa (cervical carcinoma)	–	Dual-drug-loaded nanofibers showed better antitumor effect than the single drug-loaded nanofibers	[55]

PLGA, GE, mZnO	DOX, CPT	HFIP	Blend electrospinning	HepG2 (hepatocellular carcinoma)	–	Incorporation of mZnO within PLGA/GE nanofibers reduced the burst release of DOX and improved the mechanical feature of the nanofibers	[56]
PLGA, PEO	FRA	DCM/DMF	Blend electrospinning	MCF-7 (breast cancer)	–	FRA-loaded nanofibers were more efficient in apoptosis induction compared with free FRA	[57]
P(NIPAAM-AAm-VP)	DOX	Water	Blend electrospinning	A549 (lung cancer)	–	–	[58]
PPC	PTX-loaded Ca-alginate MPs, TMZ	DCM	Emulsion electrospinning	C6 (glioma)	–	Optimal synergistic effect was achieved when the weight ratio of the two drugs was 1:1	[59]
PVP	CUR	Acetic ether	Blend electrospinning	B16 (melanoma)	Melanoma	CUR-loaded nanofibers induced cancer cell apoptosis and faded its invasion ability	[60]

AA, acetic acid; Ag NPs, silver nanoparticles; CHCl₃, chloroform; CIS, cisplatin; coPLA, poly(L-lactide-co-D,L-lactide); CPT, camptothecin; CS, chitosan; CUR, curcumin; DCA, dichloroacetate; DCM, dichloromethane; DMF, N,N-dimethylformamide; DMSO, dimethyl sulfoxide; DNR, daunorubicin; DOX, doxorubicin hydrochloride; EtOH, ethanol; FA-PCL-PEG, folate-conjugated-poly(ε-caprolactone)-poly(ethylene glycol); FRA, ferulic acid; 5-FU, 5-fluorouracil; GE, gelatin; GO, graphene oxide; GOS, gossypol; GTP, green tea polyphenols; HANPs, hydroxyapatite nanoparticles; HCPT, hydroxycamptothecin; HFIP, hexafluoro-2-propanol; IBU, ibuprofen; INDO, indomethacin; MC, methylene chloride; MeOH, methanol; MPs, microparticles; MSNs, mesoporous silica nanoparticles; MWCNTs, multiwalled carbon nanotubes; mZnO, mesoporous ZnO; NIC, niclosamide; NPs, nanoparticles; PCL, poly(ε-caprolactone); PDA, polydopamine; PEG, poly(ethylene glycol); PELA, poly(DL-lactic acid)-poly(ethylene glycol); PEO, polyethylene oxide; PGC-C18, poly(glycerol monostearate-co-caprolactone); PLA, polylactide; PLDLA, poly(L-lactide-co-D,L-lactide); PLGA, poly(lactide-co-glycolide); PLLA, poly-L-lactic acid; P(NIPAAM-AAm-VP), poly(N-isopropylacrylamide-co-acrylamide-co-vinylpyrrolidone); PPC, polypropylene carbonate; PTX, paclitaxel; PVA, polyvinyl alcohol; PVP, polyvinyl pyrrolidone; QCS, quaternized chitosan; SN-38, 7-ethyl-10-hydroxy camptothecin; TB-II, timosaponin B-II; TFE, trifluoroethanol; TMZ, temozolomide; UCNPS, NaGdF₄/Yb/Er@NaGdF₄/Yb@mSiO₂-polyethylene glycol nanoparticles.

via electrospinning. The dual anticancer drug-loaded composite nanofibers demonstrated a sustained dual drug release and a superior antitumor effect on HeLa cells compared with the single drug-loaded nanofibers [55].

To provide specific targeting to tumor cells, the local drug delivery systems can also be biofunctionalized with targeting moieties that have affinity for over-expressed/unique tumor cell markers. Thus, the active-targeting drug delivery systems can enhance therapeutic efficacy while reducing the toxicity to normal cells [63–65].

Yang et al. [32] developed an active-targeting micelle-in-nanofiber system for local cancer therapy. In this particular delivery system, DOX was encapsulated in folate-conjugated poly(ϵ -caprolactone)-poly(ethylene glycol) (FA-PCL-PEG) micelles by self-assembling. The folate (FA) ligands can bind to the folate receptors (FR) that are overexpressed on the surface of many of solid tumors. The micelles were then embedded in the core of the core-shell nanofibers by coaxial electrospinning in which the inner phase was a mixture of poly(vinyl alcohol) (PVA) and the micelles and the outer phase was cross-linked gelatin. *In vivo* studies on 4 T1 tumor-bearing mice not only showed smaller tumor volume in nanofiber treated groups than intravenous (IV) DOX-injected groups after 21 days but also once implantation of nanofibers demonstrated comparable tumor growth suppression compared with four times injection of DOX. Moreover, the folate-containing groups showed a better inhibition effect on the tumor growth, which was ascribed to the enhancement of internalization into the tumor cells via FR-mediated endocytosis.

15.3 Magnetic hyperthermia therapy

Hyperthermia therapy is a technique in which heat is applied to kill cancer cells or sensitize them to radiation and chemotherapy and therefore synergistically enhance the antitumor effect [66]. The major challenge in hyperthermia therapy is localized heating of the tumor site to the optimum temperature without overheating the surrounding healthy tissues. In order to apply localized heating and enable repeated heating upon the application of an alternating magnetic field, magnetic nanoparticles can be embedded in a variety of vehicles such as nanofibers, hydrogels, spheres, liposomes, and micelles [67,68]. Furthermore, these magnetic fibers can be employed for controlled drug delivery under the application of an alternating magnetic field amalgamating the concepts of hyperthermia therapy and chemotherapy [69,70]. Table 15.2 presents a summary of the prepared electrospun-based systems utilized for hyperthermia therapy.

Iron oxide nanoparticles (IONPs) are being applied clinically for magnetic hyperthermia in cancer treatment [75,76]. In order to improve targetability of the nanoparticles and prevent their leakage from the dead cancer cells into the surrounding healthy tissues, IONPs (nanoparticle size, 50 nm and loading concentration, 20% w/w) were incorporated in electrospun polystyrene (PS) fibers. Upon functionalization of the fiber surface with collagen, human SKOV-3 ovarian cancer cells were bound to the fibers, and they were killed by application of an alternating magnetic field during 10 min at a temperature of 45°C. The magnetic fibers could be repeatedly heated at the tumor site without the loss of the heating capacity or release of IONPs [67].

Table 15.2 Electrospun-based systems for local magnetic hyperthermia therapy

Polymer	Drug	Solvent	Method	Cancer cell (in vitro)	Highlight	References
CS	Fe ₃ O ₄ NPs	TFA/ DCM	Electrospinning, coating	Caco-2 (colon cancer)	The magnetic CS nanofibers could increase temperature to 45°C, reducing tumor cell proliferation	[71]
Alg, PEO, PVA	Fe ₃ O ₄ NPs	Water	Electrospinning, chemical coprecipitation	A-549 (lung cancer)	Alginate-based fibers were cross-linked by either “ionic” or “covalent” method followed by chemical coprecipitation of Fe ₃ O ₄ magnetite NPs	[72]
PLA	DNR, MWCNT, Fe ₃ O ₄ NPs	Acetone/ CHCl ₃	Blend electrospinning	K562 (leukemia)	Synergistic antitumor effect of magnetic hyperthermia and chemotherapy was seen	[73]
PLGA	BTZ, IONPs	HFIP	Blend electrospinning, coating	4T1 (breast cancer)	PLGA-IONP nanofibers were coated with dopamine to prepare mussel-inspired magnetic nanofibers. Then, the catechol moieties were used to bind BTZ and for pH-dependent release of BTZ	[74]
P(MMA-co-DMA),	BTZ, IONPs	DMF	Blend electrospinning	MCF-7, 4T1 (breast cancer)	The catechol moieties of the nanofibers were employed to bind BTZ that was released in a pH-dependent manner	[70]
Poly (NIPAAm-co-HMAAm)	DOX, MNPs	HFIP	Blend electrospinning	COLO 679 (melanoma)	The nanofibers were composed of a temperature-sensitive polymer containing DOX and MNPs. MNPs served as a trigger of DOX release and a source of heat	[69]
PS	IONPs	DMF/ THF	Blend electrospinning	SKOV-3 (ovarian cancer)	The nanofibers could kill all the attached cancer cells upon exposure to an alternating magnetic field in 10 min	[67]

Alg, alginate; AMF, alternating magnetic field; BTZ, bortezomib; CHCl₃, chloroform; CS, chitosan; DCM, dichloromethane; DMF, *N,N*-dimethylformamide; DNR, daunorubicin; DOX, doxorubicin hydrochloride; HFIP, hexafluoro-2-propanol; IONPs, Iron oxide nanoparticles; MNPs, magnetic nanoparticles, a mixture of magnetite (Fe₃O₄) and maghemite (γ-Fe₂O₃); MWCNTs, multiwalled carbon nanotubes; NPs, nanoparticles; PEO, polyethylene oxide; PLA, polylactide; PLGA, poly(D,L-lactide-co-glycolide); P(MMA-co-DMA), poly(methyl methacrylate-co-dopamine methacrylamide); Poly (NIPAAm-co-HMAAm), copolymer of *N*-isopropylacrylamide (NIPAAm) and *N*-hydroxymethylacrylamide(HMAAm); PS, polystyrene; PVA, polyvinyl alcohol; TFA, trifluoroacetic acid; THF, tetrahydrofuran.

In another work, temperature-responsive nanofibers made of *N*-isopropylacrylamide (NIPAAm) and *N*-hydroxymethylacrylamide (HMAAm) copolymer containing DOX and magnetic nanoparticles (MNPs, a mixture of magnetite (Fe_3O_4) and maghemite ($\gamma\text{-Fe}_2\text{O}_3$)) were fabricated. The temperature-responsive copolymer could trigger drug release through the switchable changes in the swelling ratio of the polymer network in response to “on-off” switching of an alternating magnetic field, while the self-generated heat from the MNPs was able to induce deswelling of the polymer networks (Fig. 15.1). In fact, at “on” state, the nanofibers deswelled and deformed, triggering the release of the drug molecules, whereas only negligible amounts of DOX were released during the cooling “off” process, maintaining interactions between nanofibers and DOX. Therefore, the nanofibers could kill 70% of human melanoma cells in 5 min of alternating magnetic field application by synergistic effect of the hyperthermia and chemotherapy [69].

15.4 Photothermal-chemotherapy

Photothermal therapy is a minimally invasive technique, which uses hyperthermia generated by photothermal agents from laser energy to kill cancer cells. Near-infrared (NIR) radiation is often employed in photothermal therapy owing to

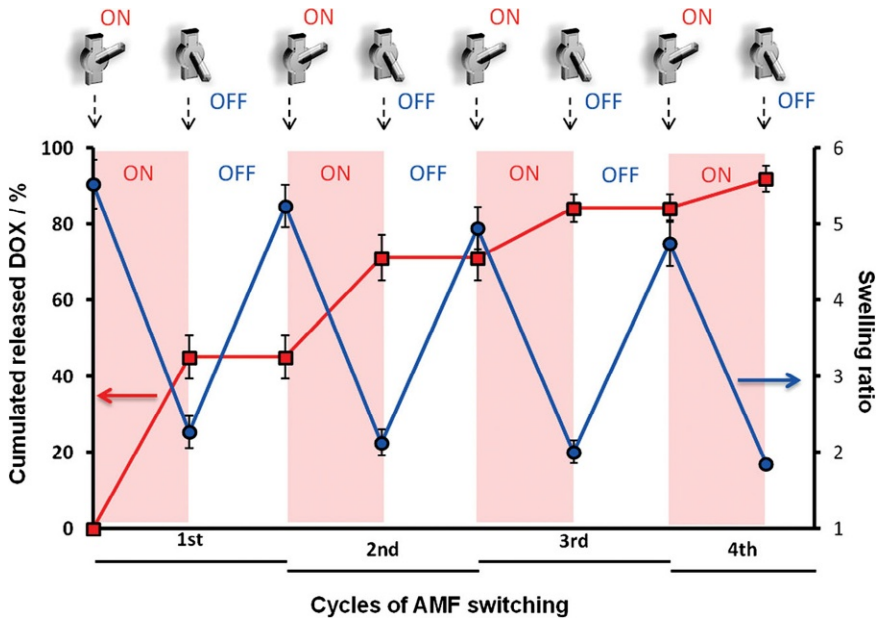


Fig. 15.1 “On-off” switchable and reversible heat profile and the corresponding swelling ratio of the cross-linked MNP nanofibers and DOX release in response to temperature. *AMF*, alternating magnetic field.

Reproduced with permission from Kim Y, Ebara M, Aoyagi T. A smart hyperthermia nanofiber with switchable drug release for inducing cancer apoptosis. *Adv Func Mater* 2013;23:5753–61.

its tissue penetration of several centimeters in biological tissues [20,77]. Recently, NIR photothermal agents such as gold (Au) nanoparticles [78,79], carbon nanotubes [20,80], polyaniline nanoparticles [81], and copper sulfides (Cu_9S_5) nanoparticles [77] have been employed in combination with chemotherapeutics to develop photothermal-chemotherapy platform (Table 15.3).

For example, in one study, multiwalled carbon nanotubes (MWCNTs), as photothermal reactive components, and DOX were incorporated into poly-L-lactic acid (PLLA) nanofibers. The NIR irradiation could not only induce cancer cell death through the local hyperthermia effect but also initiate the burst release of DOX due to the relatively low glass transition temperature ($T_g = 61.3^\circ\text{C}$) of PLLA. Viability of HeLa cells was reported to be about 70% and 20% in the case of MWCNT nanofibers and MWCNTs+DOX nanofibers, respectively, upon 10 min irradiation and 24 h incubation. Also, without irradiation, MWCNTs+DOX nanofibers showed 45% viability of the cancer cells. Therefore, the multifunctional fibers exhibited enhanced cytotoxicity both in vitro and in vivo by virtue of the combination of photothermally induced hyperthermia and chemotherapy with DOX [20].

In another work, DOX-loaded core-shell-structured $\text{Cu}_9\text{S}_5@m\text{SiO}_2$ nanoparticles were embedded into poly(ϵ -caprolactone) and gelatin (PG) nanofibers (DOX- $\text{Cu}_9\text{S}_5@m\text{SiO}_2$ PG). Therefore, DOX could be released from the mesoporous SiO_2 , and Cu_9S_5 was able to provide photothermal transformation under 980 nm laser irradiation. In addition, $\text{Cu}_9\text{S}_5@m\text{SiO}_2$ could release DOX in a pH-responsive profile owing to the more positive surface zeta potential of the SiO_2 layer at lower pH value, attenuating the electrostatic interaction between SiO_2 and DOX positive charge molecules, which results in a faster DOX release. As pH in the extracellular environment of solid tumors is usually lower than that in normal tissues because of the high rate of glycolysis in cancer cells, pH-responsive electrospun nanofibers are of interest for cancer therapy applications [83,84]. Synergistic photothermal-chemotherapy (DOX- $\text{Cu}_9\text{S}_5@m\text{SiO}_2$ PG+light) was found more efficient in tumor suppression in mice bearing the hepatoma H22 tumor compared with either treatment alone (i.e., DOX- $\text{Cu}_9\text{S}_5@m\text{SiO}_2$ PG and $\text{Cu}_9\text{S}_5@m\text{SiO}_2$ PG+light) (Fig. 15.2) [77].

15.5 Gene therapy

Gene therapy is regarded as a great opportunity for cancer treatment through changing expression of the genes that are responsible for the disease. In this realm, RNA interference (RNAi) is a promising approach for cancer treatment through several strategies including downregulation of cell-cycle-required proteins, suppression of oncogene expression, or apoptosis induction. To provide site-specific and controlled delivery of RNAi and also preserve its bioactivity, various RNAi delivery systems such as liposomes, nanoparticles, and fibrous scaffolds have been utilized [85–87].

In one study, PCL electrospun fibers were employed to deliver bioactive DNA encoding for short hairpin (sh) RNA against the cell-cycle-specific protein, Cdk2. As a result, the Cdk2i scaffold could significantly decrease Cdk2 mRNA expression in cells, corresponding to a 40% reduction in the proliferation of MCF-7 human breast cancer cells [85].

Table 15.3 Electrospun-based systems for local photothermal-chemotherapy

Polymer	Drug	Solvent	Method	Cancer cell (in vitro)	Cancer (in vivo)	Highlight	References
PCL, GE	DOX-Cu ₉ S ₅ @mSiO ₂	TFE	Blend electrospinning	HeLa (cervical carcinoma)	Hepatoma H22 Tumor	Cu ₉ S ₅ could convert optical energy into thermal energy to ablate tumor cells; meanwhile, the released DOX was able to kill tumor cells	[77]
PCL, GE	Polyaniline NPs	TFE	Blend electrospinning	HeLa (cervical carcinoma)	Hepatoma H22 Tumor	Polyaniline NPs embedded in the nanofibers could convert optical energy into thermal energy to ablate tumor cells upon 808 nm laser irradiation	[81]
PLLA	DOX, MWCNTs	CHCl ₃	Blend electrospinning	HeLa (cervical carcinoma)	Cervical carcinoma	Fibers exhibited enhanced cytotoxicity both in vitro and in vivo via the combination of photothermally induced hyperthermia by MWCNTs and chemotherapy by DOX	[20]
PLLA	Purpurin-18	CHCl ₃ /acetone	Blend electrospinning	SMMC 7721 (hepatocellular carcinoma), ECA 109 (esophageal cancer)	–	The efficacy of purpurin-18 on different cancer cell lines was similar	[82]

CHCl₃, chloroform; Cu₉S₅@mSiO₂, core-shell-structured Cu₉S₅@ mesoporous SiO₂ nanoparticles; DOX, doxorubicin hydrochloride; GE, gelatin; MWCNTs, multiwalled carbon nanotubes; NPs, nanoparticles; PCL, poly(ϵ -caprolactone); PLLA, poly-L-lactic acid; TFE, trifluoroethanol.

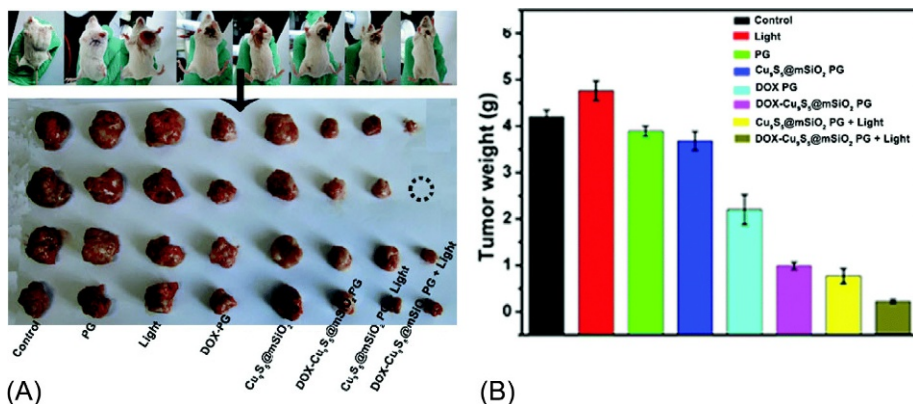


Fig. 15.2 (A) The images of representative Kunming mice with excised tumors. (B) Tumor weights after treatment with saline solution as control, PCL-gelatin nanofibers, PG, light, DOX-PG, Cu₉S₅@mSiO₂ PG, DOX-Cu₉S₅@mSiO₂ PG, Cu₉S₅@mSiO₂ PG+light, and DOX-Cu₉S₅@mSiO₂ PG+light.

Reproduced with permission from Chen Y, Hou Z, Liu B, Huang S, Li C, Lin J. DOX-Cu₉S₅@mSiO₂-PG composite fibers for orthotopic synergistic chemo- and photothermal tumor therapy. Dalton Trans 2015;44:3118–27.

In another study with aim of providing FA receptor-targeted viral transduction for cancer gene therapy, Park et al. synthesized a chitosan-PEG-FA polymer in which PEG and FA were used as a linker and a tumor-targeting ligand, respectively. Then, it was ionically cross-linked with adenovirus (Ad) by electrospinning, producing Ad/chitosan-PEG-FA nanodroplets (average size, 140 nm). The transduction efficiency of Ad/chitosan-PEG-FA was found ca. 57% higher than Ad/chitosan, implying the superiority of FA receptor-mediated endocytosis for viral transduction. In addition, reduced immune response against Ad through the conjugation with PEG polymer revealed its potential application for systemic gene delivery to distant metastatic tumors [88]. It is noteworthy to mention that chitosan and its quaternized derivatives show some anticancer effects due to their polycationic nature, and therefore, they have been widely utilized for anticancer drug delivery systems [89,90].

15.6 Circulating tumor cell capturing

Circulating tumor cells (CTCs) arising from primary tumors or tumor metastasis are considered as real-time markers for clinical cancer diagnostics. Therefore, capturing CTCs with sufficient sensitivity and specificity is an important step for early cancer diagnosis [91,92]. Recently, electrospun nanofibers functionalized with various specific biomarker molecules such as epithelial cell adhesion molecule antibody (anti-EpCAM) [92], hyaluronic acid (HA) [93], and folic acid (FA) [94] have been used to capture CTCs (Table 15.4).

Table 15.4 Electrospun-based systems for circulating tumor cell capturing

Polymer	Capturing moiety	Solvent	Method	Cancer cell (in vitro)	Highlight	References
CA	FA-modified dendrimer	Acetone/ DMF	Electrospinning, LBL	KB (epithelial carcinoma)	FA-modified dendrimers were conjugated on CA nanofibers to capture FAR-overexpressing cancer cells	[94]
PVA/PEI	LA	Water	Electrospinning	HepG2 (hepatocellular carcinoma), HeLa ^a (cervical carcinoma)	The mesh could capture ASGPR-overexpressing HepG2 cells via a ligand-receptor interaction	[95]
PVA/PEI	HA	Water	Electrospinning	HeLa (cervical carcinoma)	HA-functionalized nanofibers showed superior capability to capture CD44 receptor-overexpressing cancer cells	[93]
SA-coated TiNFs	Anti-EpCAM	–	Electrospinning, coating	HCT116 (colon cancer), BGC823 (gastric cancer), HeLa (cervical carcinoma) K562 (leukemia)	The TiNF substrate showed over 18 times cell-capture yield than the flat Si	[92]

Anti-EpCAM, epithelial-cell adhesion-molecule antibody; *CA*, cellulose acetate; *DMF*, *N,N*-dimethyl formamide; *DOX*, doxorubicin hydrochloride; *FA*, folic Acid; *FAR*, FA receptors; *GE*, gelatin; *HA*, hyaluronic acid; *LA*, lactobionic acid; *LBL*, layer-by-layer; *PEI*, polyethyleneimine; *PVA*, polyvinyl alcohol; *SA*, streptavidin; *Si*, silicon; *TiNFs*, TiO₂ nanofibers.

^aHepG2 cells with high ASGPR expression or HeLa cells without ASGPR expression.

As an illustration, Zhao et al. [93] fabricated HA-functionalized polyvinyl alcohol/polyethyleneimine (PVA/PEI) nanofibers to capture CD44 receptor-overexpressing cancer cells. HA-functionalized nanofibers demonstrated higher cell-capture efficiency (85.0% at 240 min) than nanofibers without HA (64.7% at 240 min), which was attributed to the HA-mediated targeting and binding of CD44 receptor-overexpressing HeLa cells onto the fibrous scaffolds. In a similar study, PVA/PEI nanofibers immobilized with lactobionic acid (LA) were employed to capture asialoglycoprotein receptor (ASGPR)-overexpressing HepG2 cells through the LA-mediated ligand-receptor interaction [95].

15.7 Conclusions and future perspectives

The use of biodegradable electrospun micro- and nanofibrous systems as drug carrier of anticancer agents is a promising approach for local cancer therapy. Electrospun fibers can provide high concentration of the therapeutic agents and sustained release of them at the tumor vicinity and therefore enhance the therapeutic efficacy while reducing toxicity of the systemic treatments in normal tissues. However, further studies are still needed to elucidate the long-term effects of the electrospun-based systems and their efficacy as anticancer drug carriers in animal models before clinical implementation and commercialization.

References

- [1] Cohen J, Pivodic L, Miccinesi G, Onwuteaka-Philipsen B, Naylor W, Wilson D, et al. International study of the place of death of people with cancer: a population-level comparison of 14 countries across 4 continents using death certificate data. *Br J Cancer* 2015;113:1397–404.
- [2] Bhowmik A, Nath S, Das S, Ghosh SK, Choudhury Y. ATM rs189037 (G > A) polymorphism and risk of lung cancer and head and neck cancer: a meta-analysis. *Meta Gene* 2015;6:42–8.
- [3] Norouzi M, Nazari B, Miller DW. Injectable hydrogel-based drug delivery systems for local cancer therapy. *Drug Discov Today* 2016;21:1835–49.
- [4] Shah R, Singh J, Singh D, Jaggi AS, Singh N. Sulfatase inhibitors for recidivist breast cancer treatment: a chemical review. *Eur J Med Chem* 2016;114:170–90.
- [5] Untch M, Ditsch N, Hermelink K. Immunotherapy: new options in breast cancer treatment. *Expert Rev Anticancer Ther* 2014;3:403–8.
- [6] Xiong L, Luo Q, Wang Y, Li X, Shen Z, Zhu W. An injectable drug-loaded hydrogel based on a supramolecular polymeric prodrug. *Chem Commun* 2015;51:14644–7.
- [7] Du YQ, Yang XX, Li WL, Wang J, Huang CZ. A cancer-targeted drug delivery system developed with gold nanoparticle mediated DNA–doxorubicin conjugates. *RSC Adv* 2014;4:34830–5.
- [8] Bai M, Liu S. A simple and general method for preparing antibody-PEG-PLGA sub-micron particles using electrospray technique: an in vitro study of targeted delivery of cisplatin to ovarian cancer cells. *Colloids Surf B Biointerfaces* 2014;117:346–53.
- [9] Tian R, Chen J, Niu R. The development of low-molecular weight hydrogels for applications in cancer therapy. *Nanoscale* 2014;6:3474–82.

- [10] Wolinsky JB, Colson YL, Grinstaff MW. Local drug delivery strategies for cancer treatment: gels, nanoparticles, polymeric films, rods, and wafers. *J Control Release* 2012;159:14–26.
- [11] Ignatova M, Rashkov I, Manolova N. Drug-loaded electrospun materials in wound-dressing applications and in local cancer treatment. *Expert Opin Drug Deliv* 2013;10:469–83.
- [12] Chen Z, Chen Z, Zhang A, Hu J, Wang X, Yang Z. Electrospun nanofibers for cancer diagnosis and therapy. *Biomater Sci* 2016;4:922–32.
- [13] Ta HT, Dass CR, Dunstan DE. Injectable chitosan hydrogels for localised cancer therapy. *J Control Release* 2008;126:205–16.
- [14] Orive G, Hernández RM, Gascón AR, Pedraz JL. Micro and nano drug delivery systems in cancer therapy. *Cancer Ther* 2005;3:131–8.
- [15] Davis ME, Shin DM. Nanoparticle therapeutics: an emerging treatment modality for cancer. *Nat Rev Drug Discov* 2008;7:771–82.
- [16] Peer D, Karp JM, Hong S, Farokhzad OC, Margalit R, Langer R. Nanocarriers as an emerging platform for cancer therapy. *Nat Nanotechnol* 2007;2:751–60.
- [17] Blanco E, Kessinger CW, Sumer BD, Gao J. Multifunctional micellar nanomedicine for cancer therapy. *Exp Biol Med (Maywood)* 2009;234:123–31.
- [18] Cattel L, Ceruti M, Dosio F. From conventional to stealth liposomes: a new frontier in cancer chemotherapy. *Tumori* 2003;89:237–49.
- [19] Torchilin VP. Targeted pharmaceutical nanocarriers for cancer therapy and imaging. *AAPS J* 2007;9:E128–47.
- [20] Zhang Z, Liu S, Xiong H, Jing X, Xie Z, Chen X, et al. Electrospun PLA/MWCNTs composite nanofibers for combined chemo-and photothermal therapy. *Acta Biomater* 2015;26:115–23.
- [21] Norouzi M, Boroujeni SM, Omidvarkordshouli N, Soleimani M. Advances in skin regeneration: application of electrospun scaffolds. *Adv Healthc Mater* 2015;4:1114–33.
- [22] Mirdailami O, Soleimani M, Dinarvand R, Khoshayand MR, Norouzi M, Hajarizadeh A, et al. Controlled release of rhEGF and rhbFGF from electrospun scaffolds for skin regeneration. *J Biomed Mater Res A* 2015;103:3374–85.
- [23] Norouzi M, Shabani I, Atyabi F, Soleimani M. EGF-loaded nanofibrous scaffold for skin tissue engineering applications. *Fibers Polym* 2015;16:782–7.
- [24] Norouzi M, Shabani I, Ahvaz HH, Soleimani M. PLGA/gelatin hybrid nanofibrous scaffolds encapsulating EGF for skin regeneration. *J Biomed Mater Res A* 2015;103:2225–35.
- [25] Norouzi M, Soleimani M, Shabani I, Atyabi F, Ahvaz HH, Rashidi A. Protein encapsulated in electrospun nanofibrous scaffolds for tissue engineering applications. *Polym Int* 2013;62:1250–6.
- [26] Azfarniam L, Norouzi M. Multifunctional polyester fabric using a multicomponent treatment. *Fibers Polym* 2016;17:298–304.
- [27] Yoo HS, Kim TG, Park TG. Surface-functionalized electrospun nanofibers for tissue engineering and drug delivery. *Adv Drug Deliv Rev* 2009;61:1033–42.
- [28] Ghoreishian SM, Maleknia L, Mirzapour H, Norouzi M. Antibacterial properties and color fastness of silk fabric dyed with turmeric extract. *Fibers Polym* 2013;14:201–7.
- [29] Liu D, Liu S, Jing X, Li X, Li W, Huang Y. Necrosis of cervical carcinoma by dichloroacetate released from electrospun polylactide mats. *Biomaterials* 2012;33:4362–9.
- [30] Ranganath SH, Wang C. Biodegradable microfiber implants delivering paclitaxel for post-surgical chemotherapy against malignant glioma. *Biomaterials* 2008;29:2996–3003.
- [31] Ardehshirzadeh B, Anaraki NA, Irani M, Rad LR, Shamshiri S. Controlled release of doxorubicin from electrospun PEO/chitosan/graphene oxide nanocomposite nanofibrous scaffolds. *Mater Sci Eng C* 2015;48:384–90.

- [32] Yang G, Wang J, Wang Y, Li L, Guo X, Zhou S. An implantable active-targeting micelle-in-nanofiber device for efficient and safe cancer therapy. *ACS Nano* 2015;9:1161–74.
- [33] Yan E, Fan Y, Sun Z, Gao J, Hao X, Pei S, et al. Biocompatible core-shell electrospun nanofibers as potential application for chemotherapy against ovary cancer. *Mater Sci Eng C* 2014;41:217–23.
- [34] Shao S, Li L, Yang G, Li J, Luo C, Gong T, et al. Controlled green tea polyphenols release from electrospun PCL/MWCNTs composite nanofibers. *Int J Pharm* 2011;421:310–20.
- [35] Chen Y, Liu S, Hou Z, Ma P, Yang D, Li C, et al. Multifunctional electrospinning composite fibers for orthotopic cancer treatment in vivo. *Nano Res* 2015;8:1917–31.
- [36] Zhu X, Ni S, Xia T, Yao Q, Li H, Wang B, et al. Anti-neoplastic cytotoxicity of SN-38-loaded PCL/gelatin electrospun composite nanofiber scaffolds against human glioblastoma cells in vitro. *J Pharm Sci* 2015;104:4345–54.
- [37] Dubey P, Gopinath P. Fabrication of electrospun poly (ethylene oxide)-poly (caprolactone) composite nanofibers for co-delivery of niclosamide and silver nanoparticles exhibits enhanced anti-cancer effects in vitro. *J Mater Chem B* 2016;4:726–42.
- [38] Guo G, Fu S, Zhou L, Liang H, Fan M, Luo F, et al. Preparation of curcumin loaded poly (ϵ -caprolactone)-poly (ethylene glycol)-poly (ϵ -caprolactone) nanofibers and their in vitro antitumor activity against Glioma 9L cells. *Nanoscale* 2011;3:3825–32.
- [39] Kaplan JA, Liu R, Freedman JD, Padera R, Schwartz J, Colson YL, et al. Prevention of lung cancer recurrence using cisplatin-loaded superhydrophobic nanofiber meshes. *Biomaterials* 2016;76:273–81.
- [40] Yohe ST, Herrera VL, Colson YL, Grinstaff MW. 3D superhydrophobic electrospun meshes as reinforcement materials for sustained local drug delivery against colorectal cancer cells. *J Control Release* 2012;162:92–101.
- [41] Zhang Y, Liu S, Wang X, Zhang Z, Jing X. Prevention of local liver cancer recurrence after surgery using multilayered cisplatin-loaded polylactide electrospun nanofibers. *Chin J Polym Sci* 2014;32:1111–8.
- [42] Zong S, Wang X, Yang Y, Wu W, Li H, Ma Y, et al. The use of cisplatin-loaded mucoadhesive nanofibers for local chemotherapy of cervical cancers in mice. *Eur J Pharm Biopharm* 2015;93:127–35.
- [43] Ma Y, Wang X, Zong S, Zhang Z, Xie Z, Huang Y, et al. Local, combination chemotherapy in prevention of cervical cancer recurrence after surgery by using nanofibers co-loaded with cisplatin and curcumin. *RSC Adv* 2015;5:106325–32.
- [44] Xu X, Chen X, Wang Z, Jing X. Ultrafine PEG-PLA fibers loaded with both paclitaxel and doxorubicin hydrochloride and their in vitro cytotoxicity. *Eur J Pharm Biopharm* 2009;72:18–25.
- [45] Qiu K, He C, Feng W, Wang W, Zhou X, Yin Z, et al. Doxorubicin-loaded electrospun poly (L-lactic acid)/mesoporous silica nanoparticles composite nanofibers for potential postsurgical cancer treatment. *J Mater Chem B* 2013;1:4601–11.
- [46] Zhao X, Yuan Z, Yildirim L, Zhao J, Lin ZYW, Cao Z, et al. Tumor-triggered controlled drug release from electrospun fibers using inorganic caps for inhibiting cancer relapse. *Small* 2015;11:4284–91.
- [47] Yuan Z, Zhao X, Zhao J, Pan G, Qiu W, Wang X, et al. Synergistic mediation of tumor signaling pathways in hepatocellular carcinoma therapy via dual-drug-loaded pH-responsive electrospun fibrous scaffolds. *J Mater Chem B* 2015;3:3436–46.
- [48] Zhao X, Zhao J, Lin ZYW, Pan G, Zhu Y, Cheng Y, et al. Self-coated interfacial layer at organic/inorganic phase for temporally controlling dual-drug delivery from electrospun fibers. *Colloids Surf B Biointerfaces* 2015;130:1–9.

- [49] Zhang J, Wang X, Liu T, Liu S, Jing X. Antitumor activity of electrospun polylactide nanofibers loaded with 5-fluorouracil and oxaliplatin against colorectal cancer. *Drug Deliv* 2016;23:784–90.
- [50] Huo Z, Qiu Y, Chu Z, Yin P, Lu W, Yan Y, et al. Electrospinning preparation of timosaponin B-II-Loaded PLLA nanofibers and their antitumor recurrence activities in vivo. *J Nanomater* 2015;2015:4.
- [51] Luo X, Xie C, Wang H, Liu C, Yan S, Li X. Antitumor activities of emulsion electrospun fibers with core loading of hydroxycamptothecin via intratumoral implantation. *Int J Pharm* 2012;425:19–28.
- [52] Ignatova MG, Manolova NE, Toshkova RA, Rashkov IB, Gardeva EG, Yossifova LS, et al. Electrospun nanofibrous mats containing quaternized chitosan and polylactide with in vitro antitumor activity against HeLa cells. *Biomacromolecules* 2010;11:1633–45.
- [53] Ignatova M, Kalinov K, Manolova N, Toshkova R, Rashkov I, Alexandrov M. Quaternized chitosan-coated nanofibrous implants loaded with gossypol prepared by electrospinning and their efficacy against Graffi myeloid tumor. *J Biomater Sci Polym Ed* 2014;25:287–306.
- [54] Xie J, Wang C. Electrospun micro- and nanofibers for sustained delivery of paclitaxel to treat C6 glioma in vitro. *Pharm Res* 2006;23:1817–26.
- [55] Chen M, Feng W, Lin S, He C, Gao Y, Wang H. Antitumor efficacy of a PLGA composite nanofiber embedded with doxorubicin@ MSNs and hydroxycamptothecin@ HANPs. *RSC Adv* 2014;4:53344–51.
- [56] Wei J, Hu J, Li M, Chen Y, Chen Y. Multiple drug-loaded electrospun PLGA/gelatin composite nanofibers encapsulated with mesoporous ZnO nanospheres for potential postsurgical cancer treatment. *RSC Adv* 2014;4:28011–9.
- [57] Vashisth P, Sharma M, Nikhil K, Singh H, Panwar R, Pruthi PA, et al. Antiproliferative activity of ferulic acid-encapsulated electrospun PLGA/PEO nanofibers against MCF-7 human breast carcinoma cells. *3 Biotech* 2015;5:303–15.
- [58] Salehi R, Irani M, Rashidi M, Aroujalian A, Raisi A, Eskandani M, et al. Stimuli-responsive nanofibers prepared from poly (*N*-isopropylacrylamide-acrylamide-vinylpyrrolidone) by electrospinning as an anticancer drug delivery. *Des Monomers Polym* 2013;16:515–27.
- [59] Ni S, Fan X, Wang J, Qi H, Li X. Biodegradable implants efficiently deliver combination of paclitaxel and temozolomide to glioma C6 cancer cells in vitro. *Ann Biomed Eng* 2014;42:214–21.
- [60] Wang C, Ma C, Wu Z, Liang H, Yan P, Song J, et al. Enhanced bioavailability and anticancer effect of curcumin-loaded electrospun nanofiber: in vitro and in vivo study. *Nanoscale Res Lett* 2015;10:1–10.
- [61] Norouzi M, Zare Y, Kiany P. Nanoparticles as effective flame retardants for natural and synthetic textile polymers: application, mechanism, and optimization. *Polym Rev* 2015;55:531–60.
- [62] Ghoreishian SM, Badii K, Norouzi M, Malek K. Effect of cold plasma pre-treatment on photocatalytic activity of 3D fabric loaded with nano-photocatalysts: Response surface methodology. *Appl Surf Sci* 2016;365:252–62.
- [63] Steichen SD, Calderera-Moore M, Peppas NA. A review of current nanoparticle and targeting moieties for the delivery of cancer therapeutics. *Eur J Pharm Sci* 2013;48:416–27.
- [64] Shu C, Li R, Yin Y, Yin D, Gu Y, Ding L, et al. Synergistic dual-targeting hydrogel improves targeting and anticancer effect of Taxol in vitro and in vivo. *Chem Commun* 2014;50:15423–6.

- [65] Würth R, Thellung S, Bajetto A, Mazzanti M, Florio T, Barbieri F. Drug-repositioning opportunities for cancer therapy: novel molecular targets for known compounds. *Drug Discov Today* 2015;21:190–9.
- [66] López-Noriega A, Hastings CL, Ozbakir B, O'Donnell KE, O'Brien FJ, Storm G, et al. Hyperthermia-induced drug delivery from thermosensitive liposomes encapsulated in an injectable hydrogel for local chemotherapy. *Adv Healthc Mater* 2014;3:854–9.
- [67] Huang C, Soenen SJ, Rejman J, Trekker J, Chengxun L, Lagae L, et al. Magnetic electrospun fibers for cancer therapy. *Adv Funct Mater* 2012;22:2479–86.
- [68] Laurent S, Dutz S, Häfeli UO, Mahmoudi M. Magnetic fluid hyperthermia: focus on superparamagnetic iron oxide nanoparticles. *Adv Colloid Interface Sci* 2011;166:8–23.
- [69] Kim Y, Ebara M, Aoyagi T. A smart hyperthermia nanofiber with switchable drug release for inducing cancer apoptosis. *Adv Funct Mater* 2013;23:5753–61.
- [70] GhavamiNejad A, Sasikala ARK, Unnithan AR, Thomas RG, Jeong YY, Vatankehah-Varnoosfaderani M, et al. Mussel-inspired electrospun smart magnetic nanofibers for hyperthermic chemotherapy. *Adv Funct Mater* 2015;25:2867–75.
- [71] Lin T, Lin F, Lin J. In vitro feasibility study of the use of a magnetic electrospun chitosan nanofiber composite for hyperthermia treatment of tumor cells. *Acta Biomater* 2012;8:2704–11.
- [72] Chen Y, Cheng C, Chang W, Lin Y, Lin F, Lin J. Studies of magnetic alginate-based electrospun matrices crosslinked with different methods for potential hyperthermia treatment. *Mater Sci Eng C* 2016;62:338–49.
- [73] Hosseini L, Mahboobnia K, Irani M. Fabrication of PLA/MWCNT/Fe₃O₄ composite nanofibers for leukemia cancer cells. *Int J Polym Mater* 2016;65:176–82.
- [74] Sasikala ARK, Unnithan AR, Yun Y, Park CH, Kim CS. An implantable smart magnetic nanofiber device for endoscopic hyperthermia treatment and tumor-triggered controlled drug release. *Acta Biomater* 2016;31:122–33.
- [75] Peng XH, Qian X, Mao H, Wang AY, Chen ZG, Nie S, et al. Targeted magnetic iron oxide nanoparticles for tumor imaging and therapy. *Int J Nanomedicine* 2008;3:311–21.
- [76] Mahmoudi M, Sant S, Wang B, Laurent S, Sen T. Superparamagnetic iron oxide nanoparticles (SPIONs): development, surface modification and applications in chemotherapy. *Adv Drug Deliv Rev* 2011;63:24–46.
- [77] Chen Y, Hou Z, Liu B, Huang S, Li C, Lin J. DOX-Cu₉S₅@mSiO₂-PG composite fibers for orthotopic synergistic chemo- and photothermal tumor therapy. *Dalton Trans* 2015;44:3118–27.
- [78] Jain S, Hirst D, O'sullivan J. Gold nanoparticles as novel agents for cancer therapy. *Br J Radiol* 2014;85:101–13.
- [79] You J, Zhang R, Zhang G, Zhong M, Liu Y, Van Pelt CS, et al. Photothermal-chemotherapy with doxorubicin-loaded hollow gold nanospheres: a platform for near-infrared light-triggered drug release. *J Control Release* 2012;158:319–28.
- [80] Liu S, Ko AC, Li W, Zhong W, Xing M. NIR initiated and pH sensitive single-wall carbon nanotubes for doxorubicin intracellular delivery. *J Mater Chem B* 2014;2:1125–35.
- [81] Chen Y, Li C, Hou Z, Huang S, Liu B, He F, et al. Polyaniline electrospinning composite fibers for orthotopic photothermal treatment of tumors in vivo. *New J Chem* 2015;39:4987–93.
- [82] Wu HM, Chen N, Wu ZM, Chen ZL, Yan YJ. Preparation of photosensitizer-loaded PLLA nanofibers and its anti-tumor effect for photodynamic therapy in vitro. *J Biomater Appl* 2013;27:773–9.
- [83] Liu J, Huang Y, Kumar A, Tan A, Jin S, Mozhi A, et al. pH-Sensitive nano-systems for drug delivery in cancer therapy. *Biotechnol Adv* 2014;32:693–710.

- [84] Lee ES, Na K, Bae YH. Polymeric micelle for tumor pH and folate-mediated targeting. *J Control Release* 2003;91:103–13.
- [85] Achille C, Sundaresh S, Chu B, Hadjiargyrou M. Cdk2 silencing via a DNA/PCL electrospun scaffold suppresses proliferation and increases death of breast cancer cells. *PLoS One* 2012;7:e52356.
- [86] El-Aneed A. An overview of current delivery systems in cancer gene therapy. *J Control Release* 2004;94:1–14.
- [87] Chen M, Gao S, Dong M, Song J, Yang C, Howard KA, et al. Chitosan/siRNA nanoparticles encapsulated in PLGA nanofibers for siRNA delivery. *ACS Nano* 2012;6:4835–44.
- [88] Park Y, Kang E, Kwon O, Hwang T, Park H, Lee JM, et al. Ionically crosslinked Ad/chitosan nanocomplexes processed by electrospinning for targeted cancer gene therapy. *J Control Release* 2010;148:75–82.
- [89] Hu X, Liu S, Zhou G, Huang Y, Xie Z, Jing X. Electrospinning of polymeric nanofibers for drug delivery applications. *J Control Release* 2014;185:12–21.
- [90] Hosseinzadeh H, Atyabi F, Dinarvand R, Ostad SN. Chitosan-Pluronic nanoparticles as oral delivery of anticancer gemcitabine: preparation and in vitro study. *Int J Nanomedicine* 2012;7:1851–63.
- [91] Hou S, Zhao L, Shen Q, Yu J, Ng C, Kong X, et al. Polymer nanofiber-embedded microchips for detection, isolation, and molecular analysis of single circulating melanoma cells. *Angew Chem Int Ed* 2013;52:3379–83.
- [92] Zhang N, Deng Y, Tai Q, Cheng B, Zhao L, Shen Q, et al. Electrospun TiO₂ nanofiber-based cell capture assay for detecting circulating tumor cells from colorectal and gastric cancer patients. *Adv Mater* 2012;24:2756–60.
- [93] Zhao Y, Fan Z, Shen M, Shi X. Hyaluronic acid-functionalized electrospun polyvinyl alcohol/polyethyleneimine nanofibers for cancer cell capture applications. *Adv Mater Interfaces* 2015;2:1–9.
- [94] Zhao Y, Zhu X, Liu H, Luo Y, Wang S, Shen M, et al. Dendrimer-functionalized electrospun cellulose acetate nanofibers for targeted cancer cell capture applications. *J Mater Chem B* 2014;2:7384.
- [95] Zhao Y, Fan Z, Shen M, Shi X. Capturing hepatocellular carcinoma cells using lactobionic acid-functionalized electrospun polyvinyl alcohol/polyethyleneimine nanofibers. *RSC Adv* 2015;5:70439–47.

Electrospun nanofibers for regenerative dentistry

16

D. Pankajakshan, M.T.P. Albuquerque, M.C. Bottino
Indiana University School of Dentistry, Indianapolis, IN, United States

16.1 Introduction

Periodontal disease and caries are considered major oral pathologies affecting teeth and their supporting tissues [1]. According to recent National Health and Nutrition Examination Survey (NHANES) statistics, 8.52% of adults (age 20–64) and 17.20% of seniors (age 65 and older) are afflicted with periodontal disease. Meanwhile, caries affects 42% of children (age 2–11) in their primary teeth, 92% of adults, and 93% of seniors, in their permanent dentition. These diseases remain major clinical challenges, mainly due to the limited dental tissues' self-healing ability [2].

Periodontitis is one of the most aggressive diseases that impair the integrity of the periodontium [3]. The progression of periodontitis leads to the destruction of tooth-supporting structures, ultimately leading to tooth loss [3]. The treatment of periodontitis has evolved over the years. Guided tissue and bone regeneration have been used with the aid of a physical membrane that acts as a barrier to prevent epithelial and connective tissue downgrowth into the defect, enabling the regeneration of periodontal tissues. Different processing techniques have been employed to fabricate these membranes [3]. Among them is electrospinning, a simple, versatile, and well-documented technology that has been used to fabricate nano- and micro-scale fibers [3]. Worth mentioning, the chemical characteristics of polymer(s) or blends are not compromised during electrospinning; this has allowed researchers to incorporate antimicrobial agents and bioactive particles (e.g., calcium phosphates) into different polymers and, therefore, fabricate a material with therapeutic properties [3]. Furthermore, electrospinning has also allowed for the synthesis of tissue-specific multilayered membranes or scaffolds to simultaneously amplify hard and soft periodontal tissue regeneration [4].

Another challenging clinical problem is the treatment of immature permanent teeth with pulpal necrosis. Traumatic injuries or bacterial infection of the dental pulp leads to inflammation and, if left untreated, necrosis [5]. Endodontic management of these teeth includes surgery and retrograde sealing, calcium hydroxide-induced apical closure (apexification), and, more recently, placement of an apical plug of mineral trioxide aggregate (MTA). Alternatively, encouraging regenerative outcomes achieved by evoked bleeding (EB) therapy in the treatment of necrotic immature permanent teeth, combined with the latest advances in tissue engineering, clearly suggest that establishment of a regenerative-based clinical strategy is closer than ever [5]. The idea behind

EB relies on the regenerative capacity of stem cells, which are introduced into root canals through the intentional laceration of periapical tissue after a thorough disinfection protocol. However, antibiotic pastes used for root canal disinfection prior to a regenerative strategy have been shown to negatively impair dental pulp stem cells' (DPSCs) survival [6]. To overcome the challenge of the inherent toxicity of the currently used disinfection agents, our group pioneered the concept of a cell-friendly disinfection strategy through the successful development of antibiotic-containing polymer nanofibers [5,7–15].

To provide a comprehensive update on the progress in the field, this chapter is arranged into two major parts. The first presents a brief overview of the periodontium and its pathological conditions, currently employed therapeutics used to regenerate the distinct periodontal tissues, and a review of recent advances on the use of electrospinning to develop bioactive membranes for periodontal regeneration. The second part provides a short background on the importance of disinfection in regenerative endodontics and major highlights of antibiotic-containing polymer nanofibers, their antimicrobial properties, and the future perspective of this novel intracanal drug delivery strategy in regenerative endodontics.

16.2 Periodontal disease and treatment modalities

Periodontitis affects the integrity of periodontal tissues. The periodontium is an intricate system consisting of the root cementum, periodontal ligament (PDL), alveolar bone, and dentogingival junction [16,17]. Periodontal disease occurs when bacteria-stimulated inflammation or infection of the gums (gingivitis) progressively destroys the periodontium, ultimately resulting in tooth loss. During the process, tissue integrity is compromised by the loss of soft tissue attachment to the root surface, which results in periodontal pocket formation, a deeper lesion, and subsequent loss of the alveolar bone. The progressive lesion then operates as a reservoir, favoring the growth of anaerobic bacteria (e.g., *Porphyromonas gingivalis*) [18].

Different treatment modalities have been suggested in order to regenerate periodontal tissues damaged in the case of periodontitis. As mentioned earlier, the strategy of using either synthetic or tissue-derived membranes as barriers with or without calcium phosphate-based bone graft materials has received great attention for restoring the function of a damaged or pathologically affected periodontium [3,19–21,4,22–46].

16.3 Periodontal-specific tissue engineering

Tissue engineering is an interdisciplinary field that applies the principles and methods of engineering and the life sciences toward the development of biological substitutes that restore, maintain, and improve the function of damaged tissues and organs [47]. Periodontal regeneration or periodontal tissue engineering is attributed to a complete recovery of periodontal tissues in terms of both structure and function, that is, formation of the alveolar bone, a new connective attachment through collagen fibers functionally oriented on the newly formed cementum [19,20]. Two surgical techniques have been increasingly used to restore/regenerate the different periodontal tissues,

namely, guided tissue regeneration (GTR) and guided bone regeneration (GBR) [23,28,41,43,48–53]. GTR refers to periodontal tissue regeneration, including cementum, the PDL, and the alveolar bone, whereas GBR pertains to the promotion of bone formation. In GTR, an occlusive membrane interfaces with gingival connective tissue/epithelium and a PDL/alveolar bone tissue to promote periodontal tissue regeneration. The membrane acts as a barrier when placed in the surgical site, preventing connective and epithelial tissue migration into the defect. Progenitor cells, located in the remaining PDL adjacent to the alveolar bone or blood, are then able to recolonize the root area and differentiate into a new periodontal supporting apparatus with the formation of new bone, PDL, and cementum. GBR typically refers to ridge augmentation or bone regenerative procedures that pertain to the restoration of deficient alveolar sites (e.g., an extraction site).

Ideal GTR/GBR membranes need to exhibit: (1) biocompatibility to allow for integration with the host tissues without eliciting inflammatory responses, (2) a proper degradation profile to match that of new tissue formation, (3) adequate mechanical and physical properties to allow for placement *in vivo*, and (4) sufficient sustained strength to avoid the membrane's collapse and the ability to perform their barrier function [3]. GTR/GBR membranes are divided into two groups, non-resorbable and resorbable, according to their degradation characteristics. One of the disadvantages of nonresorbable membranes is the need to perform an additional surgery to remove them, which implicates not only additional pain and discomfort but also an economic burden. In order to eliminate the second surgical procedure, resorbable barrier membranes have been developed [23,27,30,43]. The majority of synthetic polymer resorbable membranes for periodontal regeneration currently on the market are either based on polyesters (e.g., poly(glycolic acid) (PGA), poly(lactic acid) (PLA), and/or their copolymers) [27–29,36,43,54–59] or tissue-derived collagens [23,60–66].

Collagen is a major constituent of the natural extracellular matrix (ECM). Tissue-derived collagen-based membranes from the human skin, the bovine achilles tendon, or the porcine skin are important alternatives to synthetic polymers in GTR/GBR procedures due to their excellent cell affinity and biocompatibility [23,67,68]. However, type I collagen may have its limitations due to its low mechanical properties and difficulty controlling degradation. Biomechanical properties and collagen matrix stability can be enhanced by means of physical/chemical cross-linking using ultraviolet radiation, genipin, glutaraldehyde, or 1-ethyl-3-(3-dimethylaminopropyl) carbodiimide hydrochloride (EDC), among others [3].

16.4 Electrospun bioactive membranes for periodontal regeneration

16.4.1 Antimicrobial properties

Infection is the foremost reason for clinical failure of regenerative procedures. Hence, it will be advantageous to have a membrane with antimicrobial properties that tackles postsurgical infection and inflammation at the implantation site. The presence of

periodontopathogens, such as *Porphyromonas gingivalis* (*Pg*), *Prevotella intermedia*, and *Fusobacterium nucleatum* (*Fn*), may negatively affect the success of periodontal regeneration. Therefore, it is extremely important to control and/or reduce bacterial contamination of the periodontal defect in order to enhance periodontal regeneration [18,69].

A wide range of antimicrobial drugs, including but not limited to tetracycline hydrochloride (TCH), metronidazole benzoate (MET), and doxycycline (DOX), have been successfully incorporated into distinct polymer membranes to develop a material with therapeutic properties [70–72]. For example, MET is an antimicrobial drug commonly used in the treatment of periodontal infections [73]. It acts against anaerobic Gram-negative (e.g., *Porphyromonas gingivalis*) and anaerobic spore-forming Gram-positive bacilli [74]. Zamani et al. [72] fabricated poly(ϵ -caprolactone) (PCL) nanofibrous membranes loaded with MET. Of note, MET release was without a burst and was sustained for at least 19 days, which could be key to the inhibition of related bacteria and an aid in the regeneration of a new periodontium [72]. Xue et al. [75] developed MET-loaded electrospun poly(ϵ -caprolactone)-gelatin nanofibrous membranes, which showed good biocompatibility without infection following subcutaneous implantation in rabbits for 8 months.

In a recent study by our group, we evaluated the antimicrobial properties of MET-containing and ciprofloxacin (CIP)-containing polydioxanone electrospun membranes [7]. The antimicrobial properties were evaluated against those of *Pg* and *Enterococcus faecalis* (*Ef*). Cytotoxicity was assessed in human dental pulp stem cells (hDPSCs). CIP-containing membranes significantly inhibited the biofilm growth of both bacteria. Conversely, MET-containing membranes only inhibited *Pg* growth (Fig. 16.1). Agar diffusion confirmed the antimicrobial properties against specific bacteria for the antibiotic-containing membranes. Only the 25 wt% CIP-containing membranes were cytotoxic.

TCH was incorporated into poly(L-lactic acid) (PLLA) fibers by either blending or coaxial electrospinning [71]. Two relevant conclusions were drawn based on the in vitro drug release evaluation. First, it was demonstrated that threads processed from the core-shell fibers had a lower early burst and a more continuous release. Second, threads processed from the blend fibers resulted in a greater early burst release, which can be of great value in avoiding bacterial infection [71]. In another study, Mohammadi et al. [76] fabricated blend and core-shell electrospun membranes using poly-lactic-glycolic acid (PLGA), gum tragacanth (GT), and TCH. Drug release studies showed that both the fraction of GT within blend nanofibers and the core-shell structure can effectively control the TCH release rate. By incorporating TCH into core-shell nanofibers, drug release was sustained for 75 days with only 19% of the burst release within the first 2 h. The prolonged drug release, together with proven biocompatibility, antibacterial, and the mechanical properties of drug-loaded core-shell nanofibers, makes them a promising candidate for use as a drug delivery system to fight periodontal infection.

Incorporation of amoxicillin (AMX) in PCL-based electrospun nanofibers could lead to barrier membranes that can reduce or eliminate the bacterial contamination of periodontal defects. In a new study, Furtos et al. [77] reported on the

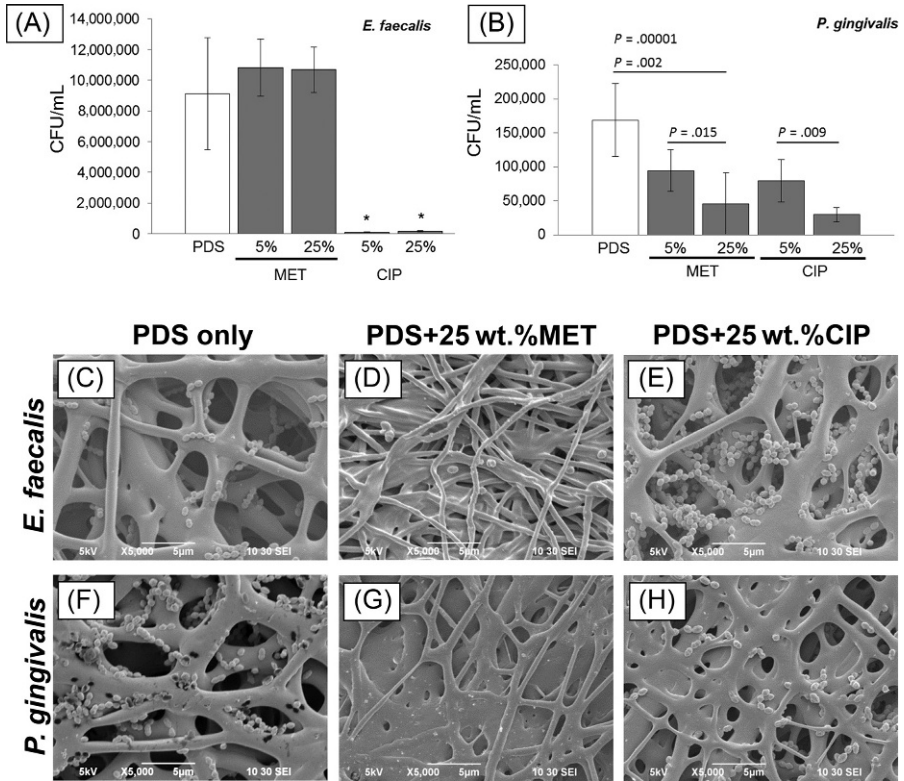


Fig. 16.1 Effects of antibiotic-containing PDS-based electrospun mats on the growth of bacteria. (A and B) Spiral plating was used to calculate CFU/mL of samples of dislodged bacteria: (A) *E. faecalis* and (B) *P. gingivalis* from biofilms containing 5 wt% CIP, 25 wt% CIP, 5 wt% MET, and 25 wt% MET and PDS (control). Significant difference is denoted with an asterisk ($*P < .05$) when compared with the control. (C–H) Representative SEM micrographs showing growth inhibition of *E. faecalis* and *P. gingivalis* on the antibiotic-containing electrospun mats [1].

synthesis of nanocomposite PCL-based membranes modified with both AMX and nanohydroxyapatite (nHAp) to endow antimicrobial and osteoconductive properties, respectively. Meanwhile, recent studies have also reported on the fabrication of electrospun membranes loaded with anti-inflammatory drugs. Farooq et al. [78] incorporated piroxicam, a nonsteroidal anti-inflammatory drug, into novel cytocompatible and biodegradable chitosan (CS)/poly(vinyl alcohol) (PVA)/hydroxyapatite (HA) electrospun composite nanofibrous membranes. In another investigation, Carter et al. [79] blended *Aloe vera*, proven for its anti-inflammatory properties, with PCL, to prepare GTR nanofibrous membranes aiming to enhance periodontal healing.

It is well recognized that antibiotics may produce some important side effects, mainly those related to bacterial strain resistance, which is a current global concern, since bacteria are becoming resistant to several antibiotic therapies. In light of this,

alternative antibacterial agents, rather than antibiotics, have been developed to translate safer regenerative technologies into clinical practice for GTR/GBR applications. Inorganic ions and metallic oxides have extensively demonstrated antibacterial properties. Silver is the most effective antibacterial metal at low concentrations and against both Gram-positive (G+) and Gram-negative (G-) bacteria. Meanwhile, several other metal oxides (e.g., copper, magnesium, titanium, and zinc) have also displayed important antibacterial activity against a wide variety of microorganisms. In this way, a recent study by our group demonstrated the successful synthesis of PCL-based electrospun membranes using ZnO as the antibacterial agent (Fig. 16.2) [80]. The antibacterial activity of the processed fibrous membranes was evaluated against known periodontopathogens, that is, *Porphyromonas gingivalis* (*Pg*) and *Fusobacterium nucleatum* (*Fn*), using agar diffusion assays. All the membranes containing different concentrations of ZnO (5, 15, and 30 wt%) presented antibacterial activity against the targeted bacteria. The membranes, when applied against *Pg*, showed similar antibacterial activity regardless of the concentration of ZnO; however, when applied against *Fn*, the most concentrated group (30 wt%) displayed higher antibacterial activity (Table 16.1).

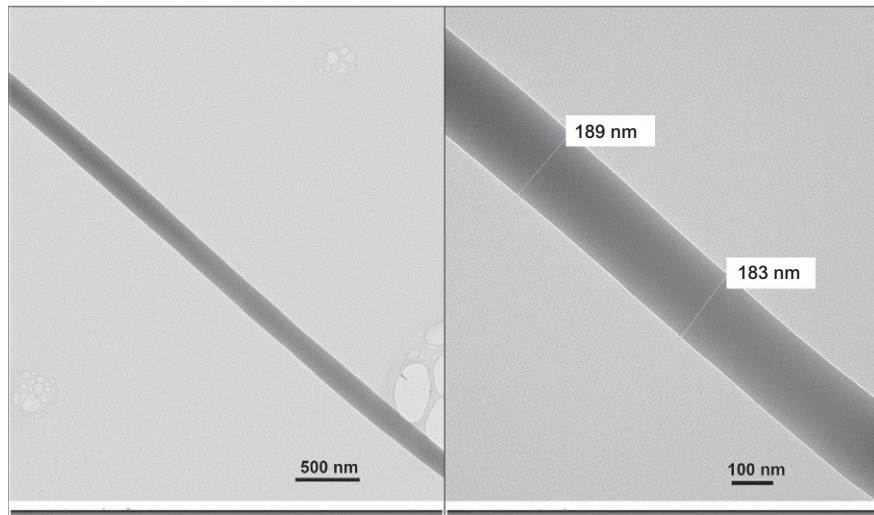
16.4.2 Calcium phosphates and bioactive glass

16.4.2.1 Hydroxyapatite (HA)

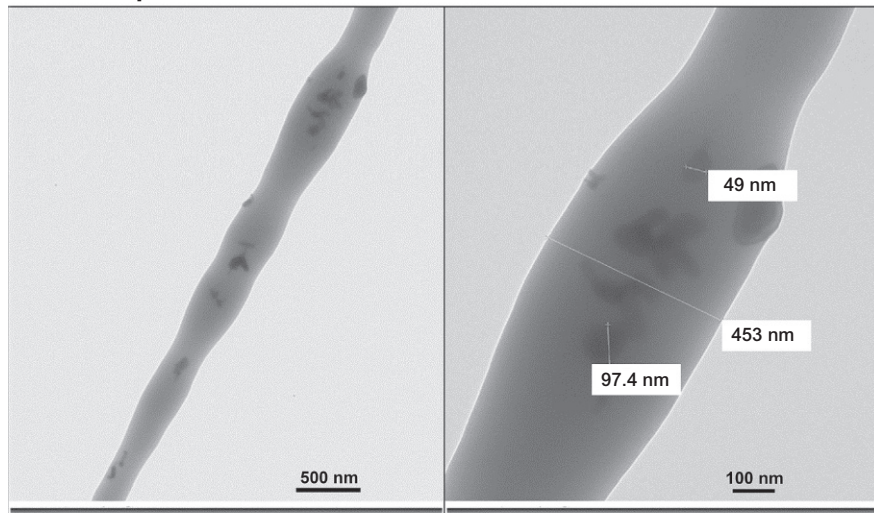
Hydroxyapatite is a naturally occurring mineral form of calcium phosphate that constitutes up to 70% of the dry weight of bone [81]. Techniques, such as coelectrospinning of HA nanoparticles [82–88], electrospaying of HA suspensions [89], and biomimetic growth of HA from simulated body fluids, have been frequently employed for fabricating fibrous composites of polymer and HA with improved mechanical properties and bioactivity, resulting in greater adhesion and proliferation of osteoblasts or mesenchymal stem cells [90,91].

Many research groups have studied the effect of nanosized hydroxyapatite (HA) particles in electrospun matrices for bone tissue regeneration in vitro. The interest in nHAp as inorganic nanofiller lies in its high surface area to volume ratio, high surface activity, biocompatibility, and ability to absorb a number of bioactive species [77,91].

Yang et al. [46] electrospun nanofibrous membranes composed of nanoapatite (nHAp) and PCL, that is, n0 (nHAp/PCL = 0:100), n25 (nHAp/PCL = 25:100), and n50 (nHAp/PCL = 50:100). The authors demonstrated that the incorporation of nanoapatite played a significant role in terms of improving membrane bioactivity and facilitating early cell differentiation [46]. Jose et al. [88] studied the effect of collagen and HA on aligned electrospun multifunctional nanofibers based on PLGA/collagen/HA by human mesenchymal stem cells' seeding. The membranes supported cell adhesion and proliferation [88]. In another study, Phipps et al. [92] showed that a bio-composite fibrous electrospun membrane comprised of PCL, collagen, and nHAp (50/30/20 weight ratio) adsorbed an increased amount of the adhesive proteins, fibronectin, and vitronectin than PCL or PCL/HA following both in vitro exposure to serum

PCL fibers

(A)

ZnO-incorporated PCL fibers

(B)

Fig. 16.2 TEM images demonstrating, respectively, the absence and the presence of ZnO nanoparticles within the neat PCL fibers (A) and ZnO-incorporated fibers (B). Images on the left and right show, respectively, magnifications of 30,000× and 98,000× [2].

Table 16.1 Mean (\pm standard deviation) of the minimal inhibition concentration (MIC) of the zinc oxide (ZnO) nanoparticles and antibacterial activity (inhibition halos, in mm) of the prepared electrospun membranes against *Porphyromonas gingivalis* (*Pg*) and *Fusobacterium nucleatum* (*Fn*) [80]

Bacteria	CHX (control)	MIC ($\mu\text{g/mL}$)		
		2500	5000	10,000
<i>Pg</i>	^A 11.7 (± 0.6) ^a	^A 8.3 (± 1.2) ^b	^A 9.0 (± 1.0) ^b	^A 8.0 (± 0.6) ^b
<i>Fn</i>	^A 10.3 (± 0.6) ^a	^B 0.0 ^c	^B 5.3 (± 0.6) ^b	^A 9.3 (± 1.2) ^a
ZnO content (wt%)	<i>Pg</i>	<i>Fn</i>		
	<i>PCL</i>	<i>PCL/GEL</i>	<i>PCL</i>	<i>PCL/GEL</i>
0	^C 0.0 ^a	^C 0.0 ^a	^D 0.0 ^a	^C 0.0 ^a
5	^B 6.3 (± 0.6) ^b	^B 7.7 (± 0.6) ^a	^C 6.7 (± 1.2) ^b	^B 11.3 (± 0.6) ^a
15	^{AB} 9.0 (± 1.0) ^a	^B 8.3 (± 0.6) ^a	^{BC} 9.0 (± 1.7) ^b	^B 11.7 (± 0.6) ^a
30	^A 11.7 (± 2.9) ^a	^B 8.3 (± 0.6) ^b	^A 14.3 (± 0.6) ^a	^A 13.7 (± 0.6) ^a
CHX (control)	^{AB} 10.0 (± 1.0) ^a	^A 11.0 (± 1.0) ^a	^B 9.7 (± 0.6) ^b	^{AB} 12.3 (± 0.6) ^a

Distinct uppercase letters in a same column and lowercase letters in a same row indicate statistically significant differences among groups tested ($P < .05$).

CHX, chlorhexidine; PCL, poly(ϵ -caprolactone); PCL/GEL, mixture of PCL and gelatin (50:50 ratio, w/w).

and placement into rat tibiae [92]. The tricomponent substrate exhibited a rapid spreading and significantly greater proliferation of cultured mesenchymal stem cells than PCL/HA, PCL, and collagen scaffolds. Moreover, cells seeded onto PCL/collagen/HA scaffolds revealed considerably higher levels of phosphorylated FAK, a marker of integrin activation known to be involved in osteoblastic differentiation signaling cascades [92].

16.4.2.2 Tricalcium phosphate (TCP)

Tricalcium phosphate is a bioceramic that is resorbed faster than synthetic HA but has weak mechanical properties [81]. Baykan et al. [93] prepared parallel concentric poly(ϵ -caprolactone)/ β -TCP composite fibrous membranes via electrospinning. In vivo findings indicated that the biomimetic multispiral membrane seeded with bone marrow-derived mesenchymal stem cells supports the ectopic formation of new bone tissue in rats.

Electrospinning has been combined with other processing techniques to obtain membranes for bone tissue regeneration. Ye et al. [94] fabricated a new hierarchical scaffold that consisted of melt-plotted PCL/ β -TCP composite and embedded electrospun collagen nanofibers. Scanning electron microscope (SEM) micrographs of the fabricated constructs indicated that the β -TCP particles were uniformly embedded in PCL struts and that electrospun collagen nanofibers were well layered between the composite struts. The collagen nanofibers and β -TCP particles in the construct provided

synergistic effects for cell activity. The work of Schneider et al. [95] investigated the use of aerosol-derived amorphous TCP nanoparticles and PLGA for the preparation of cotton, wool-like nanocomposite electrospun fibers. Overall, the membranes supported human mesenchymal stem cell proliferation and osteogenic differentiation.

16.4.2.3 Bioactive glass

Another promising material that has been used in conjunction with electrospun polymer membranes is bioactive glass, since it has the potential to induce bone formation, osteogenic proliferation, and activation of gene expression.

Silicate- and borate-based bioactive glasses have been extensively investigated as potential enhancers of bone regeneration. Although both are osteoconductive, borate-based bioactive glasses degrade faster and convert to calcium phosphate at a remarkably rapid rate, which bonds with the surrounding tissue. We recently evaluated electrospun PLA/PCL-based membranes modified with borate bioactive glass (BBG) for GBR applications [96] (Fig. 16.3). The mechanical properties of the membrane incorporated with BBG at 10 wt% were comparable or superior to that of Epi-Guide, a clinically available PLA-based membrane. The addition of BBG at 10 wt% has led to similar stiffness, but more importantly, it has led to a significantly stronger membrane when compared with Epi-Guide. Cell proliferation assays demonstrated a higher rate of preosteoblasts' proliferation on BBG-containing membranes over Epi-Guide, following 7 days of *in vitro* culture (Fig. 16.4).

Mesoporous bioactive glass particles have been incorporated with osteogenic factors or growth factors to induce osteogenic differentiation and proliferation. El-Fiqi et al. [97] fabricated electrospun PCL-gelatin fibers incorporated with mesoporous bioactive glass nanoparticles (mBG) to provide a long-term delivery of dexamethasone. The mBG-PCL membranes demonstrated excellent properties, including improved strength, elasticity, and hydrophilicity, compared with pure biopolymer matrix. The membranes demonstrated linear release kinetics of dexamethasone up to the test period (28 days) after a rapid initial release of ~30% within 24 h. PDL stem cells demonstrated increased proliferation and differentiation on the membranes *in vitro*. In another study, Kim et al. [98] found that hDPSCs could be differentiated into odontoblasts after culturing on a nanofibrous membrane consisting of PCL-gelatin and mesoporous bioactive glass nanoparticles. An increased ALP activity, mineralized nodule formation, and mRNA expressions involving ALP, osteocalcin, osteopontin, dentin sialophosphoprotein, and dentin matrix protein-1 were observed.

16.4.3 Growth factors

Successful periodontal regeneration depends on a precise interaction among a membrane or scaffold material and other key elements, such as growth factors, cells, and blood supply. The local delivery of a wide selection of growth factors (e.g., bone morphogenic protein-2 or BMP-2) has been demonstrated as enhancing both periodontal

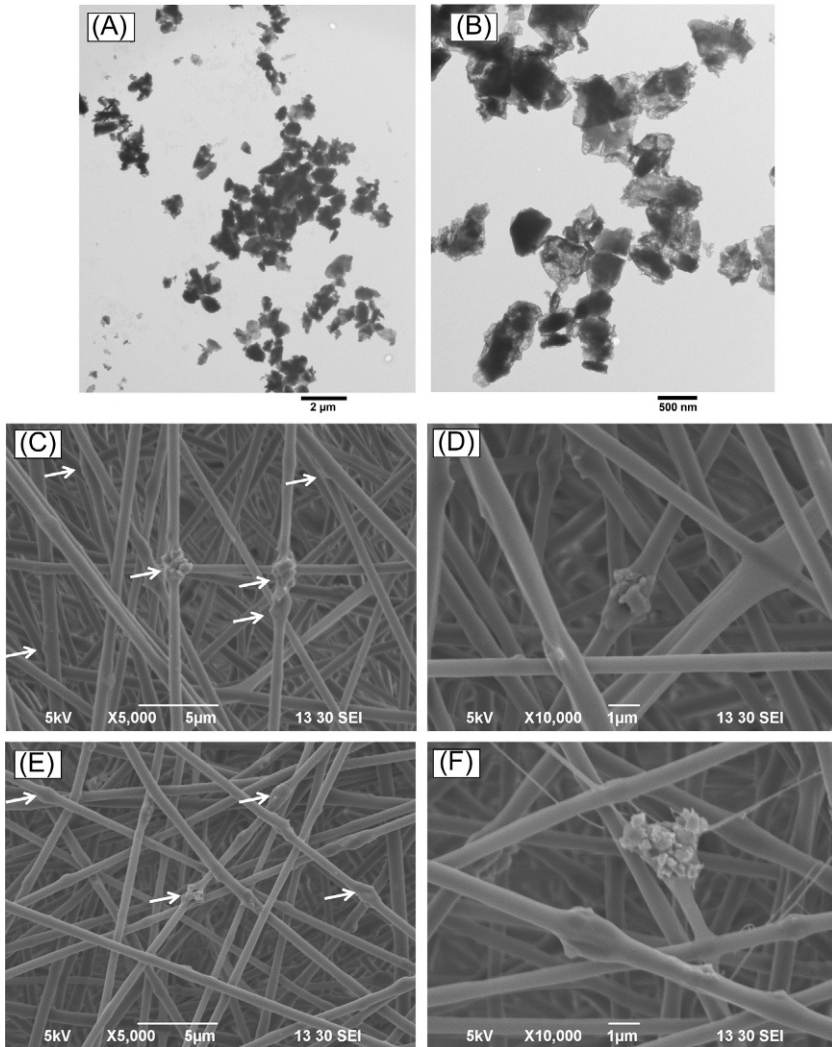


Fig. 16.3 (A and B) Representative TEM images of the borate-based bioglass (BBG) particles. (C and D) Representative SEM images of the PLA/PCL electrospun membranes modified with 5 wt% BBG at 5000 \times (C) and 10,000 \times (D) magnifications. (E and F) Representative SEM images of the PLA/PCL electrospun membranes modified with 10 wt% BBG at 5000 \times (E) and 10,000 \times (F) magnifications. The deposition of BBG on the PLA/PCL fibers is indicated by arrows in the lower magnification images [3].

healing and regeneration by modulating the cellular activity and providing stimuli to cells to differentiate and synthesize the ECM to develop new tissues.

Growth factor encapsulation has been achieved through either physical adsorption or direct blending into the polymer solution before electrospinning. Schofer et al. [99] demonstrated that incorporating BMP-2 into electrospun PLA scaffolds showed

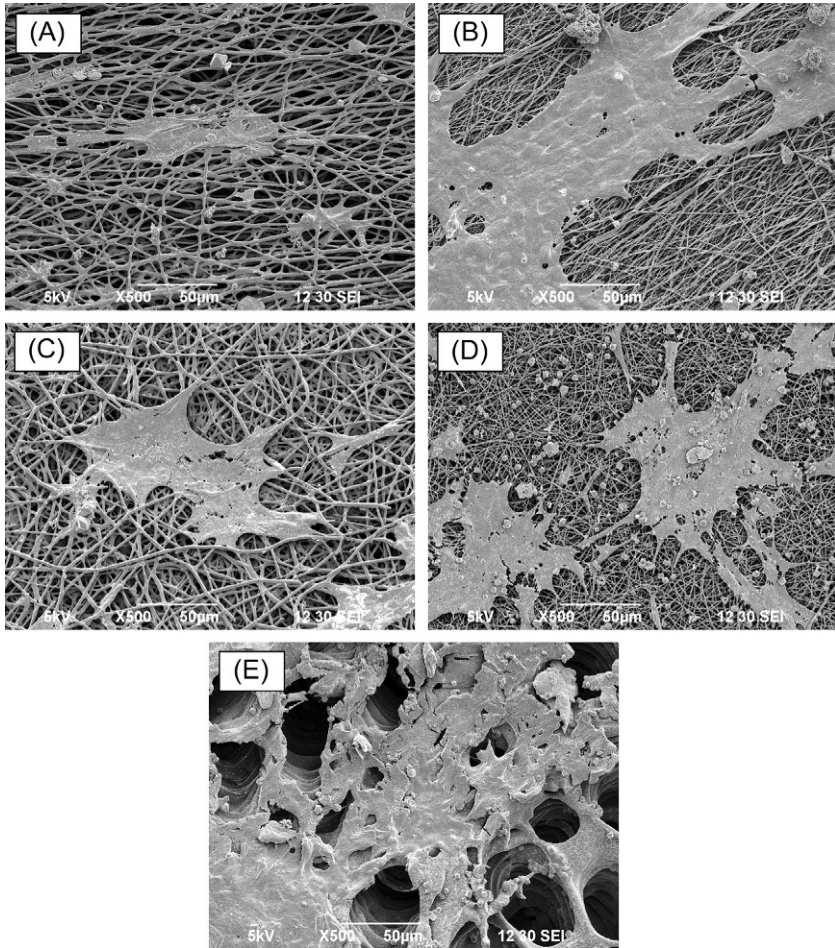


Fig. 16.4 Representative SEM images illustrating the MC3T3-E1 cell morphology after 7 days of culture: (A) PLA, (B) PCL, (C) PLA/PCL, (D) PLA/PCL + 10 wt% BBG, and (E) Epi-Guide [3].

enhanced bone regeneration and several ossification foci when implanted into critically sized calvarial defects using a rat model. After 12 weeks of implantation, osteocalcin, BMP-2, and Smad5 were significantly higher in the PLA/BMP-2 compared with the controls.

BMP-2 has also been incorporated to coaxially structured nanofibers by core-shell spinning for sustained release within the periodontal defect. Zhu et al. [100] fabricated coaxial fibers with recombinant BMP-2 using poly(ethylene glycol) as the core and PCL as the shell. A sustained release profile over a period of 24 days was achieved using this core-shell system. The membranes containing BMP-2 exhibited the fastest and most bone formation when evaluated in a rabbit cranial defect model. In another

study, Shalumon et al. [101] prepared silk fibroin/chitosan/nanohydroxyapatite/BMP-2 nanofibrous membranes by incorporating BMP-2 into the core and silk fibroin/chitosan/nHAp as the shell layer of a nanofiber with two different shell thicknesses (SCHB2-thick and SCHB-thin). The core-shell nanofibrous membranes of reduced shell thickness released higher amounts of BMP-2 and retained osteo-inductive activity toward human-bone-marrow-derived mesenchymal stem cells, highlighting its promise as a membrane for periodontal bone tissue engineering.

The potent stimulatory effects of platelet-derived growth factor (PDGF) as a chemoattractant and a mitogen, along with its ability to promote angiogenesis, position it as a key regulatory molecule in tissue repair. Phipps et al. [102] physically adsorbed PDGF-BB to blended electrospun nanofibers of PCL and collagen I with embedded nHAp particles. The membranes adsorbed greater quantities of PDGF-BB and caused sustained release for at least 8 weeks, leading to enhanced MSC chemotaxis under stringent *in vitro* conditions.

Basic fibroblast growth factor (bFGF) acts as a strong angiogenesis inducer with significant implications in bone repair. Lee et al. [103] fabricated PCL/gelatin electrospun fiber membranes onto which bFGF was immobilized via heparin to control the initial bFGF burst release. In addition to enhancing angiogenesis, bFGF incorporation enhanced bone regeneration when evaluated using a mouse calvarial critical size defect model, even at relatively small doses. In another study, Sahoo et al. [104] incorporated bFGF into PLGA nanofibers by blend electrospinning and coaxial electrospinning and found that the latter improved bFGF release to 2 weeks. However, the blended fibers demonstrated increased collagen production and upregulated gene expression of specific ECM proteins, indicating fibroblastic differentiation.

A recent strategy to promote bone regeneration was to recruit endogenous stem/progenitor cells to the injury site by increasing local concentrations of cytokines and/or chemokines at the target site, thereby regulating the mobilization, trafficking, and homing of stem/progenitor cells. Among the various cytokines or chemokines, stromal cell-derived factor-1 α (SDF-1 α), also known as chemokine (C-X-C motif) ligand 12 (CXCL12), is particularly important in mesenchymal stem cells' homing and localization within the bone marrow. Ji et al. [105] fabricated electrospun membranes for GBR applications using PCL blended with type B-gelatin and functionalized it with stromal cell-derived factor-1 α (SDF-1 α) via physical adsorption. The membranes loaded with different amounts of SDF-1 α (up to 400 ng) significantly stimulated chemotactic migration of MSCs *in vitro* without dose-dependent effects. Eight weeks after implantation in rat cranial defects, SDF-1 α -loaded membranes yielded a sixfold increase in bone formation compared with the neat membranes.

16.4.4 Functionally graded and multilayered membranes

A periodontal membrane needs to utilize a graded structure with compositional and structural gradients that meet the local functional requirements to engineer new periodontium by amplifying regeneration of the periodontal tissues while preventing gingival tissue downgrowth. With this in mind, Fujihara et al. [26] fabricated electrospun

bilayered membranes with a functional layer consisting of PCL/CaCO₃ and a PCL layer for mechanical support. PCL/CaCO₃ composite nanofibers with two different PCL to calcium carbonate (CaCO₃) ratios (PCL/CaCO₃ = 75:25 and 25:75 wt%) were spun over PCL nanofibrous membranes. It was found that the membranes could be stretched at around 200% strain without visible rupture. Moreover, the membranes supported osteoblast attachment and growth. In another study, Sundaram et al. [106] developed a bilayered construct presenting an osteoinductive layer consisting of a chitosan/2 wt% calcium sulfate membrane that can mimic and regenerate hard tissue (alveolar bone) and a PCL multiscale (micro-/nano-)electrospun membrane to mimic and regenerate soft tissue (PDL). Human dental follicle cells demonstrated osteoblastic differentiation on the layer containing calcium sulfate and fibroblastic differentiation on the PCL multiscale membranes.

A few years ago, our group reported on the fabrication of a functionally graded membrane (FGM) via sequential multilayer electrospinning [4]. The FGM consisted of a core layer (CL) and two functional surface layers (SLs) interfacing with bone (nanohydroxyapatite, nHAp) and epithelial (metronidazole, MET) tissues (Fig. 16.5). The CL comprises a neat poly(DL-lactide-co-ε-caprolactone) (PLCL) layer surrounded by two composite layers consisting of a protein/polymer ternary blend (PLCL/PLA/GEL). Hydroxyapatite nanoparticles were incorporated to enhance bone formation on the surface layer facing the bone defect, and MET, an antibiotic commonly used in the treatment of periodontitis, was added to prevent bacterial colonization on the surface layer facing the epithelial tissue. SEM images showing the morphological characterization of the FGM layers are seen in Fig. 16.6. While most biodegradable polymers are rigid and brittle, PLCL possesses exceptional elastic properties, which are critical for periodontal membranes during in vivo placement. No delamination was observed in the CL

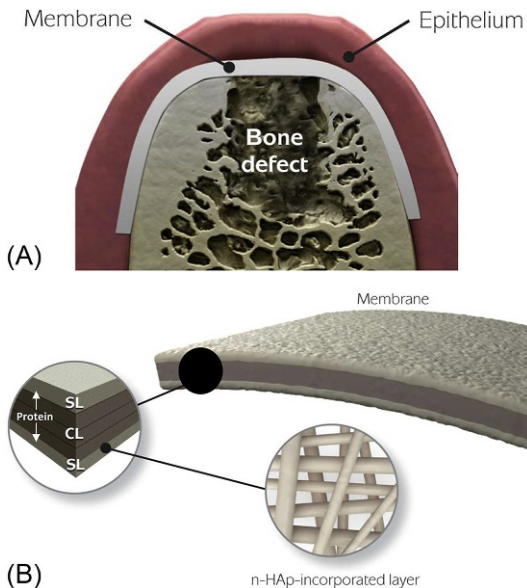


Fig. 16.5 Schematic illustration of the spatially designed and functionally graded periodontal membrane. (A) Membrane placed in a guided bone regeneration scenario. (B) Details of the core layer (CL) and the functional surface layers (SLs) interfacing bone (nHAp) and epithelial (MET) tissues. Note the chemical composition stepwise grading from the CL to SLs, that is, polymer content decreased and protein content increased [4].

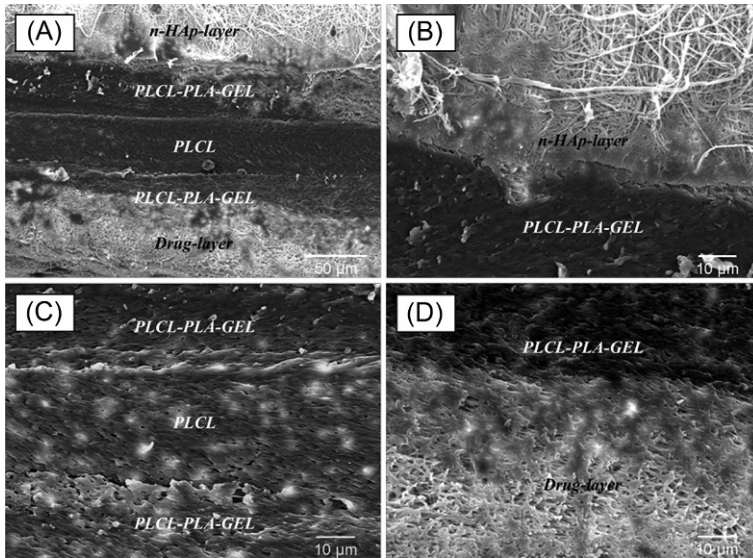


Fig. 16.6 Cross-section SEM micrographs of the FGM processed via multilayering electrospinning. (A) General view of the FGM; (B) nHAp-containing layer/PLCL/PLA/GEL interface; (C) CL structure; (D) MET-loaded layer/PLCL/PLA/GEL interface [4].

membrane, indicating that the compositionally graded layers remained intact under physiological conditions. Cross-section SEM images are shown in Fig. 16.6. The FGM exhibited a tensile strength of 3.5 MPa and a tensile modulus of 80 MPa, with a strain at break equal to 297%. The sequential electrospinning method used in this study offers an interesting route for the development of multilayered and functionally graded membranes with more predictable physicochemical, mechanical, and biological characteristics that could ultimately lead to enhanced periodontal regeneration [4].

16.5 Caries and pulpal disease

Dental trauma and the bacterial infection of dental pulp leads to inflammation, and, if left untreated, pulpal necrosis and apical periodontitis will ensue [5,107]. In the United States, over 15 million patients undergo root canal treatment each year [108], resulting in a major socioeconomic burden. Traditional root canal therapy remains the standard of care for mature, fully developed teeth with pulpal necrosis, and it involves the chemomechanical debridement and sealing of the canal system with an inert rubber-like material [109]. However, immature permanent teeth present a very unique anatomy, that is, wide-open root apex and thin root dentinal walls [5,6,107]. Given the wide-open root apex, which halts the possibility of achieving an apical seal and thin dentinal walls, performing traditional root canal therapy on necrotic immature teeth is not advisable [5,6,107]. Thus, apexification using either calcium hydroxide

(Ca(OH)₂) or MTA has been used to induce apical closure [110–112]. Although apexification supports apical closure, it neither promotes root development nor restores the immunologic competence of pulp [113,114]. Additionally, apexification eliminates any further chance for complete root development (e.g., dentinal wall thickening and apical maturation), thus increasing the chance of future root fracture [115,116].

16.5.1 The role of disinfection in regenerative endodontics

Regeneration of the pulp-dentin complex holds the promise of extending the function of the natural dentition, particularly in cases where traumatic injuries to permanent immature teeth halt root maturation and full development [5,6,117,118]. The most widely used regenerative strategy, namely, the EB method, employs intracanal medications, including triple (TAP—ciprofloxacin, metronidazole, and minocycline) and double (DAP—minocycline-free) highly concentrated antibiotic pastes, or Ca(OH)₂. The use of an antibiotic mixture in regenerative endodontic procedures was introduced in 2001 [119]. Since its advent, this intracanal antibiotic paste (i.e., TAP or DAP) has been the most widely used interappointment medicament [120]. It is worth noting that this form of medication was introduced into the clinics without precise information as to the therapeutic dose to be used, which would retain its antimicrobial effect while minimizing its toxicity on host tissues and cells, including stem cells. In regenerative endodontics, following adequate disinfection, the intentional laceration of periapical tissue is done to evoke bleeding, delivery of apical stem cells, and the subsequent formation of a fibrin-based scaffold [121]. Growth factors and stem cells from the apical area populate the scaffold, inducing tissue regeneration [5,6,107,121]. Remarkably, both root canal disinfection and blood-clot formation have been shown to play a critical role in new tissue formation and overall root maturation and development. Despite these promising results, the biological outcome of this regenerative-based treatment is rather unpredictable [119,121–125]. Bone healing and root development do not necessarily confirm formation of tissue that closely resembles the pulp-dentin complex within root canals. In fact, the histological examination of tissue formed inside the root canals of teeth treated with regenerative procedures reveals apposition of a cementum-like tissue, which is responsible for canal narrowing and an increase in length [126,127]. Additionally, the ingrowth of a connective tissue similar to the PDL, along with a bone-like tissue, was identified inside root canals [121,128,129]. These findings suggest that current endodontic regenerative protocols need careful consideration and review. Unpredictability of the histological results could relate to many factors [5,6,107,121]. The disinfection technique seems to be one of the most influential factors affecting the outcome of this regenerative-based approach [5,6,107]. There is a compelling level of data indicating that both chemical irrigants and intracanal medicaments can negatively affect the survival ability and function of dental stem cells [5,6,107]. Therefore, it would be beneficial and advantageous to use a biocompatible nanofiber-based intracanal drug delivery construct to release antibiotics at lower, yet antimicrobially effective concentrations [7].

16.5.2 Electrospun polymer nanofibers for intracanal drug delivery

In recent years, electrospinning or electrostatic spinning, a textile technology, has been employed to fabricate antibiotic-containing polymer-based nanofibers for drug delivery applications in dentistry, particularly to ablate periodontal and endodontic infections [3,5,7]. The idea behind the use of antibiotic-containing nanofibers as a three-dimensional (3D) tubular drug delivery construct [5,12,130] that can be placed inside the root canal system of necrotic teeth (Fig. 16.7) is based on the fact that the addition of low antibiotic concentrations and the slow drug release provided by these

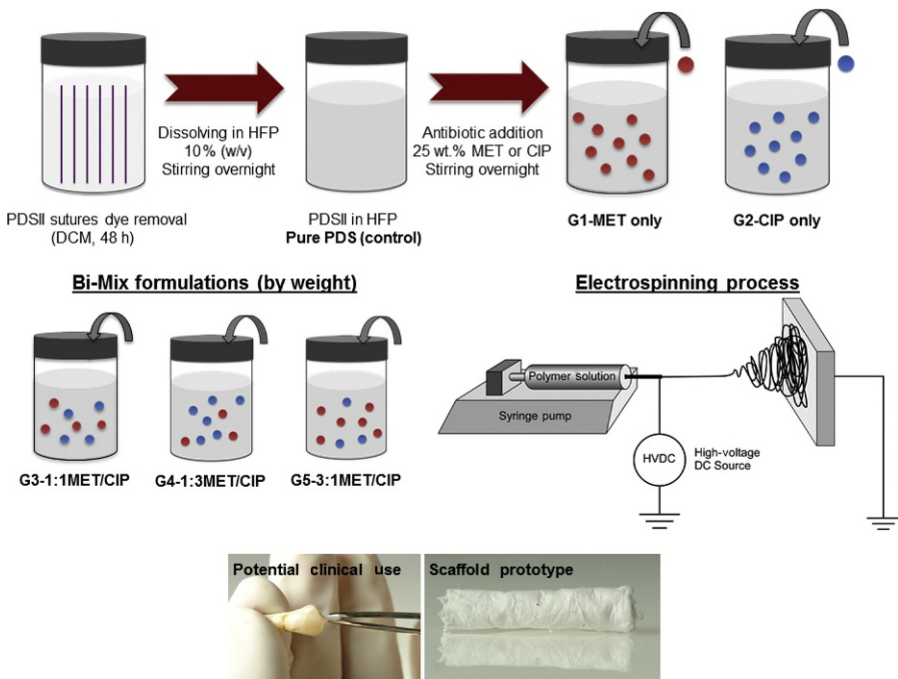


Fig. 16.7 Polydioxanone suture filaments (PDS II, Ethicon, Somerville, and NJ) are first undyed using dichloromethane (Sigma-Aldrich, St. Louis, and MO) and then dissolved in 1,1,1,3,3,3-hexafluoro-2-propanol (HFP, Sigma-Aldrich) at 10 wt% under stirring conditions. MET (Sigma-Aldrich) and CIP (Sigma-Aldrich) containing solutions are prepared by adding MET (G1) and CIP (G2) into the PDS solution at a 25 wt% relative to the total PDS weight and mixed together under vigorous stirring. Different ratios (by weight) of the two antibiotics are added to PDS solutions and mixed under vigorous stirring to obtain the following antibiotic-containing solutions: G3-1:1MET/CIP, G4-1:3MET/CIP, and G5-3:1MET/CIP. The antibiotic-containing and pure PDS (control) solutions are then electrospun under optimized parameters in a 3D tubular-shaped construct (i.e., scaffold prototype).

nanofibrous constructs will eradicate infection and thus create a bacteria-free environment favorable to tissue regeneration [5,7,9–11,13–15,130]. Worth noting, in this strategy, the antimicrobial agents could be used at much lower concentrations, as they are delivered in a predictable fashion onto the dentinal walls where microbial biofilms have been found to be present, thus being the culprit of persistent endodontic infections.

In electrospinning, a polymer solution/melt containing the desired concentration of antibiotics is prepared in order to produce nanofibers [3,5,7]. The chosen polymer solution can be incorporated with one or a combination of antibiotics, making it possible to fabricate fibers with a narrow or wide spectrum of action (e.g., ciprofloxacin (CIP), metronidazole (MET), and minocycline (MINO)) that have been shown to inhibit the growth of endodontic pathogens [7,9,13,14]. In a recent study, ciprofloxacin-containing polymer nanofibers were tested against *E. faecalis* biofilm developed on human root fragments [11]. Caries-free extracted human mandibular incisors were longitudinally sectioned to obtain two halves, each measuring $10 \times 5 \times 0.6$ mm. An *E. faecalis* suspension was inoculated on the specimens for 5 days to allow for biofilm formation, and they were then exposed (direct contact) to CIP-containing (5 and 25 wt% CIP) nanofibers. A thick biofilm mass was observed using scanning electron microscopy (SEM) along the whole root segment (i.e., cervical, middle, and apical thirds), with a remarkable concentration of bacteria on the middle third, probably due to intrinsic substrate characteristics (e.g., uniform distribution of dentinal tubules and a similar tubule diameter) (Fig. 16.8) [131]. Antimicrobial assays involving the use of colony-forming units (CFU) and SEM methodologies found that this young *E. faecalis* biofilm was susceptible to 25 wt% CIP nanofibers, demonstrating maximum bacterial biofilm elimination [11].

In an attempt to improve the antimicrobial effects of these unique nanofibers and based on several studies using TAP as the standard of care in regenerative endodontics, our group was the first to develop triple (MET, CIP, and MINO) antibiotic-containing polymer nanofibers [10]. The chosen bacteria, *A. naeslundii*, consisted of uncommon bacterial species used for in vitro studies in endodontics; however, it has been recently associated with root canal infections, particularly in cases of undeveloped traumatized teeth [132]. *A. naeslundii* was cultured on human dentin for 7 days to allow for biofilm formation on the surface and inside dentinal tubules. Infected dentin specimens exposed to triple antibiotic-containing nanofibers revealed significant bacterial death based on CLSM data when using the live/dead cell assay (Fig. 16.9) [10].

Noteworthy, the aforementioned studies focused on facultative anaerobic bacteria; however, root canal colonization, mainly in primary infections, is often composed of strict anaerobic species [133]. Therefore, recent research [15] used *Porphyromonas gingivalis* to induce a 7-day biofilm on human dentin through the careful limitation of environmental conditions (anaerobic jars). The established *P. gingivalis* biofilm was also susceptible to triple antibiotic-containing nanofibers [15]. Taken together, our studies [5,7–11,13–15] have provided abundant background information to not only test the antimicrobial efficacy of these nanofibers on multispecies biofilms in vitro but to also explore their clinical efficacy using preclinical animal models of periapical disease.

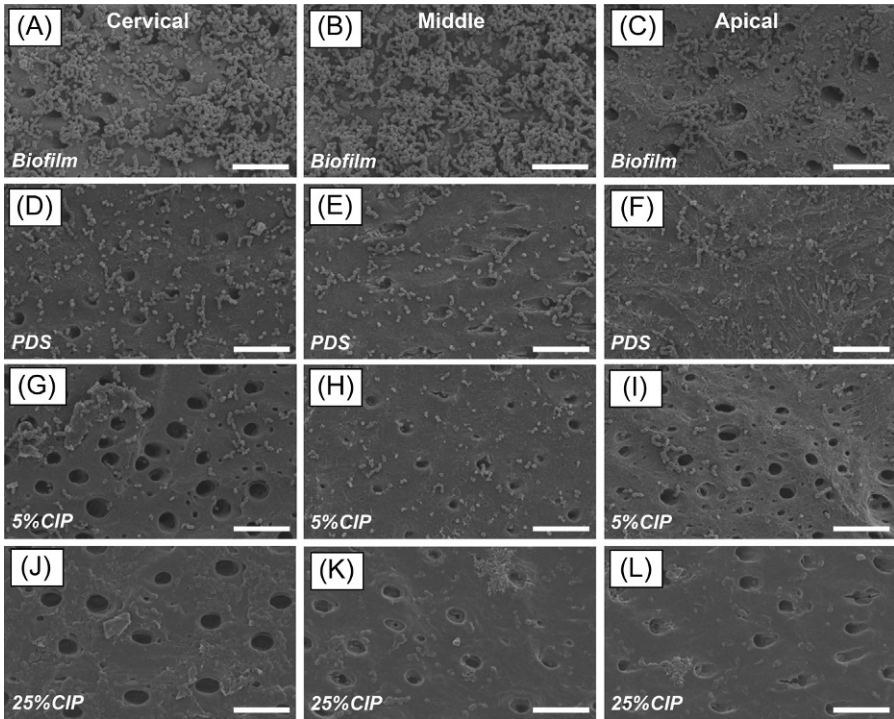


Fig. 16.8 Representative SEM images ($\times 2000$) of the radicular dentin specimen before (A–C) (i.e., biofilm) and after (D–L) scaffold exposure (i.e., PDS, PDS + 5 wt% CIP, and PDS + 25 wt% CIP) at the distinct specimen regions evaluated (cervical, middle, and apical thirds). (J–L) Dentin specimens exposed to PDS + 25 wt% CIP scaffolds displayed a bacteria-free surface, with a few dead bacteria (*white arrows*) and dentin debris (*white circles*). Scale bar = 10 μm [6].

16.6 Conclusions and future perspectives

Periodontitis is a chronic inflammatory disorder affecting nearly 50% of adults in the United States. If left untreated, it can lead to the destruction of both soft and mineralized tissues, which constitutes the periodontium. Clinical management, including but not limited to flap debridement and/or curettage, as well as regenerative-based strategies with periodontal membranes associated or not with grafting materials, has been used with distinct levels of success. Unquestionably, no single implantable biomaterial can consistently guide the coordinated growth and development of multiple tissue types, especially in very large periodontal defects. With the global population aging, it is extremely important to find novel biomaterials, particularly bioactive membranes and/or scaffolds for guided tissue/bone regeneration (GTR/GBR), to aid in the reestablishment of the health and functions of distinct periodontal tissues. Resorbable and nonresorbable membranes act as a physical barrier to avoid connective and epithelial tissue downgrowth into the

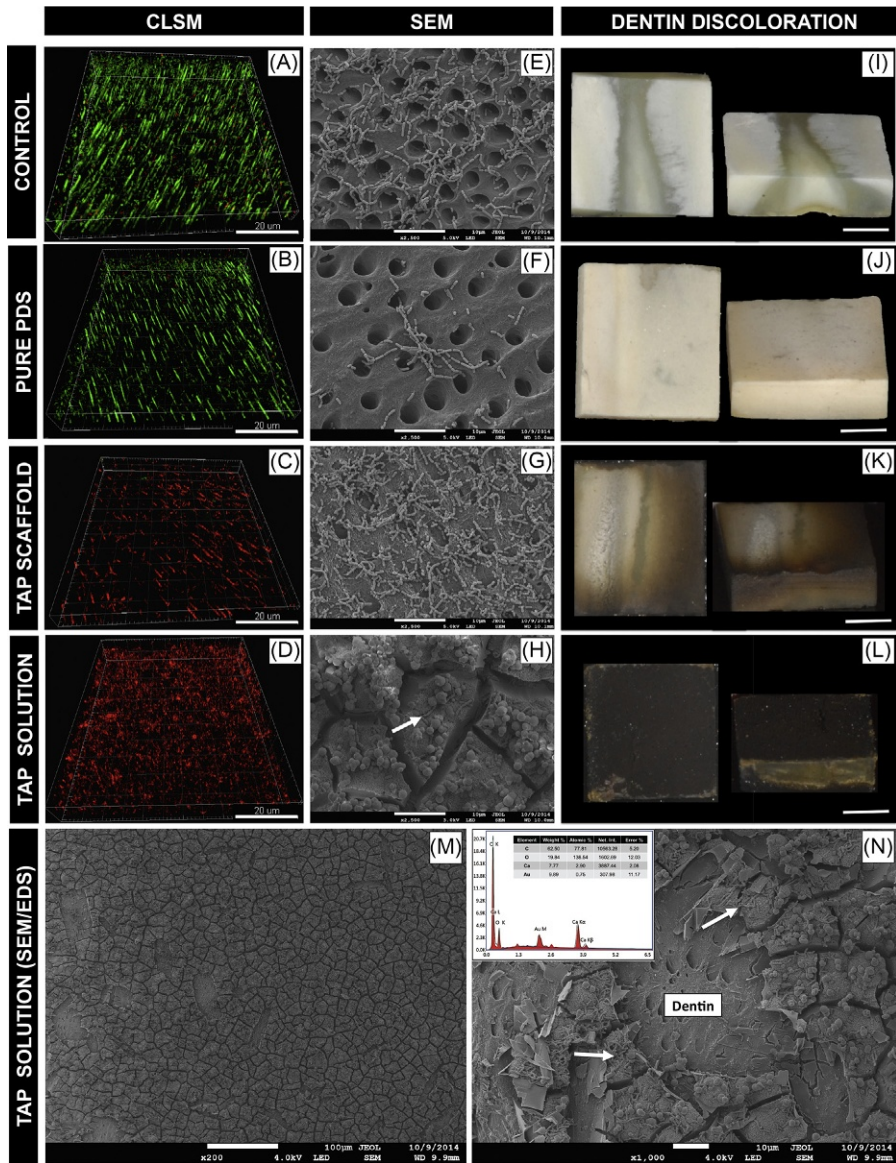


Fig. 16.9 CLSM images were collected in sequential illumination mode by using 488 and 552 nm laser lines. Fluorescent emission was collected in 2 HyD spectral detectors with filter range set up to 500–550 nm and 590–655 nm for green (SYTO9) and red dye (PI), respectively. CLSM macrophotographs of 7-day *A. naeslundii* biofilm (negative control) growth inside dentinal tubules (A), infected dentin treated with pure PDS (B), TAP scaffold (C), and TAP solution (D) for 3 days. SEM images of *A. naeslundii* biofilm on the dentin surface (negative control) (E) treated by pure PDS (F), TAP scaffold (G), and TAP solution (H). Dentin discoloration images of negative control (I), pure PDS (J), TAP scaffold (K), and TAP solution (L) groups. Representative SEM images (original magnification, $\times 200$ and $\times 1000$) of TAP solution treated dentin showing calcium-enriched (Ca) insoluble agglomerates attached to the dentin surface (M) and covering dentinal tubules (N) as demonstrated by energy-dispersive X-ray spectroscopy (EDS) analyses (*inset* EDS image N); *A. naeslundii* can be seen on the surface of this insoluble complex (*white arrows*) (N and H) [7].

defect, favoring the regeneration of periodontal tissues. These conventional membranes possess many structural, mechanical, and biofunctional limitations. Taken together, current technology and results from the literature suggest that both bioactive and multilayered nanofibrous membranes have significant potential for use in periodontal tissue engineering. Nonetheless, in order to maximize periodontal regeneration, the implantable membrane must support bone cells' infiltration from the bone-defect side. Vascularization of the biomaterial/cell construct is an essential step in tissue healing, as this process provides the nutrients and oxygen needed for bone cells to survive while facilitating removal of cell waste products.

Regarding regenerative endodontics, categorically, antibiotic mixtures have become an important intracanal medicament in cases of necrotic immature permanent teeth. However, the way they have been used remains obsolete, since microorganisms colonizing the root canal are usually not identified before the application of antibiotics, which could favor bacterial resistance toward these antibiotics. Accordingly, there is a trend in endodontic drug therapy toward determining the microbiota present in root canals and then administering specific antibiotics to properly fight the infection. Taken together, the clinical prospects associated with the design and synthesis of patient-specific cytocompatible antibiotic-containing polymer nanofibers that can be fabricated in a 3D structure (Fig. 16.7) allowing for intracanal drug delivery have gained increased attention, and in vivo preclinical studies are currently being carried out to expedite its clinical translation.

Our research team's next step is to further validate these results in preclinical large animal and eventually start clinical trials in humans. There are several technical hurdles still ahead before the use of electrospinning can be considered ready for commercial applications in dentistry. The manufacturing process and costs involved in the fabrication of bioactive multilayered membranes for periodontal regeneration and nanofibrous drug delivery systems for root canal disinfection have to be evaluated and the relevant Food and Drug Administration (FDA) and intellectual property considerations are currently being pursued.

Acknowledgments

M.C.B. acknowledges funding from the NIH/NIDCR (Grant#DE023552).

References

- [1] Caton J, Bostanci N, Remboutsika E, De Bari C, Mitsiadis TA. Future dentistry: cell therapy meets tooth and periodontal repair and regeneration. *J Cell Mol Med* 2011;15(5):1054–65.
- [2] Mitsiadis TA, Orsini G, Jimenez-Royo L. Stem cell-based approaches in dentistry. *Eur Cell Mater* 2015;30:248–57.
- [3] Bottino MC, Thomas V, Schmidt G, Vohra YK, Chu TM, Kowolik MJ, et al. Recent advances in the development of GTR/GBR membranes for periodontal regeneration—a materials perspective. *Dent Mater* 2012;28(7):703–21.

- [4] Bottino MC, Thomas V, Janowski GM. A novel spatially designed and functionally graded electrospun membrane for periodontal regeneration. *Acta Biomater* 2011;7(1):216–24.
- [5] Albuquerque MT, Valera MC, Nakashima M, Nor JE, Bottino MC. Tissue-engineering-based strategies for regenerative endodontics. *J Dent Res* 2014;93(12):1222–31.
- [6] Diogenes AR, Ruparel NB, Teixeira FB, Hargreaves KM. Translational science in disinfection for regenerative endodontics. *J Endod* 2014;40(4 Suppl.):S52–7.
- [7] Bottino MC, Kamocki K, Yassen GH, Platt JA, Vail MM, Ehrlich Y, et al. Bioactive nanofibrous scaffolds for regenerative endodontics. *J Dent Res* 2013;92(11):963–9.
- [8] Bottino MC, Arthur RA, Waeiss RA, Kamocki K, Gregson KS, Gregory RL. Biodegradable nanofibrous drug delivery systems: effects of metronidazole and ciprofloxacin on periodontopathogens and commensal oral bacteria. *Clin Oral Investig* 2014;18(9):2151–8.
- [9] Palasuk J, Kamocki K, Hippenmeyer L, Platt JA, Spolnik KJ, Gregory RL, et al. Bimix antimicrobial scaffolds for regenerative endodontics. *J Endod* 2014;40(11):1879–84.
- [10] Albuquerque MT, Ryan SJ, Munchow EA, Kamocka MM, Gregory RL, Valera MC, et al. Antimicrobial effects of novel triple antibiotic paste-mimic scaffolds on *Actinomyces naeslundii* biofilm. *J Endod* 2015;41(8):1337–43.
- [11] Albuquerque MT, Valera MC, Moreira CS, Bresciani E, de Melo RM, Bottino MC. Effects of ciprofloxacin-containing scaffolds on enterococcus faecalis biofilms. *J Endod* 2015;41(5):710–4.
- [12] Bottino MC, Yassen GH, Platt JA, Labban N, Windsor LJ, Spolnik KJ, et al. A novel three-dimensional scaffold for regenerative endodontics: materials and biological characterizations. *J Tissue Eng Regen Med* 2015;9(11):E116–23.
- [13] Kamocki K, Nor JE, Bottino MC. Effects of ciprofloxacin-containing antimicrobial scaffolds on dental pulp stem cell viability – in vitro studies. *Arch Oral Biol* 2015;60(8):1131–7.
- [14] Kamocki K, Nor JE, Bottino MC. Dental pulp stem cell responses to novel antibiotic-containing scaffolds for regenerative endodontics. *Int Endod J* 2015;48(12):1147–56.
- [15] Albuquerque MT, Evans JD, Gregory RL, Valera MC, Bottino MC. Antibacterial TAP-mimic electrospun polymer scaffold: effects on *P. gingivalis*-infected dentin biofilm. *Clin Oral Investig* 2016;20(2):387–93.
- [16] Nanci A, Bosshardt DD. Structure of periodontal tissues in health and disease. *Periodontol* 2000 2006;40:11–28.
- [17] Gillett IR, Johnson NW, Curtis MA, Griffiths GS, Sterne JAC, Carman RJ, et al. The role of histopathology in the diagnosis and prognosis of periodontal diseases. *J Clin Periodontol* 1990;17(10):673–84.
- [18] Haffajee AD, Socransky SS. Microbial etiological agents of destructive periodontal diseases. *Periodontol* 2000 1994;5:78–111.
- [19] Chen FM, Zhang J, Zhang M, An Y, Chen F, Wu ZF. A review on endogenous regenerative technology in periodontal regenerative medicine. *Biomaterials* 2010;31(31):7892–927.
- [20] Chen FM, Jin Y. Periodontal tissue engineering and regeneration: current approaches and expanding opportunities. *Tissue Eng Part B Rev* 2010;16(2):219–55.
- [21] Taba Jr. M, Jin Q, Sugai JV, Giannobile WV. Current concepts in periodontal bioengineering. *Orthod Craniofac Res* 2005;8(4):292–302.
- [22] Kikuchi M, Koyama Y, Yamada T, Imamura Y, Okada T, Shirahama N, et al. Development of guided bone regeneration membrane composed of beta-tricalcium phosphate and poly(L-lactide-co-glycolide-epsilon-caprolactone) composites. *Biomaterials* 2004;25(28):5979–86.

- [23] Behring J, Junker R, Walboomers XF, Chessnut B, Jansen JA. Toward guided tissue and bone regeneration: morphology, attachment, proliferation, and migration of cells cultured on collagen barrier membranes. A systematic review. *Odontology* 2008; 96(1):1–11.
- [24] Chen YT, Wang HL, Lopatin DE, Oneal R, MacNeil RL. Bacterial adherence to guided tissue regeneration barrier membranes exposed to the oral environment. *J Periodontol* 1997;68(2):172–9.
- [25] Chou AHK, LeGeros RZ, Chen Z, Li YH. Antibacterial effect of zinc phosphate mineralized guided bone regeneration membranes. *Implant Dent* 2007;16(1):89–100.
- [26] Fujihara K, Kotaki M, Ramakrishna S. Guided bone regeneration membrane made of polycaprolactone/calcium carbonate composite nano-fibers. *Biomaterials* 2005;26(19):4139–47.
- [27] Gentile P, Chiono V, Tonda-Turo C, Ferreira AM, Ciardelli G. Polymeric membranes for guided bone regeneration. *Biotechnol J* 2011;6(10):1187–97.
- [28] Geurs NC, Korostoff JM, Vassilopoulos PJ, Kang TH, Jeffcoat M, Kellar R, et al. Clinical and histologic assessment of lateral alveolar ridge augmentation using a synthetic long-term bioabsorbable membrane and an allograft. *J Periodontol* 2008; 79(7):1133–40.
- [29] Gielkens PFM, Schortinghuis J, de Jong JR, Paans AMJ, Ruben JL, Raghoobar GM, et al. The influence of barrier membranes on autologous bone grafts. *J Dent Res* 2008; 87(11):1048–52.
- [30] Kasaj A, Reichert C, Gotz H, Rohrig B, Smeets R, Willershausen B. In vitro evaluation of various bioabsorbable and nonresorbable barrier membranes for guided tissue regeneration. *Head Face Med* 2008;4:22.
- [31] Li JD, Zuo Y, Cheng XM, Yang WH, Wang HN, Li YB. Preparation and characterization of nano-hydroxyapatite/polyamide 66 composite GBR membrane with asymmetric porous structure. *J Mater Sci Mater Med* 2009;20(5):1031–8.
- [32] Liao S, Wang W, Uo M, Ohkawa S, Akasaka T, Tamura K, et al. A three-layered nano-carbonated hydroxyapatite/collagen/PLGA composite membrane for guided tissue regeneration. *Biomaterials* 2005;26(36):7564–71.
- [33] Liao S, Watari F, Zhu Y, Uo M, Akasaka T, Wang W, et al. The degradation of the three layered nano-carbonated hydroxyapatite/collagen/PLGA composite membrane in vitro. *Dent Mater* 2007;23(9):1120–8.
- [34] McClain PK, Schallhorn RG. Focus on furcation defects – guided tissue regeneration in combination with bone grafting. *Periodontol* 2000;22:190–212.
- [35] Milella E, Ramires PA, Brescia E, La Sala G, Di Paola L, Bruno V. Physicochemical, mechanical, and biological properties of commercial membranes for GTR. *J Biomed Mater Res* 2001;58(4):427–35.
- [36] Milella E, Barra G, Ramires PA, Leo G, Aversa P, Romito A. Poly(L-lactide)acid/alginate composite membranes for guided tissue regeneration. *J Biomed Mater Res* 2001; 57(2):248–57.
- [37] Murphy KG, Gunsolley JC. Guided tissue regeneration for the treatment of periodontal intrabony and furcation defects. A systematic review. *Ann Periodontol* 2003;8(1): 266–302.
- [38] Needleman IG, Worthington HV, Giedrys-Leeper E, Tucker RJ. Guided tissue regeneration for periodontal infra-bony defects. *Cochrane Database Syst Rev* 2006;2:29.
- [39] Park YJ, Lee YM, Park SN, Lee JY, Ku Y, Chung CP, et al. Enhanced guided bone regeneration by controlled tetracycline release from poly(L-lactide) barrier membranes. *J Biomed Mater Res* 2000;51(3):391–7.

- [40] Park JK, Yeom J, Oh EJ, Reddy M, Kim JY, Cho DW, et al. Guided bone regeneration by poly(lactic-co-glycolic acid) grafted hyaluronic acid bi-layer films for periodontal barrier applications. *Acta Biomater* 2009;5(9):3394–403.
- [41] Piattelli A, Scarano A, Russo P, Matarasso S. Evaluation of guided bone regeneration in rabbit tibia using bioresorbable and non-resorbable membranes. *Biomaterials* 1996; 17(8):791–6.
- [42] Retzeppi M, Donos N. Guided bone regeneration: biological principle and therapeutic applications. *Clin Oral Implants Res* 2010;21(6):567–76.
- [43] Sculean A, Nikolidakis D, Schwarz F. Regeneration of periodontal tissues: combinations of barrier membranes and grafting materials – biological foundation and preclinical evidence: a systematic review. *J Clin Periodontol* 2008;35:106–16.
- [44] Teng SH, Lee EJ, Wang P, Shin DS, Kim HE. Three-layered membranes of collagen/hydroxyapatite and chitosan for guided bone regeneration. *J Biomed Mater Res B Appl Biomater* 2008;87B(1):132–8.
- [45] Teng SH, Lee EJ, Yoon BH, Shin DS, Kim HE, Oh JS. Chitosan/nanohydroxyapatite composite membranes via dynamic filtration for guided bone regeneration. *J Biomed Mater Res A* 2009;88A(3):569–80.
- [46] Yang F, Both SK, Yang XC, Walboomers XF, Jansen JA. Development of an electrospun nano-apatite/PCL composite membrane for GTR/GBR application. *Acta Biomater* 2009; 5(9):3295–304.
- [47] Langer R, Vacanti JP. Tissue engineering. *Science* 1993;260(5110):920–6.
- [48] Nyman S, Lindhe J, Karring T, Rylander H. New attachment following surgical treatment of human periodontal disease. *J Clin Periodontol* 1982;9(4):290–6.
- [49] Nyman S, Gottlow J, Karring T, Lindhe J. The regenerative potential of the periodontal ligament. An experimental study in the monkey. *J Clin Periodontol* 1982;9(3):257–65.
- [50] Nyman S, Gottlow J, Lindhe J, Karring T, Wennstrom J. New attachment formation by guided tissue regeneration. *J Periodontol Res* 1987;22(3):252–4.
- [51] Karring T, Nyman S, Gottlow J, Laurell L. Development of the biological concept of guided tissue regeneration—animal and human studies. *Periodontol* 2000 1993;1:26–35.
- [52] Linde A, Alberius P, Dahlin C, Bjurstram K, Sundin Y. Osteopromotion: a soft-tissue exclusion principle using a membrane for bone healing and bone neogenesis. *J Periodontol* 1993;64(11):1116–28.
- [53] Polimeni G, Koo KT, Pringle GA, Agelan A, Safadi FF, Wikesjo UME. Histopathological observations of a polylactic acid-based device intended for guided bone/tissue regeneration. *Clin Implant Dent Relat Res* 2008;10(2):99–105.
- [54] Jovanovic SA, Nevins M. Bone formation utilizing titanium-reinforced barrier membranes. *Int J Periodontics Restorative Dent* 1995;15(1):56–69.
- [55] Coonts BA, Whitman SL, O'Donnell M, Polson AM, Bogle G, Garrett S, et al. Biodegradation and biocompatibility of a guided tissue regeneration barrier membrane formed from a liquid polymer material. *J Biomed Mater Res* 1998;42(2):303–11.
- [56] Hou LT, Yan JJ, Tsai AYM, Lao CS, Lin SJ, Liu CM. Polymer-assisted regeneration therapy with Atrisorb (R) barriers in human periodontal intrabony defects. *J Clin Periodontol* 2004;31(1):68–74.
- [57] Donos N, Kostopoulos L, Karring T. Alveolar ridge augmentation using a resorbable copolymer membrane and autogenous bone grafts – an experimental study in the rat. *Clin Oral Implant Res* 2002;13(2):203–13.
- [58] Klinge U, Klosterhalfen B, Muller M, Schumpelick V. Foreign body reaction to meshes used for the repair of abdominal wall hernias. *Eur J Surg* 1999;165(7):665–73.
- [59] Laurell L, Gottlow J. Guided tissue regeneration update. *Int Dent J* 1998;48(4):386–98.

- [60] Tal H, Kozlovsky A, Artzi Z, Nemcovsky CE, Moses O. Cross-linked and non-cross-linked collagen barrier membranes disintegrate following surgical exposure to the oral environment: a histological study in the cat. *Clin Oral Implant Res* 2008;19(8):760–6.
- [61] Bottino MC, Jose MV, Thomas V, Dean DR, Janowski GM. Freeze-dried acellular dermal matrix graft: effects of rehydration on physical, chemical, and mechanical properties. *Dent Mater* 2009;25(9):1109–15.
- [62] Bottino MC, Thomas V, Jose MV, Dean DR, Janowski GM. Acellular dermal matrix graft: synergistic effect of rehydration and natural crosslinking on mechanical properties. *J Biomed Mater Res B Appl Biomater* 2010;95B(2):276–82.
- [63] Bunyaratavej P, Wang HL. Collagen membranes: a review. *J Periodontol* 2001;72(2):215–29.
- [64] Owens K, Yukna R. Collagen membrane resorption in dogs: a comparative study. *Implant Dent* 2001;10(1):49–58.
- [65] Coic M, Placet V, Jacquet E, Meyer C. Mechanical properties of collagen membranes used in guided bone regeneration: a comparative study of three models. *Rev Stomatol Chir Maxillofac* 2010;111(5-6):286–90.
- [66] Yamada M, Kojima N, Att W, Minamikawa H, Sakurai K, Ogawa T. Improvement in the osteoblastic cellular response to a commercial collagen membrane and demineralized freeze-dried bone by an amino acid derivative: an in vitro study. *Clin Oral Implant Res* 2011;22(2):165–72.
- [67] Santos A, Goumenos G, Pascual A. Management of gingival recession by the use of an acellular dermal graft material: a 12-case series. *J Periodontol* 2005;76(11):1982–90.
- [68] Felipe M, Andrade PF, Grisi MFM, Souza SLS, Taba M, Palioto DB, et al. Comparison of two surgical procedures for use of the acellular dermal matrix graft in the treatment of gingival recession: a randomized controlled clinical study. *J Periodontol* 2007;78(7):1209–17.
- [69] Slots J, MacDonald ES, Nowzari H. Infectious aspects of periodontal regeneration. *Periodontol* 2000 1999;19:164–72.
- [70] Kenawy ER, Bowlin GL, Mansfield K, Layman J, Simpson DG, Sanders EH, et al. Release of tetracycline hydrochloride from electrospun poly(ethylene-co-vinylacetate), poly(lactic acid), and a blend. *J Control Release* 2002;81(1–2):57–64.
- [71] He CL, Huang ZM, Han XJ. Fabrication of drug-loaded electrospun aligned fibrous threads for suture applications. *J Biomed Mater Res A* 2009;89A(1):80–95.
- [72] Zamani M, Morshed M, Varshosaz J, Jannesari M. Controlled release of metronidazole benzoate from poly epsilon-caprolactone electrospun nanofibers for periodontal diseases. *Eur J Pharm Biopharm* 2010;75(2):179–85.
- [73] Freeman CD, Klutman NE, Lamp KC. Metronidazole – a therapeutic review and update. *Drugs* 1997;54(5):679–708.
- [74] El-Kamel AH, Ashri LY, Alsarra IA. Micromatrical metronidazole benzoate film as a local mucoadhesive delivery system for treatment of periodontal diseases. *AAPS PharmSciTech* 2007;8(3):11.
- [75] Xue J, Shi R, Niu Y, Gong M, Coates P, Crawford A, et al. Fabrication of drug-loaded anti-infective guided tissue regeneration membrane with adjustable biodegradation property. *Colloids Surf B Biointerfaces* 2015;135:846–54.
- [76] Ranjbar-Mohammadi M, Zamani M, Prabhakaran MP, Bahrami SH, Ramakrishna S. Electrospinning of PLGA/gum tragacanth nanofibers containing tetracycline hydrochloride for periodontal regeneration. *Mater Sci Eng, C* 2016;58:521–31.
- [77] Furtos G, Rivero G, Rapuntean S, Abraham GA. Amoxicillin-loaded electrospun nanocomposite membranes for dental applications, *J Biomed Mater Res B Appl Biomater* 2016. <http://dx.doi.org/10.1002/jbm.b.33629>.

- [78] Farooq A, Yar M, Khan AS, Shahzadi L, Siddiqi SA, Mahmood N, et al. Synthesis of piroxicam loaded novel electrospun biodegradable nanocomposite scaffolds for periodontal regeneration. *Mater Sci Eng. C* 2015;56:104–13.
- [79] Carter P, Rahman SM, Bhattarai N. Facile fabrication of aloe vera containing PCL nanofibers for barrier membrane application. *J Biomater Sci Polym Ed* 2016;27(7):692–708.
- [80] Munchow EA, Albuquerque MT, Zero B, Kamocki K, Piva E, Gregory RL, et al. Development and characterization of novel ZnO-loaded electrospun membranes for periodontal regeneration. *Dent Mater* 2015;31(9):1038–51.
- [81] Rai JJ, Kalantharakath T. Biomimetic ceramics for periodontal regeneration in infrabony defects: a systematic review. *J Int Soc Prev Community Dent* 2014;4(Suppl 2):S78–92.
- [82] Bishop A, Balazsi C, Yang JHC, Gouma PI. Biopolymer-hydroxyapatite by electrospinning. *Polym Adv Technol* 2006;17(11–12):902–6.
- [83] Thomas V, Dean DR, Vohra YK. Nanostructured biomaterials for regenerative medicine. *Curr Nanosci* 2006;2(3):155–77.
- [84] Deng XL, Sui G, Zhao ML, Chen GQ, Yang XP. Poly(L-lactic acid)/hydroxyapatite hybrid nanofibrous scaffolds prepared by electrospinning. *J Biomater Sci Polym Ed* 2007;18(1):117–30.
- [85] Thomas V, Dean DR, Jose MV, Mathew B, Chowdhury S, Vohra YK. Nanostructured biocomposite scaffolds based on collagen coelectrospun with nanohydroxyapatite. *Biomacromolecules* 2007;8(2):631–7.
- [86] Erisken C, Kalyon DM, Wang HJ. Functionally graded electrospun polycaprolactone and beta-tricalcium phosphate nanocomposites for tissue engineering applications. *Biomaterials* 2008;29(30):4065–73.
- [87] Jose MV, Thomas V, Johnson KT, Dean DR, Nyalro E. Aligned PLGA/HA nanofibrous nanocomposite scaffolds for bone tissue engineering. *Acta Biomater* 2009;5(1):305–15.
- [88] Jose MV, Thomas V, Xu YY, Bellis S, Nyairo E, Dean D. Aligned bioactive multi-component nanofibrous nanocomposite scaffolds for bone tissue engineering. *Macromol Biosci* 2010;10(4):433–44.
- [89] Gupta D, Venugopal J, Mitra S, Dev VRG, Ramakrishna S. Nanostructured biocomposite substrates by electrospinning and electrospaying for the mineralization of osteoblasts. *Biomaterials* 2009;30(11):2085–94.
- [90] Wu XN, Miao LY, Yao YF, Wu WL, Liu Y, Chen XF, et al. Electrospun fibrous scaffolds combined with nanoscale hydroxyapatite induce osteogenic differentiation of human periodontal ligament cells. *Int J Nanomed* 2014;9:4135–43.
- [91] Ribeiro N, Sousa SR, van Blitterswijk CA, Moroni L, Monteiro FJ. A biocomposite of collagen nanofibers and nanohydroxyapatite for bone regeneration. *Biofabrication* 2014;6(3):035015.
- [92] Phipps MC, Clem WC, Catledge SA, Xu Y, Hennessy KM, Thomas V, et al. Mesenchymal stem cell responses to bone-mimetic electrospun matrices composed of polycaprolactone, collagen I and nanoparticulate hydroxyapatite. *PLoS One* 2011;6(2):8.
- [93] Baykan E, Koc A, Elcin AE, Elcin YM. Evaluation of a biomimetic poly(epsilon-caprolactone)/beta-tricalcium phosphate multispiral scaffold for bone tissue engineering: in vitro and in vivo studies. *Biointerphases* 2014;9(2):029011.
- [94] Yeo M, Lee H, Kim G. Three-dimensional hierarchical composite scaffolds consisting of polycaprolactone, beta-tricalcium phosphate, and collagen nanofibers: fabrication, physical properties, and in vitro cell activity for bone tissue regeneration. *Biomacromolecules* 2011;12(2):502–10.
- [95] Schneider OD, Loher S, Brunner TJ, Uebersax L, Simonet M, Grass RN, et al. Cotton wool-like nanocomposite biomaterials prepared by electrospinning: in vitro bioactivity

- and osteogenic differentiation of human mesenchymal stem cells. *J Biomed Mater Res B Appl Biomater* 2008;84(2):350–62.
- [96] Rowe MJ, Kamocki K, Pankajakshan D, Li D, Bruzzaniti A, Thomas V, et al. Dimensionally stable and bioactive membrane for guided bone regeneration: an in vitro study. *J Biomed Mater Res B Appl Biomater* 2016;104(3):594–605.
- [97] El-Fiqi A, Kim JH, Kim HW. Osteoinductive fibrous scaffolds of biopolymer/mesoporous bioactive glass nanocarriers with excellent bioactivity and long-term delivery of osteogenic drug. *ACS Appl Mater Interfaces* 2015;7(2):1140–52.
- [98] Kim GH, Park YD, Lee SY, El-Fiqi A, Kim JJ, Lee EJ, et al. Odontogenic stimulation of human dental pulp cells with bioactive nanocomposite fiber. *J Biomater Appl* 2015;29(6):854–66.
- [99] Schofer MD, Roessler PP, Schaefer J, Theisen C, Schlimme S, Heverhagen JT, et al. Electrospun PLLA nanofiber scaffolds and their use in combination with BMP-2 for reconstruction of bone defects. *PLoS One* 2011;6(9):e25462.
- [100] Zhu H, Yu D, Zhou Y, Wang C, Gao M, Jiang H, et al. Biological activity of a nanofibrous barrier membrane containing bone morphogenetic protein formed by core-shell electrospinning as a sustained delivery vehicle. *J Biomed Mater Res B Appl Biomater* 2013;101(4):541–52.
- [101] Shalumon KT, Lai GJ, Chen CH, Chen JP. Modulation of bone-specific tissue regeneration by incorporating bone morphogenetic protein and controlling the shell thickness of silk fibroin/chitosan/nanohydroxyapatite core-shell nanofibrous membranes. *ACS Appl Mater Interfaces* 2015;7(38):21170–81.
- [102] Phipps MC, Xu Y, Bellis SL. Delivery of platelet-derived growth factor as a chemotactic factor for mesenchymal stem cells by bone-mimetic electrospun scaffolds. *PLoS One* 2012;7(7):e40831.
- [103] Lee JH, Lee YJ, Cho HJ, Kim DW, Shin H. The incorporation of bFGF mediated by heparin into PCL/gelatin composite fiber meshes for guided bone regeneration. *Drug Deliv Transl Res* 2015;5(2):146–59.
- [104] Sahoo S, Ang LT, Goh JC, Toh SL. Growth factor delivery through electrospun nanofibers in scaffolds for tissue engineering applications. *J Biomed Mater Res A* 2010;93(4):1539–50.
- [105] Ji W, Yang F, Ma J, Bouma MJ, Boerman OC, Chen Z, et al. Incorporation of stromal cell-derived factor-1alpha in PCL/gelatin electrospun membranes for guided bone regeneration. *Biomaterials* 2013;34(3):735–45.
- [106] Sundaram MN, Sowmya S, Deepthi S, Bumgardener JD, Jayakumar R. Bilayered construct for simultaneous regeneration of alveolar bone and periodontal ligament. *J Biomed Mater Res B Appl Biomater* 2016;104(4):761–70.
- [107] Galler KM. Clinical procedures for revitalization: current knowledge and considerations. *Int Endod J* 2016;49(10):926–36.
- [108] American Association of Endodontics; 2016. Available from <http://www.aae.org> [accessed 02.05.16].
- [109] Huang GT. Dental pulp and dentin tissue engineering and regeneration: advancement and challenge. *Front Biosci (Elite Ed)* 2011;3:788–800.
- [110] Cvek M. Treatment of non-vital permanent incisors with calcium hydroxide. II. Effect on external root resorption in luxated teeth compared with effect of root filling with guttupacha. A follow-up. *Odontol Revy* 1973;24(4):343–54.
- [111] Cvek M. Treatment of non-vital permanent incisors with calcium hydroxide. I. Follow-up of periapical repair and apical closure of immature roots. *Odontol Revy* 1972;23(1):27–44.

- [112] Damle SG, Bhattal H, Loomba A. Apexification of anterior teeth: a comparative evaluation of mineral trioxide aggregate and calcium hydroxide paste. *J Clin Pediatr Dent* 2012;36(3):263–8.
- [113] Jeeruphan T, Jantarat J, Yanpiset K, Suwannapan L, Khewsawai P, Hargreaves KM. Mahidol study 1: comparison of radiographic and survival outcomes of immature teeth treated with either regenerative endodontic or apexification methods: a retrospective study. *J Endod* 2012;38(10):1330–6.
- [114] Wang X, Thibodeau B, Trope M, Lin LM, Huang GT. Histologic characterization of regenerated tissues in canal space after the revitalization/revascularization procedure of immature dog teeth with apical periodontitis. *J Endod* 2010;36(1):56–63.
- [115] Andreasen JO, Farik B, Munksgaard EC. Long-term calcium hydroxide as a root canal dressing may increase risk of root fracture. *Dent Traumatol* 2002;18(3):134–7.
- [116] Cvek M. Prognosis of luxated non-vital maxillary incisors treated with calcium hydroxide and filled with gutta-percha. A retrospective clinical study. *Endod Dent Traumatol* 1992;8(2):45–55.
- [117] Diogenes A, Ruparel NB, Shiloah Y, Hargreaves KM. Regenerative endodontics: a way forward. *J Am Dent Assoc* 2016;147(5):372–80.
- [118] Albuquerque MT, Junqueira JC, Coelho MB, de Carvalho CA, Valera MC. Novel in vitro methodology for induction of *Enterococcus faecalis* biofilm on apical resorption areas. *Indian J Dent Res* 2014;25(4):535–8.
- [119] Iwaya SI, Ikawa M, Kubota M. Revascularization of an immature permanent tooth with apical periodontitis and sinus tract. *Dent Traumatol* 2001;17(4):185–7.
- [120] Kontakiotis EG, Filippatos CG, Agrafioti A. Levels of evidence for the outcome of regenerative endodontic therapy. *J Endod* 2014;40(8):1045–53.
- [121] Diogenes A, Henry MA, Teixeira FB, Hargreaves KM. An update on clinical regenerative endodontics. *Endod Top* 2013;28(1):2–23.
- [122] Banchs F, Trope M. Revascularization of immature permanent teeth with apical periodontitis: new treatment protocol? *J Endod* 2004;30(4):196–200.
- [123] Bose R, Nummikoski P, Hargreaves K. A retrospective evaluation of radiographic outcomes in immature teeth with necrotic root canal systems treated with regenerative endodontic procedures. *J Endod* 2009;35(10):1343–9.
- [124] Cehreli ZC, Isbitiren B, Sara S, Erbas G. Regenerative endodontic treatment (revascularization) of immature necrotic molars medicated with calcium hydroxide: a case series. *J Endod* 2011;37(9):1327–30.
- [125] Petrino JA, Boda KK, Shambarger S, Bowles WR, McClanahan SB. Challenges in regenerative endodontics: a case series. *J Endod* 2010;36(3):536–41.
- [126] Gomes-Filho JE, Duarte PC, Ervolino E, Mogami Bomfim SR, Xavier Abimussi CJ, Mota da Silva Santos L, et al. Histologic characterization of engineered tissues in the canal space of closed-apex teeth with apical periodontitis. *J Endod* 2013;39(12):1549–56.
- [127] Martin G, Ricucci D, Gibbs JL, Lin LM. Histological findings of revascularized/revitalized immature permanent molar with apical periodontitis using platelet-rich plasma. *J Endod* 2013;39(1):138–44.
- [128] Lin J, Shen Y, Haapasalo M. A comparative study of biofilm removal with hand, rotary nickel-titanium, and self-adjusting file instrumentation using a novel in vitro biofilm model. *J Endod* 2013;39(5):658–63.
- [129] Becerra P, Ricucci D, Loghin S, Gibbs JL, Lin LM. Histologic study of a human immature permanent premolar with chronic apical abscess after revascularization/revitalization. *J Endod* 2014;40(1):133–9.

- [130] Porter ML, Munchow EA, Albuquerque MT, Spolnik KJ, Hara AT, Bottino MC. Effects of novel 3-dimensional antibiotic-containing electrospun scaffolds on dentin discoloration. *J Endod* 2016;42(1):106–12.
- [131] Wang Z, Shen Y, Haapasalo M. Effectiveness of endodontic disinfecting solutions against young and old *Enterococcus faecalis* biofilms in dentin canals. *J Endod* 2012;38(10):1376–9.
- [132] Nagata JY, Soares AJ, Souza-Filho FJ, Zaia AA, Ferraz CC, Almeida JF, et al. Microbial evaluation of traumatized teeth treated with triple antibiotic paste or calcium hydroxide with 2% chlorhexidine gel in pulp revascularization. *J Endod* 2014;40(6):778–83.
- [133] Gomes BP, Pinheiro ET, Gade-Neto CR, Sousa EL, Ferraz CC, Zaia AA, et al. Microbiological examination of infected dental root canals. *Oral Microbiol Immunol* 2004; 19(2):71–6.

Electrospinning: A versatile technology to design biosensors and sensors for diagnostics

17

A. Macagnano*, F. De Cesare*,[†]

*IIA-National Research Council, Rome, Italy, [†]DIBAF-University of Tuscia, Viterbo, Italy

17.1 Introduction

Providing diagnosis fast and precisely through diagnostic tools (devices and tests) to prevent disease progression is a fundamental issue of modern research in medicine. For several years, the outstanding electric, optical, and magnetic properties of nanomaterials have been supporting the research and development of new strategies and approaches in medicine playing also a key role in designing cutting-edge novel technologies for diagnostics. One of the most prominent applications of nanomaterials in medicine has been their employment in image analyses and the consequent creation of exceptional diagnostic tools on purpose. Furthermore, they have been involved in the development of innovative analytic means for monitoring markers and biomarkers pertinent to human diseases. More recently, smart nanostructures have been integrated with therapies (nanotheranostics) or sensing and destruction/removal (*sensor/removal*) for simultaneously detecting and solving issues [1]. The peculiar chemical and physical features of materials at nanoscale allow them reacting with single molecules by fast, precise, and accurate identifications performed within miniaturized and easy-to-use devices.

A plethora of nanomaterials are commonly used to generate nanosensors, such as nanotubes (NTs), nanowires, nanorods (NRs), nanoparticles (NPs), and thin films made of nanocrystalline matter [2]. The high capacity of these nanomaterials for charge transfer enables nanostructured sensors to achieve low detection limits and high sensitivity values. The selection of a kind of nanomaterial for a specific sensing application depends on a multitude of physical and chemical parameters and on the type of transduction mechanism desired. Moreover, nanomaterials can be further modified to detect specific molecules (Fig. 17.1) by introducing functional groups and suitable nanodoping through several strategies to both work in distinct environments and detect a wide range of analytes, such as gases and volatile organic compounds (VOCs), metals and other inorganic ions, organic compounds, and even entire cells (i.e., microorganisms). An additional strategy improving the sensing features of sensors is to increase the specific surface of the interacting material: the higher the specific surface area of the sensing material, the higher its ability to interact, a common feature in biological sensing structures. In physiology, the features of sensing surfaces express at macroscale the properties of both their molecular structure (e.g.,

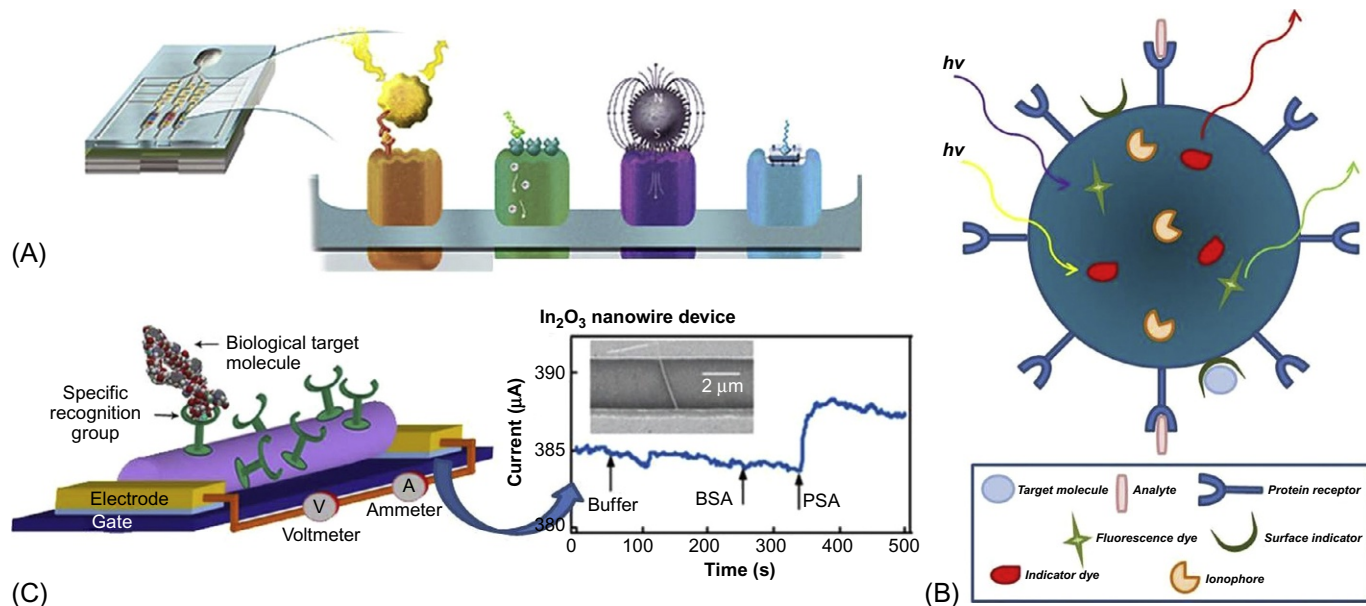


Fig. 17.1 Sketches of nanosensors and their potential multiple functionalization to detect specific and selective analytes. (A) A series of nanobiosensors based on different working principles. Specifically left to right: an optical transducer measuring light; an electrochemical transducer measuring electrical properties; a magnetic transducer measuring changes to the local magnetic field and a mechanical transducer detecting changes in motion (http://www.nanoprotech.org/?view=blog-item&item_id=16 N.R. Fuller, Sayo-Art); (B) potentials of a multidetecting nanoparticle optically active; (C) a conductive nanowire/nanotube coated with a specific recognition group sensitive only to a particular target. This recognition group could be a single stranded DNA (capable of recognizing its complementary strand), an antibody (that recognize a particular antigene), an aptamer that shows affinity for a unique target, or a protein that specifically interact with another biological molecule. The presence of this recognition group on the nanowire surface gives to the device high specificity and exclusivity toward its target. Once the nanowire-based transistor has been coated with a specific recognition group, current changes can be monitored versus time (<http://met.usc.edu/projects/nano.php>).

extended specific surface area) and composition (e.g., receptors). As a matter of fact, molecular recognition in living systems generally occurs at interfaces (cell membranes like the outer plasma membrane and internal membranes), where recognition sites mostly made of proteins/glycoproteins/lipoproteins (receptors, transporters, pumps, enzymes, etc.), carbohydrates, and polysaccharides are located. Additionally, recognition occurs intracellularly, where the binding between analytes and ligands involves various types of molecules (e.g., chelating agents) and macromolecules like nucleic acids (DNA double helix) and proteins/enzymes. Recently, the strategies used to design man-made sensors, overall electrode-based sensors, and sensing systems employ nanomaterials through variously complex techniques to closely reproduce both biological molecular recognition at interfaces [3] and mimic *in vitro* biological structures [4–8].

The recent literature has confirmed electrospinning as one of the most intriguing nanotechnologies for designing and developing smart and ultrasensitive sensing systems, for both uniqueness of the resulting nanostructures and production rate and costs. Parameters like the extremely rapid formation of fibers and fibrous scaffolds generated on a millisecond scale and the easy tuning of size and shape of fabrics until 3-D matrix production have raised great scientific interest for this technology, confirmed from the increasing number of publications in the last decade [9]. Sensors based on electrospinning showed interesting sensing properties like fast analyte adsorption, mostly resulting from the high porosity of the generated nanofibrous layer (with consequent easy diffusion through the fibrous framework) and minimized bulk effects (e.g., diffusion-desorption time and analyte entrapment). Since the diameter of fibers can roughly achieve sometimes that of interacting molecules, scientists may exploit size effects, such as quantization, and single-molecule sensitivity deriving from such tiny dimensions. As concerns the morphology of electrospun fibers, it depends on the properties of the original polymer solution (system parameters), process conditions (operational parameters), and environmental conditions. The resulting aligned or nonwoven nanofibers, arranged in 2-D or 3-D fibrous structures with tunable porosity and high specific surface area, can be grown up directly onto suitable transducers, often without further expensive modifications [10]. Furthermore, a large combination of polymer fibers by blends or core shells arrangement and by inorganic doping can be fabricated. The electrospinning apparatus can generate fibers using needles or multiple nozzles or through a needleless process, and it is also able to manage the production rate and control the jet formation, jet acceleration, and the collection of nanostructures. The further chance to customize and functionalize these micronanofibers in a postprocessing step and on a large-scale enables the electrospinning technique to match a wide range of requirements for specific sensing applications, including health monitoring and biodetection. The decoration of electrospun nanofibers by specific receptors can remarkably increase the number of recognition sites suitable for sensing, that is, available for interacting with analytes through specific binding mechanisms. Due to such an extreme versatility, electrospinning is expected to have several strategic advantages, relative to other nanotechnologies, in the fabrication of advanced tools for diagnostics and health monitoring. Obviously, due to the wide and ever increasing production of scientific papers

in this topic, this chapter is not surely exhaustive, but it likes to enhance some main strategies that researchers are pursuing to create more and more innovative and high-performance support systems to human health (Fig. 17.2).

17.2 ES-nanosensors for blood analysis

The use of blood as a diagnostic medium is a routine and prevalent medical practice, not only in providing alerts about general health status but also in furnishing detailed information on individual diseases based on specific constituent biomarkers. A crucial issue arising in diagnosing health status of individuals is that in some pathology, symptoms emerge when the disease is in an advanced stage, and possible treatments can be ineffective or heavily invasive for humans, relative to early diagnosing.

The employment of nanomaterials in diagnoses has allowed remarkable improvements like quick testing and earlier detection of diseases than other current techniques, thus providing great potentials also for point of care applications [11].

In medical diagnostic imaging, for example, the exploitation of the optical features of some NPs has already driven scientists to successfully improve disease diagnoses through biological imaging, so that clinicians can detect health problems in patients upon visible accumulations of these particles or through molecular signals upon binding of NPs with other compounds. Similarly, the binding of NPs to blood proteins and other molecules has been allowing the detection of disease indicators at a very early stage. For instance, Randeria et al. described a promising method for detecting cancer cells in the bloodstream by using NPs called nanoflares. Nanoflares were planned to bind genetic targets in cancer cells and generate light when such recognition occurs [12]. These probes are based on spherical nucleic acids and are composed of gold-NP cores and highly oriented oligonucleotide shells; these sequences are complementary to specific intracellular mRNA targets and are hybridized to fluorophore-labeled reporter strands. Nanoflares take advantage of the highly efficient fluorescence quenching properties

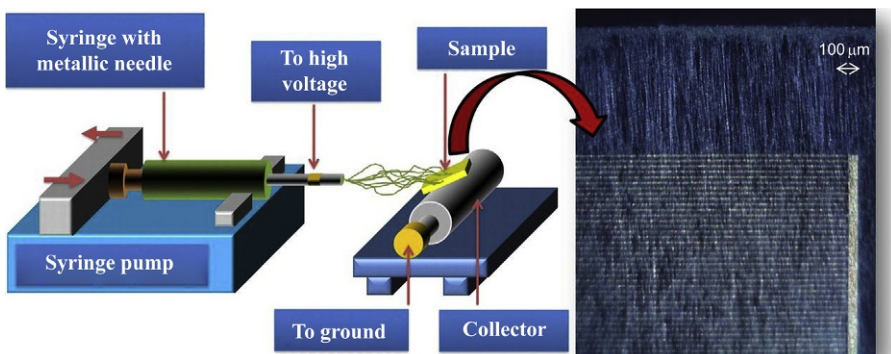


Fig. 17.2 Needle-based electrospinning process for growing up nanofibrous fabrics directly onto microchips. On the right, optical microscope image of a classical interdigitated electrode (IDE) coated with aligned fibers [10].

of gold, the rapid cellular uptake of spherical nucleic acid that occurs without the use of transfection agents and the enzymatic stability of such constructs to report a highly sensitive and specific signal in the presence of intracellular target mRNA.

Another example of strategy for early diagnosis of brain cancer uses properly functionalized magnetic NPs and magnetic resonance imaging (MRI) technology, based on the principle that when NPs bind the tumor cells or their fragments (proteins, vesicles, and nucleic acids), their magnetic properties result enhanced [13].

Abakumov et al. [13] synthesized ferric oxide (Fe_3O_4) cores coated with bovine serum albumin (BSA) to form NPs (53 ± 9 nm) and monoclonal antibodies against vascular endothelial growth factor (mAbVEGF), demonstrating that MNPs were stable and nontoxic to different cells at concentration up to 2.5 mg/mL, easily bound VEGF-positive glioma C6 cells in vitro and finally were effective in MRI visualization of the intracranial glioma.

When compared with molecular probes, nanosensors result as a combination of high sensitivity and selectivity with low toxicity, which are crucial parameters for sensing in live cells [14].

17.2.1 Cells capturing systems

Electrospinning technology, too, has been used to develop smart sensing systems for early diagnosis. The group of Hsian-Rong Tseng has developed an advanced filtering system to capture individual cancer cells circulating in the blood stream (named “NanoVelcro” chip). Circulating tumor cells (CTCs) are responsible of cancer metastasis, thus spreading cancer cells of the primary tumor to other organs of the individual’s body, so that new tumors are generated. These scientists used nanofibers of poly(lactic-co-glycolic acid) (PLGA) functionalized with antibodies capable of binding proteins located at cancer cell surface (Fig. 17.3). Consequently, they succeed in selectively entrapping cancer cells in the blood of people affected by cancer flowing through the chip and isolate and use them for further analyses. Such a system, then, works as a “liquid biopsy” of the tumor, because it identifies cancer cells in liquid medium and it also provides earlier information about potentially terminal metastases [15,16].

Similarly to what observed with antibodies, the functionalization of electrospun the fibers can be functionalized with bioreceptors, and such purpose can be achieved through several methods, depending on the final target application. A common strategy to bind and immobilize these biomolecules (such as bioreceptors and antibodies) to

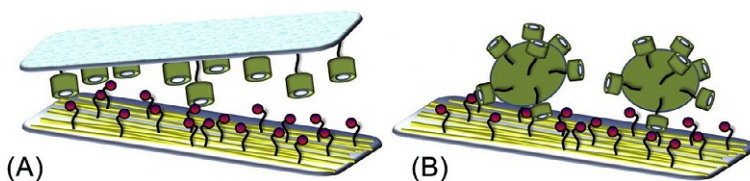


Fig. 17.3 (A) Sketch of a supramolecular Velcro chip sketch; (B) cancer cells intercepted by an ES functionalized polymer layer according to Velcro working principle.

electrospun nanofibers is based on physical or physicochemical interactions occurring between the bioreceptors and fibers. Additionally, the bioreceptors can be immobilized fixed in situ, that is, on the fibrous surface, to prevent their leaching, mostly through chemical reactions. Another method of immobilization of receptors makes use of such molecules by solving them directly into the electrospinning solution in order to obtain nanofibers with bioreceptors embedded into the electrospun polymer [17–19].

17.2.2 Glucose sensors

A lot of both chemical [20–23] and biochemical nanosensors based on electrospinning have been designed, investigated, and fabricated to detect glucose in the blood. Using chemical sensors, Zhang et al. [21] prepared a glucose sensor based on graphene oxide (GO) and electrospun NiO nanofibers (NiONFs). Indeed, the catalytic activity of metal oxides can be greatly enhanced through the incorporation of NPs of conducting materials such as carbon NTs, graphene, gold, and platinum, as well as quantum dots of various semiconductors [24–26]. Graphene, emerging as a new two-dimensional material, has captured great attention due to its high electric conductivity, huge surface area, low cost, and good thermomechanical features [27]. GO as the starting material was electrochemically reduced to go. Nafion (NA) was coated on the sensor surface to improve the antifouling ability. The addition of rGO sheets caused numerous corrugations and wrinkles of the fibers improving the electrode active area (Fig. 17.4B). As the glucose was added into the stirring buffer solution, the sensor responded rapidly

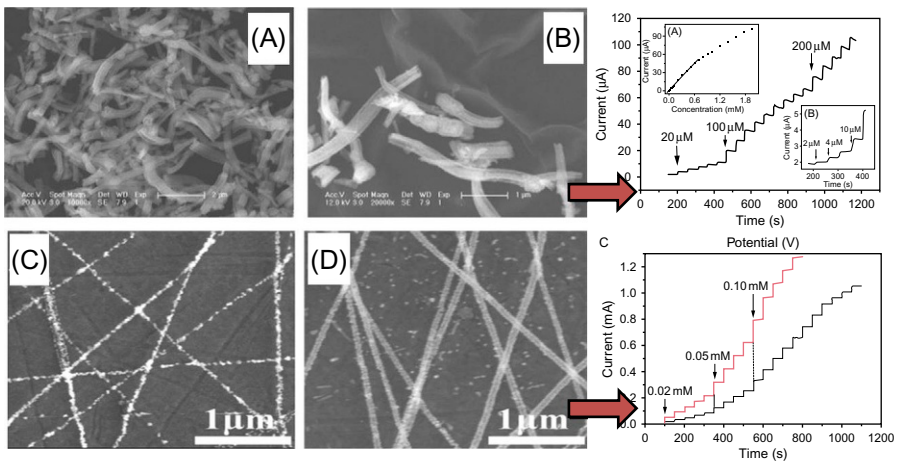


Fig. 17.4 Comparison of two nanofibrous nonenzymatic biosensors for glucose detection: SEM images of the modified electrode surface of NiONF/GCE (A) and NiONF-rGO/GCE (B) and steady-state response of the sensor on successive injection of glucose (0.60 V) [21]; SEM images of (B) CuO nanofibers and (C) Ag/CuO nanofibers and amperometric response of Ag/CuO NFs and CuO NFs sensors based on ITO, (red and black, respectively) to successive additions of glucose at an applied potential of 0.50 V [22].

achieving 95% of the steady-state current within 5 s ($S = 1100 \mu\text{A mM}^{-1} \text{cm}^{-2}$, where S denotes sensor sensitivity).

Similarly, Zhang et al. [22] developed a sensor based on Ag modified CuO NFs but using a simple two-step procedure including the electrospun of precursor NFs on to the electrodes and a subsequent calcination process. The direct preparation of CuO NFs on indium-tin oxide (ITO) electrode and the AgNPs modification ensured the fast electron transfer between the CuO NFs and the ITO electrode, enhancing the sensitivity of the sensor. The resulting Ag/CuO NFs-ITO electrode possessed fast and good response to glucose (Fig. 17.5D), making that an ideal nonenzymatic sensor for directly detect glucose ($S = 1347 \mu\text{A mM}^{-1} \text{cm}^{-2}$; LOD = 51.7 nM; and $S/N = 3$).

To measure the glucose concentration, biosensors can detect oxygen variations, pH, or H_2O_2 concentration. Specifically, oxygen sensors convert O_2 concentration

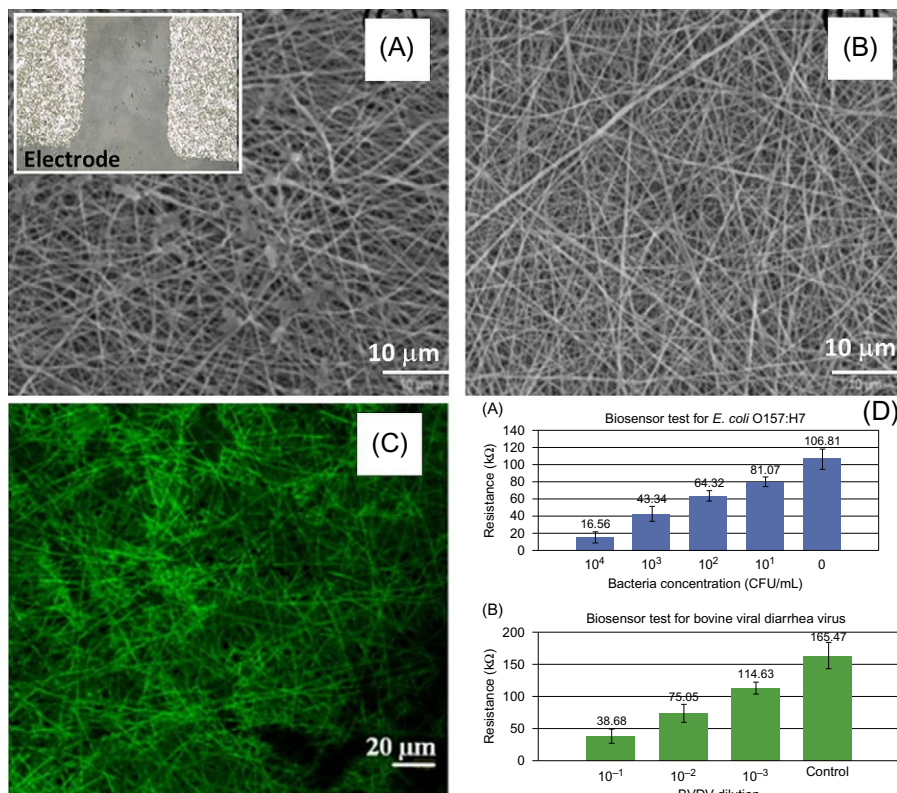


Fig. 17.5 SEM micrograph of electrospun samples after bacteria test (A) *E. coli* O157:H7 effectively captured on functionalized fiber mat (inset: Ag electrode), (B) no bacteria observed in the nanofiber mat without treatment. Nanofibers confocal laser scanning microscopy (CLSM) of fluorescein isothiocyanate (FITC) conjugated antibody/electrospun nanofibers, (C); biosensor test results for *E. coli* O157:H7 bacteria demonstrate the linear sensor response and lower detection limit of 61 CFU/mL BVDV virus, respectively (D) [28].

into electric current, pH sensors convert pH change into a voltage change, and peroxidase sensor convert H_2O_2 concentration into an electric current. The choice of the biological recognition element is the crucial decision to make when developing a novel biosensor. Similarly, the operation and storage conditions determining the half-life and stability of the sensor are important. Glucose oxidase (GOD) turned out then to be a remarkable bioreceptor for revealing glucose traces in liquids, because of its importance in food production, fermentation, and clinical diagnostics [29,30]. The first application of electrospinning technology to GOD-based biosensors is dated to 2006, when Ren et al. [31] immobilized this enzyme onto electrospun poly(vinyl alcohol) (PVA) fibrous membranes. Wu et al. also designed an easy and effective amperometric biosensor for glucose monitoring [32]. This biosensor was based on the quantitative measurement of an intermediate product of the enzyme reaction catalyzed by GOD, hydrogen peroxide (H_2O_2), which in turn was reduced by Prussian blue film (also named as “artificial peroxidase”) present in composite nanofibers (a mediator compound). Chitosan/polyvinyl alcohol composite nanofibers (CS/PVA) were selected because they generated a suitable scaffold for both enzyme immobilization (high bioaffinity) and preservation of the Prussian blue leaching out upon its layer electrodeposition onto the ITO underlayer (due to the long, straight, porous, and aligned nanofibers). Furthermore, the resulting nanofibrous layer was particularly attractive because it is composed of biocompatible, biodegradable, and nontoxic natural biopolymers. In such a structured electrospun nanobiosensor, the electrocatalytic activity occurred because the porous and high surface area of the nanomaterial enabled the diffusion of glucose to GOD. When the reaction product, that is, H_2O_2 , reached the PB layer, the PB film rapidly catalyzed H_2O_2 and substantially enhanced the electron transfer rate between GOD and the electrode. The obtained detection limit was lower than that of other enzymatic glucose sensors based on different modified nanomaterials (3.61×10^{-7} M), and the range of concentration monitored covered normal (3.6–6.1 mM) and abnormal (20 mM), glucose levels in human blood [33]. Since the immobilization of enzymes at surfaces is a crucial step in designing biosensors, immobilization should make the enzyme electroactive, stable, and with high population density. Physisorbed enzymes, indeed, frequently lose their activity due to conformational changes upon interaction at electrode surface. Conversely, covalently immobilized enzymes can show improved stability. Notwithstanding the miniaturization of electrodes, electrospinning technology can increase the gold surface of the electrochemical electrodes and globally improve their sensing performances. In the study of Marx et al. [34], a novel bioelectrode, based on electrospun nanofibers of gold with chemically immobilized fructose dehydrogenase (FDH), was presented. A solution containing poly(acrylonitrile) (PAN) and HAuCl_4 in dimethylformamide (DMF) were electrospun and collected on a rotating cylinder, then reduced by immersion in a NaBH_4 , and washed with dilute HCl and then H_2O . Therefore, gold was electrolessly deposited on the fibers by dipping the fibers in an aqueous solution containing hydroxylamine hydrochloride and HAuCl_4 . Gold fibers are incubated firstly in a cystamine solution, then in glutaraldehyde (to create suitable linkers for binding the enzyme), and finally in an FDH/PBS/glutaraldehyde solution. Such a structured biosensor was proved to be fully stable for at least 20 cycles of use with

an eightfold higher enzyme loading than conventional flat gold disk electrode biosensor. The authors reported, too, the possibility to expand the substrate variety of the fructose sensor to glucose by addition of glucose isomerase, successfully testing the performances of the sensor in serum under aerobic conditions, usually not favorable for glucose sensors based on GOD.

17.2.3 Cancer, drugs, and infectious agents' detection

DNA plays a crucial role in the life process for both retaining the global information pertaining to organisms, from cells to individuals, and participating the replication and transcription of genetic information in living cells. Therefore, specific interactions involving DNA offer promising opportunities for biomedical applications, including screening of new anticancer drugs, mutagenic factors, and genetic diseases. To magnify the responses of biosensors in terms of signals and improve their sensitivity, several strategies involving nanomaterials have been performed: NPs (e.g., metals and magnetic particles), fluorescent probes, carbon NTs, graphene, and biotin/avidin interactions.

Li et al. combined biotin with polylactic acid (PLA) through electrospinning to prepare free-standing membrane substrates for biosensors based on biotin-streptavidin-specific binding to detect pathogens. They observed that streptavidin immobilized on the membrane surface could capture a biotinylated DNA probe for binding a synthetic pathogen's DNA (*Escherichia coli*) where streptavidin had been deposited [35].

For instance, in the study of Liu et al. [36], ultrafine fibers with diameters ranging from 50 to 300 nm were prepared from a dispersion of DNA/single-walled carbon nanotubes (SWNTs)/poly(ethylene oxide) blend, and well-defined electrospun fibers were obtained, with good interaction between DNA and SWNTs (electroactive fibers). The resulting fibers also exhibited electroactive behavior and could be used as an immobilization matrix for a GOD enzyme biosensor. The sensor response was linear up to 20 mM glucose with a sensitivity of $2.4 \text{ mA cm}^2 \text{ M}^{-1}$.

In the study of Wang et al. [37] both electrospinning and NPs (i.e., MWCNTs) were included in the sensing process. Specifically, they developed a novel electrochemical biosensor based on functional composite nanofibers for the sensitive hybridization detection of p53 tumor suppressor using methylene blue (MB) as an electrochemical indicator. In human tumors, it is the most commonly mutated gene that may lead to the loss of transcriptional activation potency and the ability to bind DNA. In literature, it has been reported that about half of the cancers contain a mutation in p53. Moreover, p53 is involved in sustaining cellular homeostasis and in complex regulatory interactions [38]. Sequence-specific analysis of the p53 can help early diagnosis of cancer and consequently increase the success of the treatment. The authors used electrospinning to prepare composite nanofibers composed of carboxylate multiwalled carbon nanotubes (MWNTs) doped with nylon 6 (PA6) (MWNTs-PA6) that served as nanosized backbone for pyrrole (Py) electropolymerization. The functional composite nanofibers (MWNTs-PA6-PPy) were used as supporting scaffolds for ssDNA immobilization to dramatically increase the amount of DNA attachment and the hybridization sensitivity. First, PA6 and MWNTs were dissolved mixture of cresol and formic acid to obtain a

homogeneous solution to be electrospun. Second, the electrode was dipped in a PPy solution and subjected to electropolymerization. Finally, the MWNTs-PA6-PPy electrode was immersed into HAC solution containing ssDNA, and under a constant potential (+0.5 V), the ssDNA electrode was formed. The resulting biosensor, in effect, exhibited good sensitivity and specificity: the target wild-type p53 sequence (wtp53) could be detected as low as 50 fM, and the discrimination was up to 57.5% between the wtp53 and the mutant type p53 sequence (mtp53). Such findings resulted as a promising support for the early diagnosis of cancer development and monitoring of patient therapy.

Biosensors mainly appreciated in point of care diagnosis of diseases are commonly based on the conversion of antigen-antibody complex formation (immunosensors) into electric signals by suitable transducers. Antibodies are proteins produced by the immune system to recognize not only bacteria, viruses, parasites, and all those microorganisms or macromolecules considered extraneous to the hosting living system but also damaged or altered cells (e.g., upon mutation, infection, and cancer). Briefly, in electrochemical immunosensors, the antigen-antibody complex is converted into an electric signal (amperometric, potentiometric, or conductometric sensors), by the cooperation with redox enzymes. To allow the immunosensor to work properly, it is necessary that the enzyme employed as labeling is very close to the electrode surface. In optical biosensors, the biological sensing element responds to the interaction with the target analyte either by generating an optical signal (e.g., fluorescence) or by undergoing changes in optical properties (i.e., absorption, reflectance, emission, refractive index, and optical path), where the conjugate antibody is labeled with an optically detectable probe (e.g., a fluorophore). Microcantilevers and quartz crystal microbalances (QCMs) are commonly used for immunosensors because of the potential to microfabricate immunosensors at low cost: antigen-antibody complex can be revealed as a mass change causing a frequency shift, without using additional markers. A novel electrospun-based biosensor has been designed and optimized by Luo et al. in order to detect fragments of bacteria and viruses [28,39].

It consisted of a sequence of application-capture-absorption pads and a pair of electrodes capable of measuring the conductance of the adsorbed pathogens linked with conductive and magnetic NPs (Fig. 17.5). The electrospun material, deposited on a polyvinylidene chloride substrate, was fabricated using nitrocellulose polymer due to its biocompatibility and solubility in common solvents. The fiber surface was treated with glutaraldehyde as cross-linker for linking polyclonal antibodies. A pair of electrodes was fabricated on the capture membrane 0.5 mm apart using a spray deposition of silver paint (Fig. 17.5A, inset). The working principle is presented in Fig. 17.7. The EAPM NPs were synthesized from aniline monomer (made electrically active by acid doping) and gamma iron(III) oxide ($\gamma\text{-Fe}_2\text{O}_3$) NPs using the chemical synthesis procedure proposed by Sharma et al. [41,42] (Fig. 17.6).

The antibody modified conductive magnetic NPs were mixed and incubated with the test sample for target conjugation. After magnetic separation, the purified sample with the conductive label was carried out on the application pad forming a sandwich complex, capable of producing an electron transport path across the silver electrodes (Fig. 17.7). Due to the unique nanostructure and biocompatibility of electrospun

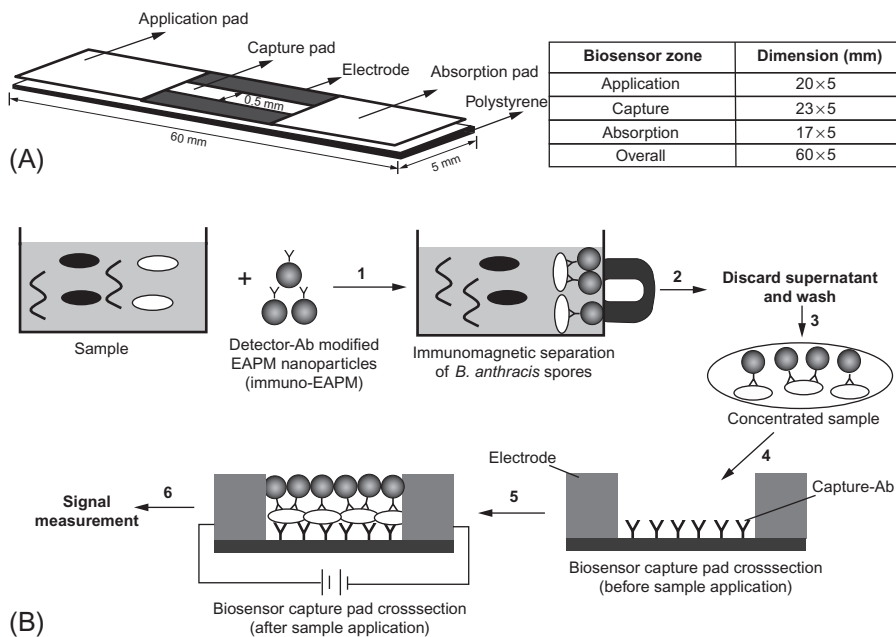


Fig. 17.6 Detection scheme of the immunosensor based on the antibody-functionalized electrospun capture membrane capable to entrap only the antigen-antibody conjugated to the magnetic/conductive nanoparticles (MNPs) [42].

nitrocellulose membranes, the biosensor showed linear detection response for *E. coli* O157:H7 and BVDV virus samples. Only an 8 min detection process was needed for each measurement. The sensitivity of the portable and low-cost biosensor was 61 CFU/mL and 103 CCID/mL for *E. coli* O157:H7 and BVDV, respectively (Fig. 17.5D).

More recently, Reinholt et al. created a biosensor based on paper (lateral flow assay, LFA) [43] using electrospun nanofibers of polylactic acid (PLA) with poly(ethylene glycol) (PEG) and a functionalized polystyrene (PS). Specifically, anti-streptavidin antibodies adsorbed on the nanofibers captured streptavidin-conjugated sulforhodamine B (SRB)-encapsulating liposomes. Varying the functional polymer concentration within the PLA base allowed the creation of separate capture zones. Also, a sandwich assay for the detection of *E. coli* O157:H7 was developed using anti-*E. coli* antibodies as capturer and reporter species with horseradish peroxidase for signal generation (LOD: 1.9×10^4 cells).

On the basis of economic criteria and the need for ultrasensitive assays, Dai et al. [40] developed very recently a novel 3-D biosensing platform based on electrospun carbon NTs/poly(methyl methacrylate) nanofibers composite biofunctionalized with α -fetoprotein (α -AFP) antibody, via electrostatic interaction. This platform was used to fabricate label-free electrochemiluminescent immunosensor to detect α -AFP. Electrochemiluminescent (ECL) technique is concerned with interplay between optical

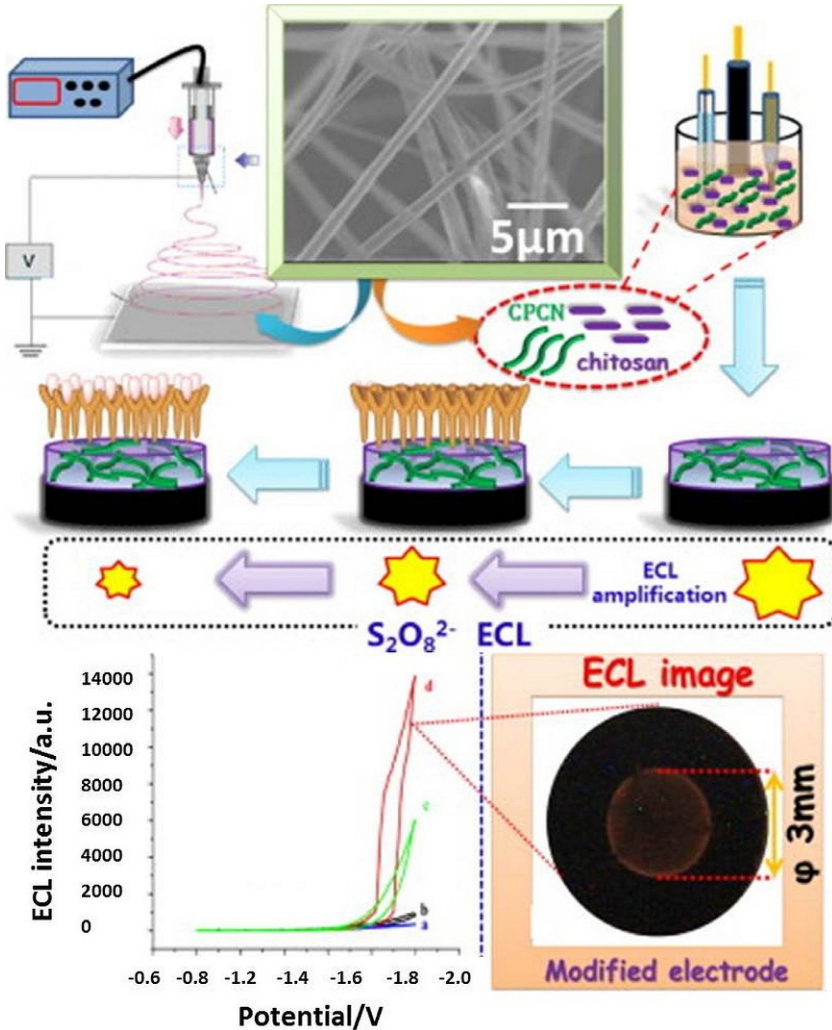


Fig. 17.7 Sketch of the working principle of the sensor (*top*); ECL intensity and potential curve of different modified electrodes in 0.1 mol/L pH 7.0 PBS solution containing 0.1 mol/L peroxydisulfate and the ECL image of peroxydisulfate at the CNTs@PNFs modified electrode [40].

information and electrochemistry: CNTs were incorporated at first in the PMMA to form conductive nanofibers through electrospinning. A three-dimensional network structure composed of chitosan, peroxydisulfate, and CNTs/PMMA nanofibers was deposited on a disk glassy carbon electrode (GCE) for sensing, benefited from the unique properties of this netlike interface (i.e., strong ECL emission of peroxydisulfate nearly 35 folds higher than GCE alone) (Fig. 17.7). When the reaction between antibody

and AFP happened, the ECL response of peroxydisulfate dramatically decreased. Such design offered a suitable carrier for immobilizing biological recognition elements with low toxicity and eco-friendliness, thus opening a promising approach to developing further electrospun nanofibers based on amplified ECL biosensors with remarkable analytic performances.

Sun et al. fabricated a 3-D immunosensor consisting in a biosensor to detect drugs, such as chloramphenicol, by immobilizing antibodies on electrospun polystyrene (PS) membranes and QCMs. Three-dimensional fibrous PS membranes comprising porous PS fibers were deposited on the electrode of QCM via electrospinning and then functionalized with sensing antibody on the membranes. The functionality of the immobilized antibodies was tested with CAP using the 3-mercaptopropionic acid (MPA) method. The antibody-functionalized MPA biosensor sensitivity increased concurrently with increasing the PS loading and the specific surface area on the QCM (a mass sensor), and its responses showed good linearity in the 5–100 ppb concentration range. The authors also observed fast response (2–3 s) to CAP, detection limit of 5 ppb, and sound capturing selectivity to CAP when tested with other antibiotics at a concentration between 5 and 200 ppb [44]. The use of electrospun sensing membrane was described in the study of Senecal et al. [45], who developed two types of electrospun capture membranes containing either carboxyl (COOH) or amine (NH₂) functional groups for covalently attaching antibodies. The carboxyl functional membrane was produced by electrospinning polyvinyl chloride (PVC) formulated, while the amine functional membrane was made through coelectrospinning of two polymers, water-soluble polyamine, and water-insoluble polyurethane. Antibodies were covalently attached to the functional groups on the membranes, and the assay was developed for detecting *Staphylococcus* enterotoxin B (SEB) and resulted in effective recognition.

An exhaustive description on biosensors and biosensing devices based on electrospinning has been reported by De Cesare et al. [19]. A recent pioneering project led by Haberer et al. (University of California, USA) is attempting to demonstrate and develop an electrospun whispering gallery mode resonator with integrated phage-based recognition elements as robust, highly sensitive multiplexed optical biosensors. The involved researchers are creating a new biosensor using laser light, engineered viruses, and advanced manufacturing techniques to more accurately detect the smallest amounts possible of biological molecules in our own blood and in other complex environments (food, water, and soil). The basic mechanism behind such advanced sensors relies on an old phenomenon: laser light is able to amplify the detection of single particles, a technique known as whispering gallery mode resonators. Whispering galleries of light work with waves of photons traveling within a circular space, or cavity. Any particles within these cavities encounter the waves thousands to millions of times, changing the light in subtle ways to be revealed. The cavity is actually a long, thin fiber with engineered viruses embedded in it. The laser is directed perpendicular to the length of the fiber, activating the sensor. The challenge is to create smooth, durable cavities simply, so they can be used for different purposes; integrating different types of phage-based recognition elements within fibers, the resulting sensors will be able to detect different kinds of molecules. Viruses are just protein-surrounding genetic materials, so they are more

stable than enzymes or antibodies. The incorporation of biorecognition elements into the fiber-based sensors will further facilitate sensing of multiple biomolecules while maintaining a small footprint and minimal sample volume. Electrospinning is well suited to incorporate biorecognition elements such as filamentous phage within the optical cavity at high concentrations. Phage-based bioreceptors provide a high density of well-organized and highly oriented analyte binding sites for high-sensitivity detection. Furthermore, they are chemically and thermally robust, tolerating a range of sensing conditions, and can be manufactured inexpensively in large quantities with a bacterial host. The integration of bioreceptors into the whispering gallery mode optical cavity will eliminate the need for biofunctionalization steps following cavity fabrication, thus minimizing manufacturing complexity, reducing biosensor footprint, and enabling straightforward multiple analyte detection. Likewise, the unsurpassed density of highly oriented bioreceptors associated with the filamentous phage and the long- and short-range ordering created by the electrospun scaffold are expected to produce fast biosensing tools with excellent sensitivity and selectivity [46] (Fig. 17.8).

17.3 ES-nanosensors for breath analysis

An alternative perspective to this approach is offered in the form of exhaled-breath gas analysis [47]. Conventional diagnostic methods such as MRI, CT, blood test, endoscope, and X-ray examination, which are expensive and sometimes painful, are usually implemented in hospitals. However, in the near future, inexpensive and simple diagnoses are expected to detect and examine diseases in the early stages.

The relationship between some human diseases and the specific odors in patients' breath has already been suggested by ancient Greek physicians. Nevertheless, such an approach has gradually been abandoned in favor of the blood tests, and only in the last thirty years, a renewal and growing interest in breath analysis for medical purposes has been rediscovered. It has been realized, in effect, that some characteristics of breath may reflect perturbations in human metabolism. Then, its analysis can be used as a sort of window through which look into the human body by a completely noninvasive strategy. This analysis is based on the assumption that the biochemical perturbations associated with metabolic diseases can be somehow "volatilized" when they reach the alveoli interfaces in the lungs and are consequently expelled from the body during

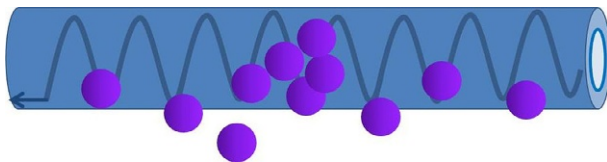


Fig. 17.8 Graphic representation of a fiber resonator: electrospinning creates long, hairlike fibers made of plastic, metal, or ceramics. The light or electromagnetic field profile of a whispering gallery mode is depicted propagating along the periphery of the fiber and subjected to interferences due to the analyte adsorption.

exhalation. Breath is mostly composed of water vapor but also comprises aerosol particles of nonvolatile biomolecules, such as leukotrienes and prostaglandins, inorganic compounds such as hydrogen peroxide, nitric oxide derivatives and hydrogen ions, inorganic gases, such as nitric oxide, ammonia, carbon monoxide and dioxide, and various VOCs. The latter ones can be produced in various organs of the human body and may result from both normal physiological and biochemical processes and pathological conditions, such as lipid peroxidation, renal failure, liver disease, perturbations of glucose or cholesterol metabolism, and even cancer. Among the about 500 compounds detected till now in breath, only few tens have been established to be potential markers of pathologies. Among them, for instance, exhaled CO has been recognized as a marker for diabetes and cardiovascular diseases, NO is a biomarker for oxidative stress including asthma, exhaled low-molecular-mass hydrocarbons (ethane and *n*-pentane) are markers for high levels of cholesterol in the blood, and ammonia is a marker of active bacterial infection of the lung or for renal and kidney malfunctioning. Thanks to major breakthroughs in new technologies (infrared, electrochemical, chemiluminescence, etc.) and the availability of very sensitive mass spectrometers, breath analysis has made considerable advances in the last century [48]. The analysis of patients breath using gas chromatography and mass spectrometry (GC-MS) has revealed VOC patterns that are associated with well-defined pathologies, that is, succeeding in identifying not only cancer-affected from healthy patients but also multiple cancer subtypes including the lung, breast, prostate, and colorectal cancer [49]. Another recent study identified a natural compound (limonene) detected in the breath as an unambiguous biomarker of early-stage cirrhosis of the liver [50]. Similarly to the hereinabove reported and extensively tested instruments for the identification of pathologies through breath analysis, nanosensor-based devices have been more recently designed and investigated as key tools to get early diagnosis, together with the opportunity to create miniaturized and portable structures, based also on high sensitivity, low power consumption and low cost, easy in manufacturing, handling, and understanding, and capability of working in platforms providing multiple information [51]. Chemoresistive or conductometric sensors have attracted a great deal of attention because of their simple structure and their ability to be miniaturized as well as their low cost and easy of fabrication. These sensors measure the change in the conductance or resistance of the sensing material caused by its interaction with the target analytes. Chemoresistive sensors have the benefit of being simple in configuration and in signal measurement.

17.3.1 NO sensors

Macagnano et al. [52] reported the potentials of a preindustrial prototype to reveal NO within the exhaled air. The core of the system was based on a nanostructured chemoresistor based on a conducting polymer (CP, PEDOT/PSS) covering a fibrous scaffold of electrospun TiO₂ nanofibers (Fig. 17.9) and capable of detecting NO (after its oxidation over trough an oxidizing cartridge), comprising pneumatic, measuring, and communicating systems, all managed by a reduced instruction set computing (RISC) microcontroller.

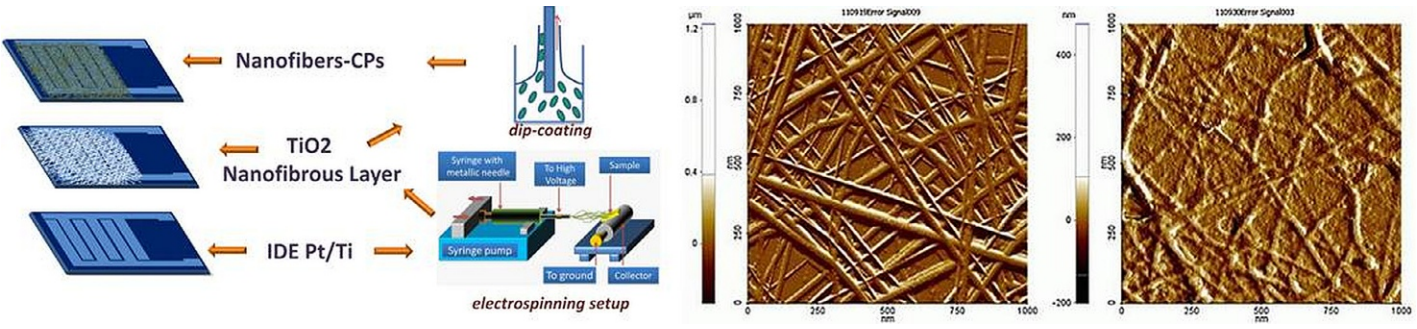


Fig. 17.9 Schematic representation of the experimental setup used to obtain chemosensors based on Pt-Ti IDEs coated with a thick nanofibrous scaffold of titania (by electrospinning) and an overlying thin layer of CP (by dipping); AFM micrograph of TiO₂ fibrous layer before and after CP dip-coating, respectively [53].

Its sensitivity, defined as the ratio between the sensor signal and the amount of gas adsorbed to the sensor surface, was calculated as the slope of the calibration curve (since the response curve was a straight line). The calculated value of the linear fitting slope of the response curve was $2.4 \pm 0.3 \times 10^2$ mA ppb⁻¹, with a limit of detection (LOD) of 6 ppb. Such indexes are parameters correlated to the affinity of the sensor toward NO_x and the limit value to generate electrically readable signals, respectively. Additionally, the sensor, powered to 0.3 V, showed further attractive features as concerns low power consumption and a relatively fast recovery of the sensor after each measurement (about 10 min). The high sensitivity of the sensors has been supposed to be related to many factors acting simultaneously: the polymer (PEDOT-PSS) sensing properties, the nanostructure arrangement, and the doping effect of the CP due to the underlying nanofibrous metal oxide (i.e., TiO₂) (Fig. 17.10) [54].

Yoo et al. [55], indeed, suggested that the junctions between the materials are capable of decreasing the energy gap and increasing the charge carriers available. Thus, the supposed mechanism occurring between NO₂, an electron withdrawing, and the p-type CP, depending on the minority of electron carriers' attraction, was favored. In the nanocomposite film, the supposed mechanism of reaction occurred at the interface between CP and TiO₂. It is, in effect, where the interacting gas, after adsorption, was capable of modulating easily the conductivity of the junction. The n-p contacts between TiO₂ nanofibers and PEDOT-PSS layer, indeed, gave the rise to CP's electronic structure changes and resulted in gas sensitivity increment. The gas delivery system was designed to both allow the sensor to be quickly pervaded by a stable concentration of NO (to assess the response time) and keep the sensor working even after removing the flow of the analyte by a recirculating system (despite the short time of the exhalation).

17.3.2 Acetone sensors

Kim et al. at KAIST developed a highly sensitive exhaled-breath sensors, using tin dioxide (SnO₂) fibers assembled from thin, wrinkled SnO₂ NTs [51]. These metal oxide nanofiber-based chemoresistive gas sensors were expected to be usable in portable real-time breath tests (Fig. 17.11). Such sensors were designed such as to diagnose diabetes or lung cancer quickly and effectively by simply breathing into a small nanofiber-based breathing sensor, mounted on a phone or other similar device.

Varying the flow rate of an electrospinning solution feed and then applying a heat treatment provided the specific arrangement of these SnO₂ fibers, called "microphase separations." Such processing resulted in nanofibers with shape like an open cylinder. Inside the cylinder, thin-film SnO₂ NTs were layered and then rolled up. A number of elongated pores ranging from 10 to 500 nm (nanometers) in length along the fiber direction were generated on purpose on the surface of the SnO₂ fibers, to allow exhaled gas molecules easily permeating the fibers. The inner and outer walls of the SnO₂ tubes were evenly coated with catalytic platinum (Pt) NPs. According to the authors, highly porous SnO₂ fibers showed fivefold higher acetone responses than that of the dense SnO₂ nanofibers.

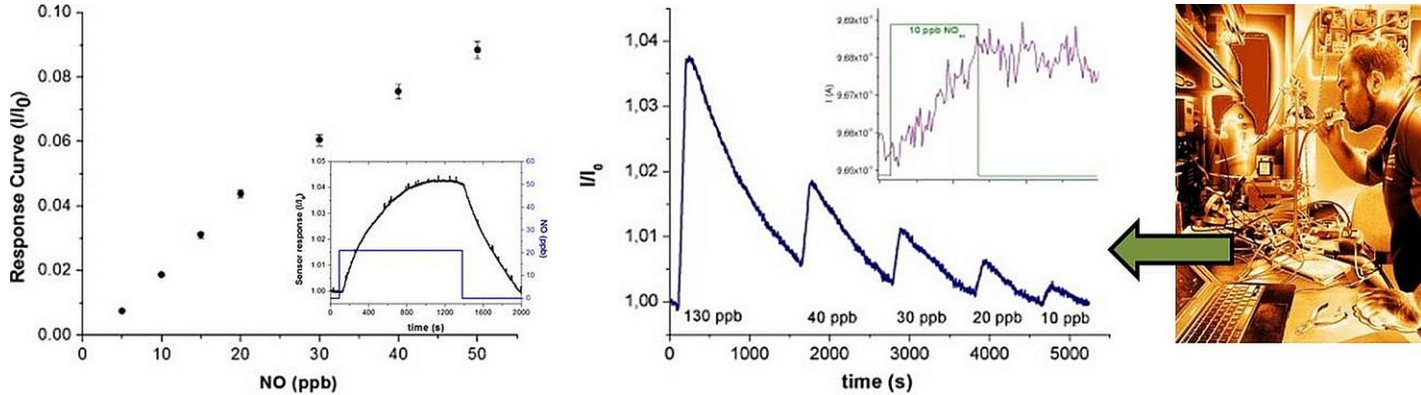


Fig. 17.10 (Left): Current changes versus increasing concentration of oxidized NO, normalized to I_0 (starting current) and (inset) current variation reported when 20 ppb of oxidized NO interacted with the sensor, at 25°C and 40% RH, normalized to the starting current value (I_0); (right): normalized sensor transient responses to decreasing concentration of NO_x (ranging between 130 and 10 ppb) for 90 s sampling under comparable environmental condition of an exhalation [54].

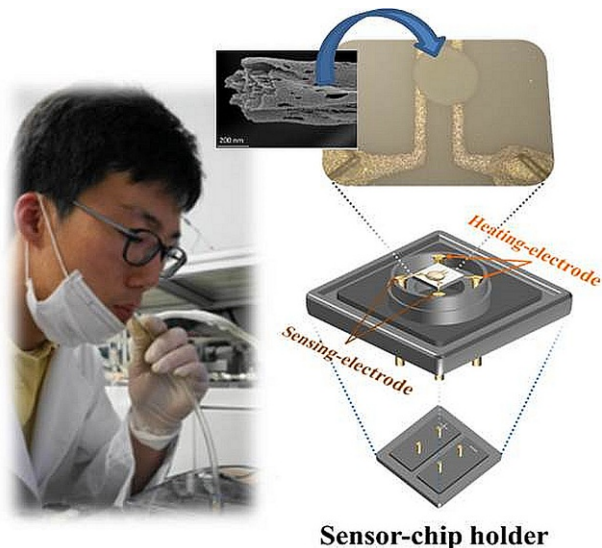


Fig. 17.11 Components of exhaled-breath sensor, showing optical microscope image (*right, top*) of exhaled-breath sensing layer coated on sensor substrate [56]. Courtesy of Prof. Il-Doo Kim, Department of Materials Science and Engineering, KAIST.

The following metal Pt doping of these tubes [57] showed a great potential for future exhaled-breath-sensor applications, detecting promptly and accurately acetone or toluene even at very low concentration—less than 100 parts per billion (ppb). The exhaled acetone level of diabetes patients exceeds 1.8 parts per million (ppm), which is two- to sixfold higher than that (0.3–0.9 ppm) of healthy people. Therefore, a highly sensitive detection that responds to acetone below 1 ppm, in the presence of other exhaled gases (and also under the humid environment of human breath), sounds as an accurate performance to diagnose diabetes.

17.3.3 Toluene and H_2S sensors

Similarly, a trace concentration of toluene (30 ppb) in exhaled breath, considered to be a distinctive early symptom of lung cancer, could be easily detected with this designed sensor. Afterward, the Kim's research group developed WO_2 semiconductive nanofibers, designed with a controlled porosity and functionalized by graphene nanoflakes, to detect further markers in breath (i.e., H_2S , halitosis) [58].

The nonwoven WO_3 NFs can be obtained by a conventional single-nozzle electrospinning of the W precursor (ammonium metatungstate hydrate)/PVP composite solution followed by high-temperature calcination. During the preparation of the electrospinning solution, insoluble PS colloids were added and dispersed homogeneously within composite electrospinning solution. After calcination, the spherical PS colloids and the PVP were eliminated, and W precursor was oxidized to form WO_3 NFs. The controlled spherical

pores distribution on the surface and inside of the WO resulted from decomposition of the spherical PS colloids (200 and 500 nm). Remarkable features of this processing improving gas-sensing performance are increased surface area due to electrospun nanofibers and facilitated gas penetration path through the pores. In addition, the sensitization effect of NOGR flakes could further enhance the sensing characteristics. The gas-sensing characteristics revealed that the PS (200 and 500)-WO₃ NFs showed a significantly enhanced H₂S (5 ppm) response, due to the increased BET surface area and easy diffusion of small and light H₂S molecules penetrating through the small pores. In contrast, PS (500)-WO₃ NFs were more sensitive to acetone (5 ppm) due to the facile penetration of the large and heavy acetone molecules through the enlarged pores. When the synthesized porous WO₃ NFs obtained by PS colloid templates were further integrated with NOGR flakes, the LOD for H₂S was improved (100 ppb H₂S) as well as the selectivity toward this analytes, because of lower responses to interfering chemicals. Finally, this work managed to verify the effective pore size and pore distribution control method in SMO nanofiber structure and the potential use of NOGR flakes without using noble metallic catalysts, which optimize the sensing characteristics for potential application in diagnosis of halitosis.

17.3.4 NH₃ and pH sensors

Also, ES sensor based on conductive polymers has recently emerged as an attractive alternative to metal and semiconducting nanowires for breath analysis. A series of polymers have been investigated for their electric features. Polyaniline has emerged as an excellent material candidate to be used as a material for a series of nanoscale applications, particularly for chemical and biological sensors [59].

Its primary chain consists of a combination of benzenoid—amine sites reacting with oxidizing substances and quinoid-imine sites reacting with reducing and protonating compounds. In the base form, all structures are insulating. Upon exposure to an acidic medium, these structures transform into salts, the highest conducting and most stabilized form being emeraldine salt.

Since electrospinning process of polyaniline is relatively hard, mainly due to its rigid backbone and relatively low molecular weight, Rutledge's group reported the successful production of continuous fibers of pure PANi doped with HCSA by coaxial electrospinning and subsequent removal of the shell polymer (poly(methyl methacrylate)). These fibers exhibited electrical conductivities as high as 130 s/cm when fully doped and were extremely sensitive to NH₃ in a response time of about 45 ± 3 s upon exposure and 63 ± 9 s for recovery upon purging. The results also showed that the measurement was reasonably reversible; the maximum $\Delta R/R_0$ value did not vary a lot over multiple cycles of exposure to the same concentration of gases, so that the fibers can be used multiple times for ammonia sensing. Alternatively, many researchers have explored the use of secondary polymers such as polyethylene oxide (PEO), polyvinylpyrrolidone (PVP), and cellulose acetate (CA) [60–62]. The choice of matrix polymer depends on the stability of the polymer, its vapor transport ability, and the affinity of the secondary component to the CP. The advantage of the fibrous matrix is that the high surface area and high porosity allow enhancement of the

percolation of analyte molecules to the CP, while the secondary component operates dually as an absorbent for target analytes and as filter for undesired interferents. Using the electrospinning technique, sensors based on polyaniline hybrids were also fabricated for both gas and pH monitoring in order to determine the suitability of these sensors in human breath analysis [63]. Due to the relationship between the pH of condensed saliva and peculiar pulmonary diseases (probably upon neutrophilic and/or eosinophilic inflammation), “breath” pH represents a parameter that could be detected in diagnostics. Indeed, the average pH of deaerated (removal of CO) exhaled-breath condensate (EBC) in healthy patients is 7.7 [64]. For patients with chronic pulmonary illnesses, the pH of EBC may decrease to 7.38 for asthma, 7.14 for bronchiectasis, and 7.24 for chronic obstructive pulmonary disease (COPD). Concurrently, researchers have found that pH can be correlated with an increase in NO released by the inflammatory cells (as in asthmatic patients). Gouma’s group described a sensor based on CA and ES-PANI capable to monitor the “headspace” of several solutions containing different pH levels. The emeraldine salt, used in these studies, was the highest conducting form of polyaniline. EDAX analyses revealed that there were sulfate ions attached to the polymer chain (consisting of half benzenoid amine and half quinoid imine units) that could act as sites for H reactivity. The results showed that as pH increased and H decreased, the films exhibited an increase in resistance by 1.7–2.0 times per pH unit (which it was correlated to a tenfold decrease in H). This increase in resistance was supposed to be associated with reduction of the electroactive sites along the polymer chain by the basic headspace. As H increased, the films became highly protonated along the imine sites yielding a decrease in the films resistance on exposure to the headspace of low pH.

17.3.5 Humidity sensors

The content of water can also be taken into account to monitor pathologies. Although literature is over abounds of studies on humidity sensors [65], those with fast response form only a small subset. The subset includes those based on inorganic materials in the form of nanostructures such as nanowires [66], NTs [67], and nanofibers of oxides [68] and of few sulfides [69]. The basic mechanism of humidity detection in the above materials is based on the change in proton/ionic conduction (resistive), dielectric constant (capacitive), refractive index (optical), frequency (impedance), or in mass, of the active material with the humidity level [70].

Mogera et al. designed an ultrafast response humidity sensor for monitoring breath humidity and flow, capable of monitoring the respiration rate (to be employed for sleep apnoea) [71].

The humidity sensor was fabricated using supramolecular nanofibers as active resistive sensing material. The nanofibers were built via self-assembly of donor and acceptor molecules (coronene tetracarboxylate and dodecyl methyl viologen, respectively) involved in charge transfer interactions. The conductivity of the nanofiber markedly varied sensitively over a wide range of relative humidities (RH) with unprecedented fast response and recovery times. Based on UV-VIS, XRD, and AFM measurements,

it was found that the stacking distance in the nanofiber decreased slightly while the charge transfer band intensity increased, all observations implying enhanced charge transfer interaction and hence the conductivity. Using two humidity sensors, a breath flow sensor was made, which could simultaneously measure RH and flow rate of exhaled nasal breath. The integrated device was tested for monitoring RH in the exhaled breath from volunteers undergoing exercise and alcohol-induced dehydration.

17.3.6 Aldehyde sensors

Inspired by the Solid Phase Microextraction (SPME) principle but provided with higher surface/volume ratio, a study of Huang et al. [72] presented a novel polystyrene/graphene (PS/G) composite nanofiber film for thin-film microextraction (TFME) for the first time. The PS/G nanofiber film was fabricated on the surface of filter paper by a facile electrospinning method. The morphology and extraction performance of the resultant composite film were investigated systematically. The PS/G nanofiber film exhibited porous fibrous structure, large surface area, and strong hydrophobicity. It was developed and investigated for the quantification of six aldehydes in human EBCs. The method showed high enrichment efficiency and fast analysis speed. Under the optimal conditions, the linear ranges of the analytes were in the range of 0.02–30 $\mu\text{mol L}^{-1}$, and the recoveries were between 79.8% and 105.6% with the relative standard deviation values lower than 16.3% ($n=5$). The limits of quantification of six aldehydes ranged from 13.8 to 64.6 nmol L^{-1} . The established method was successfully applied for the quantification of aldehyde metabolites in EBCs of lung cancer patients and healthy people. As a whole, the TFME-HPLC method is expected to be a simple, rapid, sensitive, cost-effective, noninvasive approach for the analysis of linear aliphatic aldehydes in human EBCs.

17.4 Electronic nose devices for breath analysis

More sophisticated and emerging devices can be used to detect simultaneously more biomarkers in breath and diagnose diseases. In particular, electronic noses, which are composed of cross sensitive sensor arrays, the signals of which are interpreted through pattern recognition algorithms, present several advantages, compared with other types of detecting equipment, such as portability and cost-effectiveness for handheld breath analysis devices (Fig. 17.12) [73].

Since 2003, Di Natale et al. [74] successfully investigated the use of an electronic nose composed of eight quartz microbalance gas sensors, coated with different metalloporphyrins, to check whether volatile compounds present in expired air could diagnose lung cancer. The alteration of breath composition induced by the presence of lung cancer was such to provide a complete identification of samples from diseased individuals by their prototype. Specifically, the working principle consisted in a sensor array sniffing chemicals from a sample and providing a set of signals; the pattern recognizer compared the pattern of the measurements with stored patterns of known

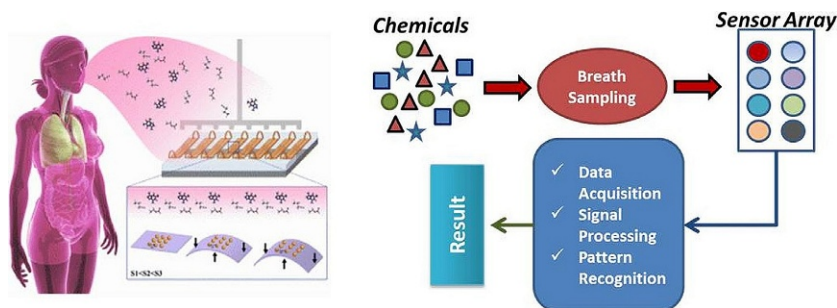


Fig. 17.12 Sketch of a breath-diagnostic array based on flexible gold-nanoparticle sensors housed in an electronic nose (*left*). Scheme of an electronic nose working principle (*right*) [73].

chemical species to identify the sniffed sample. Gas sensors tend to have very broad selectivity and respond differently to different chemical species. This is a disadvantage in many applications, but in the electronic nose, it turns into an advantage. Although every sensor in an array may respond to a given chemical, these responses will usually be different. A good sensor should fulfill a number of criteria such as having high sensitivity to the target group of chemical compounds intended for detection and relatively low selectivity in order to be sensitive to a wide number of different chemical compounds. Hundreds of different prototypes of artificial-nose devices have been developed to discriminate complex vapor mixtures containing many different types of VOCs in several applications.

The electronic-nose (e-nose) technology is able to provide a sort of fingerprint of exhaled breath (breath print, BP) by detecting VOCs through multiple sensors. In this case, individual VOCs of exhaled-breath profiles remain unidentified, but the e-nose is able to give a comprehensive VOCs profile. Variations in the concentration of the exhaled VOCs that may serve as biomarkers for specific diseases can distinguish healthy people from those who are sick. Commonly, noses designed for breath analysis make use of breath-collecting systems. These prototypes collectively represent various electronic detection (EAD) technologies that utilize different sensor types including metal oxide [75], conductive electroactive polymers [76], optical, surface acoustic wave [77], and electrochemical gas sensors [78] to the newer DNA-carbon NTs [79].

A collection of advantages and drawbacks of electronic-nose technology when compared with traditional analytic tools for breath has been more recently reported in literature by Wilson [80]. Advantages comprise features like less expensive, ease of use and operation without extensive training required, rapid results and response time, quick sensor recovery time, excellent precision, low operating costs, and large flexibility in sensor array selection [80]. Some disadvantages of e-nose instruments are the inability to identify individual compounds in complex mixtures, sensor arrays sensitive to water vapor, relatively short sensor life, difficulty in measuring analyte concentrations accurately, and somewhat lower sensitivity than instruments usually employed in analytical chemistry.

To overcome this issue, Gouma's group [81] has been working to produce e-noses (or diagnostic breathalyzers) based on ES technology exploiting highly selective semiconducting ceramic sensors to detect disease and measure specifically metabolic functions.

Semiconducting sensors based on metal oxides (MOx) are probably the most widely used sensor technology in electronic-nose applications since they display a high level of sensitivity for a range of organic vapors, offer perhaps the best balance between drift, lifetime, and sensitivity, and finally are readily available commercially in a variety of different types with broadly different specificity. Normally, they contain a heating element and a semiconductor material. Two types of semiconductor material are used: n-type semiconductors (normally oxides of zinc, tin, or iron) that respond mainly to reducing compounds and p-type semiconductors (normally oxides of nickel or cobalt) mainly responding to oxidizing compounds. Beyond the choice of the semiconductor material, the selectivity of the sensors can be modified in several ways including the doping of the interacting layer by noble metal catalysts, changing the operational temperature, and the particle size. Gouma's sensors were highly sensitive to gaseous disease-signaling markers in breath: they could detect specific molecules in parts per billion (such as ammonia, acetone, NO, and CO). The sensor chip was covered with spaghetti-like metal oxide fibers with diameters ranging from 1 to 100 nm. Oxides in the ReO_3 family such as $\alpha\text{-MoO}_3$ and $\epsilon\text{-WO}_3$ were investigated. The nanowires were synthesized by electrospinning, crystallized as it passed through, and collected on an aluminum plate.

The crystalline structure of nanofibers and the atomic configuration on their surfaces determined which compound could be detected. For instance, gases such as carbon monoxide and methane are able to stick to a nanofiber oxide the atoms of which have a tetragonal (four-sided) arrangement. Nanofibers can be made in large quantities and properly tuned during production to respond to different compounds. Once the e-nose detected its target molecule, its concentration was shown on a digital display. One sensor could detect acetone in the breath of diabetics to determine whether they need to increase their insulin doses. Another could measure nitric oxide in asthmatics' breath to detect an impending or worsening asthma attack. Gouma's group is going also to develop e-noses to detect the organic compound isoprene to measure cholesterol levels, ammonia to detect kidney disease, and a mix of ammonia and ketones to get a whiff of liver disease as well as specific alkanes and alkenes for early detection of lung cancer.

Kim's group [82] is also developing arrays of ultrasensitive and highly selective gas sensors to diagnose diseases by exhaled-breath analysis (Fig. 17.13).

The sensor technology is compatible with various types of smartphones, wearable electronic gadgets, and medical devices (Fig. 17.14).

After MOx, conducting polymers are probably the most widely used sensor technology. They have received considerable attention and have formed the basis of several of the earlier generation of commercial electronic noses. They appear promising materials since they exhibit reversible changes in conductivity at room temperature and are relatively resistant to poisoning. Zampetti et al. [83] combined electronic nose and bioinspired nanofibrous artificial epithelium principles and reported the sensing features of an array of 9 microchemoresistors (Cr-Au, 3×3) coated with electrospun

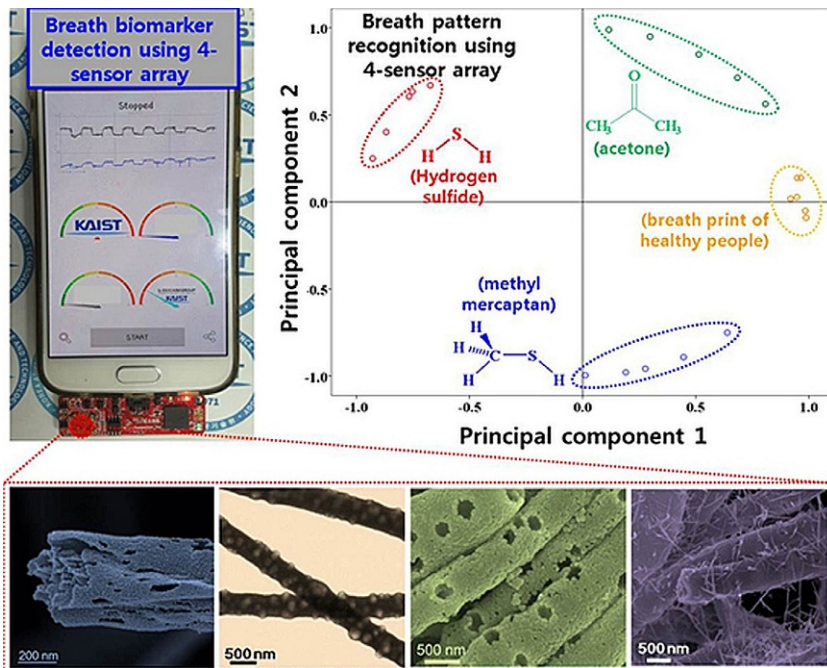


Fig. 17.13 Demonstration of breath analysis using nanofibers functionalized with various catalysts for pattern recognition of breath components such as hydrogen sulfide, acetone, and methyl mercaptan for diagnosis of diabetes and halitosis [82].

Courtesy of Prof. Il-Doo Kim, Department of Materials Science and Engineering, KAIST.

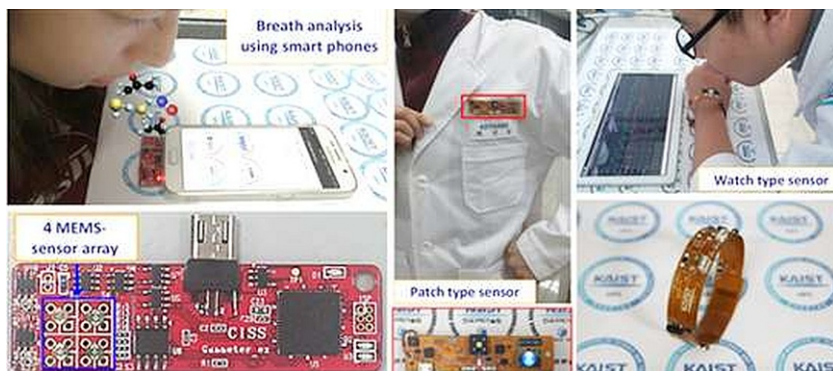


Fig. 17.14 Real-time breath analysis using portable sensor platforms such as a dongle-type sensor module, wearable patch-type sensor module, and wearable-watch-type sensor module [82].

Courtesy of Prof. Il-Doo Kim, Department of Materials Science and Engineering, KAIST.

nanofibrous CP structures. Since polyaniline is one of the most interesting CPs for its conductive features (when doped), its thermal stability, and its sensing performances, it has been selected and investigated as crucial in the construction of the sensor array. Thus, at first, blends of polyaniline and insulating host polymers were planned, prepared, and studied to verify, contemporarily, the combination of electrical conductivity of the conductive polymer and the physical properties of the host polymer. Secondly, a combination of overlaid and double-overlaid areas linked by interconnections of different fibers has been created and investigated as potential sensors. The selected overdepositions of couples of fibrous polymers, with their interconnections, introduced broader and overlapping sensitivities to different analytes, making each sensor a desirable sensing element of an artificial olfactory system. Such an interdigitated sensor array (ISA) included a plurality of nanofibers whose electric parameters were contemporarily depending on each polymer exposure to analytes and on the spatial distribution of the interlaced fibers. The choice of the hosting polymer depends on the stability of the polymer, gas/vapor transport ability, and affinity to the CP. The selected hosting polymer carriers (respectively, PVP, PEO, and PS) modified remarkably the typology of the interacting surface (diameter and length of the fibers, roughness, porosity, the presence of beads and grains, and nonwoven and/or branched framework) in addition to the different affinity to the tested analytes and thus allowed ISA getting a wider dynamic range of sensitivities. The prototype features were investigated to detect ammonia and nitrogen dioxide, useful markers in breath. The high porosity of the sensors allowed getting rapid changes in current (fast responses), when the gas was sorbed and desorbed, respectively. Since each sensor of such a nanostructured device could detect, with different sensitivity, very low concentrations of both ammonia and nitrogen dioxide (up to ppb levels), potential employments of the proposed artificial nose as a diagnostic instrument are expected to detect and reveal gases involved in metabolic diseases and released in traces from breath and skin. The sensors made of the double fibrous polymeric layer contribute to increase the variability in the sensor array broadening the sensitivity and creating a wider overlapping selectivity. The resulting LOD for NH_3 and NO_2 was confirmed to be about 250 ppb, in spite of higher values (>500 ppb) observed when only single fibrous layers (PANi-PEO, PANi-PVP, and PANi-PS) were used (Fig. 17.15).

Based on both nanofibrous chemoresistors and optical and photoconductive properties of the sensing materials, a commercial electronic nose has been fabricated and commercialized by Vaporsens [84]. Over thirty nanofibrous sensors have been developed to date to detect redox active chemicals in traces. Each sensor is able to respond differently to chemicals such as amines, oxides, aromatic compounds, and aldehydes, letting suppose potential application for health monitoring, too.

17.5 Summary and outlooks

This chapter gives a brief description of the recent results related to electrospun nanodevices designed and investigated to create novel and advanced diagnostic tools to prevent disease progression and to allow a proper and prompt therapeutic treatment.

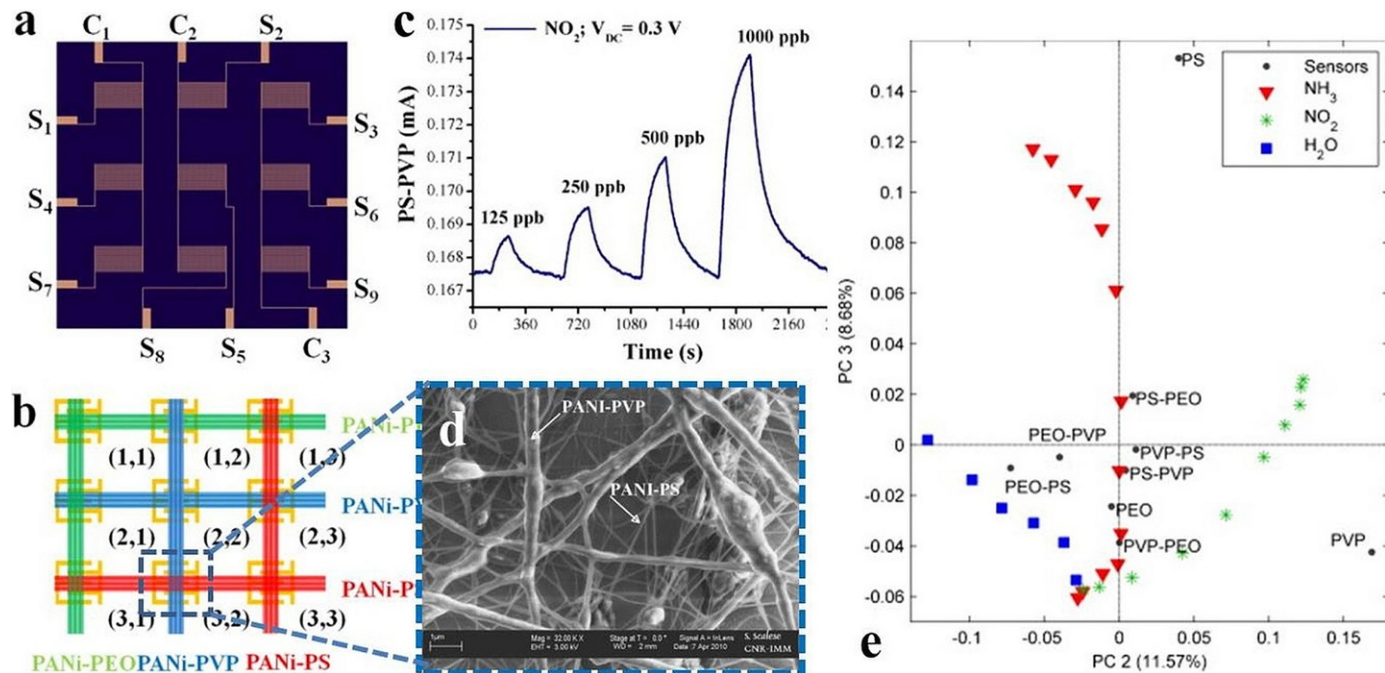


Fig. 17.15 IDEs array layout (A) and sketch of the fibrous sensor array (B); SEM micrograph of PANi-PS/PANi-PVP (under- and overlayer, respectively) (D); transient response of PANi-PS/PANi-PVP sensor in the presence of increasing concentrations of NO_2 supplied through pulses of 180 s (C); PCA bi-plot, pointing out the combined loadings and score plot, projected along the second and third principal components (E) [83].

Electrospun nanofibers have been confirmed to be an exceptional support for these detecting tools, due to their uniqueness in morphology and fibrous arrangements and to the great versatility of the ES technology in creating advanced and sophisticated sensing layers compatible with electronics and electronic nanodevices. Together with a great number of novel sensors for early detecting pathologies markers in the blood, also sensors for more noninvasive diagnostics systems are getting increasingly popular in the scientific community and on market (e.g., breath and skin monitoring) and routine analysis. Furthermore, emerging analysis methods and the development of accurate detection techniques for biomarkers provide a bright perspective for diagnosing different diseases using exhaled-breath analysis. In particular, electronic noses, which are composed of cross sensitive sensor arrays with pattern recognition algorithms, show several advantages compared with other types of analyzing equipment with respect to portability and cost-effectiveness for handheld breath analysis devices. These studies reported that ES sensors exhibit exciting performances in health disease monitoring.

According to recent literature, sensing is an area where electrospun nanofibers technologies are a great promise for industry. Despite the great potential of electrospun nanofibers, the number of commercialized products remains extremely limited.

Probably, up to now, one reason for this lack of commercialization was due to the small scale at which nanofibers could be produced using the conventional electrospinning method, which limited its use to the production of small samples within laboratories. However, the growing interest to the ES potentials, through funded projects that have facilitated the cooperation of academic world with industry, is pushing start-ups and large multinationals to recognize the commercial potential of electrospun products beyond laboratory setup. Thus, a number of companies have attempted to address the problem of nanofibers production rates and have developed new methods, adapted from conventional electrospinning, which are capable of significantly faster production than methods previously reported within academia. With these new technological advancements, the potential for the use of electrospun nanofibers in industrial applications has become more achievable, and there are a growing number of companies being formed to develop an industry for nanofibers use. Leading players in the market include Donaldson, DuPont, Ahlstrom, Hollingsworth & Vose, Johns Manville, Kuraray, Mitsubishi Rayon, Teijin, and Toray, but innovative up and coming companies involved in both the production and application of nanofibers are emerging. Significant examples comprise Elmarco, FibeRio Technology Corporation, Finetex EnE, BioInicia, Linari Engineering Srl, Nanopharma, and Revolution Fibres Ltd.

Cooperation among companies is providing successfully results. For instance, whereas functionalization of the sensing material's surface is required to impart the desired reactivity, a promising R&D collaboration, KODE Biotech Ltd (New Zealand) with Revolution Fibres reported the benefits of biofunctionalization technique with mass-produced electrospun nanofibers demonstrating the potential to revolutionize diagnostic kits worldwide—making them simple to use, simple to manufacture, and easy to be used.

Cutting-edge work by Professor Il-Do Kim at the Korea Advanced Institute of Science and Technology has widely demonstrated the mass-market potential for nanofibrous-based sensing. The especially exciting development is due to the integration of sensors platforms into USB-enabled electronic devices to allow it to be connected to smartphone devices (Samsung). It is this extra step that helps end users imagine the mass-market potential and makes future commercialization more likely.

Currently, optical and photoconductive properties of the ES sensing materials have been exploited in electronic noses and then commercialized.

The natural fit between electrospun nanofibers and the requirements for a sensing material, together with the ability to produce nanofibers from a wide range of materials and in combination with a variety of functional additives, means that ES sensors can be applied in a plethora of sensing devices, suggesting a significant commercialization potential. For instance, a recently funded project called iSMART has reported interesting developments in the commercialization nanofibrous sensors based on cost-effective and flexible electrochemical devices at commercial scale suitable for disposable medical diagnostics.

High expectations are also focused onto the new and upcoming projects that make the ES nanofibers an extremely intriguing subject, whose numerous features are still far to be fully discovered.

References

- [1] Kumar C. Nanomaterials for medical diagnosis and therapy. In: *Nanotechnologies for the life science*, vol. 10. Weinheim: Wiley-VCH Verlag GmbH & Co; 2007, p. 1–757, ISBN 978-3-527-31390-7.
- [2] Malik P, Katyal V, Malik V, Asatkar A, Inwati G, Mukherje TK. Nanobiosensors: concepts and variations. *ISRN Nanomater* 2013;2013(9). <http://dx.doi.org/10.1155/2013/327435>.
- [3] Ariga K, Ito H, Hill JP, Tsukube H. Molecular recognition: from solution science to nano/materials technology. *Chem Soc Rev* 2012;41:5800–35.
- [4] Cao G, Wang Y. Nanostructures & nanomaterials: synthesis, properties & applications. In: *World scientific series in nanoscience and nanotechnology*, vol. 2. Singapore: World Scientific; 2011. p. 596, ISBN 978-981-4322-50-8.
- [5] Kalantar-Zadeh K, Fry B. Nanotechnology-enabled sensors. New York: Springer-Verlag US; 2008. p. 490, ISBN 978-0-387-32473-9. <http://dx.doi.org/10.1007/978-0-387-68023-1>.
- [6] <http://www.nano.gov/you/nanotechnology-benefits> (N.R. Fuller, Sayo-Art).
- [7] Ray A, Kopelman R. Hydrogel nanosensors for biophotonic imaging of chemical analytes. *Nanomedicine* 2013;8(11):1829–38.
- [8] <http://met.usc.edu/projects/nano.php>.
- [9] Macagnano A, Zampetti E, Kny E. Electrospinning for high performance sensors. *Nanoscience and technology series*. Switzerland: Springer International Publisher; 2015. p. 329, ISBN 978-3-319-14405-4. <http://dx.doi.org/10.1007/978-3-319-14406-1>.
- [10] Macagnano A, Zampetti E, Pantalei S, De Cesare F, Bearzotti A, Persaud KC. Nanofibrous PANI-based conductive polymers for trace gas analysis. *Thin Solid Films* 2011;520:978–85.
- [11] <http://www.understandingnano.com/nanotechnology-medical-diagnosis.html>.

- [12] Randeria P, Briley WE, Chinen AB, Guan CM, Petrosko SH, Mirkin CA. Nanoflares as probes for cancer diagnostics. *Cancer Treat Res* 2015;166:1–22. http://dx.doi.org/10.1007/978-3-319-16555-4_1.
- [13] Abakumov MA, Nukolova NV, Sokolsky-Papkov M, Shein SA, Sandalova TO, Vishwasrao HM, et al. VEGF-targeted magnetic nanoparticles for MRI visualization of brain tumor. *Nanomedicine* 2015;11:825–33.
- [14] Kerr CA, de la Rica R. Photoluminescent nanosensors for intracellular detection. *Anal Methods* 2015;7:7067–75. <http://dx.doi.org/10.1039/C5AY00489F>.
- [15] Hou S, Zhao L, Shen Q, Yu J, Ng C, Kong X, et al. Polymer nanofibre-embedded microchips for detection, isolation, and molecular analysis of single circulating melanoma cells. *Angew Chem* 2013;52:3379–83.
- [16] Lin M, Chen J-F, Lu Y-T, Zhang Y, Song J, Hou S, et al. Nanostructure embedded microchips for detection, isolation, and characterization of circulating tumor cells. *Acc Chem Res* 2014;47:2941–50.
- [17] Uzun SD, Kayaci F, Uyar T, Timur S, Toppare L. Bioactive surface design based on functional composite electrospun nanofibres for biomolecule immobilization and biosensor applications. *ACS Appl Mater Interfaces* 2014;6(7):5235–43.
- [18] Mattanavee W, Suwanton O, Puthong S, Bunaprasert T, Hoven VP, Supaphol P. Immobilization of biomolecules on the surface of electrospun polycaprolactone fibrous scaffolds for tissue engineering. *ACS Appl Mater Interfaces* 2009;1(5):1076–85.
- [19] De Cesare F, Macagnano A. Electrospinning-based nanobiosensors. In: Macagnano A, et al., editors. *Electrospinning for high performance sensors. NanoScience and technology series*. Switzerland: Springer International Publisher; 2015. p. 225–79. http://dx.doi.org/10.1007/978-3-319-14406-1_10. [chapter 10].
- [20] Liu Y, Ding Y, Zhang Y, Lei Y. Pt–Au nanocorals, Pt nanofibres and Au microparticles prepared by electrospinning and calcination for nonenzymatic glucose sensing in neutral and alkaline environment. *Sensor Actuat B-Chem* 2012;171–172:954–61.
- [21] Zhang Y, Wang Y, Jia J, Wang J. Nonenzymatic glucose sensor based on graphene oxide and electrospun NiO nanofibres. *Sensor Actuat B-Chem* 2012;171–172:580–7.
- [22] Zhang B, Liu G, Yao A, Xiao Y, Du J, Guo Y, et al. A sensitive AgNPs/CuO nanofibres nonenzymatic glucose sensor based on electrospinning technology. *Sensor Actuat B-Chem* 2014;195:431–8.
- [23] Wang LX, Bai J, Bo XJ, Zhang XL, Guo LP. A novel glucose sensor based on ordered mesoporous carbon–Au nanoparticles nanocomposites. *Talanta* 2011;83:1386–91.
- [24] Adekunle AS, Ozoemena KI. Electron transport and electrocatalytic properties of MWCNT/nickel nanocomposites: hydrazine and diethylaminoethanethiol as analytical probes. *J Electroanal Chem* 2010;645:41–9.
- [25] Zhu CZ, Wang P, Wang L, Han L, Dong SJ. Facile synthesis of two-dimensional graphene/SnO₂/Pt ternary hybrid nanomaterials and their catalytic properties. *Nanoscale* 2011;3:4376–82.
- [26] Gu ZG, Yang SP, Li ZJ, Sun XL, Wang GL, Fang YJ, et al. An ultrasensitive hydrogen peroxide biosensor based on electrocatalytic synergy of graphene-gold nanocomposite, CdTe–CdS core-shell quantum dots and gold nanoparticles. *Anal Chim Acta* 2011;701:75–80.
- [27] Bai H, Li C, Shi GQ. Functional composite materials based on chemically converted graphene. *Adv Mater* 2011;23:1089–115.
- [28] Luo Y, Nartker S, Miller H, Hochhalter D, Wiederoder M, Wiederoder S, et al. Surface functionalization of electrospun nanofibres for detecting *E. coli* O157: H7 and BVDV cells in a direct-charge transfer biosensor. *Biosens Bioelectron* 2010;26:1612–7.

- [29] Yang MH, Yang YH, Liu B, Shen GL, Yu RQ. Amperometric glucose biosensor based on chitosan with improved selectivity and stability. *Sensor Actuat B-Chem* 2004;101:269–76.
- [30] Wang J. Electrochemical glucose biosensors. *Chem Rev* 2008;108:814–25.
- [31] Ren GL, Xu XH, Liu Q, Cheng J, Yuan XY, Wu LL, et al. Electrospun poly(vinylalcohol)/glucose oxidase biocomposite membranes for biosensor applications. *React Funct Polym* 2006;66:1559–64.
- [32] Wu J, Yin F. Sensitive enzymatic glucose biosensor fabricated by electrospinning composite nanofibres and electrodepositing Prussian blue film. *J Electroanal Chem* 2013;694:1–5.
- [33] http://www.diabetes.co.uk/diabetes_care/blood-sugar-level-ranges.html.
- [34] Marx S, Jose MV, Andersen JD, Russell AJ. Electrospun gold nanofibre electrodes for biosensors. *Biosens Bioelectron* 2011;26:2981–6.
- [35] Li D, Freya MW, Baeumner AJ. Electrospun polylactic acid nanofibre membranes as substrates for biosensor assemblies. *J Membr Sci* 2006;279(1–2):354–63.
- [36] Liu Y, Chen J, Nguyen T, Too CO, Misoska V, Wallace GG. Nanofibre mats from DNA, SWNTs, and poly(ethylene oxide) and their application in glucose biosensors. *J Electrochem Soc* 2008;155(5):K100–3.
- [37] Wang X, Wang X, Wang X, Chen F, Zhu K, Xu Q, et al. Novel electrochemical biosensor based on functional composite nanofibres for sensitive detection of p53 tumor suppressor gene. *Anal Chim Acta* 2013;765:63–9.
- [38] Vousden KH, Lane DP. p53 in health and disease. *Nat Rev Mol Cell Biol* 2007;8:275–83.
- [39] Luo Y, Nartker S, Wiederoder M, Miller H, Hochhalter D, Drzal LT, et al. Novel biosensor based on electrospun nanofibre and magnetic nanoparticles for the detection of *E. coli* O157:H7. *IEEE Trans Nanotechnol* 2012;11(4):676–81.
- [40] Dai H, Xu G, Zhang S, Gong L, Li X, Yang C, et al. Carbon nanotubes functionalized electrospun nanofibres formed 3D electrode enables highly strong ECL of peroxydisulfate and its application in immunoassay. *Biosens Bioelectron* 2014;61:575–8.
- [41] Sharma R, Lamba S, Annapoorni S, Sharma P, Inoue A. Magnetic properties of polypyrrole-coated iron oxide nanoparticles. *J Appl Phys* 2005;97(1).
- [42] Pal S, Alocilja EC. Electrically active polyaniline coated magnetic (EAPM) nanoparticle as novel transducer in biosensor for detection of *Bacillus anthracis* spores in food samples. *Biosens Bioelectron* 2009;24:1437–44.
- [43] Reinholdt SJ, Sonnenfeldt A, Naik A, Frey MW, Baeumner AJ. Developing new materials for paper-based diagnostics using electrospun nanofibres. *Anal Bioanal Chem* 2014;406:3297–304.
- [44] Sun M, Ding B, Lin J, Yu J, Sun G. Three-dimensional sensing membrane functionalized quartz crystal microbalance biosensor for chloramphenicol detection in real time. *Sensor Actuat B-Chem* 2011;160(1):428–34.
- [45] Senecal A, Magnone J, Marek P, Senecal K. Development of functional nanofibrous membrane assemblies towards biological sensing. *React Funct Polym* 2008;68:1429–34.
- [46] <http://www.livescience.com/51296-whispering-gallery-for-light-may-lead-to-clothes-that-detect-disease.html>.
- [47] Dweik RA, Amann A. Exhaled breath analysis: the new frontier in medical testing. *J Breath Res* 2008;2:030301.
- [48] Mathew TL, Pownraj P, Abdulla S, Pullithadathil B. Technologies for clinical diagnosis using expired human breath analysis. *Diagnostics* 2015;5:27–60. <http://dx.doi.org/10.3390/diagnostics5010027>.

- [49] Peng G, Hakim M, Broza YY, et al. Detection of lung, breast, colorectal, and prostate cancers from exhaled breath using a single array of nanosensors. *Br J Cancer* 2010;103:542–51.
- [50] Fernández del Río R, O'Hara ME, Holt A, Pemberton P, Shah T, Whitehouse T, et al. Volatile biomarkers in breath associated with liver cirrhosis—comparisons of pre- and post-liver transplant breath samples. *EBioMedicine* 2015;2:1243–50. <http://dx.doi.org/10.1016/j.ebiom.2015.07.027>.
- [51] Kim I-D, Choi S-J, Kim S-J, Jangm J-S. Exhaled breath sensors. In: Kyung C-M, editor. *Smart sensors for health and environment monitoring*. Dordrecht: Springer; 2015. p. 19–49, ISBN 978-94-017-9980-5.
- [52] Macagnano A, Bearzotti A, De Cesare F, Zampetti E. Sensing asthma with portable devices equipped with ultrasensitive sensors based on electrospun nanomaterials. *Electroanalysis* 2014;26:1419–29. Special Issue: electroanalysis-based clinical diagnostics.
- [53] Zampetti E, Pantalei S, Bearzotti A, Bongiorno C, De Cesarea F, Spinella C, et al. TiO₂ nanofibrous chemoresistors coated with PEDOT and PANi blends for high performance gas sensors. *Procedia Eng* 2012;47:937–40.
- [54] Zampetti E, Pantalei S, Muzyczuk A, Bearzotti A, De Cesare F, Spinella C, et al. A high sensitive NO₂ gas sensor based on PEDOT–PSS/TiO₂ nanofibres. *Sensor Actuat B-Chem* 2013;176:390–8.
- [55] Yoo KH, Han KJ, Kim J, Kang KS, Chen Y. The TiO₂ nanoparticle effect on the performance of a conducting polymer Schottky diode. *Nanotechnology* 2008;19:505202.
- [56] <http://www.kurzweilai.net/nanofibre-sensor-instantly-detects-diabetes-or-lung-cancer-in-breath>.
- [57] Shin J, Choi S-J, Lee I, Youn D-Y, Park CO, Lee J-H, et al. Thin-wall assembled SnO₂ fibers functionalized by catalytic pt nanoparticles and their superior exhaled-breath-sensing properties for the diagnosis of diabetes. *Adv Funct Mater* 2013;23:2357–67.
- [58] Choi S-J, Choi C, Kim S-J, Cho H-J, Hakim M, Jeon S, et al. Highly efficient electronic sensitization of non-oxidized graphene flakes on controlled pore-loaded WO₃ nanofibres for selective detection of H₂S molecules. *Sci Rep* 2015;5. <http://dx.doi.org/10.1038/srep08067>. Article number: 8067.
- [59] Zhang Y, Kim JJ, Chen D, Tuller HL. Electrospun polyaniline fibers as highly sensitive room temperature chemiresistive sensors for ammonia and nitrogen dioxide gases. *Adv Funct Mater* 2014;24:4005–14.
- [60] Norris ID, Shaker MM, Ko FK, Macdiarmid AG. Electrostatic of ultrafine conducting fibers: polyaniline/polyethylene oxide blends. *Synth Met* 2000;114(2):109–14.
- [61] Zhou Y, Freitag M, Hone J, Stali C. Fabrication and electrical characterization of polyaniline-based nanofibres with diameter below 30 nm. *Appl Phys Lett* 2003;83:3800–2.
- [62] Desai K, Sung C. DOE optimization and phase morphology of electrospun nanofibres of PANI/PMMA blends. In: *Proc. tech. 2004 NSTI nanotechnol. conf. trade show, Boston, MA, March 7–11, Vol. 3, p. 429–32, 9; 2004*.
- [63] Haynes AS, Gouma PI. Electrospun conducting polymer-based sensors for advanced pathogen detection. *IEEE Sens J* 2008;8:701–5.
- [64] Hostikas K, Papatheodorou G, Ganas K, Psathakis K, Penagou P, Loukides S. pH in expired breath condensate of patients with inflammatory airway disease. *Am J Respir Crit Care Med* 2002;165:1364–70.
- [65] Chen Z, Lu C. Humidity sensors: a review of materials and mechanisms. *Sensor Lett* 2005;3:274–95.

- [66] Kuang Q, Lao C, Wang ZL, Xie Z, Zheng L. High sensitivity humidity sensor based on a single SnO₂ nanowire. *J Am Chem Soc* 2007;129:6070–1.
- [67] Cheng B, Tian B, Xie C, Xiao Y, Lei S. Highly sensitive humidity sensor based on amorphous Al₂O₃ nanotubes. *J Mater Chem* 2012;21:1907–12.
- [68] Li Z, Zhang H, Zheng W, Wang W, Huang H, Wang Ce, et al. Highly sensitive and stable humidity nanosensors based on LiCl doped TiO₂ electrospun nanofibres. *J Am Chem Soc* 2008;130:5036–7.
- [69] Jiang P, Jie J, Yu Y, Wang Z, Xie C, Zhang X, et al. Aluminium doped n-type ZnS nanowires as high-performance UV and humidity sensors. *J Mater Chem* 2012;22:6856–61.
- [70] Kulwicki BM. Humidity sensors. *J Am Ceram Soc* 1991;74:697–708.
- [71] Mogera U, Sagade AA, George SJ, Kulkarni GU. Ultrafast response humidity sensor using supramolecular nanofibre and its application in monitoring breath humidity and flo. *Sci Rep* 2014;4. <http://dx.doi.org/10.1038/srep04103>. Article number: 4103.
- [72] Huang J, Deng H, Song D, Xu H. Electrospun polystyrene/graphene nanofibre film as a novel adsorbent of thin film microextraction for extraction of aldehydes in human exhaled breath condensates. *Anal Chim Acta* 2015;878:102–8.
- [73] Kahn N, Lavie O, Paz M, et al. Dynamic nanoparticle-based flexible sensors: diagnosis of ovarian carcinoma from exhaled breath. *Nano Lett* 2015;15:7023–8.
- [74] Di Natale C, Macagnano A, Martinelli E, Paolesse R, D'Arcangelo G, Roscioni C, et al. Lung cancer identification by the analysis of breath by means of an array of non-selective gas sensors. *Biosens Bioelectron* 2003;18:1209–18.
- [75] Egashira M, Shimizu Y. Odor sensing by semiconductor metal oxides. *Sensor Actuat B-Chem* 1993;13:443–6.
- [76] Hatfield JV, Neaves P, Hicks PJ, Persaud KC, Tavers P. Toward an integrated electronic nose using conducting polymer sensors. *Sensor Actuat B-Chem* 1994;18:221–8.
- [77] Staples EJ. Electronic nose simulation of olfactory response containing 500 orthogonal sensors in 10 seconds. In: *Proceedings of the 1999 IEEE ultrasonics frequency control and ferroelectrics symposium, Lake Tahoe, CA, USA; 2000*. p. 307–13.
- [78] Gardner JW, Bartlett PN. *Electronic noses: principles and applications*. Oxford: Oxford University Press; 1999. p. 221–45.
- [79] Kybert NJ, Egan L, Waldman RZ, Zeng X-N, Krein M, Preti G, et al. Analysis of sweat simulant mixtures using multiplexed arrays of DNA-carbon nanotube vapor sensors. *J Forensic Sci Criminol* 2014;1:1–6.
- [80] Wilson AD. Advances in electronic-nose technologies for the detection of volatile biomarker metabolites in the human breath. *Metabolites* 2015;5(1):140–63. Wilson AD, Baietto M. Applications and advances in electronic-nose technologies. *Sensors* 2009;9:5099–148.
- [81] Gouma PI, Stanacevic M, Simon S. An overview of the translation of selective semiconducting gas sensors from first results to automotive exhaust gas monitors to a platform for breath-based diagnostics. *Transl Mat Res* 2015;2:045001.
- [82] <http://phys.org/news/2016-03-sensitive-electronic-biosniffers-diseases-biomarkers.html>.
- [83] Zampetti E, Pantalei S, Scalese S, Bearzotti A, De Cesarea F, Spinella C, et al. Biomimetic sensing layer based on electrospun conductive polymer webs. *Biosens Bioelectron* 2011;26:2460–5.
- [84] <http://www.vaporsens.com/sensors/>.

This page intentionally left blank

Index

Note: Page numbers followed by *f* indicate figures, and *t* indicate tables.

A

- Acetone sensors, breath analysis, 401–403, 403*f*
- Additive manufacturing (AM) methods, 74
 - complex patterned architectures by, 77–83
 - 3D printer technology, 79–81, 80–81*f*
- Adipose-derived stem cell (ADSC) culture, 135
- Air-impedance electrospinning, 213, 214*f*
- Aldehyde sensors, breath analysis, 406
- Allium sativum* (AE), 168, 169*f*
- Allografts, 94, 186–187
- Angiogenic growth factors, 293
- ANIMALCLOT, 135–136
- Anticancer drugs, 137
- Antigen-antibody complex, 394
- Antimicrobial agent
 - agar/polymer electrospun, 29, 29*f*
 - AgNPs, 29–30
 - airborne fine particulates, 32
 - chitosan nanofibers, 30
 - cyclodextrins, 33–34
 - dentistry, 359–362, 361*f*, 364*t*
 - ePTFE, 32, 33*f*
 - hydrophilic drug, 28, 28*f*
 - IC formation and solution, 33–34, 35*f*
 - inhibition zone measurements, 31*f*
 - preparation, 26–28
 - silver/polyacrylonitrile, 29–30
 - titanium dioxide, 30–32, 31–32*f*
 - zinc oxide, 30
- Antimicrobial peptides (AMPs), 162, 166
- Astrocytes, 299–300, 304
- Atomic layer deposition (ALD), 32
- Autografts, 186–187, 186*f*
- AVflo, 66–68, 110
- Axon guidance, 307

B

- Bacterial cellulose (BC), 104
- Basic fibroblast growth factor (bFGF), dentistry, 368
- BBG. *See* Borate bioactive glass (BBG)
- Biased alternating current electrospinning, 216–217, 217*f*
- Bilayered nanofibrous mats (BNFs), 23
- Bioactive glass, 209–211, 365, 366–367*f*
- Biosensors, 394, 397–398
 - drugs detection, 397
 - E. coli*, 391, 391*f*, 394–395
 - for glucose detection, 390–393, 390*f*
- Bixin (Bix), 162–163
- Blend electrospinning, 5–6, 28*f*, 137, 206, 293, 331
 - bioactive agent for, 22*f*
 - polymer/drug, 117–118, 125–131
- Blood analysis, ES-nanosensors, 388–398
 - cancer, drugs, and infectious agents' detection, 393–398, 395–396*f*, 398*f*
 - CTCs capturing systems, 389–390, 389*f*
 - glucose sensors, 390–393, 390–391*f*
- Blood vessels
 - structure of, 262–266, 263*f*
 - tissue engineering, qualities of, 265–266
- Bone morphogenetic protein-2 (BMP-2), 139, 246–247, 331–332, 367–368
- Bone structure, 234
- Bone tissue engineering, 233–235
 - applications in, 93–94
 - calcium phosphates, 242–243
 - carbon nanotubes, 243–244
 - functional nanomaterials, 243
 - gelatin nanofibers, 238–239
 - human fetal osteoblast cell, 239–240, 241*f*
 - hydroxyapatite and, 239–242, 241*f*
 - magnetic nanoparticles, 244–245
 - nanodiamond, 245–246
 - PCL, 236, 240–245

- Bone tissue engineering (*Continued*)
 PLA, 236–240, 237–238*f*, 242–243
 PLACL, 238–239
 poly(L-lactic acid)/Ca-deficient
 nanohydroxyapatite, 240–242
 therapeutic applications, 246–247
- Borate bioactive glass (BBG), 365, 366–367*f*
- Bovine serum albumin (BSA), 119–120
- Brain-derived neurotrophic factor (BDNF),
 307–310
- Brain repair
 cell migration, 309–310
 cellular responses, 309
 challenges of, 299–301
 dura repair, 310–311, 311*f*
 inflammatory responses, 309
- Breath analysis
 acetone sensors, 401–403, 403*f*
 aldehyde sensors, 406
 chemoresistive/conductometric sensors,
 398–399
 conventional diagnostic methods, 398
 e-nose technology, 406–410, 407*f*, 409*f*,
 411*f*
 humidity sensors, 405–406
 NH₃ and pH sensors, 404–405
 NO sensors, 399–401, 400*f*, 402*f*
 toluene and H₂S sensors, 403–404
- Bubble-electrospinning, 64–66
- C**
- Calcium phosphates
 bone tissue engineering, 242–243
 dentistry, 357, 362–365
- Cancer treatment, 337–338
 chemotherapy, 338–344, 339–343*t*
 circulating tumor cell, 349–351, 350*t*
 gene therapy, 347–349
 local drug delivery, 337, 344
 magnetic hyperthermia, 344–346, 345*t*,
 346*f*
 photothermal-chemotherapy, 346–347,
 348*t*
- Carbon nanotubes (CNTs), 243–244, 292,
 395–397
- Cardiac fibroblast (CFs), 291–292, 291*f*
- Cardiac myocytes, 292, 293*f*
- Cardiac patch, 290–292
 angiogenic growth factors, 293
 bio-functionalized, 292–293
 synthetic and natural polymers,
 290–291
- Cardiac tissue engineering, 289–294
- Cardiomyocytes, 289–293
- Cardiovascular diseases (CVDs), 120–122,
 128–129, 289
- Caries, 357, 370–373
- Cartilage tissue, 93
- Cationized gelatin (CG), 119–120
- Cell migration, 3–4, 309–310
- Cell therapy, 289, 292
- Centrifugal spinning, 322
- Chemical vapor deposition (CVD), 120–122
- Chemokines, 208–209
- Chemotherapy, cancer, 338–344, 339–343*t*,
 346–347, 348*t*
- Chitin/chitosan, 156–157, 156*f*, 197–198
- Chondroitin 6-sulfate, 208
- Circulating tumor cells (CTCs), 349–351,
 350*t*, 389–390, 389*f*
- Cleome droserifolia* (CE), 168, 169*f*
- Coaxial electrospinning, 5–6, 8*f*, 22*f*, 89–90,
 131–132, 275–276, 291, 322–323, 344
 immiscible solvents, 324
 morphology, 4
 in nanomedicine, 329–332
 needle vs. needleless, 324–329, 325*f*
 neural tissue engineering, 307
 physical principle, 323–324
 scheme of, 325*f*
- Collagen, 181–182, 186, 193, 359
 bone tissue engineering, 236–238
 deposition, 157–159, 291–292, 291*f*
 dermal regeneration, 193
 neural tissue engineering, 307
 vascular tissue engineering, 264–267, 274,
 277–278
 wound healing applications, 150–152,
 153*f*, 160–161
- Composite polymer nanofibers, wound
 healing scaffolds, 167–173
- Contact guidance, 301–303
- Core-shell nanofibers, 322–323
 in nanomedicine, 329–332
 optimized design for, 326*f*
 porous and nonporous morphology,
 327–329

- production, 324–326
 - types, 327
 - Covalent bonding, 124–125
 - Cranial bone defects, repair of, 246–247
 - Cryo-electrospinning, 213–214, 215*f*
 - CTCs. *See* Circulating tumor cells (CTCs)
 - Curcumin (Cur), 163–164
 - Cyclodextrins (CDs), 33–34
 - Cylindrical coaxial spinning electrode, 326, 326*f*
 - Cytokines, 208–209
- D**
- Delamination, 309
 - Dentistry, 357–359
 - antimicrobial properties, 359–362, 361*f*, 364*t*
 - bioactive glass, 365, 366–367*f*
 - drug delivery, 372–373, 372*f*, 374*f*
 - functionally graded and multilayered membranes, 368–370, 369–370*f*
 - growth factors, 365–368
 - hydroxyapatite, 362–364
 - regenerative endodontics, disinfection role, 371
 - treatment modalities, 358
 - tricalcium phosphate, 364–365
 - Dermal regeneration templates (DRTs), 187–188
 - Dermal wound healing
 - air impedance, 213, 214*f*
 - alginate dressings, 186
 - allografts, 186–187
 - ambient parameters, 192*t*
 - autografts, 186–187
 - biased alternating current electrospinning, 216–217, 217*f*
 - bioactive glass, 209–211
 - chemokines, 208–209
 - chitin/chitosan, 197–198
 - composite scaffolds, 203–206
 - cryo-electrospinning, 213–214, 215*f*
 - cytokines, 208–209
 - ECM proteins, 207–208
 - electrospinning, 188–192, 191*f*
 - electrospun scaffolds for, 192–218
 - epithelial tissue regrowth, 182–183
 - gelatin, 196, 197*f*
 - gold standards, 185–187
 - inflammation, 182, 184*t*
 - manuka honey, 206–207
 - nanoparticles, 207–208
 - natural biopolymers, 199*t*
 - noncellularized wound dressings, 185–186
 - pharmaceuticals, 211–212
 - poloxamer, 202–203
 - polycaprolactone, 198–200
 - polyglycolide, 200, 200*f*
 - polylactide, 201
 - polystyrene, 201–202
 - polyvinylpyrrolidone, 203
 - pore size, increasing, 217–218
 - porogen incorporation, 215
 - processing parameters, 192*t*
 - proliferation, 183, 184*t*
 - regeneration templates, 187–188
 - remodeling phase, 184, 184*t*
 - sacrificial fiber, 215
 - silk fibroin, 194–196
 - solution parameters, 192*t*
 - synthetic polymers, 198–203, 204*t*
 - timeline and phases, 182, 183*f*
 - tissue engineered products, 187–188, 190*t*
 - typical and atypical, 182–185
 - wound care adjuncts, 185–186
 - Dermis, 179–181, 180*f*
 - Dichloroacetate (DCA), in cancer, 338
 - Dichloromethane (DCM), 139
 - Dimethyloxalylglycine (DMOG), 131–132, 131*f*
 - Dodecyltrimethylammonium bromide (DTAB), 134
 - Dopants
 - to electrospinning process, 212*t*
 - to polymers, 206–212
 - Dorsal root ganglia (DRG), 302–303
 - Doxorubicin (DOX)
 - in cancer, 338–344, 346–347, 348*t*
 - hydrochloride, 106–107, 107*f*
 - Drug adsorption, 119–120
 - Drug delivery
 - anticancer drugs, 137
 - bioactive molecules, 119, 124–125
 - biocompatibility, 117
 - cancer treatment, 337, 344
 - coaxial electrospinning, 131–132
 - commercialization prospects, 134–138

Drug delivery (*Continued*)

- core-shell nanofibers, 321–323, 331
- covalent bonding, 124–125
- DNA release, 126*f*
- drug adsorption, 119–120
- drug-encapsulating nanoparticle, 133–134
- drug-loaded micro/nanoparticles, 132–134
- drug molecules into, 117–118, 118*f*
- growth factors delivery, 136–137
- LBL assembly, 120–124
- polymer/drug blend electrospinning, 125–131
- problems in, 138–140
- Drug-loaded micro/nanoparticles, 132–134
- Dura repair, 310–311, 311*f*
- Dynamic liquid electrospinning, 217

EECM. *See* Extracellular matrix (ECM)

Elastin fibers, 181–182

Electroblowing, 60

Electrochemiluminescent (ECL) technique, 395–397, 396*f*Electronic-nose (e-nose) technology, for breath analysis, 406–410, 407*f*, 409*f*, 411*f*

- Electrospinning, 233. *See also* Nanofibers, electrospinning
 - additive manufacturing methods, 77–83
 - astrocytes interaction on, 304
 - AVflo, 66–68
 - biased alternating current electrospinning, 216–217, 217*f*
 - for biomedical applications, 45–46, 46*f*
 - biomedical products, 67*t*
 - blood analysis, nanosensors for, 388–398, 390–391*f*, 395–396*f*, 398*f*
 - bone (*see* bone tissue engineering)
 - in brain regeneration, 301*f*
 - breath analysis, nanosensors for, 398–406
 - bubble-electrospinning, 64–66
 - coaxial and double electrospinning, 50, 51*f*
 - collagen/chitosan scaffolds, 205
 - commercial products, 66–69
 - custom-designed melt electrospinning device, 88*f*
 - delivery of drug (*see* Drug delivery)
 - dermal wound healing, 188–192, 191*f*

- dopants to, 212*t*
- drug-loaded micro/nanoparticles, 132–134
- dynamic devices, 76–77
- electroblowing, 60
- electroconductive wire, 75, 76*f*
- electrohydrodynamic process, 57–58
- and electrospaying, 57–60, 87
- electrostatic field, manipulation, 74–76
- fabricated collector, 74–75, 75*f*
- fibers' orientation, 49, 49*f*
- fundamentals of, 3
- history of, 57–58
- industrial upscaling, 53
- interfiber spacing, 302–303, 303*f*
- LE-500 and LE-1000, 59–60
- Nanofiber Solutions Inc. 3-D scaffolds, 68
- needleless (*see* Needleless electrospinning)
- nozzle-based multijet electrospinning, 58–60
- parameters, 235
- patterned collector, 76, 76*f*, 82*f*, 83
- polymer solution jet, 73
- porous characteristics of, 300
- ReBOSSIS, 69
- RIVELIN Patch, 68
- sensors based on, 387–388
- setup, 73
- solvents, requirements for, 46–47, 48*t*
- spinneret geometry, 57–59, 62–64, 64*f*
- technologies and set-ups, 47–53
- tendon/ligament regeneration, 248–252, 250–251*f*
- 3D electrospun constructs, 50–53, 52*f*
- tubular scaffold, 77*f*
- variations to, 213–218
- Electrospaying, 57–60, 78–79, 87, 238–239
- Electrospun collagen skin substitutes (ECSS), 150
 - immunohistological images, 151*f*
 - skin substitutes fabricated using, 151*f*
- Electrospun nanofibrous scaffold (ENS), 45–46, 236
 - drug delivery application, 247
 - human fetal osteoblast cells, 241*f*
 - for tendon/ligament tissue engineering, 249
 - in wound healing, 150–173
- Electrospun scaffolds
 - astrocytes on, 304
 - in brain regeneration, 301*f*, 309–311

- cardiac tissue engineering, 289–294
 - conductive, 312*t*
 - for dermal wound healing, 192–218
 - fabrication parameters for, 268–270, 271*t*
 - neurons (*see* Neural tissue engineering)
 - vascular tissue (*see* Vascular tissue engineering)
 - Electrostatic field, 44, 322
 - manipulation, 74–76
 - patterned collector, 76, 76*f*
 - Emulsion electrospinning, 22*f*, 206, 293
 - Endothelial cells (ECs), 262–265, 263*f*
 - Endothelial progenitor cells (EPCs), 261–264, 272
 - Enterococcus faecalis*, 361*f*, 373
 - Epidermal growth factor (EGF), 136–137, 208
 - Epidermis, 179–180, 180*f*
 - Epi-Guide, 365, 367*f*
 - Essential oils (EOs), 33–34
 - Ethyl cellulose (EC), 8–10
 - Exhaled-breath sensors, 401, 403*f*
 - Expanded polytetrafluoroethylene (ePTFE), 32, 33*f*
 - Extended spectrum β -lactamase (ESBL), 169–170, 170*f*
 - Extracellular matrix (ECM), 3, 10, 43–44, 233
 - adhesive glycoprotein, 266–267
 - blood vessels, 262, 264–265
 - bone, 234–238
 - dermal wound healing, 207–208
 - environment, 299–300
 - fibrillar architecture, 289
 - surface functionalization using molecules, 305–307, 306*t*
- F**
- Fabrication, 43–44, 47–48
 - aligned-to-random scaffold, 74–75, 75*f*
 - FGM, 369–370
 - fibers' orientation, 49
 - parameters for electrospun scaffolds, 268–270, 271*t*
 - SF electrospun nanomatrix, 159*f*
 - 3D electrospun constructs, 50–53
 - FASTCLOT, 135–136
 - Fiber resonator, graphic representation, 397–398, 398*f*
 - Fibroblast growth factor (FGF), 136–137, 208, 249, 250–251*f*
 - Focused, low density, uncompressed nanofiber (FLUF), 217–218, 219*f*
 - Forcespinning, 322
 - Freeze-dried collagen skin substitutes (FCSS), 150
 - immunohistological images, 151*f*
 - skin substitutes fabricated using, 151*f*
 - Functionally graded membrane (FGM), 368–370, 369–370*f*
 - Fusidic acid (FA), 164–165
 - Fusobacterium nucleatum*, 361–362, 364*t*
- G**
- Gas chromatography and mass spectrometry (GC-MS), 398–399
 - Gelatin (GE), 152–153, 154*f*, 196, 197*f*
 - Gene therapy, cancer, 347–349
 - Glial cell-derived neurotrophic factor (GDNF), 307–308
 - Glial scar, 299–300, 304, 313
 - Glucose oxidase (GOD), 391–393
 - Glyceraldehyde-3-phosphate dehydrogenase (GAPDH), 124–125
 - Glycosaminoglycans (GAGs), 181, 264–265, 267
 - Gold nanoparticles (AuNPs), 292, 407*f*
 - Granulocyte macrophage colony-stimulating factor (GM-CSF), 209
 - Graphene, 313, 390–391
 - Growth cone, 301–303, 302*f*
 - Guided bone and tissue regeneration (GBR/GTR), 358–362, 365, 368
- H**
- Heart valve tissue engineering, 294
 - HeLa cells, 338–344, 347, 351
 - Hematoxylin, 153*f*
 - Hexafluoroisopropanol (HFP), 139
 - Honey, poly(vinyl alcohol), chitosan nanofibers (HPCS), 168, 169*f*
 - Human dermal microvascular endothelial cells (HDMECs), 120, 122*f*
 - Human fetal osteoblast cell, mineral depositions, 239–240, 241*f*
 - Human tendon stem/progenitor cells (hTSPCs), 250–252, 253*f*

- Human umbilical vein endothelial cells (HUVECs), 273, 275–276, 294
- Human vascular smooth muscle cells (HVSMCs), 274
- Humidity sensors, breath analysis, 405–406
- Hyaluronic acid (HA), 153–154, 208
- Hydroxyapatite (HA)
- bone tissue engineering, 239–242
 - coaxial electrospinning, 332
 - dentistry, 362–364
- Hyperthermia therapy, cancer, 344–346, 345*t*, 346*f*
- I**
- Ibuprofen, 211
- Immunosensor, 394–397, 395*f*
- Interdigitated sensor array (ISA), 408–410
- Interleukin-10 (IL-10), 208
- Iron oxide nanoparticles (IONPs), 344
- K**
- Keratinocytes, 180
- Ketoprofen (KET), 8–10
- L**
- Lavender oil (LO), 168–169
- Layer-by-layer (LBL) deposition, 117–118, 120–124, 308, 313
- Ligaments structure, 248
- Ligaments tissue engineering, 94–95, 233–234, 248
- fibroblast growth factor, 249, 250–251*f*
 - poly(D,L lactide-co-glycolide), 249, 250–251*f*
 - poly(L-lactic acid-co-ε-caprolactone), 250–252
 - polymeric microfibers, 248–249
- Local drug delivery, cancer treatment, 337, 344
- M**
- Magnetic hyperthermia, 344–346, 345*t*, 346*f*
- Magnetic nanoparticles, 389, 395*f*
- bone tissue engineering, 244–245
 - cancer therapy, 346, 346*f*
- Manuka honey, 134–135, 206–207
- Matrix metalloproteinase (MMP), 125
- MEDIFOAM, 157, 160*f*
- Melanocytes, 180
- Melt electrospinning
- bone tissue, 93–94
 - cartilage tissue, 93
 - commercial applications, 95–96
 - muscle tissue, 93
 - neural tissue, 91–92, 92*f*
 - process of, 87–89
 - skin tissue, 94
 - and solution electrospinning, 89–91
 - tendon tissue, 94–95
- 3-Mercaptopropionic acid (MPA) method, 397
- Mesoporous silica nanoparticles (MSNs), 338–344
- Methicillin-resistant *S. aureus* (MRSA), 168–170, 170*f*
- Metronidazole benzoate (MET), 360, 361*f*, 369–370
- MI. *See* Myocardial infarction (MI)
- Microcantilevers, 394
- Microfiber disks (MFD), 137–138
- Microfluidic spinning, 87
- Micropatterning, 308, 308*f*
- Multijet electrospinning, 58–60
- Multinozzle injectors, 57–59
- Multiwalled carbon nanotubes (MWNTs), 236, 237–238*f*, 243–244, 393–394
- Muscle tissue, 93
- Myocardial infarction (MI), 289, 292
- N**
- Nanodiamond, bone tissue engineering, 245–246
- Nanofibers, electrospinning
- Ag NP release profile, 9*f*
 - antimicrobial agent, 26–34
 - biocompatibility, 101
 - biomedical application of, 4–34
 - burn healing, 110*f*
 - chitosan nanoparticles, 7*f*
 - clinical applications, 101
 - clinical studies in human, 108–111, 111*t*
 - commercialization prospectus, 34–36
 - constructing scaffolds, 17*f*
 - core-shell electrospinning (*see* Coaxial electrospinning)
 - diameter and morphology, 3–4

- donor wound, 111*f*
 - doxorubicin hydrochloride, 106–107, 107*f*
 - drug delivery, 4–10
 - dynamic rotating collector, 3–4
 - fibrous membranes, shrinkage test, 17*f*
 - gross wound conditions, 104*f*
 - hybrid scaffold, 18–19, 18*f*
 - in vivo studies in animal models, 102–108, 103*f*, 109*f*
 - low pore-structure controllability, 18
 - mechanical properties, 18
 - melt-plotting method, 19*f*
 - of natural and synthetic polymers, 101
 - NO-releasing dressings, 105*f*
 - physical drug loading, 5*f*
 - in regenerative dentistry (*see* Dentistry)
 - regulatory agencies, 101–102
 - setup and preparation, 6*f*
 - surface modification techniques, 3, 11*f*
 - therapeutic process, 106*f*
 - tissue engineering, 10–19
 - triaxial electrospinning process, 10*f*
 - wound dressing, 19–26
 - Nanoflares, 388–389
 - NanoMatrix3D, 321
 - Nanomedicine, coaxial electrospinning in, 329–332
 - Nanosensors, 385–387, 386*f*, 389
 - for blood analysis, 388–398, 390–391*f*, 395–396*f*, 398*f*
 - for breath analysis, 398–406
 - Nanospider, 139–140, 324
 - NanoVelcro chip, 389, 389*f*
 - Nanoyarn, 217, 218*f*
 - Natural biopolymers, 192–198
 - Natural polymer
 - cardiac patch, 290–291
 - electrospinning, 101
 - vascular tissue engineering, 266–267
 - as wound healing scaffolds, 150–162
 - Needle coaxial electrospinning, 321–322, 324–329, 325*f*
 - Needleless electrospinning, 152–153, 154–155*f*
 - coaxial electrospinning, 321–322, 324–329, 325*f*
 - fiber generators in, 60–64, 61*f*, 64*f*
 - needle vs., 324–329, 325*f*
 - Nerve growth factor (NGF), 10–11, 13–14, 137, 307–308
 - Neural progenitor cells (NPCs), 309–310
 - Neural stem cells (NSCs), 299, 303
 - Neural tissue engineering, 91–92, 92*f*, 300–301, 301*f*
 - cell migration, 309–310
 - cellular responses, 309
 - cocultures, 304–305
 - commercialization aspects, 313–314, 314*t*
 - dura repair, 310–311, 311*f*
 - ECM molecules, 305–307, 306*t*
 - future challenges, 314–315
 - gradient/patterned coatings, 308, 308*f*
 - inflammatory responses, 309
 - neurotrophic factors, 307–308
 - passive vs. active stimulation, 312–313, 312*t*
 - recording/stimulating electrodes, 313
 - 3D in vitro platforms, 300–301, 301*f*
 - Neurite outgrowth, 301–302, 312
 - Neuronal networking, 299
 - Neurotrophic factors, 307–308
 - NO sensors, breath analysis, 399–401, 400*f*, 402*f*
 - Nozzle-based multijet electrospinning, 58–60
- P**
- Papillary dermis, 181
 - PCL/chitosan composite electrospun scaffolds, 205
 - PDGF. *See* Platelet-derived growth factor (PDGF)
 - Periodontal ligament (PDL) fibers, 107–108
 - Periodontitis, 357–359
 - antimicrobial properties, 359–362, 361*f*, 364*t*
 - bioactive glass, 365, 366–367*f*
 - drug delivery, 372–373, 372*f*, 374*f*
 - functionally graded and multilayered membranes, 368–370, 369–370*f*
 - growth factors, 365–368
 - hydroxyapatite, 362–364
 - regenerative endodontics, disinfection role, 371
 - treatment modalities, 358
 - tricalcium phosphate, 364–365
 - Pharmaceuticals, 211–212

- Phosphate-buffered saline (PBS), 119
 Photolithography, 78–79, 78f
 Photothermal therapy, cancer, 346–347, 348t
 Plasma factor VIII (FVIII), 135
 Platelet-derived growth factor (PDGF), 119
 dentistry, 368
 dermal wound healing, 208
 Platelet-rich plasma (PRP), 208–209, 210f
 dermal wound healing, 208–209
 Poloxamer, 202–203, 202f
 Poly(3-hydroxybutyrate) (PHB), 131–132
 Poly(D,L lactide-co-glycolide), 249, 250–251f
 Poly(DL-lactic acid) (PDLA), 131–132
 Poly(ϵ -caprolactone) (PCL), 91, 198–200, 200f
 bone tissue engineering, 236, 240–245
 coaxial electrospinning, 327–329, 327f
 dentistry, 360–365, 368–369
 heart valve scaffold, 294
 morphology and alignment, 14
 neural tissue engineering, 309–310
 orientation distribution, 15f
 PEG and, 124–125
 SEM micrographs, 15f
 vascular tissue engineering, 267–268, 275f, 279f
 Poly(ethylene glycol) (PEG), 132
 and PCL, 124–125
 vascular tissue engineering, 267–268
 Poly(ethylene oxide) (PEO), 193
 Poly(ethyleneimine) (PEI), 128, 129f
 Poly(lactic-co-glycolic acid) (PLGA), 16, 129–134, 133f, 164–165, 165f, 267–268, 279f
 Poly(*N*-isopropylacrylamide) (PNIPAAm), 120–123, 132
 Poly(*p*-xylylene) (PPX), 128–129, 130f
 Poly(vinyl alcohol) (PVA), 128–129, 130f, 166
 Polyamide 66 nanofibers, 82, 82f
 Polyaniline (PANI), 312
 morphology and alignment, 14
 orientation distribution, 15f
 SEM micrographs, 15f
 Poly(*N,N*-dimethylamino-2-ethyl methacrylate) (PDMAEMA) blocks, 135
 Poly(L-lactic acid)-co-poly(ϵ -caprolactone) (PLACL), 238–239
 Poly(carboxybetaine-co-methyl methacrylate) copolymer (CBMA), 21–23
 Polyethylene oxide (PEO), 157
 Polyglycolide (PGA), 200, 200f
 Polylactic acid (PLA), 128, 129f, 201
 biosensor based on paper, 393, 395
 bone tissue engineering, 236–240, 237–238f, 242–243
 chemical structure of, 201f
 nanofibers, 163–164, 164f
 Poly-L-lactic acid (PLLA), 127, 166, 167f
 Polymer/drug blend electrospinning, 125–131
 Polypropylene (PP) ring, 16
 Poly(lactic acid)/silk fibroin/nerve growth factor (PS/N)
 air plasma treatment, 12f
 fabrication, 10–11
 surface roughness and hydrophilicity, 13f
 wet-chemical etching approach, 14
 Polystyrene (PS), 201–202, 202f
 Polyurethane (PU), 165–166
 Polyvinylpyrrolidone (PVP), 203, 203f
 Porcine iliac artery endothelial cells (PIECs), 273–274
 Porogens, 215
Porphyromonas gingivalis, 359–362, 361f, 364t, 373
 Preparation rich in growth factors (PRGF), 135, 209
 Proteoglycans, 181
 Pulmonary circulation, 262–263
 Pulpal disease, 370–373
- Q**
 Quartz crystal microbalances (QCMs), 394, 397
- R**
 Rabbit conjunctival fibroblast (RCF) proliferation, 193
 ReBOSSIS, 69
 ReCell, 187–188, 189f
 Recombinant epidermal growth factor (rhEGF), 124–125
 Recombinant human PDGF-BB (rhPDGF-BB)-eluting PLGA-collagen hybrid scaffolds, 171, 172–173f

- Reduced instruction set computing (RISC)
 microcontroller, 399
- Regenerative endodontics, disinfection role
 in, 371
- Relative humidities (RH), 405–406
- Reticular dermis, 181
- Reverse transcription polymerase chain
 reaction (RT-PCR), 124–125
- RIVELIN Patch, 68
- RNA interference (RNAi), 347
- S**
- Sacrificial fibers, 215, 216*f*
- SBF. *See* Simulated body fluid (SBF)
- Scanning electron microscopy (SEM)
 bacteria test, 391*f*
 bioactive glass, 365, 367*f*
 core-shell nanofibers, 328*f*
 electrospun bilayer, 278*f*
 FGM processed via multilayering
 electrospinning, 369–370, 370*f*
 luminal surface, 277*f*
 radicular dentin specimen, 374*f*
 tendon/ligament regeneration, 250*f*
 vascular tissue engineering, 275–277, 278*f*
- Schwann cells, 304–305
- Silk fibroin (SF), 194–196, 195*f*
 bone tissue engineering, 239, 246–247
 wound healing, 157–159, 158–159*f*
- Silver nanoparticles (AgNPs), 160–161
- Silver/polyacrylonitrile (Ag/PAN), 29–30
- Simulated body fluid (SBF), 242–243
- Single-nozzle electrospinning technique, 4–5
- Single-walled carbon nanotubes (SWNTs),
 393
- Skin, anatomy and physiology, 179–182
- Skin tissue, 94
- α -Smooth muscle actin (SMA), 152–153,
 155*f*
- Smooth muscle cells (SMCs), 263–264,
 273–276
- Sol-gel process, 239–240
- Solution electrospinning, 87, 89–91,
 403–404
- Split-thickness skin graft (STSG), 189*f*
- Sprague-Dawley (SD) rat models, 152, 193,
 194*f*, 195–196, 273, 276–278, 278*f*
- Stereolithography, 79
- Stratum
 basale/germinativum, 180
 corneum, 181
 granulosum, 180–181
 lucidum, 181
 spinosum, 180
- Stromal cell-derived factor-1 α (SDF-1 α), 368
- Subventricular zone (SVZ), 299, 309–310
- SURGICLOT, 135–136
- Synthetic polymers, 198–203
 cardiac patch, 290–291
 dermal wound healing, 198–203
 electrospun nanofibers, 101
 tissue engineering, 45–46
 vascular tissue engineering, 267–268
 wound dressing, 21–23
 wound healing scaffolds, 162–166
- T**
- Taylor cone formation, 63
- TEGADERM, 165–166
- Tendons structure, 248
- Tendons tissue engineering, 94–95, 233–234,
 248
 fibroblast growth factor, 249, 250–251*f*
 poly(D,L lactide-co-glycolide), 249,
 250–251*f*
 poly(L-lactic acid-co- ϵ -caprolactone),
 250–252
 polymeric microfibers, 248–249
- Tenofovir (TFV), 139–140
- Tetrafluoroethylene (TFE), 139
- Thin-film microextraction (TFME), 406
- 3D CAD model, 79, 81, 81*f*
- 3D printer technology, 79–83, 80–81*f*
- Tin dioxide (SnO₂) fibers, 401–403
- Tissue culture plate (TCP), 13–14
- Tissue engineering (TE), 10–19
 bone (*see* Bone tissue engineering)
 cartilage tissue, 93
 3D electrospun constructs, 50–53, 52*f*
 dentistry, 358–359
 for dermal wound healing, 187–188, 190*t*
 electrospinning technologies and set-ups,
 47–53
 electrospun nanofibers, 50
 fabrication, 43–44, 47–53
 fibers' orientation, 49, 49*f*

Tissue engineering (TE) (*Continued*)

- heart valve, 294
- muscle tissue, 93
- nanofibrous scaffold architecture, 44*f*
- neural (*see* Neural tissue engineering)
- products service, 37*t*
- regenerative medicine, 43
- skin tissue, 94
- solvents, requirements for, 46–47, 48*t*
- synthetic and natural polymers, 45–46
- tendon tissue, 94–95
- vascular system (*see* Vascular tissue engineering)

Transmission electron microscopy (TEM)

- borate-based bioglass particles, 366*f*
- tendon/ligament tissue engineering, 250*f*
- ZnO nanoparticles, 361–362, 363*f*

Tricalcium phosphate (TCP), dentistry, 364–365

Tunica externa, 263–264

U

Unrestricted somatic stem cells (USSCs), 162–163

V

Valvular heart disease, 294

Vascular endothelial growth factor (VEGF), 120, 137, 265–267

- cardiac patch, 293
- dermal wound healing, 208
- electrospun systems for drug delivery, 120, 122*f*, 137

Vascular smooth muscle cells (VSMCs), 276–277

Vascular tissue engineering, 261–262

- cell sources, 275–276
- fabrication parameters and conditions, 271*t*
- factors affecting, 265
- in vivo applications of, 276–279, 277–279*f*
- mechanical properties, 273–274, 275*f*
- natural materials, 266–267
- processing parameters, 269–270
- solution parameters, 268–269

surface modification, 272–273

synthetic materials, 267–268

Vasodilation, 179

VEGF receptors (VEGFRs), 265

Vitamin A palmitate (VA), 159–160, 161*f*

Vitamin D3, 179

Vitamin E TPGS (VE), 159–160, 161*f*

Volatile organic compounds (VOCs), 398–399, 406–407

W

Weir spinner, 324–325, 326*f*Whispering gallery mode, 397–398, 398*f*

Wound dressing

- Ag-MSNs, 23–26
- coaxial electrospinning, 329–330
- core/shell approach, 21, 22*f*
- development, 147–149
- e-spun personalized nanofibrous dressing, 23–26, 25–26*f*
- gelatin nanofibers, 24*f*
- healing time, 19–20
- human-skin patterned nanofibrous mat, 26, 27*f*
- in vivo wound-healing study, 21–23, 23*f*
- polyurethane/amoxicillin nanofibers, 24*f*
- records, 20–21
- stages, 21
- synthetic polymers, 21–23
- types of wounds, 20*f*

Wound healing

- active agents, 159–160, 170–171
- challenges, 173–174
- collagen, 150–152, 153*f*, 160–161
- composite polymer nanofibers, 167–173
- electrospun nanofibers scaffolds, 149–173
- natural polymer nanofibers as, 150–162
- stages, 147, 148–149*f*
- synthetic polymer nanofibers as, 162–166

Z

Zinc oxide (ZnO)

- dermal wound healing, 208
- nanoparticles, 162–163, 163*f*

Electrospinning, an electro-hydrodynamic process, is a versatile and promising platform technology for the production of nanofibrous materials for tissue engineering and biomedical applications.

Electrospun Materials for Tissue Engineering and Biomedical Applications, examines the rapid development of electrospun materials for use in tissue engineering and biomedical applications. With a strong focus on fundamental materials science and engineering, this book also looks at successful technology transfers to the biomedical industry, highlighting biomedical products already on the market as well as the requirements to successfully commercialize electrospun materials for potential use in tissue engineering and biomedical areas.

This book is a valuable resource for materials and biomedical scientists and engineers wishing to broaden their knowledge on the tissue engineering and biomedical applications of electrospun fibrous materials.

Prof. Tamer Uyar obtained his Ph.D. degree from North Carolina State University, Fiber & Polymer Science program in 2005. Currently, he is an Associate Professor at Institute of Materials Science & Nanotechnology (UNAM) at Bilkent University, Ankara, Turkey. Prof. Uyar is very active in the field of Electrospinning of nanofiber by publishing over 100 peer-reviewed journal papers in this field with the interest of potential applications in Environmental/Filtration, Healthcare, Catalysis, Sensors, Food and Active Food Packaging, Energy, NanoTextiles and NanoAgriculture. Prof. Uyar is Founding Editor of the journal *Electrospinning* (by De Gruyter Open) and currently he is also serving in Editorial Board Member for *Scientific Reports* (by Springer Nature), Editorial Board of *Journal of Nanomaterials* (by Hindawi) and Editorial Advisory Board of *e-Polymers* (by De Gruyter). Prof. Uyar is the Vice-Chair of COST Action MP1206 for Electrospinning of nanofibers. As a young scientist, Prof. Uyar is the recipient of several prestigious International awards/fellowships including 2016 International Cyclodextrin József Szejtli Award and 2012 Fiber Society Distinguished Achievement Award and 2010 Marie Curie International Reintegration Grant (IRG) Fellowship. He also received numerous National awards given only under 40 years of age including 2014 TUBITAK Incentive Award, 2012 Turkish Academy of Sciences Outstanding Young Scientists Award (GEBIP), 2010 METU Parlar Foundation Research Incentive Award and 2009 Outstanding Young Scientist Award by FABED.

Dr. Erich Kny, an expert in materials science and technology with a focus on metals and composite materials and surface technologies, is currently the CEO of KEMYK, an independent company specializing in the commercialization of new technologies. He has published over 100 publications, 3 book contributions and several patents and has edited the conference symposium proceedings at the EMRS 2009 on Polymer Nanocomposites. Dr. Kny obtained his PhD from the University of Vienna and has many years of academic & research experience, having been head of the Engineering Department at the Austrian Research Centre for 17 years as well as a university teaching assistant in the Department of Physical Chemistry of the University of Vienna, Austria. This is complemented by his long industrial experience as deputy head of R&TD at the company Plansee in Austria. He has founded in 2007 the scientific COST network on Polymer Nanocomposites (MP701) and in 2012 the scientific COST network on electrospun nanofibres (MP1206). In both of these scientific networks he holds the position of an action chair.



WP
WOODHEAD
PUBLISHING
An imprint of Elsevier
elsevier.com/books-and-journals

ISBN 978-0-08-101022-8



9 780081 010228